NOVEL THERAPEUTIC INTERVENTIONS AGAINST INFECTIOUS DISEASES: COVID-19

EDITED BY: Sugunadevi Sakkiah, Keun Woo Lee, Chandrabose Selvaraj and Brijesh Kumar Singh

PUBLISHED IN: Frontiers in Pharmacology and Frontiers in Chemistry

frontiers Research Topics

frontiers

ISSN 1664-8714
ISBN 978-2-88974-846-4
DOI 10.3389/978-2-88974-846-4

About Frontiers

Frontiers is more than just an open-access publisher of scholarly articles: it is a pioneering approach to the world of academia, radically improving the way scholarly research is managed. The grand vision of Frontiers is a world where all people have an equal opportunity to seek, share and generate knowledge. Frontiers provides immediate and permanent online open access to all its publications, but this alone is not enough to realize our grand goals.

Frontiers Journal Series

The Frontiers Journal Series is a multi-tier and interdisciplinary set of open-access, online journals, promising a paradigm shift from the current review, selection and dissemination processes in academic publishing. All Frontiers journals are driven by researchers for researchers; therefore, they constitute a service to the scholarly community. At the same time, the Frontiers Journal Series operates on a revolutionary invention, the tiered publishing system, initially addressing specific communities of scholars, and gradually climbing up to broader public understanding, thus serving the interests of the lay society, too.

Dedication to Quality

Each Frontiers article is a landmark of the highest quality, thanks to genuinely collaborative interactions between authors and review editors, who include some of the world's best academicians. Research must be certified by peers before entering a stream of knowledge that may eventually reach the public - and shape society; therefore, Frontiers only applies the most rigorous and unbiased reviews.
Frontiers revolutionizes research publishing by freely delivering the most outstanding research, evaluated with no bias from both the academic and social point of view. By applying the most advanced information technologies, Frontiers is catapulting scholarly publishing into a new generation.

What are Frontiers Research Topics?

Frontiers Research Topics are very popular trademarks of the Frontiers Journals Series: they are collections of at least ten articles, all centered on a particular subject. With their unique mix of varied contributions from Original Research to Review Articles, Frontiers Research Topics unify the most influential researchers, the latest key findings and historical advances in a hot research area! Find out more on how to host your own Frontiers Research Topic or contribute to one as an author by contacting the Frontiers Editorial Office: frontiersin.org/about/contact

NOVEL THERAPEUTIC INTERVENTIONS AGAINST INFECTIOUS DISEASES: COVID-19

Topic Editors:
Sugunadevi Sakkiah, National Center for Toxicological Research (FDA), United States
Keun Woo Lee, Gyeongsang National University, South Korea
Chandrabose Selvaraj, Alagappa University, India
Brijesh Kumar Singh, Duke-NUS Medical School, Singapore

Citation: Sakkiah, S., Lee, K. W., Selvaraj, C., Singh, B. K., eds. (2022). Novel Therapeutic Interventions Against Infectious Diseases: COVID-19. Lausanne: Frontiers Media SA. doi: 10.3389/978-2-88974-846-4

Table of Contents

frontiers in Pharmacology

EDITORIAL
published: 14 March 2022
doi: 10.3389/fphar.2022.852078

Editorial: Novel Therapeutic Interventions Against Infectious Diseases: COVID-19

Sugunadevi Sakkiah[1]*, *Brijesh Kumar Singh*[2], *Keun Woo Lee*[3] and *Chandrabose Selvaraj*[4]*

[1]National Center for Toxicological Research, Jefferson, AR, United States, [2]Duke-NUS Medical School, Singapore, Singapore, [3]Department of Biochemistry, Gyeongsang National University, Jinju, South Korea, [4]Department of Bioinformatics, Alagappa University, Karaikudi, India

Keywords: COVID - 19, SARS – CoV – 2, drug repurpose, molecular docking, virtual screeening

Editorial on the Research Topic

Novel Therapeutic Interventions Against Infectious Diseases: COVID-19

The research topic "Novel Therapeutic Interventions Against Infectious Diseases: COVID-19" intends to examine, at the molecular level, the mechanisms of SARS-CoV-2 infection and their potential inhibition through computational or experimental approaches. Drug targets for SARS-CoV-2 infections and macromolecules responsible for the virion's binding to the host receptor protein are described in detail. The 15 research articles in this issue, each focusing on a different aspect of the fight against SARS-CoV-2, use a variety of interdisciplinary approaches, including computational chemistry, biochemical analyses, and biological activity testing. Contributing authors have searched for novel leads from the available natural substances, new chemical entities, and FDA-approved drugs to target SARS-CoV-2. Indari et al. present a comprehensive update on FDA-approved drugs for repurposing, namely chloroquine, hydroxychloroquine, remdesivir, lopinavir-ritonavir, favipiravir, ribavirin, azithromycin, umifenovir, and oseltamivir as well as convalescent plasma therapy used as antiviral therapy against SARS-CoV-2. Preclinical and clinical findings, treatment regimens, pharmacokinetics, and drug–drug interactions are discussed in this review. Some clinically approved medications have been proposed as potential anti-SARS-CoV-2 options as a result of this repurposing strategy. Yadalam et al. performed a computational study to identify the essential oil components as SARS-CoV-2 antivirals, especially in the pre-procedural mouth rinses for dental settings. Pre-procedural mouth rinses are helpful in decreasing viral particles in the oral cavity, since most of COVID-19 dissemination occurs due to the virus' presence in the mouth. Through the molecular docking and conceptual density functional theory (DFT) approach, the antiviral efficacy of essential oil components are studied against the receptor binding domain (RBD) of the spike protein. The compounds cuminal, carvacrol, myrtanol, and pinocarveol were found to be highly active by showing strong interactions with the RBD and shown to be active based on the correlation between the structure and the activity of the compounds. They recommend these components to be included as pre-procedural mouth rinses for dental procedures. Cai et al. has come up with a rehabilitation strategy by applying intermittent hypoxic preconditioning (IHP) and also showed how IHP can be a beneficial treatment strategy in the management of COVID-19. IHP, a non-drug alternative therapy for COVID-19 management, showed beneficial effects related to the impact of oxidative stress, inflammation, and the immune response. Li and Peng have reported the strategy and challenges and described recent progress in identifying broad-spectrum antivirals through drug repurposing, by classifying them into direct-acting repurposed antivirals (DARA) and host-targeting repurposed antivirals (HTRA). In addition, they have summarized and examined the

OPEN ACCESS

Edited and reviewed by:
Salvatore Salomone,
University of Catania, Italy

***Correspondence:**
Sugunadevi Sakkiah
suguna.dv@gmail.com
Chandrabose Selvaraj
selnikraj@bioclues.org

Specialty section:
This article was submitted to Experimental Pharmacology and Drug Discovery, a section of the journal Frontiers in Pharmacology

Received: *10 January 2022*
Accepted: *31 January 2022*
Published: *14 March 2022*

Citation:
Sakkiah S, Singh BK, Lee KW and Selvaraj C (2022) Editorial: Novel Therapeutic Interventions Against Infectious Diseases: COVID-19. Front. Pharmacol. 13:852078. doi: 10.3389/fphar.2022.852078

putative mechanisms of action of repurposed antivirals with potential broad-spectrum effectiveness against a range of viruses. Xiao et al. reports the potential of myricetin for the inhibition of the main protease in SARS-CoV-2, with a 3 μM IC_{50} in the enzyme assay. They also reported myricetin as having potent effect on bleomycin-induced pulmonary inflammation, by inhibiting the infiltration of inflammatory cells and the secretion of inflammatory cytokines IL-6, IL-1α, TNF-α, and IFN-γ. Rattis et al. have reviewed the therapeutic potential of curcumin, which interferes at different time points during the infection caused by SARS-CoV-2. This review has strategically contributed to the relentless search for therapies that can act on the combat of COVID-19, in addition to providing targets for future studies using the curcumin as an adjuvant treatment to COVID-19. Wang et al. stated the importance of pulmonary surfactants (PS) in treating acute respiratory distress syndrome in COVID-19. The lack of efficacy reported so far is attributed to the insufficient delivery of PS to the lungs; thus, research has been initiated to investigate new drug delivery systems for improving the PS delivery directly to the lungs. In support to that, they have integrated the data on PS with reference to pulmonary physiology and infection with its possible therapeutic benefit in COVID-19 patients. Hsu et al. have found the potency of remdesivir and cyclosporine that synergistically inhibit the human coronaviruses OC43 (HCoV-OC43) and SARS-CoV-2 by showing inhibitory activity against HCoV-OC43 in HCT-8 and MRC-5 cells. This study, suggests that the combination of remdesivir and cyclosporine merits further study as a possible treatment for COVID-19 complicated by a cytokine storm. Du et al. elucidate the add-on effect of honeysuckle for the treatment of COVID-19 with a meta-analysis. Honeysuckle combined with conventional therapy may be beneficial for the treatment of COVID-19 in improving lung CT, clinical cure rate, clinical symptoms, and laboratory indicators and reducing the rate of conversion to severe cases. Wang et al. highlight the role of high-density lipoprotein (HDL) in COVID-19 by analyzing the pathophysiological characteristics of COVID-19, the pleiotropic properties of HDL, the changes and clinical significance of HDL, and prospect of HDL-targeting therapy. They also suggest that the HDL level-raising pharmacological compounds, such as cholesteryl ester transfer protein (CETP) inhibitors and fibrates, which are already in the preclinical research stage, may be considered as potential treatments for patients with COVID-19. Basit et al. have designed the short peptides and report those peptides for blocking interactions between SARS-COV-2 and human ACE2. The RBD is highly conserved and is also a potential target for blocking its interaction with human cell surface receptor. For this, they have chosen the amino acid regions 21–40 and 65–75 of ACE2 as scaffold for the *de novo* peptide design, and those peptides are potentially strong candidates for the blocking of protein–protein interactions. Kulkarni et al. 2021 have characterized the phytocompounds from the *Ulva intestinalis* L. and report its action against the SARS-CoV-2 spike glycoprotein RBD. Some compounds, namely, 2,4-di-tert-butylphenol (2,4-DtBP); doconexent; 4,8,13-duvatriene-1,3-diol (DTD); retinoyl-β-glucuronide 6′,3′-lactone (RBGUL); and retinal had showed better binding affinity for RBD. Similarly, Kumar et al. have also identified the phytocompounds from sesame against SARS-CoV-2 main protease drug target through molecular docking and dynamics. They have identified four natural metabolites from sesame, namely, sesamin, sesaminol, sesamolin, and sesamolinol through docking and dynamics approach with the Mpro and reported their interactions insights. Rizvi et al. have shown the effect of prophylactic use of intranasal oil formulations in the hamster model of COVID-19. They have reported the prophylactic application of two intranasal formulations provided by the National Medicinal Plant Board (NMPB), anu oil and til tailya, in the hamster model of SARS-CoV-2 infection. Their molecular analysis using mRNA expression profiling indicated the reduced expression of pro-inflammatory cytokine genes, including Th1 and Th17 cytokines for both the intranasal formulations as a result of decreased viral load. Fred et al. have performed *in vitro* studies on antidepressant and antipsychotic drugs that reduce the viral infection by SARS-CoV-2. Their results show that approved drugs of antidepressants, including fluoxetine, citalopram, reboxetine, and imipramine, as well as antipsychotic compounds chlorpromazine, flupenthixol, and pimozide inhibited the infection by pseudotyped viruses with minimal effects on cell viability. Overall, the "Novel Therapeutic Interventions Against Infectious Diseases: COVID-19" research topic gives an updated summary of molecular and mechanical insights towards identifying COVID-19 therapeutic targets for the identification or repurposing of molecules to be used against the virus.

AUTHOR CONTRIBUTIONS

All authors listed have made a substantial, direct, and intellectual contribution to the work and approved it for publication.

Conflict of Interest: The authors declare that the research was conducted in the absence of any commercial or financial relationships that could be construed as a potential conflict of interest.

Publisher's Note: All claims expressed in this article are solely those of the authors and do not necessarily represent those of their affiliated organizations or those of the publisher, the editors, and the reviewers. Any product that may be evaluated in this article, or claim that may be made by its manufacturer, is not guaranteed or endorsed by the publisher.

frontiers in Pharmacology

REVIEW
published: 08 March 2021
doi: 10.3389/fphar.2021.632677

An Update on Antiviral Therapy Against SARS-CoV-2: How Far Have We Come?

Omkar Indari[1], *Shweta Jakhmola*[1], *Elangovan Manivannan*[2] *and Hem Chandra Jha*[1]*

[1]Department of Biosciences and Biomedical Engineering, Indian Institute of Technology Indore, Indore, India, [2]School of Pharmacy, Devi Ahilya Vishwavidyalaya, Indore, India

COVID-19 pandemic has spread worldwide at an exponential rate affecting millions of people instantaneously. Currently, various drugs are under investigation to treat an enormously increasing number of COVID-19 patients. This dreadful situation clearly demands an efficient strategy to quickly identify drugs for the successful treatment of COVID-19. Hence, drug repurposing is an effective approach for the rapid discovery of frontline arsenals to fight against COVID-19. Successful application of this approach has resulted in the repurposing of some clinically approved drugs as potential anti-SARS-CoV-2 candidates. Several of these drugs are either antimalarials, antivirals, antibiotics or corticosteroids and they have been repurposed based on their potential to negate virus or reduce lung inflammation. Large numbers of clinical trials have been registered to evaluate the effectiveness and clinical safety of these drugs. Till date, a few clinical studies are complete and the results are primary. WHO also conducted an international, multi-country, open-label, randomized trials-a solidarity trial for four antiviral drugs. However, solidarity trials have few limitations like no placebos were used, additionally any drug may show effectiveness for a particular population in a region which may get neglected in solidarity trial analysis. The ongoing randomized clinical trials can provide reliable long-term follow-up results that will establish both clinical safety and clinical efficacy of these drugs with respect to different regions, populations and may aid up to worldwide COVID-19 treatment research. This review presents a comprehensive update on majorly repurposed drugs namely chloroquine, hydroxychloroquine, remdesivir, lopinavir-ritonavir, favipiravir, ribavirin, azithromycin, umifenovir, oseltamivir as well as convalescent plasma therapy used against SARS-CoV-2. The review also summarizes the data recorded on the mechanism of anti-SARS-CoV-2 activity of these repurposed drugs along with the preclinical and clinical findings, therapeutic regimens, pharmacokinetics, and drug-drug interactions.

Keywords: COVID-19, SARS-CoV-2, drug repurposing, antivirals, mechanism of action, pharmacokinetics

OPEN ACCESS

Edited by:
Sugunadevi Sakkiah, National Center for Toxicological Research (FDA), United States

Reviewed by:
Arnab K. Chatterjee, Calibr at Scripps Research, United States
Farzana Liakath, University of Virginia, United States

***Correspondence:**
Hem Chandra Jha
hemcjha@iiti.ac.in

Specialty section:
This article was submitted to Experimental Pharmacology and Drug Discovery, a section of the journal Frontiers in Pharmacology

Received: *23 November 2020*
Accepted: *15 January 2021*
Published: *08 March 2021*

Citation:
Indari O, Jakhmola S, Manivannan E and Jha HC (2021) An Update on Antiviral Therapy Against SARS-CoV-2: How Far Have We Come?. Front. Pharmacol. 12:632677. doi: 10.3389/fphar.2021.632677

INTRODUCTION

The coronavirus disease of 2019 (COVID-19) pandemic has changed the scenario of the entire world, which has not been seen for a century. Influenza (H1N1 virus) outbreak of Spain that occurred in 1918 was the worst ever hit pandemic in recent history. Now, the current outbreak started in Wuhan, China, has globally spread to 219 countries and territories (WHO, 2020a). Severe acute respiratory

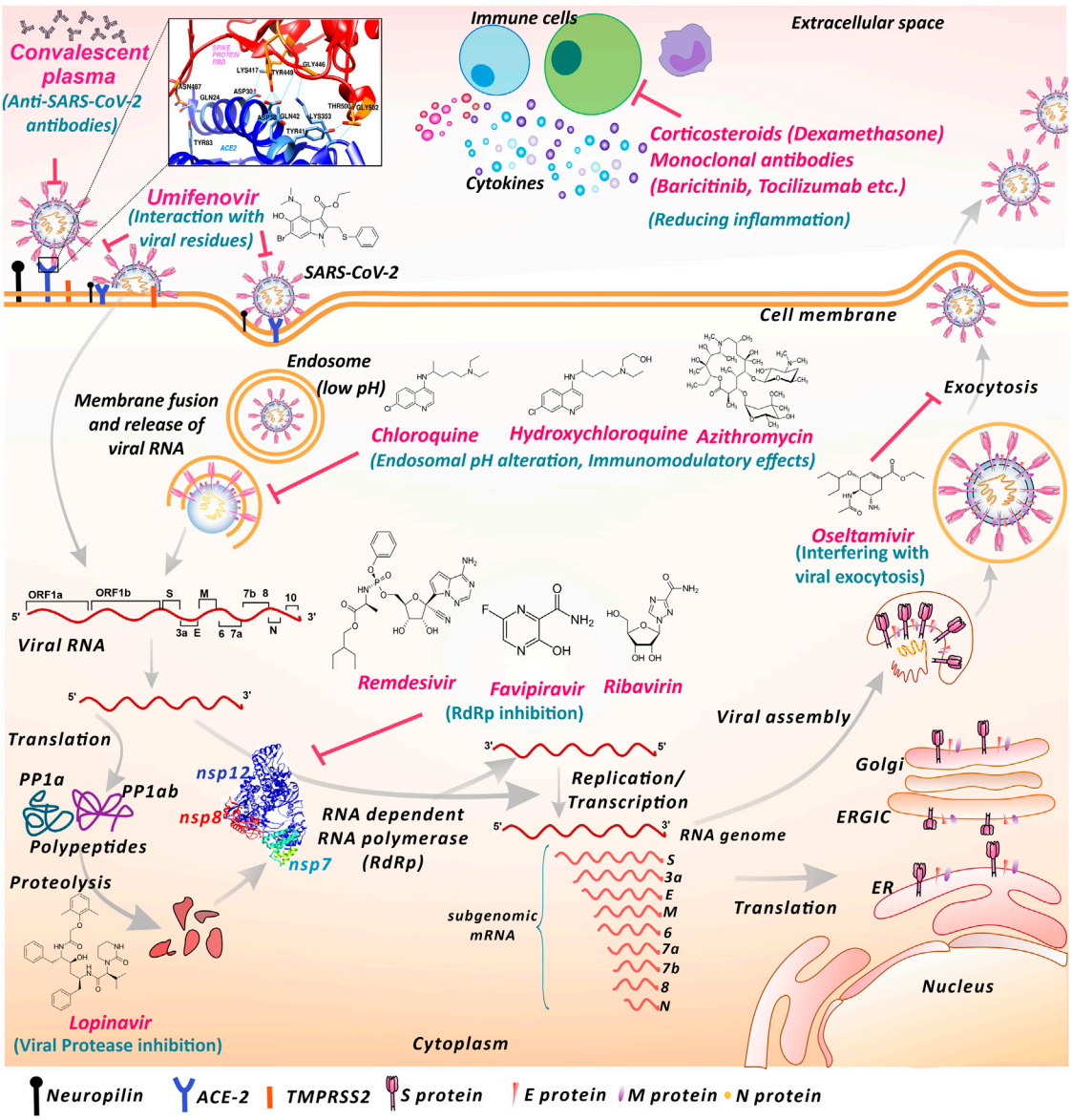

FIGURE 1 | Proposed mechanisms of repurposed drugs and therapies used against SARS-CoV-2 infection. SARS-CoV-2 interacts with cell surface receptors like ACE-2 and neuropilin to gain entry inside the cell. Umifenovir may interact with SARS-CoV-2 surface glycoproteins and lipids and obstruct the interaction with the entry receptor ACE-2. Anti-SARS-CoV-2 antibodies present in convalescent plasma may inhibit SARS-CoV-2 entry and subsequent infection transmission. Chloroquine, hydroxychloroquine and azithromycin may elevate endosomal pH and hinder viral entry and RNA release process. Chloroquine, hydroxychloroquine and azithromycin also shows immunomodulatory effects. Nucleoside inhibitors like remdesivir, favipiravir and ribavirin may inhibit RNA replication and suppress RNA-dependent RNA polymerase activity. Lopinavir may fraternize with viral protease altering the proteolysis. Oseltamivir may interplay with components involved in the exocytosis process, blocking the viral exit from the cell. Monoclonal antibodies against cytokine receptors and Corticosteroid shows anti-inflammatory actions against exaggerated immune response. (ACE-2-Angiotensin-converting enzyme 2, TMPRSS2 Transmembrane Serine protease 2, RdRp- RNA dependent RNA polymerase, ER- Endoplasmic reticulum, ERGIC- Endoplasmic reticulum-golgi intermediate complex. The displayed ACE-2-Spike interaction residues and RdRp structures are based on Protein databank structure ID: 6M0J and 6M71 respectively).

syndrome coronavirus (CoV) 2 (SARS-CoV-2), a large ssRNA virus, is the causative agent of COVID-19, which primarily attacks the respiratory tract including associated organs. Additionally, the virus has shown to impact various other organs or body systems like the gastrointestinal system, nervous system etc (Jakhmola et al., 2020a; Jakhmola et al., 2020b; Sonkar et al., 2020). Currently new variants of SARS-CoV-2 are reported from different regions of the world. In December 2020, the United Kingdom variant of SARS-CoV-2 lineage B.1.1.7, now designated as Variant of Concern 202012/01 (VOC) and the South Africa variant named 501Y.V2 have been reported to spread widely within the country and displaced the other lineages of viruses (WHO, 2020c). By the end of first COVID-19 pandemic year the VOC-202012/01 variant was

reported in 31 other countries/territories (WHO, 2020c). The receptor-binding domain of viral spike protein is essential in SARS-CoV-2 entry into the host cell via surface angiotensin-converting enzyme-2 (ACE-2) (Zhou et al., 2020) (**Figure 1**). Recently, another cell receptor Neuropilin-1 was found to be involved in SARS-CoV-2 entry (Cantuti-Castelvetri et al., 2020). The further life cycle of the virus inside the cell is similar to that of other coronaviruses. After binding to the receptor, the conformational change in the spike protein leads to virus fusion with the host cell membrane. The virus may transfer the RNA directly inside the cells or may proceed through the endosomal pathway (Simmons et al., 2005; Li, 2016; Hasan et al., 2020; Hoffmann et al., 2020). Upon translation of viral RNA, the viral replicase polyprotein PP1a and PP1ab are synthesized and cleaved into small products by viral endopeptidase (Van-Boheemen et al., 2012; Shereen et al., 2020). RNA dependent RNA polymerase (RdRp) produces subgenomic RNAs by discontinuous transcription (Hussain et al., 2005; Chen et al., 2020; Shereen et al., 2020). This further gets translated into respective viral proteins. After processing through the endoplasmic reticulum (ER), ER-Golgi intermediate compartment (ERGIC), and Golgi complex the viral RNA and proteins are assembled into virions (Lai and Cavanagh, 1997; Song et al., 2004). These virions are transported through vesicles and exocytosed for transmission. These steps of the viral life cycle are lucrative virus inhibition targets for different drugs (**Figure 1**).

Currently, no specific drug or vaccine is available for the treatment of SARS-CoV-2 infected patients. Nonetheless, drug repurposing could prove to be advantageous tactics for finding COVID-19 treatment. Benefits of drug repurposing include cost-effectiveness, elimination of some clinical trial steps, sooner on-field availability, combining the candidate drugs with other possible drugs based on prior data, and generation of new information about the existing drugs mechanisms (Agrawal, 2015). The available knowledge of previous CoVs treatments, genomic sequences, and protein modeling studies has helped researchers put forward the potential COVID-19 drug candidates. The primarily investigated drugs are either antimalarials, antivirals, antibiotics, corticosteroids, and they have been repurposed based on their potential either to negate virus, reduce lung inflammation or other disease symptoms. In particular, chloroquine (CQ) hydroxychloroquine (HCQ) and azithromycin (AZM) are majorly used against COVID-19 as they initially showed reasonably good *in vitro* and *in vivo* antiviral activity against SARS-CoV, MERS-CoV and SARS-CoV-2. Lopinavir/ritonavir (LPV/RTV), which are anti-HIV drugs, were examined for COVID-19 as they were found to be effective in earlier CoV outbreaks. Moreover, remdesivir (RDV), an experimental anti-Ebola drug, was investigated for COVID-19 and received greater attention. Based on the appreciable preliminary data, FDA has issued EUA for CQ, HCQ, and RDV (FDA, 2020b; FDA, 2020c; FDA, 2020d). However, later the EUA for CQ and HCQ was revoked while EUA for RDV was re-issued by some amendments. Similarly, favipiravir (FPV), ribavirin (RBV), umifenovir (UFV), and oseltamivir (OTV) having a broad-spectrum antiviral activity were also clinically investigated against SARS-CoV-2. WHO put forward a solidarity clinical trial, a multi-country, open-label randomized trial, for the use of HCQ, RDV, LPV/RTV, or LPV/RTV in combination with Interferon (IFN) β-1a against COVID-19 (WHO, 2020b). The recent interim results of the solidarity trial declare that all these drugs had little or no effect on overall mortality, initiation of ventilation and duration of hospital stay in hospitalized patients (Pan et al., 2020). So far, to treat severe and critical COVID-19, only corticosteroids have proven effective (WHO, 2020b). New treatment options need to be added to the solidarity trial in the future. However, solidarity trials may have few limitations like it was focused on worldwide outcomes of considered treatments. Hence, if a particular drug shows comparatively better outcome in some regions or populations that could get neglected. Therefore, there is scope to conduct the clinical studies involving various suitable drugs with different treatment regimens and combinations.

In this review, we have provided updated comprehensive information about majorly repurposed drugs which are used as antivirals to combat SARS-CoV-2 infection**.** We attempted to collate and review the studies regarding all these drugs, which are dispersed in various distinct publications. Furthermore, we have also summarized the data recorded on the mechanism of anti-SARS-CoV-2 activity of these repurposed drugs along with the preclinical and clinical findings, therapeutic regimens, pharmacokinetics, and drug-drug interactions.

SELECTED ANTIVIRALS REPURPOSING IN COVID-19 TREATMENTS

Chloroquine and Hydroxychloroquine

CQ and HCQ both belong to the 4-aminoquinoline chemical class (Devaux et al., 2020) with potential antimalarial and anti-inflammatory activities. These drugs are weak diprotic bases that increase the endosomal pH to hinder the host-virus fusion process (Devaux et al., 2020) (**Figure 1**; **Table 1**). *In vitro* studies have shown antiviral activity of CQ on MERS and SARS-CoV (Cong et al., 2018; Keyaerts et al., 2004). In addition, *in vivo* studies suggest potent activity of these drugs against human CoV-OC43, EV-A71, zika virus, and *in vitro* activity against influenza-A (Keyaerts et al., 2009; Tan et al., 2018; Li et al., 2017; Ooi et al., 2006). Recent *in vitro* studies report CQ and HCQ effectiveness against SARS-CoV-2 (Half maximal effective concentration (EC50) 2.71mM and 4.51mM, respectively) in Vero E6 cells (Liu J. et al., 2020). However, HCQ has *in vitro* activity with a lower EC50 for SARS-CoV-2 compared to CQ after 24h of growth (HCQ: 6.14μM and CQ: 23.90μM) (Yao X. et al., 2020). CQ treatment has demonstrated to reduce the recovery time and improved physiological conditions in COVID-19 patients. According to a randomized Chinese COVID-19 controlled trial, CQ (Dose 500mg bid, 15days) may work more efficiently than LPV/RTV (Huang M. et al., 2020). Another study compared the low dose (450mg bid for 1day followed by 450mg, 4days) and high dose (600mg bid, 10days) in combination with azithromycin (AZM) and OTV which determined that high dose CQ was associated with high

mortality (Borba et al., 2020). A multicentre, randomized, open-label trial from China investigated the use of HCQ (1200mg daily for 3days, followed by a maintenance dose of 800mg daily) to standard care. The interpretation included that the HCQ treated group showed inadequate response compared to control (Tang et al., 2020). The combination of HCQ and AZM resulted in early viral clearance, as demonstrated by an open-label non-randomized clinical trial (Gautret et al., 2020). A meta-analysis report stated that compared to alone HCQ, the combination of HCQ and AZM significantly increased mortality in COVID patients (Fiolet et al., 2020). A United States based observational study interpreted that HCQ treated patients did not either benefit or suffer in terms of intubation or mortality (Geleris et al., 2020). A large-scale clinical trial was conducted in United Kingdom, a Randomized Evaluation of COVID-19 Therapy (RECOVERY Trial), to investigate various drug candidates or therapies including HCQ against severe COVID-19. The result demonstrated no efficacy of HCQ against COVID-19 (Horby et al., 2020b). Surprisingly FDA issued EUA for CQ and HCQ against COVID-19 on March 28, 2020 and was revoked on June 15, 2020 (FDA, 2020b; FDA, 2020c). Major side effects of these drugs include QT prolongations, and decreased insulin clearance and resistance (FDA, 2020b; FDA, 2020c). The overuse of CQ and HCQ could possibly lead to tissue injury in the liver, retina, skeletal, and cardiac muscle cells due to their lysosomal affinity (Satarker et al., 2020; Cohen, 2020). Therefore, studies recommend that physicians avoid high doses and exercise extreme caution in the compassionate use of CQ/HCQ, either alone or in combination with other antivirals (Acharya and Sayed, 2020). Currently 88 and 267 COVID-19 associated clinical trials have been registered for CQ and HCQ respectively (ClinicalTrials.gov, 2020b; ClinicalTrials.gov, 2020d).

Lopinavir/Ritonavir

LPV/RTV are approved anti-HIV drugs that specifically target HIV protease (Chandwani and Shuter, 2008). LPV is used in combination with RTV to elevate its half-life via cytochrome P450 suppression (Chandwani and Shuter, 2008). LPV is predicted to act on the viral 3-chymotrypsin-like protease (3CLpro) (Sisay, 2020) (**Figure 1**; **Table 1**). Previous studies have established *in vitro* LPV effectiveness against SARS-CoV at 4μg/ml (Chu et al., 2004). A cumulative *in vivo* study involving LPV and RTV against MERS revealed the EC50 of the two drugs as 11.6 and 24.9μM respectively with 50% cytotoxic concentration (CC50) values >50μM (Sheahan et al., 2020). However, no *in vitro* study is available of LPV/RTV against SARS-CoV-2. In China, a clinical trial for LPV/RTV against adult hospitalized COVID-19 patients was conducted (Cao et al., 2020). The study showed no benefit of LPV/RTV (Dose: 400mg/100mg bid, 14days) treatment compared to standard care control groups (Cao et al., 2020). Although LPV/RTV treated groups exhibited less serious complications than the controls. A Japanese case-study reports successful treatment of non-severe COVID-19 pneumonia patients with LPV/RTV (Wada et al., 2020). Another study of 47 patients reported that LPV/RTV treatment improved physiological condition without adverse events (Ye et al., 2020). In the study of 120 patients, if the LPV/RTV treatment is initiated within 10days of symptom onset, it significantly reduces viral shedding (Yan et al., 2020). LPV/RTV along with IFN-α or RBV may improve the health of COVID-19 patients (Yuan et al., 2020). On the contrary, another report from Taiwan suggested that LPV/RTV treatment did not reduce the duration of viral shedding in infected patients (Cheng et al., 2020). A single-center, randomized, open-labeled, prospective clinical trial conducted by Huang *et al.* studied the effect of LPV/RTV plus IFN-α, LPV/RTV plus RBV plus IFN-α, and RBV plus IFN-α treatment on COVID-19 patients. All the three regimens showed no significant difference regarding their effectiveness against COVID-19. LPV/RTV when given in combination with RBV lead to more adverse events suggesting that these two drugs should not be administered together (Huang Y.-Q. et al., 2020). A meta-analysis study investigating randomized trials showed LPV/RTV may reduce mortality (Huang Y.-Q. et al., 2020; Verdugo-Paiva et al., 2020). Albeit some contradictory studies showed no statistically significant effect on reducing the death rate (Karolyi et al., 2020; Horby et al., 2020). A report stated the risk of bradycardia in elderly critically ill COVID-19 patients with RTV plasma overdose (Beyls et al., 2020). Adverse gastrointestinal effects such as diarrhea, nausea and vomiting have been observed in patients treated with LPV/RTV (Huang Y.-Q. et al., 2020; Liu W. et al., 2020; Vecchio et al., 2020). Therefore, it remains difficult to safely recommend LPV/RTV dose without compromising the benefit of the antiviral strategy. There is an urgency of a comprehensive pharmacokinetic/pharmacodynamic analysis for the upcoming clinical trials in similar critically ill COVID-19 patients (Lê et al., 2020). Currently, 90 clinical trials have been registered for LPV/RTV for COVID-19 (ClinicalTrials.gov, 2020e).

Remdesivir

RDV is a prodrug of an adenosine triphosphate (ATP) analog and is converted into its active form GS-441524 on administration (Al-Tawfiq et al., 2020). It was initially proposed for the Ebola virus that acted by viral replication inhibition through premature termination of RNA transcription (Al-Tawfiq et al., 2020) and hence targeting RdRp. RDV metabolites have proved useful against yellow fever virus, Dengue virus type 2, influenza A, parainfluenza 3, and various delta CoVs (Cho et al., 2012). The parent nuclei of RDV is evaluated against alpha CoV (EC50 = 0.78μM), porcine delta CoV, SARS-like bat CoVs and MERS-like bat CoVs (Murphy et al., 2018; Brown et al., 2019; Amirian and Levy, 2020). Studies on SARS and MERS infected human airway epithelial cells (EC50 ≈ 0.07μM) and animal models demonstrated the viral polymerase inhibition ability of the drug (Agostini et al., 2018). The drug is efficient at EC50, 0.77μM, and CC50 > 100μM in Vero E6 cells against SARS-CoV-2 (Wang M. et al., 2020). Studies also revealed that RDV targeted structurally analogous regions of SARS-CoV-2 polymerase (Lo et al., 2020). Several *in-vivo* reports suggested that RDV decreased viral load, reduced pathological processes, alleviated mild symptoms, and improved pulmonary lesions in SARS-CoV-2 infected animals with adverse effect (Frediansyah et al., 2020; Badgujar et al., 2020; Pruijssers et al., 2020). The

TABLE 1 | General information of repurposed drugs used against SARS-CoV-2.

Drugs	Group	Mechanism of action	Targeted virus/disease indication	Molecular target	Possible correlation to be used against COVID 19 treatment	No. of clinical trials registered	Strengths	Limitations
CQ or HCQ	Antiparasitic	Antiviral effect, immuno-modulation	*Plasmodium* sp., arthritis, CoV-OC43, enterovirus 71, zika virus	Altering endosomal pH	Activity against SARS-CoV2 and immuno-modulatory effect	88 and 267	Have shown activity against earlier outbreak CoVs	Shown to cause QTc prolongation, torsades de pointes, ventricular arrhythmia, and cardiac deaths
LPV/RTV	HIV protease inhibitor	Viral protease inhibition	HIV, SARS-CoV, MERS-CoV	Viral protease inhibition	Binding to M^{pro} protein of SARS-CoV-2	90	Have shown activity against earlier outbreak CoVs	No efficacy in multiple clinical trials including large scale clinical trials, known to cause QTc prolongation and is on the possible risk of torsades de pointes
RDV	Nucleoside analogue	Viral RNA synthesis termination	Ebola, SARS-CoV, MERS-CoV, yellow fever virus, dengue virus type 2, influenza A, parainfluenza 3, and various delta CoVs	Adenosine analogue competes with dATP in RNA synthesis	Viral replication inhibition	78	Recently discovered drug active against multiple viruses including delta CoVs, SARS and MERS CoVs, shown efficacy in recent clinical trials	Questionable safety on long term effect as the drug is recently discovered, showed no efficacy in large scale trials, known to cause acute hepatotoxic effect due to an increase in hepatic transaminase activity but no effect on QTc
FPV	Nucleoside analogue	Viral RNA synthesis inhibition	Influenza a and B viruses, arenavirus, bunyavirus, flavivirus, filoviruses and ebola virus	Guanosine analogue competes with dGTP in RNA synthesis	Viral replication inhibition	45	Active against many viruses, shown *in vitro* activity against SARS-CoV-2	Variation in FPV plasma concentration between the US and the Japanese population, shown to cause adverse effects on the fetus
RBV	Nucleoside analogue	Viral RNA synthesis inhibition	Hepatitis C virus, canine distemper virus, enterovirus 71, chikungunya virus, semliki forest virus, orthopoxvirus, influenza virus, flavi- and paramyxoviruses	Guanosine analogue competes with dGTP in RNA synthesis	Viral replication inhibition	15	Shows efficacy against MERS-CoV in animal model and used in earlier CoV outbreaks	Majorly used in combination with other drugs and is not effective against reducing mortality, shown to cause hemolytic anemia and worsening of cardiac disease to myocardial infarctions
AZM	Antibiotic	Bacterial protein synthesis inhibition, Antiviral effect	Bacteria, influenza virus, dengue virus, zika virus, ebola virus	Altering endosomal pH	Activity against SARS-CoV2, immuno-modulatory effect and interfere with viral replication	122	Active against many viruses and shown *in vitro* activity against SARS-CoV-2	Majorly used in combination with other drugs, showed adverse events, no efficacy in large scale trials, shown to cause QTc prolongation including ventricular and supraventricular arrhythmia

(Continued on following page)

TABLE 1 | (*Continued*) General information of repurposed drugs used against SARS-CoV-2.

Drugs	Group	Mechanism of action	Targeted virus/disease indication	Molecular target	Possible correlation to be used against COVID 19 treatment	No. of clinical trials registered	Strengths	Limitations
UFV	Broad spectrum antiviral	Stacking interactions with certain amino acid residues, viral glycoproteins, lipids	Influenza-A virus, respiratory syncytial virus, rhinovirus type-14, Coxsackievirus-B3 and adenovirus type-7	Stacking interactions with certain amino acid residues, viral glycoproteins, lipids	Targeting viral proteins or lipids and preventing viral entry	11	Active against SARS-CoV and SARS-CoV-2 *in vitro*, commonly used	No efficacy against COVID-19, rarely cause serious mental/mood changes but no effect on QTc
OTV	Neuraminidase inhibitor	Inhibits viral neuraminidase enzyme	Influenza a and B viruses	Component involved in exocytosis process	Virus exocytosis Inhibition	20	Commonly used drug	No efficacy against SARS-CoV-2, rarely cause serious mental/mood changes but no effect on QTc

The strength and limitations of drug used are conclusively stated comparing the reports explained in the manuscript. QTc: corrected QT interval.

recommended dose of RDV is 200mg on Day 1 and 100mg daily for 5days (for non-severe cases) to 10days (severe cases). A similar dose was considered in numerous clinical trials. A randomized, open-label, phase 3 trial investigating RDV dose for 5days vs. 10days revealed that the treatment for 5days was comparatively beneficial (Spinner et al., 2020). A double-blinded, randomized, placebo-controlled trial, determined that severe COVID-19 patients treated with RDV showed fast recovery compared to control, though statistically insignificant (Wang Y. et al., 2020). Moreover, the RDV administration is not approved globally due to questionable safety. Although SOLIDARITY trial results denote that RDV is not beneficial against COVID-19, result of some recently completed clinical trials are contrary. A double-blinded, randomized, placebo-controlled trial from the United States showed that RDV treated hospitalized patients may recover faster with comparatively less adverse events and mortality than the placebo group (Beigel et al., 2020). Prominent adverse reactions were acute respiratory failure, decreased glomerular filtration rate, lymphocytopenia, pyrexia, hyperglycemia, increased anemia, increased creatine, and liver transaminases (Beigel et al., 2020; FDA, 2020d). Result of multicentre clinical trial published at the end of first year of the pandemic, showed that RDV given in combination with baricitinib (a Janus kinase inhibitor used to hinder intracellular signaling of cytokines) was effective compared to RDV alone in terms of reducing recovery time additionally speeding improvement (Kalil et al., 2020). Based on such positive results of RDV, it has been approved to use by various authorized platforms like FDA (Mahase and McCullough, 2020). An interesting investigation showed that RDV's parent nucleotide GS-441524 is superior and less toxic than its pro-drug form and has shown efficacy in *in vivo* veterinary settings (Yan and Muller, 2020). Therefore, further investigation regarding the use of the parent nucleotide itself against COVID-19 should be driven with a faster pace. Currently, 78 COVID-19 associated clinical trials are registered with RDV (ClinicalTrials.gov, 2020g).

Favipiravir

Favipiravir (FPV), an approved influenza treatment, is a pyrazinecarboxamide derivative (Furuta et al., 2013). It also showed efficacy against arenavirus, bunyavirus, flavivirus, filoviruses, and Ebola virus (Furuta et al., 2017). The prodrug after administration is transformed by host enzymes into the ribofuranosyl triphosphate derivative (T-705-RTP), a guanine analogue and suppresses the RdRp (**Figure 1**; **Table 1**). *In vitro* effectivity of FPV against SARS or MERS viruses have not been addressed. An *in vitro* study has shown inhibition of SARS-CoV-2 by FPV (EC50 = 61.88μM; CC50 = over 400μM) (Wang X. et al., 2020). In Japan, the approved dose of FPV against influenza is 1,600mg bid on day 1, followed by 600mg bid on days 2–5 with associated side effects (PMDA, 2020). A Chinese open-label, controlled study investigated the effects of FPV (Day 1; 1600mg twice and Day 2–14; 600mg bid) vs. LPV/RTV (Day 1–14; 400mg/100mg bid). The preliminary results indicated potent FPV action and fewer adverse effects than LPV/RTV ($p < 0.001$) (Cai et al., 2020). A report suggested treatment of COVID-19 patients with FPV during times of early symptoms, helped in reducing the SARS-CoV-2 presence in nasal secretions (McCullough, 2020). However, previous clinical trials have reported the variation in FPV plasma concentration between the United States and the Japanese population (Madelain et al., 2016). Therefore, more trials regarding global use of FPV should be considered. In a Japanese study FPV also showed to control inflammatory mediators and pneumonia progression in COVID-19 patients (Yamamura et al., 2020). Severe or critical COVID-19 patients showed improvements after treating with FPV (Takahashi et al., 2020) and FPV also led to improved lung histology (Kaptein et al., 2020). However, in a meta-analysis study, FVP proved to have significant clinical and radiological

improvement without significant differences on viral clearance (Shrestha et al., 2020). For the use of FPV with respect to COVID-19, 45 clinical trials have been registered (ClinicalTrials.gov, 2020c).

Ribavirin

Ribavirin (RBV), a broad-spectrum antiviral prodrug is metabolized in host into a guanosine analog (Gish, 2006). The drug showed antiviral efficacy against canine distemper virus, hepatitis C virus, Enterovirus 71, Chikungunya virus, and Semliki Forest virus, orthopoxvirus, influenza virus, flavi- and paramyxoviruses (Elia et al., 2008; Galli et al., 2018; Li et al., 2008; Briolant et al., 2004; Smee et al., 2001; Leyssen et al., 2005). A study observed reduced replication of the MERS-CoV in rhesus macaques upon treatment with IFN-α2b and RBV (Falzarano et al., 2013). RBV in combination with LPV/RTV was used in SARS-CoV and MERS-CoV trials (Yao T. et al., 2020). In the case of SARS-CoV-2 infection, an *in vitro* study determined the EC50 of RBV as 109.50uM (Wang X. et al., 2020). A study included RBV along with LPV/RTV and IFN-α in the treatment of hospitalized COVID-19 patients (Hung et al., 2020). The triple therapy was found to be beneficial to reduce disease symptoms and virus shedding compared to groups provided LPV-RTV alone. The dose of RBV considered was 400mg bid along with 400mg/100mg of LPV/RTV + IFN-α for 14days. A study assessed the impact of sofosbuvir/daclatasvir (antivirals) compared to RBV in treatment of COVID-19 patients. The mortality was higher (33%) in COVID-19 patients treated with RBV than that of sofosbuvir/daclatasvir (Eslami et al., 2020). A retrospective cohort study comparing RBV vs. supportive therapy stated that RBV did not help in reducing the mortality rate in COVID-19 patients (Tong et al., 2020). 15 clinical trials have been registered for the use of RBV alone or in combination with other COVID-19 drugs (ClinicalTrials.gov, 2020h).

Azithromycin

Azithromycin (AZM) is a semisynthetic macrolide antibiotic belonging to the azalide class (Ballow and Amsden, 1992). It has bactericidal effects and targets the protein synthesis process of bacteria. AZM has also been shown to inhibit influenza, zika, dengue, and Ebola viruses (Damle et al., 2020; Wang M. et al., 2020). Specifically, a study showed AZM induced reduction in rhinovirus replication 7-fold in primary bronchial epithelial cells without inducing cell death (Schögler et al., 2015). The *in vitro* EC50 for AZM against SARS-CoV-2 was 2.12μM (EC90: 8.65μM) following a 72-hour incubation post-infection (MOI of 0.002) (Hughes et al., 2020). The addition of AZM with HCQ was efficient in virus elimination in COVID-19 patients (Gautret et al., 2020). The dose of 500mg on day 1 followed by 250mg/day, the next 4days was used in compliment to HCQ dose of 200mg, three times/day, for 10days. Some investigations suggested HCQ and AZM combination to be beneficial in reducing mortality in COVID-19 patients (Bonny et al., 2020; Arshad et al., 2020). A case report showed AZM provided with HCQ proved to be an effective treatment approach in pregnant women against the SARS-CoV-2 infection and associated with reduced mortality (Sisti et al., 2020). In contrast, a report from the United States stated that neither HCQ nor AZM separately or together could reduce the mortality of COVID-19 patients compared to the control group (Rosenberg et al., 2020). Moreover, treatment of AZM and HCQ was associated with greater changes in QTc in COVID-19 patients (Mercuro et al., 2020). Few other studies also reported that AZM included in treating COVID-19 patients did not provide any beneficial effect (Rodríguez-Molinero et al., 2020; Furtado et al., 2020; Cavalcanti et al., 2020). 122 clinical trials have been registered for the use of AZM alone or in combination with other drugs against COVID-19 (ClinicalTrials.gov, 2020a).

Umifenovir

Umifenovir (UFV) is an indolyl carboxylic acid widely recognized as Arbidol (Blaising et al., 2014). It is used as a treatment and prevention measure against influenza virus (Blaising et al., 2014). It has direct antiviral and host-targeting action. UFV can interact with virus protein or lipid components and may hinder different stages of the viral life cycle (Blaising et al., 2014). *In vitro* analysis of the antiviral activity of arbidol against several human respiratory viruses, namely influenza-A virus, respiratory syncytial virus, rhinovirus type-14, coxsackievirus-B3 and adenovirus type-7 is demonstrated (Shi et al., 2007). Inhibition of SARS-CoV replication on UFV treatment was demonstrated *in vitro*. UFV is also known to inhibit various isolates of zika virus in multiple cell lines (Fink et al., 2018). The inhibitory action of the drug against SARS-CoV-2 in Vero E6 cells (MOI of 0.05) has been demonstrated. The EC50 and CC50 were 4.11 and 31.79μM, respectively (Wang X. et al., 2020). Briefly, the study showed enhanced inhibitory activity at early stages compared to the post-entry stage (**Figure 1**). A small-scale study suggested post-exposure prophylaxis (PEP) use of UFV in people exposed to COVID-19 patients (Zhang et al., 2020). Another study determined that arbidol monotherapy was superior to LPV/RTV against COVID-19 (Zhu et al., 2020). COVID-19 patients provided with UFV along with LPV/RTV showed better outcomes compared to patients who received LPV/RTV only (Deng et al., 2020). A contrary study reported that UFV was not beneficial to improve the condition of the patient or viral clearance (Lian et al., 2020). Moreover, another study suggested arbidol + LPV/RTV were associated with many adverse events (Wen et al., 2020). In most of the studies, a dose of 200mg thrice a day was considered. According to a meta-analysis, UFV was not effective in terms of reducing the SARS-CoV-2 elimination from the infected patient in terms of detection in diagnostic tests and even hospital length of stay of hospitalized patients (Huang D. et al., 2020). There is no evidence to support the use of UFV for improving patient-important outcomes in patients with COVID-19. 11 registered clinical trials include UFV use in COVID-19 treatment (ClinicalTrials.gov, 2020i).

Oseltamivir

Oseltamivir (OTV) is a synthetic derivative prodrug of ethyl ester with antiviral activity (Schade et al., 2014). It acts as a neuraminidase inhibitor against the influenza virus and is also effective for various avian influenza virus strains (Ward et al., 2005). An *in vitro* OTV study on H5N1 influenza showed that the

TABLE 2 | ADMET analysis of drugs repurposed against SARS-CoV-2.

Property	Model name	Predicted value										Unit
		CQ	HCQ	AZM	RMD	RBV	LPV	RTV	FPV	UFV	OTV	
Absorption	Lipophilicity	4.81	3.78	1.90	2.31	−3.01	4.32	5.90	−0.99	5.17	1.28	Numeric (LogP)
	Water solubility	−4.249	−3.627	−4.133	−3.07	−1.71	−4.819	−3.35	−2.12	−3.98	−2.47	Numeric (log mol/L)
	Caco2 permeability	1.62	1.54	−0.21	0.63	0.42	0.06	0.37	0.62	0.83	0.93	Numeric (log papp in 10^{-6}cm/s)
	Intestinal absorption (human)	89.95	90.21	45.80	71.10	54.98	65.60	69.45	91.69	88.29	74.46	Numeric (% Absorbed)
	Skin permeability	−2.67	−2.84	−2.74	−2.73	−2.76	−2.73	−2.73	−3.2	−2.73	−3.17	Numeric (log Kp)
	P-glycoprotein substrate	Yes	Yes	Yes	Yes	No	Yes	Yes	No	Yes	No	Categorical (Yes/No)
	P-glycoprotein I inhibitor	No	No	Yes	Yes	No	Yes	Yes	No	Yes	No	Categorical (Yes/No)
	P-glycoprotein II inhibitor	No	No	No	No	No	Yes	Yes	No	Yes	No	Categorical (Yes/No)
Distribution	VDss (human)	1.33	1.07	−0.214	0.30	−0.01	−0.24	0.42	−0.21	0.72	0.04	Numeric (log L/kg)
	Fraction unbound (human)	0.19	0.24	0.51	0.005	0.78	0	0	0.78	0.12	0.59	Numeric (Fu)
	BBB permeability	0.349	0.07	−1.85	−2.05	−0.92	−0.83	−1.66	−0.12	0.03	−0.69	Numeric (log BB)
	CNS permeability	−2.19	−2.51	−3.77	−4.67	−3.75	−2.935	−3.29	−3.08	−2.19	−3.11	Numeric (log PS)
Metabolism	CYP2D6 substrate	Yes	Yes	No	No	No	No	No	No	No	No	Categorical (Yes/No)
	CYP3A4 substrate	Yes	Yes	Yes	Yes	No	Yes	Yes	No	Yes	No	Categorical (Yes/No)
	CYP1A2 inhibitior	No	Yes	No	No	No	No	No	No	No	No	Categorical (Yes/No)
	CYP2C19 inhibitior	No	No	No	No	No	Yes	No	No	Yes	No	Categorical (Yes/No)
	CYP2C9 inhibitior	No	No	No	No	No	Yes	Yes	No	No	No	Categorical (Yes/No)
	CYP2D6 inhibitior	Yes	Yes	No	No	No	No	No	No	Yes	No	Categorical (Yes/No)
	CYP3A4 inhibitior	No	No	No	No	No	Yes	Yes	No	Yes	No	Categorical (Yes/No)
Excretion	Total clearance	1.09	1.15	-0.42	0.19	0.62	0.45	0.56	0.51	0.68	0.92	Numeric (log ml/min/kg)
	Renal OCT2 substrate	Yes	No	No	No	No	No	No	No	No	No	Categorical (Yes/No)
Toxicity	AMES toxicity	Yes	Yes	No	No	No	No	No	No	No	No	Categorical (Yes/No)
	Max. Tolerated dose (human)	−0.16	−0.09	1.02	0.15	1.01	−0.29	0.09	1.29	0.33	0.47	Numeric (log mg/kg/day)
	hERG I inhibitor	No	No	No	No	No	No	No	No	No	No	Categorical (Yes/No)
	hERG II inhibitor	Yes	Yes	No	Yes	No	Yes	Yes	No	Yes	No	Categorical (Yes/No)
	Oral rat acute toxicity (LD50)	2.85	2.65	2.76	2.04	1.98	2.38	2.70	1.94	2.95	2.67	Numeric (mol/kg)
	Oral rat chronic toxicity (LOAEL)	1.02	1.40	1.99	1.63	3.09	5.94	2.23	2.02	0.73	1.09	Numeric (log mg/kg_bw/day)
	Hepatotoxicity	Yes	Yes	Yes	Yes	No	Yes	Yes	No	Yes	No	Categorical (Yes/No)
	Skin sensitization	No	No	No	No	No	No	No	No	No	No	Categorical (Yes/No)
	T.pyriformis toxicity	1.55	1.06	0.28	0.28	0.28	0.28	0.28	0.09	0.29	0.10	Numeric (log ug/L)
	Minnow toxicity	0.74	1.32	7.80	0.29	4.62	−1.50	1.787	3.40	−0.12	2.31	Numeric (log mM

The ADMET information about selected drugs is predicted using online server http://biosig.unimelb.edu.au/pkcsm/.

IC50 was 0.1–4.9nM (Govorkova et al., 2009). However, an *in vivo* study involving H5N1 infection required a longer course and higher dosage of OTV (Borio et al., 2018). No *in vitro* study against SARS-CoV-2 is conducted for OTV. The COVID-19 originated in China during flu season, and hence earlier, many patients received OTV treatment until the causative agent SARS-CoV-2 was discovered. Some current clinical trials have used OTV in combination with other major therapeutic candidates. A study showed that the drug exhibited no positive result on COVID-19 (Wang D. et al., 2020). 20 clinical trials have been registered which include OTV in the treatment panel of COVID-19 (ClinicalTrials.gov, 2020f).

OTHER POTENTIAL ANTIVIRAL DRUGS AND THERAPIES

Convalescent Plasma Therapy

Apart from antiviral drugs another probable efficient antiviral strategy includes the use of convalescent plasma collected from the recovered patients containing the anti-SARS-CoV-2 antibodies. Convalescent plasma obtained from patients recovered from COVID-19 carry receptor binding domain specific antibodies with potent antiviral activity (Robbiani et al., 2020). These antibodies can directly interact with SARS-CoV-2 proteins and could block the viral entry into the cell (**Figure 1**). In August 2020, FDA issued EUA for the use of convalescent plasma in hospitalized patients (FDA, 2021a). The samples were considered of high titer if it followed one of the following criteria-a neutralizing antibody titer of ≥250 as per Broad Institute's neutralizing antibody assay, a signal-to-cut off (S/C) of ≥12 as per Ortho VITROS IgG assay, or a level of ≥1: 2,880 in the Mount Sinai COVID-19 ELISA IgG Antibody Test (FDA, 2021a; FDA, 2021b; FDA, 2021c). Units with low titer should be specified and considered to use if high titer samples were not available. The initial dose of 200ml is recommended and further the dose is advised as per condition and requirement of the patient. However, clinical trials have used different values of titer or doses and generally convalescent plasma was examined using immunoassays instead of viral neutralization assays. For example, a study reported use of no minimum neutralizing-antibody titer and single dose of 200–500ml plasma as per the patient's condition (Joyner et al., 2020a). While in an open label phase II multicentre randomized controlled trial (PLACID Trial)

from India, two doses of 200ml with titers ranging from 1:20 to ≥1:1,280 (from immunoassay) was used. In a Chinese trial, single dose of median volume of 200–250ml with titer ≥1: 1:640 was used (Li et al., 2020). Although various studies have shown efficacy of this therapy (Ahn et al., 2020; Duan et al., 2020; Abolghasemi et al., 2020; Hegerova et al., 2020; Xia et al., 2020), some clinical trials have demonstrated that use of convalescent plasma did not reduced the hospitalization duration, severity, or mortality compared to the control groups (Simonovich et al., 2020; Li et al., 2020; Agarwal et al., 2020). Recently completed randomized, double-blind, placebo-controlled trial from Argentina showed reduced disease progression in patients treated with high titer (>1:1,000) convalescent plasma (Libster et al., 2021). Also, another multicentre study from Poland stated that convalescent plasma can be given as supportive therapy to COVID-19 patients due to availability and low frequency adverse events (Moniuszko-Malinowska et al., 2020). Another large-scale observational analysis of patients from the United States who received the convalescent plasma put forward the opinion that this therapy could be beneficial if provided in early days of symptoms onset (Joyner et al., 2020b, Effect of Convalescent Plasma on Mortality among Hospitalized Patients with COVID-19: Initial Three-Month Experience, 2020). The titers of neutralizing antibodies from donor and viral titers in recipient should be considered for providing the convalescent plasma and further clinical outcomes should be studied for optimizing the therapy. There is a lack of studies exclusively investigating the effect of convalescent plasma treatment on SARS-CoV-2 infected children or pregnant women. Additionally, the effectivity of convalescent plasma in patients infected with new SARS-CoV-2 variants also needs to be tested. The ongoing trials may shed more light on efficacy of this therapy against COVID-19 patients. However, many trials were terminated due to reduced cases in the study region. Currently, overall 172 clinical trials have been registered to investigate the use of convalescent plasma in COVID-19 patients (ClinicalTrials.gov, 2021a).

New Antiviral Candidates and Other Potential Therapies On-Board

Other than the repurposed drugs the development of anti-SARS-CoV-2 drugs has been accelerated. Recently, a hydroxymethylketone derivative PF-00835,231 showed potency to block protease of SARS-CoV-2 in pre-clinical experiments (Hoffman et al., 2020). This drug has also shown to have suitable pharmaceutical properties and has gathered as an intravenous therapy to cure the disease. Another drug AT-527, a purine nucleotide prodrug, which has shown pan-genotypic efficacy against hepatitis C infection (Good et al., 2020) has also been considered against COVID-19 in a multinational clinical trial (Clinical trial no. NCT04396106). Apart from antiviral drugs, the strategies to tackle increased inflammatory responses during COVID-19 have also been investigated in various studies. Corticosteroids, due to their potent anti-inflammatory effects have gained importance in this regard. Numerous studies investigated a glucocorticoid-dexamethasone but its importance is recently highlighted in large scale RECOVERY trial (Horby et al., 2020a) and further gained recommendation of its use from various platforms. The daily dose of 6mg dexamethasone for 10days was used for hospitalized patients and showed reduced mortality on 28th day compared to the control groups (Horby et al., 2020a). Currently there are 45 registered clinical trials for corticosteroid use against COVID-19 (ClinicalTrials.gov, 2021b).

PHARMACOKINETICS AND DRUG INTERACTIONS OF SOME REPURPOSED DRUGS

Understanding the relationship between the pharmacokinetic properties and the therapeutic effect or side-effect of a drug is clinically important (Takahashi, 2000). The bioavailability, volume of distribution, protein binding, half-life, and elimination are the key determinants of successful drug therapy. Especially in severe COVID-19 cases, complex clinical situations may arise due to multiple organ failure and the consequences of drug action cannot be predicted without sufficient pharmacokinetic data (Zaim et al., 2020; Wang T. et al., 2020). The relevant information can be obtained from preclinical and large randomized clinical trials. However, clinicians will continue to confront the challenge of deciding the dosage of repurposed drugs until the pharmacokinetics parameters are better assessed in COVID-19. Furthermore, multi-drug therapy is unavoidable in the treatment of COVID-19, especially for those patients with pre-existing diseases (Jafari et al., 2020). Therefore, drug-drug interactions (DDIs) are the major concern in clinical practice. It is too early to precisely estimate the effect of DDIs between the experimental drugs used to treat COVID-19 and other prescription drugs. Similarly, the impact of DDIs on pre-existing clinical conditions may not be clearly ruled out. Because, the currently available COVID-19 clinical results are mostly obtained from a relatively short-term study and was not performed in patients taking specific drugs for pre-existing illness (Sciaccaluga et al., 2020). Moreover, clinically significant DDIs can be rationalized in relevant studies performed on appropriate patient populations with high accuracy. Herein, we recapitulate the pharmacokinetics and DDIs of some COVID-19 repurposed drugs under consideration. Additionally, we report the *in silico* pharmacokinetics prediction of all repurposed drugs discussed in this review (**Table 2**).

Generally, the drugs are evaluated for potential risk of DDIs during drug development stage to determine the effect of cytochrome P450 (CYP) and P-glycoprotein mediated interactions (Elmeliegy et al., 2020). However, a lack of published clinical data in this area is a major setback. Some efforts are made to document the potential DDIs and they can be accessed from the COVID-19 Drug Interactions site (Liverpool COVID-19 interactions, 2021) published by the Liverpool Drug Interaction Group and the IBM Micromedex Drug Interaction Checking site (IBM Micromedex, 2021) maintained by IBM Watson Health, Greenwood Village, Colorado, United States.

Two antimalarial drugs CQ and HCQ, with or without a macrolide antibiotic AZM, have been studied in multiple clinical

trials for the treatment of COVID-19. QTc prolongation, Torsade de Pointes, ventricular arrhythmia, and cardiac deaths are major risks of CQ and HCQ. QT prolongation and potentially life-threatening arrhythmias with HCQ therapy originate from its pharmacodynamics action (O'Laughlin et al., 2016). CQ and HCQ are moderate inhibitors of cytochrome P450 (CYP) 2D6, and potential inhibitors of P-glycoprotein (P-gp) (Rendic and Guengerich, 2020). Therefore, these drugs cause a wide range of potential DDIs by altering the plasma concentration of several drugs. HCQ increases the plasma concentrations of amiodaron, dabigatran, edoxaban, cyclosporine, tacrolimus and sirolimus and decreases the bioavailability of carbamazepine and rifampicin with concomitant use (Liverpool COVID-19 interactions, 2021). The co-administration of HCQ with anti-tubercular drugs such as isoniazid or ethambutol increases the risk of peripheral neuropathy in diabetic patients. CQ and HCQ may decrease the activity of RDV and therefore co-administration of these drugs is not recommended. AZM is not metabolized by cytochromes P450 and it is not a substrate/inhibitor of CYP450. AZM is a known P-glycoprotein (P-gp) inhibitor and, if co-administered with P-gp substrates, it may result in increased serum levels requiring special therapeutic dose monitoring (Scherrmann et al., 2020).

RDV is a prodrug that inhibits viral RNA polymerases. The metabolic stability of RDV studied in various animal models showed that it was relatively stable in the intestine (t1/2 = 40.3–114.1min) but unstable in the liver (t1/2 < 3.9min) (FDA, 2020a). The hepatic instability and the complete first-pass effect prevented oral delivery of RDV. Therefore, the drug is administered through the intravenous route (IV). The IV administration of RDV (200mg) to healthy humans produced AUC0-24 values of 4.8μM/h with moderate protein binding. The *in vitro* metabolism studies of RDV suggest that it was predominantly metabolized by CYP2C8, CYP2D6, and CYP3A4. It is extensively metabolized in hepatic tissues, and the rate of metabolism by CYP3A4 alone was estimated as 42.1%. The elimination studies carried out in rats and monkeys showed that kidney and bile excretion were the major routes of elimination of RDV. It has a low potential for significant drug-drug interactions because of its rapid clearance. However, the antiviral activity effect of RDV is reduced when co-administered with CQ or HCQ (COVID-19 treatment update, FDA). It is because of the interference of CQ on the intracellular metabolic activation of RDV. Therefore, the co-administration of inhibitors of such CYPs can lead to a potentially high risk of toxic effect (Cattaneo et al., 2020). In a case study it was reported that RDV induced acute hepatotoxic effect in a male COVID-19 patient and realized the toxic effect was due to probable interaction of P-glycoprotein (P-gp) inhibitors (Leegwater et al., 2020). The clinical history of the patient described that the patient was treated with the P-gp inhibitors like chloroquine and amiodarone along with RDV. An adverse effect of an increase in hepatic transaminase activity was also observed in the clinical trial of RDV. RDV was not genotoxic, and it does not impair male fertility (Singh et al., 2020). Based on these preliminary findings, the FDA had granted a EUA for RDV for the treatment of COVID-19 patients (Ison et al., 2020; FDA, 2020d) and was last reissued on October 22, 2020 with some amendments.

The combination of LPV and RTV was approved for the treatment of HIV infection and has recently been investigated in COVID-19 patients (Jean et al., 2020). RTV-boosted LPV (400/100mg) was orally administered to COVID-19 patients. LPV is predominantly metabolized by CYP3A4 isoenzyme, and RTV is a strong inhibitor of CYP3A4 (Chen, 2005; Gregoire et al., 2020). Therefore, RTV prevented the metabolism of LPV. The concentrations of LPV in COVID-19 patients were extremely high compared with HIV-infected patients. No severe adverse events were reported in the clinical trials of LPV and RTV. However, these two drugs can inhibit metabolism and increase plasma levels of several drugs that may induce toxic effects. The potentially severe DDIs were recorded for the concurrent administration of HCQ and LPV/RTV in hospitalized COVID-19 patients (Cattaneo et al., 2020). Cattaneo, *et al.*, reported that more than fifty percent of category D based DDIs and they are attributed to LPV/RTV. The risk of QT interval prolongation by LPV/RTV therapy may be due to inhibition of human ether-a-go-go related gene (hERG) (Sciaccaluga et al., 2020). The cardiotoxicity risk ratio of LPV/RTV is double that of HCQ and AZM (Cattaneo et al., 2020). Furthermore, RTV is shown to increase in the bioavailability and half-life of immunosuppressant drugs such as tacrolimus and cyclosporine by inhibition of CYP3A (Zijp et al., 2020).

The clinical trial results of FPV showed that the peak plasma concentration was achieved at 2h after oral administration (Du and Chen, 2020). The plasma protein binding of FPV was observed 54% in humans. FPV is metabolized in the hepatic tissues majorly by aldehyde oxidase (AO), and partly by xanthine oxidase (Gowen et al., 2015). The metabolites of FPV are rapidly excreted by the kidneys. Particularly, FPV is a mechanism-based AO inhibitor and affects the action of AO in a concentration-dependent manner. Furthermore, potential DDIs between FPV, cimetidine, and zaleplon have been already reported (Renwick et al., 2002). The chances of occurring DDIs between FPV and citalopram, famciclovir, zaleplon and sulindac are higher as these drugs are also metabolized by AO (Du and Chen, 2020). *In vivo* study showed inhibitory effect of FPV on CYP2C8 isoenzyme. Therefore, more caution was necessary with anticancer agents such as tamoxifen (AO inhibitor) and paclitaxel (CYP2C8 substrate) (Jafari et al., 2020). Furthermore, a clinical study showed that FPV increases the concentrations of antidiabetic drugs such as pioglitazone or repaglinide with concomitant use that leads to the risk of hypoglycemia. Therefore, a great deal of attention must be paid by clinicians in designing the therapeutic dosage regimen.

CONCLUSION

For containing the devastating scenario of COVID-19 pandemic, the identification of potent and less toxic therapeutics for COVID-19 is a key research priority. Current research efforts are intensified on the evaluation of existing drugs against SARS-CoV-2 infection. Despite several challenges in SARS-CoV-2 infection, the drug repurposing strategy has proved its

important role in the rapid discovery of an effective treatment for COVID-19. Only judicious evaluation of these repurposed drugs may show real insights on its clinical effectiveness and clinical safety in COVID-19 patients. Furthermore, it is essential to address the issue of drug-drug interaction of the repurposed drugs in COVID-19 patients with comorbidities (Jakhmola et al., 2020c). In our knowledge, the present review adequately provides all relevant information currently needed to assist clinicians and researchers working in this area.

AUTHOR CONTRIBUTIONS

HJ and OI devised the idea of study. OI, SJ, and EM contributed to literature search. OI, SJ, and EM prepared the initial draft of manuscript. OI developed tables and figure. HJ did the proof reading, correction, modifications and final drafting.

ACKNOWLEDGMENTS

We thank the Department of Biotechnology and Ministry of Human Resource and Development, Govt. of India for the fellowship to OI and SJ, respectively, in the form of a research stipend. The funding organization has not played any role in the study design or the preparation of the manuscript. We appreciate Ms. Annu Rani and our other lab colleagues for their insights, discussions and advice. We gratefully acknowledge the Indian Institute of Technology Indore and Devi Ahilya Vishwavidyalaya, Indore for providing facilities and support.

REFERENCES

Abolghasemi, H., Eshghi, P., Cheraghali, A. M., Imani Fooladi, A. A., Bolouki Moghaddam, F., Imanizadeh, S., et al. (2020). Clinical efficacy of convalescent plasma for treatment of COVID-19 infections: results of a multicenter clinical study. *Transfus. Apher. Sci.* 59, 102875. doi:10.1016/j.transci.2020.102875

Acharya, Y., and Sayed, A. (2020). Chloroquine and hydroxychloroquine as a repurposed agent against COVID-19: a narrative review. *Ther. Adv. Infect. Dis.* 7, 2049936120947517. doi:10.1177/2049936120947517

Agarwal, A., Mukherjee, A., Kumar, G., Chatterjee, P., Bhatnagar, T., and Malhotra, P. (2020). Convalescent plasma in the management of moderate covid-19 in adults in India: open label phase II multicentre randomised controlled trial (PLACID Trial). *BMJ* 371, m3939. doi:10.1136/bmj.m3939

Agostini, M. L., Andres, E. L., Sims, A. C., Graham, R. L., Sheahan, T. P., Lu, X., et al. (2018). Coronavirus susceptibility to the antiviral remdesivir (GS-5734) is mediated by the viral polymerase and the proofreading exoribonuclease. *MBio* 9, e00221-18. doi:10.1128/mBio.00221-18

Agrawal, P. (2015). Advantages and challenges in drug Re-profiling. *J. Pharmacovigilance* s2, e002. doi:10.4172/2329-6887.s2-e002

Ahn, J. Y., Sohn, Y., Lee, S. H., Cho, Y., Hyun, J. H., Baek, Y. J., et al. (2020). Use of convalescent plasma therapy in two COVID-19 patients with acute respiratory distress syndrome in korea. *J. Korean. Med. Sci.* 35, e149. doi:10.3346/jkms.2020.35.e149

Al-Tawfiq, J. A., Al-Homoud, A. H., and Memish, Z. A. (2020). remdesivir as a possible therapeutic option for the COVID-19. *Trav. Med. Infect. Dis.* 34, 101615. doi:10.1016/j.tmaid.2020.101615

Amirian, E. S., and Levy, J. K. (2020). Current knowledge about the antivirals remdesivir (GS-5734) and GS-441524 as therapeutic options for coronaviruses. *One Health* 9, 100128. doi:10.1016/j.onehlt.2020.100128

Arshad, S., Kilgore, P., Chaudhry, Z. S., Jacobsen, G., Wang, D. D., Huitsing, K., et al. 2020). Treatment with hydroxychloroquine, azithromycin, and combination in patients hospitalized with COVID-19. *Int. J. Infect. Dis.* 97, 396–403. doi:10.1016/j.ijid.2020.06.099

Badgujar, K. C., Ram, A. H., Zanznay, R., Kadam, H., and Badgujar, V. C. (2020). Remdesivir for COVID-19: a review of pharmacology, mechanism of action, *in-vitro* activity and clinical use based on available case studies. *J. Drug Deliv. Ther.* 10, 264–270. doi:10.22270/jddt.v10i4-s.4313

Ballow, C. H., and Amsden, G. W. (1992). Azithromycin: the first azalide antibiotic. *Ann. Pharmacother.* 26, 1253–1261. doi:10.1177/106002809202601014

Beigel, J. H., Tomashek, K. M., Dodd, L. E., Mehta, A. K., Zingman, B. S., Kalil, A. C., et al. (2020). Remdesivir for the treatment of covid-19 - final report. *N. Engl. J. Med.* 383 (19), 1813–1826. doi:10.1056/NEJMoa2007764

Beyls, C., Martin, N., Hermida, A., Abou-Arab, O., and Mahjoub, Y. (2020). Lopinavir-ritonavir treatment for COVID-19 infection in intensive care unit: risk of bradycardia. *Circ. Arrhythm. Electrophysiol.* 13, e008798. doi:10.1161/CIRCEP.120.008798

Blaising, J., Polyak, S. J., and Pécheur, E. I. (2014). Arbidol as a broad-spectrum antiviral: an update. *Antivir. Res.* 107, 84–94. doi:10.1016/j.antiviral.2014.04.006

Bonny, A., Talle, M. A., Ngantcha, M., and Tayebjee, M. H. (2020). Early treatment of COVID-19 patients with hydroxychloroquine and azithromycin: a retrospective analysis of 1061 cases in Marseille, France (2020). *Trav. Med. Infect. Dis.* 35, 101738. doi:10.1016/j.tmaid.2020.101861

Borba, M. G. S., Val, F. F. A., Sampaio, V. S., Alexandre, M. A. A., Melo, G. C., Brito, M., et al. (2020). Effect of high vs low doses of chloroquine diphosphate as adjunctive therapy for patients hospitalized with severe acute respiratory syndrome coronavirus 2 (SARS-CoV-2) infection: a randomized clinical trial. *JAMA Netw. Open* 3, e208857. doi:10.1001/jamanetworkopen.2020.8857

Borio, L. L., Toner, E., and Bartlett, J. (2018). 08-11-2005 - overview of oseltamivir and key points | CBN article. Clinicians' biosecurity news | johns hopkins center for health security. Available at: https://www.centerforhealthsecurity.org/cbn/2005/cbnTOPICS_081105.html (Accessed June 25, 2020).

Briolant, S., Garin, D., Scaramozzino, N., Jouan, A., and Crance, J. M. (2004). *In vitro* inhibition of Chikungunya and Semliki Forest viruses replication by antiviral compounds: synergistic effect of interferon-alpha and ribavirin combination. *Antivir. Res* 61, 111–117. doi:10.1016/j.antiviral.2003.09.005

Brown, A. J., Won, J. J., Graham, R. L., Dinnon, K. H., 3rd, Sims, A. C., Feng, J. Y., et al. (2019). Broad spectrum antiviral remdesivir inhibits human endemic and zoonotic deltacoronaviruses with a highly divergent RNA dependent RNA polymerase. *Antivir. Res* 169, 104541. doi:10.1016/j.antiviral.2019.104541

Cai, Q., Yang, M., Liu, D., Chen, J., Shu, D., Xia, J., et al. (2020). Experimental treatment with favipiravir for COVID-19: an open-label control study. *Proc. Est. Acad. Sci. Eng.* 6 (10), 1192–1198. doi:10.1016/j.eng.2020.03.007

Cantuti-Castelvetri, L., Ojha, R., Pedro, L. D., Djannatian, M., Franz, J., Kuivanen, S., et al. (2020). Neuropilin-1 facilitates SARS-CoV-2 cell entry and infectivity. *Science* 370 (6518), 856–860. doi:10.1126/science.abd2985

Cao, B., Wang, Y., Wen, D., Liu, W., Wang, J., Fan, G., et al. (2020). A trial of lopinavir-ritonavir in adults hospitalized with severe covid-19. *N. Engl. J. Med.* 382, 1787–1799. doi:10.1056/NEJMoa2001282

Cattaneo, D., Pasina, L., Maggioni, A. P., Giacomelli, A., Oreni, L., Covizzi, A., et al. (2020). Drug-drug interactions and prescription appropriateness in patients with COVID-19: a retrospective analysis from a reference hospital in northern Italy. *Drugs Aging* 37, 925–933. doi:10.1007/s40266-020-00812-8

Cavalcanti, A. B., Zampieri, F. G., Rosa, R. G., Azevedo, L. C. P., Veiga, V. C., and Avezum, A. (2020). Hydroxychloroquine with or without azithromycin in mild-to-moderate covid-19. *N. Engl. J. Med.* 383 (21), 2041–2052. doi:10.1056/NEJMoa2019014

Chandwani, A., and Shuter, J. (2008). Lopinavir/ritonavir in the treatment of HIV-1 infection: a review. *Ther. Clin. Risk Manag.* 4, 1023–1033. doi:10.2147/tcrm.s3285

Chen, J., Wang, S., Jia, X., Bajimaya, S., Lin, H., Tam, V. H., et al. (2005). Disposition of flavonoids via recycling: comparison of intestinal versus hepatic disposition. *Drug Metab. Dispos.* 33, 1777. doi:10.1124/dmd.105.003673

Chen, Y., Liu, Q., and Guo, D. (2020). Emerging coronaviruses: genome structure, replication, and pathogenesis. *J. Med. Virol.* 92 (4), 418–423. doi:10.1002/jmv.25681

Cheng, C. Y., Lee, Y. L., Chen, C. P., Lin, Y. C., Liu, C. E., Liao, C. H., et al. (2020). Lopinavir/ritonavir did not shorten the duration of SARS CoV-2 shedding in patients with mild pneumonia in Taiwan. *J. Microbiol. Immunol. Infect.* 53, 488–492. doi:10.1016/j.jmii.2020.03.032

Cho, A., Saunders, O. L., Butler, T., Zhang, L., Xu, J., Vela, J. E., et al. (2012). Synthesis and antiviral activity of a series of 1'-substituted 4-aza-7,9-dideazaadenosine C-nucleosides. *Bioorg. Med. Chem. Lett.* 22, 2705–2707. doi:10.1016/j.bmcl.2012.02.105

Chu, C. M., Cheng, V. C., Hung, I. F., Wong, M. M., Chan, K. H., Chan, K. S., et al. (2004). Role of lopinavir/ritonavir in the treatment of SARS: initial virological and clinical findings. *Thorax* 59, 252–256. doi:10.1136/thorax.2003.012658

ClinicalTrials.gov (2020a). Azithromycin in hospitalized COVID-19 patients (AIC). Available at: https://clinicaltrials.gov/ct2/results?cond=Covid-19&term=azithromycin&cntry=&state=&city=&dist= (Accessed January 10, 2020).

ClinicalTrials.gov (2020b). Chloroquine covid-19–list results. Available at: https://clinicaltrials.gov/ct2/results?cond=Covid-19&term=chloroquine&cntry=&state=&city=&dist= (Accessed January 10, 2020).

ClinicalTrials.gov (2020c). Favipiravir covid-19. Available at: https://clinicaltrials.gov/ct2/results?cond=Covid-19&term=Favipiravir&cntry=&state=&city=&dist= (Accessed January 10, 2020).

ClinicalTrials.gov (2020d). Hydroxychloroquine covid-19. Available at: https://clinicaltrials.gov/ct2/results?cond=Covid-19&term=hydroxychloroquine&cntry=&state=&city=&dist= (Accessed January 10, 2020).

ClinicalTrials.gov (2020e). Lopinavir covid-19. Available at: https://clinicaltrials.gov/ct2/results?cond=Covid-19&term=lopinavir&cntry=&state=&city=&dist= (Accessed January 10, 2020).

ClinicalTrials.gov (2020f). Oseltamivir covid-19. Available at: https://clinicaltrials.gov/ct2/results?cond=Covid-19&term=Oseltamivir&cntry=&state=&city=&dist= (Accessed January 10, 2020).

ClinicalTrials.gov (2020g). Remdesivir covid-19. Available at: https://clinicaltrials.gov/ct2/results?cond=Covid-19&term=remdesivir&cntry=&state=&city=&dist= (Accessed January 10, 2020).

ClinicalTrials.gov (2020h). Ribavirin covid-19. Available at: https://clinicaltrials.gov/ct2/results?cond=Covid-19&term=Ribavirin&cntry=&state=&city=&dist= (Accessed January 10, 2020).

ClinicalTrials.gov (2020i). Umifenovir covid-19. Available at: https://clinicaltrials.gov/ct2/results?cond=Covid-19&term=Umifenovir&cntry=&state=&city=&dist= (Accessed January 10, 2020).

ClinicalTrials.gov (2021a). Convalescent plasma covid19. Available at: https://www.clinicaltrials.gov/ct2/results?term=convalescent+plasma&cond=Covid19 (Accessed January 13, 2021).

ClinicalTrials.gov (2021b). Dexamethasone covid19. Available at: https://www.clinicaltrials.gov/ct2/results?term=dexamethasone&cond=Covid19&Search=Apply&age_v=&gndr=&type=&rslt= (Accessed January 13, 2021).

Cohen, M. S. (2020). Hydroxychloroquine for the prevention of covid-19 - searching for evidence. *N. Engl. J. Med.* 383, 585–586. doi:10.1056/NEJMe2020388

Cong, Y., Hart, B. J., Gross, R., Zhou, H., Frieman, M., Bollinger, L., et al. (2018). MERS-CoV pathogenesis and antiviral efficacy of licensed drugs in human monocyte-derived antigen-presenting cells. *PLoS One* 13, e0194868. doi:10.1371/journal.pone.0194868

Damle, B., Vourvahis, M., Wang, E., Leaney, J., and Corrigan, B. (2020). Clinical pharmacology perspectives on the antiviral activity of azithromycin and use in COVID-19. *Clin. Pharmacol. Ther.* 108 (2), 201–211. doi:10.1002/cpt.1857

Deng, L., Li, C., Zeng, Q., Liu, X., Li, X., Zhang, H., et al. (2020). Arbidol combined with LPV/r versus LPV/r alone against Corona Virus Disease 2019: a retrospective cohort study. *J. Infect.* 9,100128. doi:10.1016/j.jinf.2020.03.002

Devaux, C. A., Rolain, J. M., Colson, P., and Raoult, D. (2020). New insights on the antiviral effects of chloroquine against coronavirus: what to expect for COVID-19?. *Int. J. Antimicrob. Agents* 55, 105938. doi:10.1016/j.ijantimicag.2020.105938

Du, Y., and Chen, X. (2020). Favipiravir: pharmacokinetics and concerns about clinical trials for 2019-nCoV infection. *Clin. Pharmacol. Ther.* 108 (2), 242–247. doi:10.1002/cpt.1844

Duan, K., Liu, B., Li, C., Zhang, H., Yu, T., Qu, J., et al. (2020). Effectiveness of convalescent plasma therapy in severe COVID-19 patients. *Proc. Natl. Acad. Sci. U.S.A.* 117, 9490–9496. doi:10.1073/pnas.2004168117

Elia, G., Belloli, C., Cirone, F., Lucente, M. S., Caruso, M., Martella, V., et al. (2008). *In vitro* efficacy of ribavirin against canine distemper virus. *Antivir. Res.* 77, 108–113. doi:10.1016/j.antiviral.2007.09.004

Elmeliegy, M., Vourvahis, M., Guo, C., and Wang, D. D. (2020). Effect of P-glycoprotein (P-gp) inducers on exposure of P-gp substrates: review of clinical drug-drug interaction studies. *Clin. Pharmacokinet.* 59, 699–714. doi:10.1007/s40262-020-00867-1

Eslami, G., Mousaviasl, S., Radmanesh, E., Jelvay, S., Bitaraf, S., Simmons, B., et al. (2020). The impact of sofosbuvir/daclatasvir or ribavirin in patients with severe COVID-19. *J. Antimicrob. Chemother.* 75, 3366–3372. doi:10.1093/jac/dkaa331

Falzarano, D., de Wit, E., Rasmussen, A. L., Feldmann, F., Okumura, A., Scott, D. P., et al. (2013). Treatment with interferon-α2b and ribavirin improves outcome in MERS-CoV-infected rhesus macaques. *Nat. Med.* 19, 1313–1317. doi:10.1038/nm.3362

FDA (2020a). FDA EAU letter -Remdesivir -COVID-19. Available at: https://www.fda.gov/media/137564/download (Accessed November 3, 2020).

FDA (2020b). FDA fact sheet -Chloroquine phosphate -COVID-19 Available at: https://www.fda.gov/media/136536/download (Accessed November 4, 2020).

FDA (2020c). FDA fact sheet -Hydroxychloroquine sulfate -COVID-19. Available at: https://www.fda.gov/media/136537/download (Accessed November 4, 2020).

FDA (2020d). FDA FACT sheet -Remdesivir -COVID-19. Available at: https://www.fda.gov/media/143189/download (Accessed November 4, 2020).

FDA (2021a). FDA EAU letter –Convalescent plasma. Available at: https://www.fda.gov/media/141477/download (Accessed January 13, 2021).

FDA (2021b). FDA EAU clinical memorandom Convalescent plasma Available at: https://www.fda.gov/media/141480/download (Accessed January 13, 2021).

FDA (2021c). FDA Fact sheet –Convalescent plasma -COVID-19. Available at: https://www.fda.gov/media/141478/download (Accessed January 13, 2021).

Fink, S. L., Vojtech, L., Wagoner, J., Slivinski, N. S. J., Jackson, K. J., Wang, R., et al. (2018). The antiviral drug arbidol inhibits zika virus. *Sci. Rep.* 8, 8989. doi:10.1038/s41598-018-27224-4

Fiolet, T., Guihur, A., Rebeaud, M., Mulot, M., Peiffer-Smadja, N., and Mahamat-Saleh, Y. (2020). Effect of hydroxychloroquine with or without azithromycin on the mortality of coronavirus disease 2019 (COVID-19) patients: a systematic review and meta-analysis. *Clin. Microbiol. Infect.* 27 (1), 19–27. doi:10.1016/j.cmi.2020.08.022

Frediansyah, A., Nainu, F., Dhama, K., Mudatsir, M., and Harapan, H. (2020). Remdesivir and its antiviral activity against COVID-19: a systematic review. *Clin. Epidemiol. Glob. Health* 9, 123–127. doi:10.1016/j.cegh.2020.07.011

Furtado, R. H. M., Berwanger, O., Fonseca, H. A., Corrêa, T. D., Ferraz, L. R., Lapa, M. G., et al. (2020). Azithromycin in addition to standard of care versus standard of care alone in the treatment of patients admitted to the hospital with severe COVID-19 in Brazil (COALITION II): a randomised clinical trial. *Lancet* 396, 959–967. doi:10.1016/s0140-6736(20)31862-6

Furuta, Y., Gowen, B. B., Takahashi, K., Shiraki, K., Smee, D. F., and Barnard, D. L. (2013). Favipiravir (T-705), a novel viral RNA polymerase inhibitor (2013). *Antivir. Res.* 100, 446–454. doi:10.1016/j.antiviral.2013.09.015

Furuta, Y., Komeno, T., and Nakamura, T. (2017). Favipiravir (T-705), a broad spectrum inhibitor of viral RNA polymerase. *Proc. Jpn. Acad. Ser. B Phys. Biol. Sci.* 93, 449–463. doi:10.2183/pjab.93.027

Galli, A., Mens, H., Gottwein, J. M., Gerstoft, J., and Bukh, J. (2018). Antiviral effect of ribavirin against HCV associated with increased frequency of G-to-A and C-to-U transitions in infectious cell culture model. *Sci. Rep.* 8, 1–13. doi:10.1038/s41598-018-22620-2

Gautret, P., Lagier, J. C., Parola, P., Meddeb, L., Mailhe, M., and Doudier, B. (2020). Hydroxychloroquine and azithromycin as a treatment of COVID-19: results of an open-label non-randomized clinical trial. *Int. J. Antimicrob. Agents* 57 (1), 106239. doi:10.1016/j.ijantimicag.2020.106239

Geleris, J., Sun, Y., Platt, J., Zucker, J., Baldwin, M., Hripcsak, G., et al. (2020). Observational study of hydroxychloroquine in hospitalized patients with covid-19. *N. Engl. J. Med.* 382, 2411–2418. doi:10.3410/f.737908482.793576143

Gish, R. G. (2006). Treating HCV with ribavirin analogues and ribavirin-like molecules. *J. Antimicrob. Chemother.* 57, 8–13. doi:10.1093/jac/dki405

Good, S. S., Moussa, A., Zhou, X.-J., Pietropaolo, K., and Sommadossi, J.-P. (2020). Preclinical evaluation of AT-527, a novel guanosine nucleotide prodrug with

potent, pan-genotypic activity against hepatitis C virus. *PLoS One* 15, e0227104. doi:10.1371/journal.pone.0227104

Govorkova, E. A., Ilyushina, N. A., McClaren, J. L., Naipospos, T. S. P., Douangngeun, B., and Webster, R. G. (2009). Susceptibility of highly pathogenic H5N1 influenza viruses to the neuraminidase inhibitor oseltamivir differs *in vitro* and in a mouse model. *Antimicrob. Agents Chemother.* 53, 3088–3096. doi:10.1128/aac.01667-08

Gowen, B. B., Sefing, E. J., Westover, J. B., Smee, D. F., Hagloch, J., Furuta, Y., et al. (2015). Alterations in favipiravir (T-705) pharmacokinetics and biodistribution in a hamster model of viral hemorrhagic fever. *Antivir. Res.* 121, 132–137. doi:10.1016/j.antiviral.2015.07.003

Gregoire, M., Le Turnier, P., Gaborit, B. J., Veyrac, G., Lecomte, R., Boutoille, D., et al. (2020). Lopinavir pharmacokinetics in COVID-19 patients. *J. Antimicrob. Chemother.* 75 (9), 2702–2704. doi:10.1093/jac/dkaa195

Hasan, A., Paray, B. A., Hussain, A., Qadir, F. A., Attar, F., Aziz, F. M., et al. (2020). A review on the cleavage priming of the spike protein on coronavirus by angiotensin-converting enzyme-2 and furin. *J. Biomol. Struct. Dyn.* 2020, 1–9. doi:10.1080/07391102.2020.1754293

Hegerova, L., Gooley, T. A., Sweerus, K. A., Maree, C., Bailey, N., Bailey, M., et al. (2020). Use of convalescent plasma in hospitalized patients with COVID-19: case series. *Blood* 136, 759–762. doi:10.1182/blood.2020006964

Hoffman, R. L., Kania, R. S., Brothers, M. A., Davies, J. F., Ferre, R. A., Gajiwala, K. S., et al. (2020). Discovery of ketone-based covalent inhibitors of coronavirus 3CL proteases for the potential therapeutic treatment of COVID-19. *J. Med. Chem.* 63, 12725–12747. doi:10.1021/acs.jmedchem.0c01063

Hoffmann, M., Kleine-Weber, H., Schroeder, S., Krüger, N., Herrler, T., Erichsen, S., et al. (2020). SARS-CoV-2 cell entry depends on ACE2 and TMPRSS2 and is blocked by a clinically proven protease inhibitor. *Cell* 181, 271–280.e8. doi:10.1016/j.cell.2020.02.052

Horby, P., Lim, W. S., Emberson, J. R., Mafham, M., Bell, J. L., Linsell, L., et al. RECOVERY Collaborative Group (2020a). Dexamethasone in hospitalized patients with covid-19 - preliminary report. *N. Engl. J. Med.* [Epub ahead of print]. doi:10.1056/NEJMoa2021436

Horby, P., Mafham, M., Linsell, L., Bell, J. L., Staplin, N., Emberson, J. R., et al. RECOVERY Collaborative Group (2020b). Effect of hydroxychloroquine in hospitalized patients with covid-19. *N. Engl. J. Med.* 383, 2030–2040. doi:10.1093/eurheartj/ehaa935

Horby, P. W., Mafham, M., Bell, J. L., Linsell, L., Staplin, N., Emberson, J., et al. (2020). Lopinavir–ritonavir in patients admitted to hospital with COVID-19 (RECOVERY): a randomised, controlled, open-label, platform trial. *Lancet* 396, 1345–1352. doi:10.1016/s0140-6736(20)32013-4

Huang, D., Yu, H., Wang, T., Yang, H., Yao, R., and Liang, Z. (2020). Efficacy and safety of umifenovir for coronavirus disease 2019 (COVID-19): a systematic review and meta-analysis. *J. Med. Virol.* 93 (1), 481–490. doi:10.1002/jmv.26256

Huang, M., Tang, T., Pang, P., Li, M., Ma, R., Lu, J., et al. (2020). Treating COVID-19 with chloroquine. *J. Mol. Cel Biol.* 12, 322–325. doi:10.1093/jmcb/mjaa014

Huang, Y.-Q., Tang, S.-Q., Xu, X.-L., Zeng, Y.-M., He, X.-Q., Li, Y., et al. (2020). No statistically apparent difference in antiviral effectiveness observed among ribavirin plus interferon-alpha, lopinavir/ritonavir plus interferon-alpha, and ribavirin plus lopinavir/ritonavir plus interferon-alpha in patients with mild to moderate coronavirus disease 2019: results of a randomized, open-labeled prospective study. *Front. Pharmacol.* 11, 1071. doi:10.3389/fphar.2020.01071

Hughes, J. H., Sweeney, K., Ahadieh, S., and Ouellet, D. (2020). Predictions of systemic, intracellular, and lung concentrations of azithromycin with different dosing regimens used in COVID-19 clinical trials. *CPT Pharmacometrics Syst. Pharmacol.* 9 (8), 435–443. doi:10.1002/psp4.12537

Hung, I. F. N., Lung, K. C., Tso, E. Y. K., Liu, R., Chung, T. W. H., Chu, M. Y., et al. (2020). Triple combination of interferon beta-1b, lopinavir–ritonavir, and ribavirin in the treatment of patients admitted to hospital with COVID-19: an open-label, randomised, phase 2 trial. *Lancet* 395, 1695–1704. doi:10.1016/S0140-6736(20)31042-4

Hussain, S., Chen, Y., Yang, Y., Xu, J., Peng, Y., Wu, Y., et al. (2005). Identification of novel subgenomic RNAs and noncanonical transcription initiation signals of severe acute respiratory syndrome coronavirus. *J. Virol.* 79 (9), 5288–5295. doi:10.1128/jvi.79.9.5288-5295.2005

IBM Micromedex (2021). IBM Watson health products: system status. Available at: https://www.micromedexsolutions.com/ (Accessed January 13, 2021).

Ison, M. G., Wolfe, C., and Boucher, H. W. (2020). Emergency use authorization of remdesivir: the need for a transparent distribution process. *JAMA* 323 (23), 2365–2366. doi:10.1001/jama.2020.8863

Jafari, A., Dadkhahfar, S., and Perseh, S. (2020). Considerations for interactions of drugs used for the treatment of COVID-19 with anti-cancer treatments. *Crit. Rev. Oncol. Hematol.* 151, 102982. doi:10.1016/j.critrevonc.2020.102982

Jakhmola, S., Indari, O., Baral, B., Kashyap, D., Varshney, N., Das, A., et al. (2020c). Comorbidity assessment is essential during COVID-19 treatment. *Front. Physiol.* 11, 984. doi:10.3389/fphys.2020.00984

Jakhmola, S., Indari, O., Chatterjee, S., and Jha, H. C. (2020a). SARS-CoV-2, an underestimated pathogen of the nervous system. *SN Compr. Clin. Med.* 2 (11), 2137–2146. doi:10.1007/s42399-020-00522-7

Jakhmola, S., Indari, O., Kashyap, D., Varshney, N., Rani, A., Sonkar, C., et al. (2020b). Recent updates on COVID-19: a holistic review. *Heliyon* 6, e05706. doi:10.1016/j.heliyon.2020.e05706

Jean, S. S., Lee, P. I., and Hsueh, P. R. (2020). Treatment options for COVID-19: the reality and challenges (2020). *J. Microbiol. Immunol. Infect.* 53, 436–443. doi:10.1016/j.jmii.2020.03.034

Joyner, M. J., Bruno, K. A., Klassen, S. A., Kunze, K. L., Johnson, P. W., Lesser, E. R., et al. (2020a). Safety update: COVID-19 convalescent plasma in 20,000 hospitalized patients. *Mayo Clin. Proc.* 95, 1888–1897. doi:10.1016/j.mayocp.2020.06.028

Joyner, M. J., Senefeld, J. W., Klassen, S. A., Mills, J. R., Johnson, P. W., Theel, E. S., et al. (2020b). Effect of convalescent plasma on mortality among hospitalized patients with COVID-19: initial three-month experience. Available at: https://ncrc.jhsph.edu/research/effect-of-convalescent-plasma-on-mortality-among-hospitalized-patients-with-covid-19-initial-three-month-experience/ (Accessed January 13, 2021).

Kalil, A. C., Patterson, T. F., Mehta, A. K., Tomashek, K. M., Wolfe, C. R., Ghazaryan, V., et al. (2020). Baricitinib plus remdesivir for hospitalized adults with covid-19. *N. Engl. J. Med.* [Epub ahead of print]. doi:10.1056/NEJMoa2031994

Kaptein, S. J. F., Jacobs, S., Langendries, L., Seldeslachts, L., ter Horst, S., Liesenborghs, L., et al. (2020). Favipiravir at high doses has potent antiviral activity in SARS-CoV-2–infected hamsters, whereas hydroxychloroquine lacks activity. *Proc. Natl. Acad. Sci.* 117, 26955–26965. doi:10.1073/pnas.2014441117

Karolyi, M., Pawelka, E., Mader, T., Omid, S., Kelani, H., Ely, S., et al. (2020). Hydroxychloroquine versus lopinavir/ritonavir in severe COVID-19 patients : results from a real-life patient cohort. *Wien. Klin. Wochenschr.* [Epub ahead of print]. doi:10.1007/s00508-020-01720-y

Keyaerts, E., Li, S., Vijgen, L., Rysman, E., Verbeeck, J., Van Ranst, M., et al. (2009). Antiviral activity of chloroquine against human coronavirus OC43 infection in newborn mice. *Antimicrob. Agents Chemother.* 53, 3416–3421. doi:10.1128/aac.01509-08

Keyaerts, E., Vijgen, L., Maes, P., Neyts, J., and Van Ranst, M. (2004). *In vitro* inhibition of severe acute respiratory syndrome coronavirus by chloroquine. *Biochem. Biophys. Res. Commun.* 323, 264–268. doi:10.1016/j.bbrc.2004.08.085

Lê, M. P., Jaquet, P., Patrier, J., Wicky, P.-H., Le Hingrat, Q., Veyrier, M., et al. (2020). Pharmacokinetics of lopinavir/ritonavir oral solution to treat COVID-19 in mechanically ventilated ICU patients. *J. Antimicrob. Chemother.* 75, 2657–2660. doi:10.1093/jac/dkaa261

Lai, M. M., and Cavanagh, D. (1997). The molecular biology of coronaviruses. *Adv. Virus Res.* 48, 1–100.

Leegwater, E., Strik, A., Wilms, E. B., Bosma, L. B. E., Burger, D. M., Ottens, T. H., et al. (2020). Drug-induced liver injury in a COVID-19 patient: potential interaction of remdesivir with P-glycoprotein inhibitors. *Clin. Infect. Dis.* [Epub ahead of print]. doi:10.1093/cid/ciaa883

Leyssen, P., Balzarini, J., De Clercq, E., and Neyts, J. (2005). The predominant mechanism by which ribavirin exerts its antiviral activity *in vitro* against flaviviruses and paramyxoviruses is mediated by inhibition of IMP dehydrogenase. *J. Virol.* 79, 1943–1947. doi:10.1128/jvi.79.3.1943-1947.2005

Li, C., Zhu, X., Ji, X., Quanquin, N., Deng, Y.-Q., Tian, M., et al. (2017). Chloroquine, a FDA-approved drug, prevents zika virus infection and its associated congenital microcephaly in mice. *EBioMedicine* 24, 189–194. doi:10.1016/j.ebiom.2017.09.034

Li, F. (2016). Structure, function, and evolution of coronavirus spike proteins. *Annu. Rev. Virol.* 3, 237–261. doi:10.1146/annurev-virology-110615-042301

Li, L., Zhang, W., Hu, Y., Tong, X., Zheng, S., Yang, J., et al. (2020). Effect of convalescent plasma therapy on time to clinical improvement in patients with severe and life-threatening COVID-19: a randomized clinical trial. *JAMA* 324, 460–470. doi:10.3410/f.738066145.793578637

Li, Z.-H., Li, C.-M., Ling, P., Shen, F.-H., Chen, S.-H., Liu, C.-C., et al. (2008). Ribavirin reduces mortality in enterovirus 71-infected mice by decreasing viral replication. *J. Infect. Dis.* 197, 854–857. doi:10.1086/527326

Lian, N., Xie, H., Lin, S., Huang, J., Zhao, J., and Lin, Q. (2020). Umifenovir treatment is not associated with improved outcomes in patients with coronavirus disease 2019: a retrospective study. *Clin. Microbiol. Infect.* 26, 917–921. doi:10.1016/j.cmi.2020.04.026

Libster, R., Pérez Marc, G., Wappner, D., Coviello, S., Bianchi, A., Braem, V., et al. (2021). Early high-titer plasma therapy to prevent severe covid-19 in older adults. *N. Engl. J. Med.* [Epub ahead of print]. doi:10.1056/NEJMoa2033700

Liu, J., Cao, R., Xu, M., Wang, X., Zhang, H., Hu, H., et al. (2020). Hydroxychloroquine, a less toxic derivative of chloroquine, is effective in inhibiting SARS-CoV-2 infection *in vitro*. *Cell Discov.* 6, 16. doi:10.1038/s41421-020-0156-0

Liu, W., Zhou, P., Chen, K., Ye, Z., Liu, F., Li, X., et al. (2020). Efficacy and safety of antiviral treatment for COVID-19 from evidence in studies of SARS-CoV-2 and other acute viral infections: a systematic review and meta-analysis. *CMAJ* 192, E734–E744. doi:10.1503/cmaj.200647

Liverpool COVID-19 interactions (2021). Interactions for colchicine and aspirin (as an antiplatelet COVID-19 adjunct therapy) are now on the checker. Available at: https://www.covid19-druginteractions.org/ (Accessed January 13, 2021).

Lo, M. K., Albariño, C. G., Perry, J. K., Chang, S., Tchesnokov, E. P., Guerrero, L., et al. (2020). Remdesivir targets a structurally analogous region of the Ebola virus and SARS-CoV-2 polymerases. *Proc. Natl. Acad. Sci. U.S.A.* 117, 26946–26954. doi:10.1073/pnas.2012294117

Madelain, V., Nguyen, T. H. T., Olivo, A., de Lamballerie, X., Guedj, J., Taburet, A.-M., et al. (2016). Ebola virus infection: review of the pharmacokinetic and pharmacodynamic properties of drugs considered for testing in human efficacy trials. *Clin. Pharmacokinet.* 55, 907–923. doi:10.1007/s40262-015-0364-1

Mahase, E. (2020). Covid-19: US approves remdesivir despite WHO trial showing lack of efficacy. *BMJ* 371, m4120. doi:10.1136/bmj.m4120

McCullough, P. A. (2020). Favipiravir and the need for early ambulatory treatment of SARS-CoV2 infection (COVID-19). *Antimicrob. Agents Chemother.* [Epub ahead of print]. doi:10.1128/AAC.02017-20

Mercuro, N. J., Yen, C. F., Shim, D. J., Maher, T. R., McCoy, C. M., Zimetbaum, P. J., et al. (2020). Risk of QT interval prolongation associated with use of hydroxychloroquine with or without concomitant azithromycin among hospitalized patients testing positive for coronavirus disease 2019 (COVID-19). *JAMA Cardiol.* [Epub ahead of print]. doi:10.1001/jamacardio.2020.1834

Moniuszko-Malinowska, A., Czupryna, P., Zarębska-Michaluk, D., Tomasiewicz, K., Pancewicz, S., Rorat, M., et al. (2020). Convalescent plasma transfusion for the treatment of COVID-19—experience from Poland: a multicenter study. *J. Clin. Med. Res.* 10, 28. doi:10.3390/jcm10010028

Murphy, B. G., Perron, M., Murakami, E., Bauer, K., Park, Y., Eckstrand, C., et al. (2018). The nucleoside analog GS-441524 strongly inhibits feline infectious peritonitis (FIP) virus in tissue culture and experimental cat infection studies. *Vet. Microbiol.* 219, 226–233. doi:10.1016/j.vetmic.2018.04.026

O'Laughlin, J. P., Mehta, P. H., and Wong, B. C. (2016). Life threatening severe QTc prolongation in patient with systemic lupus erythematosus due to hydroxychloroquine. *Case Rep. Cardiol.* 2016, 4626279. doi:10.1155/2016/4626279

Ooi, E. E., Chew, J. S. W., Loh, J. P., and Chua, R. C. S. (2006). *In vitro* inhibition of human influenza A virus replication by chloroquine. *Virol. J.* 3, 1–3. doi:10.1186/1743-422X-3-39

Pan, H., Peto, R., Henao-Restrepo, A.-M., Preziosi, M.-P., Sathiyamoorthy, V., Karim, Q. A., et al. WHO Solidarity Trial Consortium (2020). Repurposed antiviral drugs for covid-19 - interim WHO solidarity trial results. *N. Engl. J. Med.* [Epub ahead of print]. doi:10.1056/NEJMoa2023184

PMDA (2020). An evaluation report of Avigan (favipiravir), Toyama Chemical Co., Ltd. Available at: https://www.pmda.go.jp/files/000210319.pdf (Accessed November 3, 2020).

Pruijssers, A. J., George, A. S., Schäfer, A., Leist, S. R., Gralinksi, L. E., Dinnon, K. H., 3rd, et al. (2020). Remdesivir inhibits SARS-CoV-2 in human lung cells and chimeric SARS-CoV expressing the SARS-CoV-2 RNA polymerase in mice. *Cell Rep.* 32, 107940. doi:10.1016/j.celrep.2020.107940

Rendic, S., and Guengerich, F. P. (2020). Metabolism and interactions of chloroquine and hydroxychloroquine with human cytochrome P450 enzymes and drug transporters. *Curr. Drug Metab.* 21, 1127–1135. doi:10.2174/1389200221999201208211537

Renwick, A. B., Ball, S. E., Tredger, J. M., Price, R. J., Walters, D. G., Kao, J., et al. (2002). Inhibition of zaleplon metabolism by cimetidine in the human liver: *in vitro* studies with subcellular fractions and precision-cut liver slices. *Xenobiotica* 32, 849–862. doi:10.1080/00498250210158221

Robbiani, D. F., Gaebler, C., Muecksch, F., Lorenzi, J. C. C., Wang, Z., Cho, A., et al. (2020). Convergent antibody responses to SARS-CoV-2 in convalescent individuals. *Nature* 584, 437–442. doi:10.1038/s41586-020-2456-9

Rodríguez-Molinero, A., Pérez-López, C., Gálvez-Barrón, C., Miñarro, A., Macho, O., López, G. F., et al. (2020). Observational study of azithromycin in hospitalized patients with COVID-19. *PLoS One* 15, e0238681. doi:10.1371/journal.pone.0238681

Rosenberg, E. S., Dufort, E. M., Udo, T., Wilberschied, L. A., Kumar, J., Tesoriero, J., et al. (2020). Association of treatment with hydroxychloroquine or azithromycin with in-hospital mortality in patients with COVID-19 in New York state. *JAMA* 323 (24), 2493–2502. doi:10.1001/jama.2020.8630

Satarker, S., Ahuja, T., Banerjee, M., E, V. B., Dogra, S., Agarwal, T., et al. (2020). Hydroxychloroquine in COVID-19: potential mechanism of action against SARS-CoV-2. *Curr. Pharmacol. Rep.* [Epub ahead of print]. doi:10.1007/s40495-020-00231-8

Schögler, A., Kopf, B. S., Edwards, M. R., Johnston, S. L., Casaulta, C., Kieninger, E., et al. (2015). Novel antiviral properties of azithromycin in cystic fibrosis airway epithelial cells. *Eur. Respir. J.* 45, 428–439. doi:10.1183/09031936.00102014

Schade, D., Kotthaus, J., Riebling, L., Kotthaus, J., Müller-Fielitz, H., Raasch, W., et al. (2014). Development of novel potent orally bioavailable oseltamivir derivatives active against resistant influenza A. *J. Med. Chem.* 57, 759–769. doi:10.1021/jm401492x

Scherrmann, J. M. (2020). Intracellular ABCB1 as a possible mechanism to explain the synergistic effect of hydroxychloroquine-azithromycin combination in COVID-19 therapy. *AAPS J.* 22, 86. doi:10.1208/s12248-020-00465-w

Sciaccaluga, C., Cameli, M., Menci, D., Mandoli, G. E., Sisti, N., Cameli, P., et al. (2020). COVID-19 and the burning issue of drug interaction: never forget the ECG. *Postgrad. Med. J.* [Epub ahead of print]. doi:10.1136/postgradmedj-2020-138093

Sheahan, T. P., Sims, A. C., Leist, S. R., Schäfer, A., Won, J., Brown, A. J., et al. (2020). Comparative therapeutic efficacy of remdesivir and combination lopinavir, ritonavir, and interferon beta against MERS-CoV. *Nat. Commun.* 11, 222. doi:10.1038/s41467-019-13940-6

Shereen, M. A., Khan, S., Kazmi, A., Bashir, N., and Siddique, R. (2020). COVID-19 infection: origin, transmission, and characteristics of human coronaviruses. *J. Adv. Res.* [Epub ahead of print]. doi:10.1016/j.jare.2020.03.005

Shi, L., Xiong, H., He, J., Deng, H., Li, Q., Zhong, Q., et al. (2007). Antiviral activity of arbidol against influenza A virus, respiratory syncytial virus, rhinovirus, coxsackie virus and adenovirus *in vitro* and *in vivo*. *Arch. Virol.* 152, 1447–1455. doi:10.1007/s00705-007-0974-5

Shrestha, D. B., Budhathoki, P., Khadka, S., Shah, P. B., Pokharel, N., and Rashmi, P. (2020). Favipiravir versus other antiviral or standard of care for COVID-19 treatment: a rapid systematic review and meta-analysis. *Virol. J.* 17, 141. doi:10.1186/s12985-020-01412-z

Simmons, G., Gosalia, D. N., Rennekamp, A. J., Reeves, J. D., Diamond, S. L., and Bates, P. (2005). Inhibitors of cathepsin L prevent severe acute respiratory syndrome coronavirus entry. *PNAS* 102, 11876–11881. doi:10.1073/pnas.0505577102

Simonovich, V. A., Burgos Pratx, L. D., Scibona, P., Beruto, M. V., Vallone, M. G., Vázquez, C., et al. (2020). A randomized trial of convalescent plasma in covid-19 severe pneumonia. *N. Engl. J. Med.* [Epub ahead of print]. doi:10.1056/NEJMoa2031304

Singh, A. K., Singh, A., Singh, R., and Misra, A. (2020). Remdesivir in COVID-19: a critical review of pharmacology, pre-clinical and clinical studies. *Diabetes Metab. Syndr.* 14, 641–648. doi:10.1016/j.dsx.2020.05.018

Sisay, M. (2020). 3CLpro inhibitors as a potential therapeutic option for COVID-19: available evidence and ongoing clinical trials. *Pharmacol. Res.* 156, 104779. doi:10.1016/j.phrs.2020.104779

Sisti, G., Schiattarella, A., and Sisti, A. (2020). Treatment of COVID-19 pregnancy with hydroxychloroquine and azithromycin: a case report. *Acta Biomedica* 91, e2020123. doi:10.23750/abm.v91i4.10216

Smee, D. F., Bray, M., and Huggins, J. W. (2001). Antiviral activity and mode of action studies of ribavirin and mycophenolic acid against orthopoxviruses *in vitro*. *Antivir. Chem. Chemother.* 12 (6), 327–335. doi:10.1177/095632020101200602

Song, H. C., Seo, M. Y., Stadler, K., Yoo, B. J., Choo, Q. L., and Coates, S. R. (2004). Synthesis and characterization of a native, oligomeric form of recombinant severe acute respiratory syndrome coronavirus spike glycoprotein. *J. Virol.* 78, 10328–10335. doi:10.1128/JVI.78.19.10328-10335.2004

Sonkar, C., Kashyap, D., Varshney, N., Baral, B., and Jha, H. C. (2020). Impact of gastrointestinal symptoms in COVID-19: a molecular approach. *SN Compr. Clin. Med.* [Epub ahead of print]. doi:10.1007/s42399-020-00619-z

Spinner, C. D., Gottlieb, R. L., Criner, G. J., Arribas López, J. R., Cattelan, A. M., Soriano Viladomiu, A., et al. (2020). Effect of remdesivir vs standard care on clinical status at 11 Days in patients with moderate COVID-19: a randomized clinical trial. *JAMA* 324, 1048–1057. doi:10.1001/jama.2020.16349

Takahashi, H. (2000). Developmental changes in pharmacokinetics and pharmacodynamics of warfarin enantiomers in Japanese children. *Clin. Pharmacol. Ther.* 68, 541–555. doi:10.1067/mcp.2000.110977

Takahashi, H., Iwasaki, Y., Watanabe, T., Ichinose, N., Okada, Y., Oiwa, A., et al. (2020). Case studies of SARS-CoV-2 treated with favipiravir among patients in critical or severe condition. *Int. J. Infect. Dis.* 100, 283–285. doi:10.1016/j.ijid.2020.08.047

Tan, Y. W., Yam, W. K., Sun, J., and Chu, J. J. H. (2018). An evaluation of chloroquine as a broad-acting antiviral against hand, foot and mouth disease. *Antivir. Res.* 149, 143–149. doi:10.1016/j.antiviral.2017.11.017

Tang, W., Cao, Z., Han, M., Wang, Z., Chen, J., Sun, W., et al. (2020). Hydroxychloroquine in patients with mainly mild to moderate coronavirus disease 2019: open label, randomised controlled trial. *BMJ* 2020, 369. doi:10.1136/bmj.m1849

Tong, S., Su, Y., Yu, Y., Wu, C., Chen, J., Wang, S., et al. (2020). Ribavirin therapy for severe COVID-19: a retrospective cohort study. *Int. J. Antimicrob. Agents* 56, 106114. doi:10.1016/j.ijantimicag.2020.106114

van Boheemen, S., de Graaf, M., Lauber, C., Bestebroer, T. M., Raj, V. S., Zaki, A. M., et al. (2012). Genomic characterization of a newly discovered coronavirus associated with acute respiratory distress syndrome in humans. *MBio* 3, e00473-12. doi:10.1128/mBio.00473-12

Vecchio, G., Zapico, V., Catanzariti, A., Carboni Bisso, I., and Las Heras, M. (2020). Adverse effects of lopinavir/ritonavir in critically ill patients with COVID-19. *Medicina* 80, 439–441.

Verdugo-Paiva, F., Izcovich, A., Ragusa, M., and Rada, G. (2020). Lopinavir-ritonavir for COVID-19: a living systematic review. *Medwave* 20, e7967. doi:10.5867/medwave.2020.06.7966

Wada, T., Shimode, K., Hoshiyama, T., Takayama, Y., and Yamaoka, K. (2020). Three novel COVID-19 pneumonia cases successfully treated with lopinavir/ritonavir. *Front. Med.* 7 [, 2020 Epub ahead of print]. doi:10.3389/fmed.2020.00241

Wang, D., Hu, B., Hu, C., Zhu, F., Liu, X., Zhang, J., et al. (2020). Clinical characteristics of 138 hospitalized patients with 2019 novel coronavirus-infected pneumonia in wuhan, China. *JAMA* [Epub ahead of print]. doi:10.1001/jama.2020.1585

Wang, M., Cao, R., Zhang, L., Yang, X., Liu, J., Xu, M., et al. (2020). Remdesivir and chloroquine effectively inhibit the recently emerged novel coronavirus (2019-nCoV) *in vitro*. *Cell Res.* 30, 269–271. doi:10.1038/s41422-020-0282-0

Wang, T., Du, Z., Zhu, F., Cao, Z., An, Y., Gao, Y., et al. (2020). Comorbidities and multi-organ injuries in the treatment of COVID-19. *Lancet* 395, e52. doi:10.1016/S0140-6736(20)30558-4

Wang, X., Cao, R., Zhang, H., Liu, J., Xu, M., Hu, H., et al. (2020). The anti-influenza virus drug, arbidol is an efficient inhibitor of SARS-CoV-2 *in vitro*. *Cel Discov.* 6, 28. doi:10.1038/s41421-020-0169-8

Wang, Y., Zhang, D., Du, G., Du, R., Zhao, J., Jin, Y., et al. (2020). Remdesivir in adults with severe COVID-19: a randomised, double-blind, placebo-controlled, multicentre trial (2020). *Lancet* 395, 1569–1578. doi:10.1016/S0140-6736(20)31022-9

Ward, P., Small, I., Smith, J., Suter, P., and Dutkowski, R. (2005). Oseltamivir (Tamiflu) and its potential for use in the event of an influenza pandemic. *J. Antimicrob. Chemother.* 55, i5–i21. doi:10.1093/jac/dki018

Wen, C. Y., Xie, Z. W., Li, Y. P., Deng, X. L., Chen, X. T., Cao, Y., et al. (2020). Real-world efficacy and safety of lopinavir/ritonavir and arbidol in treating with COVID-19 : an observational cohort study. *Zhonghua Nei Ke Za Zhi* 59, E012. doi:10.3760/cma.j.cn112138-20200227-00147

WHO (2020a). Coronavirus Disease (COVID-19) situation reports. Available at: https://www.who.int/emergencies/diseases/novel-coronavirus-2019/situation-reports (Accessed July 3, 2020).

WHO (2020b). Solidarity clinical trial for COVID-19 treatments. Available at: https://www.who.int/emergencies/diseases/novel-coronavirus-2019/global-research-on-novel-coronavirus-2019-ncov/solidarity-clinical-trial-for-covid-19-treatments (Accessed November 4, 2020).

WHO (2020c). SARS-CoV-2 variants. Available at: http://www.who.int/csr/don/31-december-2020-sars-cov2-variants/en/ (Accessed January 13, 2021).

Xia, X., Li, K., Wu, L., Wang, Z., Zhu, M., Huang, B., et al. (2020). Improved clinical symptoms and mortality among patients with severe or critical COVID-19 after convalescent plasma transfusion. *Blood* 136, 755–759. doi:10.1182/blood.2020007079

Yamamura, H., Matsuura, H., Nakagawa, J., Fukuoka, H., Domi, H., and Chujoh, S. (2020). Effect of favipiravir and an anti-inflammatory strategy for COVID-19. *Crit. Care* 24, 413. doi:10.1186/s13054-020-03137-5

Yan, D., Liu, X.-Y., Zhu, Y.-N., Huang, L., Dan, B.-T., Zhang, G.-J., et al. (2020). Factors associated with prolonged viral shedding and impact of Lopinavir/Ritonavir treatment in hospitalised non-critically ill patients with SARS-CoV-2 infection. *Eur. Respir. J.* [Epub ahead of print]. doi:10.1183/13993003.00799-2020

Yan, V. C., and Muller, F. L. (2020). Advantages of the parent nucleoside GS-441524 over remdesivir for covid-19 treatment. *ACS Med. Chem. Lett.* 11, 1361–1366. doi:10.1021/acsmedchemlett.0c00316

Yao, T., Qian, J., Zhu, W., Wang, Y., and Wang, G. (2020). A systematic review of lopinavir therapy for SARS coronavirus and MERS coronavirus—a possible reference for coronavirus disease-19 treatment option. *J. Med. Virol.* 92, 556–563. doi:10.1002/jmv.25729

Yao, X., Ye, F., Zhang, M., Cui, C., Huang, B., Niu, P., et al. (2020). *In Vitro* antiviral activity and projection of optimized dosing design of hydroxychloroquine for the treatment of severe acute respiratory syndrome coronavirus 2 (SARS-CoV-2). *Clin. Infect. Dis.* [Epub ahead of print]. doi:10.1093/cid/ciaa237

Ye, X.-T., Luo, Y.-L., Xia, S.-C., Sun, Q.-F., Ding, J.-G., Zhou, Y., et al. (2020). Clinical efficacy of lopinavir/ritonavir in the treatment of Coronavirus disease 2019. *Eur. Rev. Med. Pharmacol. Sci.* 24, 3390–3396. doi:10.26355/eurrev_202003_20706

Yuan, J., Zou, R., Zeng, L., Kou, S., Lan, J., Li, X., et al. (2020). The correlation between viral clearance and biochemical outcomes of 94 COVID-19 infected discharged patients. *Inflamm. Res.* 69, 599–606. doi:10.1007/s00011-020-01342-0

Zaim, S., Chong, J. H., Sankaranarayanan, V., and Harky, A. (2020). COVID-19 and multiorgan response. *Curr. Probl. Cardiol.* 45, 100618. doi:10.1016/j.cpcardiol.2020.100618

Zhang, J.-N., Wang, W.-J., Peng, B., Peng, W., Zhang, Y.-S., Wang, Y.-L., et al. (2020). Potential of arbidol for post-exposure prophylaxis of COVID-19 transmission—a preliminary report of a retrospective cohort study. *Curr. Med. Sci.* [Epub ahead of print]. doi:10.1007/s11596-020-2203-3

Zhou, P., Yang, X.-L., Wang, X.-G., Hu, B., Zhang, L., Zhang, W., et al. (2020). A pneumonia outbreak associated with a new coronavirus of probable bat origin. *Nature* 579, 270–273. doi:10.1038/s41586-020-2012-7

Zhu, Z., Lu, Z., Xu, T., Chen, C., Yang, G., Zha, T., et al. (2020). Arbidol monotherapy is superior to lopinavir/ritonavir in treating COVID-19. *J. Infect.* 81, e21–e23. doi:10.1016/j.jinf.2020.03.060

Zijp, T. R., Toren-Wielema, M. L., Nannan Panday, P. V., Kosterink, J. G. W., Berger, S. P., and Touw, D. J. (2020). Important interactions of immunosuppressants with experimental therapies for novel coronavirus disease (COVID-19): how to act. *Ther. Drug Monit.* 42, 652–653. doi:10.1097/FTD.0000000000000766

Conflict of Interest: The authors declare that the research was conducted in the absence of any commercial or financial relationships that could be construed as a potential conflict of interest.

frontiers in Chemistry

ORIGINAL RESEARCH
published: 29 March 2021
doi: 10.3389/fchem.2021.642026

Antiviral Essential Oil Components Against SARS-CoV-2 in Pre-procedural Mouth Rinses for Dental Settings During COVID-19: A Computational Study

Pradeep Kumar Yadalam[1], Kalaivani Varatharajan[2], K. Rajapandian[2], Priyanka Chopra[3], Deepavalli Arumuganainar[4], Thilgavathi Nagarathnam[1], Honglae Sohn[5] and Thirumurthy Madhavan[6]**

[1]Adhiparashakthi Dental College and Hospital, Melmaruvathur, India, [2]Department of Periodontics, SRM Kattankulathur Dental College and Hospital, SRM Institute of Science and Technology, Chennai, India, [3]Faculty of Dental Sciences, SGT University, Gurugram, India, [4]Ragas Dental College and Hospital, Chennai, India, [5]Department of Chemistry and Department of Carbon Materials, Chosun University, Gwangju, South Korea, [6]Department of Genetic Engineering, Computational Biology Lab, School of Bioengineering, SRM Institute of Science and Technology, Chennai, India

OPEN ACCESS

Edited by:
Sugunadevi Sakkiah,
National Center for Toxicological Research (FDA), United States

Reviewed by:
Balachandran Manavalan,
School of Medicine, Ajou University, South Korea
Kalaiarasan Ponnusamy,
Jawaharlal Nehru University, India

***Correspondence:**
Honglae Sohn
hsohn@chosun.ac.kr
Thirumurthy Madhavan
thiru.murthyunom@gmail.com

Specialty section:
This article was submitted to Theoretical and Computational Chemistry, a section of the journal Frontiers in Chemistry

Received: 15 December 2020
Accepted: 01 February 2021
Published: 29 March 2021

Citation:
Yadalam PK, Varatharajan K, Rajapandian K, Chopra P, Arumuganainar D, Nagarathnam T, Sohn H and Madhavan T (2021) Antiviral Essential Oil Components Against SARS-CoV-2 in Pre-procedural Mouth Rinses for Dental Settings During COVID-19: A Computational Study. Front. Chem. 9:642026. doi: 10.3389/fchem.2021.642026

COVID-19 mainly spreads through cough or sneeze droplets produced by an infected person. The viral particles are mostly present in the oral cavity. The risk of contracting COVID-19 is high in the dental profession due to the nature of procedures involved that produce aerosols. Along with other measures to limit the risk of infection, pre-procedural mouth rinses are beneficial in reducing the viral particles in the oral cavity. In this study, the antiviral efficacy of essential oil components has been determined specifically against SARS-CoV-2 by molecular docking and conceptual DFT approach. Based on the binding affinities of the components against the receptor binding domain of the S1 glycoprotein, cuminal, carvacrol, myrtanol, and pinocarveol were found to be highly active. The molecular descriptor values obtained through conceptual DFT also indicated the above-mentioned components to be active based on the correlation between the structure and the activity of the compounds. Therefore, pre-procedural mouth rinses with these components included may be specifically suitable for dental procedures during the COVID-19 period.

Keywords: COVID-19, SARS-CoV-2, pre-procedural mouth rinse, antiviral, dental, molecular docking, conceptual DFT

INTRODUCTION

The outbreak of corona virus disease 2019 (COVID-19) in Wuhan, China, has impacted the world in several ways (Lai et al., 2020). This disease, caused by severe acute respiratory syndrome coronavirus 2 (SARS-CoV-2), has swiftly spread across 202 countries in the world due to its highly contagious nature (Peng et al., 2020b). As per the World Health Organization (WHO) report, there have been about 38 million confirmed cases of COVID-19, including one million deaths all over the world (as on October 16, 2020) (https://covid19.who.int/). And in India alone, there are seven million cases with about 100,000 deaths reported (as on October 12, 2020) (WHO Coronavirus Disease, 2020). Despite undertaking serious measures to contain the disease globally, it is still on the rise with no

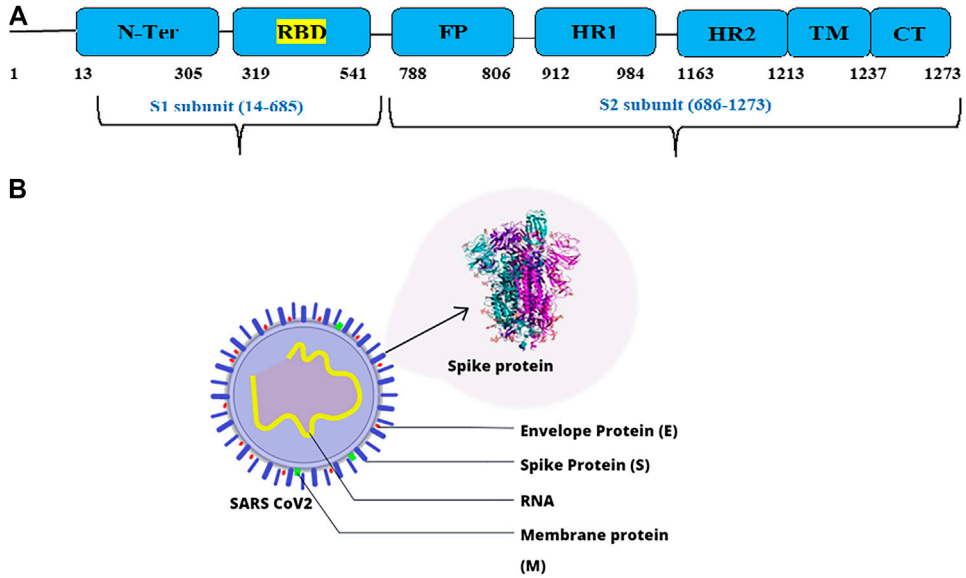

FIGURE 1 | (A) Domains of S glycoprotein. **(B)** Structure of SARS-CoV-2.

vaccine or drug to control the same. The virus spreads through direct contact with cough and sneeze droplets from an infected person or by touching contaminated surfaces and further by touching the nose or mouth (Dhand and Li, 2020). Once a person contracts the disease, the viral particles are mostly housed in the nasal cavity, oropharynx, nasopharynx, and salivary secretions (Han and Ivanovski, 2020; Krajewska Wojciechowska et al., 2020). An infected person displays symptoms such as fever, cough, and cold, a there have been reports indicating that asymptomatic carriers also spread the disease (Qu et al., 2020; Yu and Yang, 2020).

The nature of dental doctors' work mostly involves being in close proximity with patients and exposure to saliva and blood from aerosols generated from regular dental procedures, which puts them at high risk of viral infection (Li et al., 2020; Meng et al., 2020; Peng et al., 2020a). The droplets may infect the dentist if they are large in size; otherwise, they may remain suspended in the air and cause long-distance transmission in case of smaller droplets (Baghizadeh Fini, 2020). Several studies suggest that SARS-CoV-2 spike protein (1273 amino acid residues) binds to human angiotensin converting enzyme 2 (ACE-2) and utilizes it as a cellular entry receptor for binding and replication (Gurwitz, 2020; Verdecchia et al., 2020; Ziegler et al., 2020). The spike (S) protein is composed of two subunits, namely, S1 and S2. The receptor binding domain (RBD) of the S1 protein (319–541 residues) binds to the ACE-2 cell receptor, followed by fusion, which involves the S2 protein. The RBD lies in the C-terminal domain of the S1 protein, which has more residues that directly interact with the ACE-2 receptor when compared to the N-terminal domain (Huang et al., 2020). The domains of S glycoprotein and structure of SARS-CoV-2 are depicted in **Figure 1**. Hence, this region is a critical target for antibodies or antiviral compounds. ACE-2 receptors are abundantly present in the salivary glands and lungs (Xu et al., 2020). Therefore, dental professionals must exercise extreme care in terms of safety to prevent nosocomial infection. Dental societies and associations have laid down guidelines to control the transmission of the disease by suggesting dental professionals either completely stop providing dental services or postpone elective treatments and provide primary care through telemedicine services. Only emergency treatments are permitted to be performed by wearing personal protective equipment (PPE) and treating the patients with pre-procedural mouth rinse (PPMR) as a precaution to avoid any possible infection (Jevon and Shamsi, 2020; Nimbulkar et al., 2020). Recent studies have acknowledged the effectiveness of PPMR components such as povidone-iodine, 0.12%-chlorhexidine gluconate, cetylpyridinium chloride, chloroxylenol, benzalkonium chloride, and cetrimide/chlorhexidine in dental care to limit the viral load prior to treatment (Herrera et al., 2020; Meng et al., 2020). Certain essential oil (EO) components such as menthol, thymol, eugenol, and eucalyptol are common active ingredients in mouth rinses (Vlachojannis et al., 2013; Alshehri, 2018). Essential oils are a complex mixture of aromatic compounds that are known for antimicrobial activity against a host of microbes (Bakkali et al., 2008). The activity of these compounds is mostly related to their structure. Previously, numerous studies have proven the efficacy of EOs against many viruses such as herpes simplex virus (type 1 and type 2), influenza virus adenovirus type 3, and poliovirus (Minami et al., 2003; Koch et al., 2008; Swamy et al., 2016; Tariq et al., 2019). The study of synergistic activity among the EO components may lead to better antimicrobial activity. The main advantage of using EOs for therapy, against synthetic drugs, is that they fall under the GRAS (generally regarded as safe) category, whereas synthetic drugs have to undergo various levels of safety and toxicity testing,

TABLE 1 | 2D structures of the ligands (EO components).

Compound name	Structure	Compound name	Structure
α-Terpinene	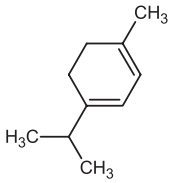	Carvacrol	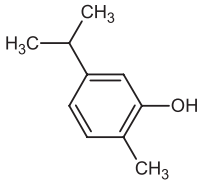
Anethole	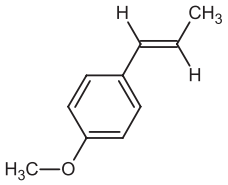	Caryophyllene	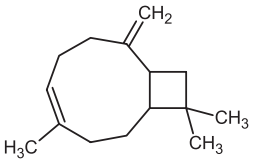
Camphene	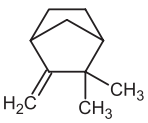	Cinnamaldehyde	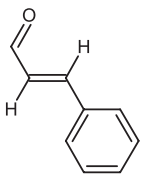
Cinnamyl acetate	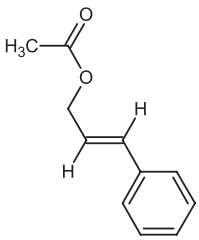	Citronellol	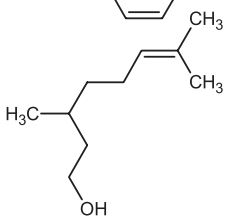
Citral	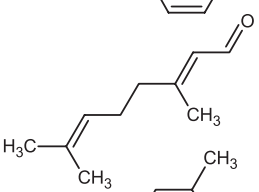	Cuminal	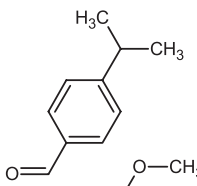
Citronellal	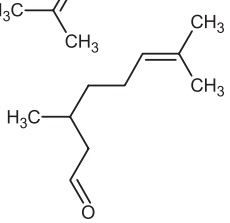	Estragole	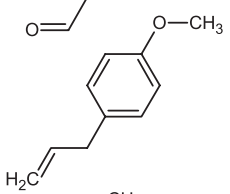
Eucalyptol	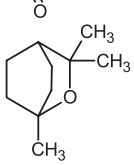	Limonene	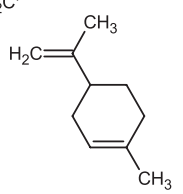
Eugenol	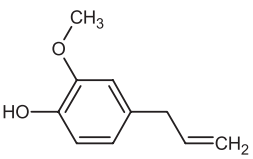	Linalool	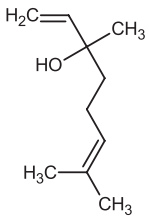

(Continued on following page)

TABLE 1 | (*Continued*) 2D structures of the ligands (EO components).

Compound name	Structure	Compound name	Structure
Fenchol	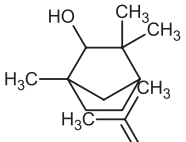	Menthol	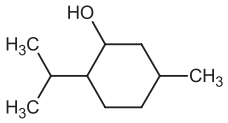
Geraniol	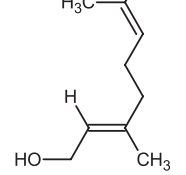	Myrtanol	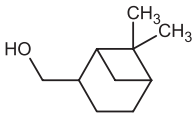
Ocimene	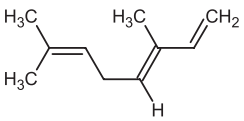	Sabinene	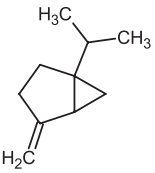
p-Cymene	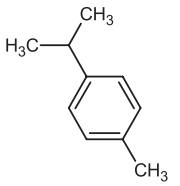	Sylvestrene	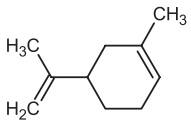
Pinocarveol	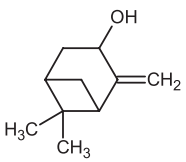	Terpinen-4-ol	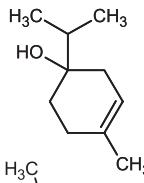
Pulegone	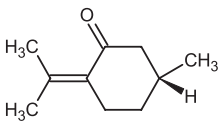	Thujene	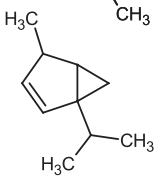
Thymol	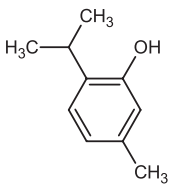	Zingiberene	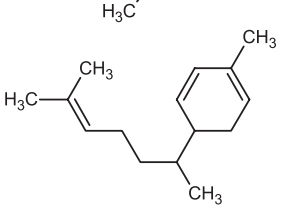

which is time-consuming. EOs are generally used for therapeutic benefits in complementary and alternative medicine (CAM) to treat infectious, non-infectious, and psychological disorders. Hence, in this study, we aim to identify EO components that are comparable or better in terms of activity, in comparison with the ones that are commonly used.

In silico techniques such as molecular docking and conceptual DFT have been employed in this study. The EO components have been docked to the RBD of the spike glycoprotein (S1) since this protein is a key target for many inhibitors because of its involvement in ACE-2 binding. The major objectives of this study are to determine the best set of inhibitors of spike protein based on the binding affinity calculations and to assess the activity of the top inhibitors based on their structure–activity relationship obtained by conceptual DFT calculations.

MATERIALS AND METHODS

Selection and Preparation of Protein Structure

The target protein considered for this study is the RBD of the SARS-CoV-2 S1 subunit, since it is primarily involved in interaction with ACE-2. The 3D structure of this protein possessing PDB ID 6M0J was retrieved from the Protein Data Bank (http://www.rcsb.org/). Initial preparation of the protein structure involved removal of water molecules and co-crystal ligands such as NAG, Cl, Zn, and ACE-2 structure which was bound to the RBD using PyMol software (http://www.pymol.org/). The protein was further prepared for docking by adding charges, energy minimization, fixing side chains and atom bumps, and using PyRx virtual screening software.

TABLE 2 | Binding affinities of the EO components with the RBD of S protein along with the H-bond and hydrophobic interactions made with the amino acid residues. EO components with better binding affinities are represented in bold.

Compound name	Binding affinity (kcal/mol)	H-bond interactions	Hydrophobic interactions
α-Terpinene	−4.3	—	Tyr449, Tyr451, Tyr453, Leu455, Phe456, Leu461, Ile468, Thr470, Ile472
Anethole	−4.8	—	
Camphene	−4.4	—	
Carvacrol	**−4.9**	Ser459	
Caryophyllene	−4.7	—	
Cinnamaldehyde	−4.6	Tyr473	
Cinnamyl acetate	−4.7	Arg454	
Citral	−4.0	Ser459	
Citronellal	−4.4	Ser459	
Citronellol	−4.4	Arg454	
Cuminal	**−4.9**	Arg457, Ser459	
Estragole	−4.7	Arg457	
Eucalyptol	−4.2	Lys458	
Eugenol	**−4.9**	Arg457, Phe456	
Fenchol	−4.6	—	
Geraniol	−4.6	Arg454, Phe456	
Limonene	−4.6	—	
Linalool	−4.7	Asp467, Ser469	
Menthol	**−5.0**	—	
Myrtanol	**−5.3**	Ser459, Lys458	
Ocimene	−4.0	—	
p-Cymene	−4.8	—	
Pinocarveol	**−5.0**	Ser469	
Pulegone	−4.8	Ser459	
Sabinene	−4.3	—	
Sylvestrene	**−5.1**	—	
Terpinen-4-ol	−4.8	Arg457, Asp467	
Thujene	−4.8	—	
Thymol	**−5.4**	Arg457, Phe456	
Zingiberene	**−5.2**	—	

Subsequently, the protein was converted to the PDBQT file format to render it readable by AutoDock Vina in PyRx software (Trott and Olson, 2010; Dallakyan and Olson, 2015).

Selection and Preparation of Ligands

The ligands chosen for this study are the components of certain EOs which are known to possess high antimicrobial activity against a broad range of microorganisms. Thymol, eucalyptol, menthol, and eugenol are widely used in most of the pre-procedural mouth rinses used by dentists (Baptista-Silva et al., 2020). These components are majorly present in thyme, eucalyptus, and clove essential oils. Therefore, other essential oil components are chosen along with these standard compounds for comparison purposes.

The 3D structure of the ligands was obtained from the PUBCHEM database (https://pubchem.ncbi.nlm.nih.gov/) in the SDF (structure data file) format. PUBCHEM is a database maintained by the NCBI, which consists of chemical and structure information of compounds that can be freely downloaded along with descriptive datasets. The ligand molecules were imported to the PyRx software using OpenBabel control (O'Boyle et al., 2011). They were prepared by adding charges and optimized using the universal force field (UFF). Furthermore, the ligands were also converted to the PDBQT format, as required by AutoDock Vina. The 2D images of the ligands are presented in **Table 1**.

Binding Site Selection and Molecular Docking

Prior to docking, selection of the appropriate binding site for the ligands is of paramount importance for deriving reliable inference from docking results. One particular binding site has been well characterized by Choudhary et al., 2020; Kulkarni et al., 2020; and Prajapat et al., 2020. Therefore, the site on the RBD with residues Tyr453, Arg454, Leu455, Lys458, Ser459, Ser469, Glu471, Pro491, Leu492, Gln493, and Tyr489 was chosen for docking of ligands. This site of the RBD of S1 protein is also involved in binding to ACE-2.

Molecular docking is performed *in silico* to assess the affinity of binding between a macromolecule and a set of small molecules based on the scores generated by the software for every interaction. In this study, docking was performed using AutoDock Vina in PyRx virtual screening open source software. AutoDock Vina is an upgraded version of AutoDock 4.0 in terms of speed and accuracy of binding mode prediction. In the PyRx software, the protein and ligand molecules to be docked are selected under the Vina Wizard control. The grid which appears on the protein is modified in dimensions according to the area around the binding site. The "Run Vina" control is selected to start the docking process. The results can be viewed under the "Analyze Results" tab and can also be exported in the CSV format to the working directory.

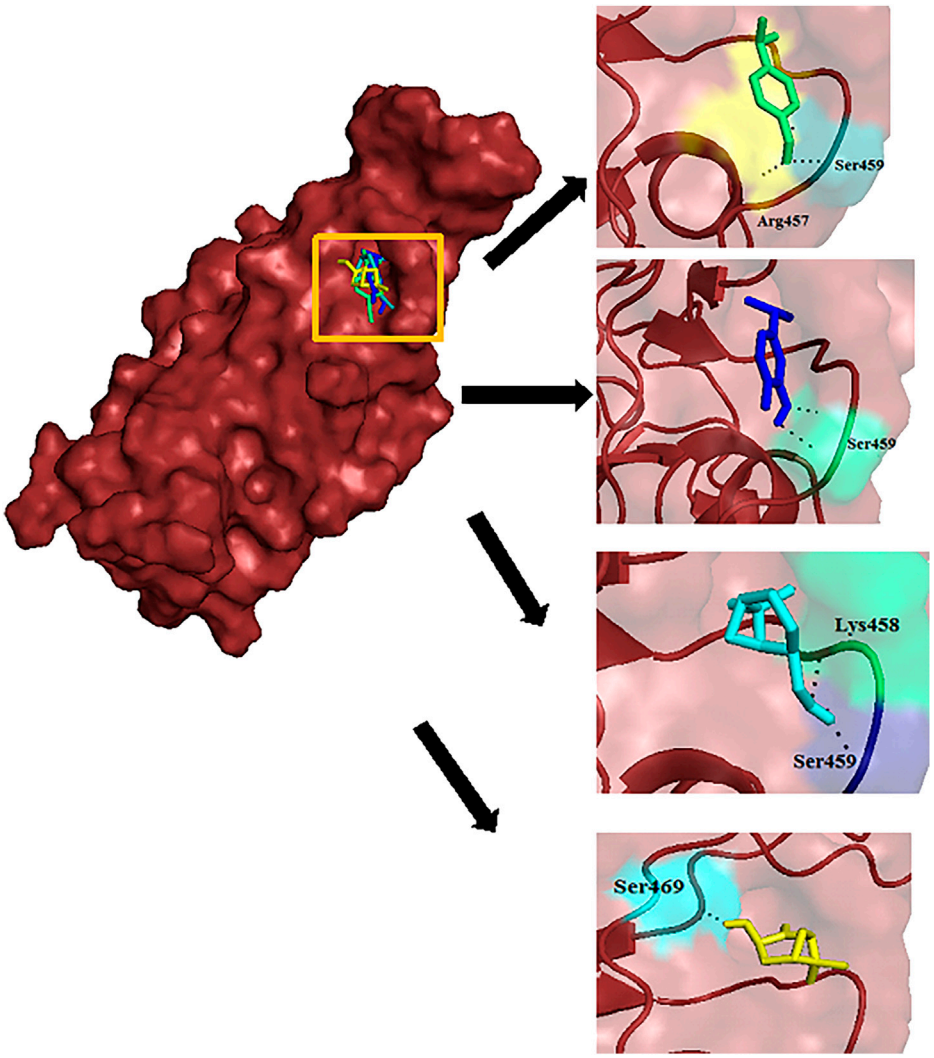

FIGURE 2 | Docked poses of cuminal (green), carvacrol (blue), myrtanol (teal), and pinocarveol (yellow) in the binding site of the RBD of S glycoprotein. The hydrogen bonding between ligands and amino acid residues is depicted.

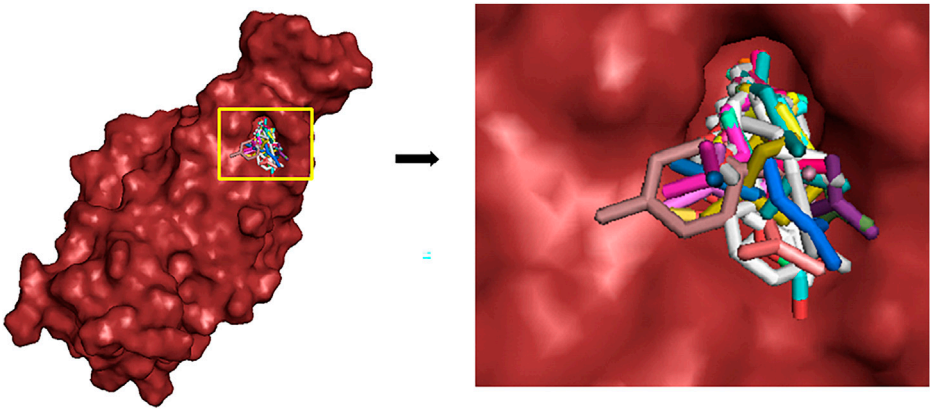

FIGURE 3 | Ligands docked in the binding site of the RBD of S protein.

TABLE 3 | Statistics of DFT based molecular descriptors of selected EO components.

Compound	Total energy (E γ) (in eV)	Molecular dipole moment (debye)	E_{HOMO}	E_{LUMO}	HOMO/ LUMO gap (ΔE)	Absolute hardness (η)	Global softness (σ)	Electronegativity (χ)	Chemical potential (μ)	Electrophilicity index (ω)
α-Terpinene	−10631.09	0.49	−5.23	−0.26	4.97	2.49	0.20	−2.75	2.75	1.52
Carvacrol	−12645.87	1.45	−5.75	0.19	5.94	2.97	0.17	−2.78	2.78	1.30
Caryophyllene	−15945.58	0.35	−5.95	0.53	6.48	3.24	0.15	−2.71	2.71	1.13
Cuminal	−12612.99	3.84	−6.83	−1.59	5.24	2.62	0.19	−4.21	4.21	3.39
Eugenol	−14658.45	1.50	−5.72	0.08	5.80	2.90	0.17	−2.82	2.82	1.37
Menthol	−12744.29	1.50	−6.90	2.01	8.91	4.45	0.11	−2.44	2.44	0.67
Myrtanol	−12710.09	1.64	−6.91	1.89	8.80	4.40	0.11	−2.51	2.51	0.72
Pinocarveol	−12676.80	1.70	−6.88	−1.50	5.38	3.48	0.14	−3.15	3.15	2.71
Sylvestrene	−10630.83	0.35	−6.13	0.77	6.91	3.45	0.14	−2.68	2.68	1.04
Thymol	−12645.82	1.45	−5.72	0.18	5.90	2.95	0.17	−2.77	2.77	1.30
Zingiberene	−15835.79	0.37	−7.96	3.89	11.86	5.93	0.08	−2.04	2.04	0.35

Conceptual DFT

Conceptual DFT (CDFT) is a subfield of DFT (density functional theory). This technique has been employed in this study to observe the chemical behavior of a molecule based on the electron density in the molecular orbitals (Geerlings and de Proft, 2008). DFT and CDFT are mainly based on the Hohenberg–Kohn theorem (Hohenberg and Kohn, 1964). About 10 different molecular descriptors are calculated as a part of the CDFT study that defines the molecular activity of the components. They are the total energy, lowest unoccupied molecular orbital (LUMO), highest occupied molecular orbital (HOMO), energy gap (ΔE), global softness (σ), absolute hardness (η), molecular dipole moment, electronegativity (χ), electrophilicity index (ω), and chemical potential (μ). These descriptors can provide prominent insights into the structure–activity relationship of molecules.

RESULTS

Molecular Docking

Docking technique essentially aids in identifying the best inhibitors to a particular protein based on the binding affinity scores generated for various conformations of the docked poses. Visualization tools such as PyMol further help in locating the ligands in the binding pocket along with the bonds exhibited with the neighboring residues. In this case, all 30 EO components were docked in the binding site specified during the docking run. Among them, carvacrol, cuminal, myrtanol, and pinocarveol displayed the best binding affinity with the spike protein with scores of −4.9 kcal/mol, −4.9 kcal/mol, −5.3 kcal/mol, and 5.0 kcal/mol, respectively, and they formed hydrogen bonding with residues Ser459, Arg457, Ser469, and Lys458. Thymol, eugenol, eucalyptol, and menthol, which were also docked for comparison purposes, scored −5.4 kcal/mol, −4.9 kcal/mol, −4.2 kcal/mol, and 5.0 kcal/mol, respectively. Zingiberene and sylvestrene too displayed good binding affinity with scores of −5.2 kcal/mol and −5.1 kcal/mol, respectively, but these components did not make any hydrogen bonds with the residues in vicinity. The stability of all the ligands in the pocket may be attributed to numerous hydrophobic residues present around the site. The docking scores along with hydrogen bonding and hydrophobic interaction information are tabulated in **Table 2**. It is clear from this study that the components proposed as top inhibitors have displayed almost similar or better activity when compared to the EO components used in conventional PPMRs. **Figure 2** illustrates the docked poses of selected inhibitors of SARS-CoV-2 with the hydrogen bonding made by them with the residues. **Figure 3** illustrates the docked poses of all the 30 ligands in the binding pocket of the RBD of S protein.

Conceptual DFT

Optimization of the EO components was performed using Gaussian 16 (Frisch et al., 2016) with B3LYP function (Becke, 1988) and 6-31G(d) basis set. The energies of the molecular orbitals represented as HOMO (E_{HOMO}) and LUMO (E_{LUMO}) were calculated on the basis of Fukui's theory (Fukui, 1982). The values of each of the descriptors were derived for the selected EO components. The HOMO and LUMO represent the ability of the compounds in donating and accepting electrons, respectively. The energy gap (ΔE) is the difference in energies between two molecules orbitals, which is given by $\Delta E = E_{LUMO} - E_{HOMO}$. ΔE essentially represents the energy needed to perform transition of molecules from the HOMO to the LUMO, and hence, it is directly proportional to the molecular reactivity (Mert et al., 2011). In this study, larger ΔE values were attributed to a wide range of E_{LUMO} values. **Table 3** provides the statistics of DFT-based molecular descriptors of selected EO components. It can be observed from the table that cuminal showed the lowest ΔE, whereas zingiberene displayed the largest ΔE. It is understood that the lower the energy gap, the higher the activity of the molecules, which can be correlated with the transition of molecules from the HOMO to the LUMO. Carvacrol, caryophyllene, pinocarveol, and sylvestrene also exhibited low ΔE. The electron density maps depicting the density of electrons in different regions of the molecules are presented in **Figure 4**. Mert et al., 2011, have pointed out that the molecular dipole moment of a molecule is directly proportional to its chemical reactivity. Cuminal has the highest dipole moment with 3.84 debye, followed by pinocarveol with 1.70 debye and myrtanol with 1.64 debye, which is higher than that of eugenol,

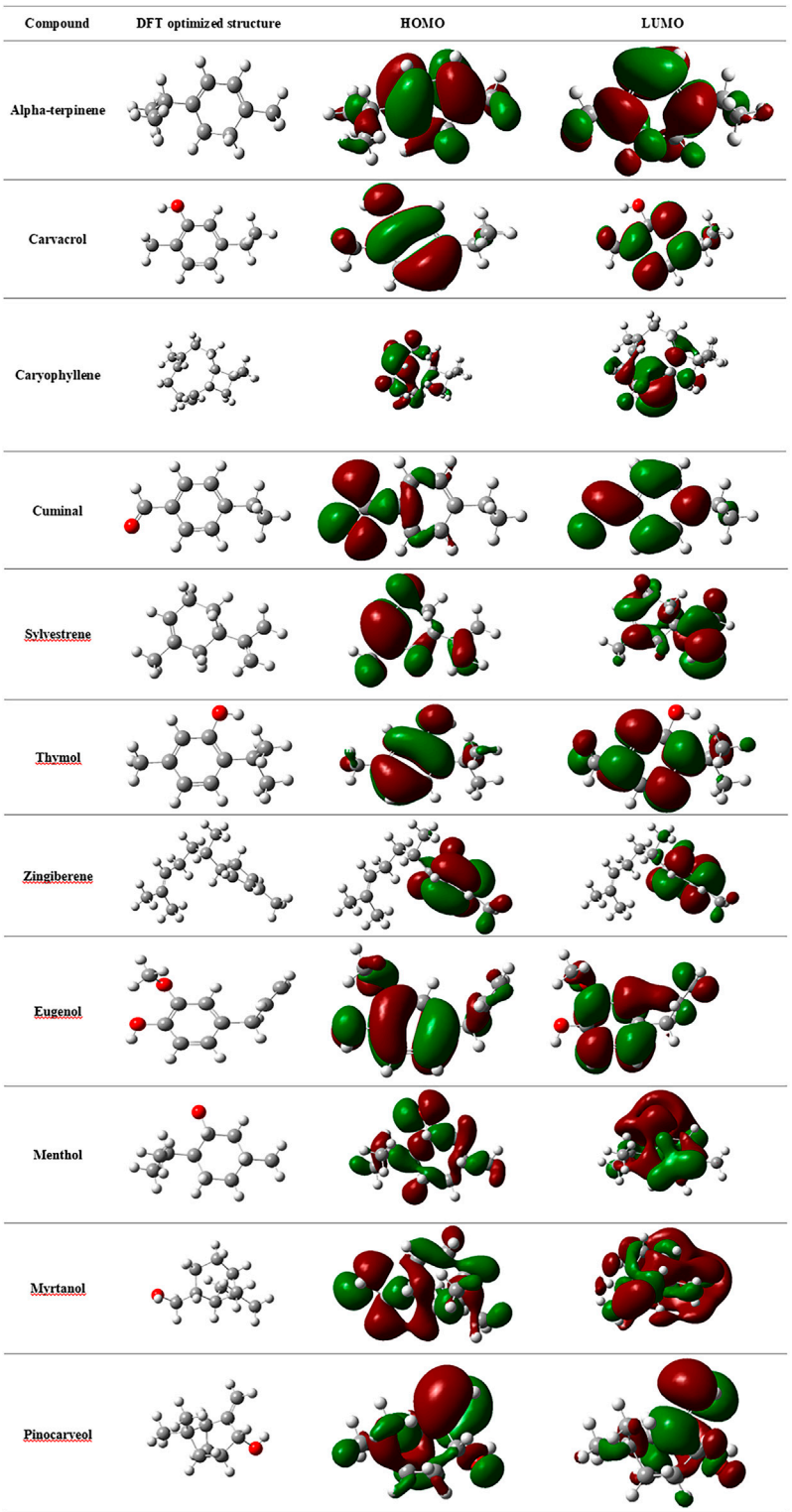

FIGURE 4 | Electron density maps of the HOMO and LUMO of selected essential oil components.

menthol, and thymol. Carvacrol and thymol scored 1.45 debye. Electronegativity of a compound is an index of the ability of a molecule to accept electrons. It is an important indicator of efficiency of inhibition of the molecule. The lower the electronegativity of a molecule is, the higher its efficiency of inhibition will be. Cuminal has the lowest electronegativity

index (−4.21). This index for other components was almost in the range of −3.15 to −2.82. The results of conceptual DFT are in agreement with the docking results.

DISCUSSION

Due to the sudden outbreak of COVID-19, the standard procedures of operation had to be modified in almost every sector, especially in the field of medicine and dentistry since they involve frontline care givers. Dental professionals have to exercise extra caution because of the high risk of nosocomial infection through aerosol-generating procedures. Although physical protection from the virus by wearing safety gear such as PPE is recommended, an effective antiviral PPMR may ensure safety even in case the patient is infected but asymptomatic. Recent literature suggests numerous mouth rinses that can effectively reduce the viral load in the oral cavity. Povidone-iodine (PVP-I) oral rinse has been found to be effective in various studies conducted by Tessema et al., 2020; Bidra et al., 2020; and Pelletier et al., 2021. Mouth rinses containing 1% PVP-I exhibited a virucidal activity higher than 99.99%, which corresponds to a reduction of viral load greater than 4 $\log_{10}$. The use of PVP-I has been contraindicated in patients with an allergy to iodine, thyroid disease, and pregnancy. Chlorhexidine (CHX) is a broad-spectrum antiseptic that has long been known to be effective against herpes simplex virus (HSV), human immunodeficiency virus (HIV), and hepatitis B virus (HBV) (Brookes et al., 2020). The effectiveness of CHX specifically against SARS-CoV-2 has not been well established yet. In comparison with PVP-I, hydrogen peroxide (H_2O_2) has been found to be less effective by a study conducted by Ather et al., 2020. Certain essential oil (EO) components such as thymol, eugenol, menthol, methyl salicylate, and eucalyptol are common major ingredients in mouth rinses recommended by the American Dental Association (ADA) (Alshehri, 2018). The activity of these components has been well established by several studies against a wide array of microbes, including viruses. The main aim of this study was to explore other components with comparable or better activity than the existing ones by *in silico* methods. Moreover, EO components are safe since they fall under the generally regarded as safe (GRAS) category. Cuminal, myrtanol, carvacrol, caryophyllene, pinocarveol, and sylvestrene were found to have inhibitory effects against SARS-CoV-2. A number of recent *in silico* studies have predicted the anitiviral activity of EO components against SARS-CoV-2. Kulkarni et al., 2020, performed a similar study with the same target protein and found that cinnamaldehyde, anethole, thymol, and carvacrol were highly active. Similar results were obtained by Asif et al., 2020, and Senthil Kumar et al., 2020. Boukhatem, 2020, have discussed how EOs could have an inhibitory effect on SARS-CoV-2, similar to the effect they have had on other viruses. Thuy et al., 2020, predicted that 17 compounds of garlic oil interacted with the viral main protease (Mpro) of SARS-CoV-2. Da Silva et al., 2020, predicted that (E,E)-α-farnesene, (E,E)-farnesol, and (E)-nerolidol interacted with SARS-CoV-2 Mpro, thereby inhibiting viral replication, out of 171 EO components. So far, no *in vitro* or *in vivo* studies have established the efficacy of these compounds. This study has resulted in predicting EO components that can increase the efficiency of conventional PPMRs by reducing the viral load in the oropharyngeal cavity, specifically against SARS-CoV-2.

CONCLUSION

Providing dental care treatment to patients, while reducing the risk of highly contagious viral infection caused by SARS-CoV-2 is a challenge for dental professionals.. Through this study, we conclude that EO components such as cuminal, carvacrol, myrtanol, caryophyllene, pinocarveol, and sylvestrene are good inhibitors of the S1 glycoprotein of coronavirus by *in silico* methods. Hence, these components can be proposed to be effective antiviral ingredients of pre-procedural mouth rinses recommended to be administered to patients for effective reduction of viral load in the oropharyngeal cavity. The futurology of this study indicates *in vitro* and *in vivo* testing of the same to confirm the antiviral efficiency of the proposed EO components, specifically against SARS-CoV-2.

DATA AVAILABILITY STATEMENT

The authors acknowledge that the data presented in this study must be deposited and made publicly available in an acceptable repository, prior to publication.

AUTHOR CONTRIBUTIONS

PY, HS, and TM contributed to the conception, design, and data acquisition. PY drafted the manuscript. KV, KR, PC, DA, and TN contributed to data analysis and have critically revised the manuscript. All authors gave final approval and agreed to be accountable for all aspects of the work.

REFERENCES

Alshehri, F. A. (2018). The use of mouthwash containing essential oils (LISTERINE®) to improve oral health: a systematic review. *Saudi Dent. J.* 30, 2–6. doi:10.1016/j.sdentj.2017.12.004

Asif, M., Saleem, M., Saadullah, M., Yaseen, H. S., and al Zarzour, R. (2020). COVID-19 and therapy with essential oils having antiviral, anti-inflammatory, and immunomodulatory properties. *Inflammopharmacology* 28, 1153–1161. doi:10.1007/s10787-020-00744-0

Ather, A., Patel, B., Ruparel, N. B., Diogenes, A., and Hargreaves, K. M. (2020). Coronavirus disease 19 (COVID-19): implications for clinical dental care. *J. Endod.* 46, 584–595. doi:10.1016/j.joen.2020.03.008

Baghizadeh Fini, M. (2020). What dentists need to know about COVID-19. *Oral Oncol.* 105, 104741. doi:10.1016/j.oraloncology.2020.104741

Bakkali, F., Averbeck, S., Averbeck, D., and Idaomar, M. (2008). Biological effects of essential oils-a review. *Food Chem. Toxicol.* 46, 446–475. doi:10.1016/j.fct.2007.09.106

Baptista-Silva, S., Borges, S., Ramos, O. L., Pintado, M., and Sarmento, B. (2020). The progress of essential oils as potential therapeutic agents: a review. *J. Essent. Oil Res.* 32, 279–295. doi:10.1080/10412905.2020.1746698

Becke, A. D. (1988). Density-functional exchange-energy approximation with correct asymptotic behavior. *Phys. Rev. A. Gen. Phys.* 38, 3098–3100. doi:10.1103/PhysRevA.38.3098

Bidra, A. S., Pelletier, J. S., Westover, J. B., Frank, S., Brown, S. M., and Tessema, B. (2020). Rapid in-vitro inactivation of severe acute respiratory syndrome coronavirus 2 (SARS-CoV-2) using povidone-iodine oral antiseptic rinse. *J. Prosthodont.* 29, 529–533. doi:10.1111/jopr.13209

Boukhatem, M. N. (2020). Effective antiviral activity of essential oils and their characteristics terpenes against coronaviruses: an update. *J. Pharmacol. Clin. Toxicol.* 8, 1–8.

Brookes, Z. L. S., Bescos, R., Belfield, L. A., Ali, K., and Roberts, A. (2020). Current uses of chlorhexidine for management of oral disease: a narrative review. *J. Dent.* 103, 103497. doi:10.1016/j.jdent.2020.103497

Choudhary, S., Malik, Y. S., and Tomar, S. (2020). Identification of SARS-CoV-2 cell entry inhibitors by drug repurposing using in silico structure-based virtual screening approach. *Front. Immunol.* 11, 1664. doi:10.3389/fimmu.2020.01664

Da Silva, J. K. R., Figueiredo, P. L. B., Byler, K. G., and Setzer, W. N. (2020). Essential oils as antiviral agents. Potential of essential oils to treat SARS-CoV-2 infection: an in-silico investigation. *Int. J. Mol. Sci.* 21, 1–37. doi:10.3390/ijms21103426

Dallakyan, S., and Olson, A. J. (2015). Small-molecule library screening by docking with PyRx. *Methods Mol. Biol.* 1263, 243–250. doi:10.1007/978-1-4939-2269-7_19

Dhand, R., and Li, J. (2020). Coughs and sneezes: their role in transmission of respiratory viral infections, including SARS-CoV-2. *Am. J. Respir. Crit. Care Med.* 202, 651–659. doi:10.1164/rccm.202004-1263PP

Frisch, M. J., Trucks, G. W., Schlegel, H. B., Scuseria, G. E., Robb, M. A., Cheeseman, J. R., et al. (2016). *Gaussian 16*, Wallingford, CT: Gaussian Inc.

Fukui, K. (1982). The role of frontier orbitals in chemical reactions (nobel lecture). *Angew. Chem. Int. Ed. Engl.* 21, 801–809. doi:10.1002/anie.198208013

Geerlings, P., and de Proft, F. (2008). Conceptual DFT: the chemical relevance of higher response functions. *Phys. Chem. Chem. Phys.* 10, 3028–3042. doi:10.1039/b717671f

Gurwitz, D. (2020). Angiotensin receptor blockers as tentative SARS-CoV-2 therapeutics. *Drug Dev. Res.* 81, 537–540. doi:10.1002/ddr.21656

Han, P., and Ivanovski, S. (2020). Saliva-friend and foe in the COVID-19 outbreak. *Diagnostics* 10, 290. doi:10.3390/diagnostics10050290

Herrera, D., Serrano, J., Roldán, S., and Sanz, M. (2020). Is the oral cavity relevant in SARS-CoV-2 pandemic? *Clin. Oral Investig.* 24, 2925–2930. doi:10.1007/s00784-020-03413-2

Hohenberg, P., and Kohn, W. (1964). Inhomogeneous electron gas. *Phys. Rev.* 136, B864. doi:10.1103/PhysRev.136.B864

Huang, Y., Yang, C., Xu, X. F., Xu, W., and Liu, S. W. (2020). Structural and functional properties of SARS-CoV-2 spike protein: potential antivirus drug development for COVID-19. *Acta Pharmacol. Sin.* 41, 1141–1149. doi:10.1038/s41401-020-0485-4

Jevon, P., and Shamsi, S. (2020). COVID-19 and medical emergencies in the dental practice. *Br. Dent J.* 229, 19–24. doi:10.1038/s41415-020-1782-5

Koch, C., Reichling, J., Schneele, J., and Schnitzler, P. (2008). Inhibitory effect of essential oils against herpes simplex virus type 2. *Phytomedicine* 15, 71–78. doi:10.1016/j.phymed.2007.09.003

Krajewska Wojciechowska, J., Krajewski, W., Zub, K., and Zatoński, T. (2020). Review of practical recommendations for otolaryngologists and head and neck surgeons during the COVID-19 pandemic. *Auris Nasus Larynx* 47, 544–558. doi:10.1016/j.anl.2020.05.022

Kulkarni, S. A., Nagarajan, S. K., Ramesh, V., Palaniyandi, V., Selvam, S. P., and Madhavan, T. (2020). Computational evaluation of major components from plant essential oils as potent inhibitors of SARS-CoV-2 spike protein. *J. Mol. Struc.* 1221, 128823. doi:10.1016/j.molstruc.2020.128823

Lai, C. C., Shih, T. P., Ko, W. C., Tang, H. J., and Hsueh, P. R. (2020). Severe acute respiratory syndrome coronavirus 2 (SARS-CoV-2) and coronavirus disease-2019 (COVID-19): the epidemic and the challenges. *Int. J. Antimicrob. Agents* 55, 105924. doi:10.1016/j.ijantimicag.2020.105924

Li, Y., Ren, B., Peng, X., Hu, T., Li, J., Gong, T., et al. (2020). Saliva is a non-negligible factor in the spread of COVID-19. *Mol. Oral Microbiol.* 35, 141–145. doi:10.1111/omi.12289

Meng, L., Hua, F., and Bian, Z. (2020). Coronavirus disease 2019 (COVID-19): emerging and future challenges for dental and oral medicine. *J. Dent. Res.* 99, 481–487. doi:10.1177/0022034520914246

Mert, B. D., Erman Mert, M., Kardaş, G., and Yazici, B. (2011). Experimental and theoretical investigation of 3-amino-1,2,4-triazole-5-thiol as a corrosion inhibitor for carbon steel in HCl medium. *Corros. Sci.* 53, 4265–4272. doi:10.1016/j.corsci.2011.08.038

Minami, M., Kita, M., Nakaya, T., Yamamoto, T., Kuriyama, H., and Imanishi, J. (2003). The inhibitory effect of essential oils on herpes simplex virus type-1 replication *in vitro*. *Microbiol. Immunol.* 47, 681–684. doi:10.1111/j.1348-0421.2003.tb03431.x

Nimbulkar, G., Dubey, N., Mandwar, S., Dharmapuria, S., Reche, A., and Chhabra, K. G. (2020). Dental practice guidelines in the precariousness of COVID-19: a review. *Int. J. Curr. Res. Rev.* 12, 82–87. doi:10.31782/IJCRR.2020.12195

O'Boyle, N. M., Banck, M., James, C. A., Morley, C., Vandermeersch, T., and Hutchison, G. R. (2011). Open babel: an open chemical toolbox. *J. Cheminform.* 3, 33. doi:10.1186/1758-2946-3-33

Pelletier, J. S., Tessema, B., Frank, S., Westover, J. B., Brown, S. M., and Capriotti, J. A. (2021). Efficacy of povidone-iodine nasal and oral antiseptic preparations against severe Acute Respiratory syndrome-coronavirus 2 (SARS-CoV-2). *Ear Nose Throat J.* 100, 192S–196S. doi:10.1177/0145561320957237

Peng, X., Xu, X., Li, Y., Cheng, L., Zhou, X., and Ren, B. (2020a). Transmission routes of 2019-nCoV and controls in dental practice. *Int. J. Oral Sci.* 12, 9. doi:10.1038/s41368-020-0075-9

Peng, Y., Li, C., Rong, Y., Chen, X., and Chen, H. (2020b). Retrospective analysis of the accuracy of predicting the alert level of COVID-19 in 202 countries using Google Trends and machine learning. *J. Glob. Health* 10, 020511. doi:10.7189/jogh.10.020511

Prajapat, M., Shekhar, N., Sarma, P., Avti, P., Singh, S., Kaur, H., et al. (2020). Virtual screening and molecular dynamics study of approved drugs as inhibitors of spike protein S1 domain and ACE2 interaction in SARS-CoV-2. *J. Mol. Graph. Model.* 101, 107716. doi:10.1016/j.jmgm.2020.107716

Qu, J., Chang, L. K., Tang, X., Du, Y., Yang, X., Liu, X., et al. (2020). Clinical characteristics of COVID-19 and its comparison with influenza pneumonia. *Acta Clinica Belgica: Int. J. Clin. Lab. Med.* 75, 348–356. doi:10.1080/17843286.2020.1798668

Senthil Kumar, K. J., Vani, M. G., Wang, C. S., Chen, C. C., Chen, Y. C., Lu, L. P., et al. (2020). Geranium and lemon essential oils and their active compounds downregulate angiotensin-converting enzyme 2 (ACE2), a SARS-CoV-2 spike receptor-binding domain, in epithelial cells. *Plants* 9, 1–12. doi:10.3390/plants9060770

Swamy, M. K., Akhtar, M. S., and Sinniah, U. R. (2016). Antimicrobial properties of plant essential oils against human pathogens and their mode of action: an updated review. *Evid. Based Complement. Alternat Med.* 2016, 3012462. doi:10.1155/2016/3012462(2016).

Tariq, S., Wani, S., Rasool, W., Shafi, K., Bhat, M. A., Prabhakar, A., et al. (2019). A comprehensive review of the antibacterial, antifungal and antiviral potential of essential oils and their chemical constituents against drug-resistant microbial pathogens. *Microb. Pathog.* 134, 103580. doi:10.1016/j.micpath.2019.103580

Tessema, B., Frank, S., and Bidra, A. (2020). SARS-CoV-2 viral inactivation using low dose povidone-iodine oral rinse-immediate application for the prosthodontic practice. *J. Prosthodont.* 29, 459. doi:10.1111/jopr.13207

Thuy, B. T. P., My, T. T. A., Hai, N. T. T., Hieu, L. T., Hoa, T. T., Thi Phuong Loan, H., et al. (2020). Investigation into SARS-CoV-2 resistance of compounds in garlic essential oil. *ACS Omega* 5, 8312–8320. doi:10.1021/acsomega.0c00772

Trott, O., and Olson, A. J. (2010). AutoDock Vina: improving the speed and accuracy of docking with a new scoring function, efficient optimization, and multithreading. *J. Comput. Chem.* 31, 455–461. doi:10.1002/jcc.21334

Verdecchia, P., Cavallini, C., Spanevello, A., and Angeli, F. (2020). The pivotal link between ACE2 deficiency and SARS-CoV-2 infection. *Eur. J. Int. Med.* 76, 14–20. doi:10.1016/j.ejim.2020.04.037

Vlachojannis, C., Winsauer, H., and Chrubasik, S. (2013). Effectiveness and safety of a mouthwash containing essential oil ingredients. *Phytother. Res.* 27, 685–691. doi:10.1002/ptr.4762

WHO Coronavirus Disease (2020). (*COVID-19) dashboard*. Available at: https://covid19.who.int/region/searo/country/ (Accessed December 05 2020).

Xu, R., Cui, B., Duan, X., Zhang, P., Zhou, X., and Yuan, Q. (2020). Saliva: potential diagnostic value and transmission of 2019-nCoV. *Int. J. Oral Sci.* 12, 11. doi:10.1038/s41368-020-0080-z

Yu, X., and Yang, R. (2020). COVID-19 transmission through asymptomatic carriers is a challenge to containment. *Influenza Other Respir. Viruses* 14, 474–475. doi:10.1111/irv.12743

Ziegler, C. G. K., Allon, S. J., Nyquist, S. K., Mbano, I. M., Miao, V. N., Tzouanas, C. N., et al. (2020). SARS-CoV-2 receptor ACE2 is an interferon-stimulated gene in human airway epithelial cells and is detected in specific cell subsets across tissues. *Cell* 181, 1016–1035.e19. doi:10.1016/j.cell.2020.04.035

Conflict of Interest: The authors declare that the research was conducted in the absence of any commercial or financial relationships that could be construed as a potential conflict of interest.

frontiers in Pharmacology

REVIEW
published: 30 April 2021
doi: 10.3389/fphar.2021.643619

Intermittent Hypoxic Preconditioning: A Potential New Powerful Strategy for COVID-19 Rehabilitation

Ming Cai[1†], Xuan Chen[2†], Jieling Shan[3†], Ruoyu Yang[4], Qi Guo[1], Xia Bi[1], Ping Xu[4], Xiangrong Shi[5], Lixi Chu[4,6]* and Liyan Wang[4]**

[1]Shanghai University of Medicine and Health Sciences Affiliated Zhoupu Hospital, Shanghai, China, [2]School of Kinesiology, Shanghai University of Sport, Shanghai, China, [3]Department of Ultrasound, Huashan Hospital, Fudan University, Shanghai, China, [4]College of Rehabilitation Science, Shanghai University of Medicine and Health Sciences, Shanghai, China, [5]Department of Pharmacology and Neuroscience, University of North Texas Health Science Center, Fort Worth, TX, United States, [6]Shanghai Sunshine Rehabilitation Center, Shanghai, China

OPEN ACCESS

Edited by:
Brijesh Kumar Singh, Duke-NUS Medical School, Singapore

Reviewed by:
Pradeep Bist, Duke-NUS Medical School, Singapore
Rupesh K. Srivastava, All India Institute of Medical Sciences, India

***Correspondence:**
Xiangrong Shi
Xiangrong.shi@unthsc.edu
Lixi Chu
chulixi2@126.com
Liyan Wang
wangly@sumhs.edu.cn

[†]These authors have contributed equally to this work

Specialty section:
This article was submitted to Respiratory Pharmacology, a section of the journal Frontiers in Pharmacology

Received: *18 December 2020*
Accepted: *15 March 2021*
Published: *30 April 2021*

Citation:
Cai M, Chen X, Shan J, Yang R, Guo Q, Bi X, Xu P, Shi X, Chu L and Wang L (2021) Intermittent Hypoxic Preconditioning: A Potential New Powerful Strategy for COVID-19 Rehabilitation. Front. Pharmacol. 12:643619. doi: 10.3389/fphar.2021.643619

COVID-19 is a highly infectious respiratory virus, which can proliferate by invading the ACE2 receptor of host cells. Clinical studies have found that the virus can cause dyspnea, pneumonia and other cardiopulmonary system damage. In severe cases, it can lead to respiratory failure and even death. Although there are currently no effective drugs or vaccines for the prevention and treatment of COVID-19, the patient's prognosis recovery can be effectively improved by ameliorating the dysfunction of the respiratory system, cardiovascular systems, and immune function. Intermittent hypoxic preconditioning (IHP) as a new non-drug treatment has been applied in the clinical and rehabilitative practice for treating chronic obstructive pulmonary disease (COPD), diabetes, coronary heart disease, heart failure, hypertension, and other diseases. Many clinical studies have confirmed that IHP can improve the cardiopulmonary function of patients and increase the cardiorespiratory fitness and the tolerance of tissues and organs to ischemia. This article introduces the physiological and biochemical functions of IHP and proposes the potential application plan of IHP for the rehabilitation of patients with COVID-19, so as to provide a better prognosis for patients and speed up the recovery of the disease. The aim of this narrative review is to propose possible causes and pathophysiology of COVID-19 based on the mechanisms of the oxidative stress, inflammation, and immune response, and to provide a new, safe and efficacious strategy for the better rehabilitation from COVID-19.

Keywords: COVID-19, intermittent hypoxic preconditioning, HIF-1α, immune response, inflammatory cytokine storm, rehabilitation

INTRODUCTION

Since the outbreak and pandemic of the highly infectious and pathogenic COVID-19, most attention has been focused on containing transmission of the coronavirus and addressing the surge of critically ill patients in acute care settings. However, in the future, emphasis will gradually transition to prognosis care and rehabilitation of COVID-19 survivors. Although COVID-19 predominantly affects the respiratory system, it's anticipated that COVID-19 may have an adverse impact on physical, cognitive, mental and social health status, which is a multisystem disease and frequently

severe and often results in death (Barker-Davies et al., 2020; Madjid et al., 2020). Rehabilitation guideline after critical illness recommends progressive rehabilitation programmes are best initiated within the first 30°days (post-acute phase) to have greatest impact on recovery, including improving respiratory function, physical exercise ability, self-care in daily living activities, as well as psychological support, etc (Group, 2009). Very little attention to the prognosis and rehabilitation therapy methods or outcomes of COVID-19 patients after discharge from acute care. So far, only one related study has been published, in which a randomized controlled trail showed that 6°weeks respiratory rehabilitation (2 sessions of 10 min per week) had beneficial to the improvement of respiratory function, endurance, quality of life, and depression following discharge from acute care (K. Liu K.et al., 2020).

The latest epidemiological analysis pointed out a lower incidence of COVID-19 and proposed a possible weaker transmission rate of severe SARS-CoV-2 among high-altitude populations (Arias-Reyes et al., 2020; Segovia-Juarez et al., 2020; Xi et al., 2020). The typical characteristic of plateau environment is hypobaric hypoxia, which could increase tissue oxygen delivery and enhance oxygen utilization. Thus, it can be argued that high-altitude residents may be somewhat tolerant to the consequences of more hypoxemia and systemic tissue hypoxia developing as a result of COVID-19 infection and subsequent lung injury. An intuitive evidence is that hypoxia can reduce the incidence of COVID-19, which may be related to the fact that hypoxia can shorten the half-life of SARS-CoV-2 virus and induce down-regulation of angiotensin-converting enzyme 2 (ACE2) expression, thereby increasing the body's resistance to viruses (Arias-Reyes et al., 2020). Of note, recently, intermittent hypoxic preconditioning (IHP) as a new non-drug treatment has been used in the clinical treatment of chronic obstructive pulmonary disease (COPD), diabetes, coronary heart disease, hypertension, and other diseases. Many clinical studies have confirmed that IHP can improve the cardiopulmonary function of patients, increase blood oxygen content and the tolerance of tissues and organs to ischemia, inhibit the overactivation of immune system, and control acute pulmonary inflammation. Based on the many beneficial functions of IHP, we speculate that IHP is expected to become a new exploration in the prognosis and rehabilitation of stable COVID-19 cases.

In this review, we briefly outlined the epidemiology, pathological features and histopathology, inflammatory cytokine storm and related damage of COVID-19. Then, we mainly focused on the potential of IHP applied in rehabilitation of COVID-19 and the prognosis based on a variety of IHP related beneficial impacts on physiological functions, and plausible mechanisms to better help the patients to recover and return to society promptly and safely.

EPIDEMIOLOGY

At December 2019, the first cases of severe acute respiratory infections of unknown origin were reported in Wuhan, China. The causative agent was identified as a novel ß-coronavirus SARS-CoV-2 and the disease was named COVID-19, which is another human infectious disease caused by coronavirus. The transmission of COVID-19 is potent and the infection rate is high. Although the outbreak of COVID-19 is better under control in China, the global situation is still in severe challenge and the confirmed infected cases are continually increased. Since the beginning of 2020, the infection has been spreading worldwide over 215 Countries, causing 115,967,664 cases and over 2,579,775 deaths (as of 09:38 am, March 7, 2021, https://covid19.who.int/), which led the WHO to declare COVID-19 a public health emergency of international concern and the current situation as a new normal for epidemic prevention and control.

The transmission of COVID-19 occurs mainly via respiratory droplets and contact routes, the incubation period ranges from 1 to 14°days with mostly 3–7°days (Guan et al., 2020). All age groups are susceptible, especially the elderly and those with chronic diseases. Now most cases are asymptomatic or mild, but they are potential sources of infection and some patients develop severe pneumonia with acute respiratory distress, septic shock, and multi-organ failure. In other words, asymptomatically infected persons and patients in incubation or recovered from COVID-19 may pose serious challenges for disease prevention and control. The overall case fatality rate is estimated to range from 1 to 16%, which depends on some important parameters such as age, underlying medical comorbidities, preparedness of health system to an outbreak, implementation of preventive measures, and country reaction time to epidemic situation (Verity et al., 2020).

PATHOLOGICAL FEATURES AND HISTOPATHOLOGY

The most common symptoms of COVID-19 are fever (98%), dry cough (76%), and myalgia or fatigue (44%) (Huang et al., 2020). Other symptoms are sputum production, arthralgia or sore throat, headache, nausea, vomiting or diarrhea (Borges do Nascimento et al., 2020). Meanwhile, clinical examination shows that severe cases are usually accompanied by obvious hypoxemia (the oxygen saturation is less than 92%) and hypocapnia, which is manifested by decreased arterial partial pressure of oxygen to the ratio of inhaled partial pressure of oxygen and lower plasma CO_2 levels (Wang D. et al., 2020; Wang M. et al., 2020). Besides, more than half of patients developed dyspnea.

Typical pulmonary imaging findings of COVID-19 cases include multifocal peripherally distributed ground-glass opacities or consolidations, interlobular septal thickening, crazy paving appearance and cystic changes. In autopsies, immunostaining shows bilateral diffuse alveolar damage with cellular fibromyxoid exudates, histological patterns in lung and extrapulmonary tissues were characterized by capillary congestion, necrosis of pneumocytes, hyaline membrane, interstitial edema, pneumocyte hyperplasia, and reactive atypia, which are accompanied by severe inflammatory response (Menter et al., 2020; Xu et al., 2020). Moreover, infiltrates express as macrophages in alveolar lumens and

lymphocytes in the interstitium are found in the lung (Song et al., 2020). Again, a lot of findings are suggestive for vascular dysfunction, in lung and other tissues. Meanwhile, COVID-19 has also been shown to be harmful to the heart, some patients are associated with cardiovascular complications such as myocardial injury (Madjid et al., 2020), cardiac arrest (Baldi et al., 2020) and acute heart failure (Tomasoni et al., 2020; Xu et al., 2020). Adverse outcomes of COVID-19 are associated with comorbidities, including hypertension, cardiovascular disease, and lung disease.

Lipids metabolism and inflammation may play key roles in the development of COVID-19. A recent study indicates that lipids are important in the envelopment and transformation of COVID-19 virus, and metabolic disorders may provide additional possibility for the virus to invade host cells (Abu-Farha et al., 2020). The aging associated with increasing chronic inflammation will also destroy the effective control of the immune system in the acute phase of COVID-19 replication (Figliozzi et al., 2020). In addition, COVID-19 will induce excessive inflammation, oxidative stress, abnormal immune responses, and other cardiovascular complications. Then, activation of immune cells will increase oxygen consumption and reduce the supply of O_2 due to vascular dysfunction, resulting in breathing difficulties and hypoxia, and even death (Cummins et al., 2016).

INFLAMMATORY CYTOKINE STORM AND RELATED DAMAGE

Chest computerized tomography (CT) scans of COVID-19 show pneumonia with abnormal findings in all cases, and the potential mechanisms are particularly complex. Clinical and preclinical research will have to explain many aspects that underlie the particular clinical presentations of COVID-19. The data so far are available to indicate that the viral infection is capable to produce an excessive immune reaction in the host. In some cases, a reaction takes place which as a whole is labeled an "inflammatory cytokine storm", including the tumor necrosis factor a (TNF-α), IL-1β, IL-6, IL-8, IL-12, interferon-gamma inducible protein (IP10), macrophage inflammatory protein 1A (MIP1A), and monocyte chemoattractant protein 1 (MCP1). Moreover, COVID-19 can bind the Toll-like receptor (TLR) to induce the release of pro-IL-1β, which is cleaved into the active mature IL-1β mediating lung inflammation, until fibrosis (Conti et al., 2020). In the early stage of the disease, characteristic laboratory findings of normal white blood cell (WBC) count or mild leukopenia, marked lymphopenia, elevated inflammatory factors (IL-2R, IL-6, TNF-α), suggest that uncontrolled inflammatory responses may further aggravate tissue damage in cardiovascular and other organs (Qin et al., 2020; Wu and McGoogan, 2020). Interestingly, lymphopenia appears to be a negative prognostic factor. The elevated neutrophil-to-lymphocyte ratio (NLR), derived NLR ratio (d-NLR) [neutrophil count divided by the result of WBC count minus neutrophil count], and platelet-to-lymphocyte ratio, can be the expression of the inflammatory storm (Yang et al., 2020). Research has shown that peripheral proinflammatory CD4 and cytotoxic granules CD8 T cells reduce in severe patients, suggesting antiviral immune responses and overactivation of T cells (Xu et al., 2020). However, the reduced T-cell numbers is negatively correlated with IL-6 and TNF-α (Diao et al., 2020). Additionally, the obviously increased levels of senescence markers (PD-1, Tim-3, CTLA-4 and TIGIT) are important signs of severe COVID-19 (Zheng H.-Y. et al., 2020). Moreover, lymphocytes may also become depleted due to the expression of pro-inflammatory cytokines by (not infected) innate immune who are recruited to the lungs and trigger hyper-inflammation, seen during the development of a "cytokine storm" (Cron and Chatham, 2020).

Study shows that excessive inflammation will make patients more prone to endothelial dysfunction and thrombotic diseases in the blood circulation (Bikdeli et al., 2020). Microvascular thrombosis in the pulmonary circulation can lead to an increased dead space. Early pulmonary fibrosis following the disease has been reported from Italy, which could be deficient oxygen-related or excessive inflammation-related. Pulmonary thrombosis has been associated with wedge-shaped infarcts in the lungs on imaging, without the evidence of deep vein thrombosis (Li et al., 2020). Virus also can induce cell death, including necrosis or pyroptosis, proinflammatory cytokine overexpression (uninfected) immune cell recruitment and activation. And COVID-19 may also (partially) escape these mechanisms through the induction of T cell apoptosis (Yi et al., 2020). Pneumonia can lead to respiratory dysfunction and hypoxaemia, which can also bring about cardiomyocyte injury (Zheng Y.-Y. et al., 2020).

TREATMENT STRATEGIES

With the rapid increase in the global prevalence and mortality of COVID-19, there is an urgent need to develop targeted therapies. Specific pharmacological treatment for COVID-19 is not currently available. Based on the previously therapeutic experience of SARS and MERS, the potential treatments for COVID-19 include antiviral drugs (anti-HIV drugs, anti-HBV and anti-HCV drugs), plasma transfusion, vaccines and so on (Li and Clercq, 2020). However, now there is no specific antiviral treatment recommended and the effective vaccines are still on the road. Therefore, the clinical efficacy of above drugs requires strictly clinical trials to prove.

In these patients experiencing worsening inflammatory-induced lung injury, there is a decrease in oxygen saturation (<93%). This seems to be the crucial phase of the disease, from this point onwards, there may be a rapid deterioration of respiratory functions. The scenario is truly incredible because, for patients who are paucisymptomatic and slightly hypoxic, the first therapeutic approach is oxygen therapy. A significant number of patients with pneumonia require passive oxygen therapy. Non-invasive ventilation and high-flow nasal oxygen therapy can be applied in mild and moderate non-hypercapnia cases. A lung-saving ventilation strategy must be implemented in acute respiratory distress syndrome and mechanically ventilated

patients. Although this strategy is effective, the worsening of respiratory failure may occur in some patients. With the drive preserved, the next step, according to logic, is the non-invasive ventilation (NIV). This therapy has a rapid success by increasing the PaO_2/FiO_2 (Partial arterial O_2 pressure, PaO_2; Fraction of inspiration O_2, FiO_2). In some patients, however, there is a sudden, unexpected worsening of clinical conditions. Patients collapse under the operator's eyes and require rapid intubation and invasive mechanical ventilation. However, after 24–48 h the patient can have a rapid improvement with an increase in P/F. Operators are therefore tempted to proceed with weaning. But very often, after an initial success, there is a new worsening of respiratory conditions, such as to require a new invasive therapy. Therefore, mechanical ventilation has also been suggested for 1–2 weeks.

The treatment is symptomatic, and oxygen therapy represents the first step for addressing respiratory impairment. Non-invasive (NIV) and invasive mechanical ventilation (IMV) may be necessary in cases of respiratory failure refractory to oxygen therapy. Another clinical trial aiming to test with the use of hyperbaric oxygen is estimated to start on April 25, 2020. The anti-inflammatory effects, which include decreased expression of IL-1β, IL-6 and TNF-α (Aricigil et al., 2018), could be beneficial to mitigate ARDS associated with COVID-19 and fibrosis development.

Although the prospective of counteracting cytokine storm is compelling, a major limitation relies on the limited understanding of the immune signaling pathways triggered by COVID-19 infection. The altered identification of signaling pathways during viral infections may help to unravel the most relevant molecular cascades implicated in biological processes mediating viral infections and to unveil key molecules that may be targeted. Thus, given the key role of the immune system in COVID-19, a deeper understanding of the mechanism behind the immune dysregulation might give us clues for the clinical management of the severe cases and for preventing the transition from mild to severe stages.

COVID-19 has been related to hypoxia and inflammation leading to endothelial dysfunction, increased permeability, and aberrant coagulation in small and large vessels, which are the early hallmarks of organ damage in patients. Moreover, thrombotic complications are a relevant cause of death in COVID-19 patients, and the interaction of SARS-CoV-2 with ACE2 possibly implies alterations of angiotensin II plasma levels. Therefore, the vascular system is increasingly being addressed as a major therapeutic target for defeating COVID-19 (Escher et al., 2020; Giannis et al., 2020).

POSSIBLE REHABILITATION STRATEGY-INTERMITTENT HYPOXIC PRECONDITIONING

In view of the above-mentioned pathological of COVID-19, a non-drug alternative therapy- intermittent hypoxic preconditioning (IHP), via increasing blood oxygen delivery and promoting tissue oxygenation response to improve severe dyspnea, may act as a significant effect on the prognosis and rehabilitation treatment of COVID-19. IHP is a method by which subjects receive exposure to short bouts (1–6 min) of moderate hypoxia (9–12% O_2), interspersed with the brief periods of normal air (Serebrovskaya, 2002). Firstly, IHP is expected to inhibit the overactivation of immune system, control acute pulmonary inflammation and improve the endogenous reparation for injured tissue, which will become a new exploration in the rehabilitation of stable COVID-19 cases. Secondly, IHP will be an ideal treatment measure of novel coronavirus infection-related acute respiratory distress syndrome. More importantly, IHP has the advantages of high safety, easy-to-accomplish and no side effects.

IHP can trigger the body's endogenous protective mechanism to make the tissues and cells highly resistant to hypoxia, to relax airways and blood vessels and to improve myocardial contractility. Moreover, it also can increase cardiopulmonary endurance, reduce the area of heart infarction, add blood vessel density and coordinate blood oxygen delivery. Therefore, it can have a strong defense and protective effect on the subsequent longer or more severe ischemia and hypoxia (Neubauer, 2001). Besides, it's also effective on improving respiratory muscle function and relieving dyspnea, alleviating disease-related anxiety and depression, and enhancing skeletal muscle function of upper and lower limbs (Ponsot et al., 2006; Bao et al., 2020). Studies have confirmed that IHP can improve the balance of the rat's immune system by activating the defenses of cells against oxidative stress and inflammation (Shi et al., 2015), and IHP is also an effective measure to reduce the damage of the cardiopulmonary system (Ding et al., 2004)

Collectively, combined with the many beneficial functions of IHP, although there is no exact method for the treatment or prevention of COVID-19, we propose that IHP can improve immunity, accelerate the recovery of patients, and reduce the occurrence of positive rejuvenation after discharge. Here, we will explore the potential mechanisms of action of a certain model of IHP in the cardiopulmonary system damage, vascular endothelial dysfunction and hemodynamics of COVID-19, and explored possible rehabilitation options for the prognosis of patients, with a view to providing a novel and effective rehabilitation method for the prognosis of patients, and better help the patients to recover and return to society more promptly and safely (**Figure 1**).

Possibility of Applying IHP to the Rehabilitation of COVID-19

Hypoxia is a "double-edged sword", mainly depending on a variety of the concentration, frequency, and duration of hypoxia exposure, can cause harm or benefit to the human body. Modest hypoxia (9–16% inspired O_2) and low cycle numbers (3–15 episodes per day) most often lead to beneficial effects, while severe hypoxia (2–8% inspired O_2) and more episodes per day (48 episodes/day) elicit progressively greater pathology (Navarrete-Opazo and Mitchell, 2014). After the appropriate intermittent hypoxic exposure, tissues and organs can form a complex and active defense mechanism against the

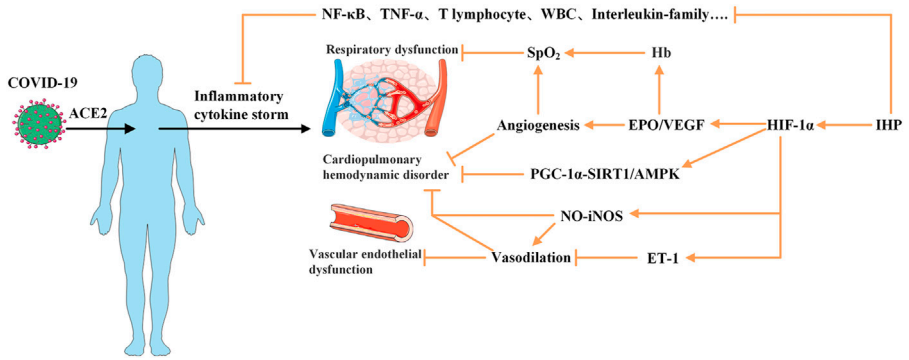

FIGURE 1 | Plausible mechanisms of intermittent hypoxia preconditioning applied for COVID-19 rehabilitation. COVID-19 virus enters the body and combines with ACE2 to produce an excessive immune reaction and to trigger "inflammatory cytokine storm," which may initiate the pathogenesis of SARS, cardiopulmonary hemodynamic disorder and vascular endothelial dysfunction. Application of IHP on patients may provide inhibitory effect on the levels of various proinflammatory factors and activate HIF-1 to promote target genes to augment EPO/VEGF expression which lead to stimulate production of red blood cell and Hb and angiogenesis to increase capacity to carry oxygen. Furthermore, activated HIF-1 may mobilize PGC-1-SIRT1/AMPK pathway and NO availability and inhibit ET-1. These factors can help reverse the virus induced cardiopulmonary hemodynamic disorder and endothelial dysfunction. ACE2, Angiotensin-converting enzyme 2; AMPK, 5'-AMP activated protein kinase; EPO, erythropoietin; ET, endothelin; Hb, hemoglobin; HIF, hypoxia-inducible factors; PGC, γ-coactivator; NF-B, nuclear factor-k-gene binding; SARS, server acute respiratory syndrome; SIRT, Sirtuin; TNF-α, Tumor Necrosis Factor-α; VEGF, vascular endothelial growth factor; WBC, white blood cell. symbol indicates an activation; symbol indicates an inhibition.

same or similar hypoxic environment, and develop resistance and tolerance, thereby to prevent or reduce the damage that it may cause (Semenza, 1999; Verges et al., 2015). This is because that IHP has the function of stimulating the body adaptive physiological changes in different modes of brief repeated exposure in a (10–16% inspired O_2) hypoxic environment. In the last decade, many clinical trials have described the powerful protective effects of IHP on the respiratory diseases. Rozova et al. confirmed that IHP (15 min 12% inspired O_2 + 15 min 21% inspired O_2/cycle, 5 cycle/d for 4 weeks) could relieve the structural damage of the lung air-blood barrier, and promote a specific type of mitosis in lung and heart tissues, then normalize the ultrastructure of lung and heart (Rozova and Mankovska, 2012). Burtscher et al. believe that the protection of IHP on chronic obstructive pulmonary disease (COPD) and coronary heart disease (CAD) benefits from its positive effects of increasing total hemoglobin, enhancing lung diffusion and lung ventilation (Burtscher et al., 2010). Vogtel et al. found that the 18 COPD patients' exercise endurance enhances, and the functions of forced expiratory volume in 1 s (FEV1), forced vital capacity (FVC) and carbon monoxide diffusing capacity (DLCO) significantly increase, when performing IHP (12–15% inspired O_2 for 15 times within 3 weeks) (Vogtel and Michels, 2010). Even if IHP is used after brain and spinal cord injury, it can also limit the further development of the disease and promote the remodeling and recovery of tissue structure and function (Baillieul et al., 2017). Many of the previous studies have suggested that IHP has a significant therapeutic effect on COPD and various lung pathological changes. In addition, studies have confirmed that IHP can not only activate hypoxia-inducible factors-1α (HIF-1α) and 5′-AMP activated protein kinase (AMPK)/SIRTl (Sirtuin1)/γ-coactivator 1α (PGC-1α) signaling cascade, but also can reduce the mRNA and protein levels of ACE2, which can significantly inhibit the number of receptors for SARS-CoV-2 virus to enter host cells, thereby to improve endothelial dysfunction, promote cardiovascular hemodynamics, inhibit excessive inflammation and immune response. These changes will be provide the benefit for the recovery from heart and lung injury and dyspnea (Zhang et al., 2009; Singh et al., 2013; Yu et al., 2018 ; Gangwar et al., 2020), and the inhibitory effect of HIF-1α on ACE2 provides a novel idea for using IHP to treat COVID-19.

IHP can Enhance the Cardiopulmonary Function

It has been showed that ACE2 plays an important role in the immune systems, and SARS-CoV-2 infects host cells through ACE2 receptors causing COVID-19 (Li et al., 2003; Zhou P. et al., 2020). The ACE2 mRNA and protein expression levels of patients with viral infections and complications of cardiopulmonary injury are significantly higher than those of uncomplicated patients, so they have a higher risk of heart disease and critical illness (Chen et al., 2020). Moreover, ACE2 is highly expressed in the heart and kidneys as well as on the lung alveolar epithelial cells, which are the principal target cells for SARS-CoV-2 and the site of dominant injury (Walls et al., 2020). It can be concluded that ACE2-related signaling pathway may play a crucial role in cardiopulmonary injury. It has been fully proven that IHP can reduce and/or reverse cardiovascular damage and cardiopulmonary dysfunction in the way of improving cardiovascular endothelial dysfunction and hemodynamics. This effect usually depends on the HIF-1 mediated downstream signaling pathway. HIF-1 consists of a constitutively expressed subunit ß and an oxygen-regulated subunit α (or its paralogs 2α and 3α). The stability and activity of the α subunit of are regulated by its post-translational modifications such as hydroxylation,

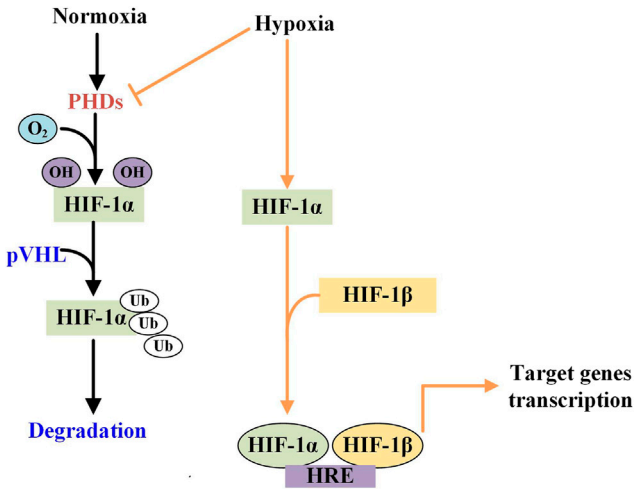

FIGURE 2 | The different effects of normoxia and hypoxiaon the HIF-1α activity. Under normoxic condition, HIF-1 is hydroxylated by prolyl hydorylase (PHD) to attach with von HippelLindau (pVHL) protein and then is degraded. While in hypoxic condition, PHD is inhibited and HIF is phosphorylated which then is translocated and become dimerises with HIF-1β in the nucleus. The heterodimer binds to the hypoxia response element (HRE) to activate the target genes transcription.

ubiquitination, acetylation, and phosphorylation. During normoxia, hydroxylation of two proline residues and acetylation of a lysine residue at the oxygen-dependent degradation domain of HIF-1α trigger its association with pVHL, thereby reducing its stability and leading to HIF-1α degradation (Kaelin and Ratcliffe, 2008). HIF-1 exists in all tissues, with highly sensitive to tissue oxygen tension (Serocki et al., 2018). In hypoxia, the αsubunit becomes stable and will be translocated to the nucleus where HIF-α heterodimerizes with HIF-1β. Then the HIF1α/β complex binds to the promoter regions of target genes containing hypoxia-responsive elements (HRE) and activates a variety of hypoxic adaptive target genes transcription (**Figure 2**).

IHP-induced hypoxia-reoxygenation cycle can activate HIF-1, thereby promoting the expression of cytoprotective proteins, such as nitric oxide synthase (NOS), erythropoietin (EPO) and vascular endothelial growth factor (VEGF) (Singh et al., 2013), and then up-regulate the synthesis of NO, promote the normalization of microvessels and improve the vasodilation function (Korkushko et al., 2010). At the same time, it can increase the number of red blood cells and improve the vascular microcirculation (Connolly et al., 1989; Krantz, 1991). Some researchers believe that the efficacy of hypoxic adaptation will decrease as patients aging (Levine et al., 1997; Korkushko et al., 2009). However, Korkushko et al. reported that IHP is also well tolerated and safe for elderly patients (Korkushko et al., 2010).

IHP can Improve the Vascular Endothelial Function

Endothelial dysfunction is a common feature of cell damage caused by virus infection, which will lead to microvascular dysfunction, in turn, inducing vasospasm or abnormal vasocontraction and thrombosis of multiple major arteries (Steinberg et al., 2012; Chen et al., 2020). Vascular endothelial cells play key roles in regulating vascular tension and peripheral resistance by synthesizing vascular "dilators" (NO etc.) and vasoconstrictors (endothelin-1, ET-1, etc.). The endothelial dysfunction is caused by the unbalanced expression of vascular endothelial factor (Virdis et al., 2011; Lytsy et al., 2013). Gel'tser et al. found that the severity of the disease was positively correlated with vascular endothelial dysfunction in extra-hospital pneumonia, which manifested as insufficient vasodilation or even contraction, and then increased the risk of cardiac hypoperfusion (Gel'tser and Brodskaia, 2005). Aguilar et al. found that applying the treatment of IHP (11.7% inspired O_2 + 21% inspired O_2, 4 cycles/d for 4˚days) could activate the antioxidant defense mechanisms to the improve the cardiovascular endothelial dysfunction of adult Wistar rats (Aguilar et al., 2018). In addition, study has shown that activation of HIF-1α can inhibit the expression of ET-1 in pulmonary artery smooth muscle cells and reduce pulmonary vasoconstriction (C. C. Wang et al., 2018). Meanwhile, IHP (4–8 h/d, 10%–12% inspired O_2) can promote the expression of inducible nitric oxide synthase (iNOS) and increase cardiac NO synthesis ability (Coulet et al., 2003; Robinson, et al., 2011). As hypoxia itself can promote the release of NO and other vasodilator factors, it meets the myocardial demand for O_2 better, which can lead local arterioles to dilate (Park et al., 2015). Lyamina et al. proved that IHP (3 min 10% inspired O_2+3 min 21% inspired O_2 for 4–10 cycles) was one of the most effective ways to stimulate the synthesis of endogenous NO, in which the antihypertensive effect was highly correlated to the increase of NO expression level (Lyamina et al., 2011). In addition, Mukharliamov et al. found that IHP (10 cycles/d for 5 min 10–14% inspired O_2 + 5 min 21% inspired O_2) combined with antihypertensive drugs significantly reduced the systolic and diastolic blood pressure of hypertensive (Mukharliamov et al., 2006). Furthermore, IHP has been proved not to cause hypertensive reaction in healthy subjects (X. Liu et al., 2017). Faulhaber et al. found that the arterial blood pressure of mild COPD was not be affected during IHP intervention (Faulhaber et al., 2015). Based on these, we hypothesize that IHP can resume the balance between the expression of NO and ET-1 in COVID-19, so as to improve the dysfunction of the cardiopulmonary vascular endothelium and accelerate the recovery.

IHP can Improve the Hemodynamics via Activating HIF-1α/EPO/VEGF Signals

The evaluation of hemodynamics is a method to detect whether the blood flow maintains the optimal oxygen delivery, to ensure good oxygen tissue perfusion, and the hemodynamics of COVID-19 may be changed for viral infection. After evaluating the erythrocyte sedimentation rate and high-sensitivity C-reactive protein (hs-CRP) level of 27 COVID-19 cases, Zhou et al. found that the erythrocyte sedimentation rate increased in 18 cases, and the hs-CRP expression added in all 27 cases, which are signs of acute pneumonia or autoimmune system damage (Zhou S. et al., 2020). Some studies also have shown that COVID-19 is characterized by increasing pulmonary capillary pressure,

which induces an increase in alveolar-capillary permeability, accompanied by the lung compliance decrease as well as the dead space adding, and even induces cardiopulmonary and other multiple organs dysfunction, ultimately resulting in death.

EPO and VEGF are glycoprotein growth factors regulated by HIF-1, and both play a variety of positive roles in coordinating hemodynamics (Krantz, 1991; Dale et al., 2014). EPO is one of the earliest discovered HIF-1α-regulated target proteins. It is mainly produced in the kidney and used to increase the number of red blood cells. The expression and secretion are closely related to tissue oxygen (Fliser and Haller, 2007). Studies have shown that IHP (6 min 10% inspired O_2+6 min 21% inspired O_2, 10 cycles) can activate HIF-1α to up-regulate the EPO activity to provide more O_2 supply for the myocardia, which in turn stimulates red blood cell production, enhances hematopoietic function and the oxygen-transport capacity (Jelkmann, 1992; Bin-Jaliah et al., 2010). Törpel et al. proved that IHP (3 h, 13.5% inspired O_2) could increase the central and peripheral EPO levels, and under the same hypoxia intensity, the EPO expression of young people is significantly higher than that of the elders. In addition to promoting red blood cell production, EPO also has other physiological functions (Törpel et al., 2019). Costa et al. treated rats with hypobaric hypoxia and found that the EPO activity was increase induced by HIF-1α. Then, it upregulated the key transcription factor Nrf2 (NF-E2-relatedfactor 2) to exert cellular antioxidant and anti-inflammatory effects, which can promote the synthesis of antioxidant enzymes and reduce the excitotoxicity of nuclear factor kappa-B (NF-κB) induced damage in rat brain and heart (Costa et al., 2013; Mallet et al., 2018). Animal model of myocardial infarction shows that EPO can reduce the infarct size and improve left ventricular function. The mechanism is mainly through the activation of phosphoinositide-3-kinase (PI3K)/protein kinase B (Akt) signal pathways to inhibit cardiomyocyte apoptosis, and mobilize endothelial progenitor cells as well as inhibiting inflammatory cell migration (Roubille et al., 2013).

VEGF, called vascular permeability factor (VPF), the gene expression can be regulated by HIF-1α to increase angiogenesis, improve hemodynamics, and increase the supply of energy substances. Paula et al. found that activating HIF-1α helped to up-regulate the VEGF gene expression for increasing the capillary density (Rodriguez-Miguelez et al., 2015). Senger et al. expounded that intraperitoneal injection of the purified VEGF could increase the vascular permeability of the peritoneal wall, diaphragm, and mesentery *in vitro* (Senger et al., 1983). Connolly et al. found that VEGF could promote the growth of new blood vessels, when injected into the healed rabbit bone graft or rat cornea (Connolly et al., 1989). Dao et al. confirmed that VEGF with exogenous nasal delivery could promote compensatory lung growth in mice, which is manifested by the significant increase of lung capacity and alveolar count (Dao et al., 2018). Fan et al. found that the organism could mediate HIF-1α/VEGF to upregulate the anti-oxidative stress activity during lung injury, which in turn activates the self-protection mechanism of angiogenesis and angioplasty (Fan et al., 2019). In addition, VEGF, cooperated with EPO, can promote angiogenesis, accelerate blood flow, and facilitate the transportation of nutrients and the removal of metabolic waste (Orth et al., 2019). Therefore, we speculate that IHP via the character of activating HIF-1α to upregulate the EPO and VEGF, can reduce the pressure of the vascular circulatory system, increase the efficiency of blood oxygen utilization, and improve the cardiopulmonary circulatory function. As a result, the COVID-19 hemodynamics will be significantly improved and the patient prognostic recovery will be promoted.

IHP can Alleviate the Dyspnea via Rectifying Inflammation and Lipid Metabolism Disorders

Evidence suggests that the levels of inflammatory markers, such as IL-6, hs-CRP, immune cells, in the fifth grade level of dyspnea is far higher than the first and second grade despite that the inflammation is not completely related to dyspnea (Garrod et al., 2007; Ryan et al., 2016). In addition, the disorder of lipid metabolism may be the other important factor for dyspnea (Gualdoni et al., 2018). Studies have confirmed that virus infection will interfere with the lipid synthesis and the related signal transduction in host cells. In this process, the virus envelopes and receptors synthesize faster to for completing the virus replication, in consequence, a series of pathological changes occurs in the cardiopulmonary and other peripheral systems (Murillo et al., 2015; Abu-Farha et al., 2020).

In addition to directly activating the HIF-1α signaling cascade, evidences show that IHP can activate the AMPK/SIRT signaling cascade, thereby activating its downstream target PGC1-α, and promoting the dephosphorylation of NF-κB, which is then play a potential protective role in the metabolization and the immune response (Yu et al., 2018; Gangwar et al., 2020). As one of the nicotinamide adenine dinucleotide (NAD+) dependent deacetylases, SIRT1 is a key factor, which is crucial in the regulation of metabolic transcription (H. Yang et al., 2015). Gao et al. confirmed that the increased transcription and expression of SIRT1 in T lymphocytes could better maintain the tolerance of peripheral T lymphocytes, thereby regulating the immune response (Gao et al., 2012). Considering of the close relationship between inflammation, lipid metabolism disorders and dyspnea, IHP may be a potential treatment for improving dyspnea and alleviating tissue hypoxia. For example, in the terms of ameliorating the dyspnea, Berezovskyi et al. performed IHP (1-2w, 3cycles/d, 15 min 12% inspired O_2+10 min 21% inspired O_2/cycle) on 55 patients (6–17 years old) with bronchospasm. The results suggest that the bronchial obstruction significantly improves along with the vital capacity enhances and breath-hold time prolongs (Berezovskyi et al., 2015). Serebrovska et al. confirmed that IHP (20 min 12% inspired O_2+5 min 21% inspired O_2/cycle, four cycle/session, 5 sessions/w) has little adverse effect on the SpO_2 of diabetes (Serebrovska T. V. et al., 2019). They also found that the IHP (3 times/d, 15 d, 6–7 min 11% inspired O_2) significantly increase the alveolar ventilation and maximum lung ventilation of healthy subjects in the sitting and supine positions, and also significantly improve hypoxic ventilation response sensitivity in hyperpnea subjects (Serebrovskaya et al., 1999).

IHP can Boost Antioxidant and Antiinflammation Capacity of COVID-19

Gangwar et al. found that the healthy subjects may have a slight inflammatory response in the early stage of IHP (4 h/d, 12%

inspired O_2) implementation. However, the levels of ROS in macrophages tend to decrease, in parallel, the secretion of the antioxidant enzyme enhances, such as glutathione at the 7th-day-IHP treatment, which indicates that the redox homeostasis mechanism is activated to inhibit oxidative stress and acute inflammatory signal response (Gangwar et al., 2020). Rudyk et al. declared that IHP could reduce the accumulation of ROS and inhibit cell apoptosis by enhancing the mitochondria resistance to the open of mitochondrial permeability transition pore (mPTP) in the old rats myocardium heart (Rudyk et al., 2004). Meanwhile, IHP can exert antioxidant protection by inhibiting the excessive formation of reactive metabolites, such as superoxide and peroxide nitrate, or by weakening the activity of stress-activated protein kinase p38 (Ryou et al., 2017). In addition to directly influencing the oxidative stress and inflammatory injury, the IHP likely indirectly reduced these damage via activating the HIF-1α-mediated downstream signals. Tian et al. manifested that the IHP (3 w, 6 h/d 11.1% inspired O_2 hypoxic exposure) could promote the expression of HIF-1α and the antioxidant ability of kidney to defense the tissue injury in diabetic rats (Tian et al., 2016). This effect may be attributed to the activation of the HIF-1α/VEGF/intranuclear nuclear factor (erythroid-derived 2, Nrf2) signaling pathway, in which the antioxidant enzymes activity enhances to reduce urine protein, inflammatory cell infiltration and glomerular interstitial damage (Chang et al., 2019). Based on the previous studies, we speculate that IHP can improve the inflammation and oxidative stress of COVID-19 by stimulating their own anti-oxidation mechanism.

The effect of hypoxia on the innate immune system and host defenses is controversial. Study has suggested that long-term exposure to hypoxic condition may be harmful to the cellular immune function and increase the risk of respiratory infections at high altitude (Walsh and Oliver, 2016). Wang et al. found that IHP (30 min/d 15% inspired O_2, 5 d/w, 4 w) could delay the aging of T lymphocyte subsets in the blood, reduce oxidative stress and the production of pro-inflammatory cytokines, and then to the greatest extent to improve immune dysfunction (Wang et al., 2011). IHP can activate the SIRT1 to promote the deacetylation of NF-κB and decrease its activity, thereby reducing the TNF-α and 1L-1β expression to enhance the adaptive immune response (Schug et al., 2010).

THE POSSIBLE APPLICATION OF IHP IN THE PROGNOSIS AND REHABILITATION OF COVID-19

Choose the Appropriate Timing to Apply IHP

All rehabilitation should be carried out under the premise of safety. Patient's heart rate, arterial oxygen saturation (SaO_2) and other indicators can be used to determine whether the patient has passed the acute phase. Due to the lack of IHP clinical interventions for COVID-19, the specific cut-in time remains to be further studied. In case a patient shows peripheral capillary oxygen saturation (SpO_2) < 88% or develops symptoms, such as cardiac arrhythmia, palpitations, sweating, chest tightness, and shortness of breath, which are deemed unsuitable for rehabilitation by the clinician, then the rehabilitation program should be terminated immediately. For mild and moderate cases, rehabilitation interventions should be introduced as early as possible. In contrast, for severe and critical cases, life-saving measures should be prioritized when the patient's condition is unstable or the disease is still progressing. In such cases, pulmonary rehabilitation interventions should be introduced only when the patient's condition has stabilized. In addition, in view of safety and human resources, movement of severely or critically ill patients should be limited to their bed or bedside. Once discharged, patients should continue individualized rehabilitation under the premise of strengthening protection and prevention against other infectious diseases such as cold. In addition, the following contraindications should be noted during IHP intervention (Serebrovskaya and Xi, 2016): ① acute phase of physical disease (myocardial infarction within the last three months, unstable angina pectoris, acute ischemic stroke within six months); ② with fever and/or acute infectious diseases and conditions that require enhanced traditional therapy; ③ compensated chronic renal failure, requiring hemodialysis; ④ three-stage hypertension, frequent hypertension; ⑤ severe peripheral blood flow disorder; ⑥ hypercapnic patient; ⑦ congenital abnormalities of the heart and great blood vessels; ⑧ thrombosis and embolism complications; ⑨ primary and secondary polycythemia; ⑩ personal intolerance to hypoxia; ⑪ mental or mental disorders.

Choose the Appropriate IHP Therapeutic Options

According to the recent research on the cardiovascular protective function of IHP, the use of IHP to improve the prognosis of COVID-19 is traceable. Patients with chronic pulmonary diseases, when exercising, as the interval for red blood cells to pass through the alveolar capillaries is shortened, the ventilation flow rate disorder increases, oxygen intake and blood oxygen saturation decreases. IHP therapy can well make up for the limitations of exercise therapy, not only can ensure the safety and effectiveness of the application, but also be more convenient for home rehabilitation. At the same time, even if the patients with mobility impairments can get the same or even better rehabilitation effect than exercise. Currently, however, there is no standard IHP treatment plan clinically developed. And in recent years, IHP intervention experiments and clinical studies also have large differences in its related parameter settings, such as the range of hypoxic concentration (from 12 to 18%), the duration of hypoxia (ranging from 15 s to 12 h), the number of cycles per day (ranging from 3 cycles to 25 cycles) etc (Serebrovskaya and Xi, 2016). Therefore, it is so important about the strict control of IHP intervention parameters. It also can set parameters according to the hypoxic sensitivity and the development of its disease, such as using the heart rate changes during the steady decline of SaO_2 to predict the individual's adaptation to hypoxia and prognosis, and select the best intervention plan.

Based on the above clinical research evidence, we set an IHP plan for the prognosis and rehabilitation of COVID-19: 3–5 min

hypoxia (10–16% inspired O_2) + 5 min normoxia (21% inspired O_2) as one cycle, 6–10 cycles per day, 3–5 times a week for a total of 8 weeks. Before the formal intervention, the patient should undergo hypoxic preconditioning training to familiarize himself with the treatment equipment and procedures, and at the same time checking the tolerance of the patient and adjusting the appropriate hypoxia concentration. During the treatment process, real-time monitoring of the patient's heart rate, blood pressure, electrocardiogram, peripheral blood oxygen saturation, lung ventilation function and other physiological indicators. Moreover, as subjects need to inhale low-oxygen gas through a breathing mask, considering the high infectivity of COVID-19, after a patient finished using the device, the disposable face mask should be replaced immediately, and the ventilation pipe and periphery of the device should be disinfected to avoid cross-infection. At the same time, the treatment clinic where the patient is located should be strictly disinfected. In addition, the following principles should be followed: patients should be evaluated comprehensively before starting the rehabilitation program by clinical experts. Evaluation and monitoring should be conducted throughout the IHP rehabilitation program. As COVID-19 patients having chronic pulmonary diseases often have excessive airway secretions, should pay attention to facilitate sputum excretion and reduce the exhaustion due to coughing. Meanwhile, more clinical research should be conducted to prove the safety and efficacy of IHP therapy among COVID-19 rehabilitated phase patients, and explore individualized treatment program.

SUMMARY AND PERSPECTIVE

Currently, evidence on the prognosis and rehabilitation of COVID-19 patients is insufficient, especially for elderly patients whose disease is complicated by other pathology or comorbidity. It remains unclear whether the impairment of multiple systemic functions is completely reversible or if the long-term existence of the virus can cause residual physical and mental dysfunction in these patients. Nonetheless, we believe that IHP not only has beneficial effect on cardiovascular protection and cardiorespiratory fitness, but also can applied as a potential protector against inflammatory stress. Timely implementing IHP intervention to restore the cardiopulmonary function of COVID-19 and to recover the autoimmunity is very important. IHP intervention program for the prognosis and rehabilitation of COVID-19 should be based on the existing condition and actual vital signs of the patients (such as blood cell parameters, blood oxygen saturation, heart rate, blood pressure, etc.) in consideration of all other underlying disorders (such as hypertension, diabetes, COPD, etc.) to set different intervention parameters to target the biological mechanism mediated by HIF-1α to activate downstream signal targets (iNOS, EPO, VEGF), and at the same time activate AMPK/SIRT1 signaling cascade, and then reduce the tissue and organ damage of patients, and improve the body's tolerance and resistance to ischemia and hypoxia. It is possible to prevent disease or reduce the virus damage if we may take IHP before attach of virus, which is critical to maintain strong immune capacity, and reduce the prevalence of various chronic diseases. The most appropriate timing and program, the efficacy and safety of IHP for rehabilitation interventions require large-scale clinical trials and further confirmation.

AUTHOR CONTRIBUTIONS

MC, XC, JS, and RY wrote the primary draft and drew the graph. XS, LC, and LW proposed the idea and revised the final version. QG, XB, and PX searched and reviewed the literatures. All authors have accepted responsibility for the entire content of this manuscript and approved its submission.

FUNDING

This work was sponsored by Scientific Research Foundation of SUMHS (SSF-21-03-008) and the grant of the funding of Youth Fund Project of Research Planning Foundation on Humanities and Social Sciences of the Ministry of Education (20YJCZH001).

REFERENCES

Abu-Farha, M., Thanaraj, T. A., Qaddoumi, M. G., Hashem, A., Abubaker, J., and Al-Mulla, F. (2020). The role of lipid metabolism in COVID-19 virus infection and as a drug target. *Ijms* 21 (10), 3544. doi:10.3390/ijms21103544

Aguilar, M., González-Candia, A., Rodríguez, J., Carrasco-Pozo, C., Cañas, D., García-Herrera, C., et al. (2018). Mechanisms of cardiovascular protection associated with intermittent hypobaric hypoxia exposure in a rat model: role of oxidative stress. *Ijms* 19 (2), 366. doi:10.3390/ijms19020366

Arias-Reyes, C., Zubieta-DeUrioste, N., Poma-Machicao, L., Aliaga-Raduan, F., Carvajal-Rodriguez, F., Dutschmann, M., et al. (2020). Does the pathogenesis of SARS-CoV-2 virus decrease at high-altitude?. *Respir. Physiol. Neurobiol.* 277, 103443. doi:10.1016/j.resp.2020.103443

Aricigil, M., Dundar, M. A., Yucel, A., Arbag, H., Arslan, A., Aktan, M., et al. (2018). Anti-inflammatory effects of hyperbaric oxygen on irradiated laryngeal tissues. *Braz. J. Otorhinolaryngol.* 84 (2), 206–211. doi:10.1016/j.bjorl.2017.02.001

Baillieul, S., Chacaroun, S., Doutreleau, S., Detante, O., Pépin, J., and Verges, S. (2017). Hypoxic conditioning and the central nervous system: a new therapeutic opportunity for brain and spinal cord injuries?. *Exp. Biol. Med. (Maywood)* 242 (11), 1198–1206. doi:10.1177/1535370217712691

Baldi, E., Sechi, G. M., Mare, C., Canevari, F., Brancaglione, A., Primi, R., et al. (2020). Out-of-Hospital cardiac arrest during the covid-19 outbreak in Italy. *N. Engl. J. Med.* 383 (5), 496–498. doi:10.1056/NEJMc2010418

Bao, X., Liu, H., Liu, H. Y., Long, Y., Tan, J. W., and Zhu, Z. M. (2020). The effect of intermittent hypoxia training on migraine: a randomized controlled trial. *Am. J. Transl Res.* 12 (7), 4059–4065. Retrieved from Available at: http://www.ncbi.nlm.nih.gov/pubmed/32774759.

Barker-Davies, R. M., O'Sullivan, O., Senaratne, K. P. P., Baker, P., Cranley, M., Dharm-Datta, S., et al. (2020). The Stanford Hall consensus statement for post-COVID-19 rehabilitation. *Br. J. Sports Med.* 54 (16), 949–959. doi:10.1136/bjsports-2020-102596

Berezovskyi, V. A., Lisukha, L. M., Lisukha, L. M., Stepanova, Y. I., and Kolpacov, I. Y. (2015). The influence of the normobaric hypoxia for the breathihg indexes of

the children lived in radioactive contaminated territories. *Fiziol Zh* 61 (3), 35–43. doi:10.15407/fz61.03.035

Bikdeli, B., Madhavan, M. V., Jimenez, D., Chuich, T., Dreyfus, I., Driggin, E., et al. (2020). COVID-19 and thrombotic or thromboembolic disease: implications for prevention, antithrombotic therapy, and follow-up. *J. Am. Coll. Cardiol.* 75 (23), 2950–2973. doi:10.1016/j.jacc.2020.04.031

Bin-Jaliah, I., Ammar, H. I., Mikhailidis, D. P., Dallak, M. A., Al-Hashem, F. H., Haidara, M. A., et al. (2010). Cardiac adaptive responses after hypoxia in an experimental model. *Angiology* 61 (2), 145–156. doi:10.1177/0003319709352486

Borges do Nascimento, I. J., Cacic, N., Abdulazeem, H. M., von Groote, T. C., Jayarajah, U., Weerasekara, I., et al. (2020). Novel coronavirus infection (COVID-19) in humans: a scoping review and meta-analysis. *Jcm* 9 (4), 941. doi:10.3390/jcm9040941

Burtscher, M., Gatterer, H., Szubski, C., Pierantozzi, E., and Faulhaber, M. (2010). Effects of interval hypoxia on exercise tolerance: special focus on patients with CAD or COPD. *Sleep Breath* 14 (3), 209–220. doi:10.1007/s11325-009-0289-8

Chang, H.-H., Hsu, S.-P., and Chien, C.-T. (2019). Intrarenal transplantation of hypoxic preconditioned mesenchymal stem cells improves glomerulonephritis through anti-oxidation, anti-ER stress, anti-inflammation, anti-apoptosis, and anti-autophagy. *Antioxidants* 9 (1), 2. doi:10.3390/antiox9010002

Chen, L., Li, X., Chen, M., Feng, Y., and Xiong, C. (2020). The ACE2 expression in human heart indicates new potential mechanism of heart injury among patients infected with SARS-CoV-2. *Cardiovasc. Res.* 116 (6), 1097–1100. doi:10.1093/cvr/cvaa078

Connolly, D. T., Heuvelman, D. M., Nelson, R., Olander, J. V., Eppley, B. L., Delfino, J. J., et al. (1989). Tumor vascular permeability factor stimulates endothelial cell growth and angiogenesis. *J. Clin. Invest.* 84 (5), 1470–1478. doi:10.1172/JCI114322

Conti, P., Ronconi, G., Caraffa, A., Gallenga, C. E., Ross, R., Frydas, I., et al. (2020). Induction of pro-inflammatory cytokines (IL-1 and IL-6) and lung inflammation by Coronavirus-19 (COVI-19 or SARS-CoV-2): anti-inflammatory strategies. *J. Biol. Regul. Homeost Agents* 34 (2), 327–331. doi:10.23812/CONTI-E

Costa, D. C., Alva, N., Trigueros, L., Gamez, A., Carbonell, T., and Rama, R. (2013). Intermittent hypobaric hypoxia induces neuroprotection in kainate-induced oxidative stress in rats. *J. Mol. Neurosci.* 50 (3), 402–410. doi:10.1007/s12031-012-9945-8

Coulet, F., Nadaud, S., Agrapart, M., and Soubrier, F. (2003). Identification of hypoxia-response element in the human endothelial nitric-oxide synthase gene promoter. *J. Biol. Chem.* 278 (47), 46230–46240. doi:10.1074/jbc.M305420200

Cron, R. Q., and Chatham, W. W. (2020). The rheumatologist's role in COVID-19. *J. Rheumatol.* 47 (5), 639–642. doi:10.3899/jrheum.200334

Cummins, E. P., Keogh, C. E., Crean, D., and Taylor, C. T. (2016). The role of HIF in immunity and inflammation. *Mol. Aspects Med.* 47-48, 24–34. doi:10.1016/j.mam.2015.12.004

Dale, E. A., Ben Mabrouk, F., and Mitchell, G. S. (2014). Unexpected benefits of intermittent hypoxia: enhanced respiratory and nonrespiratory motor function. *Physiology* 29 (1), 39–48. doi:10.1152/physiol.00012.2013

Dao, D. T., Vuong, J. T., Anez-Bustillos, L., Pan, A., Mitchell, P. D., Fell, G. L., et al. (2018). Intranasal delivery of VEGF enhances compensatory lung growth in mice. *PLoS One* 13 (6), e0198700. doi:10.1371/journal.pone.0198700

Diao, B., Wang, C., Tan, Y., Chen, X., Liu, Y., Ning, L., et al. (2020). Reduction and functional exhaustion of T cells in patients with coronavirus disease 2019 (COVID-19). *Front. Immunol.* 11, 827. doi:10.3389/fimmu.2020.00827

Ding, H.-L., Zhu, H.-F., Dong, J.-W., Zhu, W.-Z., and Zhou, Z.-N. (2004). Intermittent hypoxia protects the rat heart against ischemia/reperfusion injury by activating protein kinase C. *Life Sci.* 75 (21), 2587–2603. doi:10.1016/j.lfs.2004.07.005

Escher, R., Breakey, N., and Lämmle, B. (2020). Severe COVID-19 infection associated with endothelial activation. *Thromb. Res.* 190, 62. doi:10.1016/j.thromres.2020.04.014

Fan, J., Lv, H., Li, J., Che, Y., Xu, B., Tao, Z., et al. (2019). Roles of Nrf2/HO-1 and HIF-1α/VEGF in lung tissue injury and repair following cerebral ischemia/reperfusion injury. *J. Cel Physiol* 234 (6), 7695–7707. doi:10.1002/jcp.27767

Faulhaber, M., Gatterer, H., Haider, T., Linser, T., Netzer, N., and Burtscher, M. (2015). Heart rate and blood pressure responses during hypoxic cycles of a 3-week intermittent hypoxia breathing program in patients at risk for or with mild COPD. *Copd* 10, 339–345. doi:10.2147/COPD.S75749

Figliozzi, S., Masci, P. G., Ahmadi, N., Tondi, L., Koutli, E., Aimo, A., et al. (2020). Predictors of adverse prognosis in COVID-19: a systematic review and meta-analysis. *Eur. J. Clin. Invest.* 50 (10), e13362. doi:10.1111/eci.13362

Fliser, D., and Haller, H. (2007). Erythropoietin and treatment of non-anemic conditions-cardiovascular protection. *Semin. Hematol.* 44 (3), 212–217. doi:10.1053/j.seminhematol.2007.04.008

Gangwar, A., Paul, S., Ahmad, Y., and Bhargava, K. (2020). Intermittent hypoxia modulates redox homeostasis, lipid metabolism associated inflammatory processes and redox post-translational modifications: benefits at high altitude. *Sci. Rep.* 10 (1), 7899. doi:10.1038/s41598-020-64848-x

Gao, B., Kong, Q., Kemp, K., Zhao, Y.-S., and Fang, D. (2012). Analysis of sirtuin 1 expression reveals a molecular explanation of IL-2-mediated reversal of T-cell tolerance. *Proc. Natl. Acad. Sci.* 109 (3), 899–904. doi:10.1073/pnas.1118462109

Garrod, R., Marshall, J., Barley, E., Fredericks, S., and Hagan, G. (2007). The relationship between inflammatory markers and disability in chronic obstructive pulmonary disease (COPD). *Prim. Care Respir. J.* 16 (4), 236–240. doi:10.3132/pcrj.2007.00047

Gel'tser, B. I., and Brodskaia, T. A. (2005). [Functional condition of the vascular endothelium in patients with extrahospital pneumonia]. *Klin Med. (Mosk)* 83 (7), 19–24. Retrieved from Available at: http://www.ncbi.nlm.nih.gov/pubmed/16117419.

Giannis, D., Ziogas, I. A., and Gianni, P. (2020). Coagulation disorders in coronavirus infected patients: COVID-19, SARS-CoV-1, MERS-CoV and lessons from the past. *J. Clin. Virol.* 127, 104362. doi:10.1016/j.jcv.2020.104362

Group, G. D. (2009).Rehabilitation after critical illness, *National Institute for Health & Clinical Excellence*, 28(1). 74–80.

Gualdoni, G. A., Mayer, K. A., Kapsch, A.-M., Kreuzberg, K., Puck, A., Kienzl, P., et al. (2018). Rhinovirus induces an anabolic reprogramming in host cell metabolism essential for viral replication. *Proc. Natl. Acad. Sci. USA* 115 (30), E7158–E7165. doi:10.1073/pnas.1800525115

Guan, W.-j., Ni, Z.-y., Hu, Y., Liang, W.-h., Ou, C.-q., He, J.-x., et al. (2020). Clinical characteristics of coronavirus disease 2019 in China. *N. Engl. J. Med.* 382 (18), 1708–1720. doi:10.1056/NEJMoa2002032

Huang, C., Wang, Y., Li, X., Ren, L., Zhao, J., Hu, Y., et al. (2020). Clinical features of patients infected with 2019 novel coronavirus in Wuhan, China. *The Lancet* 395 (10223), 497–506. doi:10.1016/S0140-6736(20)30183-5

Jelkmann, W. (1992). Erythropoietin: structure, control of production, and function. *Physiol. Rev.* 72 (2), 449–489. doi:10.1152/physrev.1992.72.2.449

Kaelin, W. G., Jr., and Ratcliffe, P. J. (2008). Oxygen sensing by metazoans: the central role of the HIF hydroxylase pathway. *Mol. Cel* 30 (4), 393–402. doi:10.1016/j.molcel.2008.04.009

Korkushko, O. V., Shatilo, V. B., and Ishchuk, V. A. (2010). [Effectiveness of intermittent normabaric hypoxic trainings in elderly patients with coronary artery disease]. *Adv. Gerontol.* 23 (3), 476–482.

Korkushko, O. V., Ivanov, L. A., Pisaruk, A. V., and Chebotarev, N. D. (2009). The respiratory function of blood in elderly and old age and the factors that determine it. *Fiziol Cheloveka* 35 (2), 40–46. doi:10.1134/s0362119709020054Retrieved from Available at: http://www.ncbi.nlm.nih.gov/pubmed/19402552.

Krantz, S. (1991). Erythropoietin. *Blood* 77 (3), 419–434. doi:10.1182/blood.v77.3.419.bloodjournal773419Retrieved from Available at: http://www.ncbi.nlm.nih.gov/pubmed/1991159.

Levine, B. D., Zuckerman, J. H., and deFilippi, C. R. (1997). Effect of high-altitude exposure in the elderly. *Circulation* 96 (4), 1224–1232. doi:10.1161/01.cir.96.4.1224

Li, G., and Clercq, E. D. (2020). Therapeutic options for the 2019 novel coronavirus (2019-nCoV). *Nat. Rev. Drug Discov.* 19 (3). doi:10.1038/d41573-020-00016-0

Li, H., Liu, Z., and Ge, J. (2020). Scientific research progress of COVID-19/SARS-CoV-2 in the first five months. *J. Cel Mol Med* 24 (12), 6558–6570. doi:10.1111/jcmm.15364

Li, W., Moore, M. J., Vasilieva, N., Sui, J., Wong, S. K., Berne, M. A., et al. (2003). Angiotensin-converting enzyme 2 is a functional receptor for the SARS coronavirus. *Nature* 426 (6965), 450–454. doi:10.1038/nature02145

Liu, K., Zhang, W., Yang, Y., Zhang, J., Li, Y., and Chen, Y. (2020). Respiratory rehabilitation in elderly patients with COVID-19: a randomized controlled study. *Complement. Therapies Clin. Pract.* 39, 101166. doi:10.1016/j.ctcp.2020.101166

Liu, X., Xu, D., Hall, J. R., Ross, S., Chen, S., Liu, H., et al. (2017). Enhanced cerebral perfusion during brief exposures to cyclic intermittent hypoxemia. *J. Appl. Physiol.(1985)* 123 (6), 1689–1697. doi:10.1152/japplphysiol.00647.2017

Lyamina, N. P., Lyamina, S. V., Senchiknin, V. N., Mallet, R. T., Downey, H. F., and Manukhina, E. B. (2011). Normobaric hypoxia conditioning reduces blood pressure and normalizes nitric oxide synthesis in patients with arterial hypertension. *J. Hypertens.* 29 (11), 2265–2272. doi:10.1097/HJH.0b013e32834b5846

Lytsy, P., Lind, L., and Sundström, J. (2013). Endothelial function and risk of hypertension and blood pressure progression. *J. Hypertens.* 31 (5), 936–939. doi:10.1097/HJH.0b013e32835ed5a0

Madjid, M., Safavi-Naeini, P., Solomon, S. D., and Vardeny, O. (2020). Potential effects of coronaviruses on the cardiovascular system. *JAMA Cardiol.* 5 (7), 831–840. doi:10.1001/jamacardio.2020.1286

Mallet, R. T., Manukhina, E. B., Ruelas, S. S., Caffrey, J. L., and Downey, H. F. (2018). Cardioprotection by intermittent hypoxia conditioning: evidence, mechanisms, and therapeutic potential. *Am. J. Physiology-Heart Circulatory Physiol.* 315 (2), H216–h232. doi:10.1152/ajpheart.00060.2018

Menter, T., Haslbauer, J. D., Nienhold, R., Savic, S., Hopfer, H., Deigendesch, N., et al. (2020). Postmortem examination of COVID-19 patients reveals diffuse alveolar damage with severe capillary congestion and variegated findings in lungs and other organs suggesting vascular dysfunction. *Histopathology* 77, 198. doi:10.1111/his.14134

Mukharliamov, F. Iu., Smirnova, M. I., Bedritskiĭ, S. A., and Liadov, K. V. (2006). [Interval hypoxic training in arterial hypertension]. *Vopr Kurortol Fizioter Lech Fiz Kult* (2), 5–6. Available at: http://www.ncbi.nlm.nih.gov/pubmed/16752815.

Murillo, A., Vera-Estrella, R., Barkla, B. J., Méndez, E., and Arias, C. F. (2015). Identification of host cell factors associated with astrovirus replication in caco-2 cells. *J. Virol.* 89 (20), 10359–10370. doi:10.1128/JVI.01225-15

Navarrete-Opazo, A., and Mitchell, G. S. (2014). Therapeutic potential of intermittent hypoxia: a matter of dose. *Am. J. Physiology-Regulatory, Integr. Comp. Physiol.* 307 (10), R1181–R1197. doi:10.1152/ajpregu.00208.2014

Neubauer, J. A. (2001). Invited review: physiological and pathophysiological responses to intermittent hypoxia. *J. Appl. Physiol.(1985)* 90 (4), 1593–1599. doi:10.1152/jappl.2001.90.4.1593

Orth, M., Shenar, A. K., Scheuer, C., Braun, B. J., Herath, S. C., Holstein, J. H., et al. (2019). VEGF-loaded mineral-coated microparticles improve bone repair and are associated with increased expression of epo and RUNX-2 in murine non-unions. *J. Orthop. Res.* 37 (4), 821–831. doi:10.1002/jor.24267

Park, S. S., Hong, M., Ha, Y., Sim, J., Jhon, G.-J., Lee, Y., et al. (2015). The real-time *in vivo* electrochemical measurement of nitric oxide and carbon monoxide release upon direct epidural electrical stimulation of the rat neocortex. *Analyst* 140 (10), 3415–3421. doi:10.1039/c5an00122f

Ponsot, E., Dufour, S. P., Zoll, J., Doutrelau, S., N'Guessan, B., Geny, B., et al. (2006). Exercise training in normobaric hypoxia in endurance runners. II. Improvement of mitochondrial properties in skeletal muscle. *J. Appl. Physiol.(1985)* 100 (4), 1249–1257. doi:10.1152/japplphysiol.00361.2005

Qin, C., Zhou, L., Hu, Z., Zhang, S., Yang, S., Tao, Y., et al. (2020). Dysregulation of immune response in patients with coronavirus 2019 (COVID-19) in wuhan, China. *Clin. Infect. Dis.* 71 (15), 762–768. doi:10.1093/cid/ciaa248

Robinson, M. A., Baumgardner, J. E., and Otto, C. M. (2011). Oxygen-dependent regulation of nitric oxide production by inducible nitric oxide synthase. *Free Radic. Biol. Med.* 51 (11), 1952–1965. doi:10.1016/j.freeradbiomed.2011.08.034

Rodriguez-Miguelez, P., Lima-Cabello, E., Martínez-Flórez, S., Almar, M., Cuevas, M. J., and González-Gallego, J. (2015). Hypoxia-inducible factor-1 modulates the expression of vascular endothelial growth factor and endothelial nitric oxide synthase induced by eccentric exercise. *J. Appl. Physiol.* 118 (8), 1075–1083. doi:10.1152/japplphysiol.00780.2014*1985*

Roubille, F., Prunier, F., Barrère-Lemaire, S., Leclercq, F., Piot, C., Kritikou, E. A., et al. (2013). What is the role of erythropoietin in acute myocardial infarct? Bridging the gap between experimental models and clinical trials. *Cardiovasc. Drugs Ther.* 27 (4), 315–331. doi:10.1007/s10557-013-6461-1

Rozova, K., and Mankovska, I. (2012). The effect of intermittent hypoxic training on lung and heart tissues of healthy rats. *Pneumonol Alergol Pol.* 80 (4), 296–300. Retrieved from Available at: http://www.ncbi.nlm.nih.gov/pubmed/22714072.

Rudyk, O. V., Vavilova, H. L., Strutyns'ka, N. A., Kotsiuruba, A. V., and Sahach, V. F. (2004). [Sensitivity of phenylarsineoxide-induced mitochondrial permeability transition pore opening in the heart of old rats during intermittent hypoxic training]. *Fiziol Zh* 50 (5), 29–37.

Ryan, R., Spathis, A., Clow, A., and Booth, S. (2016). Breathlessness and inflammation. *Curr. Opin. Support. Palliat. Care* 10 (3), 242–248. doi:10.1097/SPC.0000000000000229

Ryou, M.-G., Mallet, R. T., Metzger, D. B., and Jung, M. E. (2017). Intermittent hypoxia training blunts cerebrocortical presenilin 1 overexpression and amyloid-β accumulation in ethanol-withdrawn rats. *Am. J. Physiology-Regulatory, Integr. Comp. Physiol.* 313 (1), R10–r18. doi:10.1152/ajpregu.00050.2017

Schug, T. T., Xu, Q., Gao, H., Peres-da-Silva, A., Draper, D. W., Fessler, M. B., et al. (2010). Myeloid deletion of SIRT1 induces inflammatory signaling in response to environmental stress. *Mcb* 30 (19), 4712–4721. doi:10.1128/mcb.00657-10

Segovia-Juarez, J., Castagnetto, J. M., and Gonzales, G. F. (2020). High altitude reduces infection rate of COVID-19 but not case-fatality rate. *Respir. Physiol. Neurobiol.* 281, 103494. doi:10.1016/j.resp.2020.103494

Semenza, G. L. (1999). Perspectives on oxygen sensing. *Cell* 98 (3), 281–284. doi:10.1016/s0092-8674(00)81957-1

Senger, D., Galli, S., Dvorak, A., Perruzzi, C., Harvey, V., and Dvorak, H. (1983). Tumor cells secrete a vascular permeability factor that promotes accumulation of ascites fluid. *Science* 219 (4587), 983–985. doi:10.1126/science.6823562

Serebrovska, T. V., Grib, O. N., Portnichenko, V. I., Serebrovska, Z. O., Egorov, E., and Shatylo, V. B. (2019). Intermittent hypoxia/hyperoxia versus intermittent hypoxia/normoxia: comparative study in prediabetes. *High Alt. Med. Biol.* 20 (4), 383–391. doi:10.1089/ham.2019.0053

Serebrovskaya, T. V., Swanson, R. J., Karaban, I. N., Serebrovskaya, Z. A., and Kolesnikova, E. E. (1999). Intermittent hypoxia alters hypoxic ventilatory responses. *Fiziol Zh* 45 (5), 9–18. Retrieved from Available at: http://www.ncbi.nlm.nih.gov/pubmed/10687058. doi:10.1089/15270290260131920

Serebrovskaya, T. V. (2002). Intermittent hypoxia research in the former soviet union and the commonwealth of independent States: history and review of the concept and selected applications. *High Alt. Med. Biol.* 3 (2), 205–221. doi:10.1089/15270290260131939

Serebrovskaya, T. V., and Xi, L. (2016). Intermittent hypoxia training as non-pharmacologic therapy for cardiovascular diseases: practical analysis on methods and equipment. *Exp. Biol. Med. (Maywood)* 241 (15), 1708–1723. doi:10.1177/1535370216657614

Serocki, M., Bartoszewska, S., Janaszak-Jasiecka, A., Ochocka, R. J., Collawn, J. F., and Bartoszewski, R. (2018). miRNAs regulate the HIF switch during hypoxia: a novel therapeutic target. *Angiogenesis* 21 (2), 183–202. doi:10.1007/s10456-018-9600-2

Shi, M., Cui, F., Liu, A.-J., Ma, H.-J., Cheng, M., Song, S.-X., et al. (2015). The protective effects of chronic intermittent hypobaric hypoxia pretreatment against collagen-induced arthritis in rats. *J. Inflamm.* 12, 23. doi:10.1186/s12950-015-0068-1

Singh, M., Thomas, P., Shukla, D., Tulsawani, R., Saxena, S., and Bansal, A. (2013). Effect of subchronic hypobaric hypoxia on oxidative stress in rat heart. *Appl. Biochem. Biotechnol.* 169 (8), 2405–2419. doi:10.1007/s12010-013-0141-2

Song, J.-W., Zhang, C., Fan, X., Meng, F.-P., Xu, Z., Xia, P., et al. (2020). Immunological and inflammatory profiles in mild and severe cases of COVID-19. *Nat. Commun.* 11 (1), 3410. doi:10.1038/s41467-020-17240-2

Steinberg, B. E., Goldenberg, N. M., and Lee, W. L. (2012). Do viral infections mimic bacterial sepsis? The role of microvascular permeability: a review of mechanisms and methods. *Antiviral Res.* 93 (1), 2–15. doi:10.1016/j.antiviral.2011.10.019

Tian, Y.-M., Guan, Y., Li, N., Ma, H.-J., Zhang, L., Wang, S., et al. (2016). Chronic intermittent hypobaric hypoxia ameliorates diabetic nephropathy through enhancing HIF1 signaling in rats. *Diabetes Res. Clin. Pract.* 118, 90–97. doi:10.1016/j.diabres.2016.06.021

Tomasoni, D., Italia, L., Adamo, M., Inciardi, R. M., Lombardi, C. M., Solomon, S. D., et al. (2020). COVID- 19 and heart failure: from infection to inflammation and angiotensin II stimulation. Searching for evidence from a new disease. *Eur. J. Heart Fail.* 22 (6), 957–966. doi:10.1002/ejhf.1871

Törpel, A., Peter, B., Hamacher, D., and Schega, L. (2019). Dose-response relationship of intermittent normobaric hypoxia to stimulate erythropoietin in the context of health promotion in young and old people. *Eur. J. Appl. Physiol.* 119 (5), 1065–1074. doi:10.1007/s00421-019-04096-8

Verges, S., Chacaroun, S., Godin-Ribuot, D., and Baillieul, S. (2015). Hypoxic conditioning as a new therapeutic modality. *Front. Pediatr.* 3, 58. doi:10.3389/fped.2015.00058

Verity, R., Okell, L. C., Dorigatti, I., Winskill, P., Whittaker, C., Imai, N., et al. (2020). Estimates of the severity of coronavirus disease 2019: a model-based analysis. *Lancet Infect. Dis.* 20 (6), 669–677. doi:10.1016/s1473-3099(20)30243-7

Virdis, A., Ghiadoni, L., and Taddei, S. (2011). Effects of antihypertensive treatment on endothelial function. *Curr. Hypertens. Rep.* 13 (4), 276–281. doi:10.1007/s11906-011-0207-x

Vogtel, M., and Michels, A. (2010). Role of intermittent hypoxia in the treatment of bronchial asthma and chronic obstructive pulmonary disease. *Curr. Opin. Allergy Clin. Immunol.* 10 (3), 206–213. doi:10.1097/ACI.0b013e32833903a6

Walls, A. C., Park, Y.-J., Tortorici, M. A., Wall, A., McGuire, A. T., and Veesler, D. (2020). Structure, function, and antigenicity of the SARS-CoV-2 spike glycoprotein. *Cell* 181 (2), 281–292 e286. doi:10.1016/j.cell.2020.02.058

Walsh, N. P., and Oliver, S. J. (2016). Exercise, immune function and respiratory infection: an update on the influence of training and environmental stress. *Immunol. Cel Biol* 94 (2), 132–139. doi:10.1038/icb.2015.99

Wang, C.-C., Ying, L., Barnes, E. A., Adams, E. S., Kim, F. Y., Engel, K. W., et al. (2018). Pulmonary artery smooth muscle cell HIF-1α regulates endothelin expression via microRNA-543. *Am. J. Physiology-Lung Cell Mol. Physiol.* 315 (3), L422–l431. doi:10.1152/ajplung.00475.2017

Wang, D., Hu, B., Hu, C., Zhu, F., Liu, X., Zhang, J., et al. (2020). Clinical characteristics of 138 hospitalized patients with 2019 novel coronavirus-infected pneumonia in wuhan, China. *JAMA* 323 (11), 1061–1069. doi:10.1001/jama.2020.1585

Wang, J.-S., Chen, W.-L., and Weng, T.-P. (2011). Hypoxic exercise training reduces senescent T-lymphocyte subsets in blood. *Brain Behav. Immun.* 25 (2), 270–278. doi:10.1016/j.bbi.2010.09.018

Wang, M., Zhou, Y., Zong, Z., Liang, Z., Cao, Y., Tang, H., et al. (2020). A precision medicine approach to managing 2019 novel coronavirus pneumonia. *Precis Clin. Med.* 3 (1), 14–21. doi:10.1093/pcmedi/pbaa002

Wu, Z., and McGoogan, J. M. (2020). Characteristics of and important lessons from the coronavirus disease 2019 (COVID-19) outbreak in China. *JAMA* 323 (13), 1239–1242. doi:10.1001/jama.2020.2648

Xi, A., Zhuo, M., Dai, J., Ding, Y., Ma, X., Ma, X., et al. (2020). Epidemiological and clinical characteristics of discharged patients infected with SARS-CoV-2 on the Qinghai Plateau. *J. Med. Virol.* 92, 2528. doi:10.1002/jmv.26032

Xu, Z., Shi, L., Wang, Y., Zhang, J., Huang, L., Zhang, C., et al. (2020). Pathological findings of COVID-19 associated with acute respiratory distress syndrome. *Lancet Respir. Med.* 8 (4), 420–422. doi:10.1016/s2213-2600(20)30076-x

Yang, A.-P., Liu, J.-p., Tao, W.-q., and Li, H.-m. (2020). The diagnostic and predictive role of NLR, d-NLR and PLR in COVID-19 patients. *Int. Immunopharmacology* 84, 106504. doi:10.1016/j.intimp.2020.106504

Yang, H., Bi, Y., Xue, L., Wang, J., Lu, Y., Zhang, Z., et al. (2015). Multifaceted modulation of SIRT1 in cancer and inflammation. *Crit. Rev. Oncog* 20 (1-2), 49–64. doi:10.1615/critrevoncog.2014012374

Yi, Y., Lagniton, P. N. P., Ye, S., Li, E., and Xu, R.-H. (2020). COVID-19: what has been learned and to be learned about the novel coronavirus disease. *Int. J. Biol. Sci.* 16 (10), 1753–1766. doi:10.7150/ijbs.45134

Yu, Q., Dong, L., Li, Y., and Liu, G. (2018). SIRT1 and HIF1α signaling in metabolism and immune responses. *Cancer Lett.* 418, 20–26. doi:10.1016/j.canlet.2017.12.035

Zhang, R., Wu, Y., Zhao, M., Liu, C., Zhou, L., Shen, S., et al. (2009). Role of HIF-1α in the regulation ACE and ACE2 expression in hypoxic human pulmonary artery smooth muscle cells. *Am. J. Physiology-Lung Cell Mol. Physiol.* 297 (4), L631–L640. doi:10.1152/ajplung.90415.2008

Zheng, H.-Y., Zhang, M., Yang, C.-X., Zhang, N., Wang, X.-C., Yang, X.-P., et al. (2020). Elevated exhaustion levels and reduced functional diversity of T cells in peripheral blood may predict severe progression in COVID-19 patients. *Cell Mol Immunol* 17 (5), 541–543. doi:10.1038/s41423-020-0401-3

Zheng, Y.-Y., Ma, Y.-T., Zhang, J.-Y., and Xie, X. (2020). COVID-19 and the cardiovascular system. *Nat. Rev. Cardiol.* 17 (5), 259–260. doi:10.1038/s41569-020-0360-5

Zhou, P., Yang, X.-L., Wang, X.-G., Hu, B., Zhang, L., Zhang, W., et al. (2020). A pneumonia outbreak associated with a new coronavirus of probable bat origin. *Nature* 579 (7798), 270–273. doi:10.1038/s41586-020-2012-7

Zhou, S., Wang, Y., Zhu, T., and Xia, L. (2020). CT features of coronavirus disease 2019 (COVID-19) pneumonia in 62 patients in wuhan, China. *Am. J. Roentgenology* 214 (6), 1287–1294. doi:10.2214/AJR.20.22975

Conflict of Interest: The authors declare that the research was conducted in the absence of any commercial or financial relationships that could be construed as a potential conflict of interest.

frontiers in Pharmacology

REVIEW
published: 04 May 2021
doi: 10.3389/fphar.2021.660710

Strategy, Progress, and Challenges of Drug Repurposing for Efficient Antiviral Discovery

Xinlei Li† *and Tao Peng**

State Key Laboratory of Respiratory Disease, Sino-French Hoffmann Institute, College of Basic Medicine, Guangzhou Medical University, Guangzhou, China

Emerging or re-emerging viruses are still major threats to public health. Prophylactic vaccines represent the most effective way to prevent virus infection; however, antivirals are more promising for those viruses against which vaccines are not effective enough or contemporarily unavailable. Because of the slow pace of novel antiviral discovery, the high disuse rates, and the substantial cost, repurposing of the well-characterized therapeutics, either approved or under investigation, is becoming an attractive strategy to identify the new directions to treat virus infections. In this review, we described recent progress in identifying broad-spectrum antivirals through drug repurposing. We defined the two major categories of the repurposed antivirals, direct-acting repurposed antivirals (DARA) and host-targeting repurposed antivirals (HTRA). Under each category, we summarized repurposed antivirals with potential broad-spectrum activity against a variety of viruses and discussed the possible mechanisms of action. Finally, we proposed the potential investigative directions of drug repurposing.

Keywords: drug repurposing, emerging virus, antivirals, broad spectrum, COVID-19

OPEN ACCESS

Edited by:
Sugunadevi Sakkiah, National Center for Toxicological Research (FDA), United States

Reviewed by:
Hasan Ejaz, Al Jouf University, Saudi Arabia
Nasser Hadal Alotaibi, Al Jouf University, Saudi Arabia

***Correspondence:**
Tao Peng
peng_tao@gibh.ac.cn

†***Present address:***
Xinlei Li, The Abigail Wexner Research Institute at Nationwide Children's Hospital, Columbus, OH, United States

Specialty section:
This article was submitted to Experimental Pharmacology and Drug Discovery, a section of the journal Frontiers in Pharmacology

Received: *29 January 2021*
Accepted: *16 April 2021*
Published: *04 May 2021*

Citation:
Li X and Peng T (2021) Strategy, Progress, and Challenges of Drug Repurposing for Efficient Antiviral Discovery. Front. Pharmacol. 12:660710. doi: 10.3389/fphar.2021.660710

INTRODUCTION

Since December 2019, a novel coronavirus disease 2019 (COVID-19) has rapidly spread all over the globe to cause a pandemic (Li et al., 2020b; Zhu et al., 2020). The pneumonia causative agent was identified to be a new coronavirus, severe acute respiratory syndrome coronavirus 2 (SARS-CoV-2). As of April 6, 2021, more than 130 million cases have been confirmed globally, including approximately 2.85 million deaths. The still ongoing pandemic represents the most recent example of how emerging or re-emerging human or zoonotic viruses pose a threat to public health. These viruses include but not limited to Ebola virus (EBOV), Zika virus (ZIKV), West Nile virus (WNV), yellow fever virus (YFV), dengue virus (DENV), henipaviruses (Nipah, Hendra), SARS-CoV, Middle East respiratory syndrome (MERS-CoV), Lassa virus (LASV), Crimean-Congo hemorrhagic fever virus (CCHFV), Rift Valley fever virus (RVFV), chikungunya virus (CHIKV), human immunodeficiency virus (HIV) and influenza A virus (IAV). We listed six viral families in which a number of viruses have merged or remerged in recent years to have caused or potentially cause an epidemic or pandemic, including *Coronaviridae*, *Filoviridae*, *Flaviviridae*, *Arenaviridae*, *Nairoviridae*, and *Orthomyxoviridae*. The genome structure, important viruses, and key features regarding virus-host interactions are summarized in **Table 1**.

The emerging or remerging virus outbreak has emphasized the urgent need for preventative or treatment regimens. Vaccines are recognized as a preferred promising line of defense. However, vaccine development is a complex process and multiple challenges are involved in light of the fact

TABLE 1 | Important emerging or remerging viruses.

Virus family	Genome	Important viruses	Key features/Virus-host interactions	Ref
Coronaviridae	ss (+) RNA; 26–32 kb	SARS-CoV, SARS-CoV-2, MERS-CoV, HCoV-229 E, HCoV-OC43, HCoV-NL63, HCoV-HKU1	Enveloped viruses; case fatality rate: 30% (MERS-CoV), 10% (SARS-CoV), 3% (SARS-CoV-2); receptor: ACE2 (SARS-CoV, SARS-CoV-2); DPP4 (MERS-CoV); S protein proteolytic cleavage by cathepsins or TMPRSS2 is necessary for infection; RNA proofreading is viable due to the exoribonuclease activity	de Wit et al. (2016); Chen (2020)
Flaviviridae	ss (+) RNA; 9.6–12.3 kb	DENV, ZIKV, YFV, WNV	Enveloped viruses; cause hemorrhagic fever, liver damage, congenital malformations (microcephaly); transmission by vectors like mosquitos or ticks	Mukhopadhyay et al. (2005); Barrows et al. (2018)
Filoviridae	ss (–) RNA; 19 kb	EBOV, MARV	Enveloped filamentous virions can exceed to 14,000 nm in length; cause fatal viral hemorrhagic fevers; case fatality rate: from 25 to 90%; DC-SIGN, or integrins as attachment factor; receptor: NPC1 (EBOV)	—
Arenaviridae	ss (–) RNA; segmented	LASV, JUNV	Enveloped viruses; case fatality rate: 20–30% (JUNV), 1% (LASV); entry factors: Alpha-dystroglycan, LAMP1 (LASV); cause hemorrhagic fever; virus spreads through rodents	Jae et al. (2014); Pontremoli et al. (2019)
Nairoviridae	ss (–) RNA; segmented	CCHFV	Enveloped viruses with circular genome; case fatality rate: 10–40% (CCHFV); virus entry is clathrin-, pH- and cholesterol dependent; cause hemorrhagic fever; transmission by vectors like ticks	Simon et al. (2009); Zivcec et al. (2016)
Orthomyxoviridae	ss (–) RNA; segmented	IAV (H1N1, H2N2, H5N1, H3N2, H7N9, . . .)	Enveloped viruses; genome reassortment is common; case fatality rate varies, 2–3% (1918 H1N1)	Ramos and Fernandez-Sesma (2012)

TABLE 2 | Compound library for drug repurposing.

Library	Library scale	Introduction	Refs
Prestwick chemical library	1,520	99% approved drugs (FDA, EMA and other agencies)	Ulferts et al. (2016)
NCATS pharmaceutical collection (or NCGC pharmaceutical Collection)	~3,500	2,500 approved molecules, plus about 1,000 investigational compounds	Huang et al. (2011)
ReFRAME compound library	~12,000	Containing nearly all small molecules that have reached clinical development or undergone significant preclinical profiling, 38% of which are approved drugs	Janes et al. (2018); Riva et al. (2020)
Library of pharmacologically active compounds (LOPAC), sigma	1,280	Biologically annotated collection of inhibitors, receptor ligands, pharma-developed tools, and approved drugs	Hu et al. (2014)
NIH clinical collection	727	All have a history of use in human clinical trials and known safety profiles	van Cleef et al. (2013)

that the pathogens that need to be confronted may display high genetic variability (e.g., HIV) or an identity hardly predicted in advance (e.g., SARS-CoV-2 or ZIKV). Thus, unprecedented demands have emerged on antivirals that can be rapidly available in clinical practices. In the absence of a vaccine available to use, hepatitis C virus (HCV) is supposed to be eliminated in the use of the direct-acting antivirals, which probably represents the first virus to be cured by antivirals. That strengthens the promising potential of antivirals in terms of virus treatment.

Drug repurposing (also called drug repositioning) is a strategy for identifying new uses for approved or investigational drugs that beyond the original indicative scope to facilitate antiviral development. Typically, antiviral discovery development is time and resource-consuming, which involves three major stages including drug discovery (3–6 years), preclinical studies in experimental animal models (about 3 years), clinical trials in humans from phase I to III (about 5 years). Finally, if a therapeutic succeeds to pass all the processes, it needs to get approved by the appropriate agency. It is estimated that only 5% of the candidate molecules are finally approved and up to 3 billion dollars are consumed. Given that the repurposed drugs have been proven to be safe in humans, drug repurposing likely can skip phase I and probably the phase II clinical trials. Thus, the attrition rate to be a novel antiviral is reduced, although the phase III trial is still needed. Remdesivir, an adenosine analog to inhibit EBOV RNA-dependent RNA polymerase (RdRp) (Tchesnokov et al., 2019), is the latest example. Although remdesvir did not show therapeutic activity against EBOV infection in a real-world phase III clinical trial (Nakkazi, 2018), remdesivir shows potent antiviral activity against SARS-CoV-2, SARS-CoV, and MERS-CoV *in vitro* or *in vivo* in preclinical animal models (de Wit et al.,

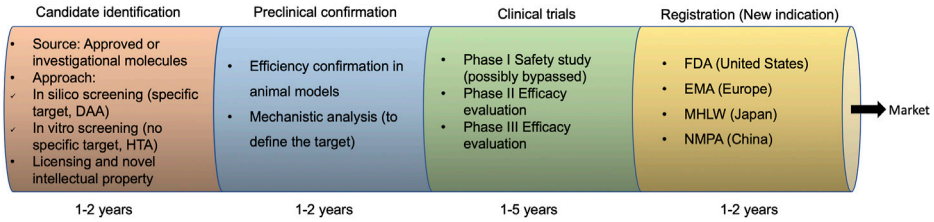

FIGURE 1 | Drug repurposing development process. DAA, direct-acting antivirals; HTA, host-targeting antivirals; FDA, Food and Drug Administration; EMA, the European Medicines Agency; MHLW, Ministry of Health, Labor, and Welfare; NMPA, National Medical Products Administration.

2020; Wang et al., 2020a). Two randomized phase III clinical trials indicate that patients who received remdesivir had a shorter time to recover (Spinner et al., 2020; Wang et al., 2020c), based upon which the U.S. Food and Drug Administration (FDA) has approved remdesivir for use in COVID-19 patients, less than 1 year after the outbreak of the pandemic. From the above example, drug repurposing could significantly facilitate antiviral development for emergency use. Given the urgent need for therapeutics for emerging or re-emerging viruses and a great number of approved or developmental therapeutics, drug repurposing represents a better way for antiviral discovery. In this review, we discussed the strategies of drug repurposing for antiviral development, summarized the promising drug candidates that have the antiviral potency with broad-spectrum activity, and analyzed the possible caveats of this strategy of drug discovery.

STRATEGIES TO DEVELOP REPURPOSED ANTIVIRALS

A typical drug repurposing strategy comprises four steps (**Figure 1**), including the identification of a candidate therapeutic for the new indication as an antiviral; antiviral efficiency confirmation and/or mechanistic analysis in preclinical animal models; antiviral efficacy evaluation in clinical trials (phase I may be not prerequisite if sufficient safety data has already been obtained as parts of the original indication); and approval of the novel indication by government agencies such as the FDA, the European Medicines Agency (EMA), Ministry of Health, Labor and Welfare (MHLW) of Japan, and National Medical Products Administration (NMPA) of China.

APPROACHES FOR ANTIVIRAL REPURPOSING

The identification of the right drug for the new indication is crucial. The major approaches involve high throughput *in silico* or *in vitro* screening. The *in silico* screening is commonly used for the identification of a compound that binds to the given target, commonly a virally encoded protein, such as RNA-dependent RNA polymerase (Patel and Kukol, 2017). The *in vitro* screening involves the high throughput antiviral screening, leading to the subsequent validation for the most potent candidates. These candidates can target host proteins or viral proteins (Kouznetsova et al., 2014; Chopra et al., 2016; Xu et al., 2016; Li et al., 2017c). For either approach, compound libraries, in particular those with approved molecules, are needed (**Table 2**). These include the Drugbank library, NIH Clinical Compound (NCC) Collection (van Cleef et al., 2013), the Prestwick Chemical Library (Ulferts et al., 2016), the Library of Pharmacologically Active Compounds (LOPAC) (Hu et al., 2014), a library of approved drugs that were assembled by the NIH Chemical Genomics Centre (NCGC) called the NCGC Pharmaceutical Collection (NPC) (Huang et al., 2011), and the ReFRAME (Repurposing, Focused Rescue, and Accelerated Medchem) Library (Janes et al., 2018). Recently, the LOPAC and ReFRAME drug libraries were successfully used for the discovery of the SARS-CoV-2 antiviral candidates (Riva et al., 2020).

CATEGORIES OF REPURPOSED ANTIVIRALS

Based on the origin and feature of the repurposed antiviral targets, two major categories are divided: direct-acting repurposed antiviral (DARA) and host-targeting repurposed antiviral (HTRA) repurposing. The representative antivirals with repurposed potentials are summarized in **Figure 2**.

Direct-Acting Repurposed Antiviral (DARA)

A large majority of antivirals approved by the FDA are direct-acting antivirals (DAA) other than host-targeting agents (HTA) (Chaudhuri et al., 2018). DARAs contain antiviral activity relying on structural similarity or identical enzymatic activity of virally encoded targets, particularly viral polymerase, protease, reverse transcriptase, or viral proteins with ion channel activity. Below we reported the advances in repurposed antivirals targeting the two important viral enzymes, RdRp and protease.

RdRp Inhibitors

Remdesivir (GS-5734)

Remdesivir was an investigational compound in the class of nucleotide analogs, which was originally developed to treat *Filoviridae* members EBOV or Marburg infection and rapidly pushed through clinical trials due to the EBOV epidemic in West Africa from 2013 through 2016. However, in August 2019,

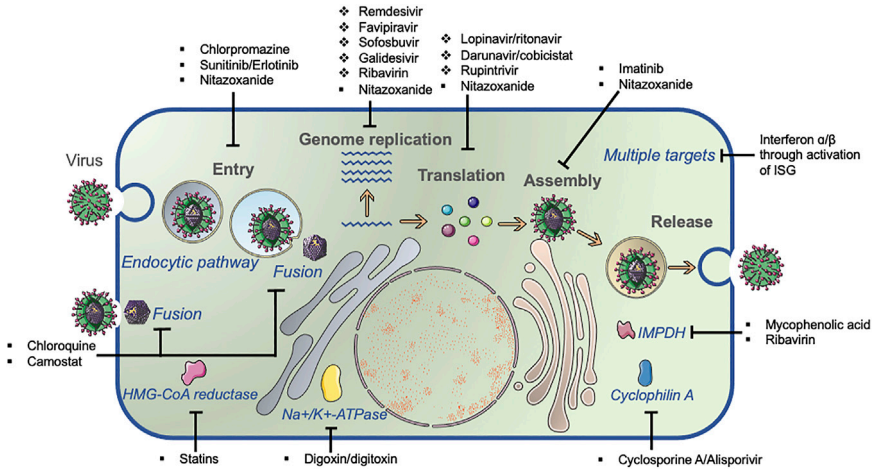

FIGURE 2 | Common viral lifecycle and broad-spectrum antiviral identification. The common viral lifecycle comprises three steps: viral entry, genome replication, and virus assembly/release. Direct-acting antivirals (DAA, ❖) and host-targeting antivirals (HTA, ■) inhibit virus replication by targeting viral protein and host molecules that are required for virus replication, respectively.

remdesivir was announced to be less effective than the other two monoclonal antibody regimens (Mulangu et al., 2019). It has also been found to show antiviral activity against other RNA viruses such as *Pneumoviridae* member RSV (EC50 = 0.019 μM); *Paramyxoviridae* Nipah virus (EC50 = 0.029 μM), Hendra virus (EC50 = 0.055 μM), parainfluenza type three virus (EC50 = 0.018 μM), MV (EC50 = 0.037 μM) and MuV viruses (EC50 = 0.79 μM); *Arenaviridae* JUNV (EC50 = 0.47 μM), LASV (EC50 = 1.48 μM); some *Flaviviridae* viruses like Kyasanur Forest disease virus (KFDV) (EC50 = 1.8 μM), Omsk Hemorrhagic Fever virus (OHFV) (EC50 = 1.2 μM), Tick-borne encephalitis (TBEV) (EC50 = 2.1 μM), and *Coronaviridae* including MERS-CoV (EC50 = 0.074 μM), SARS-CoV (EC50 = 0.069 μM), and SARS-CoV-2 (EC50 = 0.77 μM) (Warren et al., 2016; Lo et al., 2017; Sheahan et al., 2017a; Choy et al., 2020) (**Table 3**). The parent nucleoside of remdesivir, GS-441524 (1′-cyano substituted adenine nucleoside analog or Nuc) also shows a broad-spectrum but less effective antiviral activity against infections of coronaviruses like MERS-CoV and feline coronavirus (Warren et al., 2016; Pedersen et al., 2019).

Remdesivir shows prophylactic or therapeutic potency when administrated in SARS-CoV-infected mice, in which reduced viral load in lung and improved clinical symptoms and respiratory function was observed (Sheahan et al., 2017a). A similar prophylactic or therapeutic potency of remdesivir against MERS-CoV was seen in macaques or mouse models (de Wit et al., 2020; Sheahan et al., 2020). Remdesivir efficiently inhibits SARS-CoV-2 replication *in vitro* (Wang et al., 2020b), and was used as a compassionate use in the first COVID-19 case in the United States (Holshue et al., 2020) before large-scale clinical studies (NCT04280705; NCT04292899; NCT04292730; NCT04257656) were launched. One large-scale study in which hospitalized COVID-19 patients were given remdesivir for 10 days showed significantly shortened time to recovery (Beigel et al., 2020). Another study indicated that remdesivir treatment in moderate COVID-19 patients for 5 days led to symptom improvement significantly higher than the standard care group (Spinner et al., 2020). Contrarily, a smaller scale study only found remdesivir resulted in a marginally but numerically faster time to clinical improvement (Wang et al., 2020c). Based upon these clinical studies, the full and conditional use of remdesivir in hospitalized COVID-19 patients was approved by FDA in October 2020. Although World Health Organization (WHO) recommends against it, based on the interim result of the WHO Solidarity Trial.

Mechanistically, remdesivir exerts the antiviral activity through competing with ATP that is supposed to incorporate into viral RdRp for RNA replication. It results in delayed EBOV and MERS-CoV RNA chain termination at the fifth and third position, respectively after the initiation site (Warren et al., 2016; Tchesnokov et al., 2019; Gordon et al., 2020).

Ribavirin (RBV)

RBV is on the WHO's list of essential medicines, it is licensed to treat RSV infection (Committee on Infectious Diseases, 1993), or HCV infection in combination with interferon (IFN)-α or direct-acting antivirals (AASLD-IDSA HCV Guidance Panel, 2018). RBV is also effective against other hepatotropic viruses including HBV(Galban-Garcia et al., 2000) and HEV (Kamar et al., 2014; Kamar et al., 2019) in clinical studies, although no convincing activity against HBV was obtained in cell culture systems (Isorce et al., 2016). Ribavirin was clinically used to treat a variety of viral hemorrhagic fevers, including Lassa fever (McCormick et al., 1986), Crimean-Congo hemorrhagic fever (Fisher-Hoch et al., 1995), and Hantavirus infection (Ogg et al., 2013) alone or in combination with favipiravir, even though RBV might be effective only at early stages (Johnson et al., 2018; Eberhardt et al., 2019).

The clinical use of RBV as a supplement to other agents like corticosteroid for SARS-CoV treatment was documented in China and Canada (Peiris et al., 2003), while RBV had an

TABLE 3 | Approved or investigational direct-acting antivirals with repurposed potential against other virus infections.

Category	Agent name	Primary indication	Broad antiviral activity				Clinical trials	Ref
			Virus name	EC50/ EC90 (μM)	CC50 (μM)	SI		
Viral RdRp inhibitor	Remdesivir	Antiviral (EBOV, no approval)	EBOV	0.07/0.22 (Huh7 cells)	3.7	52.86	Phase III failed	Warren et al. (2016)
			JUNV	0.47/2.8	N.D.	N.D.		Warren et al. (2016)
			MERS-CoV	0.074/N.D.	>10	>135		Sheahan et al. (2017b)
			SARS-CoV	0.069/N.D.	>10	>144		Sheahan et al. (2017b)
			SARS-CoV-2	0.77/1.76	>100	>129.87	Approved for hospitalized COVID-19 patients	Wang et al. (2020b)
			RSV	0.021/0.059	6.195	395		Lo et al. (2017)
			NiV	0.029/0.053	8.294	286		Lo et al. (2017)
	Ribavirin	Antiviral (HCV, RSV)	HCV	8.4/N.D.	108	12.86	Approved	Ortega-Prieto et al. (2013)
			RSV	69.5/N.D.	N.D.	N.D.	Approved	Kim et al. (2017)
			HBV	N.D./N.D.	N.D.	N.D.	Phase I NCT04356677; phase II NCT04276688;	Isorce et al. (2016)
			HEV	6.9/50.38	N.D.	N.D.	phase III NCT04392427	Todt et al. (2018)
			ZIKA	23/281	N.D.	N.D.		Kamiyama et al. (2017)
			LASV	2.47/N.D.	>50	>20		Welch et al. (2016)
			EBOV	5.34/N.D.	>50	>9		Welch et al. (2016)
			SARS-CoV	81.9/N.D.	>819	>10		Saijo et al. (2005)
			MERS-CoV	66.9/86.6	N.D.	N.D.		Falzarano et al. (2013a)
			SARS-CoV-2	109.5/N.D.	>400	3.65	Phase II/III NCT04460443, NCT04497649; phase III NCT04392427, . . .	Wang et al. (2020b)
	Favipiravir	Antiviral (IAV)	IAV(H1N1)	1.97/3.75	>128	>64	Approved	Sleeman et al. (2010)
			LASV	29.3/43.2	>1000	>34		Oestereich et al. (2016)
			JUNV	0.79/5.0	188	239		Furuta et al. (2013)
			CCHFV	6.37/10.18	>100	>15.7		Oestereich et al. (2014b)
			RVFV	5.0/32	>980	>196		Furuta et al. (2013)
			Rabies	32.4/N.D.	N.D.	N.D.		Yamada et al. (2016)
			RSV	N.D./36	>1600	N.D.		Jochmans et al. (2016)
			EBOV	67/110	>1000	>14.9		Oestereich et al. (2014a)
			SARS-CoV-2	61.88/N.D.	>400	>6.46	Phase III: NCT04425460, NCT04373733; phase	Wang et al. (2020b)
			WNV	53/N.D.	N.D.	N.D.	IV NCT04359615.	Morrey et al. (2008)
			YFV	180/330	>6370	>19		Julander et al. (2009)
			ZIKA	22/N.D.	>637	>26		Zmurko et al. (2016)
			EV-71	68.74/N.D.	>1000	>14.55		Wang et al. (2016b)
	Sofosbuvir	Antiviral (HCV)	HCV	0.032–0.13/N.D.	N.D.	N.D.	Approved	Han et al. (2019)
			YFV	4.2/N.D.	381	90		de Freitas et al. (2019)
			DENV	1.4/6.4	>100	>71		Xu et al. (2017)
			CHIKV	1/N.D.	402	402		Ferreira et al. (2019)
			ZIKA	1.37/12.3	>200	>145		Bullard-Feibelman et al. (2017)
			HEV	1.97/N.D.	>100	>51		Netzler et al. (2019)
			HBV	—	—	—	Phase II NCT03312023	—
			SARS-CoV-2	—	—	—	Phase II/III: NCT04460443, NCT04443725; phase IV NCT04498936; . . .	—
	Galidesivir	Antiviral (EBOV, investigational)	EBOV	11.8/25.4	>11,800	>100	Preclinical	Warren et al. (2014)
			MARV	4.4/10.5	1065	242	Phase I NCT03800173	Warren et al. (2014)
			SUDV	3.4/10.3	>3400	>100		Warren et al. (2014)
			TBEV	0.95/N.D.	N.D.	N.D.		Eyer et al. (2019)
			YFV	14.1/46.8	>14,100	>100	Phase I NCT03891420	Warren et al. (2014)
			WNV	2.33/N.D.	>100	>42		Eyer et al. (2017)
			DENV	32.8/89.3	>9710	>296		Warren et al. (2014)
			ZIKA	3.8/18.2	N.D.	N.D.		Julander et al. (2017)
			RVFV	41.6/98.0	>41,600	>100		Warren et al. (2014)
			LASV	43.0/>100	>4300	>100		Warren et al. (2014)
			RSV	11.0/25.7	>980	>89		Warren et al. (2014)
			IAV(H1N1)	10.7/17	>3167	>296		Warren et al. (2014)
			SARS-CoV	57.7/>95	>17,080	>296		Warren et al. (2014)
			SARS-CoV-2	—	—	—	Phase I NCT03891420	—

(Continued on following page)

TABLE 3 | (*Continued*) Approved or investigational direct-acting antivirals with repurposed potential against other virus infections.

Category	Agent name	Primary indication	Broad antiviral activity				Clinical trials	Ref
			Virus name	EC50/ EC90 (μM)	CC50 (μM)	SI		
Viral protease inhibitor	Lopinavir/ ritonavir	Antiviral (HIV)	HIV (lopinavir)	0.018/N.D.	N.D.	N.D.	Approved	Masse et al. (2007)
			HIV (ritonavir)	0.046/N.D.	N.D.	N.D		Masse et al. (2007)
			SARS-CoV (lopinavir)	17.1/N.D.	>32	>2		de Wilde et al. (2014)
			MERS-CoV (lopinavir)	8.0/N.D.	24.4	3.1		de Wilde et al. (2014)
			SARS-CoV-2 (lopinavir)	26.63/N.D.	49.75	1.87	Phase III: NCT04372628, NCT04321174; phase IV: NCT04350684, NCT0435067; . . .	Choy et al. (2020)
	Rupintrivir	Antiviral (HRV, investigational)	HRV-100	0.022/0.032	N.D.	N.D.	Phase II completed	Binford et al. (2005)
			Echovirus-6	0.051/0.094	N.D.	N.D.		Binford et al. (2005)
			CVB2	0.022/0.088	N.D.	N.D.		Binford et al. (2005)
			CVA16/860 F	0.015/N.D.	>50	>3500		Zhang et al. (2013)
			EV71/695 F	0.014/N.D.	>50	>3500		Zhang et al. (2013)
			HCoV-229e	0.3/N.D.	>500	>1500		Kim et al. (2012)
			TGEV	2.5/N.D.	>500	>200		Kim et al. (2012)
			BOC	15.3/N.D.	>500	>32		Kim et al. (2012)
			Norovirus/ Norwalk	0.32/1.5	>50	>150		Rocha-Pereira et al. (2014)

EC50 of 81.9 μM *in vitro* (Saijo et al., 2005). RBV is also effective to inhibit MERS-CoV with an EC50 ranging from 66.9 μM (16.33 μg/ml) to 169.7 μM (41.45 μg/ml) *in vitro* (Falzarano et al., 2013a). RBV alongside IFN-α was reported to reduce the hospital mortality rate from 70 to 29% in hospitalized MERS patients at 14 days after admission (Omrani et al., 2014). RBV also shows antiviral activity against SARS-CoV-2 *in vitro* with an EC50 of 109.5 μM (Wang et al., 2020b), while another report did not find the favorable effect of RBV (Choy et al., 2020). The higher EC50 of RBV against either MERS-CoV or SARS-CoV-2 may be due to the reduced RBV uptake (Ibarra and Pfeiffer, 2009) or inabilities to accumulate sufficient amounts of phosphorylated RBV metabolites required for the effective RBV antiviral actions (Shah et al., 2010). As of early January 2021, at least seven clinical trials (phase I NCT04335123; phase II NCT04494399; phase II NCT04563208; phase II NCT04605588; NCT04664010; phase II NCT04276688; phase II/III NCT04402203) have been launched to investigate the efficacy of RBV alone or in combination with other agents for COVID-19 treatment.

Mechanistically, at least two types of antiviral machinery may be involved. Upon the uptake into cells, RBV is metabolized to form a purine RNA nucleotide-like form, which interferes with viral RNA polymerases, leading to hypermutation of RNA that reduces the viability and is lethal to RNA viruses. RBV is also an inhibitor of inosine-5′-monophosphate dehydrogenase (IMPDH), which is essential for the *de novo* synthesis of guanosine-5′-monophosphate (GMP). RBV structure may interfere with the RNA capping process that relies on natural guanosine to prevent RNA degradation. Upon the inhibition of IMPDH, RBV can lower the intracellular pool of GTP, and DNA virus replication is then inhibited. Alternatively, RBV has the potential to reduce cell death, affect type 1 cytokine production or inflammatory response, which may help combat HBV, HCV, or LASV infection (Tam et al., 1999; Oestereich et al., 2016).

Favipiravir

Favipiravir (6-fluoro-3-hydroxy-2-pyrazinecarboxamide) was firstly designed to inhibit influenza RdRp, despite of different serotypes and strains of influenza A, B, or C (Furuta et al., 2013). Favipiravir has been approved since 2014 in Japan for emergent use to treat influenza. In addition, favipiravir has shown a broad antiviral activity against other negative sense RNA viruses such as RSV (*Pneumoviridae*, EC90 = 36 μM), CCHFV (*Nairoviridae*, EC50 = 6.37 μM), LSAV (*Arenaviridae*, EC50 = 29.3 μM), JUNV (*Arenaviridae*, EC50 = 0.79 μM), Rabies virus (*Rhabdoviridae*, EC50 = 32.4 μM), EBOV (*Filoviridae*, EC50 = 67 μM), or positive sense RNA viruses like SARS-CoV-2 (*Coronaviridae*, EC50 = 61.88 μM), *Flaviviridae* ZIKA (EC50 = 22 μM), WNV (EC50 = 53 μM), YFV (EC50 = 180 μM), and enterovirus EV71 (*Picornaviridae*, EC50 = 68.74 μM) (Morrey et al., 2008; Oestereich et al., 2014a; Oestereich et al., 2014b; Jochmans et al., 2016; Oestereich et al., 2016; Yamada et al., 2016; Zmurko et al., 2016; Furuta et al., 2017; Wang et al., 2020b) (**Table 3**).

A preclinical study in EBOV-infected macaques shows a higher plasma favipiravir concentrations greater than 70–80 μg/ml or 446–509 μM were associated with reduced viral loads and extended survival rate (Guedj et al., 2018). A similar study in IFNAR−/− mice also shows a high dose [300 mg/(kg/d)] of favipiravir enhances EBOV clearance and prevents a lethal outcome (Oestereich et al., 2014a). Clinically, favipiravir showed good tolerance in EBOV patients but no strong antiviral efficacy (Sissoko et al., 2016), possibly due to the low median trough drug concentrations (46 μg/ml or 293 μM at day 2 post-treatment) (Nguyen et al., 2017). Thus, the optimal dosage and potency of favipiravir merit further investigation.

Favipiravir exhibited antiviral activity against SARS-CoV-2 *in vitro* (Wang et al., 2020b) and showed a significantly shorter viral clearance time than the control group (4 vs. 11 days) and a higher improvement in chest imaging in a non-randomized clinical study (Cai et al., 2020). Another

small-sized open-label phase II/III clinical trial (NCT04434248) also found that favipiravir enabled SARS-CoV-2 viral clearance in 62.5% of patients within 4 days, as compared to 30% of patients on a standard of care; however, the viral clearance rate by day 10 after favipiravir administration was only marginally improved (Ivashchenko et al., 2020). Although favipiravir has been approved in some countries, large-scale, placebo-controlled, double-blinded clinical trials may be still needed to further evaluate the efficacy and safety of favipiravir.

The mechanism of action of inhibiting influenza RdRp by favipiravir involves the conversion to the metabolite favipiravir ribofuranosyl-5′-triphosphate (favipiravir-RTP), which further incorporates into influenza RdRp to inhibit the polymerase activity at nanomolar to micromolar concentrations (Furuta et al., 2013). The inhibition of other viral RdRp by favipiravir may involve a similar mechanism.

Sofosbuvir

Sofosbuvir that targets HCV RdRp NS5B from 15 subtypes in six genotypes with an EC50 ranging from 0.032 to 0.13 μM is an approved oral direct-actin antiviral to treat chronic hepatitis C (Han et al., 2019). A cocktail treatment regimen containing sofosbuvir and HCV protease NS3/4A inhibitors has already been approved for pan-genotypic HCV infection. Sofosbuvir shows antiviral effects against other virus members in *Flaviviridae* family, such as ZIKA (EC50 = 4.25 μM) (Bullard-Feibelman et al., 2017; Mumtaz et al., 2017; Sacramento et al., 2017), DENV(Sacramento et al., 2017), CHIKV (EC50 = 1 μM) (Ferreira et al., 2019), and YFV (EC50 = 4.2 μM) (de Freitas et al., 2019). Strikingly, HEV, another hepatotropic virus but evolutionally distant from HCV, was reported to be susceptible to sofosbuvir (EC50 = 1.97 μM) (Todt et al., 2018; Netzler et al., 2019) (**Table 3**). A phase II clinical trial of sofosbuvir for HBV treatment (phase II NCT03312023) is also under investigation. Besides, the binding residue of sofosbuvir on coronavirus RdRp is conserved among SARS-CoV, SARS-CoV-2, and MERS-CoV(Jacome et al., 2020), although sofosbuvir did not exhibit the inhibitory effect against MERS-CoV RdRp in a cell-based reporter assay (Min et al., 2020). Sofosbuvir binds to SARS-CoV-2 RdRp and inhibits virus infection in lung and brain cells (Elfiky, 2020a), and clinical trials have initiated in multiple countries (phase II NCT04561063, phase II NCT04532931, phase II/III NCT04460443; phase II/III NCT04497649; phase III NCT04530422, phase III NCT04535869, phase IV NCT04498936).

Galidesivir (BCX4430, Immucillin-A)

Galidesivir, an imino-C-nucleoside analog, was originally developed to combat EBOV infection (Warren et al., 2014). Galidesivir strongly inhibits EBOV RdRp activity *in vitro* and post-exposure intramuscular administration of galidesivir protects mice or macaques against Ebola virus or Marburg disease (Warren et al., 2014). Currently, a phase I clinical trial (NCT03800173) for Marburg disease is being performed.

Galidesivir was subsequently identified to exhibit broad-spectrum antiviral effectiveness against other RNA virus families like *Flaviviridae* members TBEV (EC50 = 0.95 μM), YFV (EC50 = 14.1 μM), WNV (EC50 = 2.33 μM), DENV (EC50 = 32.8 μM), and ZIKA (EC50 = 3.8 μM), *Arenaviridae* (LASV, EC50 = 43.0 μM), *Phleboviridae* (RVFV, EC50 = 41.6 μM), *Pneumoviridae* (RSV, EC50 = 11.0 μM), *Orthomyxoviridae* (IAV H1N1, EC50 = 10.7 μM), and *Coronaviridae* MERS-CoV (EC50 = 68.4 μM) and SARS-CoV (EC50 = 57.7 μM) (Warren et al., 2014; Eyer et al., 2017; Julander et al., 2017; Westover et al., 2018; Eyer et al., 2019). Preclinical studies showed intramuscular or intraperitoneal administration of galidesivir in Syrian golden hamsters effectively limited systemic RVFV infection and improved survival outcomes (Westover et al., 2018). Galidesivir also showed anti-ZIKA activity in a lethal mouse model even when the treatment was initiated during the peak of viremia (Julander et al., 2017). Despite the anti-coronavirus activity *in vitro*, and the predicted strong binding of galidesivir with SARS-CoV-2 RdRp (Elfiky, 2020b), an early stage clinical showed that treatment with galidesivir offered COVID-19 patients no benefit compared to a placebo.

Viral Protease Inhibitor

Lopinavir/ritonavir (LPV/r)

LPV/r is a fixed-dose combination for HIV prevention and treatment. It combines LPV with a low dose of ritonavir (RTV), both of which are HIV protease inhibitors. In HIV-1 NL4-3 infection system *in vitro*, LPV and RTV have an EC50 of 0.018 and 0.046 μM, respectively, against HIV-1, but LPV has a much higher potency than RTV does (EC50 = 0.015 μM for LPV vs. 0.349 μM for RTV) for HIV-2 (Masse et al., 2007). RTV is also a very potent inhibitor of intestinal and hepatic cytochrome P450 3A4 (Eagling et al., 1997), which is involved in LPV catabolism. As with LPV/r, darunavir/cobicistat (DRV/c) is also a dose-fixed combination containing HIV protease inhibitor DRV and CYP3A enzymatic antagonist cobicistat (Masse et al., 2007). Low doses of RTV or cobicistat could slow down the breakdown of HIV protease inhibitors, thereby greatly increases its blood concentration.

Some viruses, like SARS-CoV, MERS-CoV, and SARS-CoV-2, encode proteases, which are structurally and functionally similar to HIV protease. LPV shows an EC50 of 17.1, 8.0, and 26.63 μM, respectively against the three coronaviruses (de Wilde et al., 2014; Choy et al., 2020) (**Table 3**). LPV/r combination shows greater anti-MERS-CoV activity than LPV does (EC50 of 8.5 vs. 11.6 μM) *in vitro* (Sheahan et al., 2020). LPV/r alongside IFN-β shows improved clinical and pathological features in a nonhuman primate MERS model (Chan et al., 2015), while prophylactic or therapeutic LPV/r-IFN-β treatment only slightly improves the disease outcomes in patients (Sheahan et al., 2020). Similarly, SARS patients receiving LPV/r were found to have an improvement in respiratory syndrome (Chu et al., 2004). However, the potency of LPV/r for SARS-CoV is only effective if administrated early but not as rescue or salvage therapy (Chan et al., 2003). Despite of its potential for COVID-19 treatment, a randomized trial showed the hospitalized COVID-19 patients did not benefit from LPV/r therapy (Cao et al., 2020).

Rupintrivir (AG-7088)

Rupintrivir is a peptidomimetic compound inhibiting viral protease activity, it is designed to combat human rhinovirus (HRV, belonging to family Piconaviridae) infection. Rupintrivir shows potent *in vitro* activity against all 48 HRV serotypes tested, with a range of EC50s of 0.007 to 0.104 μM (Binford et al., 2005). A phase II placebo-controlled randomized, double-blind trial experimentally shows the biosafety and potential efficacy in volunteers (Hayden et al., 2003). Because of a lack of efficacy in natural HRV infection in a subsequent clinical trial, further development of rupintrivir was suspended.

Rupintrivir has shown antiviral activity against a spectrum of viruses that encodes 3C or 3C-like protease, for instance, rupintrivir exhibits antiviral activities against multiple enteroviruses, including EV71 (strain 695F, EC50 = 0.014 μM), coxsackievirus B2 (CVB2, EC50 = 0.022 μM), CVA16 (strain 860F, EC50 = 0.015 μM) (Hung et al., 2011). Two studies show rupintrivir exhibits cross-genotypic inhibitory activity against either human or mouse norovirus, a member in the family *Caliciviridae*, with the EC50 of 0.32 and 13 μM, respectively (Kim et al., 2012; Rocha-Pereira et al., 2014). A molecular modeling study shows rupintrivir is capable to bind with SARS-CoV main proteinase $3CL^{pro}$ (Anand et al., 2003); however, rupintrivir fails to show good activity at even 100 μM, although some rupintrivir derivatives show better potency (IC50 = 11–39 μM) (Shie et al., 2005). Rupintrivir exerts an antiviral effect on coronaviruses including CoV-229E (EC50 = 0.3 μM), transmissible gastroenteritis virus (TGEV, EC50 = 2.5 μM), bovine coronavirus (BCV, EC50 = 15.3 μM) (**Table 3**). Rrupintrivir also showed inhibition for SARS-CoV-2 main protease with a 50% inhibitory concentration of 68 ± 7 μM (Vatansever et al., 2021).

Rupintrivir has poor aqueous solubility and low oral bioavailability in animals, the hydrolyzed metabolites are reportedly 400-fold less active than rupintrivir but predominates the biotransformation pathway. The above features may limit its potential clinical application.

Host-Targeting Antiviral (HTA) Repurposing

HTA repurposing identifies antivirals targeting to host proteins, functions, or pathways, which are required for virus life cycle including viral entry, genome replication, protein translation, and virus assembly and release. As the entire viral life cycle cannot be completed without cells, HTA may exhibit broad antiviral activity against different viruses. Based on the essential steps of a viral life cycle, four major categories of host-targeting repurposed antivirals (HTRA) are classified as below.

HTRA Aiming Virus Entry Step

The first step of the viral life cycle is to enter permissive cells. Some enveloped viruses like HIV, and Nipah virus enter cells *via* direct membrane fusion with the plasma membrane, resulting in the release of nucleocapsid directly to the cytosol (Bossart et al., 2002; Wilen et al., 2012). Bacteriophages can inject their genomes alone into bacterial cells. Except for the aforementioned two mechanisms, most viruses depend on an endocytic pathway to be internalized into cells. The involved pathways include clathrin-mediated endocytosis, caveolar/lipid raft-mediated endocytosis, or micropinocytosis, through which viruses are internalized into the early endosome, intermediate endosome, and then late endosome or lysosome in a stepwise manner. Finally, the exposure of virions either naked or enveloped to low pH and proteolytic enzymes will trigger changes in the naked virions, or membrane fusion between the organelle and enveloped viruses, to help deliver the viral genome or the intact nucleocapsid into cytosol. Aftermath, most RNA viruses replicate in different locations within the cytosol, whereas DNA viruses continue the journey to the nucleus.

Chlorpromazine (CPZ) and Other Dopamine Antagonists

CPZ is a phenothiazine used to treat psychotic disorders including schizophrenia or manic-depression in adults. CPZ can treat in children severe behavioral problems like attention deficit hyperactivity disorder. CPZ is also indicated to treat anxiety before surgery, nausea and vomiting, and chronic hiccups that do not improve following other treatments (Lopez-Munoz et al., 2005). CPZ is on the list of WHO's essential medicines, among the most effective and safest medicines. CPZ antagonizes dopamine receptors, which are divided into two classes based on which G-protein they are coupled: the D1-like class (including D1 and D5) and the D2-like class, which comprises D2, D3, and D4 receptors. CPZ can bind to and block two types of dopamine receptors, in particular D2 dopamine receptors, exerting antipsychotic activity.

CPZ has proved to inhibit clathrin-mediate endocytosis by preventing the assembly of the clathrin-coated pit on the cell surface (Wang et al., 1993). Thus, CPZ and other dopamine receptor antagonists show antiviral activity against a broad spectrum of viruses that use clathrin-mediated endocytosis to enter cells. These viruses include HIV(Bosch et al., 2008), rubella virus (Kee et al., 2004), human adenovirus (HAdV) (Diaconu et al., 2010), EV71 (Hussain et al., 2011), HAV (Rivera-Serrano et al., 2019), HEV (Yin et al., 2016a), HCV (Blanchard et al., 2006), DENV (Carro et al., 2018), ZIKA (Persaud et al., 2018; Li et al., 2020a), CSFV (Shi et al., 2016), CCHFV (Simon et al., 2009; Ferraris et al., 2015b), SFV (Pohjala et al., 2011), EBOV (Bhattacharyya et al., 2010), MERS-CoV (de Wilde et al., 2014), and SARS-CoV (Inoue et al., 2007).

HIV can either enter cells through direct viral membrane fusion with the plasma membrane, or cell-to-cell transmission and viral synapses between T cells. The latter type of HIV entry is sensitive to CPZ treatment, suggesting the involvement of clathrin-mediated endocytosis (Bosch et al., 2008). Viruses within *Flaviviridae* family, such as HCV, DENV, ZIKA, and CSFV also enter cells dependent on clathrin-mediated endocytosis and are susceptible to CPZ treatment (Zhu et al., 2012; Shi et al., 2016). Cell surface FcγR was reported to be required for antibody-dependent enhancement of DENV or ZIKV infection (Khandia et al., 2018). Interestingly, the viral entry mediated by FcγRII needs the formation of clathrin-coated vesicles whilst FcγRI-dependent viral entry is independent of clathrin (Carro et al., 2018). On the contrary, naked and enveloped viruses may comparably be sensitive to CPZ. HAV

and HEV had been recognized as naked viruses until recently the membrane-trapped viral particles were identified (Feng et al., 2013; Yin et al., 2016a). The naked and enveloped HAV or HEV are both sensitive to CPZ treatment (Yin et al., 2016a; Rivera-Serrano et al., 2019), suggesting the clathrin-mediated endocytosis is equally needed. Coronaviruses such as MERS-CoV and SARS-CoV share the same clathrin-mediated endocytosis for virus entry. In light of this, clinical studies have initiated (phase II/III NCT04354805; phase III NCT04366739) to evaluate the safety and effectiveness of CPZ for COVID-19 treatment, although observative clinical studies have suggested that CPZ at the prescribed dose may not be clinically effective for COVID-19 (Hoertel et al., 2021).

Sunitinib, Erlotinib (Receptor Tyrosine Kinase Inhibitors)

Sunitinib and erlotinib are inhibitors to receptor tyrosine kinases (RTK) that play important roles in both tumor angiogenesis and tumor cell proliferation. Sunitinib has been approved for the treatment of cancers, such as gastrointestinal stromal cell tumor, renal cell carcinoma, and imatinib-resistant gastrointestinal stromal tumor; while erlotinib is licensed to treat non-small cell lung cancer, and pancreatic cancer (Hartmann and Kanz, 2008; Neveu et al., 2015). Erlotinib is on the list of WHO's essential medicines.

The major antiviral mechanism of sunitinib involves the inhibition of adaptor protein 2 (AP2)-associated protein kinase 1 (AAK1), which phosphorylates membrane trafficking adaptor proteins AP-1 and AP-2 to enhance the binding with clathrin-associated cargos for bidirectional transport and endocytosis from the plasma membrane, respectively (Ricotta et al., 2002). The inhibition of AAK1 thereby inhibits virus entry, or assembly and release. For instance, sunitinib reportedly inhibits DENV entry and infectious virus release but not RNA replication (Bekerman et al., 2017). In a multiple cycle infection system, the EC50 against DENV1 is 0.6 μM, similar EC50s (0.3–1.2 μM) of sunitinib against other members in the family *Flaviviridae* (HCV, ZIKV, other DENV serotypes) were reported (Bekerman et al., 2017) (**Table 4**). Sunitinib is also effective against infections of other viruses including EBOV (EC50 = 0.47 μM), CHIKV (EC50 = 4.67 μM), JUNV (EC50 = 4.8 μM), HIV (EC50 = 0.8 μM), and RSV (EC50 < 0.12 μM) (Bekerman et al., 2017). Albeit sunitinib and erlotinib combinations showed no efficacy in murine models of DENV and EBOV infection (Bekerman et al., 2017).

EGFR is involved in multiple virus entry processes such as DNA viruses HBV, HPV, and RNA viruses HCV, RSV, and porcine reproductive and respiratory syndrome virus in cell cultures (Lupberger et al., 2011; Wang et al., 2016a; Iwamoto et al., 2019; Lingemann et al., 2019; Mikuličić et al., 2019). Specifically, EGFR mediates HCV entry by regulating CD81–claudin-1 associations and viral glycoprotein-dependent membrane fusion (Lupberger et al., 2011). EGFR reportedly associates with sodium taurocholate cotransporting polypeptide (NTCP), the HBV receptor on the hepatocyte cell surface, and inhibition of EGFR dramatically impairs HBV virion internalization (Iwamoto et al., 2019; Gan et al., 2020). However, a recent clinical study suggests that HBV reactivation may occur in lung cancer patients receiving erlotinib treatment (Yao et al., 2019). Therefore, the safety and efficacy of sunitinib/erlotinib need to be cautiously investigated.

Chloroquine (CQ) (Lysosomotropic Agents)

CQ is a medication primarily used to treat or prevent a non-resistant malaria infection, it is also occasionally used for amebiasis treatment. Additionally, CQ has shown anti-inflammatory properties for the clinical management of some autoimmune diseases such as rheumatoid arthritis and lupus erythematosus (Rainsford et al., 2015). CQ is on the list of WHO's essential medicines. The anti-malarial mechanism of action involves the lysosomotropic feature, which allows CQ to accumulate in an acidic digestive vacuole inside red blood cells, where CQ binds to hemes to form a toxic product resulting in cell lysis and ultimately parasite cell autodigestion. Also, because of the involvement of lysosomes in the autophagy process, the inhibition by CQ of lysosomal enzymes leads to the accumulation of the autophagy cargos that are supposed to break down in lysosomes, leading to the impairment of autophagy machinery.

Due to the lysosomotropic feature, CQ or other agents like hydroxychloroquine (HCQ) and Bafilomycin A, accumulate in lysosomes, acidic endosomes, or trans-Golgi network vesicles to elevate the pH and subsequently inhibit the residential hydrolase activity (Thome et al., 2013). Such an inhibition in lysosomal function leads to the uptake impairment of a panel of viruses. These include HCV (Ashfaq et al., 2011), DENV (Farias et al., 2014; Farias et al., 2015), ZIKA (Li et al., 2017b; Shiryaev et al., 2017), CCHFV (Ferraris et al., 2015a), CHIKV (Khan et al., 2010), MERS-CoV (Dyall et al., 2014), SARS-CoV (Keyaerts et al., 2004; Vincent et al., 2005), and SARS-CoV-2 (Wang et al., 2020b).

CQ exerts antiviral activity against DENV infection either *in vitro* (Farias et al., 2014) and *in vivo* in an infected monkey model (Farias et al., 2015). However, a double-blind and placebo-controlled trial in 307 dengue patients found that CQ does not reduce the duration of viremia and the viral NS1 antigenemia (Tricou et al., 2010). Although CQ shows antiviral activity against EBOV *in vitro*; however, CQ fails to protect against EBOV infection and disease pathogenesis in the *in vivo* guinea pig model (Dowall et al., 2015). CQ shows antiviral activity against some strains of HIV *in vitro* (Tsai et al., 1990) with an EC50 of 0.4–0.9 μM when treated in combination with hydroxyurea plus didanosine in a lymphocytic cell line (Boelaert et al., 1999). And HCQ exhibits anti-HIV activity *in vivo* (Sperber et al., 1995). The mechanism may involve the inhibition of cell-to-cell transmission of HIV, which requires clathrin-mediated endocytosis (Bosch et al., 2008), or the inhibition of p120 production at a post-transcriptional level, possibly by impairing hydrolases or other enzymes in acidic vesicles (Savarino et al., 2001).

CQ shows broad and good antiviral activity against coronavirus infection *in vitro*. However, no efficacy is observed to reduce SARS-CoV virus titers in a nonlethal mouse model (Barnard et al., 2006a). Although CQ and HCQ had drawn a lot of attention for the treatment of COVID-19, the safety or severe side effects of CQ or HCQ at a high dose is

TABLE 4 | Approved and investigational host-targeting antivirals with repurposed potential against virus infection.

Agent name	Primary indication/mechanism of action	Repurposed antiviral activity						Clinical trials	Ref
		Category	Virus name	EC50/ EC90 (μM)	CC50 (μM)	SI	Mechanism of action		
Chlorpromazine (CPZ)	Anti-psychotic; CPZ antagonizes dopamine receptors to exert antipsychotic activity	Virus entry inhibitor	SARS-CoV	8.8/N.D.	24.3	2.8	CPZ and other dopamine receptor antagonize clathrin-mediated endocytosis which is required for some virus entry	Phase II/III NCT04354805; phase III NCT04366739	de Wilde et al. (2014)
			MERS-CoV	4.9/N.D.	21.3	4.3			de Wilde et al. (2014)
			SARS-CoV-2	—	—	—			-
			HCV	N.D./N.D.	N.D.	N.D.			Blanchard et al. (2006)
			DENV	N.D./N.D.	N.D.	N.D.			Carro et al. (2018)
			ZIKA	N.D./N.D.	N.D.	N.D.			Khandia et al. (2018)
			CSFV	N.D./N.D.	N.D.	N.D.			Shi et al. (2016)
			CCHFV	10.6/N.D.	30	2.8			Ferraris et al. (2015b)
			SFV	15.7/N.D.	67.3	4.5			Pohjala et al. (2011)
			EBOV	N.D./N.D.	N.D.	N.D.			Bhattacharyya et al. (2010); Du et al. (2020)
			HAV	N.D./N.D.	N.D.	N.D.			Rivera-Serrano et al. (2019)
			HEV	N.D./N.D.	N.D.	N.D.			Yin et al. (2016a)
Chloroquine (CQ)	Anti-malaria; lysosomotropic CQ accumulates in acidic digestive vacuole inside red blood cells, where CQ binds to hemes to form a toxic product resulting in cell lysis and ultimately parasite cell autodigestion		HCV	<50/N.D.	>100	>2	As a lysosomotropic agent, CQ blocks the membrane fusion between virus and lysosomes to inhibit virus entry	Phase III: NCT04447534, NCT04360759; phase IV: NCT04362332, NCT04331600; …	Ashfaq et al. (2011)
			DENV	N.D./N.D.	N.D.	N.D.			Farias et al. (2014)
			ZIKA	7.25/N.D.	>30	>4			Ianevski et al. (2018)
			CCHFV	39.4/N.D.	1000	26.9			Ferraris et al. (2015a)
			SARS-CoV	6.5/N.D.	>100	>15			Dyall et al. (2014)
			MERS-CoV	6.28/N.D.	>10	>1.5			Dyall et al. (2014)
			SARS-CoV-2	1.13/N.D.	>100	>88.5			Wang et al. (2020b)
			EBOV	1.57/3.35	N.D.	N.D.			Du et al. (2020)
			eHAV	N.D./N.D.	N.D.	N.D.			Feng et al. (2013)
			HIV	<0.9/N.D.	N.D.	N.D.			Boelaert et al. (1999)
Sunitinib/erlotinib	Anti-tumor; inhibiting tumor cell growth by inhibiting receptor tyrosine kinase (RTK) pathways		HCV(sunitinib)	1.2/N.D.	>10	>8.3	Sunitinib/erlotinib inhibits RTKs including AAK1 or EGFR, which is invovled in intracellular vesicle trafficking that is used by some virus to enter cells	Phase I/II NCT02380625	Bekerman et al. (2017)
			HCV(erlotinib)	0.6/N.D.	>15	>25			Bekerman et al. (2017)
			DENV1(sunitinib)	0.6/N.D.	>10	>16.7			Bekerman et al. (2017)
			DENV1(erlotinib)	1.9/N.D.	>20	>10.5			Bekerman et al. (2017)
			ZIKV(sunitinib)	0.51/N.D.	14.1	27.6			Bekerman et al. (2017)
			ZIKV(erlotinib)	6.28/N.D.	>30	>4.7			Bekerman et al. (2017)
			EBOV(sunitinib)	0.47/N.D.	>10	>21.2			Bekerman et al. (2017)
			EBOV(erlotinib)	2.88/N.D.	15	5.2		Phase I/II NCT02380625	Bekerman et al. (2017)
			CHIKV(sunitinib)	4.67/N.D.	11.9	2.5			Bekerman et al. (2017)
			CHIKV(erlotinib)	0.7/N.D.	30	42.9			Bekerman et al. (2017)
			JUNV(sunitinib)	4.8/N.D.	10.4	2.2			Bekerman et al. (2017)
			JUNV(erlotinib)	1.7/N.D.	>20	>11			Bekerman et al. (2017)
			HIV(sunitinib)	0.8/N.D.	>20	>15			Bekerman et al. (2017)
			HIV(erlotinib)	2/N.D.	>20	>10			Bekerman et al. (2017)
			RSV(sunitinib)	<0.12/N.D.	12.5	>100			Bekerman et al. (2017)
			RSV(erlotinib)	<0.12/N.D.	>30	>250			Bekerman et al. (2017)
			HBV(erlotinib)	N.D./N.D.	N.D.	N.D.			Gan et al. (2020)
			SARS-CoV-2	—	—	—		Phase I: NCT02134886, NCT00890747; phase I/II: NCT02380625, NCT01835938; phase II NCT00521092; …	—
Camostat	Chronic pancreatitis and postoperative reflux esophagitis; inhibiting transmembrane protease, serine 2 (TMPRSS2)		SARS-CoV	~1/~5	>500	>500	Camostat is an inhibitor to TMPRSS2 which is required for entry of coronaviruses or influenza	Phase II/III NCT04455815; phase III NCT04355052; phase IV NCT04338906; …	Hoffmann et al. (2020b)
			MERS-CoV	~1.5/~5	>500	>300			Hoffmann et al. (2020b)
			SARS-CoV-2	~1/~5	>500	>500			Hoffmann et al. (2020b)
			IAV-A	4.4/N.D.	>1000	>200			Hosoya et al. (1992)
			IAV-B	11.7/N.D.	>1000	>85			Hosoya et al. (1992)

(Continued on following page)

TABLE 4 | (*Continued*) Approved and investigational host-targeting antivirals with repurposed potential against virus infection.

Agent name	Primary indication/mechanism of action	Repurposed antiviral activity						Clinical trials	Ref
		Category	Virus name	EC50/ EC90 (μM)	CC50 (μM)	SI	Mechanism of action		
Statins	Hypercholesterolemia; statins are HMG-CoA reductase inhibitors to reduce cholesterol biosynthesis	Virus replication inhibitor	DENV	11.9/N.D.	53.6	4.5	Statin inhibits replicase formation of	Phase II NCT02841774; phase III NCT03037372	Martinez-Gutierrez et al. (2011)
			ZIKA (cerivastatin)	0.02/N.D.	0.37	18.1	flaviviruses,		Español et al. (2019)
			ZIKA (lovastatin)	14.59/N.D.	38.76	2.66	reverse transcription of HIV; impairs		Español et al. (2019)
			HCV (lovastatin)	N.D./N.D.	N.D.	N.D.	EBOV		Ye et al. (2003)
			HIV	N.D./N.D.	N.D.	N.D.	glycoprotein processing		Giguère and Tremblay (2004); Amet et al. (2008)
			HBV (simvastatin)	5.2/N.D.	>30	>5.7			Okuyama-Dobashi et al. (2015)
			EBOV (fluvastatin)	0.89/2.48	N.D.	N.D.			Du et al. (2020)
			RSV	N.D./N.D.	N.D.	N.D.			Gower and Graham (2001); Ravi et al. (2013a)
			CVB3	N.D./N.D.	N.D.	N.D.			Werner et al. (2014)
			MV	N.D./N.D.	N.D.	N.D.			Robinzon et al. (2009)
			SARS-CoV-2	—	—	—		Phase III: NCT04486508, NCT04472611; phase IV NCT02735707; . . .	—
Digoxin	Heart failure; the cardiac glycoside can block the Na^+/K^+ ATPase ion pump activity to raise the intracellular Ca^{2+} level to improve the cardiac failure		HSV	0.13/N.D.	10.21	78.54	Digoxin impedes the immediate-early or	—	Su et al. (2008)
			HSV (digitoxin)	0.05/N.D.	10.66	213	early	—	Su et al. (2008)
			HCMV	0.036/N.D.	0.45	12.6	gene expressions of herpes viruses;	—	Kapoor et al. (2012)
			HAdV	N.D./N.D.	N.D.	N.D.	impaires JEV or EBOV	—	Grosso et al. (2017)
			HIV	0.045/0.1	>0.1	>2	RNA replication or virus entry; may also	—	Wong et al. (2013)
			HBV (digitoxin)	0.093/N.D.	1.7	18.9	inhibit coronavirus entry;	—	Okuyama-Dobashi et al. (2015)
			JEV	0.10/N.D.	>100	>969.9	inhibits arenaviruses whose replication	—	Guo et al. (2020)
			CHIKV	0.0488/N.D.	>10	>200	depends	—	Ashbrook et al. (2016)
			SINV	0.1989/N.D.	N.D.	N.D.	on Na^+/K^+ ATPase activity	—	Ashbrook et al. (2016)
			RRV	0.1265/N.D.	N.D.	N.D.		—	Ashbrook et al. (2016)
			RSV	0.026/N.D.	0.839	32.3		—	Norris et al. (2018)
			LCMV (ouabain)	0.0058/N.D.	0.0289	4.99		—	Iwasaki et al. (2018)
			LASV	N.D./N.D.	N.D.	N.D.		—	Iwasaki et al. (2018)
			JUNV	N.D./N.D.	N.D.	N.D.		—	(Iwasaki et al., 2018)
			Reovirus	0.1339/N.D.	N.D.	N.D.		—	Ashbrook et al. (2016)
			VSV	0.2387/N.D.	N.D.	N.D.		—	Ashbrook et al. (2016)
			EBOV	0.32/2.44	N.D.	N.D.		—	Du et al. (2020)
			MERS-CoV (ouabain)	N.D./N.D.	N.D.	N.D.		—	Burkard et al. (2015)
			SARS-CoV-2	0.043/N.D.	>10	>232	—	—	Cho et al. (2020)
Mycophenolic acid (MPA)	Immuno-suppression; MPA inhibits IMPDH to cause the intracellular guanosine depletion, resulting in immunosuppressive activity in lymphocyte		CHIKV	1.5/N.D.	>200	>130	MPA exerts antiviral activity through	Phase II NCT03262441	Pohjala et al. (2011)
			HCV	0.68/N.D.	73.8	108.5	IMPDH-mediated		Ye et al. (2012)
			DENV	0.3/N.D.	N.D.	N.D.	depletion of intracellular guanosine, on		Diamond et al. (2002)
			WNV (New York isolate)	2.8/0.94	>312	>111	which viral genome replication replies		Morrey et al. (2002)
			ZIKV	0.1–1/N.D.	N.D.	N.D.			Barrows et al. (2016)
			HBV	N.D./N.D.	N.D.	N.D.			Gong et al. (1999); Ying et al. (2000)
			HIV	N.D./N.D.	N.D.	N.D.			Chapuis et al. (2000)
			HEV	N.D./N.D.	N.D.	N.D.			Wang et al. (2014)
			VacV	0.7/N.D.	48	68.6			Smee et al. (2001)
			HuNoV	N.D./N.D.	N.D.	N.D.			Dang et al. (2017)
			Rotavirus	0.885/N.D.	438.07	495.05			Yin et al. (2016b)
			IAV (H1N1)	1.51/N.D.	>50	>33			To et al. (2016)
			MERS-CoV	0.53/8.15	>32	>195.12			Chan et al. (2013)
			SARS-CoV-2	0.15/N.D.	—	—			Han et al. (2021)
Cyclosporine a (CsA)	Immuno-suppression; CsA is an inhibitor to peptidylprolyl isomerase cyclophilin a (CyPA), causing the block of T cell activation though the cypa-calcineurin-nf-at pathway		HCV	0.33/N.D.	N.D.	N.D.	CyPA-dependent: CyPA interacts with	Phase III completed	Koizumi et al. (2017)
			DENV	N.D./N.D.	N.D.	N.D.	flavivirus proteins,	NCT04451239; phase I NCT04412785; phase II	Qing et al. (2009)
			MERS-CoV	3.6/N.D.	26.4	7.3	IAV M protein, nucleocapsid and Nsp1	NCT04492891; phase IV NCT0439253	de Wilde et al. (2017)
			SARS-CoV	1.3/N.D.	>50	>38.5	proteins of SARS-CoV.		de Wilde et al. (2017)
			SARS-CoV-2	0.46/3.1	>10	>21	CyPA-independent: CsA inhibits HBV		Softic et al. (2020)
			HIV	N.D./N.D.	N.D.	N.D.	entry, IAV replication		Franke et al. (1994); Hatziioannou et al. (2005)
			HBV	1.12/N.D.	>10	>8.9			Watashi et al. (2014)
			IAV	1.45/N.D.	>20	>13			Hamamoto et al. (2013)

(Continued on following page)

TABLE 4 | (*Continued*) Approved and investigational host-targeting antivirals with repurposed potential against virus infection.

Agent name	Primary indication/mechanism of action	Repurposed antiviral activity						Clinical trials	Ref
		Category	Virus name	EC50/ EC90 (μM)	CC50 (μM)	SI	Mechanism of action		
Imatinib	Anti-tumor; imatinib inhibits tyrosine kinase c-Abl to block tumor cell proliferation	Virus assembly/ release inhibitor	EBOV	N.D./N.D.	N.D.	N.D.	Imatinib decreases the budding or release of EBOV, VacV, and DENV; imatinib also inhibits CVB entry	Phase II: NCT04357613, NCT04346147; phase III: NCT04394416, NCT04422678; …	Garcia et al. (2012)
			DENV	N.D./N.D.	N.D.	N.D.			Clark et al. (2016)
			MERS-CoV	17.7/N.D.	>50	>2.8			Dyall et al. (2014)
			SARS-CoV	9.82/N.D.	>50	>5			Dyall et al. (2014)
			SARS-CoV-2	4.86/N.D.	37.3	7.7			Han et al. (2021)
			VacV	N.D./N.D.	N.D.	N.D.			Reeves et al. (2011)
Interferon α/β	Approved for antiviral (HCV, HBV) and multiple sclerosis treatment; IFN induces the production of inteferon-stimulated genes through JAK-STAT pathway	Inhibition of multiple targets	HCV (IFN-α)	*2.5/10	>10,000	>4000	IFN exerts the broad-specrum antiviral activity by inducing ISG production, which may inhibit each step of the viral life cycle		Okuse et al. (2005)
			HBV(IFN-α2)	#7754/N.D.	N.D.	N.D.		Phase I NCT03294798; phase II NCT03575208; phase IV NCT03357822, NCT04035837; …	Chen et al. (2020)
			HIV	N.D./N.D.	N.D.	N.D.		Phase 1/2 NCT0247143	Iyer et al. (2017)
			EBOV (IFN-β)	*74/N.D.	N.D.	N.D.			McCarthy et al. (2016)
			EBOV (IFN-α)	*748/N.D	N.D.	N.D.			McCarthy et al. (2016)
			DENV	*182.1/N.D.	N.D.	N.D.			Pires de Mello et al. (2018a)
			ZIKV	*407.8/N.D.	N.D.	N.D.			Pires de Mello et al. (2018b)
			SARS-CoV(IFN-α)	*4950/N.D.	>10,000	>2			Cinatl et al. (2003)
			SARS-CoV(IFN-β)	*95/N.D.	>10,000	>105			Cinatl et al. (2003)
			MERS-CoV(IFN-α-2b)	*58.08/ 320.11	N.D.	N.D.			Falzarano et al. (2013a)
			SARS-CoV-2 (IFN-α or β)	*1.35 or 0.76/N.D.	N.D.	N.D.		Phase III: NCT04492475, NCT04320238; phase IV: NCT04350671, NCT04254874; …	Mantlo et al. (2020)
Nitazoxanide	Anti-parasite; nitazoxanide interferences with the pyruvate:ferredoxin oxidoreductase (PFOR) enzyme-dependent electron transfer reaction to disrupt parasite enegery metabolism		IAV (H1N1/PR8)	3.25/N.D.	>163	>50	Nitazoxanide inhibits morphogenesis of IAV and rotavirus; post-entry steps of SeV and RSV; HBV DNA replication; viral protease activity of ZIKV or coronavirus; induce innate immune genes	Phase II NCT03905655	Rossignol et al. (2009)
			SeV	1.63/N.D.	>163	>100			Rossignol (2014)
			RSV	0.98/N.D.	>163	>166			Rossignol (2014)
			HCV	0.68/3.03	123.7	181			Korba et al. (2008)
			JEV	0.39/N.D.	60	154			Shi et al. (2014)
			ZIKV	1.48/4.0	77	52			Li et al. (2017c)
			HIV	1.63/N.D.	>100	>50			Tan et al. (2012)
			HBV	0.39/2.7	>325	>833			Korba et al. (2008)
			Rotavirus	6.5/N.D.	>163	>25			La Frazia et al. (2013)
			CHIKV	2.96/N.D.	25	8.45			Wang et al. (2016c)
			MHV	1/N.D.	>10	>10			Cao et al. (2015)
			SARS-CoV-2	2.12/N.D.	35.53	16.76		Phase III: NCT04382846, NCT04392427; phase IV: NCT04498936, NCT04406246; …	Wang et al. (2020b)

*Note: N.D. not determined. # pg/ml; * IU/ml for IFN unit.*

concerned (Borba et al., 2020; Cortegiani et al., 2020), and recent clinical studies (including WHO Solidarity trial) indicate that CQ or HCQ has little efficacy for COVID-19 (Boulware et al., 2020).

Camostat or Nafamostat Mesylate (TMPRSS2 Inhibitor)

Camostat and nafamostat are serine protease inhibitors that inhibit the transmembrane protease, serine 2 (TMPRSS2). Camostat is approved in Japan for the treatment of postoperative reflux esophagitis and chronic pancreatitis, while nafamostat is approved for pancreatitis, an anticoagulant in patients with disseminative blood vessel coagulation, hemorrhagic lesions, and hemorrhagic tendencies (Jia et al., 2005; Maruyama et al., 2011).

Camostat and nafamostat exhibit effectiveness against a broad spectrum of viruses from different families including IAV (Hosoya et al., 1992; Hosoya et al., 1993; Lee et al., 1996), myxoviruses (Hosoya et al., 1992), DENV (Rathore et al., 2019), MERS-CoV (Shirato et al., 2013), SARS-CoV (Kawase et al., 2012), and SARS-CoV-2 (Hoffmann et al., 2020b) (**Table 4**). Particularly, camostat and nafamostat are effective to inhibit type A or B IAV replication *in vitro* at a micromolar level, while showing no efficacy against other respiratory viruses tested including RSV and parainfluenza virus (Hosoya et al., 1992). Additionally, camostat mesylate at an ED50 (the survival rate of influenza virus-infected chick embryos by 50%) of 0.8 μg/g can increase the survival rate of influenza virus-infected chick embryos (Lee et al., 1996). The mechanism of camostat antiviral activity involves the inhibition of hemagglutinin (HA) cleavage, which is essential for the process of IAV infection and is achieved intracellularly or extracellularly by host proteases like TMPRSS2 (Yamaya et al., 2015).

SARS-CoV and SARS-CoV-2 both use angiotensin-converting enzyme 2 (ACE2) as a receptor, whereas MERS-CoV utilizes DDP4 as the receptor for entry (Li et al., 2003; Raj et al., 2013; Lan et al., 2020). These three coronaviruses all use two mechanisms to enter cells. One involves the direct membrane fusion at the cell surface after the virions binding to receptors, the membrane fusion is triggered by TMPRSS2 serine protease to generate a cleaved form of spike (S) protein for fusion step (Kawase et al., 2012; Shirato et al., 2013; Yamamoto et al., 2016; Hoffmann et al., 2020a). Alternatively, these viruses enter cells through the endocytic pathway in the absence of TMPRSS2, involving the cleavage and priming of S protein by cysteine protease cathepsin B/L in acidic endosomes (Simmons et al., 2005; Qian et al., 2013; Hoffmann et al., 2020a). Inhibition of both TMPRSS2 serine protease and cathepsin B/L cysteine protease activities are required for full blockade of the above coronavirus infection (Kawase et al., 2012; Hoffmann et al., 2020a), while TMPRSS2 inhibition by camostat or nafamostat only results in partial impairment in virus entry (Kawase et al., 2012; Shirato et al., 2013). Strikingly, camostat at a dose of 30 mg/g shows antiviral efficacy by improving the survival rate in a lethal SARS-CoV-infected mouse model; however, a cysteine protease inhibitor SMDC256160 at a higher dose of 50 mg/g is no effective (Zhou et al., 2015). The result suggests that TMPRSS2 rather than cathepsin B/L facilitates the spread of SARS-CoV in the infected mice. It would be of interest to evaluate the treatment efficacy of camostat or nafamostat for SARS-CoV-2 infection, and multiple clinical studies have been available for camostat (phase I/II NCT04321096; phase I/II NCT04435015; phase II NCT04353284; phase II NCT04374019; phase II NCT04470544; phase II/III NCT04455815; phase III NCT04355052; phase IV NCT04338906) and nafamostat (phase II/III NCT04352400; phase II/III NCT04418128; phase II/III NCT04473053).

HTRA Targeting Virus Replication Step

After the viral genome is uncoated from nucleocapsid, viral genome replication and protein translation occur. Positive-sense RNA viruses, for instance, coronaviruses and flaviviruses, directly use the viral genome as a template for viral protein translation using host machinery. Negative-sense RNA viruses like filoviruses and myxoviruses, need to generate positive-sense RNA by the virally encoded polymerase, and then protein translation is initiated. Retrovirus and HBV replication involve one additional step, copying RNA to DNA by using virally encoded reverse transcriptase. DNA viruses need to use a host RNA polymerase to generate RNA from the viral DNA genome for protein translation. A number of viruses replicate in specific compartments, so-called replication organelles, in the cytoplasm, involving the aberrant lipid-rich membrane rearrangement (de Wilde et al., 2018). Specifically, some flaviviruses or alphaviruses replicate on an architecture composed of single-membrane spherules (den Boon and Ahlquist, 2010); while coronaviruses or picornaviruses form double-membrane vesicles as replicase sites (de Wilde et al., 2013; van der Schaar et al., 2016). To facilitate viral genome amplification, a variety of host proteins or related pathways are required to generate a favorable environment for virus production. These host proteins or pathways that interact with viral proteins are ideal host-targeting antivirals with a potential comprehensive antiviral efficacy.

Statins (HMG-CoA Reductase Inhibitors)

Statins are reversible inhibitors of 3-hydroxy-3-methylglutaryl-CoA (HMG-CoA) reductase, a rate-limiting enzyme involved in cholesterol biosynthesis. The statins are clinically approved to reduce cholesterol levels to prevent primary and secondary cardiovascular diseases. There are various forms of statins, which include lovastatin, atorvastatin, fluvastatin, pitavastatin, pravastatin, rosuvastatin, and simvastatin. Simvastatin is on the list of the WHO's essential medicines. Statins have been reported to inhibit a panel of disparate viruses including the viruses within the family *Flaviviridae* (HCV, DENV, and ZIKV) (Ye et al., 2003; Soto-Acosta et al., 2017; Españo et al., 2019), HIV (Amet et al., 2008), HBV (Okuyama-Dobashi et al., 2015), MV (Robinzon et al., 2009), EBOV (Shrivastava-Ranjan et al., 2018), RSV (Gower and Graham, 2001), EBV (Katano et al., 2004; Cohen, 2005), PRV (Desplanques et al., 2010), SFTSV (Urata et al., 2018), and parainfluenza (Bajimaya et al., 2017), because cholesterol biosynthesis is required for the replication of these viruses.

Statins efficiently inhibit flaviviral replication either in cell cultures or in animal models. Lovastatin impairs HCV RNA replication by blocking geranylgeranylation of a host protein required for HCV replication. Statins inhibit infectious ZIKV

production as well as virus spread, possibly through the inhibition at either the early stage and the post-entry steps (Españo et al., 2019). Lovastatin impairs DENV replicase complex formation or virus assembly (Martinez-Gutierrez et al., 2011; Soto-Acosta et al., 2017). In addition, lovastatin, either prophylactically or even 48 hr post-infection significantly prolongs the survival rate of DENV-infected mice (Martinez-Gutierrez et al., 2014). Lovastatin is able to inhibit HIV reverse transcriptase activity (Mazière et al., 1994), HIV attachment (Giguère and Tremblay, 2004), or HIV virion release (Amet et al., 2008). However, drug-drug interactions are reported to exist for statins and viral protease inhibitors like HCV NS3/4A antagonists or HIV protease inhibitors (Busti et al., 2004; Chauvin et al., 2013). Thus, the efficacy of statins against Flavivirus or HIV infection in the real world needs to be further assessed.

Negative strand RNA viruses are susceptible to statins. Lovastatin shows antiviral potency in RSV-infected mice prophylactically and prevents the illness-associated weight loss (Gower and Graham, 2001), which is consistent with the observation that RSV induces HMG-CoA reductase activity and lovastatin is able to inhibit RSV replication *in vitro* (Ravi et al., 2013b). Lovastatin impairs coxackie virus B3 infection through downregulating coxsackie and adenovirus receptor expression (Werner et al., 2014). Lovastatin inhibits hPIV assembly and release but no other steps (Bajimaya et al., 2017). Statins are capable of impairing EBOV glycoprotein processing and infectious EBOV production and the glycoprotein-induced attachment (Hacke et al., 2015; Shrivastava-Ranjan et al., 2018). Retrospective clinical studies found that statins may help improve the outcome in hospitalized flu patients (Rothberg et al., 2012), although no effect was observed in IAV-infected rodent models (Kumaki et al., 2012; Belser et al., 2013; Glück et al., 2013).

Statins may benefit COVID-19 patients according to a retrospective study in 13,981 COVID-19 patients (Zhang et al., 2020). Currently, at least eight clinical trials are being on the way to continue the investigation into the efficacy of statins for COVID-19 (NCT04333407; phase II NCT04348695; phase II NCT04380402; phase II/III NCT04466241; phase III NCT04486508; phase III NCT04472611; phase III NCT04343001; phase IV NCT02735707).

Digoxin (Ion Pump Modulator)

Digoxin is a cardiac glycoside or cardiotonic steroid, on the WHO's list of essential medicines. Digoxin has been used to treat certain heart dysfunctions including atrial fibrillation, and other heart failures (Gheorghiade et al., 2006). Digoxin has been shown to block the Na^+/K^+-ATPase with an inhibitory potency around 100–200 nM (Noel et al., 2018), resulting in elevated intracellular Na^+ level, and subsequent Ca^{2+} level *via* the sodium-calcium exchanger. Digoxin and its analogs are reported to inhibit a global type of viruses, including dsDNA virus adenovirus (Grosso et al., 2017) and HSV (Dodson et al., 2007), retrovirus HIV (Wong et al., 2018), HBV (Okuyama-Dobashi et al., 2015), positive-sense alphavirus CHIKV, SINV, and RRV (Ashbrook et al., 2016), negative-sense enveloped RNA virus VSV, dsRNA naked virus reovirus (Ashbrook et al., 2016), RSV (Norris et al., 2018), arenaviruses including LCMV, LASV, and JUNV (Iwasaki et al., 2018), filovirus EBOV (Du et al., 2020), and coronaviruses (Burkard et al., 2015) (**Table 4**).

Cardiac glycoside efficiently inhibits DNA virus replication. Digoxin or ouabain exhibits herpes virus, such as HSV and HCMV, at the immediate-early or early gene expression stage, the antiviral activity replies on the inhibition in Na^+/K^+-ATPase activity (Dodson et al., 2007; Su et al., 2008; Kapoor et al., 2012), Besides, digoxin also reportedly inhibits HSV release step (Su et al., 2008). Digoxin also inhibits HAdV DNA synthesis (Grosso et al., 2017).

Other cardiac glycosides but not digoxin are able to inhibit HBV infection *in vitro,* possibly through blocking HBV preS1 protein binding to its receptor NTCP (Okuyama-Dobashi et al., 2015). Digoxin inhibits HIV protein expression in peripheral blood mononuclear cells, by a mechanism involving the impaired activity of the CLK family of SR protein kinases (Wong et al., 2013), or the modulation of MEK1/2-ERK1/2 signaling (Wong et al., 2018). In addition, digoxin may also negatively affect HIV integration in T cells (Zhyvoloup et al., 2017). As digoxin exhibits anti-HIV activity with an excellent EC50 (1.1–1.3 nM) at which it is far below the concentration in clinical use, cardiac glycosides merit further investigation to validate the efficacy for HIV treatment.

Digoxin and ouabain at nanomolar inhibit JEV infection in multiple cell culture systems, and ouabain protects against the JEV infection-induced lethality in mice (Guo et al., 2020). The inhibitory mechanism of digoxin or ouabain against (+) ssRNA virus infection may involve impaired RNA replication or virus entry (Ashbrook et al., 2016; Guo et al., 2020).

Na^+/K^+-ATPase is implicated in the entry process of coronaviruses including MHV and FIPV, cardiac glycosides like ouabain or bufalin inhibit MHV, FIPV, and MERS-CoV infections, by inhibiting virus entry and membrane fusion steps (Burkard et al., 2015). By contrast, cardiac glycosides inhibit SARS-CoV-2 at the post-entry step rather than S protein-mediated virus fusion or syncytia formation (Cho et al., 2020; Musarrat et al., 2020). Despite the excellent antiviral activity of cardiac glycosides against SARS-CoV-2 *in vitro*, no clinical trials have been initiated. One of the possible concerns is the association between digoxin use and increased all-cause mortality.

Mycophenolic Acid (MPA) (IMPDH Inhibitor)

MPA, also called mycophenolate, is an immunosuppressant approved to prevent transplant organ rejection and to treat Crohn's disease (van Gelder and Hesselink, 2015). MPA is a reversible, non-competitive inhibitor of IMPDH, which is the rate-limiting enzyme for the *de novo* synthesis of guanosine nucleotides that are substrates for DNA or RNA synthesis. MPA is more potent to inhibit type II than type I IMPDH enzyme, the former type expresses in activated lymphocytes, while the latter one in other most cells (Allison and Eugui, 2000). DNA or RNA virus replication replies on host guanosine pool, thus, MPA shows a broad spectrum antiviral activity against a variety of viruses, including HIV (Chapuis et al., 2000), HEV (Wang et al., 2014), HBV (Gong et al., 1999), BK

polyoma virus (Acott et al., 2009), HCV and flaviviruses (DENV, WNV, JEV, and ZIKA) (Diamond et al., 2002; Morrey et al., 2002; Henry et al., 2006; Sebastian et al., 2011; Ye et al., 2012; Barrows et al., 2016; Adcock et al., 2017), orthobunyaviruses (Guama and Tacaiuma viruses) (Livonesi et al., 2007), orthopoxviruses like Vaccinia virus (VacV) and cowpox (Smee et al., 2001), rotavirus (Chan et al., 2013), SINV (Scheidel and Stollar, 1991), IAV (To et al., 2016; Cho et al., 2017; Hui et al., 2018), and MERS-CoV(Chan et al., 2013) (**Table 4**).

MPA displays anti-HIV activity both *in vitro* and in HIV patients (Margolis et al., 1999; Chapuis et al., 2000), and a phase II clinical study (NCT03262441) is currently under investigation. Additionally, MPA potentiates the antiviral effect of reverse transcriptase inhibitors such as abacavir (Margolis et al., 1999). The antiviral mechanisms involve the depleted guanosine pool, as well as the induction of T cell apoptosis (Chapuis et al., 2000).

MPA is also effective for HBV, at 31.2 μM (10 μg/ml, the therapeutic concentration in serum for immunosuppressive effect) in primary hepatocytes drastically reduces the secretion of HBV DNA and HBsAg, as well as the intracellular cccDNA level (Gong et al., 1999). Moreover, MPA and RBV, another IMPDH inhibitor, enhance the anti-HBV activity of nucleoside analogs including entecavir (Ying et al., 2000; Ying et al., 2007).

Although MPA shows anti-HCV potency *in vitro* or a mouse model (Henry et al., 2006; Pan et al., 2012; Ye et al., 2012), it fails to show antiviral efficacy in a double-blinded and placebo-controlled clinical study (Firpi et al., 2003). MPA presents anti-JEV activity *in vitro* with an EC50 of 9.68 μM (3.1 μg/ml) and up to 75% protection against the lethal challenge of JEV *in vivo* (Sebastian et al., 2011). MPA effectively dampens DENV replication with an EC50 of 0.3 μM *in vitro* (Diamond et al., 2002; Manchala et al., 2019), and similarly inhibits ZIKV with the EC50 between 0.1 and 1 μM (Barrows et al., 2016), although high cytotoxicity was also observed (Adcock et al., 2017).

MPA inhibits human and avian-originated IAV *in vitro*, including IAV-A (H1N1) (pdm09/H1/415, EC_{50} = 1.51 μM), A (H3N2), A (H5N1) (Vietnam/1194/2004, EC_{50} = 0.94 μM), A (H7N9) and IAV-B (To et al., 2016; Cho et al., 2017). MPA also shows efficacy in an H5N1-infected mouse model (Cho et al., 2017).

After a repurposed drug screening, MPA exhibited good anti-MERS-CoV activity with an EC50 (0.53 μM), EC90 (8.15 μM), and high SI value (>195.12) (Chan et al., 2013). MPA in combination with IFN-β further lowers the EC50 by 1–3 times (Chan et al., 2013). Contrarily, IMPDH inhibitors including MPA slightly enhance SARS-CoV replication in the lungs (Barnard et al., 2006b). MPA enables to inhibit SARS-CoV-2 infection in different cell cultures (Kato et al., 2020; Han et al., 2021), however, no clinical evidence is available to show the efficacy of MPA in COVID-19 patients.

Cyclosporine A (CsA) (Cyclophilin Inhibitor)

CsA is an immunosuppressant firstly isolated from fungus and has been approved to treat and prevent graft-versus-host disease in bone marrow transplantation, to prevent rejection of kidney, heart, and liver, or to treat autoimmune diseases like rheumatoid arthritis and psoriasis transplants (Griffiths and Voorhees, 1990; Faulds et al., 1993). CsA was recently approved as eye drops to treat dry eye disease (Mandal et al., 2019). CsA is on the WHO's list of essential medicines. The immunomodulatory mechanism of CsA involves its binding to peptidylprolyl isomerase cyclophilin A (CyPA). The CsA-CyPA complex is able to inhibit the calcineurin phosphatase activity, the nuclear translocation of the nuclear factor of activated T cells (NF-AT), eventually block the transcription of cytokines and T cell activation (Matsuda and Koyasu, 2000). CsA and its analog like alisporivir (ALV) have shown a broad-spectrum antiviral capacity against viruses, including *Flaviviridae* members HCV and ZIKV (Watashi et al., 2003; Henry et al., 2006; Koizumi et al., 2017; Dong et al., 2019), hepatotropic viruses HBV and HEV (Wang et al., 2014; Watashi et al., 2014), HIV (Keckesova et al., 2006; Saini and Potash, 2006; Nicolás et al., 2017), coronavirus SARS-CoV, SARS-CoV-2, CoV-NL63, and MERS-CoV(de Wilde et al., 2011; Pfefferle et al., 2011; Tanaka et al., 2013; Carbajo-Lozoya et al., 2014; Guisado-Vasco et al., 2020), rotavirus (Shen et al., 2015; Yin et al., 2016b), norovirus (Dang et al., 2017), DNA virus CMV (Abdullah et al., 2018), and IAV (Hamamoto et al., 2013; Ma et al., 2016).

CsA inhibits HCV RNA replication and the antiviral capacity seems independent of its immunosuppressive effect (Watashi et al., 2003; Henry et al., 2006), as ALV, a non-immunosuppressive CsA analog, maintains the anti-HCV capacity (Crouchet et al., 2018). ALV in follow-up clinical trials (phase I to III) shows a higher sustained virological response rate than IFN and ribavirin do (Stanciu et al., 2019). However, serious side effects were more frequent in ALV-treated patients, the clinical studies were then halted. CyPA interacts with flavivirus proteins and is required for viral replication (Chatterji et al., 2009; Chatterji et al., 2010), and CsA is capable of inhibiting the infections of DENV, WNV, and YFV(Qing et al., 2009). Interestingly, CsA shows strong adulticidal activity against mosquitos, although no direct anti-ZIKV activity was found in a mosquito cell culture system (Dong et al., 2019).

CsA displays anti-HBV activity *in vitro*, and the inhibition is independent of CyPA or calcineurin (Watashi et al., 2014; Phillips et al., 2015). The inhibitory mechanism involves the block of the interactions of NTCP, the HBV entry receptor, with HBV large envelope protein (Watashi et al., 2014). CsA derivatives that maintain the anti-HBV activities but lose the impact on NTCP transporter activity have been successfully developed (Shimura et al., 2017). CyPA interacts with IAV matrix (M) protein (Liu et al., 2009), but CsA inhibits IAV or IBV infection at the steps of viral replication, IAV protein translation, or virus assembly/release, in a CyPA-independent manner (Liu et al., 2012; Hamamoto et al., 2013; Ma et al., 2016). Further preclinical and clinical studies for either virus infection are warranted later.

CyPA specifically binds to the nucleocapsid and Nsp1 proteins of SARS-CoV and is detectable in the SARS-CoV particles (Chen et al., 2005; Pfefferle et al., 2011). CsA inhibits diverse coronaviruses including SARS-CoV, MERS-CoV, HCoV-229E, HCoV-NL63, and MHV (de Wilde et al., 2011; Pfefferle et al., 2011; de Wilde et al., 2013). 16 μM CsA drastically inhibits infectious SARS-CoV production by >3log, although CsA less

than 4 μM seems to have pro-viral activity (de Wilde et al., 2011). CsA inhibits SARS-CoV RNA replication or post-entry steps (Pfefferle et al., 2011; Softic et al., 2020), and the early step is also possibly affected (de Wilde et al., 2011). Despite the encouraging results in cell culture systems, treatment with RBV and ALV does not protect from SARS-CoV infection in a mouse model (de Wilde et al., 2017). 9 μM CsA treatment completely blocks the MERS-CoV-induced cytopathology in Vero cells, and CsA in combination with IFN-α display more effective anti-MERS-CoV activity (de Wilde et al., 2013; Li et al., 2018). ALV displays antiviral activity against SARS-CoV-2 with an EC50 of 0.46 μM *in vitro* (Softic et al., 2020), and CsA in a cohort study showed a 4-fold decrease in observed mortality in hospitalized COVID-19 patients (Guisado-Vasco et al., 2020). Currently, at least four clinical trials have been in the process to evaluate the efficacy of CsA or ALV to treat COVID-19 (NCT04451239; phase I NCT04412785; phase II NCT04492891; phase IV NCT04392531). More results will be available soon.

HTRA Targeting Virus Assembly/Release Step

After a sufficient viral structure protein pool is available, viral assembly, a dynamic process driven by programmed sequential reactions is initiated, which involves interactions between the viral genomes and viral capsid proteins, and virus-host protein associations. The newly assembled nonenveloped virions disrupt the cytoskeleton to facilitate dispersal of viral progenies, whilst enveloped viruses gain their envelope from an intracellular organelle or plasma membrane to exit the cells by a budding or exocytosis process, albeit the dividing line between nonenveloped and enveloped viruses has become blurred given that non-lytic spread mechanisms have been identified for HAV, HEV, and some enteroviruses (Feng et al., 2013; Bird et al., 2014; Chen et al., 2015; Yin et al., 2016a). The host endosomal sorting complexes required for transport (ESCRT) and autophagy machinery have emerged roles to mediate the virus release despite the envelopment.

Imatinib (STI-571) (c-Abl Inhibitors)

Imatinib is a 2-phenyl amino pyrimidine derivative that functions as a specific inhibitor of many tyrosine kinases, including c-Abl, c-Kit, and platelet-derived growth factor receptor. It replaces ATP in the enzymatically active site, leading to the decreased activity of these tyrosine kinases. Imatinib is a medication used to treat cancer including chronic myelogenous leukemia, acute lymphocytic leukemia, and gastrointestinal stromal tumors. Imatinib is on the list of WHO's essential medicines. c-Abl is also implicated in the lifecycle of different viruses, and imatinib has been reported to inhibit infection of EBOV, DENV, MERS-CoV, SARS-CoV, coxsackievirus, and VacV (**Table 4**).

c-Abl1 inhibitor imatinib or nilotinib drastically decreases the budding or release of EBOV, as the inhibition of phosphorylation of the viral matrix protein VP40 (Garcia et al., 2012). Similarly, imatinib significantly dampens the extracellular enveloped VacV virion release without affecting cell-associated enveloped virions, and imatinib shows prophylactical or therapeutic antiviral effect in VacV-infected mice (Reeves et al., 2011). In addition, imatinib significantly inhibits DENV replication at the post-entry steps, reducing the production of infectious DENV (Clark et al., 2016).

Interestingly, imatinib appears to inhibit the entry step of group B coxsackieviruses (CVBs), blocking the aggregation of virions to the tight junction, where the virions subsequently initiate the internalization step to finally surmount the epithelial barrier (Coyne and Bergelson, 2006).

Imatinib or other c-Abl inhibitors nilotinib and dasatinib are able to inhibit MERS-CoV or SARS-CoV infection (Dyall et al., 2014). Specifically, imatinib and dasatinib show effectiveness against both viruses, while nilotinib is only effective for SARS-CoV (Dyall et al., 2014). Recently, imatinib was reported to inhibit SARS-CoV-2 in stem cell-differentiated lung organoids (EC50 = 4.86 μM) (Han et al., 2021). The detailed mechanism for this inhibition warrants further investigation. Currently, at least five clinical trials including three phase III studies (NCT04394416; NCT04422678; NCT04356495) have been carried out to investigate the treatment efficacy of imatinib for COVID-19.

Other Agents

Other agents that are also capable of inhibiting virus assembly/release include statins, which, as mentioned previously, inhibits virion assembly of DENV or parainfluenza, and impairs infectious HIV or EBOV release (Amet et al., 2008; Martinez-Gutierrez et al., 2011; Bajimaya et al., 2017; Shrivastava-Ranjan et al., 2018). Another example is nitazoxanide, exhibiting multiple targeting features, can inhibit assembly/release of IAV, rotavirus, and possibly paramyxoviruses (Rossignol et al., 2009; La Frazia et al., 2013; Piacentini et al., 2018).

Repurposed Agents With Multiple Targets

Some repurposed agents have more than three potential targets, either viral or host proteins. The most documented example is IFN-α/β, which is a crucial member of innate immunity, the first line to defend pathogens including viruses. Another instance is nitazoxanide, which has shown a very broad antiviral efficiency, representing divergent antiviral mechanisms for different viruses.

Interferon

Almost all viruses can induce interferon response that is mediated by different sensors including cGAS for DNA viruses; RIG-I, MDA5 for RNA viruses (Tan et al., 2018). These pattern recognition receptors recognize the invaders containing pathogen-associated molecular patterns to induce IFN, which in turn secretes out of cells and binds to receptors to induce the activation of JAK-STAT pathway. As a result, a broad spectrum of interferon-stimulated genes (ISG) is induced and exert antiviral effects through different mechanisms (Liu et al., 2013; Bailey et al., 2014; Li et al., 2017a). Clearly, the ISG network is diverse and complicated, each ISG functions in concert with others, in a combinatorial or even redundant way to combat virus infection. There are three classes of IFNs, type I, type II, and type III, distinguished by their different receptors. The type I IFNs include IFN-α, IFN-β, IFN-ε, IFN-κ, and IFN-ω; type II IFN comprises IFN-γ; and type III IFNs refer to IFN-λ1 (IL-29), IFN-λ2 (IL-28A), IFN-λ3 (IL-28B), and IFN-λ4 (Stanifer et al., 2019). IFN-α

has been used for clinical purposes against HCV and HBV for a long time, and IFN-β is approved to treat multiple sclerosis (Rice et al., 2001; Heim, 2013; Ezzikouri et al., 2020).

IFNs have been explored clinically to treat different virus infections including EBOV (Rhein et al., 2015; Konde et al., 2017; Fanunza et al., 2018; Lee et al., 2019), DENV (Pires de Mello et al., 2018a), ZIKA (Ngono and Shresta, 2018; Caine et al., 2019), MERS-CoV, SARS-CoV, and SARS-CoV-2 (Cinatl et al., 2003; Tan et al., 2004; Kindler et al., 2016; Haji Abdolvahab et al., 2021). A clinical study suggests that IFN-β-1a facilitates EBOV viral clearance and enhances survival rate (Konde et al., 2017), consistent with cell culture data that EBOV is sensitive to IFN-α or β (McCarthy et al., 2016). AG129 mice that are deficient in interferon a/β/γ signaling are more susceptible to all four serotypes of DENV (Sarathy et al., 2015; Milligan et al., 2017), suggesting the importance of IFN for DENV control. Similarly, IFN-α/β receptor (IFNAR)-deficient mice are highly susceptible to ZIKV infection (Lazear et al., 2016), and IFN-α considerately inhibits ZIKV infection *in vitro* alone or in combination with favipiravir (Pires de Mello et al., 2018b). Moreover, IFN-λ protects the female reproductive tract against ZIKV infection in mice (Caine et al., 2019).

IFNs enable to inhibit SARS-CoV or MERS-CoV in cell cultures (Cinatl et al., 2003; Falzarano et al., 2013a), and show potency in macaques infected with SARS-CoV or MERS-CoV (Haagmans et al., 2004; Falzarano et al., 2013b). A retrospective cohort study in MERS-CoV patients shows that IFN-α-2a plus RBV results in a significant survival rate at 14 days than control supportive care (Omrani et al., 2014). However, the same treatment regimen did not benefit MERS patients in another clinical study (Al-Tawfiq et al., 2014). A preliminary, uncontrolled study shows that IFN plus corticosteroids are associated with better disease outcomes in SARS patients compared to corticosteroid treatment alone (Loutfy et al., 2003). Interestingly, a dual role of IFN for SARS pathology in mice was recently reported, while delayed IFN response correlates with severe lung immunopathology and reduced survival rate, early IFN administration ameliorates immunopathology (Channappanavar et al., 2016). IFN-α or IFN-β efficiently inhibits SARS-CoV-2 infection *in vitro* (EC50 1.35 and 0.76 IU/ml, respectively) (Mantlo et al., 2020). However, the Solidarity clinical trials launched by WHO concluded that IFN does not affect overall mortality in hospitalized COVID-19 patients. In spite of that, multiple clinical studies are still in progress to evaluate the efficacy of IFNA for COVID-19 including four phase III (NCT04492475; NCT04320238; NCT04324463; NCT04315948) and five phase IV (NCT04350671; NCT04254874; NCT04350684; NCT04291729; NCT02735707) trials.

Nitazoxanide

Nitazoxanide is licensed in the United States to treat parasite infection-induced diarrhea (Ortiz et al., 2001) due to the interference with the pyruvate: ferredoxin oxidoreductase (PFOR) enzyme-dependent electron transfer reaction which is essential to anaerobic energy metabolism. Nitazoxanide reduces IAV-induced duration of clinical symptoms and viral shedding in a double-blind, randomized, and placebo-controlled phase IIb/III clinical trial (Haffizulla et al., 2014). A phase III clinical trial (NCT01610245) is then initiated. The mechanism of action of nitazoxanide against IAV infection involves the inhibition in the maturation of viral hemagglutinin (HA) at the post-translational stage, thus impairing HA intracellular trafficking and insertion into the host plasma membrane (Rossignol et al., 2009). Besides, nitazoxanide is found to clinically effective to treat infections of adenovirus (Esquer Garrigos et al., 2018), rotavirus (Rossignol and El-Gohary, 2006; Teran et al., 2009), HBV (Rossignol and Keeffe, 2008), and HCV (Rossignol et al., 2008; Elazar et al., 2009; Rossignol et al., 2010). In addition, nitazoxanide enables to inhibition of other viral infections *in vitro* including HIV (Tan et al., 2012), JEV (Shi et al., 2014), ZIKV (Cao et al., 2017; Li et al., 2017c), feline calicivirus (Fumian et al., 2018), rubella virus (Perelygina et al., 2017), CHIKV(Wang et al., 2016c), paramyxovirus SeV and RSV(Piacentini et al., 2018), coronavirus MHV, MERS-CoV, and SARS-CoV-2 (Cao et al., 2015; Rossignol, 2016; Wang et al., 2020b).

Different antiviral mechanisms are involved for nitazoxanide in the context of different virus infections. Nitazoxanide prohibits SeV or RSV fusion step after entry into cells (Piacentini et al., 2018), HBV DNA replication and viral protein synthesis (Korba et al., 2008), viral RNA replication or protein processing of HCV, ZIKV, or MHV (Rossignol and Keeffe, 2008; Cao et al., 2015; Li et al., 2017c), viral morphogenesis of IAV or rotavirus (Rossignol et al., 2009; La Frazia et al., 2013). Nitazoxanide also triggers innate immune genes, like IRF1, RIG-I, or PKR, to combat norovirus or EBOV replication (Dang et al., 2018; Jasenosky et al., 2019).

HBV or HCV is susceptible to nitazoxanide treatment. An open-label small-scale clinical trial shows the preliminary efficacy of nitazoxanide in treating chronic hepatitis B (Rossignol and Keeffe, 2008). A further phase II clinical study (NCT03905655) is currently instigated. Clinical trials in hepatitis C patients show the improved SVR rate when treated alone or in combination with IFN and/or RBV (Rossignol et al., 2008; Elazar et al., 2009; Rossignol et al., 2010).

Nitazoxanide has potent antiviral activity against coronavirus. Nitazoxanide emerges as one of the most potent antivirals against MHV after drug repurposing screening (Cao et al., 2015), similar activity is observed for MERS-CoV (Rossignol, 2016) or SARS-CoV-2 (Wang et al., 2020b). A preliminary clinical study suggests the potential efficacy of nitazoxanide for COVID-19 treatment (Rocco et al., 2021). Currently, at least 18 clinical trials have been launched to test the antiviral efficacy in COVID-19 patients including five phase III (NCT04382846; NCT04392427; NCT04343248; NCT04359680; NCT04486313) and three phase IV (NCT04498936; NCT04406246; NCT04341493) clinical studies (**Table 4**).

CHALLENGES AND PERSPECTIVE

Currently, most of the approved antivirals are used to treat infections of HIV, HCV, HBV, and IAV, very few novel antivirals for recently emerging viruses including SARS-CoV-2, MERS-CoV, EBOV, ZIKV, and DENV. Drug repurposing has

played a crucial role in pushing the approved or investigational therapeutics through clinical trials, because of higher success rate, less investment, and faster approval.

Drug repurposing is not risk-free, the success rate is reported around 30%. There are still a lot of hurdles before the repurposed drug is approved. Even though repurposed drugs could be exempted from phase I clinical trial, which mainly focuses on the drug safety evaluation, drug safety still represents one of the biggest concerns for repurposing. For instance, the safety of the drug that has been evaluated in a group of participants for the original indication does not necessarily guarantee safety in another group of people. In this scenario, drug safety may need to re-evaluate. Moreover, the dosing regimen of the repurposed drug validated previously may be different in new indications. A major obstacle to successful repurposing attributes to the higher effective concentrations in the new indication than those in the original indications. It suggests that greater harm and less benefit may be instigated. To overcome the obstacle, cocktail-based combinatorial regimens that contains at least two repurposed drugs targeting different steps of the viral lifecycle would be beneficial. In addition, drug-drug interactions may be another challenge when a repurposed drug has to use in combination with other drugs and no drug-drug interaction data is available. Thus, drug safety issue needs to be carefully appraised and addressed if necessary.

Apart from the safety issue, the intellectual property barrier is another important issue that needs to address. Commonly, drug repurposing focuses on drugs for which the patents on the original indication have been expired. For the off-patent generic drugs, a new method-of-use patent can be obtained for the new indication. However, enforceability or market exclusivity can be a major issue, as other company-manufactured generic drugs may be prescribed as off-label use for the new indication, which would be hardly prohibited. That may reduce the profit and financial incentive for drug repurposing. The off-label use can be limited if a new formulation or dosing regimen is required for the novel indication so that it cannot be easily fulfilled with the available generic versions of the drug. On the other hand, with the appropriate licensing, repurposing of drugs that are still covered by existing patent property is also achievable, even though many repurposed uses of patent drugs have been reported in the literature, which may limit the ability to gain the new patent protection. The reliable and novel evidence to support the new indication of the repurposed drug is a necessity to obtain the granted patents. Other challenges include self-medication, misuse, drug shortage, and price hike of the drugs with potential repurposed indications (Mallhi et al., 2020a; Mallhi et al., 2020b). The misuse of repurposed drugs would be devastating and should be discouraged particularly during a pandemic. The availability and affordability of these repurposed agents should also be vigilantly monitored.

With more approaches to address the safety, efficacy, and patent issues by deploying recombination therapies and reinforcing collaboration and negotiation, drug repurposing for a novel, efficient, and broad-spectrum antiviral development would strengthen the efforts to combat the emerging and re-emerging viruses.

AUTHOR CONTRIBUTIONS

XL drafted the manuscript. TP edited and revised the manuscript. All authors reviewed and approved the final version of the manuscript for publication.

ACKNOWLEDGMENTS

We express our thanks to Mike Bray, the Editor-in-chief of the journal Antiviral Research for his constructive advice to improve the manuscript. We thank support from the 111 Project (#D18010), Infinitus China, and Guangzhou Institute of Respiratory Health Open Project (Funds provided by China Evergrande Group, Project #2020GIRHHMS01).

REFERENCES

Abdullah, A. A., Abdullah, R., Nazariah, A. Z., Balakrishnan, K. N., Firdaus, J. A. F., Jamilu, A. B., et al. (2018). Cyclophilin A as a Target in the Treatment of Cytomegalovirus Infections. *Antivir. Chem. Chemother.* 26, 2040206618811413. doi:10.1177/2040206618811413

Acott, P., O'Regan, P. A., and Crocker, J. F. (2009). Suppression of Early and Chronic BK Polyoma Virus Replication by Mycophenolic Acid in Vero Cells. *Transpl. Int.* 22 (2), 225–231. doi:10.1111/j.1432-2277.2008.00766.x

Adcock, R. S., Chu, Y. K., Golden, J. E., and Chung, D. H. (2017). Evaluation of Anti-zika Virus Activities of Broad-Spectrum Antivirals and NIH Clinical Collection Compounds Using a Cell-Based, High-Throughput Screen Assay. *Antivir. Res* 138, 47–56. doi:10.1016/j.antiviral.2016.11.018

Al-Tawfiq, J. A., Momattin, H., Dib, J., and Memish, Z. A. (2014). Ribavirin and Interferon Therapy in Patients Infected with the Middle East Respiratory Syndrome Coronavirus: an Observational Study. *Int. J. Infect. Dis.* 20, 42–46. doi:10.1016/j.ijid.2013.12.003

Allison, A. C., and Eugui, E. M. (2000). Mycophenolate Mofetil and its Mechanisms of Action. *Immunopharmacology* 47 (2–3), 85–118. doi:10.1016/s0162-3109(00)00188-0

Amet, T., Nonaka, M., Dewan, M. Z., Saitoh, Y., Qi, X., Ichinose, S., et al. (2008). Statin-induced Inhibition of HIV-1 Release from Latently Infected U1 Cells Reveals a Critical Role for Protein Prenylation in HIV-1 Replication. *Microbes Infect.* 10 (5), 471–480. doi:10.1016/j.micinf.2008.01.009

Anand, K., Ziebuhr, J., Wadhwani, P., Mesters, J. R., and Hilgenfeld, R. (2003). Coronavirus Main Proteinase (3CLpro) Structure: Basis for Design of Anti-SARS Drugs. *Science* 300 (5626), 1763–1767. doi:10.1126/science.1085658

Ashbrook, A. W., Lentscher, A. J., Zamora, P. F., Silva, L. A., May, N. A., Bauer, J. A., et al. (2016). Antagonism of the Sodium-Potassium ATPase Impairs Chikungunya Virus Infection. *mBio* 7 (3). doi:10.1128/mBio.00693-16

Ashfaq, U. A., Javed, T., Rehman, S., Nawaz, Z., and Riazuddin, S. (2011). Lysosomotropic Agents as HCV Entry Inhibitors. *Virol. J.* 8, 163. doi:10.1186/1743-422x-8-163

Bailey, C. C., Zhong, G., Huang, I. C., and Farzan, M. (2014). IFITM-family Proteins: The Cell's First Line of Antiviral Defense. *Annu. Rev. Virol.* 1, 261–283. doi:10.1146/annurev-virology-031413-085537

Bajimaya, S., Hayashi, T., Frankl, T., Bryk, P., Ward, B., and Takimoto, T. (2017). Cholesterol Reducing Agents Inhibit Assembly of Type I Parainfluenza Viruses. *Virology* 501, 127–135. doi:10.1016/j.virol.2016.11.011

Barnard, D. L., Day, C. W., Bailey, K., Heiner, M., Montgomery, R., Lauridsen, L., et al. (2006b). Enhancement of the Infectivity of SARS-CoV in BALB/c Mice by IMP Dehydrogenase Inhibitors, Including Ribavirin. *Antivir. Res.* 71 (1), 53–63. doi:10.1016/j.antiviral.2006.03.001

Barnard, D. L., Day, C. W., Bailey, K., Heiner, M., Montgomery, R., Lauridsen, L., et al. (2006a). Evaluation of Immunomodulators, Interferons and Known *In Vitro* SARS-coV Inhibitors for Inhibition of SARS-coV Replication in BALB/c Mice. *Antivir. Chem. Chemother.* 17 (5), 275–284. doi:10.1177/095632020601700505

Barrows, N. J., Campos, R. K., Liao, K. C., Prasanth, K. R., Soto-Acosta, R., Yeh, S. C., et al. (2018). Biochemistry and Molecular Biology of Flaviviruses. *Chem. Rev.* 118 (8), 4448–4482. doi:10.1021/acs.chemrev.7b00719

Barrows, N. J., Campos, R. K., Powell, S. T., Prasanth, K. R., Schott-Lerner, G., Soto-Acosta, R., et al. (2016). A Screen of FDA-Approved Drugs for Inhibitors of Zika Virus Infection. *Cell Host Microbe* 20 (2), 259–270. doi:10.1016/j.chom.2016.07.004

Beigel, J. H., Tomashek, K. M., Dodd, L. E., Mehta, A. K., Zingman, B. S., Kalil, A. C., et al. (2020). Remdesivir for the Treatment of Covid-19—Preliminary Report. *N. Engl. J. Med.* 383 (19)–18131826. doi:10.1056/NEJMoa2007764

Bekerman, E., Neveu, G., Shulla, A., Brannan, J., Pu, S. Y., Wang, S., et al. (2017). Anticancer Kinase Inhibitors Impair Intracellular Viral Trafficking and Exert Broad-Spectrum Antiviral Effects. *J. Clin. Invest.* 127 (4), 1338–1352. doi:10.1172/JCI89857

Belser, J. A., Szretter, K. J., Katz, J. M., and Tumpey, T. M. (2013). Simvastatin and Oseltamivir Combination Therapy Does Not Improve the Effectiveness of Oseltamivir Alone Following Highly Pathogenic Avian H5N1 Influenza Virus Infection in Mice. *Virology* 439 (1), 42–46. doi:10.1016/j.virol.2013.01.017

Bhattacharyya, S., Warfield, K. L., Ruthel, G., Bavari, S., Aman, M. J., and Hope, T. J. (2010). Ebola Virus Uses Clathrin-Mediated Endocytosis as an Entry Pathway. *Virology* 401 (1), 18–28. doi:10.1016/j.virol.2010.02.015

Binford, S. L., Maldonado, F., Brothers, M. A., Weady, P. T., Zalman, L. S., Meador, J. W., 3rd, et al. (2005). Conservation of Amino Acids in Human Rhinovirus 3C Protease Correlates with Broad-Spectrum Antiviral Activity of Rupintrivir, a Novel Human Rhinovirus 3C Protease Inhibitor. *Antimicrob. Agents Chemother.* 49 (2), 619–626. doi:10.1128/AAC.49.2.619-626.2005

Bird, S. W., Maynard, N. D., Covert, M. W., and Kirkegaard, K. (2014). Nonlytic Viral Spread Enhanced by Autophagy Components. *Proc. Natl. Acad. Sci. U. S. A.* 111 (36), 13081–13086. doi:10.1073/pnas.1401437111

Blanchard, E., Belouzard, S., Goueslain, L., Wakita, T., Dubuisson, J., Wychowski, C., et al. (2006). Hepatitis C Virus Entry Depends on Clathrin-Mediated Endocytosis. *J. Virol.* 80 (14), 6964–6972. doi:10.1128/JVI.00024-06

Boelaert, J. R., Sperber, K., and Piette, J. (1999). Chloroquine Exerts an Additive *In Vitro* Anti-HIV Type 1 Effect when Associated with Didanosine and Hydroxyurea. *AIDS Res. Hum. Retroviruses* 15 (14), 1241–1247. doi:10.1089/088922299310133

Borba, M. G. S., Val, F. F. A., Sampaio, V. S., Alexandre, M. A. A., Melo, G. C., Brito, M., et al. (2020). Effect of High vs. Low Doses of Chloroquine Diphosphate as Adjunctive Therapy for Patients Hospitalized with Severe Acute Respiratory Syndrome Coronavirus 2 (SARS-CoV-2) Infection: A Randomized Clinical Trial. *JAMA Netw. Open* 3 (4), e208857. doi:10.1001/jamanetworkopen.2020.8857

Bosch, B., Grigorov, B., Senserrich, J., Clotet, B., Darlix, J. L., Muriaux, D., et al. (2008). A Clathrin-dynamin-dependent Endocytic Pathway for the Uptake of HIV-1 by Direct T Cell-T Cell Transmission. *Antivir. Res* 80 (2), 185–193. doi:10.1016/j.antiviral.2008.06.004

Bossart, K. N., Wang, L. F., Flora, M. N., Chua, K. B., Lam, S. K., Eaton, B. T., et al. (2002). Membrane Fusion Tropism and Heterotypic Functional Activities of the Nipah Virus and Hendra Virus Envelope Glycoproteins. *J. Virol.* 76 (22), 11186–11198. doi:10.1128/jvi.76.22.11186-11198.2002

Boulware, D. R., Pullen, M. F., Bangdiwala, A. S., Pastick, K. A., Lofgren, S. M., Okafor, E. C., et al. (2020). A Randomized Trial of Hydroxychloroquine as Postexposure Prophylaxis for Covid-19. *N. Engl. J. Med.* 383 (6), 517–525. doi:10.1056/NEJMoa2016638

Bullard-Feibelman, K. M., Govero, J., Zhu, Z., Salazar, V., Veselinovic, M., Diamond, M. S., et al. (2017). The FDA-Approved Drug Sofosbuvir Inhibits Zika Virus Infection. *Antivir. Res* 137, 134–140. doi:10.1016/j.antiviral.2016.11.023

Burkard, C., Verheije, M. H., Haagmans, B. L., van Kuppeveld, F. J., Rottier, P. J., Bosch, B. J., et al. (2015). ATP1A1-mediated Src Signaling Inhibits Coronavirus Entry into Host Cells. *J. Virol.* 89 (8), 4434–4448. doi:10.1128/JVI.03274-14

Busti, A. J., Hall, R. G., and Margolis, D. M. (2004). Atazanavir for the Treatment of Human Immunodeficiency Virus Infection. *Pharmacotherapy* 24 (12), 1732–1747. doi:10.1592/phco.24.17.1732.52347

Caine, E. A., Scheaffer, S. M., Arora, N., Zaitsev, K., Artyomov, M. N., Coyne, C. B., et al. (2019). Interferon Lambda Protects the Female Reproductive Tract against Zika Virus Infection. *Nat. Commun.* 10 (1), 280. doi:10.1038/s41467-018-07993-2

Cai, Q., Yang, M., Liu, D., Chen, J., Shu, D., Xia, J., et al. (2020). Experimental Treatment with favipiravir for COVID-19: An Open-Label Control Study. *Engineering (Beijing)* 6 (10), 1192–1198. doi:10.1016/j.eng.2020.03.007

Cao, B., Wang, Y., Wen, D., Liu, W., Wang, J., Fan, G., et al. (2020). A Trial of Lopinavir-Ritonavir in Adults Hospitalized with Severe Covid-19. *N. Engl. J. Med.* 382 (19), 1787–1799. doi:10.1056/NEJMoa2001282

Cao, J., Forrest, J. C., and Zhang, X. (2015). A Screen of the NIH Clinical Collection Small Molecule Library Identifies Potential Anti-coronavirus Drugs. *Antivir. Res* 114, 1–10. doi:10.1016/j.antiviral.2014.11.010

Cao, R. Y., Xu, Y. F., Zhang, T. H., Yang, J. J., Yuan, Y., Hao, P., et al. (2017). Pediatric Drug Nitazoxanide: A Potential Choice for Control of Zika. *Open Forum Infect. Dis.* 4 (1), ofx009. doi:10.1093/ofid/ofx009

Carbajo-Lozoya, J., Ma-Lauer, Y., Malešević, M., Theuerkorn, M., Kahlert, V., Prell, E., et al. (2014). Human Coronavirus NL63 Replication Is Cyclophilin A-dependent and Inhibited by Non-immunosuppressive Cyclosporine A-Derivatives Including Alisporivir. *Virus. Res.* 184, 44–53. doi:10.1016/j.virusres.2014.02.010

Carro, A. C., Piccini, L. E., and Damonte, E. B. (2018). Blockade of Dengue Virus Entry into Myeloid Cells by Endocytic Inhibitors in the Presence or Absence of Antibodies. *Plos Negl. Trop. Dis.* 12 (8), e0006685. doi:10.1371/journal.pntd.0006685

Chan, J. F., Chan, K. H., Kao, R. Y., To, K. K., Zheng, B. J., Li, C. P., et al. (2013). Broad-spectrum Antivirals for the Emerging Middle East Respiratory Syndrome Coronavirus. *J. Infect.* 67 (6), 606–616. doi:10.1016/j.jinf.2013.09.029

Chan, J. F., Yao, Y., Yeung, M. L., Deng, W., Bao, L., Jia, L., et al. (2015). Treatment with Lopinavir/Ritonavir or Interferon-Beta1b Improves Outcome of MERS-CoV Infection in a Nonhuman Primate Model of Common Marmoset. *J. Infect. Dis.* 212 (12), 1904–1913. doi:10.1093/infdis/jiv392

Chan, K. S., Lai, S. T., Chu, C. M., Tsui, E., Tam, C. Y., Wong, M. M., et al. (2003). Treatment of Severe Acute Respiratory Syndrome with Lopinavir/ritonavir: a Multicentre Retrospective Matched Cohort Study. *Hong Kong Med. J.* 9 (6), 399–406.

Channappanavar, R., Fehr, A. R., Vijay, R., Mack, M., Zhao, J., Meyerholz, D. K., et al. (2016). Dysregulated Type I Interferon and Inflammatory Monocyte-Macrophage Responses Cause Lethal Pneumonia in SARS-CoV-Infected Mice. *Cell Host Microbe* 19 (2), 181–193. doi:10.1016/j.chom.2016.01.007

Chapuis, A. G., Paolo Rizzardi, G., D'Agostino, C., Attinger, A., Knabenhans, C., Fleury, S., et al. (2000). Effects of Mycophenolic Acid on Human Immunodeficiency Virus Infection *In Vitro* and *In Vivo*. *Nat. Med.* 6 (7), 762–768. doi:10.1038/77489

Chatterji, U., Bobardt, M., Selvarajah, S., Yang, F., Tang, H., Sakamoto, N., et al. (2009). The Isomerase Active Site of Cyclophilin A Is Critical for Hepatitis C Virus Replication. *J. Biol. Chem.* 284 (25), 16998–17005. doi:10.1074/jbc.M109.007625

Chatterji, U., Lim, P., Bobardt, M. D., Wieland, S., Cordek, D. G., Vuagniaux, G., et al. (2010). HCV Resistance to Cyclosporin A Does Not Correlate with a Resistance of the NS5A-Cyclophilin A Interaction to Cyclophilin Inhibitors. *J. Hepatol.* 53 (1), 50–56. doi:10.1016/j.jhep.2010.01.041

Chaudhuri, S., Symons, J. A., and Deval, J. (2018). Innovation and Trends in the Development and Approval of Antiviral Medicines: 1987-2017 and beyond. *Antivir. Res.* 155, 76–88. doi:10.1016/j.antiviral.2018.05.005

Chauvin, B., Drouot, S., Barrail-Tran, A., and Taburet, A. M. (2013). Drug-drug Interactions between HMG-CoA Reductase Inhibitors (Statins) and Antiviral Protease Inhibitors. *Clin. Pharmacokinet.* 52 (10), 815–831. doi:10.1007/s40262-013-0075-4

Chen, J., Li, Y., Lai, F., Wang, Y., Sutter, K., Dittmer, U., et al. (2020). Functional Comparison of IFN-Alpha Subtypes Reveals Potent HBV Suppression by a

Concerted Action of IFN-Alpha and -gamma Signaling. *Hepatology* 73 (2), 486–502. doi:10.1002/hep.31282

Chen, J. (2020). Pathogenicity and Transmissibility of 2019-nCoV-A Quick Overview and Comparison with Other Emerging Viruses. *Microbes Infect.* 22 (2), 69–71. doi:10.1016/j.micinf.2020.01.004

Chen, Y. H., Du, W., Hagemeijer, M. C., Takvorian, P. M., Pau, C., Cali, A., et al. (2015). Phosphatidylserine vesicles enable efficient *en bloc* transmission of enteroviruses. *Cell* 160 (4), 619–630. doi:10.1016/j.cell.2015.01.032

Chen, Z., Mi, L., Xu, J., Yu, J., Wang, X., Jiang, J., et al. (2005). Function of HAb18G/CD147 in Invasion of Host Cells by Severe Acute Respiratory Syndrome Coronavirus. *J. Infect. Dis.* 191 (5), 755–760. doi:10.1086/427811

Cho, J., Lee, Y. J., Kim, J. H., Kim, S. I., Kim, S. S., Choi, B. S., et al. (2020). Antiviral Activity of Digoxin and Ouabain against SARS-CoV-2 Infection and its Implication for COVID-19. *Sci. Rep.* 10 (1), 16200. doi:10.1038/s41598-020-72879-7

Cho, J., Yi, H., Jang, E. Y., Lee, M. S., Lee, J. Y., Kang, C., et al. (2017). Mycophenolic Mofetil, an Alternative Antiviral and Immunomodulator for the Highly Pathogenic Avian Influenza H5N1 Virus Infection. *Biochem. Biophys. Res. Commun.* 494 (1-2), 298–304. doi:10.1016/j.bbrc.2017.10.037

Chopra, G., Kaushik, S., Elkin, P. L., and Samudrala, R. (2016). Combating Ebola with Repurposed Therapeutics Using the CANDO Platform. *Molecules* 21 (12), 1537. doi:10.3390/molecules21121537

Choy, K. T., Yin-Lam Wong, A., Kaewpreedee, P., Sia, S. F., Chen, D., Yan Hui, K. P., et al. (2020). Remdesivir, Lopinavir, Emetine, and Homoharringtonine Inhibit SARS-CoV-2 Replication *In Vitro*. *Antivir. Res* 178, 104786. doi:10.1016/j.antiviral.2020.104786

Chu, C. M., Cheng, V. C., Hung, I. F., Wong, M. M., Chan, K. H., Chan, K. S., et al. (2004). Role of Lopinavir/ritonavir in the Treatment of SARS: Initial Virological and Clinical Findings. *Thorax* 59 (3), 252–256. doi:10.1136/thorax.2003.012658

Cinatl, J., Morgenstern, B., Bauer, G., Chandra, P., Rabenau, H., and Doerr, H. W. (2003). Treatment of SARS with Human Interferons. *Lancet* 362 (9380), 293–294. doi:10.1016/s0140-6736(03)13973-6

Clark, M. J., Miduturu, C., Schmidt, A. G., Zhu, X., Pitts, J. D., Wang, J., et al. (2016). GNF-2 Inhibits Dengue Virus by Targeting Abl Kinases and the Viral E Protein. *Cell Chem. Biol.* 23 (4), 443–452. doi:10.1016/j.chembiol.2016.03.010

Cohen, J. I. (2005). HMG CoA Reductase Inhibitors (Statins) to Treat Epstein-Barr Virus-Driven Lymphoma. *Br. J. Cancer* 92 (9), 1593–1598. doi:10.1038/sj.bjc.6602561

Cortegiani, A., Ingoglia, G., Ippolito, M., Giarratano, A., and Einav, S. (2020). A Systematic Review on the Efficacy and Safety of Chloroquine for the Treatment of COVID-19. *J. Crit. Care* 57, 279–283. doi:10.1016/j.jcrc.2020.03.005

Coyne, C. B., and Bergelson, J. M. (2006). Virus-induced Abl and Fyn Kinase Signals Permit Coxsackievirus Entry through Epithelial Tight Junctions. *Cell* 124 (1), 119–131. doi:10.1016/j.cell.2005.10.035

Crouchet, E., Wrensch, F., Schuster, C., Zeisel, M. B., and Baumert, T. F. (2018). Host-targeting therapies for hepatitis C virus infection: current developments and future applications. *Therap. Adv. Gastroenterol.* 11, 1–15. doi:10.1177/1756284818759483

Dang, W., Xu, L., Ma, B., Chen, S., Yin, Y., Chang, K. O., et al. (2018). Nitazoxanide Inhibits Human Norovirus Replication and Synergizes with Ribavirin by Activation of Cellular Antiviral Response. *Antimicrob. Agents Chemother.* 62 (11), e00707-18. doi:10.1128/aac.00707-18

Dang, W., Yin, Y., Wang, Y., Wang, W., Su, J., Sprengers, D., et al. (2017). Inhibition of Calcineurin or IMP Dehydrogenase Exerts Moderate to Potent Antiviral Activity against Norovirus Replication. *Antimicrob. Agents Chemother.* 61 (11), e01095-17. doi:10.1128/aac.01095-17

de Freitas, C. S., Higa, L. M., Sacramento, C. Q., Ferreira, A. C., Reis, P. A., Delvecchio, R., et al. (2019). Yellow Fever Virus Is Susceptible to Sofosbuvir Both *In Vitro* and *In Vivo*. *Plos Negl. Trop. Dis.* 13 (1), e0007072. doi:10.1371/journal.pntd.0007072

de Wilde, A. H., Falzarano, D., Zevenhoven-Dobbe, J. C., Beugeling, C., Fett, C., Martellaro, C., et al. (2017). Alisporivir Inhibits MERS- and SARS-Coronavirus Replication in Cell Culture, but Not SARS-Coronavirus Infection in a Mouse Model. *Virus. Res.* 228, 7–13. doi:10.1016/j.virusres.2016.11.011

de Wilde, A. H., Jochmans, D., Posthuma, C. C., Zevenhoven-Dobbe, J. C., van Nieuwkoop, S., Bestebroer, T. M., et al. (2014). Screening of an FDA-Approved Compound Library Identifies Four Small-Molecule Inhibitors of Middle East Respiratory Syndrome Coronavirus Replication in Cell Culture. *Antimicrob. Agents Chemother.* 58 (8), 4875–4884. doi:10.1128/aac.03011-14

de Wilde, A. H., Raj, V. S., Oudshoorn, D., Bestebroer, T. M., van Nieuwkoop, S., Limpens, R., et al. (2013). MERS-coronavirus Replication Induces Severe *In Vitro* Cytopathology and Is Strongly Inhibited by Cyclosporin A or Interferon-α Treatment. *J. Gen. Virol.* 94 (Pt 8), 1749–1760. doi:10.1099/vir.0.052910-0

de Wilde, A. H., Snijder, E. J., Kikkert, M., and van Hemert, M. J. (2018). Host Factors in Coronavirus Replication. *Curr. Top. Microbiol. Immunol.* 419, 1–42. doi:10.1007/82_2017_25

de Wilde, A. H., Zevenhoven-Dobbe, J. C., van der Meer, Y., Thiel, V., Narayanan, K., Makino, S., et al. (2011). Cyclosporin A Inhibits the Replication of Diverse Coronaviruses. *J. Gen. Virol.* 92 (Pt 11), 2542–2548. doi:10.1099/vir.0.034983-0

de Wit, E., Feldmann, F., Cronin, J., Jordan, R., Okumura, A., Thomas, T., et al. (2020). Prophylactic and Therapeutic Remdesivir (GS-5734) Treatment in the Rhesus Macaque Model of MERS-CoV Infection. *Proc. Natl. Acad. Sci. U S A.* 117 (12), 6771–6776. doi:10.1073/pnas.1922083117

de Wit, E., van Doremalen, N., Falzarano, D., and Munster, V. J. (2016). SARS and MERS: Recent Insights into Emerging Coronaviruses. *Nat. Rev. Microbiol.* 14 (8), 523–534. doi:10.1038/nrmicro.2016.81

den Boon, J. A., and Ahlquist, P. (2010). Organelle-like Membrane Compartmentalization of Positive-Strand RNA Virus Replication Factories. *Annu. Rev. Microbiol.* 64, 241–256. doi:10.1146/annurev.micro.112408.134012

Desplanques, A. S., Pontes, M., De Corte, N., Verheyen, N., Nauwynck, H. J., Vercauteren, D., et al. (2010). Cholesterol Depletion Affects Infectivity and Stability of Pseudorabies Virus. *Virus. Res.* 152 (1-2), 180–183. doi:10.1016/j.virusres.2010.06.008

Diaconu, I., Cerullo, V., Escutenaire, S., Kanerva, A., Bauerschmitz, G. J., Hernandez-Alcoceba, R., et al. (2010). Human Adenovirus Replication in Immunocompetent Syrian Hamsters Can Be Attenuated with Chlorpromazine or Cidofovir. *J. Gene Med.* 12 (5), 435–445. doi:10.1002/jgm.1453

Diamond, M. S., Zachariah, M., and Harris, E. (2002). Mycophenolic Acid Inhibits Dengue Virus Infection by Preventing Replication of Viral RNA. *Virology* 304 (2), 211–221. doi:10.1006/viro.2002.1685

Committee on Infectious Diseases (1993). American Academy of Pediatrics Committee on Infectious Diseases: Use of Ribavirin in the Treatment of Respiratory Syncytial Virus Infection. *Pediatrics* 92 (3), 501–504.

Dodson, A. W., Taylor, T. J., Knipe, D. M., and Coen, D. M. (2007). Inhibitors of the Sodium Potassium ATPase that Impair Herpes Simplex Virus Replication Identified via a Chemical Screening Approach. *Virology* 366 (2), 340–348. doi:10.1016/j.virol.2007.05.001

Dong, S., Kang, S., and Dimopoulos, G. (2019). Identification of Anti-flaviviral Drugs with Mosquitocidal and Anti-zika Virus Activity in *Aedes aegypti*. *Plos Negl. Trop. Dis.* 13 (8), e0007681. doi:10.1371/journal.pntd.0007681

Dowall, S. D., Bosworth, A., Watson, R., Bewley, K., Taylor, I., Rayner, E., et al. (2015). Chloroquine Inhibited Ebola Virus Replication *In Vitro* but Failed to Protect against Infection and Disease in the *In Vivo* guinea Pig Model. *J. Gen. Virol.* 96 (12), 3484–3492. doi:10.1099/jgv.0.000309

Du, X., Zuo, X., Meng, F., Wu, F., Zhao, X., Li, C., et al. (2020). Combinatorial Screening of a Panel of FDA-Approved Drugs Identifies Several Candidates with Anti-ebola Activities. *Biochem. Biophys. Res. Commun.* 522 (4), 862–868. doi:10.1016/j.bbrc.2019.11.065

Dyall, J., Coleman, C. M., Hart, B. J., Venkataraman, T., Holbrook, M. R., Kindrachuk, J., et al. (2014). Repurposing of Clinically Developed Drugs for Treatment of Middle East Respiratory Syndrome Coronavirus Infection. *Antimicrob. Agents Chemother.* 58 (8), 4885–4893. doi:10.1128/AAC.03036-14

Eagling, V. A., Back, D. J., and Barry, M. G. (1997). Differential Inhibition of Cytochrome P450 Isoforms by the Protease Inhibitors, Ritonavir, Saquinavir and Indinavir. *Br. J. Clin. Pharmacol.* 44 (2), 190–194. doi:10.1046/j.1365-2125.1997.00644.x

Eberhardt, K. A., Mischlinger, J., Jordan, S., Groger, M., Gunther, S., and Ramharter, M. (2019). Ribavirin for the Treatment of Lassa Fever: A Systematic Review and Meta-Analysis. *Int. J. Infect. Dis.* 87, 15–20. doi:10.1016/j.ijid.2019.07.015

Elazar, M., Liu, M., McKenna, S. A., Liu, P., Gehrig, E. A., Puglisi, J. D., et al. (2009). The Anti-hepatitis C Agent Nitazoxanide Induces Phosphorylation of Eukaryotic Initiation Factor 2alpha *via* Protein Kinase Activated by Double-

Stranded RNA Activation. *Gastroenterology* 137 (5), 1827–1835. doi:10.1053/j.gastro.2009.07.056

Elfiky, A. A. (2020a). Anti-HCV, Nucleotide Inhibitors, Repurposing against COVID-19. *Life Sci.* 248, 117477. doi:10.1016/j.lfs.2020.117477

Elfiky, A. A. (2020b). Ribavirin, Remdesivir, Sofosbuvir, Galidesivir, and Tenofovir against SARS-CoV-2 RNA Dependent RNA Polymerase (RdRp): A Molecular Docking Study. *Life Sci.* 253, 117592. doi:10.1016/j.lfs.2020.117592

Españo, E., Nam, J. H., Song, E. J., Song, D., Lee, C. K., and Kim, J. K. (2019). Lipophilic Statins Inhibit Zika Virus Production in Vero Cells. *Sci. Rep.* 9 (1), 11461. doi:10.1038/s41598-019-47956-1

Esquer Garrigos, Z., Barth, D., Hamdi, A. M., Abu Saleh, O. M., and Sohail, M. R. (2018). Nitazoxanide Is a Therapeutic Option for Adenovirus-Related Enteritis in Immunocompromised Adults. *Antimicrob. Agents Chemother.* 62 (12), e01937-18. doi:10.1128/aac.01937-18

Eyer, L., Nougairède, A., Uhlířová, M., Driouich, J. S., Zouharová, D., Valdés, J. J., et al. (2019). An E460D Substitution in the NS5 Protein of Tick-Borne Encephalitis Virus Confers Resistance to the Inhibitor Galidesivir (BCX4430) and Also Attenuates the Virus for Mice. *J. Virol.* 93 (16). doi:10.1128/jvi.00367-19

Eyer, L., Zouharová, D., Širmarová, J., Fojtíková, M., Štefánik, M., Haviernik, J., et al. (2017). Antiviral Activity of the Adenosine Analogue BCX4430 against West Nile Virus and Tick-Borne Flaviviruses. *Antivir. Res* 142, 63–67. doi:10.1016/j.antiviral.2017.03.012

Ezzikouri, S., Kayesh, M. E. H., Benjelloun, S., Kohara, M., and Tsukiyama-Kohara, K. (2020). Targeting Host Innate and Adaptive Immunity to Achieve the Functional Cure of Chronic Hepatitis B. *Vaccines (Basel)* 8 (2). doi:10.3390/vaccines8020216

Falzarano, D., de Wit, E., Martellaro, C., Callison, J., Munster, V. J., and Feldmann, H. (2013a). Inhibition of Novel Beta Coronavirus Replication by a Combination of Interferon-Alpha2b and Ribavirin. *Sci. Rep.* 3, 1686. doi:10.1038/srep01686

Falzarano, D., de Wit, E., Rasmussen, A. L., Feldmann, F., Okumura, A., Scott, D. P., et al. (2013b). Treatment with Interferon-Alpha2b and Ribavirin Improves Outcome in MERS-CoV-Infected Rhesus Macaques. *Nat. Med.* 19 (10), 1313–1317. doi:10.1038/nm.3362

Fanunza, E., Frau, A., Corona, A., and Tramontano, E. (2018). Antiviral Agents against Ebola Virus Infection: Repositioning Old Drugs and Finding Novel Small Molecules. *Annu. Rep. Med. Chem.* 51, 135–173. doi:10.1016/bs.armc.2018.08.004

Farias, K. J., Machado, P. R., de Almeida Junior, R. F., de Aquino, A. A., and da Fonseca, B. A. (2014). Chloroquine Interferes with Dengue-2 Virus Replication in U937 Cells. *Microbiol. Immunol.* 58 (6), 318–326. doi:10.1111/1348-0421.12154

Farias, K. J., Machado, P. R., Muniz, J. A., Imbeloni, A. A., and da Fonseca, B. A. (2015). Antiviral Activity of Chloroquine Against Dengue Virus Type 2 Replication in *Aotus* Monkeys. *Viral Immunol.* 28 (3), 161–169. doi:10.1089/vim.2014.0090

Faulds, D., Goa, K. L., and Benfield, P. (1993). Cyclosporin. A Review of its Pharmacodynamic and Pharmacokinetic Properties, and Therapeutic Use in Immunoregulatory Disorders. *Drugs* 45 (6), 953–1040. doi:10.2165/00003495-199345060-00007

Feng, Z., Hensley, L., McKnight, K. L., Hu, F., Madden, V., Ping, L., et al. (2013). A Pathogenic Picornavirus Acquires an Envelope by Hijacking Cellular Membranes. *Nature* 496 (7445), 367–371. doi:10.1038/nature12029

Ferraris, O., Moroso, M., Pernet, O., Emonet, S., Ferrier Rembert, A., Paranhos-Baccala, G., et al. (2015a). Evaluation of Crimean-Congo Hemorrhagic Fever Virus *In Vitro* Inhibition by Chloroquine and Chlorpromazine, Two FDA Approved Molecules. *Antivir. Res* 118, 75–81. doi:10.1016/j.antiviral.2015.03.005

Ferraris, O., Moroso, M., Pernet, O., Emonet, S., Ferrier Rembert, A., Paranhos-Baccalà, G., et al. (2015b). Evaluation of Crimean-Congo Hemorrhagic Fever Virus *In Vitro* Inhibition by Chloroquine and Chlorpromazine, Two FDA Approved Molecules. *Antivir. Res.* 118, 75–81. doi:10.1016/j.antiviral.2015.03.005

Ferreira, A. C., Reis, P. A., de Freitas, C. S., Sacramento, C. Q., Villas Boas Hoelz, L., Bastos, M. M., et al. (2019). Beyond Members of the Flaviviridae Family, Sofosbuvir Also Inhibits Chikungunya Virus Replication. *Antimicrob. Agents Chemother.* 63 (2). doi:10.1128/AAC.01389-18

Firpi, R. J., Nelson, D. R., and Davis, G. L. (2003). Lack of Antiviral Effect of a Short Course of Mycophenolate Mofetil in Patients with Chronic Hepatitis C Virus Infection. *Liver Transpl.* 9 (1), 57–61. doi:10.1053/jlts.2003.50003

Fisher-Hoch, S. P., Khan, J. A., Rehman, S., Mirza, S., Khurshid, M., and McCormick, J. B. (1995). Crimean Congo-haemorrhagic Fever Treated with Oral Ribavirin. *Lancet* 346 (8973), 472–475. doi:10.1016/s0140-6736(95)91323-8

Franke, E. K., Yuan, H. E., and Luban, J. (1994). Specific Incorporation of Cyclophilin A into HIV-1 Virions. *Nature* 372 (6504), 359–362. doi:10.1038/372359a0

Fumian, T. M., Tuipulotu, D. E., Netzler, N. E., Lun, J. H., Russo, A. G., Yan, G. J. H., et al. (2018). Potential Therapeutic Agents for Feline Calicivirus Infection. *Viruses* 10 (8), 433. doi:10.3390/v10080433

Furuta, Y., Gowen, B. B., Takahashi, K., Shiraki, K., Smee, D. F., and Barnard, D. L. (2013). Favipiravir (T-705), a Novel Viral RNA Polymerase Inhibitor. *Antivir. Res* 100 (2), 446–454. doi:10.1016/j.antiviral.2013.09.015

Furuta, Y., Komeno, T., and Nakamura, T. (2017). Favipiravir (T-705), a Broad Spectrum Inhibitor of Viral RNA Polymerase. *Proc. Jpn. Acad. Ser. B Phys. Biol. Sci.* 93 (7), 449–463. doi:10.2183/pjab.93.027

Galban-Garcia, E., Vega-Sanchez, H., Gra-Oramas, B., Jorge-Riano, J. L., Soneiras-Perez, M., Haedo-Castro, D., et al. (2000). Efficacy of Ribavirin in Patients with Chronic Hepatitis B. *J. Gastroenterol.* 35 (5), 347–352. doi:10.1007/s005350050359

Gan, C. J., Li, W. F., Li, C. N., Li, L. L., Zhou, W. Y., and Peng, X. M. (2020). EGF Receptor Inhibitors Comprehensively Suppress Hepatitis B Virus by Downregulation of STAT3 Phosphorylation. *Biochem. Biophys. Rep.* 22, 100763. doi:10.1016/j.bbrep.2020.100763

Garcia, M., Cooper, A., Shi, W., Bornmann, W., Carrion, R., Kalman, D., et al. (2012). Productive Replication of Ebola Virus Is Regulated by the C-Abl1 Tyrosine Kinase. *Sci. Transl. Med.* 4 (123), 123ra124. doi:10.1126/scitranslmed.3003500

Gheorghiade, M., van Veldhuisen, D. J., and Colucci, W. S. (2006). Contemporary Use of Digoxin in the Management of Cardiovascular Disorders. *Circulation* 113 (21), 2556–2564. doi:10.1161/CIRCULATIONAHA.105.560110

Giguère, J. F., and Tremblay, M. J. (2004). Statin Compounds Reduce Human Immunodeficiency Virus Type 1 Replication by Preventing the Interaction between Virion-Associated Host Intercellular Adhesion Molecule 1 and its Natural Cell Surface Ligand LFA-1. *J. Virol.* 78 (21), 12062–12065. doi:10.1128/jvi.78.21.12062-12065.2004

Glück, B., Schmidtke, M., Walther, M., Meerbach, A., and Wutzler, P. (2013). Simvastatin Treatment Showed No Prophylactic Effect in Influenza Virus-Infected Mice. *J. Med. Virol.* 85 (11), 1978–1982. doi:10.1002/jmv.23682

Gong, Z. J., De Meyer, S., Clarysse, C., Verslype, C., Neyts, J., De Clercq, E., et al. (1999). Mycophenolic Acid, an Immunosuppressive Agent, Inhibits HBV Replication *In Vitro*. *J. Viral Hepat.* 6 (3), 229–236. doi:10.1046/j.1365-2893.1999.00163.x

Gordon, C. J., Tchesnokov, E. P., Feng, J. Y., Porter, D. P., and Gotte, M. (2020). The Antiviral Compound Remdesivir Potently Inhibits RNA-dependent RNA Polymerase from Middle East Respiratory Syndrome Coronavirus. *J. Biol. Chem.* 295 (15), 4773–4779. doi:10.1074/jbc.AC120.013056

Gower, T. L., and Graham, B. S. (2001). Antiviral Activity of Lovastatin against Respiratory Syncytial Virus *In Vivo* and *In Vitro*. *Antimicrob. Agents Chemother.* 45 (4), 1231–1237. doi:10.1128/aac.45.4.1231-1237.2001

Griffiths, C. E., and Voorhees, J. J. (1990). Cyclosporine A in the Treatment of Psoriasis: a Clinical and Mechanistic Perspective. *J. Invest. Dermatol.* 95 (5 Suppl. l), 53S–55S. doi:10.1111/1523-1747.ep12505786

Grosso, F., Stoilov, P., Lingwood, C., Brown, M., and Cochrane, A. (2017). Suppression of Adenovirus Replication by Cardiotonic Steroids. *J. Virol.* 91 (3), e01623-16. doi:10.1128/jvi.01623-16

Guedj, J., Piorkowski, G., Jacquot, F., Madelain, V., Nguyen, T. H. T., Rodallec, A., et al. (2018). Antiviral Efficacy of Favipiravir against Ebola Virus: A Translational Study in Cynomolgus Macaques. *Plos Med.* 15 (3), e1002535. doi:10.1371/journal.pmed.1002535

Guisado-Vasco, P., Valderas-Ortega, S., Carralon-Gonzalez, M. M., Roda-Santacruz, A., Gonzalez-Cortijo, L., Sotres-Fernandez, G., et al. (2020). Clinical Characteristics and Outcomes Among Hospitalized Adults with Severe COVID-19 Admitted to a Tertiary Medical Center and Receiving Antiviral, Antimalarials, Glucocorticoids, or Immunomodulation with

Tocilizumab or Cyclosporine: A Retrospective Observational Study (COQUIMA Cohort). *EClinicalMedicine* 28, 100591. doi:10.1016/j.eclinm.2020.100591

Guo, J., Jia, X., Liu, Y., Wang, S., Cao, J., Zhang, B., et al. (2020). Screening of Natural Extracts for Inhibitors against Japanese Encephalitis Virus Infection. *Antimicrob. Agents Chemother.* 64 (3), e02373-19. doi:10.1128/aac.02373-19

Haagmans, B. L., Kuiken, T., Martina, B. E., Fouchier, R. A., Rimmelzwaan, G. F., van Amerongen, G., et al. (2004). Pegylated Interferon-Alpha Protects Type 1 Pneumocytes against SARS Coronavirus Infection in Macaques. *Nat. Med.* 10 (3), 290–293. doi:10.1038/nm1001

Hacke, M., Björkholm, P., Hellwig, A., Himmels, P., Ruiz de Almodóvar, C., Brügger, B., et al. (2015). Inhibition of Ebola Virus Glycoprotein-Mediated Cytotoxicity by Targeting its Transmembrane Domain and Cholesterol. *Nat. Commun.* 6, 7688. doi:10.1038/ncomms8688

Haffizulla, J., Hartman, A., Hoppers, M., Resnick, H., Samudrala, S., Ginocchio, C., et al. (2014). Effect of Nitazoxanide in Adults and Adolescents with Acute Uncomplicated Influenza: a Double-Blind, Randomised, Placebo-Controlled, Phase 2b/3 Trial. *Lancet Infect. Dis.* 14 (7), 609–618. doi:10.1016/S1473-3099(14)70717-0

Haji Abdolvahab, M., Moradi-Kalbolandi, S., Zarei, M., Bose, D., Majidzadeh, A. K., and Farahmand, L. (2021). Potential Role of Interferons in Treating COVID-19 Patients. *Int. Immunopharmacol* 90, 107171. doi:10.1016/j.intimp.2020.107171

Hamamoto, I., Harazaki, K., Inase, N., Takaku, H., Tashiro, M., and Yamamoto, N. (2013). Cyclosporin A Inhibits the Propagation of Influenza Virus by Interfering with a Late Event in the Virus Life Cycle. *Jpn. J. Infect. Dis.* 66 (4), 276–283. doi:10.7883/yoken.66.276

Han, B., Martin, R., Xu, S., Parvangada, A., Svarovskaia, E. S., Mo, H., et al. (2019). Sofosbuvir Susceptibility of Genotype 1 to 6 HCV from DAA-Naive Subjects. *Antivir. Res.* 170, 104574. doi:10.1016/j.antiviral.2019.104574

Han, Y., Duan, X., Yang, L., Nilsson-Payant, B. E., Wang, P., Duan, F., et al. (2021). Identification of SARS-CoV-2 Inhibitors Using Lung and Colonic Organoids. *Nature* 589 (7841), 270–275. doi:10.1038/s41586-020-2901-9

Hartmann, J. T., and Kanz, L. (2008). Sunitinib and Periodic Hair Depigmentation Due to Temporary C-KIT Inhibition. *Arch. Dermatol.* 144 (11), 1525–1526. doi:10.1001/archderm.144.11.1525

Hatziioannou, T., Perez-Caballero, D., Cowan, S., and Bieniasz, P. D. (2005). Cyclophilin Interactions with Incoming Human Immunodeficiency Virus Type 1 Capsids with Opposing Effects on Infectivity in Human Cells. *J. Virol.* 79 (1), 176–183. doi:10.1128/JVI.79.1.176-183.2005

Hayden, F. G., Turner, R. B., Gwaltney, J. M., Chi-Burris, K., Gersten, M., Hsyu, P., et al. (2003). Phase II, Randomized, Double-Blind, Placebo-Controlled Studies of Ruprintrivir Nasal Spray 2-percent Suspension for Prevention and Treatment of Experimentally Induced Rhinovirus Colds in Healthy Volunteers. *Antimicrob. Agents Chemother.* 47 (12), 3907–3916. doi:10.1128/aac.47.12.3907-3916.2003

Heim, M. H. (2013). 25 Years of Interferon-Based Treatment of Chronic Hepatitis C: an Epoch Coming to an End. *Nat. Rev. Immunol.* 13 (7), 535–542. doi:10.1038/nri3463

Henry, S. D., Metselaar, H. J., Lonsdale, R. C., Kok, A., Haagmans, B. L., Tilanus, H. W., et al. (2006). Mycophenolic Acid Inhibits Hepatitis C Virus Replication and Acts in Synergy with Cyclosporin A and Interferon-Alpha. *Gastroenterology* 131 (5), 1452–1462. doi:10.1053/j.gastro.2006.08.027

Hoertel, N., Sanchez-Rico, M., Vernet, R., Jannot, A. S., Neuraz, A., Blanco, C., et al. (2021). Observational Study of Chlorpromazine in Hospitalized Patients with COVID-19. *Clin. Drug Investig.* 41 (3), 221–233. doi:10.1007/s40261-021-01001-0

Hoffmann, M., Kleine-Weber, H., Schroeder, S., Kruger, N., Herrler, T., Erichsen, S., et al. (2020a). SARS-CoV-2 Cell Entry Depends on ACE2 and TMPRSS2 and Is Blocked by a Clinically Proven Protease Inhibitor. *Cell* 181 (2), 271–280. doi:10.1016/j.cell.2020.02.052

Hoffmann, M., Kleine-Weber, H., Schroeder, S., Krüger, N., Herrler, T., Erichsen, S., et al. (2020b). SARS-CoV-2 Cell Entry Depends on ACE2 and TMPRSS2 and Is Blocked by a Clinically Proven Protease Inhibitor. *Cell* 181 (2), 271–280. doi:10.1016/j.cell.2020.02.052

Holshue, M. L., DeBolt, C., Lindquist, S., Lofy, K. H., Wiesman, J., Bruce, H., et al. (2020). First Case of 2019 Novel Coronavirus in the United States. *N. Engl. J. Med.* 382 (10), 929–936. doi:10.1056/NEJMoa2001191

Hosoya, M., Matsuyama, S., Baba, M., Suzuki, H., and Shigeta, S. (1992). Effects of Protease Inhibitors on Replication of Various Myxoviruses. *Antimicrob. Agents Chemother.* 36 (7), 1432–1436. doi:10.1128/aac.36.7.1432

Hosoya, M., Shigeta, S., Ishii, T., Suzuki, H., and De Clercq, E. (1993). Comparative Inhibitory Effects of Various Nucleoside and Nonnucleoside Analogues on Replication of Influenza Virus Types A and B *In Vitro* and *In Vivo*. *J. Infect. Dis.* 168 (3), 641–646. doi:10.1093/infdis/168.3.641

Hu, Z., Lan, K. H., He, S., Swaroop, M., Hu, X., Southall, N., et al. (2014). Novel Cell-Based Hepatitis C Virus Infection Assay for Quantitative High-Throughput Screening of Anti-hepatitis C Virus Compounds. *Antimicrob. Agents Chemother.* 58 (2), 995–1004. doi:10.1128/AAC.02094-13

Huang, R., Southall, N., Wang, Y., Yasgar, A., Shinn, P., Jadhav, A., et al. (2011). The NCGC Pharmaceutical Collection: a Comprehensive Resource of Clinically Approved Drugs Enabling Repurposing and Chemical Genomics. *Sci. Transl Med.* 3 (80), 80ps16. doi:10.1126/scitranslmed.3001862

Hui, D. S., Lee, N., Chan, P. K., and Beigel, J. H. (2018). The Role of Adjuvant Immunomodulatory Agents for Treatment of Severe Influenza. *Antivir. Res* 150, 202–216. doi:10.1016/j.antiviral.2018.01.002

Hung, H. C., Wang, H. C., Shih, S. R., Teng, I. F., Tseng, C. P., and Hsu, J. T. (2011). Synergistic Inhibition of Enterovirus 71 Replication by Interferon and Rupintrivir. *J. Infect. Dis.* 203 (12), 1784–1790. doi:10.1093/infdis/jir174

Hussain, K. M., Leong, K. L., Ng, M. M., and Chu, J. J. (2011). The Essential Role of Clathrin-Mediated Endocytosis in the Infectious Entry of Human Enterovirus 71. *J. Biol. Chem.* 286 (1), 309–321. doi:10.1074/jbc.M110.168468

Ianevski, A., Zusinaite, E., Kuivanen, S., Strand, M., Lysvand, H., Teppor, M., et al. (2018). Novel Activities of Safe-In-Human Broad-Spectrum Antiviral Agents. *Antivir. Res* 154, 174–182. doi:10.1016/j.antiviral.2018.04.016

Ibarra, K. D., and Pfeiffer, J. K. (2009). Reduced Ribavirin Antiviral Efficacy *via* Nucleoside Transporter-Mediated Drug Resistance. *J. Virol.* 83 (9), 4538–4547. doi:10.1128/JVI.02280-08

Inoue, Y., Tanaka, N., Tanaka, Y., Inoue, S., Morita, K., Zhuang, M., et al. (2007). Clathrin-dependent Entry of Severe Acute Respiratory Syndrome Coronavirus into Target Cells Expressing ACE2 with the Cytoplasmic Tail Deleted. *J. Virol.* 81 (16), 8722–8729. doi:10.1128/JVI.00253-07

Isorce, N., Testoni, B., Locatelli, M., Fresquet, J., Rivoire, M., Luangsay, S., et al. (2016). Antiviral Activity of Various Interferons and Pro-inflammatory Cytokines in Non-transformed Cultured Hepatocytes Infected with Hepatitis B Virus. *Antivir. Res* 130, 36–45. doi:10.1016/j.antiviral.2016.03.008

Ivashchenko, A. A., Dmitriev, K. A., Vostokova, N. V., Azarova, V. N., Blinow, A. A., Egorova, A. N., et al. (2020). AVIFAVIR for treatment of patients with moderate coronavirus disease 2019 (COVID-19): interim results of a phase II/III multicenter randomized clinical trial. *Clin. Infect. Dis.* ciaa1176. doi:10.1093/cid/ciaa1176

Iwamoto, M., Saso, W., Sugiyama, R., Ishii, K., Ohki, M., Nagamori, S., et al. (2019). Epidermal Growth Factor Receptor Is a Host-Entry Cofactor Triggering Hepatitis B Virus Internalization. *Proc. Natl. Acad. Sci. U. S. A.* 116 (17), 8487–8492. doi:10.1073/pnas.1811064116

Iwasaki, M., Minder, P., Cai, Y., Kuhn, J. H., Yates, J. R., 3rd, Torbett, B. E., et al. (2018). Interactome Analysis of the Lymphocytic Choriomeningitis Virus Nucleoprotein in Infected Cells Reveals ATPase Na+/K+ Transporting Subunit Alpha 1 and Prohibitin as Host-Cell Factors Involved in the Life Cycle of Mammarenaviruses. *Plos Pathog.* 14 (2), e1006892. doi:10.1371/journal.ppat.1006892

Iyer, S. S., Bibollet-Ruche, F., Sherrill-Mix, S., Learn, G. H., Plenderleith, L., Smith, A. G., et al. (2017). Resistance to Type 1 Interferons Is a Major Determinant of HIV-1 Transmission Fitness. *Proc. Natl. Acad. Sci. U. S. A.* 114 (4), E590–E599. doi:10.1073/pnas.1620144114

Jacome, R., Campillo-Balderas, J. A., Ponce de Leon, S., Becerra, A., and Lazcano, A. (2020). Sofosbuvir as a Potential Alternative to Treat the SARS-CoV-2 Epidemic. *Sci. Rep.* 10 (1), 9294. doi:10.1038/s41598-020-66440-9

Jae, L. T., Raaben, M., Herbert, A. S., Kuehne, A. I., Wirchnianski, A. S., Soh, T. K., et al. (2014). Virus Entry. Lassa Virus Entry Requires a Trigger-Induced Receptor Switch. *Science* 344 (6191), 1506–1510. doi:10.1126/science.1252480

Janes, J., Young, M. E., Chen, E., Rogers, N. H., Burgstaller-Muehlbacher, S., Hughes, L. D., et al. (2018). The ReFRAME Library as a Comprehensive Drug Repurposing Library and its Application to the Treatment of Cryptosporidiosis. *Proc. Natl. Acad. Sci. U S A.* 115 (42), 10750–10755. doi:10.1073/pnas.1810137115

Jasenosky, L. D., Cadena, C., Mire, C. E., Borisevich, V., Haridas, V., Ranjbar, S., et al. (2019). The FDA-Approved Oral Drug Nitazoxanide Amplifies Host Antiviral Responses and Inhibits Ebola Virus. *iScience* 19, 1279–1290. doi:10.1016/j.isci.2019.07.003

Jia, D., Taguchi, M., and Otsuki, M. (2005). Synthetic Protease Inhibitor Camostat Prevents and Reverses Dyslipidemia, Insulin Secretory Defects, and Histological Abnormalities of the Pancreas in Genetically Obese and Diabetic Rats. *Metabolism* 54 (5), 619–627. doi:10.1016/j.metabol.2004.12.005

Jochmans, D., van Nieuwkoop, S., Smits, S. L., Neyts, J., Fouchier, R. A., and van den Hoogen, B. G. (2016). Antiviral Activity of Favipiravir (T-705) against a Broad Range of Paramyxoviruses *In Vitro* and against Human Metapneumovirus in Hamsters. *Antimicrob. Agents Chemother.* 60 (8), 4620–4629. doi:10.1128/AAC.00709-16

Johnson, S., Henschke, N., Maayan, N., Mills, I., Buckley, B. S., Kakourou, A., et al. (2018). Ribavirin for Treating Crimean Congo Haemorrhagic Fever. *Cochrane Database Syst. Rev.* 6 (6), CD012713. doi:10.1002/14651858.CD012713.pub2

Julander, J. G., Shafer, K., Smee, D. F., Morrey, J. D., and Furuta, Y. (2009). Activity of T-705 in a Hamster Model of Yellow Fever Virus Infection in Comparison with that of a Chemically Related Compound, T-1106. *Antimicrob. Agents Chemother.* 53 (1), 202–209. doi:10.1128/AAC.01074-08

Julander, J. G., Siddharthan, V., Evans, J., Taylor, R., Tolbert, K., Apuli, C., et al. (2017). Efficacy of the Broad-Spectrum Antiviral Compound BCX4430 against Zika Virus in Cell Culture and in a Mouse Model. *Antivir. Res* 137, 14–22. doi:10.1016/j.antiviral.2016.11.003

Kamar, N., Abravanel, F., Behrendt, P., Hofmann, J., Pageaux, G. P., Barbet, C., et al. (2019). Ribavirin for Hepatitis E Virus Infection after Organ Transplantation: A Large European Retrospective Multicenter Study. *Clin. Infect. Dis.* 71 (5), 1204–1211. doi:10.1093/cid/ciz953

Kamar, N., Izopet, J., Tripon, S., Bismuth, M., Hillaire, S., Dumortier, J., et al. (2014). Ribavirin for Chronic Hepatitis E Virus Infection in Transplant Recipients. *N. Engl. J. Med.* 370 (12), 1111–1120. doi:10.1056/NEJMoa1215246

Kamiyama, N., Soma, R., Hidano, S., Watanabe, K., Umekita, H., Fukuda, C., et al. (2017). Ribavirin Inhibits Zika Virus (ZIKV) Replication *In Vitro* and Suppresses Viremia in ZIKV-Infected STAT1-Deficient Mice. *Antivir. Res* 146, 1–11. doi:10.1016/j.antiviral.2017.08.007

Kapoor, A., Cai, H., Forman, M., He, R., Shamay, M., and Arav-Boger, R. (2012). Human Cytomegalovirus Inhibition by Cardiac Glycosides: Evidence for Involvement of the HERG Gene. *Antimicrob. Agents Chemother.* 56 (9), 4891–4899. doi:10.1128/aac.00898-12

Katano, H., Pesnicak, L., and Cohen, J. I. (2004). Simvastatin Induces Apoptosis of Epstein-Barr Virus (EBV)-transformed Lymphoblastoid Cell Lines and Delays Development of EBV Lymphomas. *Proc. Natl. Acad. Sci. U. S. A.* 101 (14), 4960–4965. doi:10.1073/pnas.0305149101

Kato, F., Matsuyama, S., Kawase, M., Hishiki, T., Katoh, H., and Takeda, M. (2020). Antiviral Activities of Mycophenolic Acid and IMD-0354 against SARS-CoV-2. *Microbiol. Immunol.* 64 (9), 635–639. doi:10.1111/1348-0421.12828

Kawase, M., Shirato, K., van der Hoek, L., Taguchi, F., and Matsuyama, S. (2012). Simultaneous Treatment of Human Bronchial Epithelial Cells with Serine and Cysteine Protease Inhibitors Prevents Severe Acute Respiratory Syndrome Coronavirus Entry. *J. Virol.* 86 (12), 6537–6545. doi:10.1128/JVI.00094-12

Keckesova, Z., Ylinen, L. M., and Towers, G. J. (2006). Cyclophilin A Renders Human Immunodeficiency Virus Type 1 Sensitive to Old World Monkey but Not Human TRIM5 Alpha Antiviral Activity. *J. Virol.* 80 (10), 4683–4690. doi:10.1128/jvi.80.10.4683-4690.2006

Kee, S. H., Cho, E. J., Song, J. W., Park, K. S., Baek, L. J., and Song, K. J. (2004). Effects of Endocytosis Inhibitory Drugs on Rubella Virus Entry into VeroE6 Cells. *Microbiol. Immunol.* 48 (11), 823–829. doi:10.1111/j.1348-0421.2004.tb03614.x

Keyaerts, E., Vijgen, L., Maes, P., Neyts, J., and Van Ranst, M. (2004). *In vitro* inhibition of Severe Acute Respiratory Syndrome Coronavirus by Chloroquine. *Biochem. Biophys. Res. Commun.* 323 (1), 264–268. doi:10.1016/j.bbrc.2004.08.085

Khan, M., Santhosh, S. R., Tiwari, M., Lakshmana Rao, P. V., and Parida, M. (2010). Assessment of *In Vitro* Prophylactic and Therapeutic Efficacy of Chloroquine against Chikungunya Virus in Vero Cells. *J. Med. Virol.* 82 (5), 817–824. doi:10.1002/jmv.21663

Khandia, R., Munjal, A., Dhama, K., Karthik, K., Tiwari, R., Malik, Y. S., et al. (2018). Modulation of Dengue/Zika Virus Pathogenicity by Antibody-dependent Enhancement and Strategies to Protect against Enhancement in Zika Virus Infection. *Front. Immunol.* 9, 597. doi:10.3389/fimmu.2018.00597

Kim, Y. I., Pareek, R., Murphy, R., Harrison, L., Farrell, E., Cook, R., et al. (2017). The Antiviral Effects of RSV Fusion Inhibitor, MDT-637, on Clinical Isolates, vs. its Achievable Concentrations in the Human Respiratory Tract and Comparison to Ribavirin. *Influenza Other Respir. Viruses* 11 (6), 525–530. doi:10.1111/irv.12503

Kim, Y., Lovell, S., Tiew, K. C., Mandadapu, S. R., Alliston, K. R., Battaile, K. P., et al. (2012). Broad-spectrum Antivirals against 3C or 3C-like Proteases of Picornaviruses, Noroviruses, and Coronaviruses. *J. Virol.* 86 (21), 11754–11762. doi:10.1128/JVI.01348-12

Kindler, E., Thiel, V., and Weber, F. (2016). Interaction of SARS and MERS Coronaviruses with the Antiviral Interferon Response. *Adv. Virus. Res.* 96, 219–243. doi:10.1016/bs.aivir.2016.08.006

Koizumi, Y., Ohashi, H., Nakajima, S., Tanaka, Y., Wakita, T., Perelson, A. S., et al. (2017). Quantifying Antiviral Activity Optimizes Drug Combinations against Hepatitis C Virus Infection. *Proc. Natl. Acad. Sci. U S A.* 114 (8), 1922–1927. doi:10.1073/pnas.1610197114

Konde, M. K., Baker, D. P., Traore, F. A., Sow, M. S., Camara, A., Barry, A. A., et al. (2017). Interferon Beta-1a for the Treatment of Ebola Virus Disease: A Historically Controlled, Single-Arm Proof-Of-Concept Trial. *PLoS One* 12 (2), e0169255. doi:10.1371/journal.pone.0169255

Korba, B. E., Montero, A. B., Farrar, K., Gaye, K., Mukerjee, S., Ayers, M. S., et al. (2008). Nitazoxanide, Tizoxanide and Other Thiazolides Are Potent Inhibitors of Hepatitis B Virus and Hepatitis C Virus Replication. *Antivir. Res* 77 (1), 56–63. doi:10.1016/j.antiviral.2007.08.005

Kouznetsova, J., Sun, W., Martinez-Romero, C., Tawa, G., Shinn, P., Chen, C. Z., et al. (2014). Identification of 53 Compounds that Block Ebola Virus-like Particle Entry *via* a Repurposing Screen of Approved Drugs. *Emerg. Microbes Infect.* 3 (12), e84. doi:10.1038/emi.2014.88

Kumaki, Y., Morrey, J. D., and Barnard, D. L. (2012). Effect of Statin Treatments on Highly Pathogenic Avian Influenza H5N1, Seasonal and H1N1pdm09 Virus Infections in BALB/c Mice. *Future Virol.* 7 (8), 801–818. doi:10.2217/fvl.12.71

La Frazia, S., Ciucci, A., Arnoldi, F., Coira, M., Gianferretti, P., Angelini, M., et al. (2013). Thiazolides, a New Class of Antiviral Agents Effective against Rotavirus Infection, Target Viral Morphogenesis, Inhibiting Viroplasm Formation. *J. Virol.* 87 (20), 11096–11106. doi:10.1128/jvi.01213-13

Lan, J., Ge, J., Yu, J., Shan, S., Zhou, H., Fan, S., et al. (2020). Structure of the SARS-CoV-2 Spike Receptor-Binding Domain Bound to the ACE2 Receptor. *Nature* 581 (7807), 215–220. doi:10.1038/s41586-020-2180-5

Lazear, H. M., Govero, J., Smith, A. M., Platt, D. J., Fernandez, E., Miner, J. J., et al. (2016). A Mouse Model of Zika Virus Pathogenesis. *Cell Host Microbe* 19 (5), 720–730. doi:10.1016/j.chom.2016.03.010

Lee, J. S., Adhikari, N. K. J., Kwon, H. Y., Teo, K., Siemieniuk, R., Lamontagne, F., et al. (2019). Anti-Ebola Therapy for Patients with Ebola Virus Disease: a Systematic Review. *BMC Infect. Dis.* 19 (1), 376. doi:10.1186/s12879-019-3980-9

Lee, M. G., Kim, K. H., Park, K. Y., and Kim, J. S. (1996). Evaluation of Anti-influenza Effects of Camostat in Mice Infected with Non-adapted Human Influenza Viruses. *Arch. Virol.* 141 (10), 1979–1989. doi:10.1007/bf01718208

Li, C., Deng, Y. Q., Wang, S., Ma, F., Aliyari, R., Huang, X. Y., et al. (2017a). 25-Hydroxycholesterol Protects Host against Zika Virus Infection and its Associated Microcephaly in a Mouse Model. *Immunity* 46 (3), 446–456. doi:10.1016/j.immuni.2017.02.012

Li, C., Zhu, X., Ji, X., Quanquin, N., Deng, Y. Q., Tian, M., et al. (2017b). Chloroquine, a FDA-Approved Drug, Prevents Zika Virus Infection and its Associated Congenital Microcephaly in Mice. *EBioMedicine* 24, 189–194. doi:10.1016/j.ebiom.2017.09.034

Li, H. S., Kuok, D. I. T., Cheung, M. C., Ng, M. M. T., Ng, K. C., Hui, K. P. Y., et al. (2018). Effect of Interferon Alpha and Cyclosporine Treatment Separately and in Combination on Middle East Respiratory Syndrome Coronavirus (MERS-CoV) Replication in a Human *In-Vitro* and *Ex-Vivo* Culture Model. *Antivir. Res* 155, 89–96. doi:10.1016/j.antiviral.2018.05.007

Li, M., Zhang, D., Li, C., Zheng, Z., Fu, M., Ni, F., et al. (2020a). Characterization of Zika Virus Endocytic Pathways in Human Glioblastoma Cells. *Front. Microbiol.* 11, 242. doi:10.3389/fmicb.2020.00242

Li, Q., Guan, X., Wu, P., Wang, X., Zhou, L., Tong, Y., et al. (2020b). Early Transmission Dynamics in Wuhan, China, of Novel Coronavirus-Infected

Pneumonia. *N. Engl. J. Med.* 382 (13), 1199–1207. doi:10.1056/NEJMoa2001316

Li, W., Moore, M. J., Vasilieva, N., Sui, J., Wong, S. K., Berne, M. A., et al. (2003). Angiotensin-converting Enzyme 2 Is a Functional Receptor for the SARS Coronavirus. *Nature* 426 (6965), 450–454. doi:10.1038/nature02145

Li, Z., Brecher, M., Deng, Y. Q., Zhang, J., Sakamuru, S., Liu, B., et al. (2017c). Existing Drugs as Broad-Spectrum and Potent Inhibitors for Zika Virus by Targeting NS2B-NS3 Interaction. *Cell Res* 27 (8), 1046–1064. doi:10.1038/cr.2017.88

Lingemann, M., McCarty, T., Liu, X., Buchholz, U. J., Surman, S., Martin, S. E., et al. (2019). The Alpha-1 Subunit of the Na+,K+-ATPase (ATP1A1) Is Required for Macropinocytic Entry of Respiratory Syncytial Virus (RSV) in Human Respiratory Epithelial Cells. *Plos Pathog.* 15 (8), e1007963. doi:10.1371/journal.ppat.1007963

Liu, S. Y., Aliyari, R., Chikere, K., Li, G., Marsden, M. D., Smith, J. K., et al. (2013). Interferon-inducible Cholesterol-25-Hydroxylase Broadly Inhibits Viral Entry by Production of 25-hydroxycholesterol. *Immunity* 38 (1), 92–105. doi:10.1016/j.immuni.2012.11.005

Liu, X., Sun, L., Yu, M., Wang, Z., Xu, C., Xue, Q., et al. (2009). Cyclophilin A Interacts with Influenza A Virus M1 Protein and Impairs the Early Stage of the Viral Replication. *Cell Microbiol* 11 (5), 730–741. doi:10.1111/j.1462-5822.2009.01286.x

Liu, X., Zhao, Z., Li, Z., Xu, C., Sun, L., Chen, J., et al. (2012). Cyclosporin A Inhibits the Influenza Virus Replication through Cyclophilin A-dependent and -independent Pathways. *PLoS One* 7 (5), e37277. doi:10.1371/journal.pone.0037277

Livonesi, M. C., Moro de Sousa, R. L., and Moraes Figueiredo, L. T. (2007). *In vitro* study of Antiviral Activity of Mycophenolic Acid on Brazilian Orthobunyaviruses. *Intervirology* 50 (3), 204–208. doi:10.1159/000099219

Lo, M. K., Jordan, R., Arvey, A., Sudhamsu, J., Shrivastava-Ranjan, P., Hotard, A. L., et al. (2017). GS-5734 and its Parent Nucleoside Analog Inhibit Filo-, Pneumo-, and Paramyxoviruses. *Sci. Rep.* 7, 43395. doi:10.1038/srep43395

Lopez-Munoz, F., Alamo, C., Cuenca, E., Shen, W. W., Clervoy, P., and Rubio, G. (2005). History of the Discovery and Clinical Introduction of Chlorpromazine. *Ann. Clin. Psychiatry* 17 (3), 113–135. doi:10.1080/10401230591002002

Loutfy, M. R., Blatt, L. M., Siminovitch, K. A., Ward, S., Wolff, B., Lho, H., et al. (2003). Interferon Alfacon-1 Plus Corticosteroids in Severe Acute Respiratory Syndrome: a Preliminary Study. *JAMA* 290 (24), 3222–3228. doi:10.1001/jama.290.24.3222

Lupberger, J., Zeisel, M. B., Xiao, F., Thumann, C., Fofana, I., Zona, L., et al. (2011). EGFR and EphA2 Are Host Factors for Hepatitis C Virus Entry and Possible Targets for Antiviral Therapy. *Nat. Med.* 17 (5), 589–595. doi:10.1038/nm.2341

Ma, C., Li, F., Musharrafieh, R. G., and Wang, J. (2016). Discovery of Cyclosporine A and its Analogs as Broad-Spectrum Anti-influenza Drugs with a High *In Vitro* Genetic Barrier of Drug Resistance. *Antivir. Res* 133, 62–72. doi:10.1016/j.antiviral.2016.07.019

Mallhi, T. H., Khan, Y. H., Alotaibi, N. H., Alzarea, A. I., Alanazi, A. S., Qasim, S., et al. (2020a). Drug repurposing for COVID-19: a potential threat of self-medication and controlling measures. *Postgrad. Med. J.* 0, 1–2. doi:10.1136/postgradmedj-2020-138447

Mallhi, T. H., Liaqat, A., Abid, A., Khan, Y. H., Alotaibi, N. H., Alzarea, A. I., et al. (2020b). Multilevel Engagements of Pharmacists during the COVID-19 Pandemic: The Way Forward. *Front. Public Health* 8 (8), 561924. doi:10.3389/fpubh.2020.561924

Manchala, N. R., Dungdung, R., Trivedi, P., Unniyampurath, U., and Pilankatta, R. (2019). Mycophenolic Acid (MPA) Modulates Host Cellular Autophagy Progression in Sub Genomic Dengue Virus-2 Replicon Cells. *Microb. Pathog.* 137, 103762. doi:10.1016/j.micpath.2019.103762

Mandal, A., Gote, V., Pal, D., Ogundele, A., and Mitra, A. K. (2019). Ocular Pharmacokinetics of a Topical Ophthalmic Nanomicellar Solution of Cyclosporine [Cequa(R)] for Dry Eye Disease. *Pharm. Res.* 36 (2), 36. doi:10.1007/s11095-018-2556-5

Mantlo, E., Bukreyeva, N., Maruyama, J., Paessler, S., and Huang, C. (2020). Antiviral Activities of Type I Interferons to SARS-CoV-2 Infection. *Antivir. Res* 179, 104811. doi:10.1016/j.antiviral.2020.104811

Margolis, D., Heredia, A., Gaywee, J., Oldach, D., Drusano, G., and Redfield, R. (1999). Abacavir and Mycophenolic Acid, an Inhibitor of Inosine Monophosphate Dehydrogenase, Have Profound and Synergistic Anti-HIV Activity. *J. Acquir Immune Defic Syndr.* 21 (5), 362–370.

Martinez-Gutierrez, M., Castellanos, J. E., and Gallego-Gomez, J. C. (2011). Statins Reduce Dengue Virus Production *via* Decreased Virion Assembly. *Intervirology* 54 (4), 202–216. doi:10.1159/000321892

Martinez-Gutierrez, M., Correa-Londoño, L. A., Castellanos, J. E., Gallego-Gómez, J. C., and Osorio, J. E. (2014). Lovastatin Delays Infection and Increases Survival Rates in AG129 Mice Infected with Dengue Virus Serotype 2. *PLoS One* 9 (2), e87412. doi:10.1371/journal.pone.0087412

Maruyama, Y., Yoshida, H., Uchino, S., Yokoyama, K., Yamamoto, H., Takinami, M., et al. (2011). Nafamostat Mesilate as an Anticoagulant during Continuous Veno-Venous Hemodialysis: a Three-Year Retrospective Cohort Study. *Int. J. Artif. Organs* 34 (7), 571–576. doi:10.5301/IJAO.2011.8535

Masse, S., Lu, X., Dekhtyar, T., Lu, L., Koev, G., Gao, F., et al. (2007). *In vitro* selection and Characterization of Human Immunodeficiency Virus Type 2 with Decreased Susceptibility to Lopinavir. *Antimicrob. Agents Chemother.* 51 (9), 3075–3080. doi:10.1128/AAC.00146-07

Matsuda, S., and Koyasu, S. (2000). Mechanisms of Action of Cyclosporine. *Immunopharmacology* 47 (2-3), 119–125. doi:10.1016/s0162-3109(00)00192-2

Mazière, J. C., Landureau, J. C., Giral, P., Auclair, M., Fall, L., Lachgar, A., et al. (1994). Lovastatin Inhibits HIV-1 Expression in H9 Human T Lymphocytes Cultured in Cholesterol-Poor Medium. *Biomed. Pharmacother.* 48 (2), 63–67. doi:10.1016/0753-3322(94)90077-9

McCarthy, S. D., Majchrzak-Kita, B., Racine, T., Kozlowski, H. N., Baker, D. P., Hoenen, T., et al. (2016). A Rapid Screening Assay Identifies Monotherapy with Interferon-Ss and Combination Therapies with Nucleoside Analogs as Effective Inhibitors of Ebola Virus. *Plos Negl. Trop. Dis.* 10 (1), e0004364. doi:10.1371/journal.pntd.0004364

McCormick, J. B., King, I. J., Webb, P. A., Scribner, C. L., Craven, R. B., Johnson, K. M., et al. (1986). Lassa Fever. Effective Therapy with Ribavirin. *N. Engl. J. Med.* 314 (1), 20–26. doi:10.1056/NEJM198601023140104

Mikuličić, S., Finke, J., Boukhallouk, F., Wüstenhagen, E., Sons, D., Homsi, Y., et al. (2019). ADAM17-dependent signaling is required for oncogenic human papillomavirus entry platform assembly. *Elife* 8, e44345. doi:10.7554/eLife.44345

Milligan, G. N., Sarathy, V. V., White, M. M., Greenberg, M. B., Campbell, G. A., Pyles, R. B., et al. (2017). A Lethal Model of Disseminated Dengue Virus Type 1 Infection in AG129 Mice. *J. Gen. Virol.* 98 (10), 2507–2519. doi:10.1099/jgv.0.000923

Min, J. S., Kim, G. W., Kwon, S., and Jin, Y. H. (2020). A Cell-Based Reporter Assay for Screening Inhibitors of MERS Coronavirus RNA-dependent RNA Polymerase Activity. *J. Clin. Med.* 9 (8). doi:10.3390/jcm9082399

Morrey, J. D., Smee, D. F., Sidwell, R. W., and Tseng, C. (2002). Identification of Active Antiviral Compounds against a New York Isolate of West Nile Virus. *Antivir. Res* 55 (1), 107–116. doi:10.1016/s0166-3542(02)00013-x

Morrey, J. D., Taro, B. S., Siddharthan, V., Wang, H., Smee, D. F., Christensen, A. J., et al. (2008). Efficacy of Orally Administered T-705 Pyrazine Analog on Lethal West Nile Virus Infection in Rodents. *Antivir. Res* 80 (3), 377–379. doi:10.1016/j.antiviral.2008.07.009

Mukhopadhyay, S., Kuhn, R. J., and Rossmann, M. G. (2005). A Structural Perspective of the Flavivirus Life Cycle. *Nat. Rev. Microbiol.* 3 (1), 13–22. doi:10.1038/nrmicro1067

Mulangu, S., Dodd, L. E., Davey, R. T., Jr., Tshiani Mbaya, O., Proschan, M., Mukadi, D., et al. (2019). A Randomized, Controlled Trial of Ebola Virus Disease Therapeutics. *N. Engl. J. Med.* 381 (24), 2293–2303. doi:10.1056/NEJMoa1910993

Mumtaz, N., Jimmerson, L. C., Bushman, L. R., Kiser, J. J., Aron, G., Reusken, C., et al. (2017). Cell-line Dependent Antiviral Activity of Sofosbuvir against Zika Virus. *Antivir. Res* 146, 161–163. doi:10.1016/j.antiviral.2017.09.004

Musarrat, F., Chouljenko, V., Dahal, A., Nabi, R., Chouljenko, T., Jois, S. D., et al. (2020). The Anti-HIV Drug Nelfinavir Mesylate (Viracept) Is a Potent Inhibitor of Cell Fusion Caused by the SARS-CoV-2 Spike (S) Glycoprotein Warranting Further Evaluation as an Antiviral against COVID-19 Infections. *J. Med. Virol.* 92 (10), 2087–2095. doi:10.1002/jmv.25985

Nakkazi, E. (2018). Randomised Controlled Trial Begins for Ebola Therapeutics. *Lancet* 392 (10162), 2338. doi:10.1016/S0140-6736(18)33011-3

Netzler, N. E., Enosi Tuipulotu, D., Vasudevan, S. G., Mackenzie, J. M., and White, P. A. (2019). Antiviral Candidates for Treating Hepatitis E Virus Infection.

Antimicrob. Agents Chemother. 63 (6), e00003–00019. doi:10.1128/AAC.00003-19

Neveu, G., Ziv-Av, A., Barouch-Bentov, R., Berkerman, E., Mulholland, J., and Einav, S. (2015). AP-2-associated Protein Kinase 1 and Cyclin G-Associated Kinase Regulate Hepatitis C Virus Entry and Are Potential Drug Targets. *J. Virol.* 89 (8), 4387–4404. doi:10.1128/JVI.02705-14

Ngono, A. E., and Shresta, S. (2018). Immune Response to Dengue and Zika. *Annu. Rev. Immunol.* 36, 279–308. doi:10.1146/annurev-immunol-042617-053142

Nguyen, T. H., Guedj, J., Anglaret, X., Laouenan, C., Madelain, V., Taburet, A. M., et al. (2017). Favipiravir Pharmacokinetics in Ebola-Infected Patients of the JIKI Trial Reveals Concentrations Lower Than Targeted. *Plos Negl. Trop. Dis.* 11 (2), e0005389. doi:10.1371/journal.pntd.0005389

Nicolás, D., Ambrosioni, J., Sued, O., Brunet, M., López-Diéguez, M., Manzardo, C., et al. (2017). Cyclosporine A in Addition to Standard ART during Primary HIV-1 Infection: Pilot Randomized Clinical Trial. *J. Antimicrob. Chemother.* 72 (3), 829–836. doi:10.1093/jac/dkw462

Noel, F., Azalim, P., do Monte, F. M., Quintas, L. E. M., Katz, A., and Karlish, S. J. D. (2018). Revisiting the Binding Kinetics and Inhibitory Potency of Cardiac Glycosides on Na(+),K(+)-ATPase (Alpha1beta1): Methodological Considerations. *J. Pharmacol. Toxicol. Methods* 94 (Pt 2), 64–72. doi:10.1016/j.vascn.2018.09.001

Norris, M. J., Malhi, M., Duan, W., Ouyang, H., Granados, A., Cen, Y., et al. (2018). Targeting Intracellular Ion Homeostasis for the Control of Respiratory Syncytial Virus. *Am. J. Respir. Cel Mol Biol* 59 (6), 733–744. doi:10.1165/rcmb.2017-0345OC

Oestereich, L., Ludtke, A., Wurr, S., Rieger, T., Munoz-Fontela, C., and Gunther, S. (2014a). Successful Treatment of Advanced Ebola Virus Infection with T-705 (Favipiravir) in a Small Animal Model. *Antivir. Res* 105, 17–21. doi:10.1016/j.antiviral.2014.02.014

Oestereich, L., Rieger, T., Ludtke, A., Ruibal, P., Wurr, S., Pallasch, E., et al. (2016). Efficacy of Favipiravir Alone and in Combination with Ribavirin in a Lethal, Immunocompetent Mouse Model of Lassa Fever. *J. Infect. Dis.* 213 (6), 934–938. doi:10.1093/infdis/jiv522

Oestereich, L., Rieger, T., Neumann, M., Bernreuther, C., Lehmann, M., Krasemann, S., et al. (2014b). Evaluation of Antiviral Efficacy of Ribavirin, Arbidol, and T-705 (Favipiravir) in a Mouse Model for Crimean-Congo Hemorrhagic Fever. *Plos Negl. Trop. Dis.* 8 (5), e2804. doi:10.1371/journal.pntd.0002804

Ogg, M., Jonsson, C. B., Camp, J. V., and Hooper, J. W. (2013). Ribavirin Protects Syrian Hamsters against Lethal Hantavirus Pulmonary Syndrome-Aafter Intranasal Exposure to Andes Virus. *Viruses* 5 (11), 2704–2720. doi:10.3390/v5112704

Okuse, C., Rinaudo, J. A., Farrar, K., Wells, F., and Korba, B. E. (2005). Enhancement of Antiviral Activity against Hepatitis C Virus *In Vitro* by Interferon Combination Therapy. *Antivir. Res* 65 (1), 23–34. doi:10.1016/j.antiviral.2004.09.002

Okuyama-Dobashi, K., Kasai, H., Tanaka, T., Yamashita, A., Yasumoto, J., Chen, W., et al. (2015). Hepatitis B Virus Efficiently Infects Non-adherent Hepatoma Cells via Human Sodium Taurocholate Cotransporting Polypeptide. *Sci. Rep.* 5, 17047. doi:10.1038/srep17047

Omrani, A. S., Saad, M. M., Baig, K., Bahloul, A., Abdul-Matin, M., Alaidaroos, A. Y., et al. (2014). Ribavirin and Interferon Alfa-2a for Severe Middle East Respiratory Syndrome Coronavirus Infection: a Retrospective Cohort Study. *Lancet Infect. Dis.* 14 (11), 1090–1095. doi:10.1016/S1473-3099(14)70920-X

Ortega-Prieto, A. M., Sheldon, J., Grande-Perez, A., Tejero, H., Gregori, J., Quer, J., et al. (2013). Extinction of Hepatitis C Virus by Ribavirin in Hepatoma Cells Involves Lethal Mutagenesis. *PLoS One* 8 (8), e71039. doi:10.1371/journal.pone.0071039

Ortiz, J. J., Ayoub, A., Gargala, G., Chegne, N. L., and Favennec, L. (2001). Randomized Clinical Study of Nitazoxanide Compared to Metronidazole in the Treatment of Symptomatic Giardiasis in Children from Northern Peru. *Aliment. Pharmacol. Ther.* 15 (9), 1409–1415. doi:10.1046/j.1365-2036.2001.01066.x

Pan, Q., de Ruiter, P. E., Metselaar, H. J., Kwekkeboom, J., de Jonge, J., Tilanus, H. W., et al. (2012). Mycophenolic Acid Augments Interferon-Stimulated Gene Expression and Inhibits Hepatitis C Virus Infection *In Vitro* and *In Vivo*. *Hepatology* 55 (6), 1673–1683. doi:10.1002/hep.25562

Panel, A.-I. H. G. (2018). Hepatitis C Guidance 2018 Update: AASLD-IDSA Recommendations for Testing, Managing, and Treating Hepatitis C Virus Infection. *Clin. Infect. Dis.* 67 (10), 1477–1492. doi:10.1093/cid/ciy585

Patel, H., and Kukol, A. (2017). Evolutionary Conservation of Influenza A PB2 Sequences Reveals Potential Target Sites for Small Molecule Inhibitors. *Virology* 509, 112–120. doi:10.1016/j.virol.2017.06.009

Pedersen, N. C., Perron, M., Bannasch, M., Montgomery, E., Murakami, E., Liepnieks, M., et al. (2019). Efficacy and Safety of the Nucleoside Analog GS-441524 for Treatment of Cats with Naturally Occurring Feline Infectious Peritonitis. *J. Feline Med. Surg.* 21 (4), 271–281. doi:10.1177/1098612X19825701

Peiris, J. S., Chu, C. M., Cheng, V. C., Chan, K. S., Hung, I. F., Poon, L. L., et al. (2003). Clinical Progression and Viral Load in a Community Outbreak of Coronavirus-Associated SARS Pneumonia: a Prospective Study. *Lancet* 361 (9371), 1767–1772. doi:10.1016/s0140-6736(03)13412-5

Perelygina, L., Hautala, T., Seppänen, M., Adebayo, A., Sullivan, K. E., and Icenogle, J. (2017). Inhibition of Rubella Virus Replication by the Broad-Spectrum Drug Nitazoxanide in Cell Culture and in a Patient with a Primary Immune Deficiency. *Antivir. Res* 147, 58–66. doi:10.1016/j.antiviral.2017.09.019

Persaud, M., Martinez-Lopez, A., Buffone, C., Porcelli, S. A., and Diaz-Griffero, F. (2018). Infection by Zika Viruses Requires the Transmembrane Protein AXL, Endocytosis and Low pH. *Virology* 518, 301–312. doi:10.1016/j.virol.2018.03.009

Pfefferle, S., Schöpf, J., Kögl, M., Friedel, C. C., Müller, M. A., Carbajo-Lozoya, J., et al. (2011). The SARS-Coronavirus-Host Interactome: Identification of Cyclophilins as Target for Pan-Coronavirus Inhibitors. *Plos Pathog.* 7 (10), e1002331. doi:10.1371/journal.ppat.1002331

Phillips, S., Chokshi, S., Chatterji, U., Riva, A., Bobardt, M., Williams, R., et al. (2015). Alisporivir Inhibition of Hepatocyte Cyclophilins Reduces HBV Replication and Hepatitis B Surface Antigen Production. *Gastroenterology* 148 (2), 403–414. doi:10.1053/j.gastro.2014.10.004

Piacentini, S., La Frazia, S., Riccio, A., Pedersen, J. Z., Topai, A., Nicolotti, O., et al. (2018). Nitazoxanide Inhibits Paramyxovirus Replication by Targeting the Fusion Protein Folding: Role of Glycoprotein-specific Thiol Oxidoreductase ERp57. *Sci. Rep.* 8 (1), 10425. doi:10.1038/s41598-018-28172-9

Pires de Mello, C. P., Drusano, G. L., Rodriquez, J. L., Kaushik, A., and Brown, A. N. (2018a). Antiviral Effects of Clinically-Relevant Interferon-Alpha and Ribavirin Regimens against Dengue Virus in the Hollow Fiber Infection Model (HFIM). *Viruses* 10 (6). doi:10.3390/v10060317

Pires de Mello, C. P., Tao, X., Kim, T. H., Bulitta, J. B., Rodriquez, J. L., Pomeroy, J. J., et al. (2018b). Zika Virus Replication Is Substantially Inhibited by Novel Favipiravir and Interferon Alpha Combination Regimens. *Antimicrob. Agents Chemother.* 62 (1). doi:10.1128/AAC.01983-17

Pohjala, L., Utt, A., Varjak, M., Lulla, A., Merits, A., Ahola, T., et al. (2011). Inhibitors of Alphavirus Entry and Replication Identified with a Stable Chikungunya Replicon Cell Line and Virus-Based Assays. *PLoS One* 6 (12), e28923. doi:10.1371/journal.pone.0028923

Pontremoli, C., Forni, D., and Sironi, M. (2019). Arenavirus Genomics: Novel Insights into Viral Diversity, Origin, and Evolution. *Curr. Opin. Virol.* 34, 18–28. doi:10.1016/j.coviro.2018.11.001

Qian, Z., Dominguez, S. R., and Holmes, K. V. (2013). Role of the Spike Glycoprotein of Human Middle East Respiratory Syndrome Coronavirus (MERS-CoV) in Virus Entry and Syncytia Formation. *PLoS One* 8 (10), e76469. doi:10.1371/journal.pone.0076469

Qing, M., Yang, F., Zhang, B., Zou, G., Robida, J. M., Yuan, Z., et al. (2009). Cyclosporine Inhibits Flavivirus Replication through Blocking the Interaction between Host Cyclophilins and Viral NS5 Protein. *Antimicrob. Agents Chemother.* 53 (8), 3226–3235. doi:10.1128/AAC.00189-09

Rainsford, K. D., Parke, A. L., Clifford-Rashotte, M., and Kean, W. F. (2015). Therapy and Pharmacological Properties of Hydroxychloroquine and Chloroquine in Treatment of Systemic Lupus Erythematosus, Rheumatoid Arthritis and Related Diseases. *Inflammopharmacology* 23 (5), 231–269. doi:10.1007/s10787-015-0239-y

Raj, V. S., Mou, H., Smits, S. L., Dekkers, D. H., Müller, M. A., Dijkman, R., et al. (2013). Dipeptidyl Peptidase 4 Is a Functional Receptor for the Emerging Human Coronavirus-EMC. *Nature* 495 (7440), 251–254. doi:10.1038/nature12005

Ramos, I., and Fernandez-Sesma, A. (2012). Cell Receptors for Influenza a Viruses and the Innate Immune Response. *Front. Microbiol.* 3, 117. doi:10.3389/fmicb.2012.00117

Rathore, A. P., Mantri, C. K., Aman, S. A., Syenina, A., Ooi, J., Jagaraj, C. J., et al. (2019). Dengue Virus-Elicited Tryptase Induces Endothelial Permeability and Shock. *J. Clin. Invest.* 130 (10), 4180–4193. doi:10.1172/jci128426

Ravi, L. I., Li, L., Wong, P. S., Sutejo, R., Tan, B. H., and Sugrue, R. J. (2013a). Lovastatin Treatment Mitigates the Pro-inflammatory Cytokine Response in Respiratory Syncytial Virus Infected Macrophage Cells. *Antivir. Res* 98 (2), 332–343. doi:10.1016/j.antiviral.2013.03.015

Ravi, L. I., Liang, L., Wong, P. S., Brown, G., Tan, B. H., and Sugrue, R. J. (2013b). Increased Hydroxymethylglutaryl Coenzyme A Reductase Activity during Respiratory Syncytial Virus Infection Mediates Actin Dependent Intercellular Virus Transmission. *Antivir. Res* 100 (1), 259–268. doi:10.1016/j.antiviral.2013.08.012

Reeves, P. M., Smith, S. K., Olson, V. A., Thorne, S. H., Bornmann, W., Damon, I. K., et al. (2011). *Variola* and Monkeypox Viruses Utilize Conserved Mechanisms of Virion Motility and Release that Depend on Abl and SRC Family Tyrosine Kinases. *J. Virol.* 85 (1), 21–31. doi:10.1128/JVI.01814-10

Rhein, B. A., Powers, L. S., Rogers, K., Anantpadma, M., Singh, B. K., Sakurai, Y., et al. (2015). Interferon-γ Inhibits Ebola Virus Infection. *Plos Pathog.* 11 (11), e1005263. doi:10.1371/journal.ppat.1005263

Rice, G. P., Incorvaia, B., Munari, L., Ebers, G., Polman, C., D'Amico, R., et al. (2001). Interferon in Relapsing-Remitting Multiple Sclerosis. *Cochrane Database Syst. Rev.* 4, CD002002. doi:10.1002/14651858.CD002002

Ricotta, D., Conner, S. D., Schmid, S. L., von Figura, K., and Honing, S. (2002). Phosphorylation of the AP2 Mu Subunit by AAK1 Mediates High Affinity Binding to Membrane Protein Sorting Signals. *J. Cel Biol.* 156 (5), 791–795. doi:10.1083/jcb.200111068

Riva, L., Yuan, S., Yin, X., Martin-Sancho, L., Matsunaga, N., Pache, L., et al. (2020). Discovery of SARS-CoV-2 Antiviral Drugs through Large-Scale Compound Repurposing. *Nature* 586 (7827), 113–119. doi:10.1038/s41586-020-2577-1

Rivera-Serrano, E. E., Gonzalez-Lopez, O., Das, A., and Lemon, S. M. (2019). Cellular Entry and Uncoating of Naked and Quasi-Enveloped Human Hepatoviruses. *Elife* 8, e43983. doi:10.7554/eLife.43983

Robinzon, S., Dafa-Berger, A., Dyer, M. D., Paeper, B., Proll, S. C., Teal, T. H., et al. (2009). Impaired Cholesterol Biosynthesis in a Neuronal Cell Line Persistently Infected with Measles Virus. *J. Virol.* 83 (11), 5495–5504. doi:10.1128/jvi.01880-08

Rocco, P. R. M., Silva, P. L., Cruz, F. F., Junior, M., Tierno, P., Moura, M. A., et al. (2021). Early Use of Nitazoxanide in Mild Covid-19 Disease: Randomised, Placebo-Controlled Trial. *Eur. Respir. J.* doi:10.1183/13993003.03725-2020

Rocha-Pereira, J., Nascimento, M. S., Ma, Q., Hilgenfeld, R., Neyts, J., and Jochmans, D. (2014). The Enterovirus Protease Inhibitor Rupintrivir Exerts Cross-Genotypic Anti-norovirus Activity and Clears Cells from the Norovirus Replicon. *Antimicrob. Agents Chemother.* 58 (8), 4675–4681. doi:10.1128/AAC.02546-13

Rossignol, J. F., and El-Gohary, Y. M. (2006). Nitazoxanide in the Treatment of Viral Gastroenteritis: a Randomized Double-Blind Placebo-Controlled Clinical Trial. *Aliment. Pharmacol. Ther.* 24 (10), 1423–1430. doi:10.1111/j.1365-2036.2006.03128.x

Rossignol, J. F., Elfert, A., and Keeffe, E. B. (2010). Treatment of Chronic Hepatitis C Using a 4-week Lead-In with Nitazoxanide before Peginterferon Plus Nitazoxanide. *J. Clin. Gastroenterol.* 44 (7), 504–509. doi:10.1097/MCG.0b013e3181bf9b15

Rossignol, J. F., Kabil, S. M., El-Gohary, Y., Elfert, A., and Keeffe, E. B. (2008). Clinical Trial: Randomized, Double-Blind, Placebo-Controlled Study of Nitazoxanide Monotherapy for the Treatment of Patients with Chronic Hepatitis C Genotype 4. *Aliment. Pharmacol. Ther.* 28 (5), 574–580. doi:10.1111/j.1365-2036.2008.03781.x

Rossignol, J. F., and Keeffe, E. B. (2008). Thiazolides: a New Class of Drugs for the Treatment of Chronic Hepatitis B and C. *Future Microbiol.* 3 (5), 539–545. doi:10.2217/17460913.3.5.539

Rossignol, J. F., La Frazia, S., Chiappa, L., Ciucci, A., and Santoro, M. G. (2009). Thiazolides, a New Class of Anti-influenza Molecules Targeting Viral Hemagglutinin at the Post-translational Level. *J. Biol. Chem.* 284 (43), 29798–29808. doi:10.1074/jbc.M109.029470

Rossignol, J. F. (2016). Nitazoxanide, a New Drug Candidate for the Treatment of Middle East Respiratory Syndrome Coronavirus. *J. Infect. Public Health* 9 (3), 227–230. doi:10.1016/j.jiph.2016.04.001

Rossignol, J. F. (2014). Nitazoxanide: a First-In-Class Broad-Spectrum Antiviral Agent. *Antivir. Res* 110, 94–103. doi:10.1016/j.antiviral.2014.07.014

Rothberg, M. B., Bigelow, C., Pekow, P. S., and Lindenauer, P. K. (2012). Association between Statins Given in Hospital and Mortality in Pneumonia Patients. *J. Gen. Intern. Med.* 27 (3), 280–286. doi:10.1007/s11606-011-1826-2

Sacramento, C. Q., de Melo, G. R., de Freitas, C. S., Rocha, N., Hoelz, L. V., Miranda, M., et al. (2017). The Clinically Approved Antiviral Drug Sofosbuvir Inhibits Zika Virus Replication. *Sci. Rep.* 7, 40920. doi:10.1038/srep40920

Saijo, M., Morikawa, S., Fukushi, S., Mizutani, T., Hasegawa, H., Nagata, N., et al. (2005). Inhibitory Effect of Mizoribine and Ribavirin on the Replication of Severe Acute Respiratory Syndrome (SARS)-associated Coronavirus. *Antivir. Res* 66 (2-3), 159–163. doi:10.1016/j.antiviral.2005.01.003

Saini, M., and Potash, M. J. (2006). Novel Activities of Cyclophilin A and Cyclosporin A during HIV-1 Infection of Primary Lymphocytes and Macrophages. *J. Immunol.* 177 (1), 443–449. doi:10.4049/jimmunol.177.1.443

Sarathy, V. V., White, M., Li, L., Gorder, S. R., Pyles, R. B., Campbell, G. A., et al. (2015). A Lethal Murine Infection Model for Dengue Virus 3 in AG129 Mice Deficient in Type I and II Interferon Receptors Leads to Systemic Disease. *J. Virol.* 89 (2), 1254–1266. doi:10.1128/JVI.01320-14

Savarino, A., Gennero, L., Sperber, K., and Boelaert, J. R. (2001). The Anti-HIV-1 Activity of Chloroquine. *J. Clin. Virol.* 20 (3), 131–135. doi:10.1016/s1386-6532(00)00139-6

Scheidel, L. M., and Stollar, V. (1991). Mutations that Confer Resistance to Mycophenolic Acid and Ribavirin on Sindbis Virus Map to the Nonstructural Protein nsP1. *Virology* 181 (2), 490–499. doi:10.1016/0042-6822(91)90881-b

Sebastian, L., Madhusudana, S. N., Ravi, V., and Desai, A. (2011). Mycophenolic Acid Inhibits Replication of Japanese Encephalitis Virus. *Chemotherapy* 57 (1), 56–61. doi:10.1159/000321483

Shah, N. R., Sunderland, A., and Grdzelishvili, V. Z. (2010). Cell Type Mediated Resistance of Vesicular Stomatitis Virus and Sendai Virus to Ribavirin. *PLoS One* 5 (6), e11265. doi:10.1371/journal.pone.0011265

Sheahan, T. P., Sims, A. C., Graham, R. L., Menachery, V. D., Gralinski, L. E., Case, J. B., et al. (2017a). Broad-spectrum Antiviral GS-5734 Inhibits Both Epidemic and Zoonotic Coronaviruses. *Sci. Transl Med.* 9 (396), eaal3653. doi:10.1126/scitranslmed.aal3653

Sheahan, T. P., Sims, A. C., Graham, R. L., Menachery, V. D., Gralinski, L. E., Case, J. B., et al. (2017b). Broad-spectrum Antiviral GS-5734 Inhibits Both Epidemic and Zoonotic Coronaviruses. *Sci. Transl Med.* 9 (396). doi:10.1126/scitranslmed.aal3653

Sheahan, T. P., Sims, A. C., Leist, S. R., Schafer, A., Won, J., Brown, A. J., et al. (2020). Comparative Therapeutic Efficacy of Remdesivir and Combination Lopinavir, Ritonavir, and Interferon Beta against MERS-CoV. *Nat. Commun.* 11 (1), 222. doi:10.1038/s41467-019-13940-6

Shen, Z., Tian, Z., He, H., Zhang, J., Li, J., and Wu, Y. (2015). Antiviral Effects of Cyclosporine A in Neonatal Mice with Rotavirus-Induced Diarrhea. *J. Pediatr. Gastroenterol. Nutr.* 60 (1), 11–17. doi:10.1097/mpg.0000000000000493

Shi, B. J., Liu, C. C., Zhou, J., Wang, S. Q., Gao, Z. C., Zhang, X. M., et al. (2016). Entry of Classical Swine Fever Virus into PK-15 Cells *via* a pH-, Dynamin-, and Cholesterol-dependent, Clathrin-Mediated Endocytic Pathway that Requires Rab5 and Rab7. *J. Virol.* 90 (20), 9194–9208. doi:10.1128/jvi.00688-16

Shi, Z., Wei, J., Deng, X., Li, S., Qiu, Y., Shao, D., et al. (2014). Nitazoxanide Inhibits the Replication of Japanese Encephalitis Virus in Cultured Cells and in a Mouse Model. *Virol. J.* 11, 10. doi:10.1186/1743-422x-11-10

Shie, J. J., Fang, J. M., Kuo, T. H., Kuo, C. J., Liang, P. H., Huang, H. J., et al. (2005). Inhibition of the Severe Acute Respiratory Syndrome 3CL Protease by Peptidomimetic Alpha, beta-Unsaturated Esters. *Bioorg. Med. Chem.* 13 (17), 5240–5252. doi:10.1016/j.bmc.2005.05.065

Shimura, S., Watashi, K., Fukano, K., Peel, M., Sluder, A., Kawai, F., et al. (2017). Cyclosporin Derivatives Inhibit Hepatitis B Virus Entry without Interfering with NTCP Transporter Activity. *J. Hepatol.* 66 (4), 685–692. doi:10.1016/j.jhep.2016.11.009

Shirato, K., Kawase, M., and Matsuyama, S. (2013). Middle East Respiratory Syndrome Coronavirus Infection Mediated by the Transmembrane Serine Protease TMPRSS2. *J. Virol.* 87 (23), 12552–12561. doi:10.1128/jvi.01890-13

Shiryaev, S. A., Mesci, P., Pinto, A., Fernandes, I., Sheets, N., Shresta, S., et al. (2017). Repurposing of the Anti-malaria Drug Chloroquine for Zika Virus Treatment and Prophylaxis. *Sci. Rep.* 7 (1), 15771. doi:10.1038/s41598-017-15467-6

Shrivastava-Ranjan, P., Flint, M., Bergeron, É., McElroy, A. K., Chatterjee, P., Albariño, C. G., et al. (2018). Statins Suppress Ebola Virus Infectivity by Interfering with Glycoprotein Processing. *mBio* 9 (3). doi:10.1128/mBio.00660-18

Simmons, G., Gosalia, D. N., Rennekamp, A. J., Reeves, J. D., Diamond, S. L., and Bates, P. (2005). Inhibitors of Cathepsin L Prevent Severe Acute Respiratory Syndrome Coronavirus Entry. *Proc. Natl. Acad. Sci. U. S. A.* 102 (33), 11876–11881. doi:10.1073/pnas.0505577102

Simon, M., Johansson, C., and Mirazimi, A. (2009). Crimean-Congo Hemorrhagic Fever Virus Entry and Replication Is Clathrin-, pH- and Cholesterol-dependent. *J. Gen. Virol.* 90 (Pt 1), 210–215. doi:10.1099/vir.0.006387-0

Sissoko, D., Laouenan, C., Folkesson, E., M'Lebing, A. B., Beavogui, A. H., Baize, S., et al. (2016). Experimental Treatment with Favipiravir for Ebola Virus Disease (The JIKI Trial): A Historically Controlled, Single-Arm Proof-Of-Concept Trial in Guinea. *Plos Med.* 13 (3), e1001967. doi:10.1371/journal.pmed.1001967

Sleeman, K., Mishin, V. P., Deyde, V. M., Furuta, Y., Klimov, A. I., and Gubareva, L. V. (2010). *In vitro* antiviral Activity of Favipiravir (T-705) against Drug-Resistant Influenza and 2009 A(H1N1) Viruses. *Antimicrob. Agents Chemother.* 54 (6), 2517–2524. doi:10.1128/AAC.01739-09

Smee, D. F., Bray, M., and Huggins, J. W. (2001). Antiviral Activity and Mode of Action Studies of Ribavirin and Mycophenolic Acid against Orthopoxviruses *In Vitro*. *Antivir. Chem. Chemother.* 12 (6), 327–335. doi:10.1177/095632020101200602

Softic, L., Brillet, R., Berry, F., Ahnou, N., Nevers, Q., Morin-Dewaele, M., et al. (2020). Inhibition of SARS-CoV-2 Infection by the Cyclophilin Inhibitor Alisporivir (Debio 025). *Antimicrob. Agents Chemother.* 64 (7), e0087620. doi:10.1128/AAC.00876-20

Soto-Acosta, R., Bautista-Carbajal, P., Cervantes-Salazar, M., Angel-Ambrocio, A. H., and Del Angel, R. M. (2017). DENV Up-Regulates the HMG-CoA Reductase Activity through the Impairment of AMPK Phosphorylation: A Potential Antiviral Target. *Plos Pathog.* 13 (4), e1006257. doi:10.1371/journal.ppat.1006257

Sperber, K., Louie, M., Kraus, T., Proner, J., Sapira, E., Lin, S., et al. (1995). Hydroxychloroquine Treatment of Patients with Human Immunodeficiency Virus Type 1. *Clin. Ther.* 17 (4), 622–636. doi:10.1016/0149-2918(95)80039-5

Spinner, C. D., Gottlieb, R. L., Criner, G. J., Arribas Lopez, J. R., Cattelan, A. M., Soriano Viladomiu, A., et al. (2020). Effect of Remdesivir vs Standard Care on Clinical Status at 11 Days in Patients with Moderate COVID-19: A Randomized Clinical Trial. *JAMA* 324 (11), 1048–1057. doi:10.1001/jama.2020.16349

Stanciu, C., Trifan, A., Muzica, C., and Sfarti, C. (2019). Efficacy and Safety of Alisporivir for the Treatment of Hepatitis C Infection. *Expert Opin. Pharmacother.* 20 (4), 379–384. doi:10.1080/14656566.2018.1560424

Stanifer, M. L., Pervolaraki, K., and Boulant, S. (2019). Differential Regulation of Type I and Type III Interferon Signaling. *Int. J. Mol. Sci.* 20 (6), 1445. doi:10.3390/ijms20061445

Su, C. T., Hsu, J. T., Hsieh, H. P., Lin, P. H., Chen, T. C., Kao, C. L., et al. (2008). Anti-HSV Activity of Digitoxin and its Possible Mechanisms. *Antivir. Res* 79 (1), 62–70. doi:10.1016/j.antiviral.2008.01.156

Tam, R. C., Pai, B., Bard, J., Lim, C., Averett, D. R., Phan, U. T., et al. (1999). Ribavirin Polarizes Human T Cell Responses towards a Type 1 Cytokine Profile. *J. Hepatol.* 30 (3), 376–382. doi:10.1016/s0168-8278(99)80093-2

Tan, E. L., Ooi, E. E., Lin, C. Y., Tan, H. C., Ling, A. E., Lim, B., et al. (2004). Inhibition of SARS Coronavirus Infection *In Vitro* with Clinically Approved Antiviral Drugs. *Emerg. Infect. Dis.* 10 (4), 581–586. doi:10.3201/eid1004.030458

Tan, X., Hu, L., Luquette, L. J., 3rd, Gao, G., Liu, Y., Qu, H., et al. (2012). Systematic Identification of Synergistic Drug Pairs Targeting HIV. *Nat. Biotechnol.* 30 (11), 1125–1130. doi:10.1038/nbt.2391

Tan, X., Sun, L., Chen, J., and Chen, Z. J. (2018). Detection of Microbial Infections through Innate Immune Sensing of Nucleic Acids. *Annu. Rev. Microbiol.* 72, 447–478. doi:10.1146/annurev-micro-102215-095605

Tanaka, Y., Sato, Y., and Sasaki, T. (2013). Suppression of Coronavirus Replication by Cyclophilin Inhibitors. *Viruses* 5 (5), 1250–1260. doi:10.3390/v5051250

Tchesnokov, E. P., Feng, J. Y., Porter, D. P., and Gotte, M. (2019). Mechanism of Inhibition of Ebola Virus RNA-dependent RNA Polymerase by Remdesivir. *Viruses* 11 (4). doi:10.3390/v11040326

Teran, C. G., Teran-Escalera, C. N., and Villarroel, P. (2009). Nitazoxanide vs. Probiotics for the Treatment of Acute Rotavirus Diarrhea in Children: a Randomized, Single-Blind, Controlled Trial in Bolivian Children. *Int. J. Infect. Dis.* 13 (4), 518–523. doi:10.1016/j.ijid.2008.09.014

Thome, R., Lopes, S. C., Costa, F. T., and Verinaud, L. (2013). Chloroquine: Modes of Action of an Undervalued Drug. *Immunol. Lett.* 153 (1-2), 50–57. doi:10.1016/j.imlet.2013.07.004

To, K. K. W., Mok, K. Y., Chan, A. S. F., Cheung, N. N., Wang, P., Lui, Y. M., et al. (2016). Mycophenolic Acid, an Immunomodulator, Has Potent and Broad-Spectrum *In Vitro* Antiviral Activity against Pandemic, Seasonal and Avian Influenza Viruses Affecting Humans. *J. Gen. Virol.* 97 (8), 1807–1817. doi:10.1099/jgv.0.000512

Todt, D., Moeller, N., Praditya, D., Kinast, V., Friesland, M., Engelmann, M., et al. (2018). The Natural Compound Silvestrol Inhibits Hepatitis E Virus (HEV) Replication *In Vitro* and *In Vivo*. *Antivir. Res* 157, 151–158. doi:10.1016/j.antiviral.2018.07.010

Tricou, V., Minh, N. N., Van, T. P., Lee, S. J., Farrar, J., Wills, B., et al. (2010). A Randomized Controlled Trial of Chloroquine for the Treatment of Dengue in Vietnamese Adults. *Plos Negl. Trop. Dis.* 4 (8), e785. doi:10.1371/journal.pntd.0000785

Tsai, W. P., Nara, P. L., Kung, H. F., and Oroszlan, S. (1990). Inhibition of Human Immunodeficiency Virus Infectivity by Chloroquine. *AIDS Res. Hum. Retroviruses* 6 (4), 481–489. doi:10.1089/aid.1990.6.481

Ulferts, R., de Boer, S. M., van der Linden, L., Bauer, L., Lyoo, H. R., Mate, M. J., et al. (2016). Screening of a Library of FDA-Approved Drugs Identifies Several Enterovirus Replication Inhibitors that Target Viral Protein 2C. *Antimicrob. Agents Chemother.* 60 (5), 2627–2638. doi:10.1128/AAC.02182-15

Urata, S., Uno, Y., Kurosaki, Y., and Yasuda, J. (2018). The Cholesterol, Fatty Acid and Triglyceride Synthesis Pathways Regulated by Site 1 Protease (S1P) Are Required for Efficient Replication of Severe Fever with Thrombocytopenia Syndrome Virus. *Biochem. Biophys. Res. Commun.* 503 (2), 631–636. doi:10.1016/j.bbrc.2018.06.053

van Cleef, K. W., Overheul, G. J., Thomassen, M. C., Kaptein, S. J., Davidson, A. D., Jacobs, M., et al. (2013). Identification of a New Dengue Virus Inhibitor that Targets the Viral NS4B Protein and Restricts Genomic RNA Replication. *Antivir. Res* 99 (2), 165–171. doi:10.1016/j.antiviral.2013.05.011

van der Schaar, H. M., Dorobantu, C. M., Albulescu, L., Strating, J., and van Kuppeveld, F. J. M. (2016). Fat(al) Attraction: Picornaviruses Usurp Lipid Transfer at Membrane Contact Sites to Create Replication Organelles. *Trends Microbiol.* 24 (7), 535–546. doi:10.1016/j.tim.2016.02.017

van Gelder, T., and Hesselink, D. A. (2015). Mycophenolate Revisited. *Transpl. Int.* 28 (5), 508–515. doi:10.1111/tri.12554

Vatansever, E. C., Yang, K. S., Drelich, A. K., Kratch, K. C., Cho, C. C., Kempaiah, K. R., et al. (2021). Bepridil Is Potent against SARS-CoV-2 *In Vitro*. *Proc. Natl. Acad. Sci. U S A.* 118 (10), e2012201118. doi:10.1073/pnas.2012201118

Vincent, M. J., Bergeron, E., Benjannet, S., Erickson, B. R., Rollin, P. E., Ksiazek, T. G., et al. (2005). Chloroquine Is a Potent Inhibitor of SARS Coronavirus Infection and Spread. *Virol. J.* 2, 69. doi:10.1186/1743-422x-2-69

Wang, L. H., Rothberg, K. G., and Anderson, R. G. (1993). Mis-assembly of Clathrin Lattices on Endosomes Reveals a Regulatory Switch for Coated Pit Formation. *J. Cel Biol* 123 (5), 1107–1117. doi:10.1083/jcb.123.5.1107

Wang, M., Cao, R., Zhang, L., Yang, X., Liu, J., Xu, M., et al. (2020a). Remdesivir and Chloroquine Effectively Inhibit the Recently Emerged Novel Coronavirus (2019-nCoV) *In Vitro*. *Cel Res* 30 (3), 269–271. doi:10.1038/s41422-020-0282-0

Wang, M., Cao, R., Zhang, L., Yang, X., Liu, J., Xu, M., et al. (2020b). Remdesivir and Chloroquine Effectively Inhibit the Recently Emerged Novel Coronavirus (2019-nCoV) *In Vitro*. *Cel Res* 30 (3), 269–271. doi:10.1038/s41422-020-0282-0

Wang, R., Wang, X., Ni, B., Huan, C. C., Wu, J. Q., Wen, L. B., et al. (2016a). Syndecan-4, a PRRSV Attachment Factor, Mediates PRRSV Entry through its Interaction with EGFR. *Biochem. Biophys. Res. Commun.* 475 (2), 230–237. doi:10.1016/j.bbrc.2016.05.084

Wang, Y., Li, G., Yuan, S., Gao, Q., Lan, K., Altmeyer, R., et al. (2016b). *In Vitro* Assessment of Combinations of Enterovirus Inhibitors against Enterovirus 71. *Antimicrob. Agents Chemother.* 60 (9), 5357–5367. doi:10.1128/AAC.01073-16

Wang, Y. M., Lu, J. W., Lin, C. C., Chin, Y. F., Wu, T. Y., Lin, L. I., et al. (2016c). Antiviral Activities of Niclosamide and Nitazoxanide against Chikungunya Virus Entry and Transmission. *Antivir. Res* 135, 81–90. doi:10.1016/j.antiviral.2016.10.003

Wang, Y., Zhang, D., Du, G., Du, R., Zhao, J., Jin, Y., et al. (2020c). Remdesivir in Adults with Severe COVID-19: a Randomised, Double-Blind, Placebo-Controlled, Multicentre Trial. *Lancet* 395 (10236), 1569–1578. doi:10.1016/s0140-6736(20)31022-9

Wang, Y., Zhou, X., Debing, Y., Chen, K., Van Der Laan, L. J., Neyts, J., et al. (2014). Calcineurin Inhibitors Stimulate and Mycophenolic Acid Inhibits Replication of Hepatitis E Virus. *Gastroenterology* 146 (7), 1775–1783. doi:10.1053/j.gastro.2014.02.036

Warren, T. K., Jordan, R., Lo, M. K., Ray, A. S., Mackman, R. L., Soloveva, V., et al. (2016). Therapeutic Efficacy of the Small Molecule GS-5734 against Ebola Virus in Rhesus Monkeys. *Nature* 531 (7594), 381–385. doi:10.1038/nature17180

Warren, T. K., Wells, J., Panchal, R. G., Stuthman, K. S., Garza, N. L., Van Tongeren, S. A., et al. (2014). Protection against Filovirus Diseases by a Novel Broad-Spectrum Nucleoside Analogue BCX4430. *Nature* 508 (7496), 402–405. doi:10.1038/nature13027

Watashi, K., Hijikata, M., Hosaka, M., Yamaji, M., and Shimotohno, K. (2003). Cyclosporin A Suppresses Replication of Hepatitis C Virus Genome in Cultured Hepatocytes. *Hepatology* 38 (5), 1282–1288. doi:10.1053/jhep.2003.50449

Watashi, K., Sluder, A., Daito, T., Matsunaga, S., Ryo, A., Nagamori, S., et al. (2014). Cyclosporin A and its Analogs Inhibit Hepatitis B Virus Entry into Cultured Hepatocytes through Targeting a Membrane Transporter, Sodium Taurocholate Cotransporting Polypeptide (NTCP). *Hepatology* 59 (5), 1726–1737. doi:10.1002/hep.26982

Welch, S. R., Guerrero, L. W., Chakrabarti, A. K., McMullan, L. K., Flint, M., Bluemling, G. R., et al. (2016). Lassa and Ebola Virus Inhibitors Identified Using Minigenome and Recombinant Virus Reporter Systems. *Antivir. Res* 136, 9–18. doi:10.1016/j.antiviral.2016.10.007

Werner, B., Dittmann, S., Funke, C., Überla, K., Piper, C., Niehaus, K., et al. (2014). Effect of Lovastatin on Coxsackievirus B3 Infection in Human Endothelial Cells. *Inflamm. Res.* 63 (4), 267–276. doi:10.1007/s00011-013-0695-z

Westover, J. B., Mathis, A., Taylor, R., Wandersee, L., Bailey, K. W., Sefing, E. J., et al. (2018). Galidesivir Limits Rift Valley Fever Virus Infection and Disease in Syrian Golden Hamsters. *Antivir. Res* 156, 38–45. doi:10.1016/j.antiviral.2018.05.013

Wilen, C. B., Tilton, J. C., and Doms, R. W. (2012). HIV: Cell Binding and Entry. *Cold Spring Harb Perspect. Med.* 2 (8), a006866. doi:10.1101/cshperspect.a006866

Wong, R. W., Balachandran, A., Ostrowski, M. A., and Cochrane, A. (2013). Digoxin Suppresses HIV-1 Replication by Altering Viral RNA Processing. *Plos Pathog.* 9 (3), e1003241. doi:10.1371/journal.ppat.1003241

Wong, R. W., Lingwood, C. A., Ostrowski, M. A., Cabral, T., and Cochrane, A. (2018). Cardiac Glycoside/aglycones Inhibit HIV-1 Gene Expression by a Mechanism Requiring MEK1/2-Erk1/2 Signaling. *Sci. Rep.* 8 (1), 850. doi:10.1038/s41598-018-19298-x

Xu, H. T., Colby-Germinario, S. P., Hassounah, S. A., Fogarty, C., Osman, N., Palanisamy, N., et al. (2017). Evaluation of Sofosbuvir (Beta-D-2'-Deoxy-2'-Alpha-Fluoro-2'-Beta-C-Methyluridine) as an Inhibitor of Dengue Virus Replication. *Sci. Rep.* 7 (1), 6345. doi:10.1038/s41598-017-06612-2

Xu, M., Lee, E. M., Wen, Z., Cheng, Y., Huang, W. K., Qian, X., et al. (2016). Identification of Small-Molecule Inhibitors of Zika Virus Infection and Induced Neural Cell Death *via* a Drug Repurposing Screen. *Nat. Med.* 22 (10), 1101–1107. doi:10.1038/nm.4184

Yamada, K., Noguchi, K., Komeno, T., Furuta, Y., and Nishizono, A. (2016). Efficacy of Favipiravir (T-705) in Rabies Postexposure Prophylaxis. *J. Infect. Dis.* 213 (8), 1253–1261. doi:10.1093/infdis/jiv586

Yamamoto, M., Matsuyama, S., Li, X., Takeda, M., Kawaguchi, Y., Inoue, J. I., et al. (2016). Identification of Nafamostat as a Potent Inhibitor of Middle East Respiratory Syndrome Coronavirus S Protein-Mediated Membrane Fusion Using the Split-Protein-Based Cell-Cell Fusion Assay. *Antimicrob. Agents Chemother.* 60 (11), 6532–6539. doi:10.1128/AAC.01043-16

Yamaya, M., Shimotai, Y., Hatachi, Y., Lusamba Kalonji, N., Tando, Y., Kitajima, Y., et al. (2015). The Serine Protease Inhibitor Camostat Inhibits Influenza Virus Replication and Cytokine Production in Primary Cultures of Human Tracheal Epithelial Cells. *Pulm. Pharmacol. Ther.* 33, 66–74. doi:10.1016/j.pupt.2015.07.001

Yao, Z. H., Liao, W. Y., Ho, C. C., Chen, K. Y., Shih, J. Y., Chen, J. S., et al. (2019). Incidence of Hepatitis B Reactivation during Epidermal Growth Factor Receptor Tyrosine Kinase Inhibitor Treatment in Non-small-cell Lung Cancer Patients. *Eur. J. Cancer* 117, 107–115. doi:10.1016/j.ejca.2019.05.032

Ye, J., Wang, C., Sumpter, R., Jr., Brown, M. S., Goldstein, J. L., and Gale, M., Jr. (2003). Disruption of Hepatitis C Virus RNA Replication through Inhibition of Host Protein Geranylgeranylation. *Proc. Natl. Acad. Sci. U. S. A.* 100 (26), 15865–15870. doi:10.1073/pnas.2237238100

Ye, L., Li, J., Zhang, T., Wang, X., Wang, Y., Zhou, Y., et al. (2012). Mycophenolate Mofetil Inhibits Hepatitis C Virus Replication in Human Hepatic Cells. *Virus. Res.* 168 (1-2), 33–40. doi:10.1016/j.virusres.2012.06.009

Yin, X., Ambardekar, C., Lu, Y., and Feng, Z. (2016a). Distinct Entry Mechanisms for Nonenveloped and Quasi-Enveloped Hepatitis E Viruses. *J. Virol.* 90 (8), 4232–4242. doi:10.1128/JVI.02804-15

Yin, Y., Wang, Y., Dang, W., Xu, L., Su, J., Zhou, X., et al. (2016b). Mycophenolic Acid Potently Inhibits Rotavirus Infection with a High Barrier to Resistance Development. *Antivir. Res* 133, 41–49. doi:10.1016/j.antiviral.2016.07.017

Ying, C., Colonno, R., De Clercq, E., and Neyts, J. (2007). Ribavirin and Mycophenolic Acid Markedly Potentiate the Anti-hepatitis B Virus Activity of Entecavir. *Antivir. Res* 73 (3), 192–196. doi:10.1016/j.antiviral.2006.10.003

Ying, C., De Clercq, E., and Neyts, J. (2000). Ribavirin and Mycophenolic Acid Potentiate the Activity of Guanine- and Diaminopurine-Based Nucleoside Analogues against Hepatitis B Virus. *Antivir. Res* 48 (2), 117–124. doi:10.1016/s0166-3542(00)00121-2

Zhang, X. J., Qin, J. J., Cheng, X., Shen, L., Zhao, Y. C., Yuan, Y., et al. (2020). In-Hospital Use of Statins Is Associated with a Reduced Risk of Mortality Among Individuals with COVID-19. *Cell Metab* 32 (2), 176–187. doi:10.1016/j.cmet.2020.06.015

Zhang, X., Song, Z., Qin, B., Zhang, X., Chen, L., Hu, Y., et al. (2013). Rupintrivir Is a Promising Candidate for Treating Severe Cases of Enterovirus-71 Infection: Evaluation of Antiviral Efficacy in a Murine Infection Model. *Antivir. Res* 97 (3), 264–269. doi:10.1016/j.antiviral.2012.12.029

Zhou, Y., Vedantham, P., Lu, K., Agudelo, J., Carrion, R., Jr., Nunneley, J. W., et al. (2015). Protease Inhibitors Targeting Coronavirus and Filovirus Entry. *Antivir. Res* 116, 76–84. doi:10.1016/j.antiviral.2015.01.011

Zhu, N., Zhang, D., Wang, W., Li, X., Yang, B., Song, J., et al. China Novel Coronavirus Investigating and Research Team (2020). A Novel Coronavirus from Patients with Pneumonia in China, 2019. *N. Engl. J. Med.* 382, 727–733. doi:10.1056/NEJMoa2001017

Zhu, Y. Z., Xu, Q. Q., Wu, D. G., Ren, H., Zhao, P., Lao, W. G., et al. (2012). Japanese Encephalitis Virus Enters Rat Neuroblastoma Cells via a pH-dependent, Dynamin and Caveola-Mediated Endocytosis Pathway. *J. Virol.* 86 (24), 13407–13422. doi:10.1128/JVI.00903-12

Zhyvoloup, A., Melamed, A., Anderson, I., Planas, D., Lee, C. H., Kriston-Vizi, J., et al. (2017). Digoxin Reveals a Functional Connection between HIV-1 Integration Preference and T-Cell Activation. *Plos Pathog.* 13 (7), e1006460. doi:10.1371/journal.ppat.1006460

Zivcec, M., Scholte, F. E., Spiropoulou, C. F., Spengler, J. R., and Bergeron, E. (2016). Molecular Insights into Crimean-Congo Hemorrhagic Fever Virus. *Viruses* 8 (4), 106. doi:10.3390/v8040106

Zmurko, J., Marques, R. E., Schols, D., Verbeken, E., Kaptein, S. J., and Neyts, J. (2016). The Viral Polymerase Inhibitor 7-Deaza-2'-C-Methyladenosine Is a Potent Inhibitor of *In Vitro* Zika Virus Replication and Delays Disease Progression in a Robust Mouse Infection Model. *Plos Negl. Trop. Dis.* 10 (5), e0004695. doi:10.1371/journal.pntd.0004695

Conflict of Interest: The authors declare that the research was conducted in the absence of any commercial or financial relationships that could be construed as a potential conflict of interest.

GLOSSARY

BOC bovine coronavirus
CCHFV Crimean-Congo hemorrhagic fever virus
CHIKV chikungunya virus
CVA16 Coxsackievirus A16
CVB1 Coxsackievirus B1
DENV dengue virus
EBOV Ebola virus
EBV Epstein-Barr virus
EV71 enterovirus 71
FIPV feline infectious peritonitis virus
HBV hepatitis B virus
HCoV-229E human coronavirus 229E
HCV hepatitis C virus
HEV hepatitis E virus
HIV human immunodeficiency virus
hPIV human parainfluenza virus
HRV human rhinovirus
HSV herpes simplex virus
HuNoV human Norovirus
IAV influenza A virus
JEV Japanese encephalitis virus
JUNV Junin virus
KFDV Kyasanur Forest disease virus
LASV Lassa virus
LCMV lymphocytic choriomeningitis virus
MARV Marburg virus
MERS-CoV Middle East respiratory syndrome
MHV murine hepatitis virus
MuV Mumps virus
MV Measles virus
OHFV Omsk Hemorrhagic Fever virus
PRV pseudorabies virus
RRV Ross River virus
RSV respiratory syncytial virus
RVFV Rift Valley fever virus
SARS-CoV severe acute respiratory syndrome coronavirus
SARS-CoV-2 severe acute respiratory syndrome coronavirus-2
SFTSV Severe fever with thrombocytopenia syndrome virus
SFV Semliki Forest virus
SINV sindbis virus
SUDV Sudan virus
TBEV Tick-borne encephalitis (TBEV)
TGEV transmissible gastroenteritis virus
VZV varicella zoster virus
WNV West Nile virus
YFV yellow fever virus
ZIKV Zika virus

frontiers in Pharmacology

REVIEW
published: 07 May 2021
doi: 10.3389/fphar.2021.675287

Curcumin as a Potential Treatment for COVID-19

Bruna A. C. Rattis[1,2], *Simone G. Ramos*[1] *and Mara R. N. Celes*[1,2]*

[1]Department of Pathology, Faculty of Medicine of Ribeirão Preto, University of São Paulo, Ribeirão Preto, Brazil, [2]Department of Bioscience and Technology, Institute of Tropical Pathology and Public Health, Federal University of Goias, Goiania, Brazil

Coronavirus disease 2019 (COVID-19) is an infectious disease that rapidly spread throughout the world leading to high mortality rates. Despite the knowledge of previous diseases caused by viruses of the same family, such as MERS and SARS-CoV, management and treatment of patients with COVID-19 is a challenge. One of the best strategies around the world to help combat the COVID-19 has been directed to drug repositioning; however, these drugs are not specific to this new virus. Additionally, the pathophysiology of COVID-19 is highly heterogeneous, and the way of SARS-CoV-2 modulates the different systems in the host remains unidentified, despite recent discoveries. This complex and multifactorial response requires a comprehensive therapeutic approach, enabling the integration and refinement of therapeutic responses of a given single compound that has several action potentials. In this context, natural compounds, such as Curcumin, have shown beneficial effects on the progression of inflammatory diseases due to its numerous action mechanisms: antiviral, anti-inflammatory, anticoagulant, antiplatelet, and cytoprotective. These and many other effects of curcumin make it a promising target in the adjuvant treatment of COVID-19. Hence, the purpose of this review is to specifically point out how curcumin could interfere at different times/points during the infection caused by SARS-CoV-2, providing a substantial contribution of curcumin as a new adjuvant therapy for the treatment of COVID-19.

Keywords: curcumin, COVID-19, SARS-CoV-2, new therapies, ACE2

OPEN ACCESS

Edited by:
Sugunadevi Sakkiah, National Center for Toxicological Research (FDA), United States

Reviewed by:
Dumith Chequer Bou-Habib, Oswaldo Cruz Foundation (Fiocruz), Brazil
Sebastian Schloer, University of Münster, Germany
Jyoti Batra, Monash University, Australia

***Correspondence:**
Mara R. N. Celes
mrubia_celes@ufg.br

Specialty section:
This article was submitted to Experimental Pharmacology and Drug Discovery, a section of the journal Frontiers in Pharmacology

Received: *02 March 2021*
Accepted: *21 April 2021*
Published: *07 May 2021*

Citation:
Rattis BAC, Ramos SG and Celes MRN (2021) Curcumin as a Potential Treatment for COVID-19. Front. Pharmacol. 12:675287. doi: 10.3389/fphar.2021.675287

INTRODUCTION

Coronavirus disease 19 (COVID-19/2019-nCoV) is caused by the severe acute respiratory syndrome coronavirus 2 (SARS-CoV-2). The clinical manifestation of COVID-19 range from asymptomatic upper respiratory tract infection to critical illness and pneumonia associated with acute respiratory distress syndrome (ARDS) (Guan et al., 2020). The main risk factors associated with greater severity and mortality caused by COVID-19 include hypertension, diabetes mellitus, cardiovascular disease (CVD), advanced age, and obesity (Simonnet et al., 2020; Wu and McGoogan, 2020; Zhou et al., 2020).

SARS-CoV-2 is an enveloped β-coronavirus composed of four structural proteins: spike (S), envelope (E), membrane (M), and nucleocapsid (N) proteins (Chen et al., 2020). Entry of the virus into the host cell occurs through the cleavage of protein S into two subunits (S1 and S2) where SARS-CoV-2 develops a multibasic site at the S1-S2 boundary, which is cleaved by furin to form protein S for processing by TMPRSS2 (Hoffmann et al., 2020). The amino-terminal S1 subunit contains a receptor-binding domain (RBD) that is responsible for binding to the cell surface receptor, angiotensin-converting enzyme 2 (ACE2) (Wrapp et al., 2020; Xia et al., 2020). The membrane-

anchored S2 subunit is composed of the fusion peptide (FP), heptapeptide repeat sequences 1 and 2 (HR1/HR2), transmembrane domain (TM), and cytoplasmic domain. These components are responsible for viral fusion and cell invasion (Huang Y. et al., 2020; Xia et al., 2020). After the RBD domain is attached to ACE2, the S2 subunit changes its conformation and moves closer to the viral envelope and cell membrane for viral fusion and entry (Huang Y. et al., 2020). In the host, ACE2 is widely expressed in the lungs, heart, liver, vascular endothelium, kidneys, and gut. It is an important regulator of the renin-angiotensin-aldosterone system (RAAS), and promotes the conversion of angiotensin I (Ang I) to Ang (1–9) and Ang II to Ang (1–7) (D'ardes et al., 2020; Gheblawi et al., 2020). Ang (1–7) has an important physiological role and promotes vasodilation, including anti-hypertrophic, anti-inflammatory, anti-oxidant, anti-thrombotic, and anti-fibrotic effects (Imai et al., 2005; Kuba et al., 2005; Chung et al., 2020; D'ardes et al., 2020). The conversion of Ang II to Ang (1–7) regulates the concentration of Ang II-mediated by ACE2. When available, Ang II binds to the ATR1 receptor, thereby promoting harmful pro-inflammatory effects, such as hypertrophy, oxidative stress, and vasoconstriction (Imai et al., 2005; Kuba et al., 2005; Chung et al., 2020; D'ardes et al., 2020). Therefore, the negative regulation of ACE2, promoted by the binding of SARS-CoV-2, results in increased levels of Ang II (Imai et al., 2005; Kuba et al., 2005; D'ardes et al., 2020).

The current drugs approved by the Food and Drug Administration (FDA) for the treatment of patients with COVID-19 prior to the writing of this manuscript are: Fresenius Medical, multiFiltrate PRO System and multiBic/multiPlus Solutions (Fresenius Medical Care); Fresenius Kabi Propoven 2% (Fresenius Kabi USA, LLC.); REGIOCIT replacement solution that contains citrate for regional citrate anticoagulation (RCA) of the extracorporeal circuit (Baxter Healthcare Corporation); COVID-19 convalescent plasma (Office of the Assistant Secretary for Preparedness and Response US Department of Health and Human Services); remdesivir (Veklury) (Gilead Sciences, Inc.); bamlanivimab (Eli Lilly and Company); baricitinib (Olumiant) in combination with remdesivir (Veklury) (Eli Lilly and Company); REGEN-COV (casirivimab and imdevimab) (Regeneron Pharmaceuticals); bamlanivimab and etesevimab (Eli Lilly and Company); and Propofol-Lipuro 1% (B. Braun Melsungen AG), as obtained from the regulators database (https://www.fda.gov/).

Drug repurposing has been viewed as a promising strategy for combating COVID-19. Several factors, such as molecular recognition, binding affinity, and interactions, are calculated during computational drug design and development. Virtual screening was performed with approximately 3,410 drugs approved by the FDA. However, remdesivir was yet to be approved at the time, but has since been analyzed (Beck et al., 2020). The aforementioned and other studies suggested that remdesivir is a potential antiviral agent against SARS-CoV-2, following the demonstration of its affinity to target sites of the virus, including RNA-dependent RNA polymerase (RdRP), helicase, 3-to -5 exonuclease, 2-O-ribose methyltransferase, and endoRNAse from SARS-CoV-2 and SARS-CoV-2 main protease (Mpro, also called 3CLpro) (Beck et al., 2020; Elfiky, 2020). Following this methodology, curcumin displayed promising results, making it a strong candidate for *in vitro* and *in vivo* studies against SARS-CoV-2.

Natural compounds based on medicinal plants and traditional Chinese medicine (TCM) formulas with antiviral action against coronavirus have been investigated. These compounds presented several targets against SARS-Cov and Middle East Respiratory Syndrome (MERS), such as (1) spike (S) glycoprotein, (2) papain-like protease (PLpro), and (3) nucleocapsid (N) proteins. Among these compounds, including the specific viral targets, are ginsenoside-Rb1 (1), hirsutenone (2), tanshinones I–VII (2), with anti-SARS-CoV action, and resveratrol (3) with anti-MERS activity (Wu et al., 2004; Park et al., 2012; Park et al., 2012; Lin et al., 2017). Numerous therapeutic effects of the natural polyphenol, curcumin, have been reported, including potential chemotherapeutic, antioxidant, antiviral, antibacterial, and anti-inflammatory properties (Paciello et al., 2020). Clinical studies have demonstrated the effects of nanoencapsulated curcumin in patients with COVID-19. In the aforementioned study, a significant reduction in clinical manifestations of COVID-19 (fever, cough, and dyspnea) was observed in the group treated with nanocurcumin (patients with mild and severe disease) (Tahmasebi et al., 2020; Valizadeh et al., 2020). In addition, nanocurcumin reduced the mortality rate of these patients. However, the mortality rate of the placebo group was significantly higher than that of the two groups (patients with light and severe disease) treated with nanocurcumin (Tahmasebi et al., 2020; Valizadeh et al., 2020). Currently, another study involving patients with COVID-19 treated with nanoencapsulated curcumin is ongoing (Hassaniazad et al., 2020). Therefore, this manuscript provides a review of the biological effects of curcumin in diseases that arise following SARS-CoV-2 infection.

IN SILICO MODELS PREDICTING THE ANTIVIRAL EFFECTS OF CURCUMIN AGAINST SARS-COV-2

The antiviral effects of curcumin have been widely explored, and the viruses to which curcumin has antiviral action are shown in **Figure 1**. Curcumin prevents the binding of the influenza A virus (IAV) (Chen et al., 2010; Ou et al., 2013), dengue virus (Balasubramanian et al., 2019), zika virus, and chikungunya virus (Mounce et al., 2017) to host cells. Curcumin inhibits the entry of the hepatitis C virus (HCV) (Chen et al., 2012; Anggakusuma et al., 2014), human norovirus (HuNoV) (Yang et al., 2016), viral hemorrhagic septicemia virus in fish (VHSV) (Jeong et al., 2015), and bovine herpesvirus 1 (BHV-1) (ZHU et al., 2015). Furthermore, the curcumin hinders viral genome replication and transcription of the respiratory syncytial virus (RSV) (Obata et al., 2013; Yang et al., 2016) and Japanese encephalitis virus (JEV) (Dutta et al., 2009), and interferes with the translation and assembly of the Epstein-Barr virus (EBV) (Hergenhahn et al., 2002), human cytomegalovirus

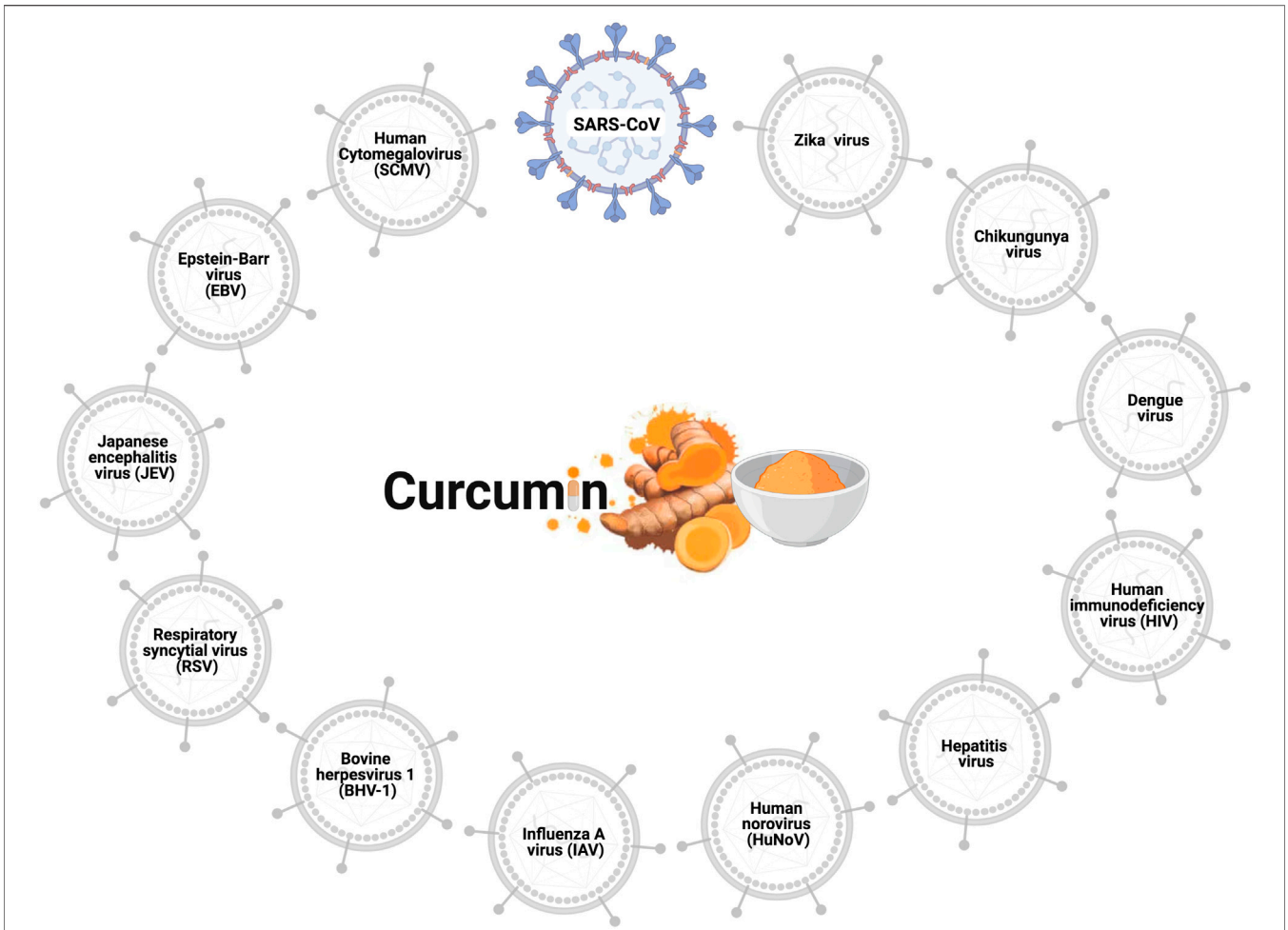

FIGURE 1 | Antiviral effects of curcumin. Curcumin prevents cell infection and viral replication in the SARS-CoV, influenza A virus (IAV), zika virus, chikungunya virus, hepatitis C virus (HCV), human norovirus (HuNoV), viral hemorrhagic septicemia virus in fish (VHSV), bovine herpesvirus 1 (BHV-1), respiratory syncytial virus (RSV), Japanese encephalitis virus (JEV), Epstein-Barr virus (EBV), human cytomegalovirus (HCMV), and human immunodeficiency virus (HIV).

(HCMV) (Lv et al., 2014a; Lv et al., 2014b), and human immunodeficiency virus (HIV) (Gupta et al., 2011; Ali and Banerjea, 2016). *In vitro* analyses revealed the antiviral action of curcumin against the SARS-CoV virus in Vero-E6 cells; this natural polyphenol could inhibit viral replication at concentrations of 3–10 μM (Wen et al., 2007). Based on such data regarding antiviral activity, researchers using in silico prediction models evaluated the potential of curcumin against the binding proteins of SARS-CoV-2 and its cellular receptors.

The SARS-CoV-2 S glycoprotein is responsible for the interaction between the virus and the host cell, promoting fusion and internalization of the virus via the ACE2 receptor. Thus, both the S glycoprotein and ACE2 are potential targets for the treatment of COVID-19. *In silico* analysis showed that curcumin has a high-affinity for interaction with the S glycoprotein through the establishment of six hydrogen bonds (Maurya et al., 2020). In this study, curcumin obtained higher scores than the control compounds, such as nafamostat and hydroxychloroquine (Maurya et al., 2020). In addition, curcumin displayed an affinity for ACE2. Moreover, docking results showed that curcumin interacted with the active site of the protein, in addition to forming two hydrogen bonds (Maurya et al., 2020). Similarly, curcumin demonstrated a better affinity for ACE2 than the control compounds, such as captopril and hydroxychloroquine (Maurya et al., 2020).

The transmembrane protein serine protease 2 (TMPRSS2) facilitates the entry of SARS-CoV-2 from the spike protein (Hoffmann et al., 2020). *In silico* analyses focusing on TMPRSS2 showed that curcumin forms four hydrophobic interactions and an H-bond with TMPRSS2 (Motohashi et al., 2020). These findings corroborated results of *in vitro* studies where curcumin treatment led to the downregulation of TMPRSS2 in prostate cancer cells (Zhang et al., 2007; Thangapazham et al., 2008).

The main protease (Mpro) of SARS-CoV-2 is indispensable in maturation and viral replication, and is a promising target in the treatment of SARS-CoV-2. The proteins that are matured by Mpro include RNA-dependent RNA polymerase (RdRp, Nsp12)

and helicase (Nsp13), which depend on the cleavage of Mpro (Rut et al., 2020). Inhibition of Mpro prevents viral replication; thus, compounds with inhibitory effects on Mpro have become attractive targets for the treatment of COVID-19 (Zhang S. et al., 2020; Anand et al., 2003). To identify compounds with potential binding to Mpro, an *in-silico* study using docking was carried out to evaluate a series of compounds, including the drugs currently used in the treatment of COVID-19. In this study, two compounds with a high affinity for Mpro were used as controls: N3 and O6K (HUYNH; WANG; LUAN, 2020). Among the compounds tested, including chloroquine, entecavir, hydroxychloroquine, and remdesivir, curcumin surprisingly formed the most stable complex with SARS-CoV-2 Mpro, and the affinity score was comparable to that of the N3 control (Huynh et al., 2020).

The entry of SARS-CoV-2 through the endosome requires an endosomal environment with an acidic pH that is promoted by the endosomal proteases, cathepsin B and L, and ion channels, particularly the vacuolar ATPase pump (V-ATPase), which is crucial in regulating endosomal pH (Aslam and Ladilov, 2020; Khan et al., 2020). Curcumin has been shown to be a potential pH controlling agent, decreasing the expression of V-ATPase, which causes an increase in pH in tumor cells (Vishvakarma et al., 2011).

In vitro results of the antiviral action of curcumin on SARS-CoV and the data from *in silico* analyses reinforce the hypothesis

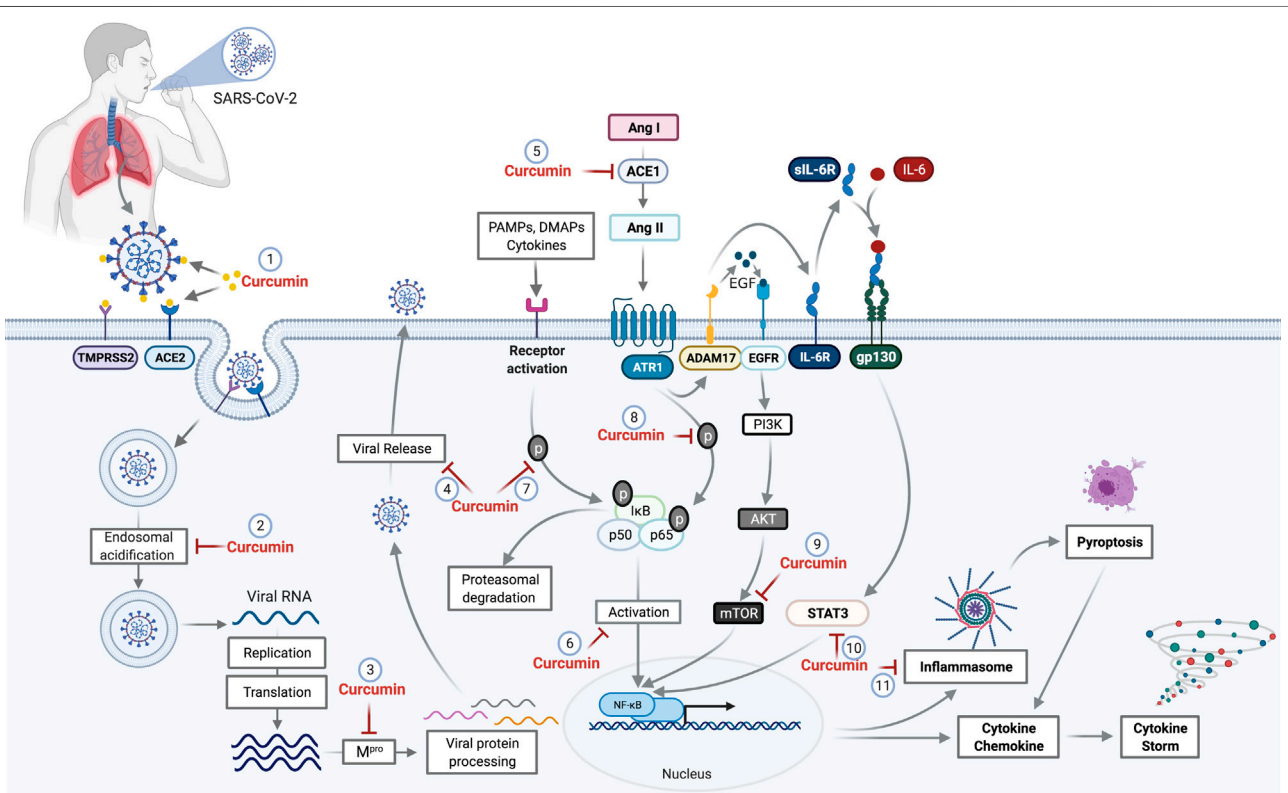

FIGURE 2 | Potential curcumin targets as antiviral and anti-inflammatory in SARS-CoV-2 infection. The first antiviral effect of curcumin against SARS-CoV-2 is its potential for preventing the binding of viral S protein to the ACE2 receptor and initiate the host cell infection process (1). After penetrating the host cell via endosomes, the virus begins the replication process that requires an acid endosomal environment to initiate the proteolytic process of viral proteins and subsequent release to the external environment. Curcumin acts by inhibiting the Endosomal acidification (2) and processing of the viral proteins (Mpro), necessary for viral release (3,4). Further, the inhibition of ACE mediated by curcumin (5) prevents the increase of Ang II levels. Curcumin inhibits NF-κB (6) through the inhibition of different pathways. The binding of PAMPs, DAMPs, and cytokines that leads to IkB phosphorylation and proteasomal degradation is one of those pathways that cause NF-κB activation. Curcumin prevents both IkB phosphorylation and p65 subunit from the NF-κB (8), which consequently prevents NF-κB activation. The activation of ADAM17 by the AngII-ATR1 axis promotes the interaction between EGF and EGFR receptor, which promotes the activation of the PI3K/AKT/mTOR axis resulting in NF-κB activation. Curcumin acts as a potential inhibitor for mTOR (9), preventing the NF-κB pathway activation. ADAM17-mediated signaling also triggers the release of soluble interleukin 6-receptor, forming a complex with IL-6 (sIL-6R-IL-6) that binds to glycoprotein gp130. This complex binding (sIL-6R-IL-6+gp130) activates the signal transduction pathways responsible to induce the activators of transcription 3 (STAT3). Activation of STAT3 results in activation of NF-κB, which can be prevented by the curcumin (10). The NF-κB activation induces a protein complex formation, knowns as inflammasome, which can lead to cell death through pyroptosis, a pathway to cell death mediated by the activation of caspase-1. However, curcumin can cause the inhibition of inflammasome formation (11) by the inhibition of NF-κB. Abbreviations: TMPRSS2, transmembrane protease, serine 2; ACE1, angiotensin-converting enzyme 1; ACE2, angiotensin-converting enzyme 2; Mpro, main protease; PAMPs, pathogen-associated molecular pattern; DAMPs, damage-associated molecular patterns; ANG I, angiotensin I; Ang II, angiotensin II; ATR1, angiotensin II (AII) receptor 1; ADAM17, a disintegrin and metalloproteinase 17; EGF, epidermal growth factor; EGFR, epidermal growth factor receptor; IL-6R, interleukin 6 receptor; sIL-6R, soluble Interleukin 6 receptor; gp130, glycoprotein 130; PI3K, phosphoinositide 3-kinase; AKT, protein kinase B; mTOR, mammalian target of rapamycin; STAT3, signal transducers and activators of transcription; NF-κB, factor nuclear kappa B.

of the potential activity against SARS-CoV-2. Thus, this review aims to encourage evaluation of the effect of curcumin on cells infected by SARS-CoV-2 and the replication of the virus using *in vitro* and *in vivo* models, and in randomized clinical trials. The possible interaction sites of curcumin with SARS-CoV-2 in the host cells are shown in **Figure 2**.

EFFECTS OF CURCUMIN IN THE COVID-19-INDUCED INFLAMMATORY PROCESS

The inflammatory process of COVID-19 is complex and multifactorial. Patients with the severe form of the disease can be affected by a hyperinflammatory condition called a cytokine storm, highlighting the need for anti-inflammatory treatment to alleviate the hyperactivation of the immune response, which induces this cytokine storm. Focusing on the anti-inflammatory action of curcumin, two studies were conducted with patients with COVID-19. In the first study, the research group investigated the modulation of pro-inflammatory cytokines by nanocurcumin. Patients with COVID-19 showed high mRNA expression and secretion of cytokines, IL-1β, IL-6, TNF-α, and IL-18, but showed a significant reduction in IL-6 and IL-1β after treatment with nanocurcumin (Valizadeh et al., 2020). Subsequently, exploring the modulatory mechanisms of nanocurcumin, the researchers demonstrated that the number of Th17 cells, gene expression, and serum Th17-mediated factors level (IL-17, IL-21, IL-23, and GM-CSF) were significantly reduced in both stages of the disease in the group of patients with COVID-19 treated with nanocurcumin (Tahmasebi et al., 2020).

Despite the rapid scientific progress regarding the pathophysiology of COVID-19, the precise mechanisms that trigger the exacerbated inflammatory response observed in some of the patients have not yet been completely elucidated. However, several hypotheses attempt to explain such changes. The nuclear factor-kappa B (NF-κB) pathway is directly involved in this inflammatory process and can stimulate the production of pro-inflammatory cytokines when activated. Recent findings led to concerns regarding the overstimulation of the NF-κB pathway and its potential contribution to the emergence of cytokine storms. Studies have shown that NF-κB can be activated directly by SARS-CoV-2 from Toll-like receptors (TLRs) and RAAS system components (Mahmudpour et al., 2020). In such situations, the SARS-CoV envelope (E) and nucleocapsid (N) proteins were shown to be directly related to NF-κB activation (Liao et al., 2005; DeDiego et al., 2014). Consequently, when this protein was deleted in a genetically modified virus, a reduction in NF-κB activation was observed (DeDiego et al., 2014).

Activation of the AngII-AT1R axis causes NF-κB activation (Crowley and Rudemiller, 2017). The AngII-AT1R axis is directly involved in the pro-inflammatory response by acting on the main pathways that lead to the release of cytokines and chemokines. The increase in AngII stimulates the phosphorylation of the NF-κB p65 subunit, leading to its activation and the subsequent release of cytokines (IL-6, IL-1ß, IL-10, and TNF-α) (Ruiz-Ortega et al., 2001; Skurk et al., 2004). The AngII-AT1R axis activates disintegrin and metalloprotease 17 (ADAM17), processing the membrane form of IL-6Rα to its soluble form (sIL-6Rα) through epidermal growth factor (EGFR). The sIL-6Rα-IL-6 complex leads to gp130-mediated STAT3 activation (Eguchi et al., 2018; Murakami et al., 2019), with STAT3 being essential for the complete activation of the NF-κB pathway, in conjunction with the main pathway stimulator, IL-6 (Murakami et al., 2019). The cytokines, TNF and IL-1, also trigger signals that cause the translocation of NF-κB to the nucleus by activating genes involved in the production of inflammatory mediators (Crowley & Rudemiller, 2017). Curcumin blocks STAT3-mediated NF-κB activation, and the consequent reduction in pro-inflammatory cytokines disrupts the positive feedback between pro-inflammatory cytokines and NF-κB (Alexandrow et al., 2012; Rahardjo et al., 2014; Ma et al., 2015; Yadav et al., 2015).

NF-κB is inactive in the cell cytoplasm because of its association with the IκB protein complex. In the presence of stimuli (PAMPs, DAMPs, and cytokines), IκB undergoes phosphorylation and proteasomal degradation that dissociates the NF-κB complex, allowing NF-κB to translocate into the nucleus, leading to the expression of chemokines and pro-inflammatory cytokines (Solt and May, 2008). Curcumin acts by inhibiting the phosphorylation of IκB through inhibiting translocation and the consequent activation of NF-κB (Karunaweera et al., 2015; Wang et al., 2018; Cheemanapalli et al., 2019). Owing to NF-κB inhibition, there is a reduction in the production of inflammatory cytokines, such as IL-1α, IL-6, and TNF-α (Rahardjo et al., 2014; Ma et al., 2015; Yadav et al., 2015).

Viral infections commonly activate inflammasomes. SARS-CoV has been shown to express at least three proteins that activate the NLRP3-type inflammasome (NOD-, LRR-, and pyrin domain-containing protein 3): envelope protein (E), Open Reading Frame-3a (ORF3a), and Open Reading Frame-8b (ORF8b) (Nieto-Torres et al., 2015; Chen et al., 2019; Shi et al., 2019). Protein E and ORF3a stimulate NF-κB signaling, thereby promoting the release of pro-inflammatory cytokines, such as IL-1β, IL-8, and IL-18, and priminf NLRP3 expression to reach the functional level (Kanzawa et al., 2006; DeDiego et al., 2014; Siu et al., 2019). The amino acid sequence of protein E is 94.7% conserved in SARS-CoV and SARS-CoV-2, indicating the possibility of inflammasome activation in patients with COVID-19 (Chan et al., 2020; Lu et al., 2020). A recent study demonstrated that active caspase-1 (Casp1p20), IL-1β, IL-18, IL-6, and lactate dehydrogenase (LDH) were increased in the serum of patients with COVID-19, and that Casp1p20 and IL-18 are products derived from inflammasomes (Rodrigues et al., 2021). The researchers also found active inflammasome NLRP3 in peripheral blood mononuclear cells (PBMCs) and in the tissues of deceased patients at autopsy. The levels of IL-18 and Casp1p20 were higher in patients who had severe disease, indicating a worse prognosis (Rodrigues et al., 2021). Therefore, the regulation of NF-κB by curcumin inhibits the formation of inflammasomes, specifically NLRP3, decreasing the secretion of IL-1β and IL-18 (Yin et al., 2018).

Another regulator of NF-κB is the mammalian target of rapamycin (mTOR) pathway. mTOR is comprised of two complexes, mTORC1, which is sensitive to rapamycin inhibition through the Raptor protein that is associated with mTORC1, and mTORC2, which is associated with Rictor protein, and has low sensitivity to rapamycin (Saxton and Sabatini, 2017). In lipopolysaccharide sepsis models, the inhibition of mTOR by rapamycin resulted in decreased phosphorylation of the p65 subunit of NF-κB, with a consequent reduction in cytokines and pro-inflammatory chemokines, such as IL-1β, IL-18, IL-6, TNF-α, MCP-1, and led to the reduced expression of the NLRP3 inflammasome (Temiz-Resitoglu et al., 2017; Jia et al., 2019). Although rapamycin is already used as an immunosuppressant in the treatment of transplant patients, it has numerous adverse effects and is associated with a high cost. Curcumin is a potential target inhibitor of the mTOR pathway and can promote the inhibition of both the mTORC1 and mTORC2 complexes (Beevers et al., 2009). Curcumin at low doses was found to suppress the mTORC1-Raptor interaction, leading to inhibition of the mTORC1 complex. Curcumin also promoted interruption of the mTORC2-Rictor interaction at higher doses, thereby inhibiting mTORC2 (Beevers et al., 2006; Beevers et al., 2009; Johnson et al., 2009).

The anti-inflammatory mechanisms of curcumin have been extensively investigated in clinical studies of several inflammatory diseases, such as Crohn's disease, ulcerative proctitis, ulcerative colitis, irritable bowel syndrome, rheumatoid arthritis, postoperative inflammation, gastric ulcer, *Helicobacter pylori* infection, and idiopathic inflammatory orbital pseudotumor (Gupta et al., 2013). Evaluating the mechanisms of action of curcumin already described in both experimental and clinical trials, which can potentially benefit patients with dysregulated immune responses in COVID-19, seems to be an innovative strategy. The mechanisms of action of curcumin and its potential effects on COVID-19 are showed in **Figure 2**.

CURCUMIN IN HEMOSTATIC DISORDERS

A growing number of studies have reported thromboembolic events in patients hospitalized due to COVID-19. High D-dimer levels are considered to be a common marker for increased thrombotic propensity and poor prognosis (Paliogiannis et al., 2020; Zhou et al., 2020). Increased platelet activation and viral RNA detectable in the blood are associated with platelet hyperactivity, leading to abnormal blood clotting. These causes have been associated with thromboembolic prognosis in patients with COVID-19 (Zhang L. et al., 2020). The following signs of hypercoagulability have been observed in these patients: prolonged prothrombin time (PT), activated partial thromboplastin time (APTT), and elevated levels of D-dimer and other fibrin degradation products (FDP) (Tang et al., 2020). In such cases, antithrombin (AT) activity has been reported to be lower than normal (Tang et al., 2020). Human platelets express ACE2 and TMPRSS2 receptors. SARS-CoV-2 binds to these receptors and promotes platelet activation (Zhang L. et al., 2020).

Endothelial cells express the necessary receptors for SARS-CoV-2 to bind and infect cells, causing cell damage and apoptosis. Damage to the vascular endothelium exposes pro-coagulating factors, such as collagen and von Willebrand factor (vWF), and stimulates the release of tissue factor (TF) (Grobler et al., 2020; Iba et al., 2020). Platelets express specific receptors for these molecules, including glycoprotein VI (GPVI) which binds to sub-endothelial collagen, and glycoprotein (GP) Ib-IX-V which binds to vWF (Falati et al., 1999; Grobler et al., 2020). In addition, activated platelets express P-selectin, which binds to monocytes and circulating neutrophils *via* the PSGL-1 receptor, causing activated monocytes to express TF and activated neutrophils (McFadyen et al., 2020). Curcumin exerts a critical antiplatelet effect, preventing platelet adhesion to the vascular endothelium and subendothelium, in addition to reducing the expression of P-selectin and GP VI (Zhang et al., 2008; Mayanglambam et al., 2010).

Activated neutrophils release extracellular neutrophil traps (NETs). This process is accompanied by cell death (NETosis) and can exacerbate the inflammatory response (Schönrich and Raftery, 2016; Bonaventura et al., 2018). NETs can contribute to the formation of clots and thrombi *via* platelet-dependent or independent pathways. The latter can cause total blood vessel occlusion, resulting in organ damage (Jiménez-Alcázar et al., 2017; Gómez-Moreno et al., 2018). Studies have shown that defects in NET degradation cause partial or total obstruction of blood vessels in the lungs (Jiménez-Alcázar et al., 2017). Furthermore, analyses of lung tissue collected at autopsy from patients with acute respiratory distress syndrome and sepsis revealed the presence of NET components in the observed clots (chromatin and myeloperoxidase), indicating that NETs can form intravascular clots in humans (Jiménez-Alcázar et al., 2017). The products released from NETs can also be cytotoxic to endothelial cells, leading to the recruitment of more NETs, which contributes to a thrombo-inflammatory response (Gómez-Moreno et al., 2018). Curcumin treatment, both *in vitro* and *in vivo*, was demonstrated to inhibit the function of NETs and reduce neutrophilic infiltration in a murine air pouch model induced by LPS (Antoine et al., 2013). In addition, the reduction in expression of P-selectin promoted by curcumin may be a key mechanism in the reduction of NETS; this is because platelets use P-selectin to bind to neutrophils, thereby promoting neutrophilic activation (Zhang et al., 2008; McFadyen et al., 2020).

In endothelial cells associated with the airways, the increased concentration of Ang II causes TF to be upregulated, with consequent activation of the pro-coagulant response (Nishimura et al., 1997). TF is expressed after vascular injury or activation of endothelial cells. Inflammatory mediators, such as TNF-α and IL-1β, are important inducers of TF in endothelial cells (Pendurthi et al., 1997). When expressed, TF serves as a receptor for factor VIIa, and the binding of factor VIIa to TF initiates the coagulation cascade. This leads to thrombin generation and sequential clot formation with the deposition of fibrin protofibrils (Hergenhahn et al., 2002; Butenas et al., 2008; D'Alessandro et al., 2018; Sathler, 2020).

Treatment of human endothelial cells with curcumin inhibited the expression of TF induced by TNF-α, LPS, and thrombin (Pendurthi et al., 1997). Curcumin was also found to inhibit platelet aggregation induced by arachidonic acid, adrenaline, and collagen (Srivastava et al., 1995). These findings corroborate those of another study that revealed the inhibition of platelet agonists, viz. epinephrine-induced platelet aggregation, platelet-activating factor (PAF), and arachidonic acid, with curcumin (Shah et al., 1999). Furthermore, curcumin has been shown to inhibit the formation of thromboxane A2 (TXA2) by platelets (Shah et al., 1999). Platelet aggregation is stimulated by TXA2 produced by active platelets, and promotes the activation of other platelets. Pretreatment of platelets with curcumin inhibited platelet aggregation induced by the calcium ionophore A-23187, following curcumin interfering with the mobilization of intracellular Ca^{2+}, which is essential for platelet aggregation (Shah et al., 1999). Curcumin has also been shown to decrease the levels of D-dimers, circulating platelets, and inhibit diesel exhaust particles (DEP) (Nemmar et al., 2012).

Curcumin administration in an *in vivo* model of disseminated intravascular coagulation (DIC) reduced the circulating levels of TNF-α, preventing the consumption of peripheral platelets and plasma fibrinogen (Chen et al., 2007). Curcumin also reduced the deposition of fibrin in the renal glomeruli, a characteristic finding of DIC with curcumin (Chen et al., 2007). In a clinical study, a 10 mg curcumin injection administered for 15 days was sufficient to reduce plasma fibrinogen levels (Ramirez Boscá et al., 2000).

Procoagulant and pro-thrombotic events are recurrent in patients with COVID-19 and can cause significant damage. Curcumin, a well-tolerated natural compound, is a promising candidate for studies in the context of COVID-19 disorder hemostatic. In fact, several *in vitro* and *in vivo* studies have reported its anticoagulant and antithrombotic effects. Therefore, the mechanisms described in the management of other diseases can be reused for new studies regarding hemostatic disorders induced by SARS-CoV-2 deserving further investigation. The molecular mechanisms underlying the targets of curcumin

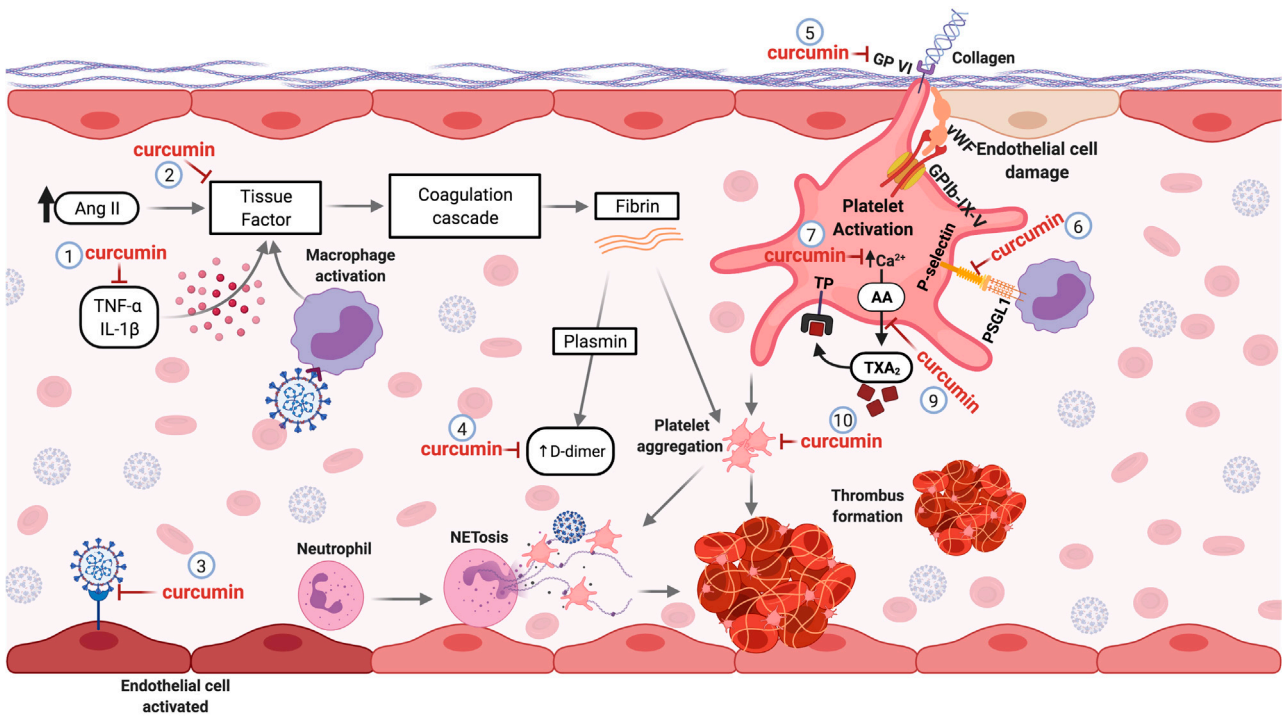

FIGURE 3 | Curcumin as a Potential antithrombotic in hemostatic disorders induced by SARS-CoV-2. Pro-inflammatory cytokines and Ang II elevated levels can induce the production of tissue factor (TF) by the endothelial cells, initiating the coagulation cascade. Curcumin decreases pro-inflammatory cytokines (1) and inhibits TF expression (2) in the vascular endothelium, avoiding the activation of the coagulation cascade. The affinity of curcumin by the SARS-CoV-2 protein S and ACE2 binding can prevent the infection and activation of endothelial cells (3). During the activation of the coagulation cascade, fibrinolysis can occur, generating D-dimers. Curcumin treatment decreases fibrin deposition and D-dimer levels formation (4). Lesions of the endothelial cells can expose the subendothelial collagen, which can be recognized by the platelet's receptor (GP-VI), leading to platelet cell activation. Curcumin can inhibit the GP-VI receptor, reducing and/or abolishing the platelet activation by binding to collagen (5). The interaction of platelets with monocytes through binding the P-selectin-PSGL-1 receptor promotes monocyte activation, causing an increase of TF expression. Curcumin inhibits this interaction by inhibiting P-selectin in platelets (6). The mobilization of intracellular calcium mediates platelet aggregation. Curcumin prevents calcium-mediated platelet aggregation (7). Besides, curcumin inhibits the thromboxane A2 (TXA2) generation (9) released by activated platelets to stimulate other platelet activation. Thus, curcumin inhibits platelet aggregation (10). Abbreviations: TNF-α, tumor necrosis factor alpha; IL-1β, interleukin 1 beta; Ang II, angiotensin II; GPVI, glycoprotein VI; vWF, Von Willebrand factor; GPIb-IX-V, glycoprotein (GP) Ib-IX-V; PSGL-1, P-selectin glycoprotein ligand-1; AA, arachidonic acid; TXA2, thromboxane A2; TP, thromboxane receptor.

involved thrombotic and coagulant disorders caused by COVID-19 are illustrated in **Figure 3**.

CURCUMIN AS A POTENTIAL AGENT AGAINST PULMONARY IMPAIRMENT

Alveolar type II (ATII) cells are the primary target of SARS-CoV-2 infection, triggering the apoptotic death of target cells and subsequent infection of adjacent ATII alveolar cells (Mason, 2020). The inflammatory process, together with cellular damage, results in the appearance of multinucleated giant cells and a fibrin-rich hyaline membrane, which causes diffuse alveolar damage that can progress to acute respiratory distress syndrome (ARDS) (Dushianthan et al., 2011). In a model of lung injury induced by benzo (a) pyrene (BaP), curcumin reduced the death of ATII cells and decreased the levels of pro-inflammatory cytokines (TNF-α, IL-6, and C-reactive protein) in serum (Almatroodi et al., 2020).

In more severe cases, patients with COVID-19 may require mechanical ventilation (MV) (Fan et al., 2020). However, inadequate MV can worsen pulmonary pathology. Ventilator-induced lung injury (VILI) causes lung expansion conversion into biochemical signals, resulting in increased activation of inflammatory cells (Silva et al., 2015). Experimentally, it has been shown that curcumin reverses the damage caused by VILI, reducing edema and lung injury. This effect was found to be mediated by the inhibition of NF-κB and the reestablishment of the redox balance from recovery of total antioxidative capacity (Wang et al., 2018).

High levels of circulating NETs have been detected in intubated patients with COVID-19 (Middleton et al., 2020). A correlation between severity and NETs has been established, suggesting that NETs contribute to COVID-19-related lung injury. In addition, platelet colocalization with citrullinated histone $H3^{+}$ and NETs indicated the presence of NETosis in pulmonary microthrombi of patients who died of COVID-19 (Middleton et al., 2020). In the lungs, NETs have a cytotoxic effect on epithelial cells, endothelial cells, and connective tissue, which can aggravate pulmonary pathology (Saffarzadeh et al., 2012). In sepsis and ARDS, NETs cause cell damage and microthrombi, potentially resulting in multiple organ dysfunction and death (Czaikoski et al., 2016; Lefrançais et al., 2018; Papayannopoulos, 2018). In experimental studies involving ARDS due to polymicrobial sepsis (CLP), curcumin decreased the apoptosis of lung cells and attenuated the severity of lung injury. IL-17A acts on ATII cells causing them to release CXCL-1, in turn inducing neutrophil aggregation. Curcumin treatment reduced the levels of IL-17A and neutrophils in the lungs (Chai et al., 2020).

Regulatory T cells (Tregs) are essential regulators of the inflammatory process and generate an adequate immune microenvironment through their anti-inflammatory and anti-apoptotic functions (Lin et al., 2018). Curcumin induces the differentiation of naïve $CD4^{+}$ T cells to Tregs by regulating the expression of IL-10 (Chai et al., 2020). IL-10 is an anti-inflammatory cytokine that promotes macrophage reprogramming from an inflammatory profile (M1) to a repeating profile (M2) by suppressing the mTORC1 complex. M2 macrophages decrease the inflammatory process and stimulate tissue repair in sepsis-induced LPA (Ip et al., 2017). Macrophages with the M1 phenotype are essential for controlling viral replication. However, limiting immunopathological reactions through the M2 phenotype is essential (Sang et al., 2015). In a COVID-19 study, severely ill patients showed a higher frequency of type M1 macrophages than patients with moderate infection or healthy control subjects who presented higher frequencies of type M2 macrophages (Liao et al., 2020). Curcumin promotes a decrease in M1 and an increase in M2 macrophages in septic lungs, indicating its potential effect on macrophage polarization (Chai et al., 2020).

In an *in vivo* model of lung injury mediated by cyclophosphamide, treatment with curcumin reduced lung injury and restored the oxidant-antioxidant balance by reducing lipid peroxidation (Ashry et al., 2013). In LPS-induced acute lung injury (ALI), treatment with curcumin decreased pulmonary edema, increased PaO_2, and improved lung function (Cheng et al., 2018). ALI can be a consequence of hemorrhagic shock and resuscitation (HSR). Animals subjected to HSR and treated with curcumin showed a reduction in the levels of reactive oxygen species, TNF-α, and neutrophilic infiltrates. Such finding indicates that the treatment provided a protective pulmonary barrier function (Yu-Wung Yeh and Wang, 2020). ALI and ARDS studies in animals with sepsis showed that treatment with curcumin attenuated lung damage and decreased proinflammatory cytokine levels (Xiao et al., 2012; Xu et al., 2013; Liu et al., 2017).

Although clinical studies have not reported the direct effects of curcumin on respiratory impairment, the decrease in clinical manifestations (fever, cough, and dyspnea) in patients with COVID-19 is a promising indicator that encourages further investigations (Tahmasebi et al., 2020; Valizadeh et al., 2020). Many clinical trials have established the therapeutic potential of curcumin, either as a single agent or in combination with other drugs in various diseases, owing to its effect on diverse cell signaling pathways. The possible curcumin action sites that can be targeted after SARS-CoV-2-induced changes in the lungs are illustrated in **Figure 4**.

CARDIOPROTECTIVE EFFECTS OF CURCUMIN

Clinical reports involving some of the first patients with COVID-19 from the Wuhan province of China showed that 5 of the 41 patients had changes in levels of highly sensitive cardiac troponin I (hs-cTnI), indicating myocardial injury (Huang C. et al., 2020). Interestingly, some patients sought medical assistance after cardiac symptoms (palpitations and chest tightness) rather than the classic symptoms of COVID-19 (fever and cough) (Deng et al., 2020; Stefanini et al., 2020). In children, COVID-19 can cause a hyperinflammatory syndrome similar to Kawasaki disease (Riphagen et al., 2020).

Underlying CVD significantly increases the mortality rate of patients with COVID-19. One study showed that patients with COVID-19, CVD, and increased troponin T levels had a mortality rate of 69.4%; however, the mortality rate of patients

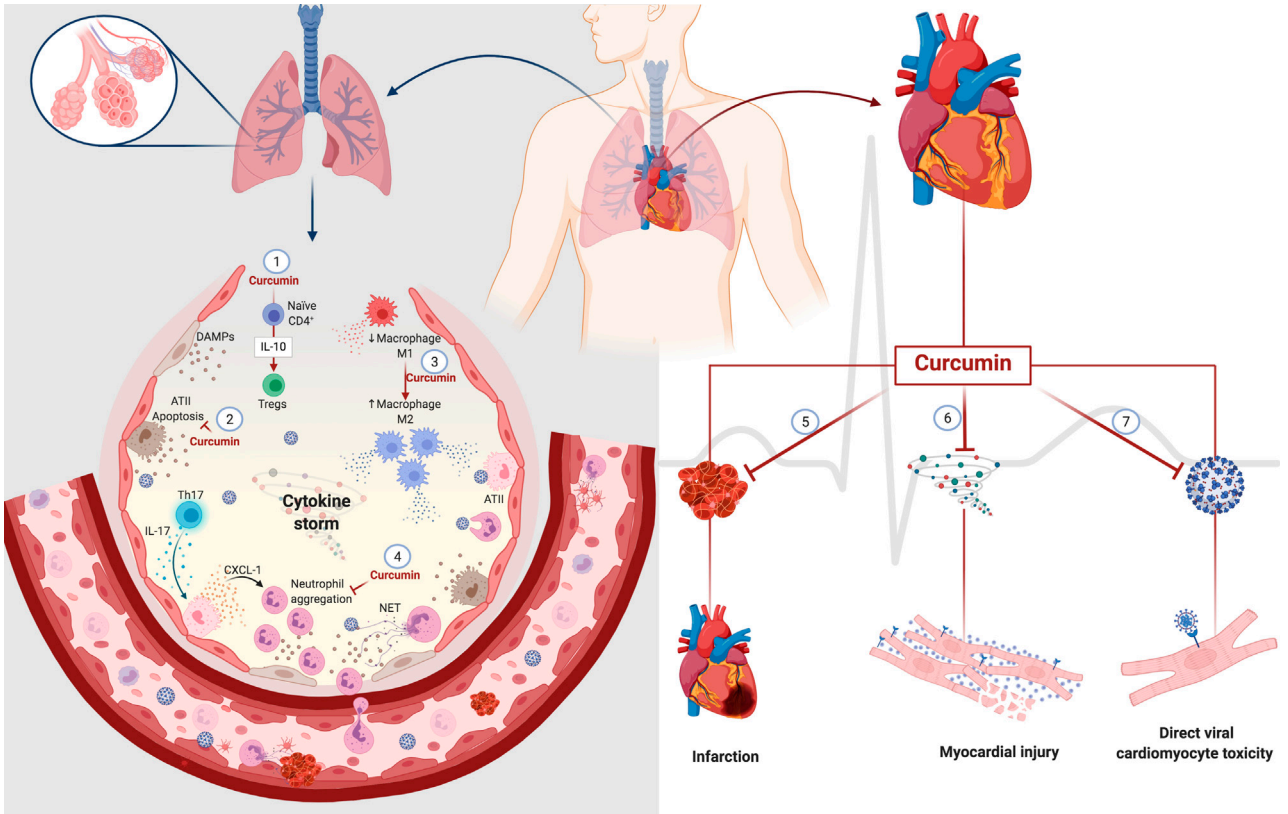

FIGURE 4 | Potential curcumin in cell damage caused by SARS-CoV-2 in the lung and heart. Curcumin promotes differentiation from naïve CD4+T-cell to Tregs through the modulation of IL-10 (1). The cytoprotective role of curcumin decreases the death of type II alveolar cells (ATII) with a consequent decrease in the release of DAMPs (2). Curcumin also mediates macrophages' polarization, decreasing the population of inflammatory macrophages M1 to macrophages M2 that participate in the resolving and reparative process (3). The presence of Th17 cells promotes the activation of ATII cells through IL-17. In turn, activated ATII cells release a chemoattractant for neutrophils that causes neutrophil aggregation. Curcumin decreases IL-17 levels with a consequent decrease in neutrophil aggregates. The anticoagulant and antithrombotic effects of curcumin can have protective effects on the heart, decreasing the heart attack risk (5). The anti-inflammatory action of curcumin can prevent damage to cardiomyocytes caused by an excess of inflammatory mediators, known as a cytokine storm (6). Its affinity for protein S and ACE2 can prevent the direct infection of cardiomyocytes by SARS-CoV-2 (7). Abbreviations: ATII, alveolar type II cells; Tregs, regulatory T cells; Th17, T helper 17 cells; CXCL-1, chemokine ligand 1; NET, neutrophil extracellular traps.

with COVID-19 with increased levels of troponin T without CVD was 37.5% (Guo et al., 2020).

The cardiac events reportedly caused by COVID-19 include acute myocardial injury, heart failure, acute coronary syndrome, infarction, and arrhythmia (Lang et al., 2020; Amirfakhryan and Safari, 2021). The hypotheses surrounding cardiovascular involvement in COVID-19 involve direct infection of cardiac cells by SARS-CoV-2, injury mediated by the inflammatory process, reduced oxygen supply, hypoxia, microthrombi, and stress cardiomyopathy (Lang et al., 2020; Amirfakhryan and Safari, 2021). Histopathological analysis of the heart of a patient with COVID-19 revealed cardiac tissue with a fibrin thrombus in a perforating vein associated with myocardial infarction, myocardial necrosis (transmural), and neutrophilic infiltrates (Rapkiewicz et al., 2020).

In experimental models of sepsis, curcumin proved to be effective at improving the survival parameters, reducing hypovolemia levels observed in the late phase of sepsis, suppression of hyperglycemia in the acute phase, and attenuation of hypoglycemia in the late stage (Silva et al., 2017). Curcumin also attenuated heart damage induced by sepsis; improved cardiac function and body temperature (Yang et al., 2013); and reduced troponin I levels and the product of lipid peroxidation, suggesting its reduction of oxidative damage (Yang et al., 2013).

The restoration of blood flow in the ischemic myocardium can exacerbate tissue injury and result in a poorly adaptive tissue process (Vinten-Johansen et al., 2005; Prasad et al., 2009). First, oxidative stress activates metalloproteinases (MMPs) that promote degradation of the extracellular matrix (ECM). This results in the progressive expansion of the infarction, thinning of the ventricular wall, and dilation of the chamber (Wang et al., 2012). The cure for the infarction involves deposition of collagen, forming a fibrotic and non-functional scar. In an experimental model of ischemia and reperfusion, treatment with curcumin reduced ECM degradation by MMPs and increased the synthesis of collagen and the accumulation of myofibroblasts (Wang et al., 2012). Consequently, there was an improvement in cardiac function, reduced left ventricle dilation, and increased wall thickness (Wang et al., 2012).

An increased number of studies evaluating post-COVID-19 sequelae warns of cardiovascular symptoms, such as chest pain and palpitations (Schneider, 2020; Carvalho-Schneider et al., 2021; Halpin et al., 2021; Huang et al., 2021; Vallejo et al., 2021). The cumulative incidence of thrombosis (2.5% at 30 days after discharge), including segmental pulmonary embolism, intracardiac thrombus, thrombosed arteriovenous fistula, and ischemic stroke, were reported in a single-center study in the United States with 163 patients (Patell et al., 2020). The 6-month post-evaluation of COVID-19 showed that patients suffer from long-term sequelae of the disease, including venous thromboembolic diseases (cardiovascular and cerebrovascular events) (Huang et al., 2021). Currently, there are no reports of curcumin in cardiac changes resulted from COVID-19. However, based on data published on other diseases and cardiac disorders, we hypothesize that curcumin may be a promising agent in preventing cardiovascular damage caused by SARS-CoV-2 infection, as summarized in **Figure 4**.

CONCLUSION

Due to the uncountable mechanisms of action addressed in this and other reviews, it has been reinforced that curcumin could serve as an adjuvant drug in COVID-19 treatment (Babaei et al., 2020; Manoharan et al., 2020; Roy et al., 2020; Soni et al., 2020; Zahedipour et al., 2020; Saeedi-Boroujeni et al., 2021; Thimmulappa et al., 2021). The multiplicity of pathophysiological responses induced by SARS-CoV-2 highlights the need for a combination of different drugs as a treatment strategy (i.e., there is no single "magic pill" for the cure of COVID-19). Curcumin is a well-tolerated natural compound in humans, even at high concentrations (Dhillon et al., 2008; Kanai et al., 2011; Gupta et al., 2013). Thus, its combination with drugs that are already approved for use appears logical. Curcumin is a well-tolerated natural compound in humans, even at high concentrations (Dhillon et al., 2008; Kanai et al., 2011; Gupta et al., 2013). Thus, its combination with drugs that are already approved for use appears logical. The first results from the studies regarding the effect of curcumin in patients with COVID-19 are promising. However, several questions need to be answered: 1) Does curcumin prevent SARS-CoV-2 infection of the host cells? 2) Does curcumin treatment attenuate respiratory and cardiovascular system commitment? 3) Is the curcumin able to reestablish hemostatic homeostasis?

Despite the absence of specific studies addressing the mechanism of action of curcumin in the treatment of COVID-19, currently, the world is experiencing an uncommon situation, which has led researchers and physicians to evaluate the available knowledge to the other diseases, in an attempt to design more promising pathways against SARS-CoV-2. In conclusion, this review strategically contributes to the relentless search for therapies that can act on combat of COVID-19, in addition to providing targets for future studies using the curcumin as an adjuvant treatment to COVID-19.

AUTHOR CONTRIBUTIONS

BR: Conceptualization, Writing—original draft, author of illustrations. SR: Conceptualization, Writing—review and editing, Funding acquisition. MC: Conceptualization, Writing—review and editing, Funding acquisition, Supervision.

FUNDING

This work was supported by grants from the Fundação de Amparo a Pesquisa do Estado de Goiás (FAPEG/BRAZIL) (2017/1026700006-8) and Coordenação de Aperfeiçoamento de Pessoal de Nível Superior (CAPES/Brazil) (88882.378587/2019-01).

ACKNOWLEDGMENTS

The authors acknowledge the Coordenação de Aperfeiçoamento de Pessoal de Nível Superior (CAPES/Brazil) [88882.378587/2019-01] and Fundação de Amparo a Pesquisa do Estado de Goiás (FAPEG/BRAZIL) [2017/1026700006-8] for supporting funds. The authors also acknowledge the BioRender for making it possible to create the illustrations.

REFERENCES

Alexandrow, M. G., Song, L. J., Altiok, S., Gray, J., Haura, E. B., and Kumar, N. B. (2012). Curcumin. *Eur. J. Cancer Prev.* 21, 407–412. doi:10.1097/CEJ.0b013e32834ef194

Ali, A., and Banerjea, A. C. (2016). Curcumin Inhibits HIV-1 by Promoting Tat Protein Degradation. *Sci. Rep.* 6, 1–9. doi:10.1038/srep27539

Almatroodi, S. A., Alrumaihi, F., Alsahli, M. A., Alhommrani, M. F., Khan, A., and Rahmani, A. H. (2020). Curcumin, an Active Constituent of Turmeric Spice: Implication in the Prevention of Lung Injury Induced by Benzo(a) Pyrene (BAP) in Rats. *Molecules* 25, 724–819. doi:10.3390/molecules25030724

Amirfakhryan, H., and Safari, F. (2021). Outbreak of SARS-CoV2: Pathogenesis of Infection and Cardiovascular Involvement. *Hellenic J. Cardiol.* 62, 13–23. doi:10.1016/j.hjc.2020.05.007

Anand, K., Ziebuhr, J., Wadhwani, P., Mesters, J. R., and Hilgenfeld, R. (2003). Coronavirus Main Proteinase (3CLpro) Structure: Basis for Design of Anti-SARS Drugs. *Science* 300, 1763–1767. doi:10.1126/science.1085658

Anggakusuma, C. C., Schang, L. M., Rachmawati, H., Frentzen, A., Pfaender, S., Behrendt, P., et al. (2014). Turmeric Curcumin Inhibits Entry of All Hepatitis C Virus Genotypes into Human Liver Cells. *Gut* 63, 1137–1149. doi:10.1136/gutjnl-2012-304299

Antoine, F., Simard, J.-C., and Girard, D. (2013). Curcumin Inhibits Agent-Induced Human Neutrophil Functions In Vitro and Lipopolysaccharide-Induced Neutrophilic Infiltration In Vivo. *Int. Immunopharmacology* 17, 1101–1107. doi:10.1016/j.intimp.2013.09.024

Ashry, N. A., Gameil, N. M., and Suddek, G. M. (2013). Modulation of Cyclophosphamide-Induced Early Lung Injury by Allicin. *Pharm. Biol.* 51, 806–811. doi:10.3109/13880209.2013.766895

Aslam, M., and Ladilov, Y. (2020). Targeting the sAC-dependent cAMP Pool to Prevent SARS-Cov-2 Infection. *Cells* 9, 1962–2014. doi:10.3390/cells9091962

Babaei, F., Nassiri-Asl, M., and Hosseinzadeh, H. (2020). Curcumin (A Constituent of Turmeric): New Treatment Option against COVID-19. *Food Sci. Nutr.* 8, 5215–5227. doi:10.1002/fsn3.1858

Balasubramanian, A., Pilankatta, R., Teramoto, T., Sajith, A. M., Nwulia, E., Kulkarni, A., et al. (2019). Inhibition of Dengue Virus by Curcuminoids. *Antiviral Res.* 162, 71–78. doi:10.1016/j.antiviral.2018.12.002

Beck, B. R., Shin, B., Choi, Y., Park, S., and Kang, K. (2020). Predicting Commercially Available Antiviral Drugs that May Act on the Novel Coronavirus (SARS-CoV-2) through a Drug-Target Interaction Deep Learning Model. *Comput. Struct. Biotechnol. J.* 18, 784–790. doi:10.1016/j.csbj.2020.03.025

Beevers, C. S., Chen, L., Liu, L., Luo, Y., Webster, N. J. G., and Huang, S. (2009). Curcumin Disrupts the Mammalian Target of Rapamycin-Raptor Complex. *Cancer Res.* 69, 1000–1008. doi:10.1158/0008-5472.CAN-08-2367

Beevers, C. S., Li, F., Liu, L., and Huang, S. (2006). Curcumin Inhibits the Mammalian Target of Rapamycin-Mediated Signaling Pathways in Cancer Cells. *Int. J. Cancer* 119, 757–764. doi:10.1002/ijc.21932

Bonaventura, A., Liberale, L., Carbone, F., Vecchié, A., Diaz-Cañestro, C., Camici, G., et al. (2018). The Pathophysiological Role of Neutrophil Extracellular Traps in Inflammatory Diseases. *Thromb. Haemost.* 118, 006–027. doi:10.1160/TH17-09-0630

Butenas, S., Orfeo, T., and Mann, K. G. (2008). Tissue Factor Activity and Function in Blood Coagulation. *Thromb. Res.* 122, S42–S46. doi:10.1016/S0049-3848(08)70018-5

Carvalho-Schneider, C., Laurent, E., Lemaignen, A., Beaufils, E., Bourbao-Tournois, C., Laribi, S., et al. (2021). Follow-up of Adults with Noncritical COVID-19 Two Months after Symptom Onset. *Clin. Microbiol. Infect.* 27, 258–263. doi:10.1016/j.cmi.2020.09.052

Chai, Y.-s., Chen, Y.-q., Lin, S.-h., Xie, K., Wang, C.-j., Yang, Y.-z., et al. (2020). Curcumin Regulates the Differentiation of Naïve CD4+T Cells and Activates IL-10 Immune Modulation against Acute Lung Injury in Mice. *Biomed. Pharmacother.* 125, 109946. doi:10.1016/j.biopha.2020.109946

Chan, J. F.-W., Kok, K.-H., Zhu, Z., Chu, H., To, K. K.-W., Yuan, S., et al. (2020). Genomic Characterization of the 2019 Novel Human-Pathogenic Coronavirus Isolated from a Patient with Atypical Pneumonia after Visiting Wuhan. *Emerging Microbes Infect.* 9, 221–236. doi:10.1080/22221751.2020.1719902

Cheemanapalli, S., Chinthakunta, N., Shaikh, N. M., Shivaranjani, V., Pamuru, R. R., and Chitta, S. K. (2019). Comparative Binding Studies of Curcumin and Tangeretin on Up-Stream Elements of NF-kB Cascade: a Combined Molecular Docking Approach. *Netw. Model. Anal. Health Inform. Bioinforma* 8, 1–11. doi:10.1007/s13721-019-0196-2

Chen, D.-Y., Shien, J.-H., Tiley, L., Chiou, S.-S., Wang, S.-Y., Chang, T.-J., et al. (2010). Curcumin Inhibits Influenza Virus Infection and Haemagglutination Activity. *Food Chem.* 119, 1346–1351. doi:10.1016/j.foodchem.2009.09.011

Chen, H.-W., Kuo, H.-T., Chai, C.-Y., Ou, J.-L., and Yang, R.-C. (2007). Pretreatment of Curcumin Attenuates Coagulopathy and Renal Injury in LPS-Induced Endotoxemia. *J. Endotoxin Res.* 13, 15–23. doi:10.1177/0968051907078605

Chen, I.-Y., Moriyama, M., Chang, M.-F., and Ichinohe, T. (2019). Severe Acute Respiratory Syndrome Coronavirus Viroporin 3a Activates the NLRP3 Inflammasome. *Front. Microbiol.* 10, 1–9. doi:10.3389/fmicb.2019.00050

Chen, M.-H., Lee, M.-Y., Chuang, J.-J., Li, Y.-Z., Ning, S.-T., Chen, J.-C., et al. (2012). Curcumin Inhibits HCV Replication by Induction of Heme Oxygenase-1 and Suppression of AKT. *Int. J. Mol. Med.* 30, 1021–1028. doi:10.3892/ijmm.2012.1096

Chen, Y., Liu, Q., and Guo, D. (2020). Emerging Coronaviruses: Genome Structure, Replication, and Pathogenesis. *J. Med. Virol.* 92, 418–423. doi:10.1002/jmv.25681

Cheng, K., Yang, A., Hu, X., Zhu, D., and Liu, K. (2018). Curcumin Attenuates Pulmonary Inflammation in Lipopolysaccharide Induced Acute Lung Injury in Neonatal Rat Model by Activating Peroxisome Proliferator-Activated Receptor γ (PPARγ) Pathway. *Med. Sci. Monit.* 24, 1178–1184. doi:10.12659/MSM.908714

Chung, M. K., Karnik, S., Saef, J., Bergmann, C., Barnard, J., Lederman, M. M., et al. (2020). SARS-CoV-2 and ACE2: The Biology and Clinical Data Settling the ARB and ACEI Controversy. *EBioMedicine* 58, 102907. doi:10.1016/j.ebiom.2020.102907

Crowley, S. D., and Rudemiller, N. P. (2017). Immunologic Effects of the Renin-Angiotensin System. *Jasn* 28, 1350–1361. doi:10.1681/ASN.2016101066

Czaikoski, P. G., Mota, J. M. S. C., Nascimento, D. C., Sônego, F., Castanheira, F. V. e. S., Melo, P. H., et al. (2016). Neutrophil Extracellular Traps Induce Organ Damage during Experimental and Clinical Sepsis. *PLoS One* 11, e0148142. doi:10.1371/journal.pone.0148142

D'Alessandro, E., Posma, J. J. N., Spronk, H. M. H., and ten Cate, H. (2018). Tissue Factor (:Factor VIIa) in the Heart and Vasculature: More Than an Envelope. *Thromb. Res.* 168, 130–137. doi:10.1016/j.thromres.2018.06.020

D'ardes, D., Boccatonda, A., Rossi, I., Guagnano, M. T., Santilli, F., Cipollone, F., et al. (2020). COVID-19 and RAS: Unravelling an Unclear Relationship. *Int. J. Mol. Sci.* 21, 1–8. doi:10.3390/ijms21083003

DeDiego, M. L., Nieto-Torres, J. L., Regla-Nava, J. A., Jimenez-Guardeno, J. M., Fernandez-Delgado, R., Fett, C., et al. (2014). Inhibition of NF- B-Mediated Inflammation in Severe Acute Respiratory Syndrome Coronavirus-Infected Mice Increases Survival. *J. Virol.* 88, 913–924. doi:10.1128/jvi.02576-13

Deng, Q., Hu, B., Zhang, Y., Wang, H., Zhou, X., Hu, W., et al. (2020). Suspected Myocardial Injury in Patients with COVID-19: Evidence from Front-Line Clinical Observation in Wuhan, China. *Int. J. Cardiol.* 311, 116–121. doi:10.1016/j.ijcard.2020.03.087

Dhillon, N., Aggarwal, B. B., Newman, R. A., Wolff, R. A., Kunnumakkara, A. B., Abbruzzese, J. L., et al. (2008). Phase II Trial of Curcumin in Patients with Advanced Pancreatic Cancer. *Clin. Cancer Res.* 14, 4491–4499. doi:10.1158/1078-0432.CCR-08-0024

Dushianthan, A., Grocott, M. P. W., Postle, A. D., and Cusack, R. (2011). Acute Respiratory Distress Syndrome and Acute Lung Injury. *Postgrad. Med. J.* 87, 612–622. doi:10.1136/pgmj.2011.118398

Dutta, K., Ghosh, D., and Basu, A. (2009). Curcumin Protects Neuronal Cells from Japanese Encephalitis Virus-Mediated Cell Death and Also Inhibits Infective Viral Particle Formation by Dysregulation of Ubiquitin-Proteasome System. *J. Neuroimmune Pharmacol.* 4, 328–337. doi:10.1007/s11481-009-9158-2

Eguchi, S., Kawai, T., Scalia, R., and Rizzo, V. (2018). Understanding Angiotensin II Type 1 Receptor Signaling in Vascular Pathophysiology. *Hypertension* 71, 804–810. doi:10.1161/HYPERTENSIONAHA.118.10266

Elfiky, A. A. (2020). Ribavirin, Remdesivir, Sofosbuvir, Galidesivir, and Tenofovir against SARS-CoV-2 RNA Dependent RNA Polymerase (RdRp): A Molecular Docking Study. *Life Sci.* 253, 117592. doi:10.1016/j.lfs.2020.117592

Falati, S., Edmead, C. E., and Poole, A. W. (1999). Glycoprotein Ib-V-IX, a Receptor for von Willebrand Factor, Couples Physically and Functionally to the Fc Receptor γ-Chain, Fyn, and Lyn to Activate Human Platelets. *Blood* 94, 1648–1656. doi:10.1182/blood.v94.5.1648

Fan, E., Beitler, J. R., Brochard, L., Calfee, C. S., Ferguson, N. D., Slutsky, A. S., et al. (2020). COVID-19-associated Acute Respiratory Distress Syndrome: Is a Different Approach to Management Warranted? *Lancet Respir. Med.* 8, 816–821. doi:10.1016/S2213-2600(20)30304-0

Gheblawi, M., Wang, K., Viveiros, A., Nguyen, Q., Zhong, J.-C., Turner, A. J., et al. (2020). Angiotensin-Converting Enzyme 2: SARS-CoV-2 Receptor and Regulator of the Renin-Angiotensin System. *Circ. Res.* 126, 1456–1474. doi:10.1161/CIRCRESAHA.120.317015

Gómez-Moreno, D., Adrover, J. M., and Hidalgo, A. (2018). Neutrophils as Effectors of Vascular Inflammation. *Eur. J. Clin. Invest.* 48, e12940–14. doi:10.1111/eci.12940

Grobler, C., Maphumulo, S. C., Grobbelaar, L. M., Bredenkamp, J. C., Laubscher, G. J., Lourens, P. J., et al. (2020). Covid-19: The rollercoaster of fibrin(ogen), d-dimer, von willebrand factor, p-selectin and their interactions with endothelial cells, platelets and erythrocytes. *Int J Mol Sci.* 21, 5168–5225. doi:10.3390/ijms21145168

Guan, W.-j., Ni, Z.-y., Hu, Y., Liang, W.-h., Ou, C.-q., He, J.-x., et al. (2020). Clinical Characteristics of Coronavirus Disease 2019 in China. *N. Engl. J. Med.* 382, 1708–1720. doi:10.1056/NEJMoa2002032

Guo, T., Fan, Y., Chen, M., Wu, X., Zhang, L., He, T., et al. (2020). Cardiovascular Implications of Fatal Outcomes of Patients with Coronavirus Disease 2019 (COVID-19). *JAMA Cardiol.* 5, 811–818. doi:10.1001/jamacardio.2020.1017

Gupta, P., Garg, P., and Roy, N. (2011). Comparative Docking and CoMFA Analysis of Curcumine Derivatives as HIV-1 Integrase Inhibitors. *Mol. Divers.* 15, 733–750. doi:10.1007/s11030-011-9304-7

Gupta, S. C., Patchva, S., and Aggarwal, B. B. (2013). Therapeutic Roles of Curcumin: Lessons Learned from Clinical Trials. *AAPS J.* 15, 195–218. doi:10.1208/s12248-012-9432-8

Halpin, S. J., McIvor, C., Whyatt, G., Adams, A., Harvey, O., McLean, L., et al. (2021). Postdischarge Symptoms and Rehabilitation Needs in Survivors of COVID-19 Infection: A Cross-sectional Evaluation. *J. Med. Virol.* 93, 1013–1022. doi:10.1002/jmv.26368

Hassaniazad, M., Inchehsablagh, B. R., Kamali, H., Tousi, A., Eftekhar, E., Jaafari, M. R., et al. (2020). The Clinical Effect of Nano Micelles Containing Curcumin as a Therapeutic Supplement in Patients with COVID-19 and the Immune Responses Balance Changes Following Treatment: A Structured Summary of a Study Protocol for a Randomised Controlled Trial. *Trials* 21, 20–22. doi:10.1186/s13063-020-04824-y

Hergenhahn, M., Soto, U., Weninger, A., Polack, A., Hsu, C.-H., Cheng, A.-L., et al. (2002). The Chemopreventive Compound Curcumin Is an Efficient Inhibitor of Epstein-Barr Virus BZLF1 Transcription in Raji DR-LUC Cells*. *Mol. Carcinog.* 33, 137–145. doi:10.1002/mc.10029

Hoffmann, M., Kleine-Weber, H., Schroeder, S., Krüger, N., Herrler, T., Erichsen, S., et al. (2020). SARS-CoV-2 Cell Entry Depends on ACE2 and TMPRSS2 and Is Blocked by a Clinically Proven Protease Inhibitor. *Cell* 181, 271–280. doi:10.1016/j.cell.2020.02.052

Huang, C., Huang, L., Wang, Y., Li, X., Ren, L., Gu, X., et al. (2021). 6-month Consequences of COVID-19 in Patients Discharged from Hospital: a Cohort Study. *The Lancet* 397, 220–232. doi:10.1016/S0140-6736(20)32656-8

Huang, C., Wang, Y., Li, X., Ren, L., Zhao, J., Hu, Y., et al. (2020). Clinical Features of Patients Infected with 2019 Novel Coronavirus in Wuhan, China. *The Lancet* 395, 497–506. doi:10.1016/S0140-6736(20)30183-5

Huynh, T., Wang, H., and Luan, B. (2020). In Silico Exploration of the Molecular Mechanism of Clinically Oriented Drugs for Possibly Inhibiting SARS-CoV-2's Main Protease. *J. Phys. Chem. Lett.* 11, 4413–4420. doi:10.1021/acs.jpclett.0c00994

Iba, T., Connors, J. M., and Levy, J. H. (2020). The Coagulopathy, Endotheliopathy, and Vasculitis of COVID-19. *Inflamm. Res.* 69, 1181–1189. doi:10.1007/s00011-020-01401-6

Imai, Y., Kuba, K., Rao, S., Huan, Y., Guo, F., Guan, B., et al. (2005). Angiotensin-converting Enzyme 2 Protects from Severe Acute Lung Failure. *Nature* 436, 112–116. doi:10.1038/nature03712

Ip, W. K. E., Hoshi, N., Shouval, D. S., Snapper, S., and Medzhitov, R. (2017). Anti-inflammatory Effect of IL-10 Mediated by Metabolic Reprogramming of Macrophages. *Science* 356, 513–519. doi:10.1126/science.aal3535

Jeong, E.-H., Vaidya, B., Cho, S.-Y., Park, M.-A., Kaewintajuk, K., Kim, S. R., et al. (2015). Identification of Regulators of the Early Stage of Viral Hemorrhagic Septicemia Virus Infection during Curcumin Treatment. *Fish Shellfish Immunol.* 45, 184–193. doi:10.1016/j.fsi.2015.03.042

Jia, X., Cao, B., An, Y., Zhang, X., and Wang, C. (2019). Rapamycin Ameliorates Lipopolysaccharide-Induced Acute Lung Injury by Inhibiting IL-1β and IL-18 Production. *Int. Immunopharmacology* 67, 211–219. doi:10.1016/j.intimp.2018.12.017

Jiménez-Alcázar, M., Rangaswamy, C., Panda, R., Bitterling, J., Simsek, Y. J., Long, A. T., et al. (2017). Host DNases Prevent Vascular Occlusion by Neutrophil Extracellular Traps. *Science* 358, 1202–1206. doi:10.1126/science.aam8897

Johnson, S. M., Gulhati, P., Arrieta, I., Wang, X., Uchida, T., Gao, T., et al. (2009). Curcumin Inhibits Proliferation of Colorectal Carcinoma by Modulating Akt/mTOR Signaling. *Anticancer Res.* 29, 3185–3190.

Kanai, M., Yoshimura, K., Asada, M., Imaizumi, A., Suzuki, C., Matsumoto, S., et al. (2011). A Phase I/II Study of Gemcitabine-Based Chemotherapy Plus Curcumin for Patients with Gemcitabine-Resistant Pancreatic Cancer. *Cancer Chemother. Pharmacol.* 68, 157–164. doi:10.1007/s00280-010-1470-2

Kanzawa, N., Nishigaki, K., Hayashi, T., Ishii, Y., Furukawa, S., Niiro, A., et al. (2006). Augmentation of Chemokine Production by Severe Acute Respiratory Syndrome Coronavirus 3a/X1 and 7a/X4 Proteins through NF-Kb Activation. *FEBS Lett.* 580, 6807–6812. doi:10.1016/j.febslet.2006.11.046

Karunaweera, N., Raju, R., Gyengesi, E., and Münch, G. (2015). Plant Polyphenols as Inhibitors of NF-Îob Induced Cytokine Productionâ€"a Potential Anti-inflammatory Treatment for Alzheimer's Disease? *Front. Mol. Neurosci.* 8, 1–5. doi:10.3389/fnmol.2015.00024

Khan, N., Chen, X., and Geiger, J. D. (2020). Role of Endolysosomes in Severe Acute Respiratory Syndrome Coronavirus-2 Infection and Coronavirus Disease 2019 Pathogenesis: Implications for Potential Treatments. *Front. Pharmacol.* 11, 1–13. doi:10.3389/fphar.2020.595888

Kuba, K., Imai, Y., Rao, S., Gao, H., Guo, F., Guan, B., et al. (2005). A Crucial Role of Angiotensin Converting Enzyme 2 (ACE2) in SARS Coronavirus-Induced Lung Injury. *Nat. Med.* 11, 875–879. doi:10.1038/nm1267

Lang, J. P., Wang, X., Moura, F. A., Siddiqi, H. K., Morrow, D. A., and Bohula, E. A. (2020). A Current Review of COVID-19 for the Cardiovascular Specialist. *Am. Heart J.* 226, 29–44. doi:10.1016/j.ahj.2020.04.025

Lefrançais, E., Mallavia, B., Zhuo, H., Calfee, C. S., and Looney, M. R. (2018). Maladaptive Role of Neutrophil Extracellular Traps in Pathogen-Induced Lung Injury. *JCI Insight* 3, 1–15. doi:10.1172/jci.insight.98178

Liao, M., Liu, Y., Yuan, J., Wen, Y., Xu, G., Zhao, J., et al. (2020). Single-cell Landscape of Bronchoalveolar Immune Cells in Patients with COVID-19. *Nat. Med.* 26, 842–844. doi:10.1038/s41591-020-0901-9

Liao, Q.-J., Ye, L.-B., Timani, K. A., Zeng, Y.-C., She, Y.-L., Ye, L., et al. (2005). Activation of NF-kappaB by the Full-Length Nucleocapsid Protein of the SARS Coronavirus. *Acta Biochim. Biophys. Sinica* 37, 607–612. doi:10.1111/j.1745-7270.2005.00082.x

Lin, S., Wu, H., Wang, C., Xiao, Z., and Xu, F. (2018). Regulatory T Cells and Acute Lung Injury: Cytokines, Uncontrolled Inflammation, and Therapeutic Implications. *Front. Immunol.* 9, 1–10. doi:10.3389/fimmu.2018.01545

Liu, Y.-F., Yang, C.-W., Liu, H., Sui, S.-G., and Li, X.-D. (2017). Efficacy and Therapeutic Potential of Curcumin against Sepsis-Induced Chronic Lung Injury in Male Albino Rats. *J. Nutr. Health Aging* 21, 307–313. doi:10.1007/s12603-016-0722-1

Lu, R., Zhao, X., Li, J., Niu, P., Yang, B., Wu, H., et al. (2020). Genomic Characterisation and Epidemiology of 2019 Novel Coronavirus: Implications for Virus Origins and Receptor Binding. *The Lancet* 395, 565–574. doi:10.1016/S0140-6736(20)30251-8

Lv, Y., Lei, N., Wang, D., An, Z., Li, G., Han, F., et al. (2014b). Protective Effect of Curcumin against Cytomegalovirus Infection in Balb/c Mice. *Environ. Toxicol. Pharmacol.* 37, 1140–1147. doi:10.1016/j.etap.2014.04.017

Ma, T., Guo, C. J., Zhao, X., Wu, L., Sun, S. X., and Jin, Q. H. (2015). The Effect of Curcumin on NF-Kb Expression in Rat with Lumbar Intervertebral Disc Degeneration. *Eur. Rev. Med. Pharmacol. Sci.* 19, 1305–1314.

Mahmudpour, M., Roozbeh, J., Keshavarz, M., Farrokhi, S., and Nabipour, I. (2020). COVID-19 Cytokine Storm: The Anger of Inflammation. *Cytokine* 133, 155151. doi:10.1016/j.cyto.2020.155151

Manoharan, Y., Haridas, V., Vasanthakumar, K. C., Muthu, S., Thavoorullah, F. F., and Shetty, P. (2020). Curcumin: a Wonder Drug as a Preventive Measure for COVID19 Management. *Ind. J. Clin. Biochem.* 35, 373–375. doi:10.1007/s12291-020-00902-9

Mason, R. J. (2020). Pathogenesis of COVID-19 from a Cell Biology Perspective. *Eur. Respir. J.* 55, 2000607–2000611. doi:10.1183/13993003.00607-2020

Maurya, V. K., Kumar, S., Prasad, A. K., Bhatt, M. L. B., and Saxena, S. K. (2020). Structure-based Drug Designing for Potential Antiviral Activity of Selected Natural Products from Ayurveda against SARS-CoV-2 Spike Glycoprotein and its Cellular Receptor. *VirusDis.* 31, 179–193. doi:10.1007/s13337-020-00598-8

Mayanglambam, A., Dangelmaier, C. A., Thomas, D., Damodar Reddy, C., Daniel, J. L., and Kunapuli, S. P. (2010). Curcumin Inhibits GPVI-Mediated Platelet Activation by Interfering with the Kinase Activity of Syk and the Subsequent Activation of PLCγ2. *Platelets* 21, 211–220. doi:10.3109/09537100903528269

McFadyen, J. D., Stevens, H., and Peter, K. (2020). The Emerging Threat of (Micro) Thrombosis in COVID-19 and its Therapeutic Implications. *Circ. Res.* 127, 571–587. doi:10.1161/CIRCRESAHA.120.317447

Middleton, E. A., He, X.-Y., Denorme, F., Campbell, R. A., Ng, D., Salvatore, S. P., et al. (2020). Neutrophil Extracellular Traps Contribute to Immunothrombosis in COVID-19 Acute Respiratory Distress Syndrome. *Blood* 136, 1169–1179. doi:10.1182/blood.2020007008

Motohashi, N., Vanam, A., and Gollapudi, R. (2020). In Silico Study of Curcumin and Folic Acid as Potent Inhibitors of Human Transmembrane Protease Serine 2 in the Treatment of COVID-19. *INNOSC Theranostics Pharmacol. Sci.* 3, 3–9. doi:10.36922/itps.v3i2.935

Mounce, B. C., Cesaro, T., Carrau, L., Vallet, T., and Vignuzzi, M. (2017). Curcumin Inhibits Zika and Chikungunya Virus Infection by Inhibiting Cell Binding. *Antiviral Res.* 142, 148–157. doi:10.1016/j.antiviral.2017.03.014

Murakami, M., Kamimura, D., and Hirano, T. (2019). Pleiotropy and Specificity: Insights from the Interleukin 6 Family of Cytokines. *Immunity* 50, 812–831. doi:10.1016/j.immuni.2019.03.027

Nemmar, A., Subramaniyan, D., and Ali, B. H. (2012). Protective Effect of Curcumin on Pulmonary and Cardiovascular Effects Induced by Repeated Exposure to Diesel Exhaust Particles in Mice. *PLoS One* 7, e39554. doi:10.1371/journal.pone.0039554

Nieto-Torres, J. L., Verdiá-Báguena, C., Jimenez-Guardeño, J. M., Regla-Nava, J. A., Castaño-Rodriguez, C., Fernandez-Delgado, R., et al. (2015). Severe Acute Respiratory Syndrome Coronavirus E Protein Transports Calcium Ions and Activates the NLRP3 Inflammasome. *Virology* 485, 330–339. doi:10.1016/j.virol.2015.08.010

Nishimura, H., Tsuji, H., Masuda, H., Nakagawa, K., Nakahara, Y., Kitamura, H., et al. (1997). Angiotensin II Increases Plasminogen Activator Inhibitor-1 and Tissue Factor mRNA Expression without Changing that of Tissue Type Plasminogen Activator or Tissue Factor Pathway Inhibitor in Cultured Rat Aortic Endothelial Cells. *Thromb. Haemost.* 77, 1189–1195. doi:10.1055/s-0038-1656136

Obata, K., Kojima, T., Masaki, T., Okabayashi, T., Yokota, S., Hirakawa, S., et al. (2013). Curcumin Prevents Replication of Respiratory Syncytial Virus and the Epithelial Responses to it in Human Nasal Epithelial Cells. *PLoS One* 8, e70225–14. doi:10.1371/journal.pone.0070225

Ou, J.-L., Mizushina, Y., Wang, S.-Y., Chuang, D.-Y., Nadar, M., and Hsu, W.-L. (2013). Structure-activity Relationship Analysis of Curcumin Analogues on Anti-influenza Virus Activity. *FEBS J.* 280, 5829–5840. doi:10.1111/febs.12503

Paciello, F., Fetoni, A. R., Mezzogori, D., Rolesi, R., Di Pino, A., Paludetti, G., et al. (2020). The Dual Role of Curcumin and Ferulic Acid in Counteracting Chemoresistance and Cisplatin-Induced Ototoxicity. *Sci. Rep.* 10, 1063. doi:10.1038/s41598-020-57965-0

Paliogiannis, P., Mangoni, A. A., Dettori, P., Nasrallah, G. K., Pintus, G., and Zinellu, A. (2020). D-dimer Concentrations and COVID-19 Severity: A Systematic Review and Meta-Analysis. *Front. Public Health* 8, 1–7. doi:10.3389/fpubh.2020.00432

Papayannopoulos, V. (2018). Neutrophil Extracellular Traps in Immunity and Disease. *Nat. Rev. Immunol.* 18, 134–147. doi:10.1038/nri.2017.105

Park, J.-Y., Jae Jeong, H., Hoon Kim, J., Min Kim, Y., Park, S.-J., Kim, D., et al. (2012). Diarylheptanoids from Alnus Japonica Inhibit Papain-like Protease of Severe Acute Respiratory Syndrome Coronavirus. *Biol. Pharm. Bull.* 35, 2036–2042. doi:10.1248/bpb.b12-00623

Park, J.-Y., Kim, J. H., Kim, Y. M., Jeong, H. J., Kim, D. W., Park, K. H., et al. (2012). Tanshinones as Selective and Slow-Binding Inhibitors for SARS-CoV Cysteine Proteases. *Bioorg. Med. Chem.* 20, 5928–5935. doi:10.1016/j.bmc.2012.07.038

Patell, R., Bogue, T., Koshy, A., Bindal, P., Merrill, M., Aird, W. C., et al. (2020). Postdischarge Thrombosis and Hemorrhage in Patients with COVID-19. *Blood* 136, 1342–1346. doi:10.1182/blood.2020007938

Pendurthi, U. R., Williams, J. T., and Rao, L. V. M. (1997). Inhibition of Tissue Factor Gene Activation in Cultured Endothelial Cells by Curcumin. *Arterioscler Thromb Vasc Biol.* 17, 3406–3413. doi:10.1161/01.ATV.17.12.3406

Prasad, A., Stone, G. W., Holmes, D. R., and Gersh, B. (2009). Reperfusion Injury, Microvascular Dysfunction, and Cardioprotection. *Circulation* 120, 2105–2112. doi:10.1161/CIRCULATIONAHA.108.814640

Rahardjo, B., Widjajanto, E., Sujuti, H., and Keman, K. (2014). Curcumin Decreased Level of Proinflammatory Cytokines in Monocyte Cultures Exposed to Preeclamptic Plasma by Affecting the Transcription Factors NF-Kb and PPAR-γ. *Biomarkers Genomic Med.* 6, 105–115. doi:10.1016/j.bgm.2014.06.002

Ramirez Boscá, A., Soler, A., Carrión-Gutiérrez, M. A., Pamies Mira, D., Pardo Zapata, J., Diaz-Alperi, J., et al. (2000). An Hydroalcoholic Extract of Curcuma Longa Lowers the Abnormally High Values of Human-Plasma Fibrinogen. *Mech. Ageing Dev.* 114, 207–210. doi:10.1016/S0047-6374(00)00089-0

Rapkiewicz, A. V., Mai, X., Carsons, S. E., Pittaluga, S., Kleiner, D. E., Berger, J. S., et al. (2020). Megakaryocytes and Platelet-Fibrin Thrombi Characterize Multi-Organ Thrombosis at Autopsy in COVID-19: A Case Series. *EClinicalMedicine* 24, 100434. doi:10.1016/j.eclinm.2020.100434

Riphagen, S., Gomez, X., Gonzalez-Martinez, C., Wilkinson, N., and Theocharis, P. (2020). Hyperinflammatory Shock in Children during COVID-19 Pandemic. *The Lancet* 395, 1607–1608. doi:10.1016/S0140-6736(20)31094-1

Rodrigues, T. S., de Sá, K. S. G., Ishimoto, A. Y., Becerra, A., Oliveira, S., Almeida, L., et al. (2021). Inflammasomes Are Activated in Response to SARS-CoV-2 Infection and Are Associated with COVID-19 Severity in Patients. *J. Exp. Med.* 218. doi:10.1084/jem.20201707

Roy, A., Sarkar, B., Celik, C., Ghosh, A., Basu, U., Jana, M., et al. (2020). Can Concomitant Use of Zinc and Curcumin with Other Immunity-boosting Nutraceuticals Be the Arsenal against COVID -19? *Phytotherapy Res.* 34, 2425–2428. doi:10.1002/ptr.6766

Ruiz-Ortega, M., Lorenzo, O., Suzuki, Y., Rupérez, M., and Egido, J. (2001). Proinflammatory Actions of Angiotensins. *Curr. Opin. Nephrol. Hypertens.* 10, 321–329. doi:10.1097/00041552-200105000-00005

Rut, W., Groborz, K., Zhang, L., Sun, X., Zmudzinski, M., Pawlik, B., et al. (2020). SARS-CoV-2 Mpro Inhibitors and Activity-Based Probes for Patient-Sample Imaging. *Nat. Chem. Biol.* 17, 222–228. doi:10.1038/s41589-020-00689-z

Lin, S.-C., Ho, C.-T., Chuo, W.-H., Li, S., Wang, T. T., and Lin, C.-C. (2017), Effective Inhibition of MERS-CoV Infection by Resveratrol, *BMC Infect. Dis.* 17, 1–10. doi:10.1186/s12879-017-2253-8

Saeedi-Boroujeni, A., Mahmoudian-Sani, M. R., Bahadoram, M., and Alghasi, A. (2021). COVID-19: A Case for Inhibiting NLRP3 Inflammasome, Suppression of Inflammation with Curcumin? *Basic Clin. Pharmacol. Toxicol.* 128, 37–45. doi:10.1111/bcpt.13503

Saffarzadeh, M., Juenemann, C., Queisser, M. A., Lochnit, G., Barreto, G., Galuska, S. P., et al. (2012). Neutrophil Extracellular Traps Directly Induce Epithelial and Endothelial Cell Death: A Predominant Role of Histones. *PLoS One* 7, e32366. doi:10.1371/journal.pone.0032366

Sang, Y., Miller, L. C., and Blecha, F. (2015). Macrophage Polarization in Virus-Host Interactions. *J. Clin. Cel. Immunol.* 6, 139–148. doi:10.4172/2155-9899.1000311

Sathler, P. C. (2020). Hemostatic Abnormalities in Covid-19: A Guided Review. *Acad. Bras. Ciênc.* 92, 1–16. doi:10.1590/0001-3765202020200834

Saxton, R. A., and Sabatini, D. M. (2017). mTOR Signaling in Growth, Metabolism, and Disease. *Cell* 168, 960–976. doi:10.1016/j.cell.2017.02.004

Schneider, E. C. (2020). Failing the Test - the Tragic Data Gap Undermining the U.S. Pandemic Response. *N. Engl. J. Med.* 383, 299–302. doi:10.1056/nejmp2014836

Schönrich, G., and Raftery, M. J. (2016). Neutrophil Extracellular Traps Go Viral. *Front. Immunol.* 7, 11–14. doi:10.3389/fimmu.2016.00366

Shah, B. H., Nawaz, Z., Pertani, S. A., Roomi, A., Mahmood, H., Saeed, S. A., et al. (1999). Inhibitory Effect of Curcumin, a Food Spice from Turmeric, on Platelet-Activating Factor- and Arachidonic Acid-Mediated Platelet Aggregation through Inhibition of Thromboxane Formation and Ca2+ Signaling. *Biochem. Pharmacol.* 58, 1167–1172. doi:10.1016/S0006-2952(99)00206-3

Shi, C.-S., Nabar, N. R., Huang, N.-N., and Kehrl, J. H. (2019). SARS-coronavirus Open Reading Frame-8b Triggers Intracellular Stress Pathways and Activates NLRP3 Inflammasomes. *Cell Death Discov.* 5. doi:10.1038/s41420-019-0181-7

Silva, L. S. d., Catalão, C. H. R., Felippotti, T. T., Oliveira- Pelegrin, G. R. d., Petenusci, S., De Freitas, L. A. P., et al. (2017). Curcumin Suppresses Inflammatory Cytokines and Heat Shock Protein 70 Release and Improves Metabolic Parameters during Experimental Sepsis. *Pharm. Biol.* 55, 269–276. doi:10.1080/13880209.2016.1260598

Silva, P. L., Negrini, D., and Macêdo Rocco, P. R. (2015). Mechanisms of Ventilator-Induced Lung Injury in Healthy Lungs. *Best Pract. Res. Clin. Anaesthesiology* 29, 301–313. doi:10.1016/j.bpa.2015.08.004

Simonnet, A., Chetboun, M., Poissy, J., Raverdy, V., Noulette, J., Duhamel, A., et al. (2020). High Prevalence of Obesity in Severe Acute Respiratory Syndrome Coronavirus-2 (SARS-CoV-2) Requiring Invasive Mechanical Ventilation. *Obesity* 28, 1195–1199. doi:10.1002/oby.22831

Siu, K. L., Yuen, K. S., Castano-Rodriguez, C., Ye, Z. W., Yeung, M. L., Fung, S. Y., et al. (2019). Severe Acute Respiratory Syndrome Coronavirus ORF3a Protein Activates the NLRP3 Inflammasome by Promoting TRAF3-dependent Ubiquitination of ASC. *FASEB j.* 33, 8865–8877. doi:10.1096/fj.201802418R

Skurk, T., Van Harmelen, V., and Hauner, H. (2004). Angiotensin II Stimulates the Release of Interleukin-6 and Interleukin-8 from Cultured Human Adipocytes by Activation of NF-Kb. *Arterioscler Thromb Vasc Biol.* 24, 1199–1203. doi:10.1161/01.ATV.0000131266.38312.2e

Solt, L. A., and May, M. J. (2008). The IκB Kinase Complex: Master Regulator of NF-Kb Signaling. *Immunol. Res.* 42, 3–18. doi:10.1007/s12026-008-8025-1

Soni, V. K., Mehta, A., Ratre, Y. K., Tiwari, A. K., Amit, A., Singh, R. P., et al. (2020). Curcumin, a Traditional Spice Component, Can Hold the Promise against COVID-19? *Eur. J. Pharmacol.* 886, 173551. doi:10.1016/j.ejphar.2020.173551

Srivastava, K. C., Bordia, A., and Verma, S. K. (1995). Curcumin, a Major Component of Food Spice Turmeric (*Curcuma longa*) Inhibits Aggregation and Alters Eicosanoid Metabolism in Human Blood Platelets. *Prostaglandins, Leukot. Essent. Fatty Acids* 52, 223–227. doi:10.1016/0952-3278(95)90040-3

Stefanini, G. G., Montorfano, M., Trabattoni, D., Andreini, D., Ferrante, G., Ancona, M., et al. (2020). ST-Elevation Myocardial Infarction in Patients With COVID-19. *Circulation* 141, 2113–2116. doi:10.1161/CIRCULATIONAHA.120.047525

Tahmasebi, S., El-Esawi, M. A., Mahmoud, Z. H., Timoshin, A., Valizadeh, H., Roshangar, L., et al. (2020). Immunomodulatory Effects of Nanocurcumin on Th17 Cell Responses in Mild and Severe COVID-19 Patients. *J. Cel. Physiol.* 236, 5325–5338. doi:10.1002/jcp.30233

Tang, N., Li, D., Wang, X., and Sun, Z. (2020). Abnormal Coagulation Parameters Are Associated with Poor Prognosis in Patients with Novel Coronavirus Pneumonia. *J. Thromb. Haemost.* 18, 844–847. doi:10.1111/jth.14768

Temiz-Resitoglu, M., Kucukkavruk, S. P., Guden, D. S., Cecen, P., Sari, A. N., Tunctan, B., et al. (2017). Activation of mTOR/IκB-A/nf-Kb Pathway Contributes to LPS-Induced Hypotension and Inflammation in Rats. *Eur. J. Pharmacol.* 802, 7–19. doi:10.1016/j.ejphar.2017.02.034

Thangapazham, R. L., Shaheduzzaman, S., Kim, K.-H., Passi, N., Tadese, A., Vahey, M., et al. (2008). Androgen Responsive and Refractory Prostate Cancer Cells Exhibit Distinct Curcumin Regulated Transcriptome. *Cancer Biol. Ther.* 7, 1427–1435. doi:10.4161/cbt.7.9.6469

Thimmulappa, R. K., Mudnakudu-Nagaraju, K. K., Shivamallu, C., Subramaniam, K. J. T., Radhakrishnan, A., Bhojraj, S., et al. (2021). Antiviral and Immunomodulatory Activity of Curcumin: A Case for Prophylactic Therapy for COVID-19. *Heliyon* 7, e06350. doi:10.1016/j.heliyon.2021.e06350

Valizadeh, H., Abdolmohammadi-vahid, S., Danshina, S., Ziya Gencer, M., Ammari, A., Sadeghi, A., et al. (2020). Nano-curcumin Therapy, a Promising Method in Modulating Inflammatory Cytokines in COVID-19 Patients. *Int. Immunopharmacology* 89, 107088. doi:10.1016/j.intimp.2020.107088

Vallejo, N., Teis, A., Mateu, L., and Bayés-Genís, A. (2021). Persistent Chest Pain after Recovery of COVID-19: Microvascular Disease-Related Angina? *Eur. Hear. J. - Case Rep.* 5, 4–5. doi:10.1093/ehjcr/ytab105

Vinten-Johansen, J., Zhao, Z.-Q., Zatta, A. J., Kin, H., Halkos, M. E., and Kerendi, F. (2005). Postconditioning A New Link in Nature's Armor against Myocardial Ischemia-Reperfusion Injury. *Basic Res. Cardiol.* 100, 295–310. doi:10.1007/s00395-005-0523-x

Vishvakarma, N. K., Kumar, A., and Singh, S. M. (2011). Role of Curcumin-dependent Modulation of Tumor Microenvironment of a Murine T Cell Lymphoma in Altered Regulation of Tumor Cell Survival. *Toxicol. Appl. Pharmacol.* 252, 298–306. doi:10.1016/j.taap.2011.03.002

Wang, N.-P., Wang, Z.-F., Tootle, S., Philip, T., and Zhao, Z.-Q. (2012). Curcumin Promotes Cardiac Repair and Ameliorates Cardiac Dysfunction Following Myocardial Infarction. *Br. J. Pharmacol.* 167, 1550–1562. doi:10.1111/j.1476-5381.2012.02109.x

Wang, X., An, X., Wang, X., Bao, C., Li, J., Yang, D., et al. (2018). Curcumin Ameliorated Ventilator-Induced Lung Injury in Rats. *Biomed. Pharmacother.* 98, 754–761. doi:10.1016/j.biopha.2017.12.100

Wang, Y., Tang, Q., Duan, P., and Yang, L. (2018). Curcumin as a Therapeutic Agent for Blocking NF-Kb Activation in Ulcerative Colitis. *Immunopharmacology and Immunotoxicology* 40, 476–482. doi:10.1080/08923973.2018.1469145

Wen, C.-C., Kuo, Y.-H., Jan, J.-T., Liang, P.-H., Wang, S.-Y., Liu, H.-G., et al. (2007). Specific Plant Terpenoids and Lignoids Possess Potent Antiviral Activities against Severe Acute Respiratory Syndrome Coronavirus. *J. Med. Chem.* 50, 4087–4095. doi:10.1021/jm070295s

Wrapp, D., Wang, N., Corbett, K. S., Goldsmith, J. A., Hsieh, C.-L., Abiona, O., et al. (2020). Cryo-EM Structure of the 2019-nCoV Spike in the Prefusion Conformation. *Science* 367, 1260–1263. doi:10.1126/science.aax090210.1126/science.abb2507

Wu, C.-Y., Jan, J.-T., Ma, S.-H., Kuo, C.-J., Juan, H.-F., Cheng, Y.-S. E., et al. (2004). Small Molecules Targeting Severe Acute Respiratory Syndrome Human Coronavirus. *Proc. Natl. Acad. Sci.* 101, 10012–10017. doi:10.1073/pnas.0403596101

Wu, Z., and McGoogan, J. M. (2020). Characteristics of and Important Lessons from the Coronavirus Disease 2019 (COVID-19) Outbreak in China. *Jama* 323, 1239–1242. doi:10.1001/jama.2020.2648

Xia, S., Liu, M., Wang, C., Xu, W., Lan, Q., Feng, S., et al. (2020). Inhibition of SARS-CoV-2 (Previously 2019-nCoV) Infection by a Highly Potent Pan-Coronavirus Fusion Inhibitor Targeting its Spike Protein that Harbors a High Capacity to Mediate Membrane Fusion. *Cell Res* 30, 343–355. doi:10.1038/s41422-020-0305-x

Xia, S., Zhu, Y., Liu, M., Lan, Q., Xu, W., Wu, Y., et al. (2020). Fusion Mechanism of 2019-nCoV and Fusion Inhibitors Targeting HR1 Domain in Spike Protein. *Cell Mol Immunol* 17, 765–767. doi:10.1038/s41423-020-0374-2

Xiao, X., Yang, M., Sun, D., and Sun, S. (2012). Curcumin Protects against Sepsis-Induced Acute Lung Injury in Rats. *J. Surg. Res.* 176, e31–e39. doi:10.1016/j.jss.2011.11.1032

Xu, F., Lin, S.-h., Yang, Y.-z., Guo, R., Cao, J., and Liu, Q. (2013). The Effect of Curcumin on Sepsis-Induced Acute Lung Injury in a Rat Model through the Inhibition of the TGF-B1/smad3 Pathway. *Int. Immunopharmaco.* 16, 1–6. doi:10.1016/j.intimp.2013.03.014

Yadav, R., Jee, B., and Awasthi, S. K. (2015). Curcumin Suppresses the Production of Pro-inflammatory Cytokine Interleukin-18 in Lipopolysaccharide Stimulated Murine Macrophage-like Cells. *Ind. J. Clin. Biochem.* 30, 109–112. doi:10.1007/s12291-014-0452-2

Yang, C., Wu, K., Li, S.-H., and You, Q. (2013). Protective Effect of Curcumin against Cardiac Dysfunction in Sepsis Rats. *Pharm. Biol.* 51, 482–487. doi:10.3109/13880209.2012.742116

Yang, M., Lee, G., Si, J., Lee, S.-J., You, H., and Ko, G. (2016). Curcumin Shows Antiviral Properties against Norovirus. *Molecules* 21, 1401. doi:10.3390/molecules21101401

Yang, X. X., Li, C. M., and Huang, C. Z. (2016). Curcumin Modified Silver Nanoparticles for Highly Efficient Inhibition of Respiratory Syncytial Virus Infection. *Nanoscale* 8, 3040–3048. doi:10.1039/c5nr07918g

Huang, Y., Yang, C., Xu, X.-F., Xu, W., and Liu, S.-W. (2020). Structural and Functional Properties of SARS-CoV-2 Spike Protein: Potential Antivirus Drug Development for COVID-19, *Acta Pharmacol. Sin.* 41, 1–9doi:10.1038/s41401-020-0485-4

Yin, H., Guo, Q., Li, X., Tang, T., Li, C., Wang, H., et al. (2018). Curcumin Suppresses IL-1β Secretion and Prevents Inflammation through Inhibition of the NLRP3 Inflammasome. *J.Immunol.* 200, 2835–2846. doi:10.4049/jimmunol.1701495

Lv, Y., An, Z., Chen, H., Wang, Z., and Liu, L. (2014a), Mechanism of Curcumin Resistance to Human Cytomegalovirus in HELF Cells, *BMC Complement. Altern. Med.* 14, 1–7. doi:10.1186/1472-6882-14-284

Yu-Wung Yeh, D., and Wang, J.-J. (2020). Curcumin Attenuates Hemorrhagic Shock and Blood Replenish Resuscitation-Induced Impairment of Pulmonary Barrier Function by Increasing SIRT1 and Reducing Malondialdehyde and TNF-α Contents and Neutrophil Infiltration in Lung in a Dose-dependent Fashion. *Transplant. Proc.* 52, 1875–1879. doi:10.1016/j.transproceed.2020.01.133

Zahedipour, F., Hosseini, S. A., Sathyapalan, T., Majeed, M., Jamialahmadi, T., Al-Rasadi, K., et al. (2020). Potential Effects of Curcumin in the Treatment of COVID -19 Infection. *Phytotherapy Res.* 34, 2911–2920. doi:10.1002/ptr.6738

Zhang, H.-n., Yu, C.-x., Zhang, P.-j., Chen, W.-w., Jiang, A.-l., Kong, F., et al. (2007). Curcumin Down Regulates Homeobox Gene NKX3.1 in Prostate Cancer Cell LNCaP. *Acta Pharmacologica Sinica* 28, 423–430. doi:10.1111/j.1745-7254.2007.00501.x

Zhang, L., Gu, Z.-l., Qin, Z.-h., and Liang, Z.-q. (2008). Effect of Curcumin on the Adhesion of Platelets to Brain Microvascular Endothelial Cellsin Vitro1. *Acta Pharmacol. Sin.* 29, 800–807. doi:10.1111/j.1745-7254.2008.00813.x

Zhang, L., Lin, D., Sun, X., Curth, U., Drosten, C., Sauerhering, L., et al. (2020). Crystal Structure of SARS-CoV-2 Main Protease Provides a Basis for Design of Improved α-ketoamide Inhibitors. *Science* 368, 409–412. doi:10.1126/science.abb3405

Zhang, S., Liu, Y., Wang, X., Yang, L., Li, H., Wang, Y., et al. (2020). SARS-CoV-2 Binds Platelet ACE2 to Enhance Thrombosis in COVID-19. *J. Hematol. Oncol.* 13, 120. doi:10.1186/s13045-020-00954-7

Zhou, F., Yu, T., Du, R., Fan, G., Liu, Y., Liu, Z., et al. (2020). Clinical Course and Risk Factors for Mortality of Adult Inpatients with COVID-19 in Wuhan, China: a Retrospective Cohort Study. *The Lancet* 395, 1054–1062. doi:10.1016/S0140-6736(20)30566-3

Zhu, L., Ding, X., Zhang, D., Yuan, C., Wang, J., Ndegwa, E., et al. (2015). Curcumin Inhibits Bovine Herpesvirus Type 1 Entry into MDBK Cells. *Acta Virol.* 59, 221–227. doi:10.4149/av_2015_03_221

Conflict of Interest: The authors declare that the research was conducted in the absence of any commercial or financial relationships that could be construed as a potential conflict of interest.

frontiers in Pharmacology

ORIGINAL RESEARCH
published: 17 June 2021
doi: 10.3389/fphar.2021.669642

Myricetin Inhibits SARS-CoV-2 Viral Replication by Targeting M^{pro} and Ameliorates Pulmonary Inflammation

Ting Xiao[1,2†], Mengqi Cui[1,2†], Caijuan Zheng[1†], Ming Wang[1†], Ronghao Sun[1†], Dandi Gao[1,2], Jiali Bao[1,2], Shanfa Ren[1,2], Bo Yang[3], Jianping Lin[1], Xiaoping Li[3], Dongmei Li[1], Cheng Yang[1,2]* and Honggang Zhou[1,2]**

[1]State Key Laboratory of Medicinal Chemical Biology, College of Pharmacy and Tianjin Key Laboratory of Molecular Drug Research, Nankai University, Haihe Education Park, Tianjin, China, [2]Tianjin Key Laboratory of Molecular Drug Research, Tianjin International Joint Academy of Biomedicine, Tianjin, China, [3]Department of Thoracic Surgery, Tianjin First Central Hospital, Nankai University, Tianjin, China

OPEN ACCESS

Edited by:
Sugunadevi Sakkiah,
National Center for Toxicological Research (FDA), United States

Reviewed by:
Vinicius Cardoso Soares,
Federal University of Rio de Janeiro, Brazil
Li Xiao Feng,
Peking University Shenzhen Hospital, China
Mahmoud A. A. Ibrahim,
Minia University, Egypt

***Correspondence:**
Dongmei Li
dongmeili@nankai.edu.cn
Cheng Yang
cheng.yang@nankai.edu.cn
Honggang Zhou
honggang.zhou@nankai.edu.cn

†These authors have contributed equally to this work

Specialty section:
This article was submitted to Respiratory Pharmacology, a section of the journal Frontiers in Pharmacology

Received: 19 February 2021
Accepted: 16 April 2021
Published: 17 June 2021

Citation:
Xiao T, Cui M, Zheng C, Wang M, Sun R, Gao D, Bao J, Ren S, Yang B, Lin J, Li X, Li D, Yang C and Zhou H (2021) Myricetin Inhibits SARS-CoV-2 Viral Replication by Targeting M^{pro} and Ameliorates Pulmonary Inflammation. Front. Pharmacol. 12:669642. doi: 10.3389/fphar.2021.669642

The coronavirus disease 2019 (COVID-19) has spread widely around the world and has seriously affected the human health of tens of millions of people. In view of lacking anti-virus drugs target to SARS-CoV-2, there is an urgent need to develop effective new drugs. In this study, we reported our discovery of SARS-CoV-2 M^{pro} inhibitors. We selected 15 natural compounds, including 7 flavonoids, 3 coumarins, 2 terpenoids, one henolic, one aldehyde and one steroid compound for molecular docking and enzymatic screening. Myricetin were identified to have potent inhibit activity with IC_{50} 3.684 ± 0.076 μM in the enzyme assay. The binding pose of Myricetin with SARS-CoV-2 M^{pro} was identified using molecular docking method. In the binding pocket of SARS-CoV-2 M^{pro}, the chromone ring of Myricetin interacts with His41 through π-π stacking, and the 3'-, 4'- and 7-hydroxyl of Myricetin interact with Phe140, Glu166and Asp187 through hydrogen bonds. Significantly, our results showed that Myricetin has potent effect on bleomycin-induced pulmonary inflammation by inhibiting the infiltration of inflammatory cells and the secretion of inflammatory cytokines IL-6, IL-1α, TNF-α and IFN-γ. Overall, Myricetin may be a potential drug for anti-virus and symptomatic treatment of COVID-19.

Keywords: COVID-19, SARS-CoV-2, 3CLpro (Mpro), myricetin, pulmonary inflammation

INTRODUCTION

The new type of coronavirus pneumonia is called COVID-19, which is a viral respiratory disease caused by the SARS-CoV-2 infection (Mittal et al., 2020; Wang et al., 2020). COVID-19 caused a global health emergency and was declared a pandemic by the World Health Organization (Ciotti et al., 2019; Kumar et al., 2020). The spread of COVID-19 brought great harm and social impact (Tandon, 2020). As of December 1, 2020, the cumulative number of confirmed cases has near to 70 millions all over the world. The overall mortality reaches about 2.19% (Cucinotta and Vanelli, 2020). Based on the data from the Chinese National Reporting System, as of February 20, 2020, 80% of the reported confirmed cases were without pneumonie, or had mild to mode rate pneumonia; about 15% had severe pneumonia (Park, 2020). Although some mild patients can heal on their own, there are still many patients who progress rapidly in the later stages, and develop into acute respiratory distress syndrome and fibrosis (Ozma et al., 2020). And now, there are still no specific

medicines and effective therapeutic methods. Therefore, there is an urgent need to developing specific drugs for COVID-19.

SARS-CoV-2 is a single positive-stranded RNA virus, it contains about 30,000 basic group and 14 open reading frames (ORFs), which can coding replicases, four structural proteins (Spike, Envelope, Membrane and Nucleocapsid protein), 16 non-structural proteins (NSPs) and nine accessory proteins (Boopathi et al., 2020; Mittal et al., 2020; Sarma et al., 2020). NSPs play an important role in the replication and transcription cycle of the virus. NSP5 is the main protease of SARS-CoV-2, also called 3CLpro, it is essential for viral polyproteins processing and maturation (Anand et al., 2003; Jin et al., 2020; Liu et al., 2020; Zhang et al., 2020), therefore, it is recognized as an important potential drug target (De Clercq and Li, 2016).

Natural products (NPs) received great attention by scientific to discover potential drugs for the treatment of various diseases, such as cancer (Cragg et al., 1997), HIV (Kurapati et al., 2015), malaria (Clark, 1996) and cardiovascular disease (Mashour et al., 1998). And recently, a large of studies reported the screening result of NPs as anti-SARS-CoV-2 inhibitors based on *in-silico* drug discovery approaches (Ibrahim et al., 2020; Joshi et al., 2020; Li et al., 2020), but there are few reports on the directly inhibition of enzyme activity. We identified Myricetin as a potent inhibitor of SARS-CoV-2 M^{pro} from 15 NPs by molecular docking and enzymatic assay in this study. Myricetin also exhibit potent anti-inflammation effect on bleomycin-treated mice. It suggests that Myricetin might be a promising candidate for COVID-19 therapy.

METHOD

Drugs and Reagents

The 15 test compounds were mainly obtained from Pusi Biotechnology Co. Ltd. (Chengdu, China). The enzyme activity inhibitor screening kit was purchased from Beyotime Biotechnology (Shanghai, China).

Molecular Docking

The crystal structure (PDB ID: 6LZE) of SARS-CoV-2 M^{pro}, which was resolved by Dai et al. (Dai et al., 2020), was extracted from the RCSB Protein Data Bank (PDB). Then, the protein structure was prepared using the Protein Preparation Wizard module in Schrodinger 2017 (Bhachoo and Beuming, 2017) to remove all crystallographic water molecules, correct side chains with missing atoms, add hydrogen atoms and assign protonation states and partial charges with the OPLS_2005 force field. The Protein Preparation Wizard module of Schrödinger was applied to add hydrogen. The protonation states for the hydroxyl, Asn, Gln, and His were optimized using the ProtAssign module of Schrödinger. After that, the protein structure was minimized until the root-mean-square deviation (RMSD) of the nonhydrogen atoms reached less than 0.3 Å. The structures of the 15 natural compounds and 17 chemical compounds were prepared using the LigPrep module of the Schrodinger 2017 molecular modeling package to add hydrogen atoms, convert 2D structures to 3D, generate stereoisomers and determine the ionization state at pH 7.0 ± 2.0 with Epik. Using the prepared receptor structure, a receptor grid was generated around the original ligand site of the crystal structure. Then, the 15 natural compounds and 17 chemical compounds were docked to the receptor using the Glide XP protocol.

Protease Activity Assay

Enzyme activity inhibitor screening adopts fluorescence resonance energy transfer method. The protease assays were performed in 96-well black flat-bottomed plates with a final volume of 100 µl. The SARS-CoV-2 M^{pro}, at a final concentration of 0.3 µM was pre-incubated for 5 min at 37°C with different compounds, at a final concentration of 50 µM in the assay buffer (50 mM Tris, 150 mM NaCl, 1 mM EDTA, 1% glycerol, PH7.3). The FRET substrate, Dabcyl-KTSAVLQSGFRKME-Edans (Jin et al., 2020), is added at a final concentration of 20 µM to the enzymatic reaction mixture for 10 min at 37°C. The blank control well consists of 93 µl assay buffer, 5 µl DMSO and 2 µl Substrate. Enzyme activity control well contains of 92 µl assay buffer, 1 µl M^{pro}, 5 µl DMSO and 2 µl Substrate, sample wells are 92 µl assay buffer, 1 µl M^{pro}, 5 µl compound and 2 µl Substrate. After incubating at 37°C for 5 min in the dark, the fluorescence signals (excitation/emission, 340 nm/490 nm) of released EDANS were measured using a multiscan spectrum (Thermo, United States). The results were plotted as dose inhibition curves using nonlinear regression with a variable slope to determine the IC_{50} values by GraghPad Prism 7.0.

Molecular Dynamics Simulation

To investigate the stability of Myricetin inside the active site of SARS-CoV-2 M^{pro}, molecular dynamics (MD) simulation was performed on the binding complex of SARS-CoV-2 M^{pro} with Myricetin obtained from the molecular docking. The MD simulation was carried out using the PMEMD module of AMBER18. The AMBER FF14SB force field (Maier et al., 2015) was used for SARS-CoV-2 M^{pro} and the GAFF force field (Wang et al., 2004) was used for Myricetin. The binding complex was neutralized by adding sodium counterions and was solvated in a rectangular box of TIP3P water molecules, with a minimal distance of 12 Å from the protein to the box boundary. The system was subject to energy minimization for 10,000 steps. Next, the complex was gradually heated from 0 to 310 K, followed by equilibration for 5 ns using NVT ensemble, and the protein and ligand were constrained with a force constraint of 50 kcal mol^{-1}·$Å^{-2}$. Then, the system was equilibrated for 30 ns using the NPT ensemble with constraint force constant gradually decreased and finally removed for the production MD simulation. The production MD at 310 K was kept running 100 ns to obtain a stable MD trajectory. During the MD simulation, a 12 Å nonbonded interaction cutoff was used, the SHAKE algorithm integration was used to constrain covalent bonds that involved hydrogen atoms and the particle mesh Ewald (PME) method was applied to treat long-range electrostatic interactions. The frames were saved every 5000 steps for analysis. Binding free energy between the SARS-CoV-2 M^{pro} and Myricetin was calculated with the MM-GBSA method.

TABLE 1 | List of drug molecular docking and primary FRET assay against SARS-CoV-2 M^{pro}.

Flavonoids compounds

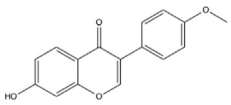

Formononetin(1)
docking score (−5.988)

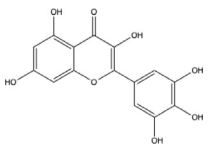

Myricetin(2)
docking score (−8.473)

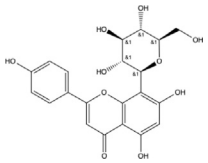

Vitexin(3)
docking score (−8.359)

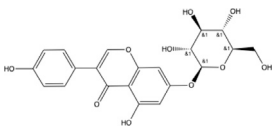

Genistin(4)
docking score (−7.934)

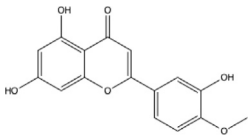

Diosmetin(5)
docking score (−7.761)

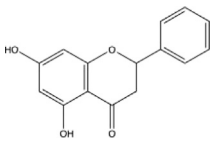

Pinocembrin(6)
docking score (−6.748)

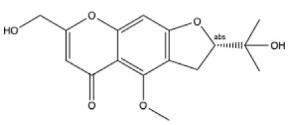

Cimifugin(7)
docking score (−6.578)

Coumarins compounds

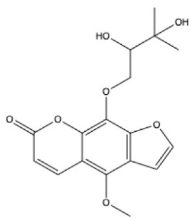

Byakangelicin(8)
docking score (−7.177)

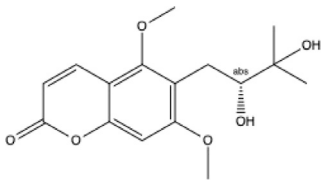

Toddalolactone(9)
docking score (−6.527)

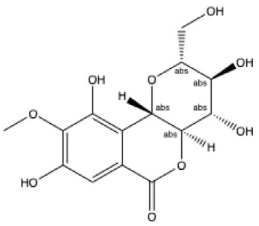

Bengenin(10)
docking score (−6.143)

Terpenoid

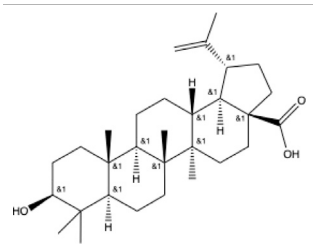

Betulinic acid(11)
docking score (−3.623)

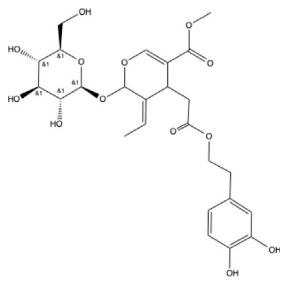

Oleuropein(12)
docking score (−10.33)

Henolic compound

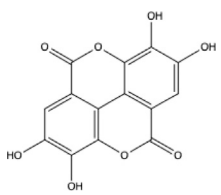

Ellagic acid(13) docking score (−7.222)

Aldehyde compound

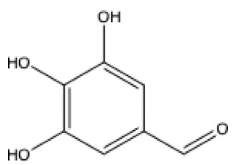

3,4,5-Trihydroxybenzaldehyde(14)
docking score (−3.828)

Steroid

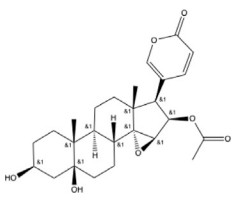

Cinobufotalin(15) docking score (−4.24)

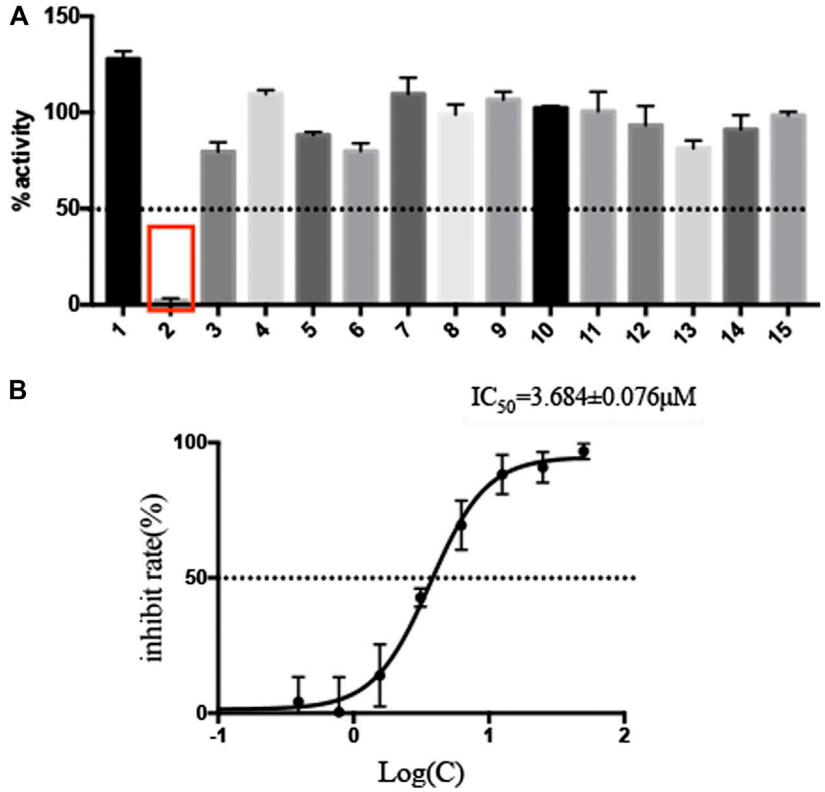

FIGURE 1 | Screening of natural compounds against SARS-CoV-2 M^{pro} and the inhibitory activity of Myricetin *in vitro*. **(A)**. 50 μM compound was pre-incubated with 0.3 μM SARS-CoV-2 M^{pro} at 37°C for 10 min, and then 20 μM FRET substrate was added to the reaction mixture to initiate the reaction. The excitation wavelength is 340 nm and the emission wavelength is 490 nm for fluorescence measurement. Results Inhibition rate (%) = (RFU100% enzyme activity control-RFU sample)/(RFU100% enzyme activity control-RFU blank control) × 100%. The results are average ± standard deviation of three repeats. **(B)** The inhibitory assay of Myricetin show efficient inhibition for M^{pro}. Error bars: mean ± S.D. of three independent replicates.

Cytotoxicity Assay

BEAS-2B cells were cultured at 37°C with 5% CO2 in a humid atmosphere. BEAS-2B cells were maintained in 96-well plates at 5×10^4 cells/ml, and were cultured with serially twice diluted Myricetin for 48 h. 15 μl MTT reagent was added in each well of 96-well plate, Cell viability was measured after 4 h of culture at 37°C. The resulting formazan crystals were dissolved with 120 μl of DMSO solution. The value of OD was measured at a wavelength of 570 nm by using Thermo Scientific™ Multiskan™ FC (New York, NY, United States). These experimental results were repeated at least three times.

Animals and Bleomycin Administration

Male C57BL/six mice (6–8 weeks, 20–25 g) were purchased from Charles River Laboratory (Beijing, China). All animal feeding and testing procedures comply with the criteria approved by the Institutional Animal Care and Use Committee (IACUC) of Nankai University (Permit No. SYXK 2014-0003). Mice were exposed to a controlled temperature (22–26°C), humidity (60 ± 2%)and a 12 h cycle of light and dark, giving them free access to food and water.

Mice were intratracheal injected with bleomycin (BLM). In short, mice were anesthetized by intraperitoneal injection of 1% pentobarbital sodium, followed by intratracheal injection of 2.5 U/kg bleomycin (BLM, China Hanfai Manufacturing Co., LTD.) with sterile insulin syringe. After injection, the mice were immediately raised and gently flapped to evenly distribute the liquid in the lungs. In the control group, the same method was used to inject the same amount of normal saline (0.9% NaCl), the 30 mice were randomly divided into six groups, with five mice in each group: control group, BLM model group, BLM + pirfenidone (PFD) group (200 mg/kg), BLM + Myricetin group (25 mg/kg), BLM + Myricetin group (50 mg/kg), BLM + Myricetin group (100 mg/kg). Pirfenidone was used as positive control. The drug Pirfenidone or Myricetin was given daily intragastric administration 1–7 days after BLM injury, the control group and BLM model group were given the same amount of normal saline. Mice were euthanized on the eighth day after administration to assess pulmonary inflammation.

Bronchoalveolar Lavage Fluid

The lungs were laved with PBS to collect bronchoalveolar lavage fluid (BALF), underwent lavage through a blunt needle attached to a syringe, which worked as a trachea cannula in the airway. Bronchoalveolar lavage fluid (BALF) was collected by washing the

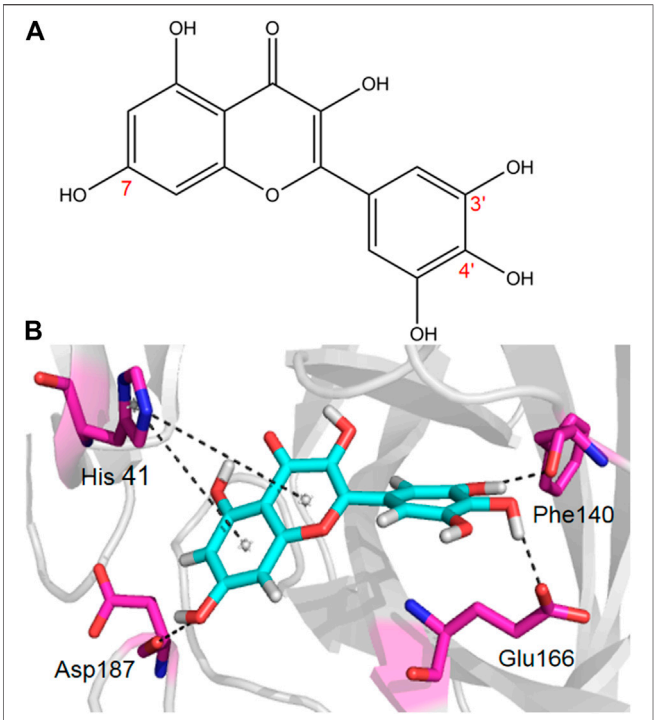

FIGURE 2 | The binding mode of Myricetin in SARS-CoV-2 Mpro. Hydrogen bonds and π-π interactions between Myricetin and SARS-CoV-2 M^{pro} are represented by dashed lines.

lung through a tracheal intubation. The lungs were washed twice times, and each time 1 ml PBS was used,rinse once and twice for the second time. The BALF was centrifuged at 3,000 rpm for 10 min and collected the supernatant and stored at −80°C. The supernatant was used for inflammatory factor analysis. The precipitated cells were resuspended with 1 ml red blood cell lysis buffer. H&E staining was performed on each suspension smear, and cell classification and count were performed. Neutrophils, macrophages and lymphocytes were counted under an optical microscope using standard morphological standards.

Histological Examination

The left lung was fixed with 10% paraformaldehyde for 24 h, the excess tissues were removed and embedded in paraffin. Lung sections were prepared (4 μm), hematoxylin -eosin (H&E) staining (Zsbio, China) for histological examination.

ELISA Detection

The supernatant of BALF was used to detect the concentration of inflammatory factors including IL-1α, IFN-γ, IL-6, TNF-α and IL-4 using enzyme-linked immunosorbent assay (ELISA) kits (Jianglai biotech, shanghai, China) in accordance with the manufacturer's protocol.

Statistical Analysis

Statistical analysis was performed using GraphPad Prism 7.0 software. Differences between experimental and control group were assessed by Student's *t* test. Significant differences among multiple groups were detected by one-way ANOVA. P <0.05 was considered as statistically significance, $^{*}P$ <0.05, $^{**}P$ <0.01, $^{***}P$ <0.001, NS: nonsignificant.

RESULTS

Molecular Docking

We docked the 15 natural compounds and 17 chemical compounds to the crystal structure of SARS-CoV-2 M^{pro}. The 2D structures of the 15 natural compounds and the corresponding Glide XP docking scores are listed in **Table 1** and the 2D structures of the 17 chemical compounds and the corresponding Glide XP docking scores are listed in **Supplementary Table S1**. Among them, four compounds (i.e. Myricetin, Vitexin, Genistin and Oleuropein) show docking scores lower than −8.0, which indicates that these compounds might have effective inhibition on SARS-CoV-2 M^{pro} activity.

Fluorescence Resonance Energy Transfer (FRET)-Based Screening Assay

The selected 15 natural compounds belong to 6 different categories, 7 compounds are flavonoids, 3 compounds are coumarins. 2 compounds is terpenoid, one is henolic, one is aldehyde and one is steroid. We screened these 15 natural compounds and 17 chemical compounds by fluorescence resonance energy transfer enzymatic assay at a final concentration of 50 μM (**Figure 1A** and **Supplementary Figure S3**). We identified that Myricetin has effective inhibition on enzymatic activity, the inhibition rate reached 97.79%, but, other compounds did not show obvious inhibitory activity, including Oleuropein, Vitexin and Genistin with low molecular docking scores.

Myricetin Inhibit the SARS-CoV-2 M^{pro} Activity and Its Structural Basis

Given the encouraging results from the primary screening, we then further characterized the inhibitory activity of Myricetin in a dose gradient and the Myricetin inhibited SARS-CoV-2 M^{pro} with 50% inhibitory concentration values (IC_{50}) of 3.684 ± 0.076 μM (**Figure 1B**). As the positive control, Ebselen inhibited M^{pro} with IC_{50} of 0.5417 ± 0.0306 μM (**Supplementary Figure S4**). We measured the cell toxicity of Myricetin to BEAS-2B cell, after treated with Myricetin for 48 h, Myricetin had no cytotoxicity within 50 μM (**Supplementary Figure S2**). We also identified the structural basis of Myricetin and M^{pro}. To investigate the stability of Myricetin inside the active site of SARS-CoV-2 M^{pro}, we performed 100 ns MD simulation on the binding complex of SARS-CoV-2 M^{pro} with Myricetin. The revealed binding mode of Myricetin with SARS-CoV-2 M^{pro} is depicted in **Figure 2**, and the interaction details between Myricetin and SARS-CoV-2 M^{pro} over time are shown in **Supplementary Figure S5**. The calculated RMSD shows the stability of the system (**Supplementary Figure S5A**). RMSF

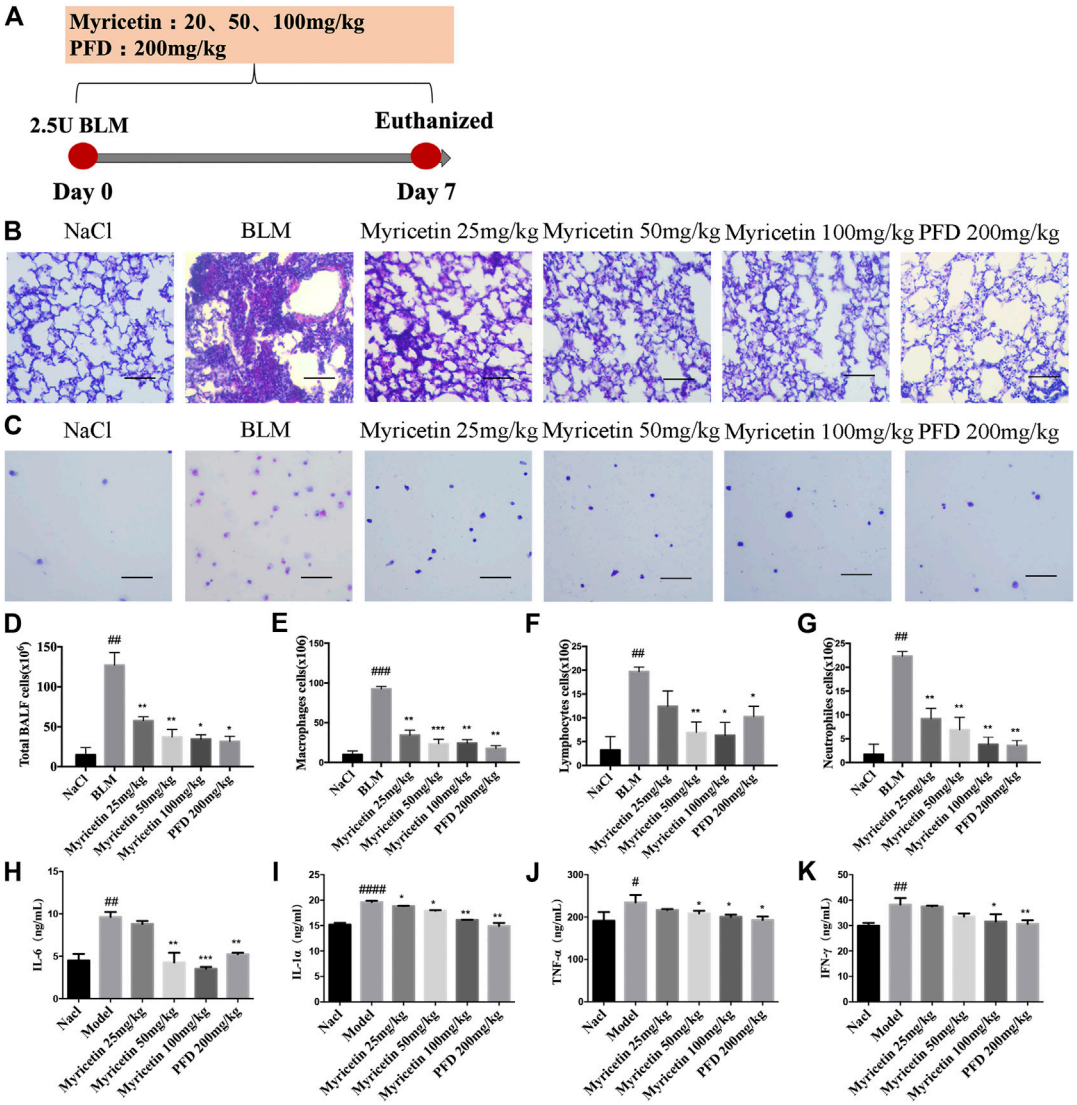

FIGURE 3 | Myricetin reduces the inflammatory response in BLM-treated mice. **(A)** Dosing regimen in BLM-induced inflammatory model. **(B–C)** H&E staining of left lung tissues (B, Scale: 50 μm) and inflammatory cells in BALF (C, Scale: 20 μm) of each group. **(D)** Total number of cells from BALF in each group. **(E)** Counts of macrophages in BALF. **(F)** Counts of lymphocytes in BALF. **(G)** Counts of Neutrophiles in BALF. **(H–K)** The expression of inflammatory factors including IL-6, IL-1α, TNF-α and IFN-γ in BALF were detected by ELISA. Data are shown as mean ± SD. # represent the difference between NaCl and BLM-treated group, ##$P < 0.01$, ###$P < 0.001$, ####$P < 0.0001$. * represent the difference between BLM-treated and treatment group, *$P < 0.05$, **$P < 0.01$, ***$P < 0.001$, ****$P < 0.0001$.

shows fluctuations are at the N-terminal and C-terminal ends of the protein (**Supplementary Figure S5B**). The chromone ring of Myricetin interacts with the imidazole side chain of His41 through π-π stacking (with the centroids distance of ~6.1 Å, **Supplementary Figure S5C**). The 3'– and 4'–hydroxyl of Myricetin form hydrogen bonds with the backbone oxygen of Phe140 and the side chain carboxyl oxygen of Glu166 (with the hydrogen bond lengths of ~2.3 Å and ~2.0 Å, **Supplementary Figures S5D,E**). The 7-hydroxyl of Myricetin forms a hydrogen bond with the backbone oxygen of Asp187 (with the hydrogen bond length of ~2.4 Å, **Supplementary Figure S5F**). These values indicate that Myricetin maintains its position in the binding pocket of SARS-CoV-2 M^{pro}. The binding free energy of Myricetin with SARS-CoV-2 Mpro is −32.98 kcal/mol calculated using the MMGBSA method. We also performed docking and MD simulation for the control drug Ebselen in the same binding pocket of Myricetin (i.e. the Cys145 site). The binding pose of Ebselen in the Cys145 pocket is shown in **Supplementary Figure S6A**. The benzisoselenazolone ring and the benzene ring of Ebselen interact with the imidazole side chain of His41 through π-π stacking (with the centroids distance of ~4.8 and ~5.4 Å, **Supplementary Figures S6B,C**) in this pocket, and the binding free energy is only −17.68 kcal/mol. Fortunately, we found that the crystal structure of Ebselen bound to SARS-CoV-2 M^{pro} was just deposited in the protein data bank quite recently (PDBID: 7BFB). In this structure, Ebselens covalently bind to SARS-CoV-2 M^{pro}

through four binding sites, e.g. the Cys44 site, the Cys145 site, the Cys156 site and the Cys300 site. The aforementioned binding mode (in **Supplementary Figure S6A**) only reflects the binding of Ebselen in the Cys145 site. The molecular size of Ebselen is small, it can easily reach these four Cys sites in SARS-CoV-2 M^{pro}. Moreover, the sulfydryl group of Cys is quite active, when Ebselen enters the active site, they will react quickly and form the covalent complex. These provide the structural basis for Ebselen having lower IC_{50} than other ligands.

Myricetin Reduced the Inflammatory Response in Bleomycin-Treated Mice and Macrophage

To study the anti-inflammatory effect of Myricetin on lung injury, a BLM-induced lung injury model was established. The drug was administered continuously for 7 days, and pirfenidone was used as a positive control (**Figure 3A**). The results of H&E staining in lung biopsy showed that Myricetin significantly improved the infiltration of inflammatory cells in BLM damaged lung tissue (**Figure 3B**). In the BALF of BLM-treated mice, the total number of inflammatory cells and the number of different inflammatory cells were significantly up-regulated, while the number of inflammatory cells in Myricetin-treated mice was significantly down-regulated in a dose dependent manner. The effect of high dose Myricetin (100 mg/kg) is similar to that of the positive drug pirfenidone (**Figures 3C–G**). In addition, the expression levels of inflammatory factors such as IL-6, TNF-α,IFN-γ and IL-1α in BALF were measured, and the results showed that Myricetin significantly inhibited the expression levels of inflammatory factors (**Figures 3H–K**). These data showed that Myricetin reduced lung inflammation in BLM-induced mice.

DISCUSSION

The popularity of coronavirus disease 2019 (COVID-19) has given rise to an urgent need for new therapy strategies (Wu et al., 2020). At present, there is no available specific drugs targeting SARS-CoV-2 (Luo et al., 2020), but new drug candidates targeting the SARS-CoV-2 M^{pro} to inhibit the viral replication are being explored with the X-ray crystal structure was reported (Garg and Roy, 2020; Jin et al., 2020; Ma et al., 2020; Zhang et al., 2020). Now, a large number of compounds have been screened by structure-based virtual screening, including FDA approved drug libraries (Kandeel and Al-Nazawi, 2020), drug candidates in clinical trials (Mahanta et al., 2020) and other pharmacologically active compounds (Vijayakumar et al., 2020). Lopinavir and nelfinavir (Costanzo et al., 2020; Reiner et al., 2020), the FDA approved antiretroviral drug used against HIV, showed excellent binding affinity with the M^{pro} through virtual screening and *in silico* studies. However, it were proved that they have no inhibitory activity at 20 μM by FRET-based assay (Hung et al., 2020), which reflecting the fact that no benefit was observed in patients with severe COVID-19. Tens of thousands of phytochemicals and Chinese medicinal agents, such as flavonoids, garlic, naturally occurring coumarin derivatives and green tea polyphenols, have been determined to have higher affinity than some marketed drugs and may be promising candidates, but their usefulness for targeting M^{pro} needs experimental validation and clinical manifestation (Ghosh et al., 2020; Joshi et al., 2020; Li et al., 2020).

We compared the binding affinity of 15 natural compounds, contain of flavonoids, coumarins, terpenoids, henolic, aldehyde and steriod compounds, with SARS-CoV-2 M^{pro} through virtual analysis. Oleuropein, Myricetin and vitexin have high affinity with M^{pro}, however, only Myricetin exhibit significant inhibition with IC_{50} 3.684 ± 0.076 μM by FRET-based assay. Structurally, Myricetin can interact with His41 through π-π stacking and form hydrogen bonds with Phe140, Glu166 and Asp187 in the catalytic center of SARS-CoV-2 M^{pro}. This result indicates that the anti-viral activity test based on experiments are necessary for developing more effective and reliable anti-SARS-CoV-2 drugs.

COVID-19 is an inflammatory disease caused by SARS-CoV-2 (Zhu et al., 2020). Excessive inflammation is central to a poor prognosis, and associated with inflammatory mediators such as IL-6 and lactate dehydrogenase (LDH) (Conti et al., 2020; Rodrigues et al., 2021). Here, we further evaluated the effect of Myricetin on pulmonary inflammation with bleomycin treated mice. The results showed that Myricetin can effective inhibit the infiltration of inflammatory cells and the secretion of inflammatory factors in the lung, especially lymphocytes and IL-6.

CONCLUSION

In a word, Myricetin may be an potential candidate drug for COVID-19 therapy by both anti-SARS-CoV-2 and anti-inflammation. Small-molecule bioactive natural products could be a useful source of SARS-CoV-2 M^{pro} inhibitors and an effective first line of defense against COVID-19.

DATA AVAILABILITY STATEMENT

The datasets presented in this study can be found in online repositories. The names of the repository/repositories and accession numbers can be found in the article/**Supplementary Material**.

ETHICS STATEMENT

The animal study was reviewed and approved by the Institutional Animal Care and Use Committee (IACUC) of Nankai University (Permit No. SYXK 2014-0003).

AUTHOR CONTRIBUTIONS

HZ, CY, and DL contributed to the conception and design. TX, MC, CZ, MW, and RS contributed to the collection and assembly of data. DG, JB, SR, and JL contributed to the data analysis and

interpretation. BY and XL contributed to the data revision. TX and MC contributed to the manuscript writing. All author read and approved the final manuscript.

FUNDING

This study was supported by The National Natural Science Foundation of China (Grant 82070060), The Fundamental Research Funds for the Central University (Grant 735-63201241) and (Grant 735-63201239).

SUPPLEMENTARY MATERIAL

The Supplementary Material for this article can be found online at: https://www.frontiersin.org/articles/10.3389/fphar.2021.669642/full#supplementary-material

REFERENCES

Anand, K., Ziebuhr, J., Wadhwani, P., Mesters, J. R., and Hilgenfeld, R. (2003). Coronavirus Main Proteinase (3CLpro) Structure: Basis for Design of Anti-SARS Drugs. *Science* 300, 1763–1767. doi:10.1126/science.1085658

Bhachoo, J., and Beuming, T. (2017). Investigating Protein-Peptide Interactions Using the Schrödinger Computational Suite. *Methods Mol. Biol.* 1561, 235–254. doi:10.1007/978-1-4939-6798-8_14

Boopathi, S., Poma, A. B., and Kolandaivel, P. (2020). Novel 2019 Coronavirus Structure, Mechanism of Action, Antiviral Drug Promises and Rule Out against its Treatment. *J. Biomol. Struct. Dyn.* 2020, 1–10. doi:10.1080/07391102.2020.1758788

Ciotti, M., Angeletti, S., Minieri, M., Giovannetti, M., Benvenuto, D., Pascarella, S., et al. (2019). COVID-19 Outbreak: An Overview. *Chemotherapy* 64, 215–223. doi:10.1159/000507423

Clark, A. M. (1996). Natural Products as a Resource for New Drugs. *Pharm. Res.* 13, 1133–1141. doi:10.1023/a:1016091631721

Conti, P., Ronconi, G., Caraffa, A., Gallenga, C. E., Ross, R., Frydas, I., et al. (2020). Induction of Pro-inflammatory Cytokines (IL-1 and IL-6) and Lung Inflammation by Coronavirus-19 (COVI-19 or SARS-CoV-2): Anti-inflammatory Strategies. *J. Biol. Regul. Homeost Agents* 34, 327–331. doi:10.23812/CONTI-E

Costanzo, M., De Giglio, M. A. R., and Roviello, G. N. (2020). SARS-CoV-2: Recent Reports on Antiviral Therapies Based on Lopinavir/Ritonavir, Darunavir/Umifenovir, Hydroxychloroquine, Remdesivir, Favipiravir and Other Drugs for the Treatment of the New Coronavirus. *Curr. Med. Chem.* 27, 4536–4541. doi:10.2174/0929867327666200416131117

Cragg, G. M., Newman, D. J., and Snader, K. M. (1997). Natural Products in Drug Discovery and Development. *J. Nat. Prod.* 60, 52–60. doi:10.1021/np9604893

Cucinotta, D., and Vanelli, M. (2020). WHO Declares COVID-19 a Pandemic. *Acta Biomed.* 91, 157–160. doi:10.23750/abm.v91i1.9397

Dai, W., Zhang, B., Jiang, X-M., Su, H., Li, J., Zhao, Y., et al. (2020). Structure-based Design of Antiviral Drug Candidates Targeting the SARS-CoV-2 Main Protease. *Science* 368, 1331–1335. doi:10.1126/science.abb4489

De Clercq, E., and Li, G. (2016). Approved Antiviral Drugs over the Past 50 Years. *Clin. Microbiol. Rev.* 29, 695–747. doi:10.1128/cmr.00102-15

Garg, S., and Roy, A. (2020). In Silico analysis of Selected Alkaloids against Main Protease (Mpro) of SARS-CoV-2. *Chem.-Biol. Interact.* 332, 109309. doi:10.1016/j.cbi.2020.109309

Ghosh, R., Chakraborty, A., Biswas, A., and Chowdhuri, S. (2020). Evaluation of Green Tea Polyphenols as Novel Corona Virus (SARS CoV-2) Main Protease (Mpro) Inhibitors–Anin Silicodocking and Molecular Dynamics Simulation Study. *J. Biomol. Struct. Dyn.*, 1–13. doi:10.1080/07391102.2020.1779818

Hung, H. C., Ke, Y. Y., Huang, S. Y., Huang, P. N., Kung, Y. A., Chang, T. Y., et al. (2020). Discovery of M Protease Inhibitors Encoded by SARS-CoV-2. *Antimicrob. Agents Chemother.* 64, e00872. doi:10.1128/aac.00872-20

Ibrahim, M. A. A., Abdeljawaad, K. A. A., Abdelrahman, A. H. M., and Hegazy, M-E. F. (2020). Natural-like Products as Potential SARS-CoV-2 Mpro Inhibitors: In-Silico Drug Discovery. *J. Biomol. Struct. Dyn.* 1–13. doi:10.1080/07391102.2020.1790037

Jin, Z., Du, X., Xu, Y., Deng, Y., Liu, M., Zhao, Y., et al. (2020). Structure of Mpro from SARS-CoV-2 and Discovery of its Inhibitors. *Nature* 582, 289–293. doi:10.1038/s41586-020-2223-y

Joshi, T., Joshi, T., Sharma, P., Mathpal, S., Pundir, H., Bhatt, V., et al. (2020). In Silico screening of Natural Compounds against COVID-19 by Targeting Mpro and ACE2 Using Molecular Docking. *Eur. Rev. Med. Pharmacol. Sci.* 24, 4529–4536. doi:10.26355/eurrev_202004_21036

Kandeel, M., and Al-Nazawi, M. (2020). Virtual Screening and Repurposing of FDA Approved Drugs against COVID-19 Main Protease. *Life Sci.* 251, 117627. doi:10.1016/j.lfs.2020.117627

Kumar, S., Poonam, and Rathi, B. (2020). Coronavirus Disease COVID-19: A New Threat to Public Health. *Curr. Top. Med. Chem.* 20, 599–600. doi:10.2174/1568026620999200305144319

Kurapati, K. R., Atluri, V. S., Samikkannu, T., Garcia, G., and Nair, M. P. (2015). Natural Products as Anti-HIV Agents and Role in HIV-Associated Neurocognitive Disorders (HAND): A Brief Overview. *Front. Microbiol.* 6, 1444. doi:10.3389/fmicb.2015.01444

Li, S., Liu, C., Guo, F., Taleb, S. J., Tong, M., and Shang, D. (2020). Traditional Chinese Medicine as Potential Therapy for COVID-19. *Am. J. Chin. Med.* 48, 1263–1277. doi:10.1142/s0192415x20500627

Liu, C., Zhou, Q., Li, Y., Garner, L. V., Watkins, S. P., Carter, L. J., et al. (2020). Research and Development on Therapeutic Agents and Vaccines for COVID-19 and Related Human Coronavirus Diseases. *ACS Cent. Sci.* 6, 315–331. doi:10.1021/acscentsci.0c00272

Luo, H., Tang, Q-L., Shang, Y-X., Liang, S-B., Yang, M., Robinson, N., et al. (2020). Can Chinese Medicine Be Used for Prevention of Corona Virus Disease 2019 (COVID-19)? A Review of Historical Classics, Research Evidence and Current Prevention Programs. *Chin. J. Integr. Med.* 26, 243–250. doi:10.1007/s11655-020-3192-6

Ma, C., Sacco, M. D., Hurst, B., Townsend, J. A., Hu, Y., Szeto, T., et al. (2020). Boceprevir, GC-376, and Calpain Inhibitors II, XII Inhibit SARS-CoV-2 Viral Replication by Targeting the Viral Main Protease. *Cell Res.* 30, 678–692. doi:10.1038/s41422-020-0356-z

Mahanta, S., Chowdhury, P., Gogoi, N., Goswami, N., Borah, D., Kumar, R., et al. (2020). Potential Anti-viral Activity of Approved Repurposed Drug against Main Protease of SARS-CoV-2: Anin Silicobased Approach. *J. Biomol. Struct. Dyn.* 1–10. doi:10.1080/07391102.2020.1768902

Maier, J. A., Martinez, C., Kasavajhala, K., Wickstrom, L., Hauser, K. E., and Simmerling, C. (2015). ff14SB: Improving the Accuracy of Protein Side Chain and Backbone Parameters from ff99SB. *J. Chem. Theor. Comput.* 11, 3696–3713. doi:10.1021/acs.jctc.5b00255

Mashour, N. H., Lin, G. I., and Frishman, W. H. (1998). Herbal Medicine for the Treatment of Cardiovascular Disease. *Arch. Intern. Med.* 158, 2225–2234. doi:10.1001/archinte.158.20.2225

Mittal, L., Kumari, A., Srivastava, M., Singh, M., and Asthana, S. (2020). Identification of Potential Molecules against COVID-19 Main Protease through Structure-Guided Virtual Screening Approach. *J. Biomol. Struct. Dyn.* 1–19. doi:10.1080/07391102.2020.1768151

Ozma, M. A., Maroufi, P., Khodadadi, E., Kose, S., Esposito, I., Ganbarov, K., et al. (2020). Clinical Manifestation, Diagnosis, Prevention and Control of SARS-CoV-2 (COVID-19) during the Outbreak Period. *Infez Med.* 28, 153–165.

Park, S. E. (2020). Epidemiology, Virology, and Clinical Features of Severe Acute Respiratory Syndrome -coronavirus-2 (SARS-CoV-2; Coronavirus Disease-19). *Clin. Exp. Pediatr.* 63, 119–124. doi:10.3345/cep.2020.00493

Reiner, Ž., Hatamipour, M., Banach, M., Pirro, M., Al-Rasadi, K., Jamialahmadi, T., et al. (2020). Statins and the COVID-19 Main Protease: In Silico Evidence on Direct Interaction. *Arch Med. Sci.* 16, 490–496. doi:10.5114/aoms.2020.94655

Rodrigues, T. S., de Sa, K. S. G., Ishimoto, A. Y., Becerra, A., Oliveira, S., Almeida, L., et al. (2021). Inflammasomes Are Activated in Response to SARS-CoV-2 Infection and Are Associated with COVID-19 Severity in Patients. *J. Exp. Med.* 218, e20201707. doi:10.1084/jem.20201707

Sarma, P., Shekhar, N., Prajapat, M., Avti, P., Kaur, H., Kumar, S., et al. (2020). In-silico Homology Assisted Identification of Inhibitor of RNA Binding against 2019-nCoV N-Protein (N Terminal Domain). *J. Biomol. Struct. Dyn.* 1–9. doi:10.1080/07391102.2020.1753580

Tandon, P. N. (2020). COVID-19: Impact on Health of People & Wealth of Nations. *Indian J. Med. Res.* 151, 121–123. doi:10.4103/ijmr.IJMR_664_20

Vijayakumar, B. G., Ramesh, D., Joji, A., Jayachandra Prakasan, J., and Kannan, T. (2020). In Silico pharmacokinetic and Molecular Docking Studies of Natural Flavonoids and Synthetic Indole Chalcones against Essential Proteins of SARS-CoV-2. *Eur. J. Pharmacol.* 886, 173448. doi:10.1016/j.ejphar.2020.173448

Wang, J., Wolf, R. M., Caldwell, J. W., Kollman, P. A., and Case, D. A. (2004). Development and Testing of a General Amber Force Field. *J. Comput. Chem.* 25, 1157–1174. doi:10.1002/jcc.20035

Wang, D., Hu, B., Hu, C., Zhu, F., Liu, X., Zhang, J., et al. (2020). Clinical Characteristics of 138 Hospitalized Patients with 2019 Novel Coronavirus-Infected Pneumonia in Wuhan, China. *JAMA* 323, 1061–1069. doi:10.1001/jama.2020.1585

Wu, F., Zhao, S., Yu, B., Chen, Y-M., Wang, W., Song, Z-G., et al. (2020). A New Coronavirus Associated with Human Respiratory Disease in China. *Nature* 579, 265–269. doi:10.1038/s41586-020-2008-3

Zhang, L., Lin, D., Sun, X., Curth, U., Drosten, C., Sauerhering, L., et al. (2020). Crystal Structure of SARS-CoV-2 Main Protease Provides a Basis for Design of Improved α-ketoamide Inhibitors. *Science* 368, 409–412. doi:10.1126/science.abb3405

Zhu, N., Zhang, D., Wang, W., Li, X., Yang, B., Song, J., et al. (2020). A Novel Coronavirus from Patients with Pneumonia in China, 2019. *N. Engl. J. Med.* 382, 727–733. doi:10.1056/nejmoa2001017

Conflict of Interest: The authors declare that the research was conducted in the absence of any commercial or financial relationships that could be construed as a potential conflict of interest.

frontiers in Pharmacology

REVIEW
published: 29 June 2021
doi: 10.3389/fphar.2021.698905

The Role of Pulmonary Surfactants in the Treatment of Acute Respiratory Distress Syndrome in COVID-19

Shengguang Wang[1†], *Zhen Li*[1†], *Xinyu Wang*[1], *Shiming Zhang*[1], *Peng Gao*[1*] *and Zuorong Shi*[2*]

[1]School of Pharmacy, Shandong University of Traditional Chinese Medicine, Jinan, China, [2]School of Chinese Medicine, Shandong University of Traditional Chinese Medicine, Jinan, China

OPEN ACCESS

Edited by:
Chandrabose Selvaraj, Alagappa University, India

Reviewed by:
Gopinath Krishnasamy, University of Turku, Finland
Bikash Kumar Paul, Mawlana Bhashani Science and Technology University, Bangladesh
Pradeep Kumar, University of the Witwatersrand, South Africa

***Correspondence:**
Peng Gao
48395504@qq.com
Zuorong Shi
zuorongsh@163.com

[†]These authors have contributed equally to this work and share first authorship

Specialty section:
This article was submitted to Respiratory Pharmacology, a section of the journal Frontiers in Pharmacology

Received: 22 April 2021
Accepted: 17 June 2021
Published: 29 June 2021

Citation:
Wang S, Li Z, Wang X, Zhang S, Gao P and Shi Z (2021) The Role of Pulmonary Surfactants in the Treatment of Acute Respiratory Distress Syndrome in COVID-19. Front. Pharmacol. 12:698905. doi: 10.3389/fphar.2021.698905

Lung alveolar type-II (AT-II) cells produce pulmonary surfactant (PS), consisting of proteins and lipids. The lipids in PS are primarily responsible for reducing the air-fluid surface tension inside the alveoli of the lungs and to prevent atelectasis. The proteins are of two types: hydrophilic and hydrophobic. Hydrophilic surfactants are primarily responsible for opsonisation, thereby protecting the lungs from microbial and environmental contaminants. Hydrophobic surfactants are primarily responsible for respiratory function. Severe acute respiratory syndrome coronavirus-2 (SARS-CoV-2) enters the lungs through ACE-2 receptors on lungs and replicates in AT-II cells leading to the etiology of Coronavirus disease – 2019 (COVID-19). The SARS-CoV-2 virus damages the AT-II cells and results in decreased production of PS. The clinical symptoms of acute respiratory distress syndrome (ARDS) in COVID-19 patients are like those of neonatal respiratory distress syndrome (NRDS). The PS treatment is first-line treatment option for NRDS and found to be well tolerated in ARDS patients with inconclusive efficacy. Over the past 70°years, a lot of research is underway to produce natural/synthetic PS and developing systems for delivering PS directly to the lungs, in addition to finding the association between PS levels and respiratory illnesses. In the present COVID-19 pandemic situation, the scientific community all over the world is searching for the effective therapeutic options to improve the clinical outcomes. With a strong scientific and evidence-based background on role of PS in lung homeostasis and infection, few clinical trials were initiated to evaluate the functions of PS in COVID-19. Here, we connect the data on PS with reference to pulmonary physiology and infection with its possible therapeutic benefit in COVID-19 patients.

Keywords: pulmonary surfactant, COVID-19, SARS-cov-2, ARDS, NRDS

Abbreviations: AA, amino acid; ACE-2, angiotensin converting enzyme 2; ARDS, acute respiratory distress syndrome; AT-II, alveolar type-II; COVID-19, Coronavirus disease 2019; CPAP, continuous positive airway pressure; DAD, diffuse alveolar disease; DPPC, dipalmitoyl phosphatidylcholine; HIV, human immunodeficiency virus; NCT, National Clinical Trials; NL, neutral lipid; NRDS, neonatal respiratory distress syndrome; PC, phosphatidylcholine; PE, phosphatidylethanolamine; PG, phosphatidylglycerol; PL, phospholipid; POPG, palmitoyloleoyl phosphatidylglycerol; PS, pulmonary surfactant; RDS, respiratory distress syndrome; RSV, respiratory syncytial virus; SARS-CoV-2, Severe acute respiratory syndrome coronavirus 2; SP, surfactant protein.

INTRODUCTION

Human pulmonary surfactant (PS) is an endogenous lipoprotein complex produced naturally in the lungs. PS forms a layer on the alveolar epithelium and is responsible in reducing surface tension at the air-fluid interface on the alveolar surface (Agassandian and Mallampalli, 2013). The reduced alveolar surface tension will allow the expansion of alveoli and allows gas exchange (Seadler et al., 2020). Human PS contains phospholipids, mainly dipalmitoylphosphatidylcholine (DPPC), and surfactant proteins-A, B, C, and D. The PS is present as a barrier when inhaled particle and noxious agents come in contact with it and enhances the clearance of particles. PS also participate in host defense against infections and inflammation. The loss or deficiency in endogenous surfactant is implicated with respiratory disorders (Wert et al., 2009). During the gestation period, the production of endogenous lung surfactant results in lowering alveolar surface tension and stabilizes the alveoli to prevent the lung from collapsing at resting transpulmonary pressures. Premature infants are highly likely to be PS deficient, which causes increased surface tension leading to lung collapse and results in neonatal respiratory distress syndrome (NRDS). NRDS is associated with fast breathing, increased heart rate and apoxia, which in certain cases may lead to death (Khawar and Marwaha, 2021). PS therapy is currently the first-line treatment for NRDS.

During the COVID-19 pandemic, patients admitted in intensive care units are mainly those with clinical symptoms of acute respiratory distress syndrome (ARDS). The severe acute respiratory syndrome coronavirus (SARS-CoV)-2-induced lung injury in COVID-19 patients may lead to respiratory failure. Emerging evidence on respiratory mechanisms suggests that clinical symptoms of ARDS in COVID-19 patients resemble to those of NRDS caused by surfactant deficiency.

In this review, we connect the current understanding of the pathophysiology of lungs in COVID-19 patients with the possible role of PS in circumventing ARDS symptoms in COVID-19 patients.

PULMONARY SURFACTANT IN LUNG HOMEOSTASIS

PS is an important biosurfactant in human. PS lines the alveoli and terminal bronchioles, thereby protecting the lungs from

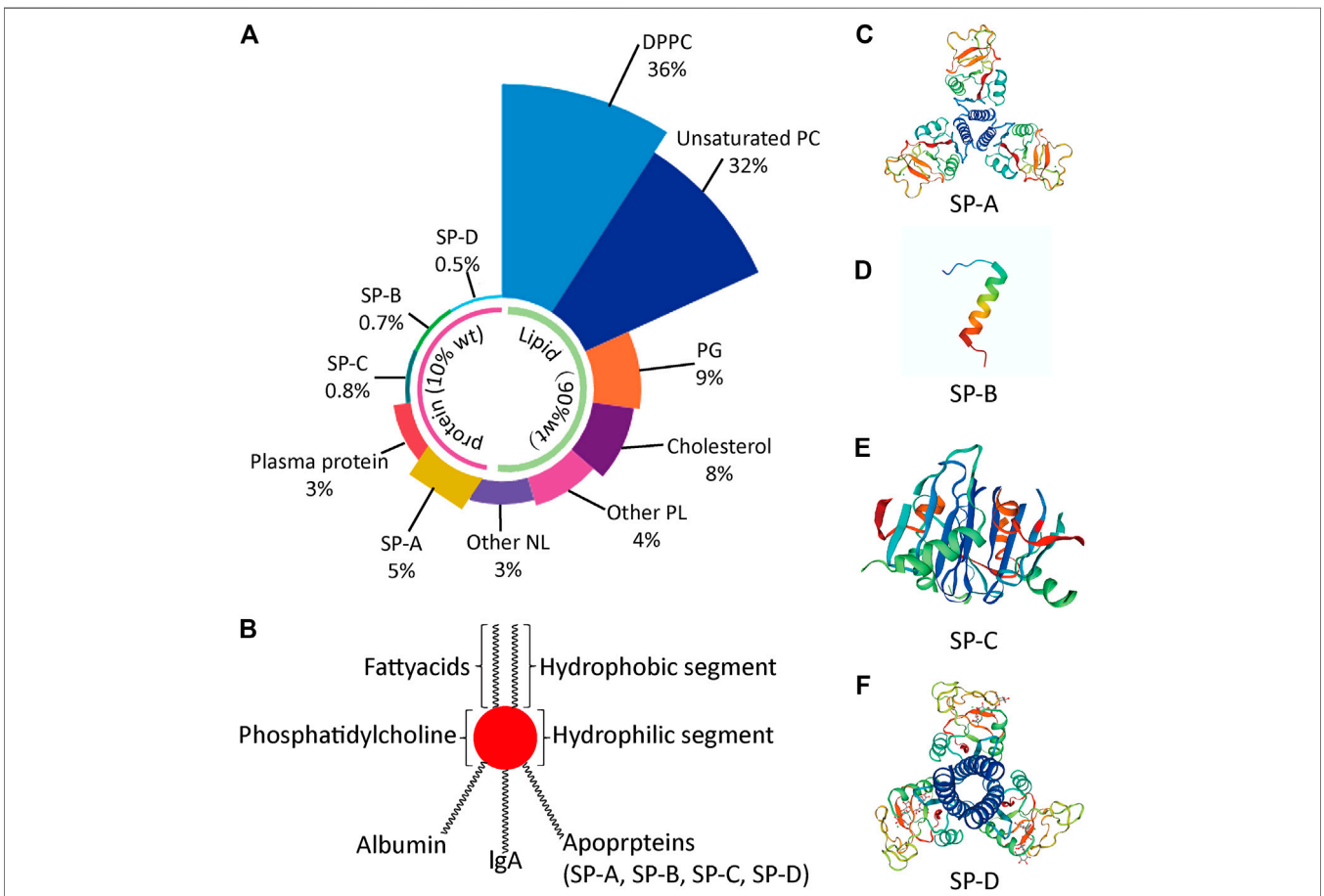

FIGURE 1 | Lung pulmonary surfactant (PS) **(A)** Relative precent of various components in PS **(B)** Representative structure of PS **(C)** Molecular representation of surfactant protein (SP)-A **(D)** Molecular representation of SP-B **(E)** Molecular representation of SP-C **(F)** Molecular representation of SP-D. DPPC, dipalmitoyl phosphatidylcholine; NL, neutral lipid; PC, phosphatidylcholine; PG, phosphatidylglycerol; PL, phospholipid; SP, surfactant protein.

TABLE 1 | Characteristics and details of pulmonary surfactant proteins and surfactant lipids.

Name	Size	Chemistry	Major functions	Ref
SP-A	28–36 kDa	Hydrophilic Octadecameric glycoprotein, acidic	Involved in facilitating phagocytosis, inhibition of phospholipase A_2 activity and maintaining surfactant integrity during lung injury	[1]
SP-B	8 kDa	Hydrophobic. Disulfide linked homodimer with 79 amino acids (AA)	Involved in decreasing the surface tension and enhancing adsorption of PL at air-water interface. Deficiency results in severe respiratory failure	[2]
SP-C	4.2 kDa	Hydrophobic. α-helical protein with 35 AA	Involved in stabilizing phospholipids, increasing the viscosity of air-water interfacial film Deficiency results in minimal effect on respiratory function	[2]
SP-D	43 kDa	Hydrophilic. Dodecameric glycoprotein with 4 trimmers	Involved in regulating surfactant metabolism and promotes phagocytosis by alveolar cells	[3]
1,2-Dipalmitoyl-sn-glycero-3-phosphatidylcholine	734.05 $gmol^{-1}$	PC16:0/16:0, $C_{40}H_{80}NO_8P$	Involved in the generation of near-zero surface tension	[3]
1-Palmitoyl-2-oleoyl-sn-glycero-3-phosphocholine (POPC)	760.09 $gmol^{-1}$	PC 16:0/18:1 $C_{42}H_{82}NO_8P$	Involved in making the membrane fluid at body temperature	[3,4]
1-Palmitoyl-2-palmitoleoyl-sn-glycero-3-phosphocholine (PPPC)	732.04 $gmol^{-1}$	PC 16:0/16:1, $C_{40}H_{78}NO_8P$	Involved in regulating respiratory rate and surface dynamics of surfactant	[3,4]
1-Palmitoyl-2-myristoyl-sn-glycero-3-phosphocholine	706 $gmol^{-1}$	PC16:0/14:0, $C_{38}H_{76}NO_8P$	Involved in regulating respiratory rate and alveolar macrophages function to improve protection	[4,5]
1,2-Dipalmitoyl- sn-glycero-3-phosphoglycerol (DPPG)	722.98 $gmol^{-1}$	$C_{38}H_{75}O_{10}P$	Involved in reducing permeability of benzo [*a*]pyrene	[4,5]
1-Palmitoyl-2-oleoyl-sn-glycero-3-phosphoglycerol (POPG)	749.02 $gmol^{-1}$	$C_{40}H_{77}O_{10}P$	The most abundant PG in human *p*S. Enhances fluidization of film, inhibits macrophage proinflammatory responses and antiviral	[4,5]
Phosphatidylserine	792.09 $gmol^{-1}$	$C_{42}H_{82}NO_{10}P$	Involved in determining the cellular and subcellular distribution of quinidine	[2,4]
PE	299.22 $gmol^{-1}$	$C_9H_{18}NO_8P$	Involved in stabilizing membrane protein by initiation of lateral pressure and curvature stress	[2,4]
Phosphatidylinositol	334.21 $gmol^{-1}$	$C_9H_{19}O_{11}P$	Involved in increasing the rate of alveolar fluid clearance and stabilization of surfactant mono layer	[4,6]
Cholesterol	386.66 $gmol^{-1}$	$C_{17}H_{46}O$	Involved in increasing the surfactant fluidity	[4,7]

Note: AA, amino acid; DPPC, dipalmityl phophotidylcholine; PE, phosphatidylethanolamine; PS, Pulmonary surfactant; SP, surfactant protein; C, Carbon; H, Hydrogen: O, Oxygen; p, *Phosphorus; N, Nitrogen.*

References.

[1] J.A. Whitsett, The molecular era of surfactant biology, Neonatology. 105 (2014) 337–343. doi:10.1159/000360649.

[2] F.P.S. Yu, D. Islam, J. Sikora, S. Dworski, J. Gurka, L. López-Vásquez, M. Liu, W.M. Kuebler, T. Levade, H. Zhang, J.A. Medin, Chronic lung injury and impaired pulmonary function in a mouse model of acid ceramidase deficiency., Am. J. Physiol. Lung Cell. Mol. Physiol. 314 (2018) L406–L420. doi:10.1152/ajplung.00223.2017.

[3] F. Wang, J. Liu, H. Zeng, Interactions of particulate matter and pulmonary surfactant: Implications for human health., Adv. Colloid Interface Sci. 284 (2020) 102,244. doi:10.1016/j.cis.2020.102,244.

[4] S.E. Wert, J.A. Whitsett, L.M. Nogee, Genetic disorders of surfactant dysfunction, Pediatr. Dev. Pathol. 12 (2009) 253–274. doi:10.2350/09–01-0,586.1.

[5] U. Klenz, M. Saleem, M.C. Meyer, H.J. Galla, Influence of lipid saturation grade and headgroup charge: A refined lung surfactant adsorption model, Biophys. J. 95 (2008) 699–709. doi:10.1529/biophysj.108.131,102.

[6] D.R. Voelker, M. Numata, Phospholipid regulation of innate immunity and respiratory viral infection., J. Biol. Chem. 294 (2019) 4,282–4,289. doi:10.1074/jbc.AW118.003229.

[7] A. Kelly, C. McCarthy, Pulmonary Alveolar Proteinosis Syndrome., Semin. Respir. Crit. Care Med. 41 (2020) 288–298. doi:10.1055/s-0039–3402,727.

atelectasis (Han and Mallampalli, 2015). PS is synthesized in type II alveolar epithelial cells, stored in lamellar bodies, and is secreted via exocytosis into the alveolar lumen. PS is a complex mixture comprising 90% lipids and 10% surfactant proteins by weight. The lipids are made of DPPC (36%), unsaturated phosphatidylcholine (PC; 32%), phosphatidylglycerol (PG; 8%), cholesterol (7%), other phospholipids (PL; 4%) and other neutral lipids (NL; 3%). The surfactant proteins consist of plasma protein (3%), surfactant protein (SP)-A (5%), SP-B (0.7%), SP-C (0.8%) and SP-D (0.5%) as depicted in **Figure 1A**) (Bernhard, 2016).

The PS lipids forms a monolayer at the air-fluid interface, reduces the surface tension to a minimum of <10 mN/m and thus, prevents the collapse of alveoli and maintains the alveolar stability (Sunde et al., 2017). The main active component of PS lipids is DPPC.

The SPs are classified into hydrophilic SPs (SP-A and SP-D) and hydrophobic SPs (SP-B and SP-C; **Figures 1C–F**). The details of SPs and PS lipids are provided in **Table 1** (Wang et al., 2020). SP-A and SP-D are highly ordered collagen-like oligomeric glycoprotein belonging to collectin family. These two SPs are part of innate immune response and protect the lungs against inhaled chemicals and microorganisms via stimulating phagocytosis by alveolar macrophages. They are also involved in surfactant metabolism. SP-A is the most abundant SP and accounts for 2–3% w/w of total SPs. It does not have any effect on surface tension at air-fluid interface in alveoli. However, it enhances the phospholipid absorption process to the air-fluid interface, regulates the PS secretion by AT-II cells, binds specific carbohydrate moieties found on lipids and on the surface of microorganisms and prevents the inhibition of surfactant function by plasma proteins which are leaked into the alveolar

space (Echaide et al., 2017). The encoded protein may also be involved in surfactant metabolism. SP-B and SP-C are apolipoproteins comprising of 1–2% w/w of total SPs (Echaide et al., 2017). These are involved in the spreading of the surfactant layer at the air-fluid interface and thus reduce the surface tension (Weaver and Conkright, 2001). The SP-B enhances the rate of spreading and increases the stability of monolayers.

PULMONARY SURFACTANT DEFICIENCY/ DYSFUNCTION

In anticipation of birth during gestation period, the alveoli start producing PS in 24th week and reaches to the peak production in 34th week. The endogenous cortisol stimulates the production of PS during gestation. Premature infants, especially those born before 34th weeks, have immature lungs and are deficient in *p*S. These infants have difficulty in breathing and develop a condition called NRDS (Nogee, 2019). Pregnant women who are at the risk of premature delivery are given betamethasone for 48 h before delivery to improve the lung maturity and reduce the risk of developing NRDS. The genetic disorders comprising the mutations in SP-B and SP-C are reported to cause surfactant dysfunction, leading to the development of NRDS. Observational studies suggested that humans with ARDS have altered PS composition and its functions. AT-II epithelial cells are reported to be the primary site of influenza virus replication. Mice infected with influenza virus have shown lower amounts of phosphatidylcholine and alters the metabolism of PS, which are attributed to the development of ARDS (Woods et al., 2016).

The effects of SP deficiencies or dysfunctions is paramount in the pathogenesis of neonatal respiratory diseases (Verlato et al., 2018). In neonates, SP-A is critical in lung immune system while SP-B is important in sustaining respiratory physiology. It was also substantiated that there is a significant lack of surfactant protein found in preterm newborns with RDS or had experienced failure in extubation than that of newborns with normal functioning lungs (Ballard et al., 2019). It is also known that polymorphisms of SP-A, B and D showed association with idiopathic pulmonary fibrosis and various other pulmonary diseases. Chang et al. reported that SP-A +186A/G and SP-B 1580C/T polymorphisms results in the elevated risk of preterm NRDS; on the other hand, polymorphisms of SP-B −18A/C, SP-D Met11 ThrT/C, and Ala160 ThrG/A genes are not associated to the risk of NRDS (Chang et al., 2016).

The beneficial use of surfactant protein as a treatment in neonates with RDS has been a breakthrough and has been studied in-depth for neonatal medicine in the past 3 decades (Speer et al., 2013). Thus, it is logical to hypothesize that restoration of PS does improve the lung function (Echaide et al., 2017) and circumvent the symptoms of NRDS in infants and ARDS in adults.

APPLICATIONS OF PULMONARY SURFACTANT

The primary application of pulmonary surfactants is in the treatment of NRDS in premature infants. However, the studies did not demonstrate significant benefit of pulmonary surfactants in ARDS. Meta-analysis of randomized controlled trials for the effect of surfactant in adult patients with ARDS (Ballard et al., 2019) revealed neither improvements in the mortality nor improvement in oxygenation. Marcel Filoche et al. proposed that insufficient delivery of PS to the lungs in adults could be the reason for showing the efficacy in adults (Speer et al., 2013). One of the postulations put forward to explain the observed differences in clinical efficacy of PS in NRDS and ARDS is that in case of NRDS, the surfactants are administered well in advance before the RDS becomes severe in infants who are at the risk of developing NRDS. Thus, it is worth to explore the option of checking the efficacy of PS in early stages of ARDS. However, this approach requires the identification of patients who are at the stage of developing ARDS. Thus, identification of PS levels in serum would predict the occurrence of ARDS.

The clinical efficacy of PS is also being actively investigated in other pulmonary diseases such as asthma and pneumonia (Choi et al., 2020). One study reported that PS improved lung function in an acute asthma exacerbation but not in stable asthma (Tepper et al., 2012). One study reported the administration of PS improved oxygenation in Gram-negative lobar pneumonia and in HIV-infected patients with P. carinii pneumonia or RSV pneumonia (Han and Mallampalli, 2015). Another study reported that PS improved the pulmonary function in adult patient with stable chronic bronchitis (Agudelo et al., 2020). In addition, PS is reported to decrease the cytokine release, synthesis of inflammatory mediators, lymphocyte proliferation, immunoglobulin production, and expression of adhesion molecules. Another study reported PS improves the anti-inflammatory effect of amikacin. All the above observations suggest the possible role of surfactants in modulating the immune responses in pulmonary diseases.

The SP-A and SP-D are reported to bind to viruses (influenza A, human immunodeficiency virus (HIV), respiratory syncytial virus (RSV), SARS-CoV) and inhibit their activity of the viruses through viral neutralization, agglutination, and enhanced phagocytosis (Cañadas et al., 2020).

THERAPEUTIC PULMONARY SURFACTANTS

There are two types of therapeutic PS: natural and synthetic. Natural PS are derived from animals while synthetic PS contain peptides that mimic SP-B and SP-C. Therapeutic PS are the first-line treatment option for NRDS (Whitsett, 2014; Hentschel et al., 2020). The natural therapeutic PS are being sourced from bovine, porcine, and human amniotic fluid. Currently the use of human amniotic fluid for sourcing therapeutic PS are halted mainly because of non-availability and cost. The advantage of natural surfactants is that they contain surfactant-associated proteins and thus results in better spreading and lung defense properties.

Due to the difficulties in sourcing animal derived surfactant, well-defined synthetic surfactants were developed. Initially, the synthesis of artificial SP-B and SP-C used for the treatment of neonatal RDS was indeed challenging. It was also reported that

TABLE 2 | Clinical trials on pulmonary surfactants for the treatment of ARDS in COVID-19 patients.

Surfactant	Dose	Administration route	Study type	Primary purpose	NCT number
Poractant alfa	50 mg/kg only once	Bronchial fibroscopy	Interventional	Treatment using Curosurf® in adult acute respiratory distress syndrome due to COVID-19	NCT04384731
Poractant alfa	30 mg/kg once a day for 3 days	Endotracheal intubation	Interventional	Treatment using poractant alfa - curosurf for SARS-cov-19 ARDS (Covid-19)	NCT04502433
Bovine lung extract surfactant	50 mg/kg once a day for 3 days	Endotracheal intubation	Interventional	Treatment using London's exogenous surfactant study for COVID-19 (LESSCOVID)	NCT04375735
Bovine lung extract surfactant	150 mg twice a day for 5 days	Inhalation	Observational	Treatment using Surfactant-BL in adult ARDS due to COVID-19	NCT04568018
Lucinactant	80 mg	Injection	Interventional	Treatment by assessing the safety and preliminary tolerability of lyophilized lucinactant in adults with Covid-19	NCT04389671
COVSurf	N/A	N/A	Interventional	Treatment using delivery of the surfactant to the lungs	NCT04362059
Exogenous surfactant		Inhalation	Interventional	Evaluation of the effect of exogenous surfactant through nebulizer mask on clinical outcomes in Covid-19 patients	NCT04847375
Biological: AT-100 (rhSP-D)	75 or 150 mg once a day for 7 days	Intratracheal administration	Interventional	Treatment: Safety study on AT-100 in treating adults with severe COVID-19 infection	NCT04659122

Note: N/A, Not applicable; ARDS, Acute Respiratory Distress Syndrome; NCT, National Clinical Trials.

synthetic surfactant containing only one protein has not found success (Johansson and Curstedt, 2019). Both synthetic and natural surfactants are found to be effective in RDS with natural surfactants containing SP-B and SP-C are found to be superior in clinical efficacy.

To date, the list of natural surfactants, and synthetic surfactants developed for the treatment of respiratory infections are shown in **Table 2**. First generation synthetic surfactants were prepared in combination of DPPC with either egg phosphatidylglycerol (ALEC®) or hexadecanol and tyloxapol (Exosurf®) (Zhang et al., 2011). However, the first-generation surfactants do not contain either SP-B or SP-C peptide mimics, thus limiting their clinical efficacy. The second-generation of synthetic surfactants contain either SP-B (Surfaxin®) or SP-C (Venticute®) peptide (Bae et al., 2016). The second-generation of synthetic surfactants are found to be clinically effective, suggesting the presence of SP-B and SP-C in surfactants are essential.

Colfosceril palmitate is a first generation commercially available artificial surfactant (Law et al., 2014; Sardesai et al., 2017). At present, it is under the state of cancellation in the post-marketing stage because of adverse effects. In addition to being useful in RDS, it has also shown to significantly reduce the risk of pneumothoraces, pulmonary interstitial emphysema and mortality, bronchopulmonary dysplasia, intraventricular hemorrhage and patent ductus arteriosus. Sinapultide, also known as KL4 peptide, mimics human SP-B. It is administered as its aqueous dispersion with the phospholipids. Lucinactant is a synthetic surfactant containing sinapultide, and lipids, DPPC, palmitoyloleoyl phosphatidylglycerol (POPG) and a palmitic acid. Pumactant is another synthetic surfactant containing naturally occurring phospholipids DPPC and PG.

Calfactant is a natural pulmonary surfactant from calf lungs containing phosphatidylcholine, SP-B and SP-C. Beractant is another natural pulmonary surfactant from bovine lungs containing phosphotidylcholine, triglycerides, fatty acids, SP-B and SP-C. Portactant alfa is another natural pulmonary surfactant from porcine lungs containing phosphatidylcholine, dipaImitoylphosphatidylcholine, SP-B and SP-C.

PULMONARY SURFACTANTS IN COVID-19

SARS-CoV-2 enters the body through lungs via binding of viral spike protein with angiotensin converting enzyme 2 (ACE-2) receptor (Mason, 2020). After entry, SARS-CoV-2 is postulated to destroy type II alveolar cells, the site for the synthesis of pulmonary surfactants, resulting in decreased production of *p*S. Decreased surfactant production causes atelectasis and reduced the pulmonary compliance. The patients with Coronavirus disease 2019 (COVID-19) are presented with clinical symptoms which are very similar to those observed in NRDS (Nieman et al., 2018; Schousboe et al., 2020) for which deficiency in PS is the primary cause (**Figure 2**). Decreased concentration of PS, altered composition of PS and mutations in PS are reported to be the critical factors in COVID-19 mortality (Weiskirchen, 2020). Mirastschijski et al. has suggested to include pulmonary surfactants therapy in the early stages together with standard ARDS care. Preliminary observations from lung autopsies of COVID-19 patients found that pulmonary surfactant increased blood oxygenation, reduced pulmonary edema, and ameliorated the excessive inflammatory reaction (Mirastschijski et al., 2020). In addition, PS is reported to have the ability to recognize the SARS-CoV-2 spike protein and thereby activate the macrophages for phagocytosis (Matera et al., 2020). This evidence motivated the interventional clinical trials to investigate the clinical effectiveness of PS in COVID-19 patients.

Gattinoni et al. (Gattinoni et al., 2020) has classified COVID-19 patients into two different groups; one group develops acute respiratory distress syndrome (ARDS) with low compliance and another group develops non-ARDS with normal compliance. Gene expression studies on lung biopsy cells in COVID-19 patients have confirmed the downregulation of pulmonary surfactant proteins and their metabolism which has provided a

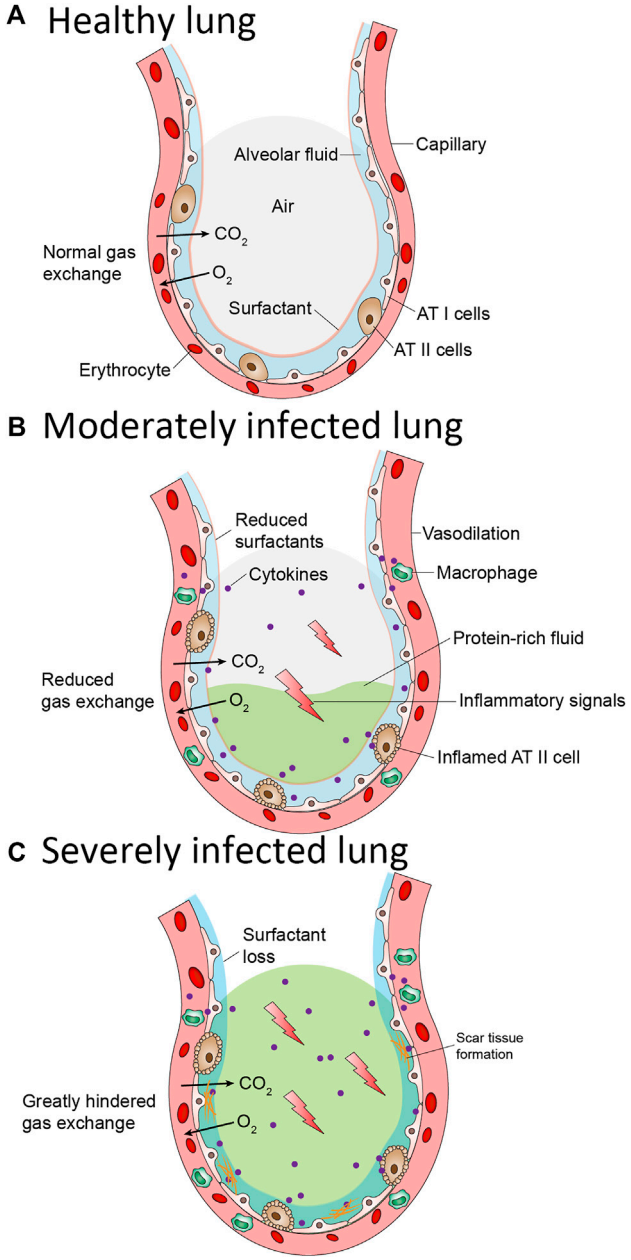

FIGURE 2 | Pathological changes in the lung alveolus during COVID-19 **(A)** Normal alveolus is wrapped with capillaries containing red blood cells. Oxygen in the alveolus is exchanged with carbon dioxide in the capillaries. The alveolus surface contains alveolar Type I and Type II cells. Type I cells enables gas exchange. Type II cells secrete pulmonary surfactant (PS). PS lines the alveolus and prevent it from collapsing **(B)** In a moderately infected lung, Alveolar Type II cells are inflamed resulting in reduced pulmonary surfactant. Surface tension and pressure increase inside the alveolus affecting the gas exchange. Vasodilation of the capillary occurs resulting in the release of inflammatory cytokines and accumulation of protein-rich fluid inside the alveolus **(C)** In severely infected lung, the alveolar type II cells become more inflamed thereby resulting in complete loss of pulmonary surfactant. Scar tissue on the alveolar surface began to form. The release of inflammatory cytokines is increased, and more protein-rich fluid accumulate inside the alveolus. The oxygen/carbon dioxide exchange is greatly hindered and thus patients in this stage must undergo intubation as an aid to breathe.

scientific base to advocate further studies on investigating the usefulness of surfactant therapy in COVID-19 patients (Islam and Khan, 2020). Clinical trials are underway to determine the association of SP-D levels (NCT04618861) and SP genetic variants (NCT04650191) with severity of COVID-19 infection (Surfactant Protein D Levels in Covid-19 Infection: Case-Control Study; Surfactant Protein Genetic Variants in COVID-19 Infection) and the results are not yet available.

Peter et al. (Schousboe et al., 2020) has postulated that COVID-19 patients with pulmonary surfactant deficiency develop symptoms resembling neonatal respiratory distress syndrome (NRDS). A clinical trial (NCT04609488) is underway to determine the levels of surfactant proteins in COVID-19 patients to delineate the association between surfactant deficiency and progression of COVID-19 disease.

Lung surfactant therapy is a standard, safe and effective therapy for the treatment of ARDS in neonates, however clinical trials on recombinant SP-C based surfactant was found to be ineffective in the treatment of ARDS in adults (Spragg et al., 2004). The natural surfactants, compared to synthetic surfactants, are reported to be superior in improving the blood oxygenation and shortening the ventilation time in infants (Ainsworth et al., 2000; Been and Zimmermann, 2007). These observations suggest that early administration of natural surfactant to COVID-19 patients might be beneficial to improve the pulmonary function (Mirastschijski et al., 2020).

A recent review article by Francesco et al. (Cattel et al., 2021) has highlighted the potential use of exogenous surfactants early in the treatment of COVID-19 ARDS. Kumar et al. (Kumar, 2020) has proposed an innovative hypothesis that co-aerosolized exogenous pulmonary surfactant and ambroxol can be a potential therapeutic option for the treatment of COVID-19 ARDS. The hypothesis was made based on reported evidences on beneficial effects of exogenous surfactants (Davidson et al., 2006; Dushianthan et al., 2012; Zhang et al., 2013; Meng et al., 2019) and ambroxol (Malerba and Ragnoli, 2008; Paleari et al., 2011; Kantar et al., 2020) in the treatment of ARDS. However, this hypothesis is yet to be tested. A prospective observational cohort study revealed that autoimmunity in severe COVID-19 patients is mediated through binding of immunoglobulin A (IgA) antibodies to human surfactant protein B (SP-B) and surfactant protein C (SP-C) leading to reduced levels of pulmonary surfactant (Sinnberg et al., 2021).

Abbas et al. (Abbasi et al., 2021) has made a serendipitous observation that non-invasive ventilation improved the survival of mice with bacterial pneumonia and the improved survival is associated with the expression of surfactant protein A. Majority of the COVID-19 patients are also reported to be co-infect with other pathogens (Hughes et al., 2020; Jiang et al., 2020; Kim et al., 2020; Roh et al., 2021) and many research papers (Floros and Phelps, 2020; Tekos et al., 2020; Xu et al., 2020) have highlighted that SP-A variants have shown beneficial effects in the treatment of ARDS in COVID-19 patients under different scenarios. Thus, in an opinion article by Abbs et al. (Abbasi et al., 2021), the team has expressed that non-invasive ventilation using high-flow nasal cannula (HFNC) may be beneficial for COVID-19 patients which

TABLE 3 | List of natural and synthetic surfactant proteins.

Trade name	Surfactant	Type
Curosurf®	Porcine surfactant	Natural
Survanta®	Modified version of bovine surfactant	Natural
ALEC®	Combination of DPPC and egg phosphatidylglycerol	Synthetic
Exosurf®	Combination of DPPC with hexadecanol and tyloxapol	Synthetic
Surfaxin®	SP-B analog KL4	Synthetic
Venticute®	Recombinant human surfactant protein C	Synthetic

warrants further laboratory and clinical studies to confirm (Abbasi et al., 2021).

A clinical study (Choreño-Parra et al., 2021) has concluded that serum SP-D level is high only in pandemic influenza A (H1N1) but not in COVID-19. However, contradicting to this study, another clinical study (Kerget et al., 2020) has concluded that human SP-D levels is higher in individuals with COVID-19 compared to those without COVID-19. The contradictory results from these two studies may be due to differences in the population demographics, and objectives of the study. Thus, more clinical studies are warranted to confirm the association between SP-D levels and progression of COVID-19 infection.

In a case study of a 48-year-old-male non-smoker COVID-19 patient with comorbidities of hyperlipidemia and prediabetes (Heching et al., 2021), it is reported that administration of surfactant (Calfactant) directly to the lungs has improved oxygenation. This observation rises a hope that surfactant therapy would be beneficial for treating ARDS in COVID-19 and thus warrant further detailed investigations to confirm the therapeutic efficacy of surfactants in COVID-19 patients.

The recombinant fragment of human lung surfactant protein D (rfhSP-D) is reported to be more potent than remdesivir, an antiviral, in inhibiting the replication and infectivity of SARS-CoV-2 and the activity is found to mediated through down regulation of RdRp gene expression (Hsieh et al., 2021; Madan et al., 2021).

Computational fluid dynamics simulation studies (Kitaoka et al., 2021) using 3D human airway models has predicted that wedge instillation of pulmonary surfactant from subsegmental bronchi is better than conventional method to deliver the effective concentration of pulmonary surfactant to the lungs to protect them from COVID-19 infection.

Hideyuki has put forward a hypothesis (Takano, 2020) based on cumulative scientific evidences that pulmonary surfactants or synthetic surfactants or surfactant production stimulants may be effective for either prophylaxis or treatment for COVID-19. However, this hypothesis is yet to be tested and validated in clinic.

CLINICAL TRIALS ON PULMONARY SURFACTANTS IN COVID-19 PATIENTS

Based on the data retrieved from https://clinicaltrials.gov/, accessed on June 15, 2021, the details of on-going clinical trials in surfactants related to COVID-19 are provided in **Table 3**. Three surfactant products: poractant alfa, bovine lung extract surfactant (BLSE), and lucinactant are in phase I/II trials to test their efficacy in improving the clinical outcomes of ARDS in COVID-19 patients. There are two trials that are underway on poractant alfa using two different routes of administration: bronchial fibroscopy and endotracheal intubation. Another two trials are underway on BLSE using two different routes of administration: endotracheal intubation and inhalation. As for lucinactant, one trial is underway, and it is administered via injection only. In addition, two trials are going on to determine the levels of surfactants present in the lungs and serum of COVID-19 patients with the objective of finding the association between the surfactant levels and ARDS symptoms. Lastly, one clinical trial is underway to determine the efficacy of new drug delivery system directly to the lungs using COVsurf.

CONCLUSION

SARS-CoV-2 uses ACE-2 receptor on lungs for entry and alveolar type II cells for replication. Infection with SARS-CoV-2 causes ARDS which may lead to respiratory failure. AT II cells are the sites of pulmonary surfactant production. Lack of PS is the principal cause for NRDS and viral infections are known to reduce PS levels in lungs. PS therapy is the mainstay for NRDS treatment across the world for many years. The results from clinical trials on the efficacy and safety PS in adults with ARDS were not significant in terms of clinical outcomes but they were proven to be safe. The lack of efficacy is attributed to the insufficient delivery of PS to the lungs and thus research has been initiated to investigate new drug delivery systems for improving the PS delivery directly to the lungs. Serum PS levels were found to be low in COVID-19 patients and ARDS clinical symptoms in COVID-19 were found to be like those of NRDS. The science of pulmonary surfactant has come a long way since it was discovered in the 1950s and provides very strong theoretical evidence suggesting that PS could play a role in COVID-19 treatment. In the current COVID-19 pandemic crisis, researchers and health care workers across the globe have been working hard to find a solution to end the pandemic. Few clinical trials are in progress to test the efficacy of three pulmonary surfactants in improving the clinical outcomes in COVID-19 patients, to determine the association between surfactant levels and severity of ARDS in COVID-19 patients, and new drug delivery systems for improved and safe delivery of PS in COVID-19 patients.

AUTHOR CONTRIBUTIONS

SW and ZL searched the literature, collected the data, and drafted the manuscript. SW, ZL, XW, and SZ contributed to analysis and manuscript preparation. SZ, PG, and ZS helped in checking the figures and tables. SZ and XW downloaded the documents and made classification. SZ, PG, and ZS contributed comments for version of the manuscript. All authors contributed to the article and approved the submitted version.

FUNDING

This research was funded by National Major Science and Technology Projects of China, 2018ZX09721004-011.

REFERENCES

Abbasi, A., Phelps, D. S., Ravi, R., and Floros, J. (2021). Can Prophylactic High Flow of Humidified and Warmed Filtered Air Improve Survival from Bacterial Pneumonia and Sars-Cov-2 in Elderly Individuals? the Role of Surfactant Protein a. *Antioxidants* 10, 640. doi:10.3390/antiox10050640

Agassandian, M., and Mallampalli, R. K. (2013). Surfactant Phospholipid Metabolism. *Biochim. Biophys. Acta (Bba) - Mol. Cel Biol. Lipids* 1831, 612–625. doi:10.1016/j.bbalip.2012.09.010

Agudelo, C. W., Kumley, B. K., Area-Gomez, E., Xu, Y., Dabo, A. J., Geraghty, P., et al. (2020). Decreased Surfactant Lipids Correlate with Lung Function in Chronic Obstructive Pulmonary Disease (COPD). *PLoS One* 15, e0228279. doi:10.1371/journal.pone.0228279

Ainsworth, S., Beresford, M., Milligan, D., Shaw, N., Matthews, J., Fenton, A., et al. (2000). Pumactant and Poractant Alfa for Treatment of Respiratory Distress Syndrome in Neonates Born at 25-29 Weeks' Gestation: a Randomised Trial. *The Lancet* 355, 1387–1392. doi:10.1016/S0140-6736(00)02136-X

Bae, C.-W., Chung, S.-H., and Choi, Y.-S. (2016). Development of a Synthetic Surfactant Using a Surfactant Protein-C Peptide Analog: *In Vitro* Studies of Surface Physical Properties. *Yonsei Med. J.* 57, 203–208. doi:10.3349/ymj.2016.57.1.203

Ballard, P. L., Keller, R. L., Keller, R. L., Truog, W. E., Chapin, C., Horneman, H., et al. (2019). Surfactant Status and Respiratory Outcome in Premature Infants Receiving Late Surfactant Treatment. *Pediatr. Res.* 85, 305–311. doi:10.1038/s41390-018-0144-3

Been, J. V., and Zimmermann, L. J. I. (2007). What's New in Surfactant? *Eur. J. Pediatr.* 166, 889–899. doi:10.1007/s00431-007-0501-4

Bernhard, W. (2016). Lung Surfactant: Function and Composition in the Context of Development and Respiratory Physiology. *Ann. Anat. - Anatomischer Anzeiger* 208, 146–150. doi:10.1016/j.aanat.2016.08.003

Cañadas, O., Olmeda, B., Alonso, A., and Pérez-Gil, J. (2020). Lipid-Protein and Protein-Protein Interactions in the Pulmonary Surfactant System and Their Role in Lung Homeostasis. *Ijms* 21, 3708. doi:10.3390/ijms21103708

Cattel, F., Giordano, S., Bertiond, C., Lupia, T., Corcione, S., Scaldaferri, M., et al. (2021). Use of Exogenous Pulmonary Surfactant in Acute Respiratory Distress Syndrome (ARDS): Role in SARS-CoV-2-Related Lung Injury. *Respir. Physiol. Neurobiol.* 288, 103645. doi:10.1016/j.resp.2021.103645

Chang, H.-Y., Li, F., Li, F.-S., Zheng, C.-Z., Lei, Y.-Z., and Wang, J. (2016). Genetic Polymorphisms of SP-A, SP-B, and SP-D and Risk of Respiratory Distress Syndrome in Preterm Neonates. *Med. Sci. Monit.* 22, 5091–5100. doi:10.12659/msm.898553

Choi, Y., Jang, J., and Park, H.-S. (2020). Pulmonary Surfactants: a New Therapeutic Target in Asthma. *Curr. Allergy Asthma Rep.* 20, 1–8. doi:10.1007/s11882-020-00968-8

Choreño-Parra, J. A., Jiménez-Álvarez, L. A., Ramírez-Martínez, G., Cruz-Lagunas, A., Thapa, M., Fernández-López, L. A., et al. (2021). Expression of Surfactant Protein D Distinguishes Severe Pandemic Influenza A(H1N1) from Coronavirus Disease 2019. *J. Infect. Dis.* 223, jiab113. doi:10.1093/infdis/jiab113

Davidson, W., Dorscheid, D., Spragg, R., Schulzer, M., Mak, E., and Ayas, N. (2006). Exogenous Pulmonary Surfactant for the Treatment of Adult Patients with Acute Respiratory Distress Syndrome: Results of a Meta-Analysis. *Crit. Care* 10, R41. doi:10.1186/cc4851

Dushianthan, A., Cusack, R., Goss, V., Postle, A. D., and Grocott, M. P. (2012). Clinical Review: Exogenous Surfactant Therapy for Acute Lung Injury/acute Respiratory Distress Syndrome - where Do We Go from Here? *Crit. Care* 16, 238. doi:10.1186/cc11512

Echaide, M., Autilio, C., Arroyo, R., and Perez-Gil, J. (2017). Restoring Pulmonary Surfactant Membranes and Films at the Respiratory Surface. *Biochim. Biophys. Acta (Bba) - Biomembranes* 1859, 1725–1739. doi:10.1016/j.bbamem.2017.03.015

Floros, J., and Phelps, D. S. (2020). Is the Role of Lung Innate Immune Molecules, SP-A1 and SP-A2, and of the Alveolar Macrophage Being Overlooked in COVID-19. *COVID-19 Diverse Outcomes. Pneumon.* 33, 1–5. doi:10.1016/s0925-4439(98)00077-5

Gattinoni, L., Chiumello, D., and Rossi, S. (2020). COVID-19 Pneumonia: ARDS or Not? *Crit. Care* 24, 154. doi:10.1186/s13054-020-02880-z

Han, S., and Mallampalli, R. K. (2015). The Role of Surfactant in Lung Disease and Host Defense against Pulmonary Infections. *Ann. ATS* 12, 765–774. doi:10.1513/AnnalsATS.201411-507FR

Heching, M., Lev, S., Shitenberg, D., Dicker, D., and Kramer, M. R. (2021). Surfactant for the Treatment of ARDS in a Patient with Coronavirus Disease 2019. *Chest* S0012-3692, 00100–8. doi:10.1016/j.chest.2021.01.028

Hentschel, R., Bohlin, K., van Kaam, A., Fuchs, H., and Danhaive, O. (2020). Surfactant Replacement Therapy: from Biological Basis to Current Clinical Practice. *Pediatr. Res.* 88, 176–183. doi:10.1038/s41390-020-0750-8

Hsieh, M.-H., Beirag, N., Murugaiah, V., Chou, Y.-C., Kuo, W.-S., Kao, H.-F., et al. (2021). Human Surfactant Protein D Binds Spike Protein and Acts as an Entry Inhibitor of SARS-CoV-2 Pseudotyped Viral Particles. *Front. Immunol.* 12, 641360. doi:10.3389/fimmu.2021.641360

Hughes, S., Troise, O., Donaldson, H., Mughal, N., and Moore, L. S. P. (2020). Bacterial and Fungal Coinfection Among Hospitalized Patients with COVID-19: a Retrospective Cohort Study in a UK Secondary-Care Setting. *Clin. Microbiol. Infect.* 26, 1395–1399. doi:10.1016/j.cmi.2020.06.025

Islam, A. B. M. M. K., and Khan, M. A.-A.-K. (2020). Lung Transcriptome of a COVID-19 Patient and Systems Biology Predictions Suggest Impaired Surfactant Production Which May be Druggable by Surfactant Therapy. *Sci. Rep.* 10, 19395. doi:10.1038/s41598-020-76404-8

Jiang, S., Liu, P., Xiong, G., Yang, Z., Wang, M., Li, Y., et al. (2020). Coinfection of SARS-CoV-2 and Multiple Respiratory Pathogens in Children. *Clin. Chem. Lab. Med.* 58, 1160–1161. doi:10.1515/cclm-2020-0434

Johansson, J., and Curstedt, T. (2019). Synthetic Surfactants with SP-B and SP-C Analogues to Enable Worldwide Treatment of Neonatal Respiratory Distress Syndrome and Other Lung Diseases. *J. Intern. Med.* 285, 165–186. doi:10.1111/joim.12845

Kantar, A., Klimek, L., Cazan, D., Sperl, A., Sent, U., and Mesquita, M. (2020). Ambroxol for the Treatment of Children with Acute and Chronic Respiratory Diseases: an Overview of Efficacy and Safety. *Multidis Res. Med.* 15, 511. doi:10.4081/mrm.2020.511

Kerget, B., Kerget, F., Koçak, A. O., Kızıltunç, A., Araz, Ö., Uçar, E. Y., et al. (2020). Are Serum Interleukin 6 and Surfactant Protein D Levels Associated with the Clinical Course of COVID-19? *Lung* 198, 777–784. doi:10.1007/s00408-020-00393-8

Khawar, H., and Marwaha, K. (2021). *Surfactant - PubMed*. Fairfield, Iowa: StatPearls Publishing.

Kim, D., Quinn, J., Pinsky, B., Shah, N. H., and Brown, I. (2020). Rates of Co-infection between SARS-CoV-2 and Other Respiratory Pathogens. California: Stanford, *Jama* 323, 2085–2086. doi:10.1001/jama.2020.6266

Kitaoka, H., Kobayashi, H., Takimoto, T., and Kijima, T. (2021). Proposal of Selective Wedge Instillation of Pulmonary Surfactant for COVID-19 Pneumonia Based on Computational Fluid Dynamics Simulation. *BMC Pulm. Med.* 21, 1–5. doi:10.1186/s12890-021-01435-4

Kumar, P. (2020). Co-aerosolized Pulmonary Surfactant and Ambroxol for COVID-19 ARDS Intervention: What Are We Waiting for? *Front. Bioeng. Biotechnol.* 8, 577172. doi:10.3389/fbioe.2020.577172

Law, V., Knox, C., Djoumbou, Y., Jewison, T., Guo, A. C., Liu, Y., et al. (2014). DrugBank 4.0: Shedding New Light on Drug Metabolism. *Nucl. Acids Res.* 42, D1091–D1097. doi:10.1093/nar/gkt1068

Madan, T., Biswas, B., Varghese, P. M., Subedi, R., Pandit, H., Idicula-Thomas, S., et al. (2021). A Recombinant Fragment of Human Surfactant Protein D Binds Spike Protein and Inhibits Infectivity and Replication of SARS-CoV-2 in Clinical Samples. *Am. J. Respir. Cel Mol. Biol.* [Epub ahead of print]. doi:10.1165/rcmb.2021-0005oc

Malerba, M., and Ragnoli, B. (2008). Ambroxol in the 21st century: Pharmacological and Clinical Update. *Expert Opin. Drug Metab. Toxicol.* 4, 1119–1129. doi:10.1517/17425255.4.8.1119

Mason, R. J. (2020). Thoughts on the Alveolar Phase of COVID-19. *Am. J. Physiology-Lung Cell Mol. Physiol.* 319, L115–L120. doi:10.1152/ajplung.00126.2020

Matera, M. G., Rogliani, P., Calzetta, L., and Cazzola, M. (2020). Pharmacological Management of COVID-19 Patients with ARDS (CARDS): A Narrative Review. *Respir. Med.* 171, 106114. doi:10.1016/j.rmed.2020.106114

Meng, S.-S., Chang, W., Lu, Z.-H., Xie, J.-F., Qiu, H.-B., Yang, Y., et al. (2019). Effect of Surfactant Administration on Outcomes of Adult Patients in Acute

Respiratory Distress Syndrome: A Meta-Analysis of Randomized Controlled Trials. *BMC Pulm. Med.* 19, 9. doi:10.1186/s12890-018-0761-y

Mirastschijski, U., Dembinski, R., and Maedler, K. (2020). Lung Surfactant for Pulmonary Barrier Restoration in Patients with COVID-19 Pneumonia. *Front. Med.* 7, 1–4. doi:10.3389/fmed.2020.00254

NCT04618861 *Surfactant Protein D Levels in Covid-19 Infection: Case-Control Study* ClinicalTrials.Gov. Available at: https://clinicaltrials.gov/show/NCT04618861 (Accessed November 6, 2020).

NCT04650191 *Surfactant Protein Genetic Variants in COVID-19 Infection*. Available at: https://ezp2.imu.edu.my/login?url=https://search.ebscohost.com/login.aspx?direct=true&db=edsclt&AN=edsclt.NCT04650191&site=eds-live (Accessed Dcemeber 2, 2020).

Nieman, G. F., Andrews, P., Satalin, J., Wilcox, K., Kollisch-Singule, M., Madden, M., et al. (2018). Acute Lung Injury: How to Stabilize a Broken Lung. *Crit. Care* 22, 1–11. doi:10.1186/s13054-018-2051-8

Nogee, L. M. (2019). Genetic Causes of Surfactant Protein Abnormalities. *Curr. Opin. Pediatr.* 31, 330–339. doi:10.1097/MOP.0000000000000751

Paleari, D., Rossi, G. A., Nicolini, G., and Olivieri, D. (2011). Ambroxol: A Multifaceted Molecule with Additional Therapeutic Potentials in Respiratory Disorders of Childhood. *Expert Opin. Drug Discov.* 6, 1203–1214. doi:10.1517/17460441.2011.629646

Roh, K. H., Kim, Y. K., Kim, S.-W., Kang, E.-R., Yang, Y.-J., Jung, S.-K., et al. (2021). Coinfections with Respiratory Pathogens Among COVID-19 Patients in Korea. *Can. J. Infect. Dis. Med. Microbiol.* 2021, 1–9. doi:10.1155/2021/6651045

Sardesai, S., Biniwale, M., Wertheimer, F., Garingo, A., and Ramanathan, R. (2017). Evolution of Surfactant Therapy for Respiratory Distress Syndrome: Past, Present, and Future. *Pediatr. Res.* 81, 240–248. doi:10.1038/pr.2016.203

Schousboe, P., Wiese, L., Heiring, C., Verder, H., Poorisrisak, P., Verder, P., et al. (2020). Assessment of Pulmonary Surfactant in COVID-19 Patients. *Crit. Care* 24, 4–5. doi:10.1186/s13054-020-03268-9

Seadler, B. D., Kaushik, R., and Sharma, S. (2020). Physiology, Alveolar Tension. FL: Treasure Island, StatPearls Publishing. Available at: http://www.ncbi.nlm.nih.gov/pubmed/30969647 (Accessed November 25, 2020).

Sinnberg, T., Lichtensteiger, C., Ali, O. H., Pop, O. T., Gilardi, M., Risch, L., et al. (2021). IgA Autoantibodies Target Pulmonary Surfactant in Patients with Severe COVID-19. *Matthias S. Matter 6 Lukas Flatz* 17, 19. doi:10.1101/2021.02.02.21250940

Speer, C. P., Sweet, D. G., and Halliday, H. L. (2013). Surfactant Therapy: Past, Present and Future. *Early Hum. Dev.* 89, S22–S24. doi:10.1016/S0378-3782(13)70008-2

Spragg, R. G., Lewis, J. F., Walmrath, H.-D., Johannigman, J., Bellingan, G., Laterre, P.-F., et al. (2004). Effect of Recombinant Surfactant Protein C-Based Surfactant on the Acute Respiratory Distress Syndrome. *N. Engl. J. Med.* 351, 884–892. doi:10.1056/nejmoa033181

Sunde, M., Pham, C. L. L., and Kwan, A. H. (2017). Molecular Characteristics and Biological Functions of Surface-Active and Surfactant Proteins. *Annu. Rev. Biochem.* 86, 585–608. doi:10.1146/annurev-biochem-061516-044847

Takano, H. (2020). Pulmonary Surfactant Itself Must Be a strong Defender against SARS-CoV-2. *Med. Hypotheses* 144, 110020. doi:10.1016/j.mehy.2020.110020

Tekos, F., Skaperda, Z., Goutzourelas, N., Phelps, D. S., Floros, J., and Kouretas, D. (2020). The Importance of Redox Status in the Frame of Lifestyle Approaches and the Genetics of the Lung Innate Immune Molecules, SP-A1 and SP-A2, on Differential Outcomes of Covid-19 Infection. *Antioxidants* 9, 784, 1–22. doi:10.3390/antiox9090784

Tepper, R. S., Wise, R. S., Covar, R., Irvin, C. G., Kercsmar, C. M., Kraft, M., et al. (2012). Asthma Outcomes: Pulmonary Physiology. *J. Allergy Clin. Immunol.* 129, S65–S87. doi:10.1016/j.jaci.2011.12.986

Verlato, G., Simonato, M., Giambelluca, S., Fantinato, M., Correani, A., Cavicchiolo, M. E., et al. (2018). Surfactant Components and Tracheal Aspirate Inflammatory Markers in Preterm Infants with Respiratory Distress Syndrome. *J. Pediatr.* 203, 442–446. doi:10.1016/j.jpeds.2018.08.019

Wang, F., Liu, J., and Zeng, H. (2020). Interactions of Particulate Matter and Pulmonary Surfactant: Implications for Human Health. *Adv. Colloid Interf. Sci.* 284, 102244. doi:10.1016/j.cis.2020.102244

Weaver, T. E., and Conkright, J. J. (2001). Function of Surfactant Proteins B and C. *Annu. Rev. Physiol.* 63, 555–578. doi:10.1146/annurev.physiol.63.1.555

Weiskirchen, R. (2020). Severity of Coronavirus Disease 2019 (COVID-19): Does Surfactant Matter? *Front. Microbiol.* 11, 1905. doi:10.3389/fmicb.2020.01905

Wert, S. E., Whitsett, J. A., and Nogee, L. M. (2009). Genetic Disorders of Surfactant Dysfunction. *Pediatr. Dev. Pathol.* 12, 253–274. doi:10.2350/09-01-0586.1

Whitsett, J. A. (2014). The Molecular Era of Surfactant Biology. *Neonatology* 105, 337–343. doi:10.1159/000360649

Woods, P. S., Doolittle, L. M., Rosas, L. E., Joseph, L. M., Calomeni, E. P., and Davis, I. C. (2016). Lethal H1N1 Influenza a Virus Infection Alters the Murine Alveolar Type II Cell Surfactant Lipidome. *Am. J. Physiology-Lung Cell Mol. Physiol.* 311, L1160–L1169. doi:10.1152/ajplung.00339.2016

Xu, H. N., Lin, Z., Gandhi, C. K., Amatya, S., Wang, Y., Li, L. Z., et al. (2020). Sex and SP-A2 Dependent NAD(H) Redox Alterations in Mouse Alveolar Macrophages in Response to Ozone Exposure: Potential Implications for COVID-19. *Antioxidants* 9, 915–919. doi:10.3390/antiox9100915

Zhang, H., Fan, Q., Wang, Y. E., Neal, C. R., and Zuo, Y. Y. (2011). Comparative Study of Clinical Pulmonary Surfactants Using Atomic Force Microscopy. *Biochim. Biophys. Acta (Bba) - Biomembranes* 1808, 1832–1842. doi:10.1016/j.bbamem.2011.03.006

Zhang, L.-N., Sun, J.-P., xue, X.-Y., and Wang, J.-X. (2013). Exogenous Pulmonary Surfactant for Acute Respiratory Distress Syndrome in Adults: A Systematic Review and Meta-Analysis. *Exp. Ther. Med.* 5, 237–242. doi:10.3892/etm.2012.746

Conflict of Interest: The authors declare that the research was conducted in the absence of any commercial or financial relationships that could be construed as a potential conflict of interest.

frontiers in Pharmacology

REVIEW
published: 16 July 2021
doi: 10.3389/fphar.2021.720283

The Role of High-Density Lipoprotein in COVID-19

*Guyi Wang[1], Jiayi Deng[1], Jinxiu Li[1], Chenfang Wu[1], Haiyun Dong[1], Shangjie Wu[2] and Yanjun Zhong[1]**

[1]Department of Critical Care Medicine, The Second Xiangya Hospital, Central South University, Changsha, China, [2]Department of Respiratory, The Second Xiangya Hospital, Central South University, Changsha, China

The current Coronavirus disease 2019 (COVID-19) pandemic has become a global challenge. Managing a large number of acutely ill patients in a short time, whilst reducing the fatality rate and dealing with complications, brings unique difficulties. The most striking pathophysiological features of patients with severe COVID-19 are dysregulated immune responses and abnormal coagulation function, which can result in multiple-organ failure and death. Normally metabolized high-density lipoprotein (HDL) performs several functions, including reverse cholesterol transport, direct binding to lipopolysaccharide (LPS) to neutralize LPS activity, regulation of inflammatory response, anti-thrombotic effects, antioxidant, and anti-apoptotic properties. Clinical data shows that significantly decreased HDL levels in patients with COVID-19 are correlated with both disease severity and mortality. However, the role of HDL in COVID-19 and its specific mechanism remain unclear. In this analysis, we review current evidence mainly in the following areas: firstly, the pathophysiological characteristics of COVID-19, secondly, the pleiotropic properties of HDL, thirdly, the changes and clinical significance of HDL in COVID-19, and fourthly the prospect of HDL-targeting therapy in COVID-19 to clarify the role of HDL in the pathogenesis of COVID-19 and discuss the potential of HDL therapy in COVID-19.

Keywords: COVID-19, SARS-CoV-2, lipoproteins, HDL, angiotensin-converting enzyme 2

OPEN ACCESS

Edited by:
Brijesh Kumar Singh, Duke-NUS Medical School, Singapore

Reviewed by:
Abhigyan Satyam, Harvard Medical School, United States
Kristen M. Tecson, Baylor Scott & White Research Institute (BSWRI), United States

****Correspondence:***
Yanjun Zhong
zhongyanjun@csu.edu.cn

Specialty section:
This article was submitted to Experimental Pharmacology and Drug Discovery, a section of the journal Frontiers in Pharmacology

Received: *04 June 2021*
Accepted: *06 July 2021*
Published: *16 July 2021*

Citation:
Wang G, Deng J, Li J, Wu C, Dong H, Wu S and Zhong Y (2021) The Role of High-Density Lipoprotein in COVID-19. Front. Pharmacol. 12:720283. doi: 10.3389/fphar.2021.720283

INTRODUCTION

Coronavirus disease 2019 (COVID-19), caused by severe acute respiratory syndrome coronavirus 2 (SARS-CoV-2), outbroke in Wuhan in late 2019 (Guan W.-J. et al., 2020; Wang et al., 2020a; Huang C. et al., 2020; Hui et al., 2020; Lu et al., 2020). It has since spread worldwide (Albarello et al., 2020; Giunta et al., 2020; Young et al., 2020). By June 30, 2021, more than 180 million people have been infected with SARS-CoV-2, and nearly four million have died globally (WHO, 2021a). The COVID-19 pandemic has become a significant burden on global healthcare systems. Patients with COVID-19 with underlying metabolic dysfunction, such as type 2 diabetes and non-alcoholic fatty liver disease, have a higher risk of poor outcomes (Guan W.-j. et al., 2020; Mahamid et al., 2020; Ji et al., 2021). A decline in total cholesterol, high-density lipoprotein (HDL), and low-density lipoprotein (LDL) levels in patients with COVID-19 has been observed in several studies, including our previous research (Wei et al., 2020a; Wang et al., 2020b). Our data also shows that among the several lipids named above, only HDL was associated with the severity of COVID-19 (Wang G. et al., 2020). In this review, we aim to analyze the available evidence about how HDL dysfunction is associated with infection, including a focus on COVID-19.

SARS-COV-2

SARS-CoV-2 is a positive-sense, single-stranded RNA virus, surrounded by an envelope (Han et al., 2020; Kočar et al., 2021). SARS-CoV-2 is reported to share 79.6% homology with SARS-CoV (Zhou F. et al., 2020). The highly pathogenic CoVs, including Middle East Respiratory Syndrome (MERS) CoV, SARS-CoV-1, and SARS-CoV-2, mainly invade the lower respiratory tract through the upper respiratory tract and result in fatal pneumonia (Han et al., 2020).

SARS-CoV-2 entry into susceptible host tissue cells depends on the host cell angiotensin-converting-enzyme 2 (ACE2) receptor via the spike (S) protein, followed by S protein cleaving and membrane fusion (Chambers et al., 2020). ACE2 is widely expressed in human tissues, including in lung alveolar epithelial cells, small intestinal epithelial cells, vascular endothelial cells and smooth muscle cells within the lung, kidney, intestines, and other organs (Kočar et al., 2021).

PATHOPHYSIOLOGICAL CHARACTERISTICS OF COVID-19

COVID-19 causes significant infection-related morbidity and mortality. There have been about 33 million positive cases and nearly 600 thousand deaths in America (WHO, 2021b), while in China, there have been about 118 thousand positive cases and about five thousand deaths (WHO, 2021c). A recent meta-analysis of 212 studies from 11 countries/regions involving 281,461 individuals showed about 22.9% of patients with COVID-19 had severe disease and 5.6% patients die (Li J. et al., 2021). The most striking pathophysiological feature of patients with severe COVID-19 is a dysregulated immune response, characterized by lymphopenia and a cytokine storm, which results in acute respiratory distress syndrome, hepatic dysfunction, multiple-organ failure, and ultimately death. Abnormal coagulation function is also a prominent feature in severe COVID-19 cases (Beltrán-García et al., 2020; José et al., 2020; Song et al., 2020; Zafer et al., 2021).

Dysregulated Immune Responses

SARS-CoV-2 may activate both innate and adaptive immune responses in patients, including lymphopenia, cytokine release syndrome, and abnormal activation of macrophages and their complement system (Jamal et al., 2021). Lymphopenia, involving a drastic reduction in T-cells and B cells (Qin et al., 2020a; Tan et al., 2020; Xu et al., 2020), is a common feature in patients with severe COVID-19. This is possibly triggered by SARS-CoV-2-induced activation of apoptosis in lymphocytes (Xiong et al., 2020).

Patients with COVID-19 have also shown monocyte/macrophages morphological and physiological changes. These monocytes were characterized by mixed M1/M2 polarization, relatively elevated $CD80^+$ and $CD206^+$ expression, and higher secretion of interleukin (IL)-6, IL-10, and tumor necrosis factor (TNF)-α (Zhang D. et al., 2021). Macrophages infiltrated into the lungs of patients with COVID-19 were mostly type 1 (Yao et al., 2020). Monocytes obtained from patients with COVID-19 were shown to express ACE2 receptors, suggesting SARS-CoV-2 may directly infect and affect monocytes and macrophages in COVID-19 (Zhang Y. et al., 2021). Additionally, cytokine storms were common in patients with severe COVID-19. Patients exhibited increased cytokine secretion, particularly IL-2, IL-4, IL-6, IL-10, TNF-α, and interferon (IFN)-γ (Qin et al., 2020b). The possible causes of this cytokine release syndrome could be a dysregulated immune response incapable of controlling the production of excessive amounts of cytokines and chemokine.

The complement system was also considered to play a pivotal role in COVID-19. A recent study showed that complement components of the classical (C1q, C4d) and alternative (Factor H, C3d) pathways were deposited in the lungs of people with COVID-19, indicating the activation of complement system in COVID-19 (Satyam et al., 2021). Early clinical reports indicates that C3 inhibition therapy holds potential anti-inflammatory properties in COVID-19 (Mastaglio et al., 2020; Satyam and Tsokos, 2020) and anti-complement C5 therapy in patients with severe COVID-19 lead to a drop in inflammatory markers and a successful recovery (Diurno et al., 2020; Satyam and Tsokos, 2020).

Abnormal Coagulation

Abnormal coagulation function is also a prominent feature in severe COVID-19 cases. Severe COVID-19 was associated with widespread activation of the coagulation system, corroborated by elevated activated partial thromboplastin time (APTT) and prothrombin time (PT) along with markedly elevated D-dimer levels (Tang et al., 2020; Zhou P. et al., 2020). Severe endothelial injury and widespread thrombosis with microangiopathy are evident in lungs from patients with COVID-19 (Ackermann et al., 2020). Possible causes include a direct attack by the virus on the endothelial cells via ACE-2 receptors (Ackermann et al., 2020), and cytokine storms such as TNF and IL-6, which are potent activators of the tissue factor (TF)-dependent coagulation cascade (Tijburg et al., 1991; Kerr et al., 2001).

COMPOSITION, METABOLISM AND FUNCTION OF HDL

HDL is a type of lipoprotein with an extremely heterogeneous composition, density, and particle size, containing cholesterol, phospholipids, triglycerides, and apolipoproteins. It was first isolated from blood in the 1960s by ultracentrifugation. Among all types of human plasma lipoproteins, HDL, mainly synthesized in the liver and small intestine, has the highest density and smallest volume in the circulatory system. Apolipoprotein A-I (ApoA-I) is the main structural protein component of HDL, and other protein components such as serum amyloid A (SAA), lecithin cholesterol acyltransferase (LCAT), paraoxonase-1 (PON-1) and cholesterol ester transfer protein (CETP) also participate in the metabolic process of HDL (Gordon et al., 1989; Ginsberg, 1998; Tosheska Trajkovska and Topuzovska, 2017).

Reverse Cholesterol Transport

Normally metabolized HDL has various functions. The most important and well characterized function is the regulation of reverse cholesterol transport. During the formation and maturation of HDL, its main functional protein, ApoA-I, continuously binds to free cholesterol in tissue cells, and is then transported to the liver. Thus, cholesterol is excreted from the body's tissue cells through a series of transport and transformation processes, which reduces the cholesterol level in the body and delays the occurrence and progression of coronary heart disease (Gordon et al., 1989; Rader, 2003; Tosheska Trajkovska and Topuzovska, 2017).

Direct Binding to Lipopolysaccharide and Neutralizing LPS Activity

LPS is the chief component of the outer membrane of Gram-negative bacteria. Numerous studies have found that HDL prevents systemic endotoxemia by binding and neutralizing LPS (Parker et al., 1995), which is considered to be the main mechanism of HDL's antimicrobial effect (Ulevitch et al., 1979; Freudenberg et al., 1980). Early studies have shown that HDL can prevent the activation of peripheral blood monocytes and macrophages by LPS, and reduce the synthesis and secretion of inflammatory cytokines such as TNF-α and IL-1β (Levine et al., 1993). *In vivo* studies have shown that the initiation of intravenous infusion of recombinant HDL prior to induction of endotoxemia in healthy volunteers significantly reduced TNF, IL-6, and IL-8 levels, as well as reducing endotoxin-induced clinical symptoms and leukocyte activation (Pajkrt et al., 1996). A recent study showed that, compared with normal mice, ApoA-I (the main component of HDL) knockout mice showed increased production of inflammatory cytokines, decreased ability to neutralize and clear LPS, and reduced survival (Guo et al., 2013). In addition to binding and neutralizing LPS, HDL also promotes LPS clearance, mainly binding with SR-B1 and mediating LPS intake. It has been reported that in LPS-induced endotoxemia and cecal ligation and puncture (CLP) sepsis models *in vitro*, SR-B1 gene deletion mice showed decreased endotoxin clearance (Cai et al., 2008; Guo et al., 2009).

Regulation of Inflammatory Response

HDL may also be a key regulator of inflammatory response. *In-vitro* cell experiments show that HDL inhibits a subset of LPS-stimulated macrophage genes that regulate the type I interferon response via microarray analysis (Suzuki et al., 2010). HDL also down-regulates the expression of Toll-like receptor (TLR)-induced pro-inflammatory cytokines through the transcriptional regulator activating transcription factor 3 (ATF3) (De Nardo et al., 2014). Transgenic mice with 2-fold-elevated plasma HDL levels had lower plasma cytokine levels, and improved survival rates in an endotoxemia mouse model (Levine et al., 1993).

Anti-Thrombotic Effects

HDL can act as a regulator of platelet and coagulation responses in a variety of ways. Numerous epidemiological studies have established an inverse correlation between HDL levels and the risk of thrombosis (Sharrett et al., 2001; Deguchi et al., 2005; Lüscher et al., 2014), and many studies have explored the mechanisms involved. HDL stimulates NO and prostacyclin production in endothelial cells which are both inhibitors of platelet activation (Van Sickle et al., 1986; Yuhanna et al., 2001; Calabresi et al., 2003). Endothelial cells express TF after thrombin-induction in acute coronary syndromes, and HDL presents an atheroprotective effect by inhibiting thrombin-induced human endothelial TF expression (Viswambharan et al., 2004). HDL, mainly ApoA-I, also protects endothelial cells against oxidized LDL (oxLDL) and prevents its apoptosis (Suc et al., 1997). Additionally, purified HDL enhances inactivation of coagulation factor Va by activated protein C (APC) and protein S (Griffin et al., 1999). ApoA-I also neutralizes the procoagulant properties of anionic phospholipids, and incorporation of ApoA-I in anionic vesicles prevents the formation of the prothrombinase complex (Oslakovic et al., 2009; Oslakovic et al., 2010).

Antioxidant and Anti-Apoptotic Properties

HDL can prevent intracellular reactive oxygen species (ROS) production, triggered by oxLDL or H_2O_2, thereby inhibiting the subsequent proteasome activation, and NF-kappa B activation (Robbesyn et al., 2003). HDL exerts a protective effect against oxidative damage induced by copper ions (Ferretti et al., 2003). Additionally, PON-1 is an HDL-associated esterase, which protects lipoproteins against oxidation. It is demonstrated that PON-1-deficient mice were susceptible to oxidative stress and HDL isolated from these mice were unable to prevent LDL oxidation (Shih et al., 1998).

HDL was shown to have the capacity to inhibit apoptosis of endothelial cells induced by oxLDL (Suc et al., 1997). HDL also prevented caspase-3 and caspase-9 activation, as well as apoptotic alterations of the plasma membrane (Nofer et al., 2001). In addition, HDL reduced cardiomyocyte apoptosis in a mouse model of myocardial ischemia/reperfusion (Theilmeier et al., 2006).

HDL CHANGES DURING HUMAN INFECTION

Changes in Levels or Functions of HDL

Levels and functions of HDL changed significantly in patients infected with different pathogens. Multiple studies show HDL decreased in many infections, including sepsis, nosocomial infections, dengue, Helicobacter pylori infection, and HIV infection (Canturk et al., 2002; van Leeuwen et al., 2003; Chien et al., 2005; Rose et al., 2006; Jia et al., 2009; Aragonès et al., 2010; Baker et al., 2010; Zou et al., 2016; Cirstea et al., 2017; Tanaka et al., 2017; Barrientos-Arenas et al., 2018). The explanations includes decreased HDL synthesis, over-consumption of HDL particles, or HDL redistribution from intravascular to extravascular space (Pirillo et al., 2015; Tanaka et al., 2020a; Cao et al., 2020). Infection not only leads to a decrease in HDL levels, but also affects its function. HDL from HIV+ individuals has reduced antioxidant function (Angelovich

et al., 2017), modified HDL metabolism, and reduced functionality of reverse cholesterol transport (Rose et al., 2008). In mice models, HDL loses its anti-inflammatory properties after acute influenza infection (Van Lenten et al., 2001).

Relationship Between HDL, Susceptibility of Infection and Outcome

Low serum HDL levels seem to be associated with a higher risk of infectious diseases, including sepsis (Shor et al., 2008; Grion et al., 2010), nosocomial infection after surgery (Delgado-Rodriguez et al., 1997; Canturk et al., 2002), and in-hospital infection in patients with acute ischemic stroke (Rodríguez-Sanz et al., 2013). Furthermore, a prospective population-based cohort study involving more than 100,000 patients showed a U-shaped association of HDL with the risk of infectious disease, and that both high and low levels of HDL were related with a high risk of infection (Madsen et al., 2018). In addition, mortality rates, intensive care unit (ICU) stay, and length of hospital stay, all increased among septic patients with lower levels of HDL or ApoA-I (Chien et al., 2005; Montero-Chacón et al., 2020). Low HDL level at admission was also associated with severe sepsis (Grion et al., 2010). Lower HDL may herald a bad outcome, while higher levels of HDL seem to have a protective effect toward infection.

Therapeutic Strategy Targeting HDL in Infection

Due to the important role of HDL in infection, therapeutic strategy targeting HDL is considered as a possible new approach to the treatment of infection. Reconstituted HDL was shown to reduce inflammation and bacterial burden, attenuate organ injury and improve survival in experimental septic models (Levine et al., 1993; McDonald et al., 2003; Tanaka et al., 2020b; Tanaka et al., 2020c). Trypanosome lytic factor, as a minor subfraction of HDL, ameliorates Leishmania infection, possibly due to the ability to selectively damage pathogens in phagolysosomes (Samanovic et al., 2009). CETP is a key regulator of HDL levels. Its gain-of-function variant was significantly associated with an increased risk of mortality in sepsis (Trinder et al., 2019). CETP inhibitor Anacetrapib preserved levels of HDL and ApoA-I and increased the survival rate in CLP sepsis models (Trinder et al., 2021).

ASSOCIATION BETWEEN HDL AND COVID-19

Alteration of HDL Level in Patients With COVID-19

A large number of studies have shown a close correlation of HDL with COVID-19, which were summarized in **Table 1**. The serum HDL level in patients with COVID-19 was lower than that in healthy controls (Huang et al., 2021). A genome-wide association study (GWAS) summary analysis of 7362 COVID-19 participants from the United Kingdom Biobank, showed that individuals with a lower level of HDL were more vulnerable to SARS-CoV-2 infection (Zhang D. et al., 2021). A clinical observational study also found that lower HDL levels were related to a higher risk of SARS-CoV-2 infection (Aung et al., 2020), while higher HDL levels were associated with a lower risk of SARS-CoV-2 infection (Ho et al., 2020).

Changes of HDL Function in Patients With COVID-19

In addition to HDL levels, the composition and functions of HDL in COVID-19 were also changed. ApoA-I and PON-1 were less abundant in patients with COVID-19, whereas, using proteomic analyses, SAA and alpha-1 antitrypsin were found to be higher (Begue et al., 2021). HDL from patients with COVID-19 showed less protection in TNF-α treated endothelial cells (Begue et al., 2021). Generally, patients with diabetes and elderly patients showed a higher extent of glycation (Kawasaki et al., 2002; Park and Cho, 2011). Glycated HDL showed much lower antivirus activity against SARS-CoV-2 than that of native HDL, which may explain why older patients and patients with underlying conditions such as diabetes are more likely to develop severe illness and death in COVID-19 (Cho et al., 2021).

Relationship of HDL With the Outcomes of Patients With COVID-19

Additionally, HDL or ApoA-I levels were significantly lower in severe, critically ill and mortality groups compared to patients with mild COVID-19 (Wang et al., 2020b; Huang C. et al., 2020; Ouyang et al., 2020; Xie et al., 2020; Zhang Q. et al., 2020; Hilser et al., 2021; Li J. et al., 2021; Turgay Yıldırım and Kaya, 2021). This suggests that HDL is associated with COVID-19 severity and risk of death (Tanaka et al., 2020b; Hu et al., 2020; Wang et al., 2020; Wei X. et al., 2020; Zhang B. et al., 2020). During ICU hospitalization in patients with COVID-19, in cases of bacterial superinfection, low HDL concentrations were also found to be correlated with higher mortality (Tanaka et al., 2020c). Significantly, in patients with severe COVID-19, a gradual increase of HDL levels during hospitalization could suggest a path to gradual recovery (Qin et al., 2020a). Moreover, HDL levels influenced the virus shedding duration in patients with COVID-19 (Ding et al., 2020) and may predict the risk of hospitalization for COVID-19 (Hamer et al., 2020; Lassale et al., 2021). This data strongly suggests that high HDL levels might be beneficial in patients with COVID-19 through its antiviral activity.

The Possible Mechanism of HDL Action in COVID-19

Lipid metabolism plays an essential role during SARS-CoV-2 infection. Cholesterol is widely shown to interact with SARS-CoV-2 S protein (Kočar et al., 2021). The accumulation of lipids was observed in SARS-CoV-2 infected cells, both *in vitro* and in the lungs of patients of COVID-19 (Nardacci et al., 2021). In a cell experiment *in vitro*, HDL showed an obvious antiviral effect on

TABLE 1 | Changes in HDL levels in patients with COVID-19.

Author	Country	Number of patients	Time point	Comparison of HDL levels
Wang (Wang et al. (2020a)	China	228	Within 24 h after admission	COVID-19 patients vs healthy control: median, 0.78 vs 1.37 mmol/L, $p < 0.001$ Severe vs non-severe patients: median, 0.69 vs 0.79 mmol/L, $p = 0.032$
Huang (Huang et al. (2021)	China	218	The 1st day of admission	COVID-19 patients vs healthy control: mean, 1.02 vs 1.52 mmol/L, $p < 0.05$ Severe vs non-severe patients: mean, 0.83 vs 1.15 mmol/L, $p < 0.05$
Zhang (Zhang B. et al. (2020)	China	74	Not known	Severe vs non-severe patients: median, 0.92 vs 1.08 mmol/L, $p = 0.021$
Xie (Xie et al. (2020)	China	62	Not known	Severe vs non-severe patients with CVD: median, 1.1 vs 1.4 mmol/L Severe vs non-severe patients without CVD: median, 1.1 vs 1.3 mmol/L
Hu (Hu et al. (2020)	China	114	On admission	COVID-19 patients vs healthy control: mean, 1.08 vs 1.27 mmol/L, $p < 0.001$ Severe vs non-severe patients: median, 1.01 vs 1.21 mmol/L, $p < 0.001$
Wei (Wei et al. (2020b)	China	597	Not known	Mild vs severe vs critical patients: median, 50 vs 50 vs 36 mg/dL, $p < 0.05$
Tanaka (Tanaka et al. (2020a)	France	48	Upon ICU admission	Alive vs dead patients on day 28: median, 0.6 vs 0.5 mmol/L, $p = 0.036$
Huang (Huang W. et al. (2020)	China	2,623	At admission	Critical vs non-critical patients: median, 0.86 vs 0.95 mmol/L, $p < 0.001$
Sun (Sun et al. (2020)	China	99	Within 24 h of admission	Mild vs severe: median, 1.18 vs 0.94, $p < 0.001$
Ouyang (Ouyang et al. (2020)	China	107	Last result	Survivors vs non-survivors: average, 1.07 vs 0.79 mmol/L, $p = 0.006$
Li (Li Y. et al. (2021)	China	424	Not known	Survivors vs non-survivors: median, 0.9 vs 0.8, $p = 0.001$
Turgay (Turgay Yıldırım and Kaya (2021)	Turkey	139	At admission	Survivors vs non-survivors: median, 44.0 vs 28.5 mg/dL, $p < 0.001$

Abbreviations: HDL, high-density lipoprotein; COVID-19, Coronavirus disease 2019.

SARS-CoV-2 via cytopathic effect (CPE) and inhibition activity tests (Cho et al., 2021). Although HDL is believed to play a protective role in infection, some studies have come to the opposite conclusion. Several studies showed HDL facilitated SARS-CoV-2 infection. It was found that HDL significantly increased cell-surface SARS-CoV-2-S binding, viral entry and replication *in vitro* through SR-B1. Blockade of the cholesterol-binding site on SARS-CoV-2 or treatment with HDL SR-B1 antagonists, inhibits HDL-enhanced SARS-CoV-2 infection (Wei et al., 2020a). Another study showed that pretreatment of 293T cells with an HDL antagonist, in the presence of HDL, strongly inhibited the entry of SARS-CoV-2 into host cells (Wei et al., 2020). It suggested that the down-regulation of HDL levels in patients with COVID-19 may be due to HDL consumption during viral invasion, and HDL or SR-B1 could be treatment targets for COVID-19. However, future studies will need to explore the molecular nature of the interaction between HDL and SARS-CoV-2.

Additionally, clinical data showed influencing the inflammatory response may be one of the mechanisms of HDL involvement in the pathophysiology of COVID-19. Severe COVID-19 is considered to be a sepsis induced by SARS-CoV-2 (Colantuoni et al., 2020; Lin, 2020; Shenoy, 2020), which is characterized by excessive inflammation and multiple-organ failure. It is reported that a marked increase in inflammatory factors occurs in COVID-19, including C-reactive protein (CRP), IL-6, TNF-α, etc. (Song et al., 2020; Zafer et al., 2021). ApoA-1 and HDL levels were shown to be negatively correlated with CRP and IL-6 levels in patients with COVID-19 (Hu et al., 2020; Sun et al., 2020), suggesting that the increased inflammatory response related to reduced HDL levels is one of the pathogenic mechanisms of COVID-19.

Moreover, apoptosis, oxidative stress and abnormal blood coagulation are all involved in the pathophysiological process of COVID-19 (Tang et al., 2020; Cizmecioglu et al., 2021; Mehri et al., 2021), and multiple studies demonstrated HDL had anti-thrombotic, anti-apoptotic and anti-oxidative effects (Tanaka et al., 2020a), which offers a possibility that HDL may also regulate these pathways in COVID-19. However, further research is needed to confirm these conclusions.

Therapeutic Strategy of COVID-19 Through Targeting HDL

Until now effective therapeutic interventions for COVID-19 are limited. Drug repurposing could identify potential treatments in a short time, which has become an important approach to explore therapeutic agents for COVID-19 (Kost-Alimova et al., 2020). As many studies have found that HDL is closely linked to COVID-19, some related randomized controlled trial (RCT) studies remain ongoing (**Table 2**). Omega-3 polyunsaturated fatty acids (PUFAs) improve lipid metabolism by reducing triglyceride and increasing HDL (Yanai et al., 2018), which enhance patient's immune function and reduce inflammatory

TABLE 2 | Clinical studies about drugs that affect HDL on patients with COVID-19.

Therapy	ClinicalTrials.gov Identifier	Mechanism of action	Effect on HDL
Dalcetrapib	NCT04676867	CETP inhibitor	Raise HDL levels
Omega3-FA	NCT04658433	Multifactorial	Raise HDL levels or affect HDL metabolism
	NCT04553705		
	NCT04483271		
Fenofibrate	NCT04517396	PPAR-alpha activator	Raise HDL levels
Atorvastatin	NCT04801940	HMG-CoA reductase inhibitors	Raise HDL levels
	NCT04631536		
	NCT04486508		
	NCT04466241		
	NCT04380402		
Rosuvastatin	NCT04472611	HMG-CoA reductase inhibitors	Raise HDL levels
	NCT04359095		
Simvastatin	NCT04348695	HMG-CoA reductase inhibitors	Raise HDL levels
	NCT04343001		

Abbreviations: HDL, high-density lipoprotein; COVID-19, Coronavirus disease 2019; HMG-CoA, 3-hydroxy-3-methylglutaryl coenzyme A; CETP, cholesteryl ester transfer protein; PPAR, peroxisome proliferator-activated receptor; FA, fatty acids.

responses (Ni et al., 2020; Sorokin et al., 2020). Subsequently, as it is considered to have a positive role in the treatment of COVID-19, it has become the most studied lipid-regulating drug in COVID-19. Statins, including Atorvastatin, Rosuvastatin, and Simvastatin also showed HDL-increasing capacity (Jones et al., 2003; Miller et al., 2004; Rosenson, 2005; Sasaki et al., 2013), and are one of the current research hotspots of COVID-19. Moreover, RCT studies on the effects of two classic HDL-increasing drugs, CETP inhibitor Dalcetrapib and Fenofibrate, in patients with COVID-19, are also underway. Other HDL-raising pharmacological compounds such as LCAT, have been also considered as potential therapies for COVID-19 (Sorokin et al., 2020).

CONCLUSION

COVID-19 has spread globally and caused significant morbidity and mortality. Patients with severe COVID-19 are characterized by a dysregulated immune response and abnormal coagulation function, which results in organ dysfunction and ultimately death. HDL possesses several well-documented functions, including regulating immune response, neutralizing endotoxins, anti-oxidation, anti-apoptosis, and anti-thrombosis formation. Multiple studies showed that HDL level, composition and functions were greatly changed in COVID-19 and lower HDL level was correlated with higher risks of severity and mortality, indicating that high HDL levels might be beneficial in COVID-19. HDL level-raising pharmacological compounds such as CETP inhibitors and fibrates are considered to be potential treatments for patients with COVID-19, and they are already in the preclinical research stage. Until now, there are still relatively few studies on the mechanisms about the protective role of HDL in COVID-19. Notably, many studies related to sepsis support that increasing the levels of HDL in septic patients may be a feasible treatment target. However, simply increasing the level of HDL does not seem to be enough to restore the function of HDL. Therefore, we still need to comprehensively understand the mechanism of HDL action in COVID-19 and improve new strategies for the treatment of patients with COVID-19, by further in-depth study on the composition, structure, and function of HDL in COVID-19.

AUTHOR CONTRIBUTIONS

Conceptualization, YZ and GW; methodology, YZ; software, JD; validation, YZ; formal analysis, YZ; investigation, JD; resources, JD; data curation, YZ; writing–original draft preparation, GW; writing–review and editing, YZ; supervision, JL, CW, HD, and SW. All authors have read and agreed to the published version of the manuscript.

FUNDING

This research was funded by Scientific Research Project of Hunan Provincial Health Commission, grant number 202117010786.

REFERENCES

Ackermann, M., Verleden, S. E., Kuehnel, M., Haverich, A., Welte, T., Laenger, F., et al. (2020). Pulmonary Vascular Endothelialitis, Thrombosis, and Angiogenesis in Covid-19. *N. Engl. J. Med.* 383, 120–128. doi:10.1056/NEJMoa2015432

Albarello, F., Pianura, E., Di Stefano, F., Cristofaro, M., Petrone, A., Marchioni, L., et al. (2020). 2019-novel Coronavirus Severe Adult Respiratory Distress Syndrome in Two Cases in Italy: An Uncommon Radiological Presentation. *Int. J. Infect. Dis.* 93, 192–197. doi:10.1016/j.ijid.2020.02.043

Angelovich, T. A., Hearps, A. C., Oda, M. N., Borja, M. S., Huynh, D., Homann, S., et al. (2017). Dysfunctional High-Density Lipoprotein from HIV+ Individuals Promotes Monocyte-Derived Foam Cell Formation *In Vitro*. *Aids* 31, 2331–2336. doi:10.1097/qad.0000000000001642

Aragonès, G., Beltrán-Debón, R., Rull, A., Rodríguez-Sanabria, F., Fernández-Sender, L., Camps, J., et al. (2010). Human Immunodeficiency Virus-Infection Induces Major Changes in High-Density Lipoprotein Particle Size Distribution

and Composition: The Effect of Antiretroviral Treatment and Disease Severity. *Clin. Chem. Lab. Med.* 48, 1147–1152. doi:10.1515/cclm.2010.218

Aung, N., Khanji, M. Y., Munroe, P. B., and Petersen, S. E. (2020). Causal Inference for Genetic Obesity, Cardiometabolic Profile and COVID-19 Susceptibility: A Mendelian Randomization Study. *Front. Genet.* 11, 586308. doi:10.3389/fgene.2020.586308

Baker, J., Ayenew, W., Quick, H., Hullsiek, K. H., Tracy, R., Henry, K., et al. (2010). High-Density Lipoprotein Particles and Markers of Inflammation and Thrombotic Activity in Patients with Untreated HIV Infection. *J. Infect. Dis.* 201, 285–292. doi:10.1086/649560

Barrientos-Arenas, E., Henao-García, V., Giraldo, D. M., Cardona, M. M., Urcuqui-Inchima, S., Castaño, J. C., et al. (2018). Modulación de los niveles de lipoproteínas de alta densidad y las citoquinas IL-1β e IL-6 en pacientes con dengue. *Rev. Peru Med. Exp. Salud Publica* 35, 15–24. doi:10.17843/rpmesp.2018.351.3568

Begue, F., Tanaka, S., Mouktadi, Z., Rondeau, P., Veeren, B., Diotel, N., et al. (2021). Altered High-Density Lipoprotein Composition and Functions During Severe COVID-19. *Sci. Rep.* 11, 2291. doi:10.1038/s41598-021-81638-1

Beltrán-García, J., Osca-Verdegal, R., Pallardó, F. V., Ferreres, J., Rodríguez, M., Mulet, S., et al. (2020). Oxidative Stress and Inflammation in COVID-19-Associated Sepsis: The Potential Role of Anti-oxidant Therapy in Avoiding Disease Progression. *Antioxidants* 9, 936. doi:10.3390/antiox9100936

Cai, L., Ji, A., De Beer, F. C., Tannock, L. R., and Van Der Westhuyzen, D. R. (2008). SR-BI Protects against Endotoxemia in Mice through its Roles in Glucocorticoid Production and Hepatic Clearance. *J. Clin. Invest.* 118, 364–375. doi:10.1172/jci31539

Calabresi, L., Rossoni, G., Gomaraschi, M., Sisto, F., Berti, F., and Franceschini, G. (2003). High-Density Lipoproteins Protect Isolated Rat Hearts From Ischemia-Reperfusion Injury by Reducing Cardiac Tumor Necrosis Factor-α Content and Enhancing Prostaglandin Release. *Circ. Res.* 92, 330–337. doi:10.1161/01.res.0000054201.60308.1a

Canturk, N., Canturk, Z., Okay, E., Yirmibesoglu, O., and Eraldemir, B. (2002). Risk of Nosocomial Infections and Effects of Total Cholesterol, HDL Cholesterol in Surgical Patients. *Clin. Nutr.* 21, 431–436. doi:10.1054/clnu.2002.0575

Cao, X., Yin, R., Albrecht, H., Fan, D., and Tan, W. (2020). Cholesterol: A New Game Player Accelerating Endothelial Injuries Caused by SARS-CoV-2? *Am. J. Physiol. Endocrinol. Metab.* 319, E197–e202. doi:10.1152/ajpendo.00255.2020

Chambers, J. P., Yu, J., Valdes, J. J., and Arulanandam, B. P. (2020). SARS-CoV-2, Early Entry Events. *J. Pathog.* 2020, 1–11. doi:10.1155/2020/9238696

Chien, J.-Y., Jerng, J.-S., Yu, C.-J., and Yang, P.-C. (2005). Low Serum Level of High-Density Lipoprotein Cholesterol Is a Poor Prognostic Factor for Severe Sepsis*. *Crit. Care Med.* 33, 1688–1693. doi:10.1097/01.ccm.0000171183.79525.6b

Cho, K.-H., Kim, J.-R., Lee, I.-C., and Kwon, H.-J. (2021). Native High-Density Lipoproteins (HDL) With Higher Paraoxonase Exerts a Potent Antiviral Effect against SARS-CoV-2 (COVID-19), While Glycated HDL Lost the Antiviral Activity. *Antioxidants* 10, 209. doi:10.3390/antiox10020209

Cirstea, M., Walley, K. R., Russell, J. A., Brunham, L. R., Genga, K. R., and Boyd, J. H. (2017). Decreased High-Density Lipoprotein Cholesterol Level Is an Early Prognostic Marker for Organ Dysfunction and Death in Patients with Suspected Sepsis. *J. Crit. Care* 38, 289–294. doi:10.1016/j.jcrc.2016.11.041

Cizmecioglu, A., Akay Cizmecioglu, H., Goktepe, M. H., Emsen, A., Korkmaz, C., Esenkaya Tasbent, F., et al. (2021). Apoptosis-induced T-cell Lymphopenia Is Related to COVID-19 Severity. *J. Med. Virol.* 93, 2867–2874. doi:10.1002/jmv.26742

Colantuoni, A., Martini, R., Caprari, P., Ballestri, M., Capecchi, P. L., Gnasso, A., et al. (2020). COVID-19 Sepsis and Microcirculation Dysfunction. *Front. Physiol.* 11, 747. doi:10.3389/fphys.2020.00747

De Nardo, D., Labzin, L. I., Kono, H., Seki, R., Schmidt, S. V., Beyer, M., et al. (2014). High-Density Lipoprotein Mediates Anti-inflammatory Reprogramming of Macrophages Via the Transcriptional Regulator ATF3. *Nat. Immunol.* 15, 152–160. doi:10.1038/ni.2784

Deguchi, H., Pecheniuk, N. M., Elias, D. J., Averell, P. M., and Griffin, J. H. (2005). High-Density Lipoprotein Deficiency and Dyslipoproteinemia Associated with Venous Thrombosis in Men. *Circulation* 112, 893–899. doi:10.1161/circulationaha.104.521344

Delgado-Rodríguez, M., Medina-Cuadros, M., Martínez-Gallego, G., and Sillero-Arenas, M. (1997). Total Cholesterol, HDL-Cholesterol, and Risk of Nosocomial Infection: A Prospective Study in Surgical Patients. *Infect. Control. Hosp. Epidemiol.* 18, 9–18. doi:10.1086/647494

Ding, X., Zhang, J., Liu, L., Yuan, X., Zang, X., Lu, F., et al. (2020). High-density Lipoprotein Cholesterol as a Factor Affecting Virus Clearance in Covid-19 Patients. *Respir. Med.* 175, 106218. doi:10.1016/j.rmed.2020.106218

Diurno, F., Numis, F. G., Porta, G., Cirillo, F., Maddaluno, S., Ragozzino, A., et al. (2020). Eculizumab Treatment in Patients with COVID-19: Preliminary Results from Real Life ASL Napoli 2 Nord Experience. *Eur. Rev. Med. Pharmacol. Sci.* 24, 4040–4047. doi:10.26355/eurrev_202004_20875

Ferretti, G., Bacchetti, T., Moroni, C., Vignini, A., and Curatola, G. (2003). Protective Effect of Human HDL against Cu(2+)-Induced Oxidation of Astrocytes. *J. Trace Elem. Med. Biol.* 17 Suppl 1 (Suppl. 1), 25–30.

Freudenberg, M. A., Bøg-Hansen, T. C., Back, U., and Galanos, C. (1980). Interaction of Lipopolysaccharides with Plasma High-Density Lipoprotein in Rats. *Infect. Immun.* 28, 373–380. doi:10.1128/iai.28.2.373-380.1980

Ginsberg, H. N. (1998). Lipoprotein Physiology. *Endocrinol. Metab. Clin. North America* 27, 503–519. doi:10.1016/s0889-8529(05)70023-2

Giunta, R. E., Frank, K., Costa, H., Demirdöver, C., Di Benedetto, G., Elander, A., et al. (2020). The COVID-19 Pandemic and its Impact on Plastic Surgery in Europe - an ESPRAS Survey. *Handchir Mikrochir Plast. Chir* 52, 221–232. doi:10.1055/a-1169-4443

Gordon, D. J., Probstfield, J. L., Garrison, R. J., Neaton, J. D., Castelli, W. P., Knoke, J. D., et al. (1989). High-density Lipoprotein Cholesterol and Cardiovascular Disease. Four Prospective American Studies. *Circulation* 79, 8–15. doi:10.1161/01.cir.79.1.8

Griffin, J. H., Kojima, K., Banka, C. L., Curtiss, L. K., and Fernández, J. A. (1999). High-density Lipoprotein Enhancement of Anticoagulant Activities of Plasma Protein S and Activated Protein C. *J. Clin. Invest.* 103, 219–227. doi:10.1172/jci5006

Grion, C. M. C., Cardoso, L. T. Q., Perazolo, T. F., Garcia, A. S., Barbosa, D. S., Morimoto, H. K., et al. (2010). Lipoproteins and CETP Levels as Risk Factors for Severe Sepsis in Hospitalized Patients. *Eur. J. Clin. Invest.* 40, 330–338. doi:10.1111/j.1365-2362.2010.02269.x

Guan, W.-J., Liang, W.-H., Zhao, Y., Liang, H.-R., Chen, Z.-S., Li, Y.-M., et al. (2020a). Comorbidity and its Impact on 1,590 Patients with COVID-19 in China: A Nationwide Analysis. *Eur. Respir. J.* 55 (5), 20027664. doi:10.1101/2020.02.25.20027664

Guan, W.-j., Ni, Z.-y., Hu, Y., Liang, W.-h., Ou, C.-q., He, J.-x., et al. (2020b). Clinical Characteristics of Coronavirus Disease 2019 in China. *N. Engl. J. Med.* 382, 1708–1720. doi:10.1056/NEJMoa2002032

Guo, L., Song, Z., Li, M., Wu, Q., Wang, D., Feng, H., et al. (2009). Scavenger Receptor BI Protects against Septic Death through its Role in Modulating Inflammatory Response. *J. Biol. Chem.* 284, 19826–19834. doi:10.1074/jbc.M109.020933

Guo, L., Ai, J., Zheng, Z., Howatt, D. A., Daugherty, A., Huang, B., et al. (2013). High Density Lipoprotein Protects against Polymicrobe-Induced Sepsis in Mice*. *J. Biol. Chem.* 288, 17947–17953. doi:10.1074/jbc.M112.442699

Hamer, M., Gale, C. R., Kivimäki, M., and Batty, G. D. (2020). Overweight, Obesity, and Risk of Hospitalization for COVID-19: A Community-Based Cohort Study of Adults in the United Kingdom. *Proc. Natl. Acad. Sci. USA.* 117, 21011–21013. doi:10.1073/pnas.2011086117

Han, Q., Lin, Q., Jin, S., and You, L. (2020). Coronavirus 2019-nCoV: A Brief Perspective from the Front Line. *J. Infect.* 80, 373–377. doi:10.1016/j.jinf.2020.02.010

Hilser, J. R., Han, Y., Biswas, S., Gukasyan, J., Cai, Z., Zhu, R., et al. (2021). Association of Serum HDL-Cholesterol and Apolipoprotein A1 Levels with Risk of Severe SARS-CoV-2 Infection. *J. lipid Res.* 62, 100061. doi:10.1016/j.jlr.2021.100061

Ho, F. K., Celis-Morales, C. A., Gray, S. R., Katikireddi, S. V., Niedzwiedz, C. L., Hastie, C., et al. (2020). Modifiable and Non-modifiable Risk Factors for COVID-19, and Comparison to Risk Factors for Influenza and Pneumonia: Results from a UK Biobank Prospective Cohort Study. *BMJ open* 10, e040402. doi:10.1136/bmjopen-2020-040402

Hu, X., Chen, D., Wu, L., He, G., and Ye, W. (2020). Declined Serum High Density Lipoprotein Cholesterol Is Associated with the Severity of COVID-19 Infection. *Clinica Chim. Acta* 510, 105–110. doi:10.1016/j.cca.2020.07.015

Huang, C., Wang, Y., Li, X., Ren, L., Zhao, J., Hu, Y., et al. (2020). Clinical Features of Patients Infected with 2019 Novel Coronavirus in Wuhan, China. *The Lancet* 395, 497–506. doi:10.1016/S0140-6736(20)30183-5

Huang, S., Zhou, C., Yuan, Z., Xiao, H., and Wu, X. (2021). The Clinical Value of High-Density Lipoprotein in the Evaluation of New Coronavirus Pneumonia. *Adv. Clin. Exp. Med.* 30, 153–156. doi:10.17219/acem/130606

Huang, W., Li, C., Wang, Z., Wang, H., Zhou, N., Jiang, J., et al. (2020). Decreased Serum Albumin Level Indicates Poor Prognosis of COVID-19 Patients: Hepatic Injury Analysis from 2,623 Hospitalized Cases. *Sci. China Life Sci.* 63, 1678–1687. doi:10.1007/s11427-020-1733-4

Hui, D. S., I Azhar, E., Madani, T. A., Ntoumi, F., Kock, R., Dar, O., et al. (2020). The Continuing 2019-nCoV Epidemic Threat of Novel Coronaviruses to Global Health - the Latest 2019 Novel Coronavirus Outbreak in Wuhan, China. *Int. J. Infect. Dis.* 91, 264–266. doi:10.1016/j.ijid.2020.01.009

Jamal, M., Bangash, H. I., Habiba, M., Lei, Y., Xie, T., Sun, J., et al. (2021). Immune Dysregulation and System Pathology in COVID-19. *Virulence* 12, 918–936. doi:10.1080/21505594.2021.1898790

Ji, D., Zhang, M., Qin, E., Zhang, L., Xu, J., Wang, Y., et al. (2021). Letter to the Editor: Obesity, Diabetes, Non-alcoholic Fatty Liver Disease and Metabolic Dysfunction Associated Fatty Liver Disease Are Proinflammatory Hypercoagulable States Associated with Severe Disease and Thrombosis in Covid-19. *Metabolism* 115, 154437. doi:10.1016/j.metabol.2020.154437

Jia, E.-Z., Zhao, F.-J., Hao, B., Zhu, T.-B., Wang, L.-S., Chen, B., et al. (2009). *Helicobacter pylori* Infection Is Associated with Decreased Serum Levels of High Density Lipoprotein, but Not with the Severity of Coronary Atherosclerosis. *Lipids Health Dis.* 8, 59. doi:10.1186/1476-511x-8-59

Jones, P. H., Davidson, M. H., Stein, E. A., Bays, H. E., Mckenney, J. M., Miller, E., et al. (2003). Comparison of the Efficacy and Safety of Rosuvastatin versus Atorvastatin, Simvastatin, and Pravastatin across Doses (STELLAR**STELLAR = Statin Therapies for Elevated Lipid Levels Compared across Doses to Rosuvastatin. Trial). *Am. J. Cardiol.* 92, 152–160. doi:10.1016/s0002-9149(03)00530-7

José, R. J., Williams, A., Manuel, A., Brown, J. S., and Chambers, R. C. (2020). Targeting Coagulation Activation in Severe COVID-19 Pneumonia: Lessons from Bacterial Pneumonia and Sepsis. *Eur. Respir. Rev.* 29, 200240. doi:10.1183/16000617.0240-2020

Kawasaki, T., Akanuma, H., and Yamanouchi, T. (2002). Increased Fructose Concentrations in Blood and Urine in Patients with Diabetes. *Diabetes Care* 25, 353–357. doi:10.2337/diacare.25.2.353

Kerr, R., Stirling, D., and Ludlam, C. A. (2001). Interleukin 6 and Haemostasis. *Br. J. Haematol.* 115, 3–12. doi:10.1046/j.1365-2141.2001.03061.x

Kočar, E., Režen, T., and Rozman, D. (2021). Cholesterol, Lipoproteins, and COVID-19: Basic Concepts and Clinical Applications. *Biochim. Biophys. Acta Mol. Cel Biol Lipids* 1866, 158849. doi:10.1016/j.bbalip.2020.158849

Kost-Alimova, M., Sidhom, E.-H., Satyam, A., Chamberlain, B. T., Dvela-Levitt, M., Melanson, M., et al. (2020). A High-Content Screen for Mucin-1-Reducing Compounds Identifies Fostamatinib as a Candidate for Rapid Repurposing for Acute Lung Injury. *Cel Rep. Med.* 1, 100137. doi:10.1016/j.xcrm.2020.100137

Lassale, C., Hamer, M., Hernáez, Á., Gale, C. R., and Batty, G. D. (2021). Association of Pre-pandemic High-Density Lipoprotein Cholesterol with Risk of COVID-19 Hospitalisation and Death: the UK Biobank Cohort Study. *medRxiv*. doi:10.1101/2021.01.20.21250152

Levine, D. M., Parker, T. S., Donnelly, T. M., Walsh, A., and Rubin, A. L. (1993). *In Vivo* protection against Endotoxin by Plasma High Density Lipoprotein. *Proc. Natl. Acad. Sci.* 90, 12040–12044. doi:10.1073/pnas.90.24.12040

Li, J., Huang, D. Q., Zou, B., Yang, H., Hui, W. Z., Rui, F., et al. (2021). Epidemiology of COVID-19: A Systematic Review and Meta-analysis of Clinical Characteristics, Risk Factors, and Outcomes. *J. Med. Virol.* 93, 1449–1458. doi:10.1002/jmv.26424

Li, Y., Zhang, Y., Lu, R., Dai, M., Shen, M., Zhang, J., et al. (2021). Lipid Metabolism Changes in Patients with Severe COVID-19. *Clinica Chim. Acta* 517, 66–73. doi:10.1016/j.cca.2021.02.011

Lin, H.-Y. (2020). The Severe COVID-19: A Sepsis Induced by Viral Infection? and its Immunomodulatory Therapy. *Chin. J. Traumatol.* 23, 190–195. doi:10.1016/j.cjtee.2020.06.002

Lu, H., Stratton, C. W., and Tang, Y. W. (2020). Outbreak of Pneumonia of Unknown Etiology in Wuhan, China: The Mystery and the Miracle. *J. Med. Virol.* 92, 401–402. doi:10.1002/jmv.25678

Lüscher, T. F., Landmesser, U., Von Eckardstein, A., and Fogelman, A. M. (2014). High-Density Lipoprotein. *Circ. Res.* 114, 171–182. doi:10.1161/circresaha.114.300935

Madsen, C. M., Varbo, A., Tybjærg-Hansen, A., Frikke-Schmidt, R., and Nordestgaard, B. G. (2018). U-shaped Relationship of HDL and Risk of Infectious Disease: Two Prospective Population-Based Cohort Studies. *Eur. Heart J.* 39, 1181–1190. doi:10.1093/eurheartj/ehx665

Mahamid, M., Nseir, W., Khoury, T., Mahamid, B., Nubania, A., Sub-Laban, K., et al. (2020). Nonalcoholic Fatty Liver Disease Is Associated with COVID-19 Severity Independently of Metabolic Syndrome. *Eur. J. Gastroenterol. Hepatol.* doi:10.1097/meg.0000000000001902

Mastaglio, S., Ruggeri, A., Risitano, A. M., Angelillo, P., Yancopoulou, D., Mastellos, D. C., et al. (2020). The First Case of COVID-19 Treated with the Complement C3 Inhibitor AMY-101. *Clin. Immunol.* 215, 108450. doi:10.1016/j.clim.2020.108450

McDonald, M. C., Dhadly, P., Cockerill, G. W., Cuzzocrea, S., Mota-Filipe, H., Hinds, C. J., et al. (2003). Reconstituted High-Density Lipoprotein Attenuates Organ Injury and Adhesion Molecule Expression in a Rodent Model of Endotoxic Shock. *Shock* 20, 551–557. doi:10.1097/01.shk.0000097249.97298.a3

Mehri, F., Rahbar, A. H., Ghane, E. T., Souri, B., and Esfahani, M. (2021). The Comparison of Oxidative Markers between Covid-19 Patients and Healthy Subjects. *Arch. Med. Res.* S0188-4409 (0121), 00126–00120. doi:10.1016/j.arcmed.2021.06.004

Miller, M., Dobs, A., Yuan, Z., Battisti, W. P., Borisute, H., and Palmisano, J. (2004). Effectiveness of Simvastatin Therapy in Raising HDL-C in Patients with Type 2 Diabetes and Low HDL-C. *Curr. Med. Res. Opin.* 20, 1087–1094. doi:10.1185/030079904125004105

Montero-Chacón, L. B., Padilla-Cuadra, J. I., Chiou, S. H., and Torrealba-Acosta, G. (2020). High-Density Lipoprotein, Mean Platelet Volume, and Uric Acid as Biomarkers for Outcomes in Patients With Sepsis: An Observational Study. *J. Intensive Care Med.* 35, 636–642. doi:10.1177/0885066618772825

Nardacci, R., Colavita, F., Castilletti, C., Lapa, D., Matusali, G., Meschi, S., et al. (2021). Evidences for Lipid Involvement in SARS-CoV-2 Cytopathogenesis. *Cell Death Dis.* 12, 263. doi:10.1038/s41419-021-03527-9

Ni, C., Cao, J., Li, D., Wu, W., Cao, L., and Zhu, C. (2020). Parenteral Nutrition Effects of Omega-3 Fatty Acids on C-Reactive Protein, High-Density Lipoprotein, Lymphocyte Characteristics and the Treatment of Critically Ill Patients. *Cel Mol Biol. (Noisy-le-grand)* 66, 52–56. doi:10.14715/cmb/2020.66.3.8

Nofer, J.-R., Levkau, B., Wolinska, I., Junker, R., Fobker, M., Von Eckardstein, A., et al. (2001). Suppression of Endothelial Cell Apoptosis by High Density Lipoproteins (HDL) and HDL-Associated Lysosphingolipids. *J. Biol. Chem.* 276, 34480–34485. doi:10.1074/jbc.M103782200

Oslakovic, C., Krisinger, M. J., Andersson, A., Jauhiainen, M., Ehnholm, C., and Dahlbäck, B. (2009). Anionic Phospholipids Lose Their Procoagulant Properties when Incorporated into High Density Lipoproteins. *J. Biol. Chem.* 284, 5896–5904. doi:10.1074/jbc.M807286200

Oslakovic, C., Jauhiainen, M., Ehnholm, C., and Dahlbäck, B. (2010). The Role of Phospholipid Transfer Protein in Lipoprotein-Mediated Neutralization of the Procoagulant Effect of Anionic Liposomes. *J. Thromb. Haemost. : JTH* 8, 766–772. doi:10.1111/j.1538-7836.2010.03744.x

Ouyang, S.-M., Zhu, H.-Q., Xie, Y.-N., Zou, Z.-S., Zuo, H.-M., Rao, Y.-W., et al. (2020). Temporal Changes in Laboratory Markers of Survivors and Non-survivors of Adult Inpatients with COVID-19. *BMC Infect. Dis.* 20, 952. doi:10.1186/s12879-020-05678-0

Pajkrt, D., Doran, J. E., Koster, F., Lerch, P. G., Arnet, B., Van Der Poll, T., et al. (1996). Antiinflammatory Effects of Reconstituted High-Density Lipoprotein during Human Endotoxemia. *J. Exp. Med.* 184, 1601–1608. doi:10.1084/jem.184.5.1601

Park, K.-H., and Cho, K.-H. (2011). High-density Lipoprotein (HDL) from Elderly and Reconstituted HDL Containing Glycated Apolipoproteins A-I Share Proatherosclerotic and Prosenescent Properties with Increased Cholesterol Influx. *Journals Gerontol. Ser. A: Biol. Sci. Med. Sci.* 66A, 511–520. doi:10.1093/gerona/glr016

Parker, T. S., Levine, D. M., Chang, J. C., Laxer, J., Coffin, C. C., and Rubin, A. L. (1995). Reconstituted High-Density Lipoprotein Neutralizes Gram-Negative Bacterial Lipopolysaccharides in Human Whole Blood. *Infect. Immun.* 63, 253–258. doi:10.1128/iai.63.1.253-258.1995

Pirillo, A., Catapano, A. L., and Norata, G. D. (2015). HDL in Infectious Diseases and Sepsis. *Handbook Exp. Pharmacol.* 224, 483–508. doi:10.1007/978-3-319-09665-0_15

Qin, C., Minghan, H., Ziwen, Z., and Yukun, L. (2020a). Alteration of Lipid Profile and Value of Lipids in the Prediction of the Length of Hospital Stay in COVID-19 Pneumonia Patients. *Food Sci. Nutr.* 8, 6144–6152. doi:10.1002/fsn3.1907

Qin, C., Zhou, L., Hu, Z., Zhang, S., Yang, S., Tao, Y., et al. (2020b). Dysregulation of Immune Response in Patients With Coronavirus 2019 (COVID-19) in Wuhan, China. *Clin. Infect. Dis.* 71, 762–768. doi:10.1093/cid/ciaa248

Rader, D. J. (2003). Regulation of Reverse Cholesterol Transport and Clinical Implications. *Am. J. Cardiol.* 92, 42–49. doi:10.1016/s0002-9149(03)00615-5

Robbesyn, F., Garcia, V., Auge, N., Vieira, O., Frisach, M. F., Salvayre, R., et al. (2003). HDL Counterbalance the Proinflammatory Effect of Oxidized LDL by Inhibiting Intracellular Reactive Oxygen Species Rise, Proteasome Activation, and Subsequent NF-κB Activation in Smooth Muscle Cells. *FASEB j.* 17, 743–745. doi:10.1096/fj.02-0240fje

Rodríguez-Sanz, A., Fuentes, B., Martínez-Sánchez, P., Prefasi, D., Martínez-Martínez, M., Correas, E., et al. (2013). High-density Lipoprotein: a Novel Marker for Risk of In-Hospital Infection in Acute Ischemic Stroke Patients? *Cerebrovasc. Dis.* 35, 291–297. doi:10.1159/000347077

Rose, H., Woolley, I., Hoy, J., Dart, A., Bryant, B., Mijch, A., et al. (2006). HIV Infection and High-Density Lipoprotein: the Effect of the Disease vs the Effect of Treatment. *Metabolism* 55, 90–95. doi:10.1016/j.metabol.2005.07.012

Rose, H., Hoy, J., Woolley, I., Tchoua, U., Bukrinsky, M., Dart, A., et al. (2008). HIV Infection and High Density Lipoprotein Metabolism. *Atherosclerosis* 199, 79–86. doi:10.1016/j.atherosclerosis.2007.10.018

Rosenson, R. S. (2005). HDL-C and the Diabetic Patient: Target for Therapeutic Intervention? *Diabetes Res. Clin. Pract.* 68 (Suppl. 2), S36–S42. doi:10.1016/j.diabres.2005.03.013

Samanovic, M., Molina-Portela, M. P., Chessler, A.-D. C., Burleigh, B. A., and Raper, J. (2009). Trypanosome Lytic Factor, an Antimicrobial High-Density Lipoprotein, Ameliorates Leishmania Infection. *Plos Pathog.* 5, e1000276. doi:10.1371/journal.ppat.1000276

Sasaki, J., Otonari, T., Uchida, Y., Ikeda, Y., Biro, S., and Kono, S. (2013). Effects of Pravastatin and Atorvastatin on HDL Cholesterol and Glucose Metabolism in Patients with Dyslipidemia and Glucose Intolerance: the PRAT Study. *Jat* 20, 368–379. doi:10.5551/jat.13532

Satyam, A., and Tsokos, G. C. (2020). Curb Complement to Cure COVID-19. *Clin. Immunol.* 221, 108603. doi:10.1016/j.clim.2020.108603

Satyam, A., Tsokos, M. G., Brook, O. R., Hecht, J. L., Moulton, V. R., and Tsokos, G. C. (2021). Activation of Classical and Alternative Complement Pathways in the Pathogenesis of Lung Injury in COVID-19. *Clin. Immunol.* 226, 108716. doi:10.1016/j.clim.2021.108716

Sharrett, A. R., Ballantyne, C. M., Coady, S. A., Heiss, G., Sorlie, P. D., Catellier, D., et al. (2001). Coronary Heart Disease Prediction From Lipoprotein Cholesterol Levels, Triglycerides, Lipoprotein(a), Apolipoproteins A-I and B, and HDL Density Subfractions. *Circulation* 104, 1108–1113. doi:10.1161/hc3501.095214

Shenoy, S. (2020). Coronavirus (Covid-19) Sepsis: Revisiting Mitochondrial Dysfunction in Pathogenesis, Aging, Inflammation, and Mortality. *Inflamm. Res.* 69, 1077–1085. doi:10.1007/s00011-020-01389-z

Shih, D. M., Gu, L., Xia, Y.-R., Navab, M., Li, W.-F., Hama, S., et al. (1998). Mice Lacking Serum Paraoxonase Are Susceptible to Organophosphate Toxicity and Atherosclerosis. *Nature* 394, 284–287. doi:10.1038/28406

Shor, R., Wainstein, J., Oz, D., Boaz, M., Matas, Z., Fux, A., et al. (2008). Low HDL Levels and the Risk of Death, Sepsis and Malignancy. *Clin. Res. Cardiol.* 97, 227–233. doi:10.1007/s00392-007-0611-z

Song, C.-Y., Xu, J., He, J.-Q., and Lu, Y.-Q. (2020). Immune Dysfunction Following COVID-19, Especially in Severe Patients. *Sci. Rep.* 10, 15838. doi:10.1038/s41598-020-72718-9

Sorokin, A. V., Karathanasis, S. K., Yang, Z. H., Freeman, L., Kotani, K., and Remaley, A. T. (2020). COVID-19-Associated Dyslipidemia: Implications for Mechanism of Impaired Resolution and Novel Therapeutic Approaches. *FASEB j.* 34, 9843–9853. doi:10.1096/fj.202001451

Suc, I., Escargueil-Blanc, I., Troly, M., Salvayre, R., and Nègre-Salvayre, A. (1997). HDL and ApoA Prevent Cell Death of Endothelial Cells Induced by Oxidized LDL. *Atvb* 17, 2158–2166. doi:10.1161/01.atv.17.10.2158

Sun, J. T., Chen, Z., Nie, P., Ge, H., Shen, L., Yang, F., et al. (2020). Lipid Profile Features and Their Associations With Disease Severity and Mortality in Patients With COVID-19. *Front. Cardiovasc. Med.* 7, 584987. doi:10.3389/fcvm.2020.584987

Suzuki, M., Pritchard, D. K., Becker, L., Hoofnagle, A. N., Tanimura, N., Bammler, T. K., et al. (2010). High-density Lipoprotein Suppresses the Type I Interferon Response, a Family of Potent Antiviral Immunoregulators, in Macrophages Challenged with Lipopolysaccharide. *Circulation* 122, 1919–1927. doi:10.1161/circulationaha.110.961193

Tan, M., Liu, Y., Zhou, R., Deng, X., Li, F., Liang, K., et al. (2020). Immunopathological Characteristics of Coronavirus Disease 2019 Cases in Guangzhou, China. *Immunology* 160, 261–268. doi:10.1111/imm.13223

Tanaka, S., Labreuche, J., Drumez, E., Harrois, A., Hamada, S., Vigué, B., et al. (2017). Low HDL Levels in Sepsis versus Trauma Patients in Intensive Care Unit. *Ann. Intensive Care* 7, 60. doi:10.1186/s13613-017-0284-3

Tanaka, S., Couret, D., Tran-Dinh, A., Duranteau, J., Montravers, P., Schwendeman, A., et al. (2020a). High-density Lipoproteins during Sepsis: from Bench to Bedside. *Crit. Care* 24, 134. doi:10.1186/s13054-020-02860-3

Tanaka, S., De Tymowski, C., Assadi, M., Zappella, N., Jean-Baptiste, S., Robert, T., et al. (2020b). Lipoprotein Concentrations Over Time in the Intensive Care Unit COVID-19 Patients: Results from the ApoCOVID Study. *PloS one* 15, e0239573. doi:10.1371/journal.pone.0239573

Tanaka, S., Genève, C., Zappella, N., Yong-Sang, J., Planesse, C., Louedec, L., et al. (2020c). Reconstituted High-Density Lipoprotein Therapy Improves Survival in Mouse Models of Sepsis. *Anesthesiology* 132, 825–838. doi:10.1097/aln.0000000000003155

Tang, N., Li, D., Wang, X., and Sun, Z. (2020). Abnormal Coagulation Parameters Are Associated with Poor Prognosis in Patients with Novel Coronavirus Pneumonia. *J. Thromb. Haemost.* 18, 844–847. doi:10.1111/jth.14768

Theilmeier, G., Schmidt, C., Herrmann, J., Keul, P., Schäfers, M., Herrgott, I., et al. (2006). High-Density Lipoproteins and Their Constituent, Sphingosine-1-Phosphate, Directly Protect the Heart against Ischemia/Reperfusion Injury *In Vivo* via the S1P 3 Lysophospholipid Receptor. *Circulation* 114, 1403–1409. doi:10.1161/circulationaha.105.607135

Tijburg, P. N., Ryan, J., Stern, D. M., Wollitzky, B., Rimon, S., Rimon, A., et al. (1991). Activation of the Coagulation Mechanism on Tumor Necrosis Factor-Stimulated Cultured Endothelial Cells and Their Extracellular Matrix. The Role of Flow and Factor IX/IXa. *J. Biol. Chem.* 266, 12067–12074. doi:10.1016/s0021-9258(18)99066-6

Tosheska Trajkovska, K., and Topuzovska, S. (2017). High-density Lipoprotein Metabolism and Reverse Cholesterol Transport: Strategies for Raising HDL Cholesterol. *Anatol J. Cardiol.* 18, 149–154. doi:10.14744/AnatolJCardiol.2017.7608

Trinder, M., Genga, K. R., Kong, H. J., Blauw, L. L., Lo, C., Li, X., et al. (2019). Cholesteryl Ester Transfer Protein Influences High-Density Lipoprotein Levels and Survival in Sepsis. *Am. J. Respir. Crit. Care Med.* 199, 854–862. doi:10.1164/rccm.201806-1157OC

Trinder, M., Wang, Y., Madsen, C. M., Ponomarev, T., Bohunek, L., Daisely, B. A., et al. (2021). Inhibition of Cholesteryl Ester Transfer Protein Preserves High-Density Lipoprotein Cholesterol and Improves Survival in Sepsis. *Circulation* 143, 921–934. doi:10.1161/circulationaha.120.048568

Turgay Yıldırım, Ö., and Kaya, Ş. (2021). The Atherogenic index of Plasma as a Predictor of Mortality in Patients with COVID-19. *Heart Lung : J. Crit. Care* 50, 329–333. doi:10.1016/j.hrtlng.2021.01.016

Ulevitch, R. J., Johnston, A. R., and Weinstein, D. B. (1979). New Function for High Density Lipoproteins. Their Participation in Intravascular Reactions of Bacterial Lipopolysaccharides. *J. Clin. Invest.* 64, 1516–1524. doi:10.1172/jci109610

van Leeuwen, H. J., Heezius, E. C. J. M., Dallinga, G. M., Van Strijp, J. A. G., Verhoef, J., and Van Kessel, K. P. M. (2003). Lipoprotein Metabolism in Patients with Severe Sepsis. *Crit. Care Med.* 31, 1359–1366. doi:10.1097/01.ccm.0000059724.08290.51

Van Lenten, B. J., Wagner, A. C., Nayak, D. P., Hama, S., Navab, M., and Fogelman, A. M. (2001). High-density Lipoprotein Loses its Anti-inflammatory Properties during Acute Influenza a Infection. *Circulation* 103, 2283–2288. doi:10.1161/01.cir.103.18.2283

Van Sickle, W. A., Wilcox, H. G., Malik, K. U., and Nasjletti, A. (1986). High Density Lipoprotein-Induced Cardiac Prostacyclin Synthesis *In Vitro*: Relationship to Cardiac Arachidonate Mobilization. *J. Lipid Res.* 27, 517–522.

Viswambharan, H., Ming, X.-F., Zhu, S., Hubsch, A., Lerch, P., Vergères, G., et al. (2004). Reconstituted High-Density Lipoprotein Inhibits Thrombin-Induced Endothelial Tissue Factor Expression through Inhibition of RhoA and

Stimulation of Phosphatidylinositol 3-kinase but Not Akt/endothelial Nitric Oxide Synthase. *Circ. Res.* 94, 918–925. doi:10.1161/01.res.0000124302.20396.b7

Wang, D., Hu, B., Hu, C., Zhu, F., Liu, X., Zhang, J., et al. (2020a). Clinical Characteristics of 138 Hospitalized Patients With 2019 Novel Coronavirus-Infected Pneumonia in Wuhan, China. *Jama* 323, 1061–1069. doi:10.1001/jama.2020.1585

Wang, D., Li, R., Wang, J., Jiang, Q., Gao, C., Yang, J., et al. (2020b). Correlation Analysis between Disease Severity and Clinical and Biochemical Characteristics of 143 Cases of COVID-19 in Wuhan, China: a Descriptive Study. *BMC Infect. Dis.* 20, 519. doi:10.1186/s12879-020-05242-w

Wang, G., Zhang, Q., Zhao, X., Dong, H., Wu, C., Wu, F., et al. (2020). Low High-Density Lipoprotein Level Is Correlated with the Severity of COVID-19 Patients: an Observational Study. *Lipids Health Dis.* 19, 204. doi:10.1186/s12944-020-01382-9

Wei, C., Wan, L., Yan, Q., Wang, X., Zhang, J., Yang, X., et al. (2020a). HDL-scavenger Receptor B Type 1 Facilitates SARS-CoV-2 Entry. *Nat. Metab.* 2, 1391–1400. doi:10.1038/s42255-020-00324-0

Wei, C., Wan, L., Zhang, Y., Fan, C., and Zhong, H. (2020b). *Cholesterol Metabolism–Impact for SARS-CoV-2 Infection Prognosis, Entry, and Antiviral Therapies*. [Epub ahead of print]. doi:10.1101/2020.04.16.20068528

Wei, X., Zeng, W., Su, J., Wan, H., Yu, X., Cao, X., et al. (2020). Hypolipidemia Is Associated with the Severity of COVID-19. *J. Clin. Lipidol.* 14, 297–304. doi:10.1016/j.jacl.2020.04.008

WHO(2021a). *Coronavirus (COVID-19) Overview*. Available at: https://covid19.who.int/ (Accessed June 30, 2021).

WHO(2021b). *Coronavirus Disease (COVID-19) Situation Dashboard of China*. Available at: https://covid19.who.int/region/wpro/country/cn (Accessed June 30, 2021).

WHO (2021c). *Coronavirus Disease (COVID-19) Situation Dashboard of United States of America*. Available at: https://covid19.who.int/region/amro/country/us (Accessed June 30, 2021).

Xie, Y., You, Q., Wu, C., Cao, S., Qu, G., Yan, X., et al. (2020). Impact of Cardiovascular Disease on Clinical Characteristics and Outcomes of Coronavirus Disease 2019 (COVID-19). *Circ. J.* 84, 1277–1283. doi:10.1253/circj.CJ-20-0348

Xiong, Y., Liu, Y., Cao, L., Wang, D., Guo, M., Jiang, A., et al. (2020). Transcriptomic Characteristics of Bronchoalveolar Lavage Fluid and Peripheral Blood Mononuclear Cells in COVID-19 Patients. *Emerg. Microbes Infect.* 9, 761–770. doi:10.1080/22221751.2020.1747363

Xu, Z., Shi, L., Wang, Y., Zhang, J., Huang, L., Zhang, C., et al. (2020). Pathological Findings of COVID-19 Associated with Acute Respiratory Distress Syndrome. *Lancet Respir. Med.* 8, 420–422. doi:10.1016/s2213-2600(20)30076-x

Yanai, H., Masui, Y., Katsuyama, H., Adachi, H., Kawaguchi, A., Hakoshima, M., et al. (2018). An Improvement of Cardiovascular Risk Factors by Omega-3 Polyunsaturated Fatty Acids. *J. Clin. Med. Res.* 10, 281–289. doi:10.14740/jocmr3362w

Yao, X. H., Li, T. Y., He, Z. C., Ping, Y. F., Liu, H. W., Yu, S. C., et al. (2020). [A Pathological Report of Three COVID-19 Cases by Minimal Invasive Autopsies]. *Zhonghua Bing Li Xue Za Zhi* 49, 411–417. doi:10.3760/cma.j.cn112151-20200312-00193

Young, B. E., Ong, S. W. X., Kalimuddin, S., Low, J. G., Tan, S. Y., Loh, J., et al. (2020). Epidemiologic Features and Clinical Course of Patients Infected With SARS-CoV-2 in Singapore. *Jama* 323, 1488–1494. doi:10.1001/jama.2020.3204

Yuhanna, I. S., Zhu, Y., Cox, B. E., Hahner, L. D., Osborne-Lawrence, S., Lu, P., et al. (2001). High-Density Lipoprotein Binding to Scavenger Receptor-BI Activates Endothelial Nitric Oxide Synthase. *Nat. Med.* 7, 853–857. doi:10.1038/89986

Zafer, M. M., El-Mahallawy, H. A., and Ashour, H. M. (2021). Severe COVID-19 and Sepsis: Immune Pathogenesis and Laboratory Markers. *Microorganisms* 9, 159. doi:10.3390/microorganisms9010159

Zhang, B., Dong, C., Li, S., Song, X., Wei, W., and Liu, L. (2020). Triglyceride to High-Density Lipoprotein Cholesterol Ratio Is an Important Determinant of Cardiovascular Risk and Poor Prognosis in Coronavirus Disease-19: A Retrospective Case Series Study. *Dmso* 13, 3925–3936. doi:10.2147/dmso.s268992

Zhang, D., Guo, R., Lei, L., Liu, H., Wang, Y., Wang, Y., et al. (2021). Frontline Science: COVID-19 Infection Induces Readily Detectable Morphologic and Inflammation-related Phenotypic Changes in Peripheral Blood Monocytes. *J. Leukoc. Biol.* 109, 13–22. doi:10.1002/jlb.4hi0720-470r

Zhang, Q., Wei, Y., Chen, M., Wan, Q., and Chen, X. (2020). Clinical Analysis of Risk Factors for Severe COVID-19 Patients With Type 2 Diabetes. *J. Diabetes Complications* 34, 107666. doi:10.1016/j.jdiacomp.2020.107666

Zhang, Y., Yang, H., Li, S., Li, W.-D., Wang, J., and Wang, Y. (2021). Association Analysis Framework of Genetic and Exposure Risks for COVID-19 in Middle-Aged and Elderly Adults. *Mech. ageing Dev.* 194, 111433. doi:10.1016/j.mad.2021.111433

Zhou, F., Yu, T., Du, R., Fan, G., Liu, Y., Liu, Z., et al. (2020). Clinical Course and Risk Factors for Mortality of Adult Inpatients with COVID-19 in Wuhan, China: A Retrospective Cohort Study. *Lancet* 395, 1054–1062. doi:10.1016/s0140-6736(20)30566-3

Zhou, P., Yang, X.-L., Wang, X.-G., Hu, B., Zhang, L., Zhang, W., et al. (2020). A Pneumonia Outbreak Associated with a New Coronavirus of Probable Bat Origin. *Nature* 579, 270–273. doi:10.1038/s41586-020-2012-7

Zou, G., He, J., Ren, B., Xu, F., Xu, G., and Zhang, W. (2016). The delta High-Density Lipoprotein Cholesterol Ratio: A Novel Parameter for Gram-Negative Sepsis. *Springerplus* 5, 1044. doi:10.1186/s40064-016-2685-4

Conflict of Interest: The authors declare that the research was conducted in the absence of any commercial or financial relationships that could be construed as a potential conflict of interest.

frontiers in Pharmacology

ORIGINAL RESEARCH
published: 13 August 2021
doi: 10.3389/fphar.2021.706901

Remdesivir and Cyclosporine Synergistically Inhibit the Human Coronaviruses OC43 and SARS-CoV-2

*Hsing-Yu Hsu[1†], Cheng-Wei Yang[1†], Yue-Zhi Lee[1†], Yi-Ling Lin[2†], Sui-Yuan Chang[3†], Ruey-Bing Yang[2], Jian-Jong Liang[2], Tai-Ling Chao[3], Chun-Che Liao[2], Han-Chieh Kao[3], Szu-Huei Wu[1], Jang-Yang Chang[1], Huey-Kang Sytwu[4], Chiung-Tong Chen[1] and Shiow-Ju Lee[1]**

[1]Institute of Biotechnology and Pharmaceutical Research, National Health Research Institutes, Miaoli, Taiwan, [2]Institute of Biomedical Sciences, Academia Sinica, Taipei, Taiwan, [3]Institute of Clinical Laboratory Sciences and Medical Biotechnology, College of Medicine, National Taiwan University, Taipei, Taiwan, [4]National Institute of Infectious Diseases and Vaccinology, National Health Research Institutes, Miaoli, Taiwan

OPEN ACCESS

Edited by:
Brijesh Kumar Singh, Duke-NUS Medical School, Singapore

Reviewed by:
Rupesh K. Srivastava, All India Institute of Medical Sciences, New Delhi, India
Sebastian Schloer, University of Münster, Germany

***Correspondence:**
Shiow-Ju Lee
slee@nhri.org.tw

†These authors have contributed equally to this work

Specialty section:
This article was submitted to Experimental Pharmacology and Drug Discovery, a section of the journal Frontiers in Pharmacology

Received: *08 May 2021*
Accepted: *31 July 2021*
Published: *13 August 2021*

Citation:
Hsu H-Y, Yang C-W, Lee Y-Z, Lin Y-L, Chang S-Y, Yang R-B, Liang J-J, Chao T-L, Liao C-C, Kao H-C, Wu S-H, Chang J-Y, Sytwu H-K, Chen C-T and Lee S-J (2021) Remdesivir and Cyclosporine Synergistically Inhibit the Human Coronaviruses OC43 and SARS-CoV-2. Front. Pharmacol. 12:706901. doi: 10.3389/fphar.2021.706901

Remdesivir, a prodrug targeting RNA-dependent-RNA-polymerase, and cyclosporine, a calcineurin inhibitor, individually exerted inhibitory activity against human coronavirus OC43 (HCoV-OC43) in HCT-8 and MRC-5 cells at EC_{50} values of 96 ± 34 ~ 85 ± 23 nM and 2,920 ± 364 ~ 4,419 ± 490 nM, respectively. When combined, these two drugs synergistically inhibited HCoV-OC43 in both HCT-8 and MRC-5 cells assayed by immunofluorescence assay (IFA). Remdesivir and cyclosporine also separately reduced IL-6 production induced by HCoV-OC43 in human lung fibroblasts MRC-5 cells with EC_{50} values of 224 ± 53 nM and 1,292 ± 352 nM, respectively; and synergistically reduced it when combined. Similar trends were observed for SARS-CoV-2, which were 1) separately inhibited by remdesivir and cyclosporine with respective EC_{50} values of 3,962 ± 303 nM and 7,213 ± 143 nM by IFA, and 291 ± 91 nM and 6,767 ± 1,827 nM by a plaque-formation assay; and 2) synergistically inhibited by their combination, again by IFA and plaque-formation assay. Collectively, these results suggest that the combination of remdesivir and cyclosporine merits further study as a possible treatment for COVID-19 complexed with a cytokine storm.

Keywords: COVID-19, cyclosporine, IL-6, IL-8, OC43, remdesivir, SARS-CoV-2, synergistic

INTRODUCTION

COVID-19 has affected more than 176.887 million people in 194 countries and caused over 3.84 million deaths (as of 2021-06-18 https://www.cdc.gov.tw/) since its emergence at the end of 2019. This disease is caused by infection with Severe Acute Respiratory Syndrome Coronavirus 2 (SARS-CoV-2), and disease progression is usually complexed with a cytokine storm and/or organ dysfunction (McElvaney et al., 2020).

Interleukin-6 (IL-6) and other cytokines are increased in patients with COVID-19, and IL-6 was also found to be a hallmark predictor for COVID-19 progression. (Chen et al., 2020; McElvaney et al., 2020; Yang et al., 2020). Tocilizumab, a monoclonal antibody against IL-6 receptor (IL6-R) is an immunosuppressive drug originally developed for the treatment of rheumatoid arthritis (Scott, 2017) and systemic juvenile idiopathic arthritis (De Benedetti et al., 2012), but is currently under development as an alternative therapy for COVID-19 patients who are at risk of a cytokine storm (Rosas et al., 2021).

Recently, preliminarily data showed tocilizumab to be associated with significant clinical improvement and a reduction in mortality (Klopfenstein et al., 2020; Toniati et al., 2020; Xu et al., 2020). Therefore, mitigation of the cytokine storm that occurs in COVID-19 patients is a sound therapeutic strategy.

Remdesivir targets SARS-CoV-2 itself, inhibiting viral RNA-dependent-RNA-polymerase (RdRp) (Gordon et al., 2020; Pruijssers et al., 2020) and was the first approved treatment for COVID-19, although its efficacy is restricted to a shortening in the time to recovery of hospitalized patients (Beigel et al., 2020). Nonetheless, COVID-19 symptoms and mortality can be ameliorated by anti-inflammatory or immunomodulatory agents (Fatima et al., 2020; Tomazini et al., 2020). Thus, the combination treatment of remdesivir with existing anti-inflammatory or immunomodulatory agents may exert an especially therapeutic effect COVID-19 patients and merits further exploration.

The repurposing of existing drugs to take advantage of their known safety profiles and associated commercial supply chains is an important strategy to expedite the discovery of effective and safe COVID-19 treatments. Moreover, the combination of existing drugs with remdesivir may also improve its effectiveness. SARS-CoV-2 related experiments are regulated and can only be performed in biosafety-level-3 (BSL-3) or higher laboratories, but the number, resources, and capacities of such laboratories are very limited. Therefore, we used the alternative coronaviruses swine transmissible gastroenteritis virus and human flu coronavirus OC43 (HCoV-OC43) as SARS-CoV-2 surrogates, to assay drugs for anti-viral activity prior to testing with SARS-CoV-2 itself. About 230 prescription drugs covered by Taiwan Health Insurance were screened, cyclosporine, an immunosuppressant widely used to prevent organ transplant rejection (Beauchesne et al., 2007; Wu et al., 2018), was found to significantly reduce infection by coronaviruses. Cyclosporine was first isolated from the fungus *Tolypocladium inflatum* (*T. inflatum*) in soil samples by scientists from the Norwegian Sandoz Pharmaceutical Company in 1969 (Beauchesne et al., 2007) (Yang et al., 2018). It is a lactam comprising 11 amino acids (including a D-amino acid) and is synthesized by ciclosporin synthetase, in contrast to most peptides that are synthesized by the ribosomes (Yang et al., 2018). Cyclosporine suppresses the activity of the immune system by inhibiting the activity and growth of T cells (Liddicoat and Lavelle, 2019) as well as IL-6 production (Stephanou et al., 1992; Iacono et al., 1997; Golling et al., 2009). NF-κB suppression by cyclosporine inhibits the production of proinflammatory cytokines (Meyer et al., 1997; Du et al., 2009; Jerkins et al., 2020).

Herein, we examine the inhibitory activities of combined treatments of remdesivir and cyclosporine against IL-6 cytokine production and the HCoV-OC43 and SARS-CoV-2. The results obtained suggest a potential regimen for combating COVID-19 complexed with a cytokine storm.

MATERIALS AND METHODS

Chemicals and Antibodies

DMSO (D1435, ≥99.5%), crystal violet (C0775, dye content ≥90%), and methylcellulose (#M0387) were purchased from Sigma-Aldrich (St. Louis, MO, United States); remdesivir (GS-5734) (S8932, 99.3%, HPLC) and cyclosporine A (cyclosporine) (S2286, 99.6%, HPLC) from Selleckchem (Houston, TX, United States); Goat anti-human IgG-Alexa Fluor 488 (A11013), Hochest 333258 (H3569), and DAPI (D1306) from Invitrogen (Thermo Fisher Scientific, Waltham, MA, United States); and 10% formaldehyde solution from Marcon™ Chemicals (#H121-08). The antibody against nucleocapsid (N) protein of HCoV-OC43 (Mab9013) was purchased from Merck Millipore (Burlington, MA, United States), and fluorescein isothiocyanate (FITC)-conjugated anti-mouse immunoglobulin (#55499) from MP Biomedicals (Irvine, CA, United States). Anti-SARS-CoV-2 N protein antibodies were provided by Dr An-Suei Yang of the Genomics Research Center, Academia Sinica.

Cell Lines, Virus, Western Analysis and Immunofluorescence Assay for HCoV-OC43

Human colon adenocarcinoma cell line HCT-8 (ATCC® CCL-244™) and human lung fibroblasts cell line MRC-5 (ATCC® CCL-171™) were obtained from American Type Culture Collection (ATCC), passaged within 6 months of receipt, and established as stocks in the cell bank at an early passage, to ensure cell line-specific characteristics. The subsequent 4th to 20th passages of HCT-8 cells and 7th to 16th passages of MRC-5 cells were used in this study. Heat inactivated premium grade fetal bovine serum (FBS) from VWR Life Science Seradigm (Radnor, PA, United States) was used to culture MRC-5 cells and FBS from Biological Industries Inc. (Cromwell, CT, United States) was used for the HCT-8 cell culture to obtain optimal culture conditions. HCoV-OC43 (ATCC® VR1558™) was grown and propagated in HCT-8 cells cultured with DMEM and 2% FBS. Time course experiments for the detection of HCoV-OC43 N protein with the antibody Mab9013, western blot [as described (Yang et al., 2020)], and IFA were performed with the samples at the indicated time points. For compound treatment studies, HCT-8 or MRC-5 cells were seeded in 96-well plates and then cultured in DMEM or MEM medium containing 2% FBS, respectively. Cells were pretreated with serial dilutions of remdesivir and cyclosporine at the indicated concentrations for 0.5 h prior to HCoV-OC43 infection at an MOI of 0.05. At 30 h.p.i., the resulting adherent cells were then fixed with 4% formaldehyde, permeabilized with 100% methanol, and subsequently subjected to IFA analyses with an antibody against HCoV-OC43 N protein (Mab9013) and FITC-conjugated anti-mouse immunoglobulin (#55499) (green), and the EC_{50} values determined as described (Yang et al., 2020). CC_{50} values were determined by staining nuclei blue with Hoechst dye and then determining relative cell viability using the number of nuclei in the vehicle control as 100%. Fluorescent signals were detected and quantified using the ImageXpress Micro XLS Widefield High-Content Analysis System (Molecular Device). The fluorescent signal was normalized with cell viability to calculate the infection rate that no compound treatment was set at 100%. Synergy scores for combined treatments were calculated using SynergyFinder (https://synergyfinder.fimm.fi/).

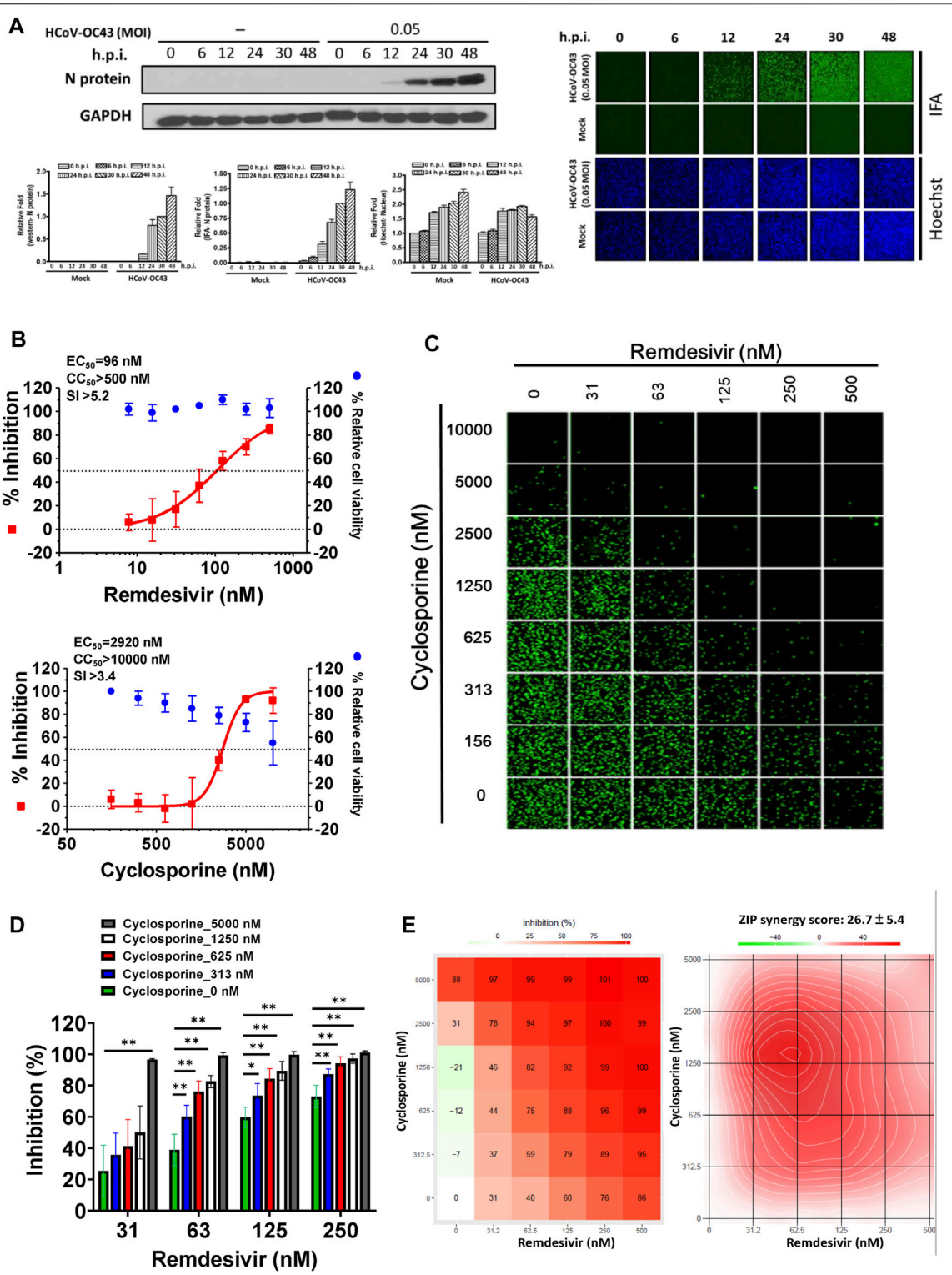

FIGURE 1 | Single or combined treatment of remdesivir and cyclosporine profoundly reduced HCoV-OC43 infection as assayed by immunofluorescence (IFAs) in human HCT-8 colorectal carcinoma cells. **(A)** Time course of HCoV-OC43 N protein expression in infected HCT-8 cells. Western analysis and IFA were performed against an antibody against HCoV-OC43 N protein (Mab9013) with the samples at the indicated time points. **(B)** Single treatments of remdesivir and cyclosporine reduced HCoV-OC43 infection in HCT-8 cells in a dose dependent manner. **(C–E)** Combined treatments of remdesivir and cyclosporine synergistically reduced the HCoV-OC43 infection in HCT-8 cells. IFAs were performed with an antibody against N protein (green) of HCoV-OC43 in HCoV-OC43 (0.05 MOI) infected HCT-8 cells at 30 h.p.i. treated with vehicle (0.5% DMSO) or compounds as indicated. Nuclei (blue) were counter stained with Hoechst dye and used to determine the relative cell

(*Continued*)

FIGURE 1 | viability by using the number of nuclei in vehicle control as 100% (**Supplementary Figure S1**). The fluorescent signal was normalized with cell viability to calculate the infection rate that no compound treatment was set at 100%. HCT-8 cells were seeded the day before compound treatment or HCoV-OC43 infection. The tested compounds were added to the wells 1 h prior to the addition of HCoV-OC43 at an MOI of 0.05 and the resulting cultures incubated for an additional 30 h at 37°C. AVE ±SD of three independent experiments are shown **(A, B, D)** The statistical significance was evaluated using one-way ANOVA followed by Tukey's multiple comparison test. * and ** denote statistical significance of $p < 0.05$, and $p < 0.01$ respectively. IFA images shown are representative of three independent experiments **(C)**. Shown inhibition % (AVE) and synergy scores (AVE ± SD) are from three independent experiments **(E)** analyzed *via* SynergyFinder (https://synergyfinder.fimm.fi/).

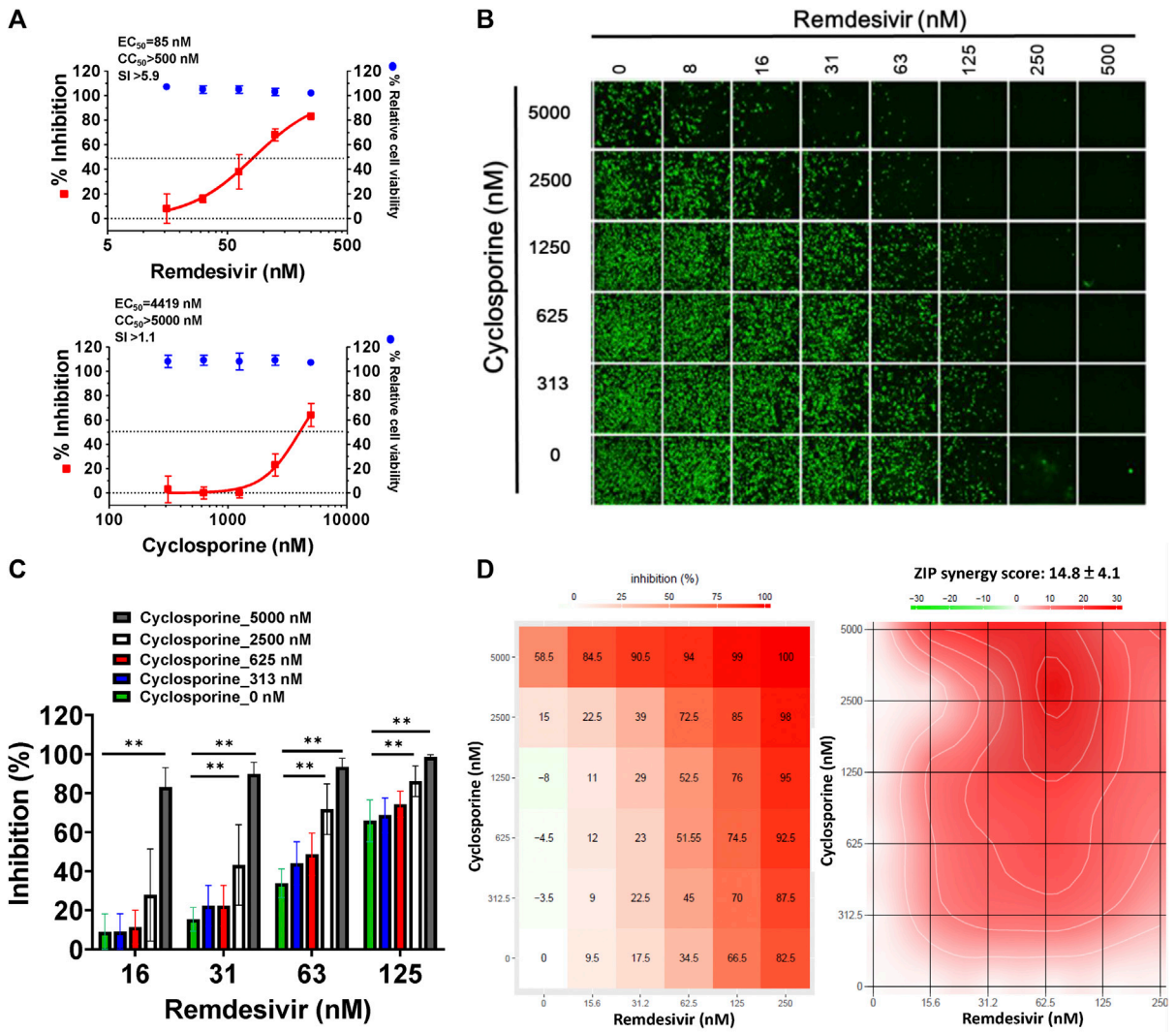

FIGURE 2 | Single or combined treatments of remdesivir and cyclosporine profoundly reduced HCoV-OC43 infection in human fetal lung fibroblast MRC-5 cells assayed by IFA. **(A)** Single treatments of remdesivir and cyclosporine reduced HCoV-OC43 infection in MRC-5 cells in a dose dependent manner. **(B–D)** Combined treatments of remdesivir and cyclosporine synergistically reduced the HCoV-OC43 infection in MRC-5 cells. IFAs were performed with an antibody against N protein (green) of HCoV-OC43 in HCoV-OC43 (0.05 MOI) infected MRC-5 cells at 30 h.p.i. treated with vehicle (0.5% DMSO) or compounds as indicated. Nuclei (blue) were counter stained with Hoechst dye and used to determine the relative cell viability by using the number of nuclei in vehicle control as 100% (**Supplementary Figure S2**). The fluorescent signal of IFA was normalized with cell viability to calculate the infection rate that no compound treatment was set at 100%. MRC-5 cells were seeded the day before compound treatment or HCoV-OC43 infection. Tested compounds were added to the wells 1 h prior to the addition of HCoV-OC43 at an MOI of 0.05. The resulting cultures were then incubated for an additional 30 h at 37°C. AVE ± SD of three independent experiments are shown **(A and C)**. The statistical significance was evaluated using one-way ANOVA followed by Tukey's multiple comparison test. * and ** denote statistical significance of $p < 0.05$, and $p < 0.01$ respectively. IFA images shown are representative of three independent experiments **(B)**. Shown inhibition % (AVE) and synergy scores (AVE ± SD) are from three independent experiments **(D)** analyzed *via* SynergyFinder (https://synergyfinder.fimm.fi/).

TABLE 1 | Antiviral activities and IL-6 reduction of remdesivir and cyclosporine against HCoV-OC43 and SARS-CoV-2. Shown are AVE ± SD from three independent experiments.

CoV	Cell line	Assay	EC50 (nM)	
			Remdesivir	Cyclosporine
HCoV-OC43	HCT-8	Viral activity by IFA	96 ± 34	2,920 ± 364
HCoV-OC43	MRC-5	Viral activity by IFA	85 ± 23	4,419 ± 490
SARS-CoV-2	Vero E6	Viral activity by IFA	3,962 ± 303	7,213 ± 143
SARS-CoV-2	Vero E6	Viral plaque formation	291 ± 91	6,767 ± 1827
HCoV-OC43	MRC-5	IL-6 by ELISA	224 ± 53	1,292 ± 352

TABLE 2 | The synergistic inhibition of HCoV-OC43, SARS-CoV-2, and IL-6 production by remdesivir and cyclosporine. Synergy scores were calculated and analyzed by SynergyFinder, ZIP method. Shown synergy scores are AVE ± SD from three independent experiments.

CoV	Cell line	Assay	Synergy score	Most synergistic area score
HCoV-OC43	HCT-8	Viral activity by IFA	26.7 ± 5.4	43.1
HCoV-OC43	MRC-5	Viral activity by IFA	14.8 ± 4.1	19.8
SARS-CoV-2	Vero E6	Viral activity by IFA	25.0 ± 2.5	65.5
SARS-CoV-2	Vero E6	Viral plaque formation	43.7 ± 14.9	46.2
HCoV-OC43	MRC-5	IL-6 by ELISA	13.0 ± 5.7	25.8

Cell Line, Virus, IFA, and Plaque Assay for SARS-CoV-2

For IFA used in the SARS-CoV-2 study, Vero E6 cells (BCRC number: 60476; derived from ATCC CRL-1586) were passaged within 6 months of receipt and the 4th–15th passages used. Cells were pretreated with each compound at the indicated concentration for 1 h at 37°C and then adsorbed with SARS-CoV-2 (TCDC#4) (sequence available on the GISAID website) at 100 PFU (MOI = 0.01) for 1 h at 37°C as described (Yang et al., 2020). The virus-containing supernatants were removed and then fresh medium containing each compound at the indicated concentrations added to the cells. After incubation for 1 day, cells were fixed and immunostained with anti-SARS-CoV-2 N protein antibody (provided by Dr An-Suei Yang) plus anti-human IgG-Alexa Fluor 488 (A11013, Invitrogen) (green). Nuclei were counter-stained with DAPI (blue); the number of nuclei in vehicle control (no compound treatment) was defined as 100%; and then relative cell viability and CC_{50} values were determined. The fluorescent signal was quantified by high-content imaging and the infection rate and EC_{50} values calculated using normalized values with respective cell viability; the infection rate was defined to be 100% for samples where no compound was added. For combined treatments, the synergy scores were calculated by SynergyFinder (https://synergyfinder.fimm.fi/).

Plaque assays for SARS-CoV-2 were performed as described (Yang et al., 2020). Briefly, Vero E6 cells were seeded 1 day before infection with SARS-CoV-2 for 1 h at 37°C. Subsequently, viruses were removed and the infected cells were covered with overlay media containing 1% methylcellulose (Sigma, cat #M0387) and the test compounds at the indicated concentrations. At 5–7 days post infection, cells were fixed overnight, the overlay media was removed, the resulting cells were stained with crystal violet, and the plaques were counted. Plaque numbers were corrected by plaque size: for a plaque size 50% smaller than the vehicle control, the plaque counted for 0.5 plaque; for a plaque size 75% smaller than the vehicle control, the plaque counted for 0.25 plaque. The percentage of inhibition was calculated as [1–(VD/VC)] × 100%, where VD and VC refer to the virus titer in the presence and absence of the test compound, respectively. The cell viability was determined as described (Kuo et al., 2021) by measurement of relative alkaline phosphatase activity; viability was defined to be 100% for samples where no compounded was added.

Interleukin 6 Cytokine Measurement

IL-6 cytokine levels in the culture supernatants of HCoV-OC43 infected MRC-5 cells at 30 h.p.i. were detected and quantified. Test supernatants were diluted to the requisite concentrations using human IL-6 enzyme-linked immunosorbent assay kits (ARG80110) from arigo Biolaboratories Corp. (Hsinchu, Taiwan) per the manufacturer's recommendations.

Drug Combination Study

Viral inhibition by remdesivir, cyclosporine, and their combinations as measured by IFA or plaque assay was assessed by a drug dose-response matrix. Average synergy scores were obtained via the online tool SynergyFinder (https://synergyfinder.fimm.fi/). ZIP synergy scores were calculated and plotted from three independent experiments. The interaction between two drugs was considered antagonistic for ZIP synergy scores of less than −10; likely to be additional for scores between −10 and 10; and synergistic for ZIP synergy scores of greater than 10.

Statistical Analysis

The statistical significance between the two groups was evaluated using one-way ANOVA followed by Tukey's multiple comparison test in GraphPad Prism (version 8) software; The two-tailed unpaired Student's t test was used evaluated the dose effect of single drug treatment on IL-6 production. * and ** denote statistical significance of $p < 0.05$, and $p < 0.01$ respectively.

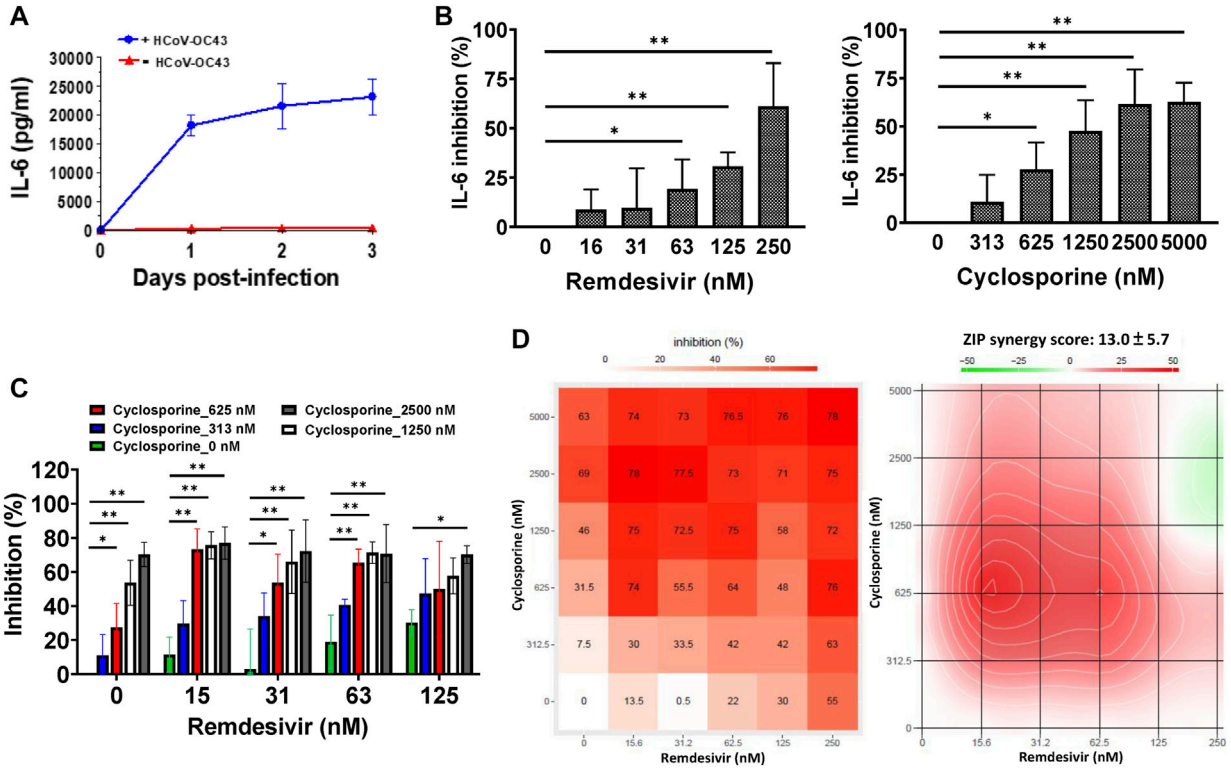

FIGURE 3 | Reduction of IL-6 levels by single and combined treatments of remdesivir and cyclosporine in HCoV-OC43 infected human MRC-5 fetal lung fibroblast cells. **(A)** IL-6 production induced by HCoV-OC43 infection in MRC-5 cells over 3 days. **(B)** Dose dependent reduction of IL-6 levels by remdesivir and cyclosporine treatments in HCoV-OC43 infected MRC-5 cells at 30 h.p.i. Shown are the AVE ± SD from three independent experiments **(A–C)** The two-tailed unpaired Student's t test was used evaluated the dose effect of single drug treatment on IL-6 production. **(C and D)** Synergistic reduction of IL-6 levels produced by HCoV-OC43 infected MRC-5 cells treatment with the combination of remdesivir and cyclosporine. MRC-5 cells were seeded the day before compound treatment or HCoV-OC43 infection. The tested compounds were added to the wells 1 h prior to the addition of HCoV-OC43 at an MOI of 0.05. The resulting cultures were then incubated for an additional 30 h **(B–D)**, or as indicated **(A)**, at 37°C. Subsequently, the culture supernatants were subjected to detection and quantitation of IL-6 by ELISA. AVE ± SD from three independent experiments **(A–C)** are shown; The statistical significance was evaluated using one-way ANOVA followed by Tukey's multiple comparison test. * and ** denote statistical significance of $p < 0.05$, and $p < 0.01$ respectively **(B and C)**. Shown inhibition % (AVE) and synergy scores (AVE ± SD) are from three independent experiments **(D)** analyzed *via* SynergyFinder (https://synergyfinder.fimm.fi/).

TABLE 3 | IL-6 production in human colorectal carcinoma HCT-8 and human fetal lung fibroblast MRC-5 cells with or without HCoV-OC43 infection at 30 h.p.i. Shown are AVE ± SD from three independent experiments.

Cell line	HCoV-OC43 infection	IL-6 quantitative range
HCT-8	–	<minimum 1.5 pg/ml
HCT-8	+	minimum 1.5 pg/ml
MRC-5	–	303 ± 66 pg/ml
MRC-5	+	18,186 ± 1,895 pg/ml

RESULTS

Inhibitory Effects of Remdesivir and Cyclosporine, Alone and in Combination, on HCoV-OC43 in Human HCT-8 Colorectal Carcinoma Cells and Human MRC-5 Fetal Lung Fibroblast Cells (IFA)

As shown in **Figure 1A**, the replication of OC43 in infected HCT-8 cells rose with time over a period of 48 h as examined by western analysis and IFA. To investigate the anti-coronaviral effects of remdesivir and cyclosporine, human colorectal carcinoma cells HCT-8 and human fetal fibroblast cells MRC-5 were infected by HCoV-OC43 at an MOI of 0.05 and incubated at various concentrations of the indicated compounds for 30 h. As shown in **Figures 1B**, **2A** and **Table 1**, remdesivir and cyclosporine inhibited HCoV-OC43 in a dose dependent manner with EC_{50} values of 96 ± 34 nM and 2,920 ± 364 nM in HCT-8 cells and 85 ± 23 nM and 4,419 ± 490 nM in human MRC-5 fetal lung fibroblast cells, respectively.

The combined effects of remdesivir and cyclosporine against HCoV-OC43 were also investigated at various concentrations of each (**Figures 1C**, **2B**). The results revealed that these two drugs exerted a significantly synergistic effect when administered in combination (**Figures 1D**, **2C**), with synergy scores of 26.7 ± 5.4 and 14.8 ± 4.1, and most synergistic area scores of 43.1 and 19.8 against HCoV-OC43 in HCT-8 and MRC-5 cells respectively, as assayed by IFA (**Figures 1C**, **2B**) and analyzed by SynergyFinder (**Figures 1E**, **2D**; **Table 2**).

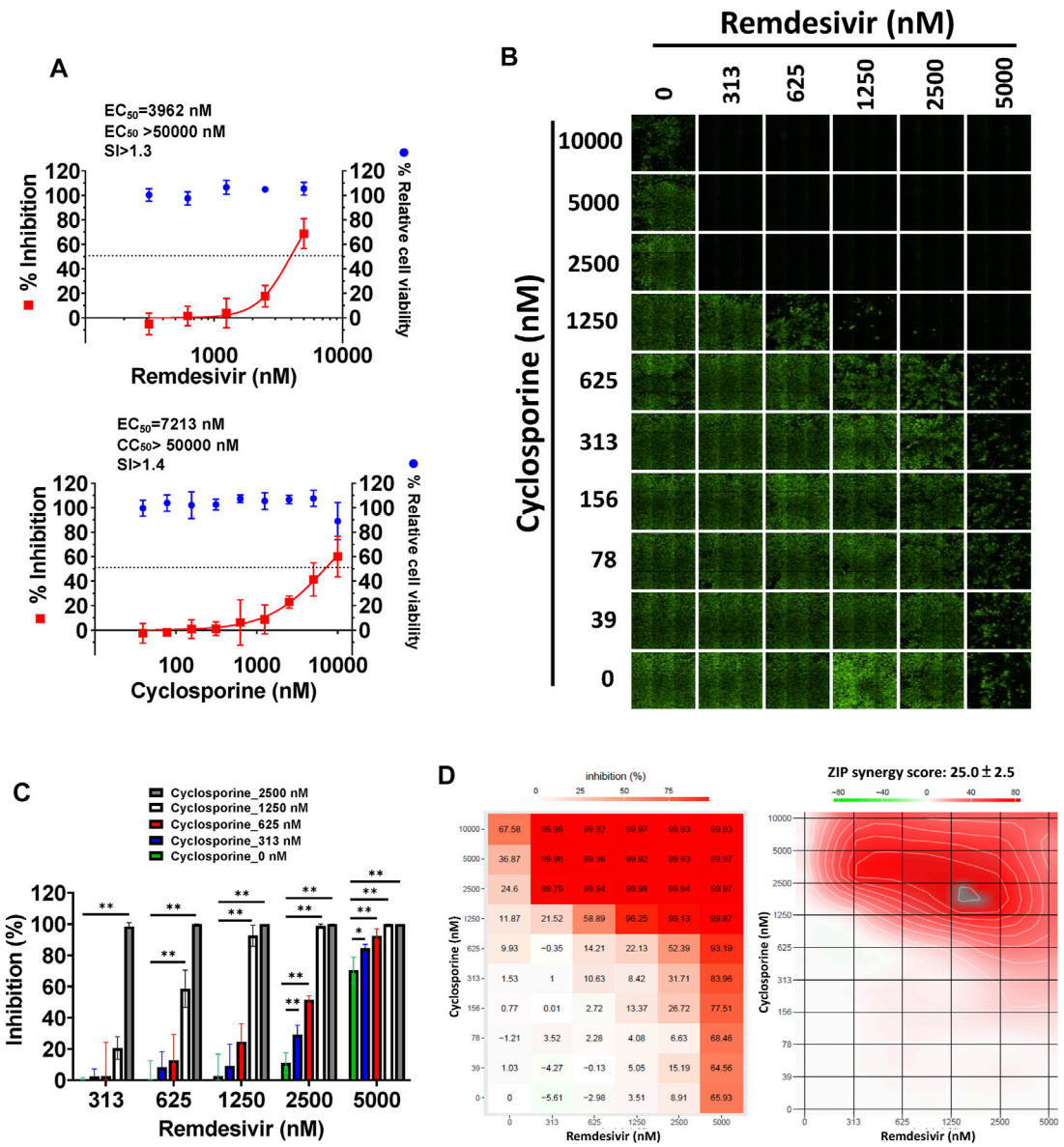

FIGURE 4 | Single or combined treatments of remdesivir and cyclosporine profoundly reduced SARS-CoV-2 infection of Vero E6 cells assayed by IFA. **(A)** Single treatments of remdesivir and cyclosporine reduced SARS-CoV-2 infection of Vero E6 cells in a dose dependent manner. **(B–D)** Combined treatments of remdesivir and cyclosporine synergistically reduced SARS-CoV-2 infection in Vero E6 cells. IFAs were performed with antibody against SARS-CoV-2 N (green) and DAPI staining (blue) for the Vero E6 host live cells. Vero E6 cells were treated with each compound at the indicated concentrations for 1 h at 37°C. The cells were adsorbed with SARS-CoV-2 (TCDC#4) at MOI = 0.01 for 1 h at 37°C. After virus adsorption, the cells were washed with PBS and fresh medium with each compound added at the indicated concentrations and then incubated for 1 day. The cells were fixed with 4% paraformaldehyde and permeabilized with 0.5% Triton X-100. The cells were stained with anti-SARS-CoV-2 N protein antibody and anti-human IgG-Alexa Fluor 488 (green). Nuclei were counter stained with DAPI (blue) and used to determine the relative cell viability by using the number of nuclei in vehicle control as 100% (**Supplementary Figure S3**). N protein expression was measured using a high-content image analysis system (Molecular Devices). The fluorescent signal was normalized with cell viability to calculate the infection rate that no compound treatment was set at 100%. EC_{50} and CC_{50} values were calculated by Prism software. Shown are the AVE ± SD from three independent experiments **(A and C)** * and ** denote statistical significance of $p < 0.05$, and $p < 0.01$ respectively. Shown results of IFA are representative of three independent experiments **(B)**. Shown inhibition % (AVE) and synergy scores (AVE ± SD) are from three independent experiments **(D)** analyzed *via* SynergyFinder (https://synergyfinder.fimm.fi/).

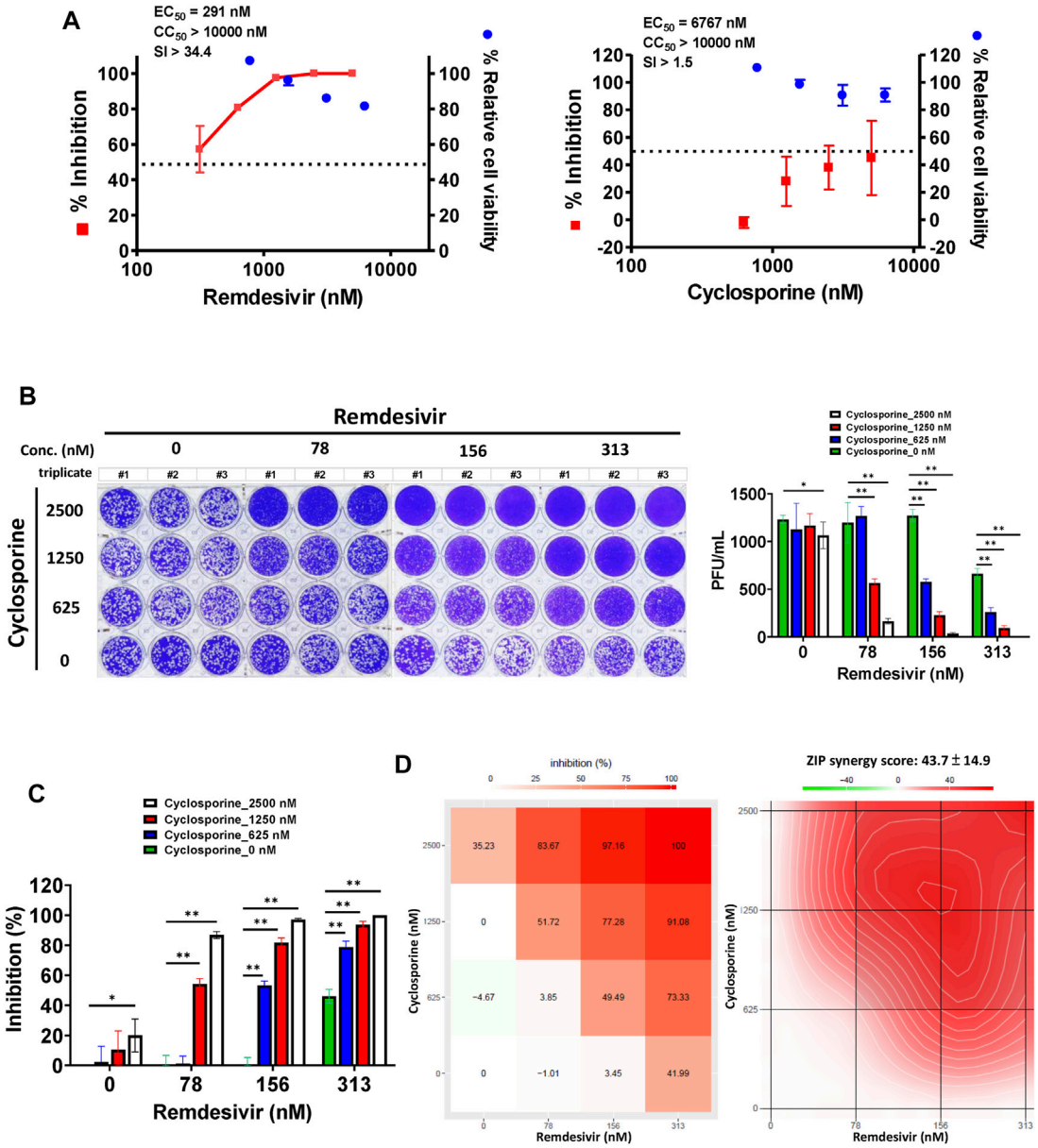

FIGURE 5 | Single or combined treatment with remdesivir and cyclosporine synergistically reduced infectious SARS-CoV-2 viral loads as determined by plaque formation assays. **(A)** Single treatment of SARS-CoV-2-infected Vero E6 cells with remdesivir and cyclosporine reduced the number of plaque-forming units in a dose dependent manner. **(B)** Combined treatment of SARS-CoV-2-infected Vero E6 cells with remdesivir and cyclosporine significantly decreased plaque formation caused by SARS-CoV-2. **(C and D)** Combined treatment of SARS-CoV-2-infected Vero E6 cells with remdesivir and cyclosporine synergistically reduced SARS-CoV-2 viral loads. Plaque assays were performed in triplicate using 24-well tissue culture plates. Vero E6 cells were seeded in DMEM with 10% FBS and antibiotics 1 day before infection. SARS-CoV-2 was added to the cell monolayer for 1 h at 37°C. Subsequently, viruses were removed and the cell monolayer was washed once with PBS before covering with overlay media containing 1% methylcellulose (Sigma, cat#M0387) and the test compounds at indicated concentrations for 5–7 days. The cells were fixed with 10% formaldehyde solution (Marcon™ Chemicals, cat #H121-08) overnight. After removal of overlay media, the cells were stained with crystal violet and the plaques were counted. The percentage of inhibition was calculated as [1–(VD/VC)] × 100%, where VD and VC refer to the virus titer in the presence and absence of the test compound, respectively. The inhibition in plaque formation results shown are representative of three independent experiments, each in triplicate **(B)**. Cell viability was determined as described (Kuo et al., 2021) by measurement of relative alkaline phosphatase activity; viability in the absence of compound treatment was set as 100%. AVE ± SD of three independent experiments were shown **(A and C)**; The statistical significance was evaluated using one-way ANOVA followed by Tukey's multiple comparison test. * and ** were used to denote the statistical significance for $p < 0.05$, and $p < 0.01$ respectively **(C)**. Shown inhibition % (AVE) and synergy scores (AVE ± SD) are from three independent experiments **(D)** analyzed *via* SynergyFinder (https://synergyfinder.fimm.fi/).

Inhibitory Effects of Remdesivir and Cyclosporine, Alone and in Combination, on IL-6 Cytokine Production in HCoV-OC43 Infected Human MRC-5 Fetal Lung Fibroblast Cells

Since IL-6 is a pivotal biomarker in COVID-19 disease progression (Henry et al., 2020; McElvaney et al., 2020), we examined IL-6 levels in HCoV-OC43-infected and -uninfected HCT-8 and MRC-5 cells. Greater than 20,000 pg/ml of IL-6 was found to be produced by HCoV-OC43-infected MRC-5 cells over the course of 3 days (**Figure 3A**); IL-6 levels in uninfected MRC-5 cells were very low (**Figure 3A**; **Table 3**). However, IL-6 was not detected in the culture supernatants of HCoV-OC43-infected or uninfected HCT-8 cells (**Table 3**). Therefore, the effects of remdesivir and cyclosporine on IL-6 cytokine production were examined in HCoV-OC43-infected MRC-5 cells at 30 h.p.i. over a time period equivalent to the time needed for the HCoV-OC43-infected human MRC-5 fetal lung fibroblast cells to produce 18,186 ± 1,895 pg/ml of IL-6 (**Table 3**).

As shown in **Figure 3B** and **Table 1**, remdesivir and cyclosporine separately reduced IL-6 production in MRC-5 cells infected with HCoV-OC43 at 30 h.p.i. in a dose dependent manner, with EC_{50} values of 224 ± 53 nM and 1,292 ± 352 nM, respectively. Similarly, the combined effects of remdesivir and cyclosporine on HCoV-OC43-induced IL-6 production were investigated at varying concentrations of each. The results showed that these two drugs exerted a significantly synergistic reduction of IL-6 production by HCoV-OC43-infected MRC-5 cells when administered in combination (**Figure 3C**), with a synergy score of 13.0 ± 5.7 and a most synergistic area score of 25.8, as assayed by ELISA and analyzed by SynergyFinder (**Figure 3D**; **Table 2**).

Inhibitory Effects of Remdesivir and Cyclosporine, Alone and in Combination, on SARS-CoV-2 in Vero E6 Cells

We further examined whether the combination of remdesivir and cyclosporine could synergistically inhibit SARS-CoV-2. Two disparate assays (IFA and plaque formation) were performed to examine the single and combined inhibitory effects of remdesivir and cyclosporine on SARS-CoV-2 in Vero E6 cells.

As shown in **Figure 4A** and **Table 1**, remdesivir and cyclosporine exhibited dose-dependent SARS-CoV-2 inhibition with respective EC_{50} values of, 3,962 ± 303 nM and 7,213 ± 143 nM in Vero E6 cells at 1 day post-infection (d.p.i.) with an antibody against SARS-CoV-2 N protein. The combined effects of remdesivir and cyclosporine against SARS-CoV-2 were then investigated at various concentrations of each. The results revealed that the inhibitory effects of these two drugs against SARS-CoV-2 in Vero E6 cells, as assayed by IFA at 1 d.p.i. (**Figure 4B**), were significantly synergistic (**Figure 4C**) with a synergy score of 25.0 ± 2.5 (analyzed by SynergyFinder) and a most synergistic area score of 65.5 (**Figure 4D** and **Table 2**).

A plaque formation assay was also undertaken, to examine the combined effect of remdesivir and cyclosporine on the SARS-CoV-2 infectious dose at 5–7 d.p.i. in Vero E6 cells (**Figure 5**). The plaque formation assay is traditionally used to determine the infectious virus dose–the number of plaque-forming units in a virus sample. Plaque formation in culture plates of SARS-CoV-2-infected confluent Vero E6 cells took 5–7 days. Plaques were counted manually and the numbers corrected based on the sizes of plaques as described in Methods. Remdesivir and cyclosporine were again found to separately inhibit SARS-CoV-2 in a dose dependent manner with respective EC_{50} values of 291 ± 91 nM and 6,767 ± 1,827 nM (**Figure 5A**; **Table 1**). Their combined inhibitory effect was found to be significantly synergistic as shown in **Figures 5B,C**, with a synergy score of 43.7 ± 14.9 and a most synergistic area score of 46.2 analyzed by SynergyFinder (**Figure 5D**; **Table 2**).

CONCLUSION AND DISCUSSIONS

Remdesivir is a prodrug which is metabolized into a nucleoside triphosphate that irreversibly bonds with the RdRp of SARS-CoV-2, blocking viral transcription after cell entry (Shannon et al., 2020; Hanafin et al., 2021). It is used clinically for the treatment of COVID-19 patients, but its efficacy is limited (Beigel et al., 2020; Goldman et al., 2020; Spinner et al., 2020) and its mechanism of action does not address the cytokine storm that also accompanies the disease progression of COVID-19 (McElvaney et al., 2020). Blockade of key pathogenic cytokines in COVID-19 patients should ameliorate disease progression and exert viral inhibition. Elevated IL-6 levels in COVID-19 patients play an important role in disease progression and severity (Henry et al., 2020; McElvaney et al., 2020), and the IL-6 inhibitor tocilizumab is a potential alternative therapy for COVID-19 patients experiencing a cytokine storm (Klopfenstein et al., 2020; Toniati et al., 2020; Xu et al., 2020). However, more controlled clinical trials are needed to confirm its efficacy and safety (Campochiaro et al., 2020; Lan et al., 2020; Stone et al., 2020).

Simultaneous reduction of coronaviral loads and mitigation of the cytokine storm may constitute an efficacious treatment of severe COVID-19. Herein, we identified the immunosuppressant cyclosporine by screening for inhibitors of HCoV-OC43, and found that it exerted a significantly synergistic inhibitory effect against HCoV-OC43 and SARS-CoV-2 in combination with remdesivir (**Figures 1**, **2**, **4**, **5**; **Tables 1**, **2**). These drugs also reduced coronavirus IL-6 production synergistically, when used in combination (**Figure 3**; **Tables 2**, **3**). Whereas cyclosporine reduces IL-6 *via* down-regulation of its production (Stephanou et al., 1992; Iacono et al., 1997) (which contributes to its anti-viral activity), remdesivir targets coronaviral RdRp (Gordon et al., 2020; Pruijssers et al., 2020) to reduce viral loads and thereby reducing IL-6 production. In combination, these drugs are capable of profoundly reducing coronaviral loads and IL-6 production in a synergistic manner. Furthermore, the doses of

cyclosporine (3.6–4.8 mg/kg) which correspond to the measured EC_{50} values (3–4 μM) or lower, when in combination with remdesivir, are actually lower than those in current clinical use (~15 mg/kg for the initial dose and 5–10 mg/kg for the maintenance doses), which result in cyclosporine plasma concentrations of 250–1000 ng/ml (Novais Sandimmune®, https://www.rxlist.com/sandimmune-drug.htm#side_effects). Similarly, the EC_{50} values of remdesivir herein are also equivalent or lower than those in current clinical use (100–200 mg) (Grein et al., 2020). Thus, the cyclosporine and remdesivir levels measured in this study are of clinical significance.

The synergy of the combinations of remdesivir with itraconazole (an anti-fungal), fluoxetine (Schloer et al., 2021) (an anti-depressant), or calcium-channel blocker diltiazem (Pizzorno et al., 2020) respectively was reported, but the effects were only marginal [synergy scores ~12 analyzed by SynergyFinder (Pizzorno et al., 2020; Schloer et al., 2021)]. On the other hand, Janus kinases (JAKs) play a critical role in the cytokine storm of severe COVID-19 patients (Luo et al., 2020) and the combined treatment of remdesivir with the JAK inhibitor baricitinib was found to further reduce recovery time and improve the clinical status of severe COVID-19 patients compared to remdesivir alone (Kalil et al., 2020). Therefore, the synergistic effect of the combined treatment of remdesivir and cyclosporine in reducing coronaviral load and IL-6 levels identified herein merits further study for application in moderately or severely ill COVID-19-patients whose SARS-CoV-2 infection is complexed with a cytokine storm, as well as other applicable conditions identified in the future.

These results validate our strategy of treating COVID-19 with two drugs–one to address viral load, and the other cellular factors. The search for other combined treatments for patients with different progressive and pathogenic stages of COVID-19 merit further exploration.

DATA AVAILABILITY STATEMENT

The original contributions presented in the study are included in the article/**Supplementary Material**, further inquiries can be directed to the corresponding author.

AUTHOR CONTRIBUTIONS

H-YH, C-WY, and Y-ZL performed most of the biochemistry, and molecular biology experiments. J-JL, C-CL, T-LC, H-CK, and S-HW performed part of the biochemistry, and molecular biology experiments. S-JL, C-WY, Y-ZL, H-YH, Y-LL, and S-YC designed experiments and analyzed the obtained results; interpreted the data and wrote the manuscript. R-BY, J-YC, H-KS and C-TC were involved in composition of the manuscript. S-JL supervised the experimental design, the interpretation of the data, and the composition of the manuscript.

FUNDING

This work was funded by the National Health Research Institutes, Taiwan, R.O.C.; Academia Sinica (AS-CFII-108-102); the Ministry of Science and Technology, Taiwan, R.O.C (MOST 109-2327-B-400-003; MOST 109-3114-Y-001-001; MOST 109-2811-B-400-518; MOST109-2327-B-002–009); and the Ministry of Health and Welfare, Taiwan, R.O.C. for an emergent grant of COVID-19.

ACKNOWLEDGMENTS

The authors gratefully acknowledge Kung-Yee Liang, National Health Research Institutes, for his full support on this work. We also would like to acknowledge Taiwan CDC for providing SARS-CoV-2 TCDC#4 (hCoV-19/Taiwan/4/2020) and the services provided by the Biosafety Level-3 Laboratory of the First Core Laboratory, National Taiwan University College of Medicine and by IBMS P3 facility at Academia Sinica.

SUPPLEMENTARY MATERIAL

The Supplementary Material for this article can be found online at: https://www.frontiersin.org/articles/10.3389/fphar.2021.706901/full#supplementary-material

REFERENCES

Beauchesne, P. R., Chung, N. S. C., and Wasan, K. M. (2007). Cyclosporine A: a Review of Current Oral and Intravenous Delivery Systems. *Drug Dev. Ind. Pharm.* 33 (3), 211–220. doi:10.1080/03639040601155665

Beigel, J. H., Tomashek, K. M., Dodd, L. E., Mehta, A. K., Zingman, B. S., Kalil, A. C., et al. (2020). Remdesivir for the Treatment of Covid-19 - Final Report. *N. Engl. J. Med.* 383 (19), 1813–1826. doi:10.1056/nejmoa2007764

Campochiaro, C., Della-Torre, E., Cavalli, G., De Luca, G., Ripa, M., Boffini, N., et al. (2020). Efficacy and Safety of Tocilizumab in Severe COVID-19 Patients: a Single-centre Retrospective Cohort Study. *Eur. J. Intern. Med.* 76, 43–49. doi:10.1016/j.ejim.2020.05.021

Chen, L., Wang, G., Tan, J., Cao, Y., Long, X., Luo, H., et al. (2020). Scoring Cytokine Storm by the Levels of MCP-3 and IL-8 Accurately Distinguished COVID-19 Patients with High Mortality. *Signal. Transduction Targeted Therapy* 5 (1), 292. doi:10.1038/s41392-020-00433-y

De Benedetti, F., Brunner, H. I., Ruperto, N., Kenwright, A., Wright, S., Calvo, I., et al. (2012). Randomized Trial of Tocilizumab in Systemic Juvenile Idiopathic Arthritis. *N. Engl. J. Med.* 367 (25), 2385–2395. doi:10.1056/nejmoa1112802

Du, S., Hiramatsu, N., Hayakawa, K., Kasai, A., Okamura, M., Huang, T., et al. (2009). Suppression of NF-Kb by Cyclosporin A and Tacrolimus (FK506) via Induction of the C/EBP Family: Implication for Unfolded Protein Response. *J. Immunol.* 182 (11), 7201–7211. doi:10.4049/jimmunol.0801772

Fatima, S. A., Asif, M., Khan, K. A., Siddique, N., and Khan, A. Z. (2020). Comparison of Efficacy of Dexamethasone and Methylprednisolone in Moderate to Severe Covid 19 Disease. *Ann. Med. Surg. (Lond)* 60, 413–416. doi:10.1016/j.amsu.2020.11.027

Goldman, J. D., Lye, D. C. B., Hui, D. S., Marks, K. M., Bruno, R., Montejano, R., et al. (2020). Remdesivir for 5 or 10 Days in Patients with Severe Covid-19. *N. Engl. J. Med.* 383 (19), 1827–1837. doi:10.1056/nejmoa2015301

Golling, M., Sadeghi, M., Zipperle, S., Fonouni, H., Golriz, M., and Mehrabi, A. (2009). In Vitrocytokine Responses in Liver Transplant Recipients Treated with

Cyclosporine A and Tacrolimus. *Clin. Transplant.* 23 (Suppl. 21), 83–91. doi:10.1111/j.1399-0012.2009.01114.x

Gordon, C. J., Tchesnokov, E. P., Woolner, E., Perry, J. K., Feng, J. Y., Porter, D. P., et al. (2020). Remdesivir Is a Direct-Acting Antiviral that Inhibits RNA-dependent RNA Polymerase from Severe Acute Respiratory Syndrome Coronavirus 2 with High Potency. *J. Biol. Chem.* 295 (20), 6785–6797. doi:10.1074/jbc.ra120.013679

Grein, J., Ohmagari, N., Shin, D., Diaz, G., Asperges, E., Castagna, A., et al. (2020). Compassionate Use of Remdesivir for Patients with Severe Covid-19. *N. Engl. J. Med.* 382, 2327–2336. doi:10.1056/nejmoa2007016

Hanafin, P. O., Jermain, B., Hickey, A. J., Kabanov, A. V., Kashuba, A. D., Sheahan, T. P., et al. (2021). A Mechanism-based Pharmacokinetic Model of Remdesivir Leveraging Interspecies Scaling to Simulate COVID-19 Treatment in Humans. *CPT Pharmacometrics Syst. Pharmacol.* 10 (2), 89–99. doi:10.1002/psp4.12584

Henry, B. M., de Oliveira, M. H. S., Benoit, S., Plebani, M., and Lippi, G. (2020). Hematologic, Biochemical and Immune Biomarker Abnormalities Associated with Severe Illness and Mortality in Coronavirus Disease 2019 (COVID-19): a Meta-Analysis. *Clin. Chem. Lab. Med.* 58 (7), 1021–1028. doi:10.1515/cclm-2020-0369

Iacono, A., Dauber, J., Keenan, R., Spichty, K., Cai, J., Grgurich, W., et al. (1997). Interleukin 6 and Interferon-?? Gene Expression in Lung Transplant Recipients with Refractory Acute Cellular Rejection. *Transplantation* 64 (2), 263–269. doi:10.1097/00007890-199707270-00015

Jerkins, G. W., Pattar, G. R., and Kannarr, S. R. (2020). A Review of Topical Cyclosporine A Formulations-A Disease-Modifying Agent for Keratoconjunctivitis Sicca. *Clin. Ophthalmol.* 14, 481–489. doi:10.2147/opth.s228070

Kalil, A. C., Patterson, T. F., Mehta, A. K., Tomashek, K. M., Wolfe, C. R., Ghazaryan, V., et al. (2020). Baricitinib Plus Remdesivir for Hospitalized Adults with Covid-19. *N. Engl. J. Med.* 384 (9), 795–807. doi:10.1056/NEJMoa2031994

Klopfenstein, T., Zayet, S., Lohse, A., Balblanc, J.-C., Badie, J., Royer, P.-Y., et al. (2020). Tocilizumab Therapy Reduced Intensive Care Unit Admissions And/or Mortality in COVID-19 Patients. *Médecine et Maladies Infectieuses* 50 (5), 397–400. doi:10.1016/j.medmal.2020.05.001

Kuo, C. J., Chao, T. L., Kao, H. C., Tsai, Y. M., Liu, Y. K., Wang, L. H., et al. (2021). Kinetic Characterization and Inhibitor Screening for the Proteases Leading to Identification of Drugs against SARS-CoV-2. *Antimicrob. Agents Chemother.* 65 (4), e02577. doi:10.1128/aac.02577-20

Lan, S.-H., Lai, C.-C., Huang, H.-T., Chang, S.-P., Lu, L.-C., and Hsueh, P.-R. (2020). Tocilizumab for Severe COVID-19: a Systematic Review and Meta-Analysis. *Int. J. Antimicrob. Agents* 56 (3), 106103. doi:10.1016/j.ijantimicag.2020.106103

Liddicoat, A. M., and Lavelle, E. C. (2019). Modulation of Innate Immunity by Cyclosporine A. *Biochem. Pharmacol.* 163, 472–480. doi:10.1016/j.bcp.2019.03.022

Luo, W., Li, Y.-X., Jiang, L.-J., Chen, Q., Wang, T., and Ye, D.-W. (2020). Targeting JAK-STAT Signaling to Control Cytokine Release Syndrome in COVID-19. *Trends Pharmacological Sciences* 41 (8), 531–543. doi:10.1016/j.tips.2020.06.007

McElvaney, O. J., McEvoy, N. L., McElvaney, O. F., Carroll, T. P., Murphy, M. P., Dunlea, D. M., et al. (2020). Characterization of the Inflammatory Response to Severe COVID-19 Illness. *Am. J. Respir. Crit. Care Med.* 202 (6), 812–821. doi:10.1164/rccm.202005-1583oc

Meyer, S., Kohler, N. G., and Joly, A. (1997). Cyclosporine A Is an Uncompetitive Inhibitor of Proteasome Activity and Prevents NF-Kb Activation. *FEBS Lett.* 413 (2), 354–358. doi:10.1016/s0014-5793(97)00930-7

Pizzorno, A., Padey, B., Dubois, J., Julien, T., Traversier, A., Dulière, V., et al. (2020). *In Vitro* evaluation of Antiviral Activity of Single and Combined Repurposable Drugs against SARS-CoV-2. *Antivir. Res.* 181, 104878. doi:10.1016/j.antiviral.2020.104878

Pruijssers, A. J., George, A. S., Schäfer, A., Leist, S. R., Gralinksi, L. E., Dinnon, K. H., et al. (2020). Remdesivir Inhibits SARS-CoV-2 in Human Lung Cells and Chimeric SARS-CoV Expressing the SARS-CoV-2 RNA Polymerase in Mice. *Cel Rep.* 32 (3), 107940. doi:10.1016/j.celrep.2020.107940

Rosas, I. O., Bräu, N., Waters, M., Go, R. C., Hunter, B. D., Bhagani, S., et al. (2021). Tocilizumab in Hospitalized Patients with Severe Covid-19 Pneumonia. *N. Engl. J. Med.* 384 (16), 1503–1516. doi:10.1056/nejmoa2028700

Schloer, S., Brunotte, L., Mecate-Zambrano, A., Zheng, S., Tang, J., Ludwig, S., et al. (2021). Drug Synergy of Combinatory Treatment with Remdesivir and the Repurposed Drugs Fluoxetine and Itraconazole Effectively Impairs SARS-CoV-2 Infection *In Vitro*. *Br. J. Pharmacol.* 178 (11), 2339–2350. doi:10.1111/bph.15418

Scott, L. J. (2017). Tocilizumab: A Review in Rheumatoid Arthritis. *Drugs* 77 (17), 1865–1879. doi:10.1007/s40265-017-0829-7

Shannon, A., Le, N. T.-T., Selisko, B., Eydoux, C., Alvarez, K., Guillemot, J.-C., et al. (2020). Remdesivir and SARS-CoV-2: Structural Requirements at Both Nsp12 RdRp and Nsp14 Exonuclease Active-Sites. *Antivir. Res.* 178, 104793. doi:10.1016/j.antiviral.2020.104793

Spinner, C. D., Gottlieb, R. L., Criner, G. J., Arribas López, J. R., Cattelan, A. M., Soriano Viladomiu, A., et al. (2020). Effect of Remdesivir vs Standard Care on Clinical Status at 11 Days in Patients with Moderate COVID-19. *Jama* 324 (11), 1048–1057. doi:10.1001/jama.2020.16349

Stephanou, A., Sarlis, N. J., Knight, R. A., Lightman, S. L., and Chowdrey, H. S. (1992). Effects of Cyclosporine A on the Hypothalamic-Pituitary-Adrenal axis and Anterior Pituitary Interleukin-6 mRNA Expression during Chronic Inflammatory Stress in the Rat. *J. neuroimmunology* 41 (2), 215–222. doi:10.1016/0165-5728(92)90072-s

Stone, J. H., Frigault, M. J., Serling-Boyd, N. J., Fernandes, A. D., Harvey, L., Foulkes, A. S., et al. (2020). Efficacy of Tocilizumab in Patients Hospitalized with Covid-19. *N. Engl. J. Med.* 383 (24), 2333–2344. doi:10.1056/nejmoa2028836

Tomazini, B. M., Maia, I. S., Cavalcanti, A. B., Berwanger, O., Rosa, R. G., Veiga, V. C., et al. (2020). Effect of Dexamethasone on Days Alive and Ventilator-free in Patients with Moderate or Severe Acute Respiratory Distress Syndrome and COVID-19. *Jama* 324 (13), 1307–1316. doi:10.1001/jama.2020.17021

Toniati, P., Piva, S., Cattalini, M., Garrafa, E., Regola, F., Castelli, F., et al. (2020). Tocilizumab for the Treatment of Severe COVID-19 Pneumonia with Hyperinflammatory Syndrome and Acute Respiratory Failure: A Single center Study of 100 Patients in Brescia, Italy. *Autoimmun. Rev.* 19 (7), 102568. doi:10.1016/j.autrev.2020.102568

Wu, Q., Wang, X., Nepovimova, E., Wang, Y., Yang, H., and Kuca, K. (2018). Mechanism of Cyclosporine A Nephrotoxicity: Oxidative Stress, Autophagy, and Signalings. *Food Chem. Toxicol.* 118, 889–907. doi:10.1016/j.fct.2018.06.054

Xu, X., Han, M., Li, T., Sun, W., Wang, D., Fu, B., et al. (2020). Effective Treatment of Severe COVID-19 Patients with Tocilizumab. *Proc. Natl. Acad. Sci. USA* 117 (20), 10970–10975. doi:10.1073/pnas.2005615117

Yang, C-W., Lee, Y-Z., Hsu, H-Y., Jan, J-T., Lin, Y-L., Chang, S-Y., et al. (2020). Inhibition of SARS-CoV-2 by Highly Potent Broad-Spectrum Anti-coronaviral Tylophorine-Based Derivatives. *Front. Pharmacol.* 11 (2056), 606097. doi:10.3389/fphar.2020.606097

Yang, C.-W., Hsu, H.-Y., Chang, H.-Y., Lee, Y.-Z., and Lee, S.-J. (2020). Natural Cardenolides Suppress Coronaviral Replication by Downregulating JAK1 via a Na+/K+-ATPase Independent Proteolysis. *Biochem. Pharmacol.* 180, 114122. doi:10.1016/j.bcp.2020.114122

Yang, X., Feng, P., Yin, Y., Bushley, K., Spatafora, J. W., and Wang, C. (2018). Cyclosporine Biosynthesis in Tolypocladium Inflatum Benefits Fungal Adaptation to the Environment. *mBio* 9 (5), e01211–01218. doi:10.1128/mbio.01211-18

Yang, Y., Shen, C., Li, J., Yuan, J., Wei, J., Huang, F., et al. (2020). Plasma IP-10 and MCP-3 Levels Are Highly Associated with Disease Severity and Predict the Progression of COVID-19. *J. Allergy Clin. Immunol.* 146 (1), 119–127. doi:10.1016/j.jaci.2020.04.027

Conflict of Interest: The authors declare that the research was conducted in the absence of any commercial or financial relationships that could be construed as a potential conflict of interest.

Publisher's Note: All claims expressed in this article are solely those of the authors and do not necessarily represent those of their affiliated organizations, or those of the publisher, the editors and the reviewers. Any product that may be evaluated in this article, or claim that may be made by its manufacturer, is not guaranteed or endorsed by the publisher.

frontiers in Pharmacology

ORIGINAL RESEARCH
published: 27 August 2021
doi: 10.3389/fphar.2021.731828

Designing Short Peptides to Block the Interaction of SARS-CoV-2 and Human ACE2 for COVID-19 Therapeutics

Abdul Basit[1†], *Asad Mustafa Karim*[2†], *Muhammad Asif*[1], *Tanveer Ali*[3], *Jung Hun Lee*[4], *Jeong Ho Jeon*[4], *Shafiq ur Rehman*[1*] and *Sang Hee Lee*[4*]

[1]Institute of Microbiology and Molecular Genetics, University of the Punjab, Lahore, Pakistan, [2]Department of Bioscience and Biotechnology, The University of Suwon, Hwaseong, South Korea, [3]Department of Host Defense, Graduate School of Medicine, University of the Ryukyus, Nishihara, Japan, [4]National Leading Research Laboratory, Department of Biological Sciences, Myongji University, Yongin, South Korea

OPEN ACCESS

Edited by:
Sugunadevi Sakkiah, National Center for Toxicological Research (FDA), United States

Reviewed by:
Gowthaman Uthaman, University of Massachusetts Medical School, United States
Ciro Leonardo Pierri, University of Bari Aldo Moro, Italy

***Correspondence:**
Shafiq ur Rehman
shafiq.mmg@pu.edu.pk
Sang Hee Lee
sangheelee@mju.ac.kr

[†]These authors have contributed equally to this work

Specialty section:
This article was submitted to Respiratory Pharmacology, a section of the journal Frontiers in Pharmacology

Received: 28 June 2021
Accepted: 17 August 2021
Published: 27 August 2021

Citation:
Basit A, Karim AM, Asif M, Ali T, Lee JH, Jeon JH, Rehman Su and Lee SH (2021) Designing Short Peptides to Block the Interaction of SARS-CoV-2 and Human ACE2 for COVID-19 Therapeutics. Front. Pharmacol. 12:731828. doi: 10.3389/fphar.2021.731828

To date, the current COVID-19 pandemic caused by SARS-CoV-2 has infected 99.2 million while killed 2.2 million people throughout the world and is still spreading widely. The unavailability of potential therapeutics against this virus urges to search and develop new drugs. SARS-CoV-2 enters human cells by interacting with human angiotensin-converting enzyme 2 (ACE2) receptor expressed on human cell surface through utilizing receptor-binding domain (RBD) of its spike glycoprotein. The RBD is highly conserved and is also a potential target for blocking its interaction with human cell surface receptor. We designed short peptides on the basis of our previously reported truncated ACE2 (tACE2) for increasing the binding affinity as well as the binding interaction network with RBD. These peptides can selectively bind to RBD with much higher affinities than the cell surface receptor. Thus, these can block all the binding residues required for binding to cell surface receptor. We used selected amino acid regions (21–40 and 65–75) of ACE2 as scaffold for the *de novo* peptide design. Our designed peptide Pep1 showed interactions with RBD covering almost all of its binding residues with significantly higher binding affinity (–13.2 kcal mol^{-1}) than the cell surface receptor. The molecular dynamics (MD) simulation results showed that designed peptides form a stabilized complex with RBD. We suggest that blocking the RBD through *de novo* designed peptides can serve as a potential candidate for COVID-19 treatment after further clinical investigations.

Keywords: COVID-19, SARS-CoV-2, RBD, designed peptide, s glycoprotein

INTRODUCTION

Severe acute respiratory syndrome-coronavirus 2 (SARS-CoV-2) is the enveloped and positive-stranded RNA virus (Muralidharan et al., 2021). SARS-CoV-2 was emerged and started causing coronavirus disease 2019 (COVID-19). Hence, it is the utmost public health emergency at present with no treatment available so far, with an urgent need of potent drug against COVID-19 (Muralidharan et al., 2021). Currently, SARS-CoV-2 has affected the whole world and possibly it can re-emerge in the future with some virus beneficial mutations which might lead to more-worst outcome. Coronaviruses use spike (S) glycoprotein to attach and fuse with host cells, followed by

entry into the cell. The interaction between the receptor-binding domain (RBD) of S protein and the human angiotensin-converting enzyme 2 (ACE2) happens while the S protein is in the pre-fusion conformation. The binding of the S protein in pre-fusion conformation with ACE2 triggers the cleavage of the S protein in two large domains: the N-terminal domain that remains attached to ACE2 and the C-terminal domain which folds in the so called post-fusion conformation (6-helix bundle fusion core) determining host-cell invasion (viral membrane fusion process) (Mercurio et al., 2021). A recent study has diagnosed SARS-CoV-2 in serum, urine and fecal samples with a low detection rate (Kim et al., 2020; Wang et al., 2020). Although it is challenging to determine whether the urinary tract, bladder or blood cells are also infected by SARS-CoV-2, virtual screening of RBD with cell surface receptor can raise the possibility of fecal/urine-respiratory infection.

Interestingly, the SARS-CoV-1 and -2 bind with cell surface receptor through RBD (a highly conserved region of S protein) (Singh et al., 2020), which suggests this domain a suitable target for drug designing (Lizbeth et al., 2020). The structural insights of SARS-CoV-2 and ACE2 interactions have been extensively studied (Lan et al., 2020; Yan et al., 2020). The RBD residues critical for interaction with ACE2 are located at position 417, 458, 493–498, and 500–502 (Chan et al., 2020; Lan et al., 2020; Yan et al., 2020; Basit et al., 2021). This suggests that almost similar binding residues of RBD are used to interact with cell surface receptor. The overall sequence of RBD is highly conserved with more than 99.9% homology with worldwide sequences of RBD reported (Basit et al., 2021). Structural elucidation has also confirmed the highly conserved nature of RBD (Lan et al., 2020). Blocking the binding residues of RBD can impede the SARS-CoV-2 to infect the human cells (Huang et al., 2020). The interactions between RBD and cell surface receptor have been extensively elucidated (Chan et al., 2020; Wan et al., 2020; Yan et al., 2020), which can be exploited to design peptide-based inhibitors targeting binding residues of RBD. Several studies have reported peptides for blocking the fusion of SARS-CoV-2 RBD with human cell surface receptor and for targeting the HR1 domain, which have shown successful inhibitory effects (Du et al., 2009; Xia et al., 2019; Han and Kral, 2020; Karoyan et al., 2021). Previous studies have shown that the residues of ACE2 at position 21–40 and 76 are optimal for binding with RBD (Huang et al., 2020; Basit et al., 2021). There are several other peptides reported for blocking RBD of SARS-CoV-2 and SARS-CoV-1 (Han et al., 2006; Chan et al., 2020). However, these peptides may not cover all the binding residues of RBD. Engineering the optimal regions of ACE2 and expanding their binding interaction network can significantly block the infection of SARS-CoV-2 into human cells. *De novo* protein design is a novel approach used to optimize the binding interface of protein-protein interactions by mutating the residues into favorable mutants which provide new binding interactions with increased binding affinity and preserved secondary structure (Chevalier et al., 2017). Recently, Huang et al. (2020), redesigned the previously reported two natural peptides from ACE2 through EvoDesign (Pearce et al., 2019) and produced a hybrid peptide with improved binding affinity for RBD and showed interactions with residues Y453, F456, Y473, A475, N487, and Y489 of RBD.

In the current study, we aimed to design peptides on the basis of our previously reported truncated ACE2 (tACE2) (Basit et al., 2021) by using EvoDesign, a *de novo* peptide design approach, to increase not only the binding affinity but also extend the binding interaction network with RBD. We have selected two regions of ACE2 (21–40 and 65–75) as a template for *de novo* peptide design (Wan et al., 2020). We designed two peptides, Pep1 and Pep2 for binding with RBD and determined their binding affinity and complex stability through protein-protein docking and molecular dynamics (MD) simulations. The present study will open a new path for designing therapeutic peptides against COVID-19.

MATERIALS AND METHODS

Designing COVID-19 Therapeutic Peptides

The three-dimensional (3D) structure (protein data bank [PDB] ID: 6m17) of RBD of SARS-CoV-2 S glycoprotein was obtained from PDB database. Two peptides (Pep1 and Pep2) were deigned against the binding residues at position 417, 453, 458, 493–498, and 500–505 of RBD (Yan et al., 2020). The amino acid position 21–40 of tACE2 binds with the binding residues 493–498 and 501–505 of RBD (Basit et al., 2021), while 65–75 amino acid region of tACE2 interacts with binding residues 417, 453. and 458 of RBD (Lizbeth et al., 2020). Therefore, we selected these two fragments of ACE2 from amino acid position 21–40 and 65–75 as scaffold1 and scaffold2, respectively, for *de novo* peptide design to further enhance their binding affinity for RBD. The 3D structure of the scaffold peptides were produced through I-TASSER (Yang et al., 2015) and optimized for energy minimization through FoldX (Schymkowitz et al., 2005). The optimized scaffold structures were submitted as template to EvoDesign server (https://zhanglab.ccmb.med.umich.edu/EvoDesign/) using interface design. The template modeling-score (TM-score) >0. 5 indicates that the designed peptide has similar fold to that of scaffold while the value < 0.2 correspond to those of randomly chosen unrelated proteins (Pierce et al., 2014). EvoDesign outputs the top 10 sequences selected from the largest clusters. The top ten designed sequences obtained for each peptide was sorted based on TM-score, sequence identity and lowest free energy. The sequence with the lowest free energy was considered as favorable design. However, we selected Pep1 and Pep2 from their corresponding top 10 sequences based on their Z-score and HADDOCK-score calculated by HADDOCK server (https://wenmr.science.uu.nl/haddock2.4/). The 3D models of the designed peptides were produced through I-TASSER (Yang et al., 2015). The selected designed peptides were analyzed for their fold similarity through template modeling alignment (TM-align) (Zhang and Skolnick, 2005).

Docking of RBD With Designed Peptides

Protein-protein docking of the designed peptides with RBD was performed through HADDOCK, a flexible protein-protein docking tool (van Zundert et al., 2016). The structures of designed peptides were optimized before docking for amino

acid side chain clashes and energy minimization by using FoldX (Schymkowitz et al., 2005). HADDOCK performs protein-protein docking by retrieving information from experimentally determined protein-protein complexes. The energy function used by HADDOCK consists on combination of interaction energies and HADDOCK-score, which is a combination of non-bonded intermolecular interactions (Vangone et al., 2017). All the generated docking poses were analyzed through PyMOL (Schrodinger, 2010). The best docked complex of RBD with designed peptides were selected on the basis of HADDOCK-score and were further analyzed for binding affinity ΔG (kcal mol^{-1}) and complex stability by using an online protein binding energy prediction server (https://bianca.science.uu.nl/prodigy/), PRODIGY (Xue et al., 2016). Dissociation constant Kd (M) was determined as previously described (Basit et al., 2021). The peptides-RBD docked complexes with higher binding affinity were subjected to MD simulation to further confirm complex stability.

Determination of RBD-Peptide Complex Stability Through MD Simulation

MD simulation of RBD in complex with designed peptides (Pep1 and Pep2) was performed through GROMACS 5.0.4 (Van Der Spoel et al., 2005; Abraham et al., 2015) using CHARM 27.0 force field (Huang and MacKerell, 2013). The protein complex was solvated in TIP3P cube box water model (volume: 596.38 nm^3 and density: 994.63 g L^{-1}) to provide an aqueous environment with a total 55,386 water molecules. The protein complex was centered in the box with a distance of at least 1.0 nm from the simulation box edge, while 1.0 nm distance between the atoms with non-bonded interactions was maintained. To neutralize the total charge of the system, one Cl^- ion was added to the box followed by energy minimization to remove conflict between the atoms (Ross et al., 2018). The system now containing 3141 protein atoms in addition to one Cl^- ion and 55,386 water molecules, was subjected to energy minimization using steepest descent method for 20,000 steps and then equilibrated through canonical ensemble (NVT: moles (N), volume (V) and temperature (T)) and isothermal-isobaric ensemble (NPT: moles (N), pressure (P) and temperature (T)) at constant temperature (300 K) and pressure (1 bar), respectively for 100 ps. Particle Mesh Ewald (PME) with grid spacing 0.16 nm were used for long-range electrostatics (Huang and MacKerell, 2013). MD simulation was then run for 100 ns at 300 K. Root mean square deviation (RMSD), root mean square fluctuation (RMSF)and radius of gyration (Rg) plots were produced through gnuplot (http://www.gnuplot.info/).

RESULTS AND DISCUSSION

De Novo Design of Inhibitory Peptides Against RBD

RBD of spike glycoprotein mediates the entry of SARS-CoV-2 into the human respiratory cells by interacting with cell surface receptor ACE2 (Lan et al., 2020). Therefore, blocking the interaction residues of RBD might block its interaction with ACE2, hence making it unable to infect human cells. The RBD of SARS-CoV-2 and SARS-CoV-1 is highly conserved (Li et al., 2020) and mainly uses residues 417, 453, 458, 490, 493–495, 498, 501, and 502 for binding to ACE2 (Lan et al., 2020; Yan et al., 2020). Therefore, blocking the binding residues of RBD through inhibitory peptides can potentially block entry of SARS-CoV-2 into the human cells and can also be useful against future pandemic if caused by newly emerged coronaviruses due to the conserved nature of RBD (Lan et al., 2020). Thereby, targeting the RBD to block its interaction with ACE2 is ideal choice for SARS-CoV-2 drug discovery. At present, much research has been focused on non-invasive routes such as nasal, pulmonary, oral, ocular, and rectal for administering peptides (Ibraheem et al., 2014). Unfortunately, the widespread use of peptides as drugs is still faced by many obstacles such as low bioavailability, short half-life in the blood stream, *in vivo* instability, and numerous other problems. In order to overcome these hurdled and improve peptide drug efficacy, various strategies have been developed such as permeability enhancement, enzyme inhibition, and protection by encapsulation (Ibraheem et al., 2014).

Previously, we targeted these nine residues of RBD to be blocked through tACE2 (Basit et al., 2021). However, the current study involved re-designing the binding interface of tACE2 to produce shorter peptide with more binding affinity and covering all the binding residues of RBD (Fosgerau and Hoffmann, 2015). Short therapeutic peptides have gain interest because they have many advantages, such as low molecular weight, selectivity for a specific target, cells with minimal toxicity (Ellert-Miklaszewska et al., 2017). Furthermore, the use of chimeric peptides encompassing disease-targeting and cell-penetrating elements can increase specificity and efficacy of drug delivery together with reducing toxicity (Ellert-Miklaszewska et al., 2017).

The RBD binding residues 490, 493–495, 498, 501, 502 are clustered at one region (region1) while 417 and 458 are clustered at the other region (region2). Therefore, either two peptides can block these two regions or single peptide with extended binding network can hinder interaction between RBD and cell surface receptor.

The residues of ACE2 at amino acid position 21–40 (scafold1) and 65–75 (scafold2) were re-designed and produced 10 *de novo* sequences for each scaffold. Two best sequences (Pep1 and Pep2) were selected from top-10 *de novo* sequences produced by EvoDesign from scaffold1 and scaffold2, respectively. The TM-score 0.61 of Pep1 (those of Pep3-10) indicate its similar fold to that of scaffold1, while Pep2 TM-score was 0.16 indicating its different fold than the scaffold2 structure. The Lower RMSD of Pep1 (0.58 Å) is in agreement with its TM-score, while Pep2 showed RMSD 2.12 Å, which indicate slight deviation of secondary structure from its scaffold (**Figure 1**). Similarly, the amino acid sequence of Pep1 showed 30% similarity while Pep2 showed 20% similarity with its corresponding native sequence (**Table 1**). The designed peptides with high similarity to their native sequence usually exhibit higher binding affinity towards its partner protein (Huang et al., 2020). We further investigated the

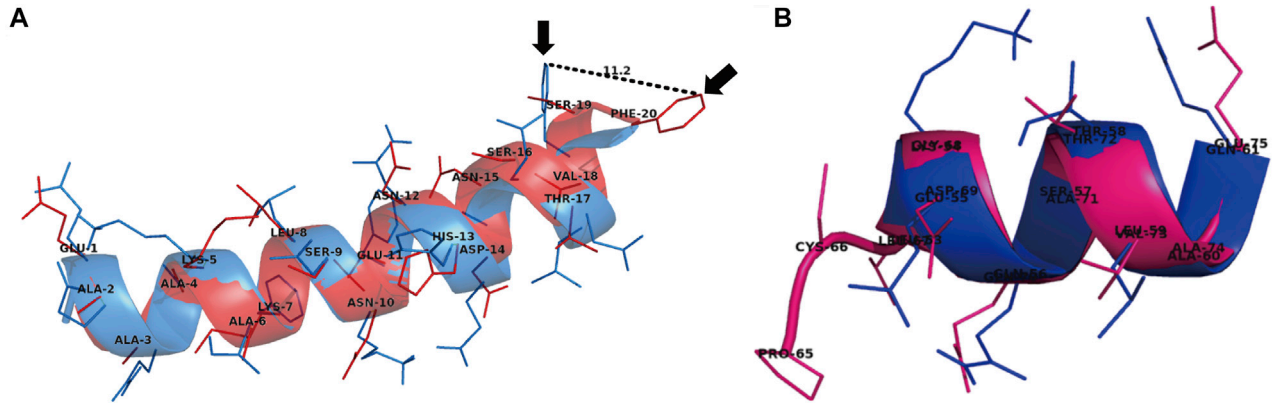

FIGURE 1 | Superimposed models of *de novo* designed peptides showing comparison of their secondary structures to those of two scaffolds (selected amino acid regions [21–40 and 65–75] of ACE2) structure. **(A)** The Pep1 (red) superimposed on tACE2 showed almost similar secondary structure with C-α backbone RMSD 0.58 Å to the wild type tACE2. However, the changes (arrows) in positions of Pep1 residues' R groups with respect to scaffold (blue) were observed, as shown the Phe20 side chain of ACE2 is moved 11.2 Å away from the Phe20 side chain of Pep1, which provide a favorable position for binding with Lys458 of RBD of SARS-CoV-2 spike glycoprotein. **(B)** The Pep2 (pink) showed notable different secondary structure composition from scaffold (dark blue) with C-α backbone RMSD 2.12 Å.

TABLE 1 | Summary of the *de novo* designed peptides produced by using ACE2 as scaffold.

Designed peptide	Sequence	TM-score[a]	Sequence identity (%)	RMSD[b]	Binding affinity (kcal mol^{-1})	Number of binding residues in RBD covered by the designed peptide
tACE2 fragment (scaffold1)	I_{21}EEQAKTFLDKFNHEAEDLF$_{40}$	—	—	—	−10.2	7
Pep1	EAAAKAKLSNENHDNSTVSF	0.61	30	0.58	−13.2	11
tACE2 fragment (scaffold2)	A_{65}GDKWSAFLKE$_{75}$	—	—	—	−7.6	3
Pep2	PCLGDQATVAE	0.16	20	2.12	−9.2	3
Pep3	EEAAKTTLANENSDNCFLSF	0.68	40	0.68	−12.8	10
Pep4	EQAAKATLANENSDNGFLSF	0.64	30	0.51	−11.2	9
Pep5	ESAAKAQLRQEDTENAAVMY	0.60	30	0.58	−11.8	8
Pep6	EAAAKSILSNENNDNSTASF	0.62	25	0.60	−10.92	7
Pep7	EENSCSFLAALFSEASCQSK	0.65	30	0.48	−11.8	8
Pep8	EFQQGCFISAADNCQSEISY	0.50	20	0.55	−11.5	8
Pep9	EKLTYSALQAEKTSSSPQSG	0.58	10	1.8	−10.8	6
Pep10	EHHAASKLMGIDQESAMIAL	0.61	20	0.78	−12.3	8

[a]*Template modeling-score (TM-score) indicates the fold similarity between two structures (each peptide and ACE2). A TM-scores >0.5 correspond to almost similar fold while the value < 0.2 indicate randomly chosen unrelated proteins.*

[b]*Root mean square deviation (RMSD) calculated by TM-align shows the structural variations of two superimposed structures (each peptide and ACE2).*

binding pattern and affinity of the designed peptides for RBD through protein-protein docking.

Protein-Protein Docking

To test the binding properties, protein-protein docking of the designed peptides with RBD was performed through HADDOCK. The HADDOCK-scores (the more negative the better binding affinity) of Pep1 and Pep2 were −119 and −111, respectively, when docked with RBD. The HADDOCK-score of Pep1 is greater than that of the intact ACE2 (−111) docked with RBD (Basit et al., 2021). The docking RMSD of Pep1 and Pep2 in complex with RBD were 0.6 and 0.8, respectively, showing the high likelihood of the docked complexes with native one (Vangone et al., 2017).

Our docking results showed that nine residues Ala2, Lys7, Ans10-Asp14, Ser16, and Phe20 of Pep1 interact with Arg403, Lys417, Tyr453, Lys458, Gln493-Gly496, Gln498, Thr500, Asn501, and Tyr505 residues of RBD (**Figures 2A–C**), while Leu67-Asp69, Thr72 and Glu75 of Pep2 interact with Arg404, Lys417, Tyr495 and Tyr 505 of RBD (**Figures 2D,E**). Similarly, seven residues of wild type tACE2 scaffold (Glu23, Glu24, Lys31, His34, Glu35, Glu37, and Asp38) showed binding interactions with Seven residues (Tyr453, Lys458, Asn487, Tyr489, Gln498, Thr500 and Gly502) of RBD **(Supplementary Figure S1).** These results confirm that Pep1 not only cover 11 the binding residues of RBD involved in interaction with human ACE2 (**Table 1**) but also other residues at position 403, 417, and 493–498, that may

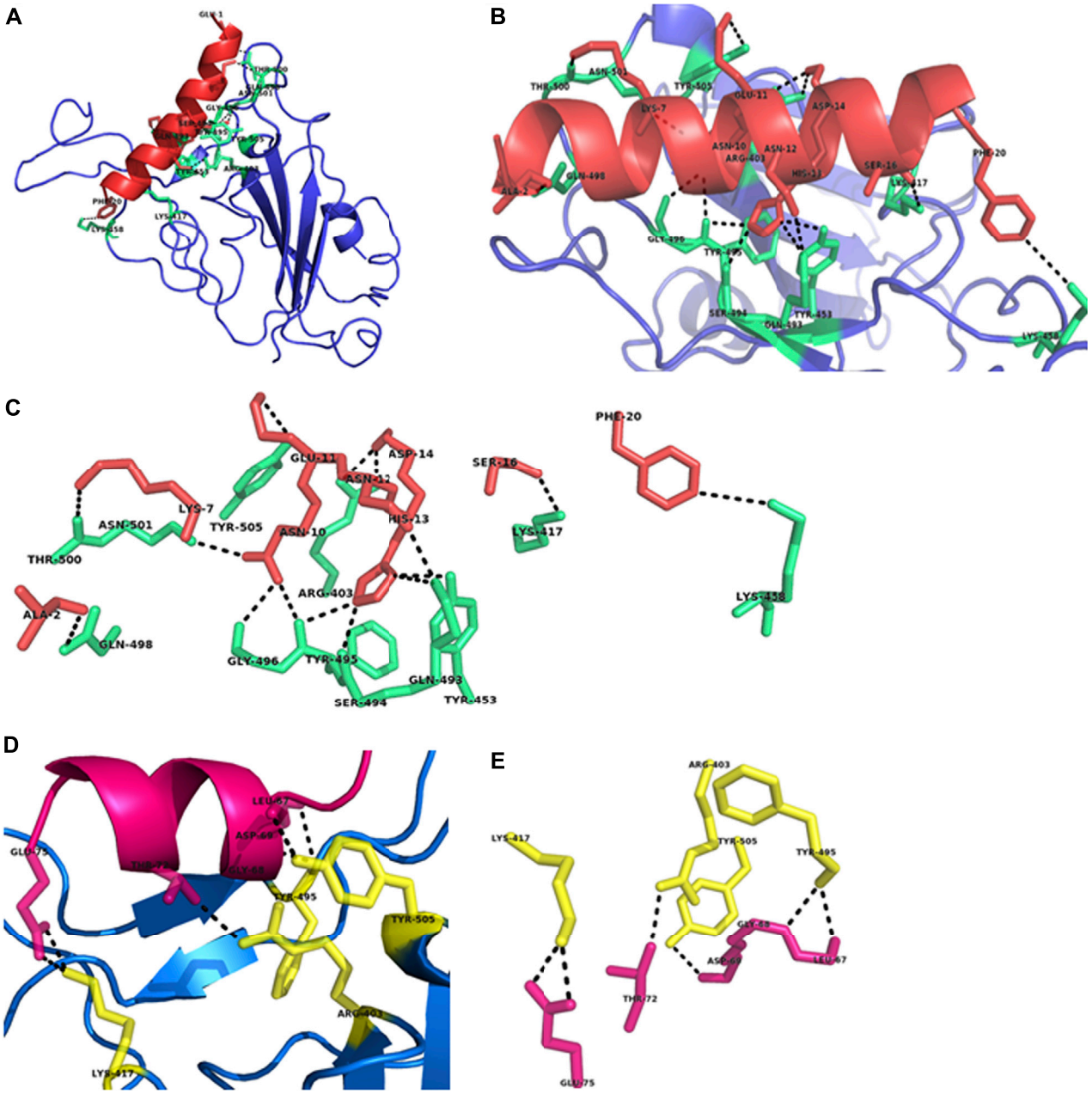

FIGURE 2 | Structural analysis of the designed peptides (Pep1 and Pep2) in complex with RBD of SARS-CoV-2 spike glycoprotein. **(A)** Pep1-RBD complex shows the positioning of designed peptide Pep1 (red) in the binding interface of RBD (blue). **(B)** Pep1 comprises on a single helical structure (red) showing their interactions with the RBD binding residues shown in green. **(C)** The residues of Pep1 involved in binding interactions with RBD residues (green). **(D)** Pep2-RBD complex shows the positioning of Pep2 (pink) at the binding interface of RBD (blue). **(E)** The residues of Pep2 involved in binding interactions with RBD residues (yellow). All interactions are denoted by black lines.

involve in interaction with human receptors, making this peptide ideal for further clinical investigation for its therapeutic potential.

Previous studies have shown that binding residues of RBD are located at two distinct position, region1 (490, 493–495, 498, 501, 502) and region2 (417 and 458) (Lan et al., 2020; Basit et al., 2021). Interestingly, our *de novo* designed peptide Pep1 showed binding with region1 as well as region2 residues (**Figure 2C**). The superimposition of docked Pep1 with its scaffold showed that redesigning moved the Phe20 into the favorable position for interaction with Lys458 of RBD, while mutation Ala16Ser results in interaction with Lys417 of RBD (**Figures 1**, **2C**). Both of these residues are located at region2 and reported to be critical for interaction with RBD (Lan et al., 2020). The superimposition of designed peptides Pep3-10 with scaffold showed average RMSD 0.2 A˚, suggesting their almost similar C-α backbone with deviation in R group positioning **(Supplementary Figure S2).**

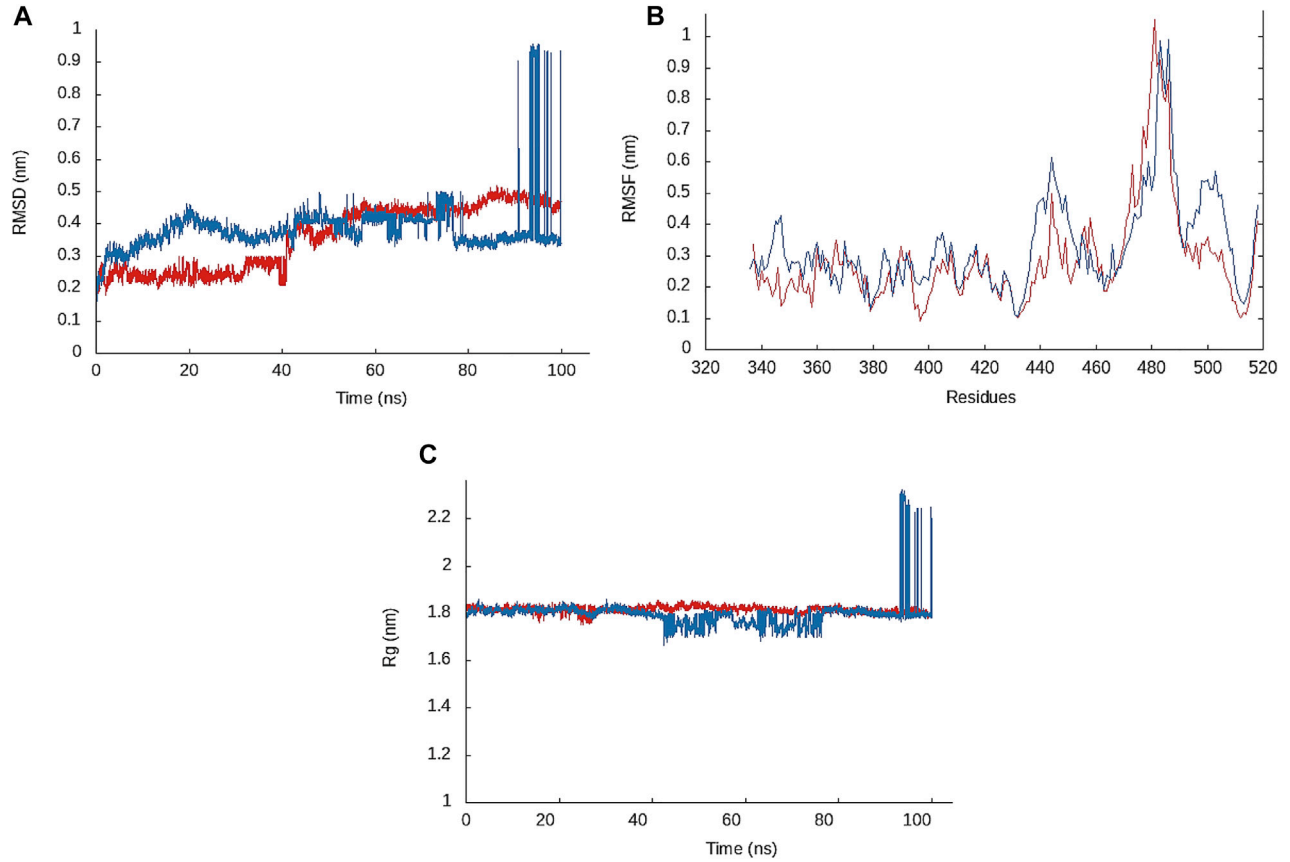

FIGURE 3 | (A) RMSD plot of the Pep1-RBD complex (red) and Pep2-RBD complex (blue) backbone atoms. **(B)** Root mean square fluctuation (RMSF) plot showing fluctuation of residues side chains of RBD in complex with Pep1 (red) and Pep2 (blue). **(C)** Radius of gyration (Rg) plot of Pep1-RBD (red) and Pep2-RBD complex (blue).

The *de novo* design approach created optimum mutation which increased binding network of the designed peptide Pep1, resulting in successful blocking of the RBD binding residues required for interaction with human cell surface receptor.

Binding Affinity of Designed Peptides for ACE2

We further determined the binding affinity of the designed peptides for RBD and complex stability. The binding affinity showed by Pep1 for RBD was −13.2 kcal mol^{-1} at 36°C as optimum temperature which is greater than the binding affinity of wild type tACE2 (−10.7 kcal mol^{-1}) (Basit et al., 2021) and scaffold tACE2 (−11.2 kcal mol^{-1}). It seems that the favorable mutations and side chain rearrangement resulted in dramatic increase in binding affinity of Pep1 for RBD. The binding affinity of other designed peptides (Pep3-10) with RBD was found lower than Pep1 and almost higher than the scaffold (**Table 1**). We further determined the dissociation constant K_d values of peptide-receptor complexes. The Pep1-RBD complex showed K_d value 3.9×10^{-10} M, which is lower than the previously reported K_d values of inhibitory peptide (P8: 2.4×10^{-9} M) proposed for S protein of SARS-CoV-2 (Karoyan et al., 2021) and wild type tACE2-RBD complex (Basit et al., 2021). The smaller K_d value indicates high stability and strong binding affinity between protein-protein complex (Johnson et al., 2007). The lower K_d value of Pep1-RBD complex suggest that the designed peptide Pep1 are tightly bound to the corresponding region of RBD. Binding affinity of Pep2-RBD complex was found lower than the Pep1-RBD complex. This indicates that region 21–40 of tACE2 has important role in binding with RBD.

MD Simulation Showed Stability of Designed Peptides-RBD Complex

To investigate the structural stability and dynamic behavior of the designed peptides in complex with RBD, we performed MD simulation of the RBD in complex with Pep1 and Pep2. The docking conformation with lowest energy was subjected to MD simulation. To investigate structural stability of the complex, RMSD plot of the complex backbone was produced. The RMSD values of Pep1-RBD complex remained 0.2–0.25 nm initially for 40 ns and then increased up to 0.4–0.5 nm for 60–100 ns of MD run. Similarly, the RMSD values of Pep2-RBD complex remained 0.3–0.4 nm during initial 90 ns while slightly increased up to 0.95 nm during 90–100 ns (**Figure 3A**). In general, the RMSD

≤0.3 nm during a 20 ns MD run indicates strong complex stability (Rao et al., 2007; Rani et al., 2016). Overall, a uniform lower RMSD of Pep1-RBD complex indicates that Pep1 bind more tightly to RBD than the Pep2. The RMSD value of Pep1-RBD complex is also lower than the previously reported therapeutic peptide (peptide inhibitor 4: 0.8 nm) for SARS-CoV-2 treatment (Han and Kral, 2020). RMSF determined in the docked complexes shows residues flexibility. The high RMSF values indicate the mobility of residue side chains in relation to their average position (Muralidharan et al., 2021). The RMSF plot of Pep1-RBD complex shows that the residues of RBD at position 358, 417, and 490–500 showing lower fluctuation (nm) than the Pep2-RBD complex. The overall RMSF value of Pep1-RBD complex is less than 0.2 nm in region 1 & II window, which is lower than the RMSF value (0.35 nm) of RBD when bound to intact ACE2 (Basit et al., 2021). The residues involved in binding interaction with lower RMSF values indicates the most stable region of the complex (Ardalan et al., 2018). The lower RMSF values of RBD binding residues indicate that Pep1 form a stable complex with RBD, as RMSF value < 0.4 nm reveals complex stability (Maqsood et al., 2020).

Rg value was determined to describe the structural integrity and folding behavior of the designed peptides in complex with RBD. A low Rg value reveals better structural integrity and folding behavior (Bhowmick et al., 2020; Chatterjee et al., 2020). Pep1-RBD complex showed a uniform and stable Rg value between 1.80–1.84 nm throughout a 100 ns MD run, while the Rg value of Pep2-RBD complex increased to 2.23 nm during 90–100 ns. The overall Rg values for both peptides remained between 1.80–1.84 nm during 0–89 ns, which is lower than the Rg value (2.2 nm) showed by intact ACE2-RBD complex (Basit et al., 2021), which indicates structural integrity of Pep1-and Pep2-RBD complex (**Figure 3C**). Overall, the MD simulation results suggests that the *de novo* designed peptides form a stabilized complex with RBD and propose their potential to block the SARS-CoV-2 spike glycoprotein for interaction with human cell surface receptor.

CONCLUSION

SARS-CoV-2 infects human cells through their receptor binding domain of its spike glycoprotein by interacting with cell surface receptor, ACE2. The *de novo* peptide design opens a new path for producing more potential therapeutic peptides that can mask the RBD critical residues required for interaction with human cell surface receptor, making the SARS-CoV-2 unable to infect human cells. Our *de novo* designed peptides covering 11binding residues of RBD with increased binding affinity and complex stability. A stabilized interactions network was shown by Pep1and Pep2. The designed peptides can be tested experimentally for their binding affinity towards spike glycoprotein, followed by analyzing their potential to inhibit the targeted human cell line from SARS-CoV-2 pseudoparticles infection, live virus infection inhibition in cell culture, followed by assessment of its potential inhibitory activity in animal model of infection.

DATA AVAILABILITY STATEMENT

The original contributions presented in the study are included in the article/**Supplementary Material**, further inquiries can be directed to the corresponding authors.

AUTHOR CONTRIBUTIONS

Conceptualization, AB, SuR, and SHL; data collection, AB, AMK, MA, TA, JHL, and JHJ; data analysis, AB, AMK, MA, TA, JHL, and JHJ; writing—original draft preparation, AB, AMK, MA, TA, JHL, JHJ, SuR, and SHL; writing—review and editing, AB, AMK, MA, TA, JHL, JHJ, SuR, and SHL; supervision, SuR and SHL; funding acquisition, SHL All authors have read and agreed to the published version of the manuscript.

FUNDING

This work was supported by research grants from the Bio and Medical Technology Development Program of the National Research Foundation of Korea (NRF) funded by the Ministry of Science, Information and Communications Technology (MSIT; grant No. NRF-2017M3A9E4078014); and from the NRF funded by the MSIT (grant Nos. NRF-2021R1A2C3004826 and NRF-2019R1C1C1008615).

SUPPLEMENTARY MATERIAL

The Supplementary Material for this article can be found online at: https://www.frontiersin.org/articles/10.3389/fphar.2021.731828/full#supplementary-material

REFERENCES

Abraham, M. J., Murtola, T., Schulz, R., Páll, S., Smith, J. C., Hess, B., et al. (2015). GROMACS: High Performance Molecular Simulations through Multi-Level Parallelism from Laptops to Supercomputers. *SoftwareX* 1-2, 19–25. doi:10.1016/j.softx.2015.06.001

Ardalan, N., Mirzaie, S., Sepahi, A. A., and Khavari-Nejad, R. A. (2018). Novel Mutant of *Escherichia coli* Asparaginase II to Reduction of the Glutaminase Activity in Treatment of Acute Lymphocytic Leukemia by Molecular Dynamics Simulations and QM-MM Studies. *Med. Hypotheses* 112, 7–17. doi:10.1016/j.mehy.2018.01.004

Basit, A., Ali, T., and Rehman, S. U. (2021). Truncated Human Angiotensin Converting Enzyme 2; a Potential Inhibitor of SARS-CoV-2 Spike Glycoprotein and Potent COVID-19 Therapeutic Agent. *J. Biomol. Struct. Dyn.* 39, 3605–3614. doi:10.1080/07391102.2020.1768150

Bhowmick, S., Alfaris, N. A., Altamimi, J. Z., Alothman, Z. A., Aldayel, T. S., Wabaidur, S. M., et al. (2020). Screening and Analysis of Bioactive Food Compounds for Modulating the CDK2 Protein for Cell Cycle Arrest: Multi-Cheminformatics Approaches for Anticancer Therapeutics. *J. Mol. Struct.* 1216, 128316. doi:10.1016/j.molstruc.2020.128316

Chan, K. K., Dorosky, D., Sharma, P., Abbasi, S. A., Dye, J. M., Kranz, D. M., et al. (2020). Engineering Human ACE2 to Optimize Binding to the Spike Protein of SARS Coronavirus 2. *Science* 369, 1261–1265. doi:10.1126/science.abc0870

Chatterjee, S., Maity, A., Chowdhury, S., Islam, M. A., Muttinini, R. K., and Sen, D. (2020). In Silico analysis and Identification of Promising Hits against 2019 Novel Coronavirus 3C-like Main Protease Enzyme. *J. Biomol. Struct. Dyn.* 39, 5290–5303. doi:10.1080/07391102.2020.1787228

Chevalier, A., Silva, D. A., Rocklin, G. J., Hicks, D. R., Vergara, R., Murapa, P., et al. (2017). Massively Parallel De Novo Protein Design for Targeted Therapeutics. *Nature* 550, 74–79. doi:10.1038/nature23912

Du, L., He, Y., Zhou, Y., Liu, S., Zheng, B. J., and Jiang, S. (2009). The Spike Protein of SARS-CoV-Aa Target for Vaccine and Therapeutic Development. *Nat. Rev. Microbiol.* 7, 226–236. doi:10.1038/nrmicro2090

Ellert-Miklaszewska, A., Poleszak, K., and Kaminska, B. (2017). Short Peptides Interfering with Signaling Pathways as New Therapeutic Tools for Cancer Treatment. *Future Med. Chem.* 9, 199–221. doi:10.4155/fmc-2016-0189

Fosgerau, K., and Hoffmann, T. (2015). Peptide Therapeutics: Current Status and Future Directions. *Drug Discov.* Today 20, 122–128. doi:10.1016/j.drudis.2014.10.003

Han, D. P., Penn-Nicholson, A., and Cho, M. W. (2006). Identification of Critical Determinants on ACE2 for SARS-CoV Entry and Development of a Potent Entry Inhibitor. *Virology* 350, 15–25. doi:10.1016/j.virol.2006.01.029

Han, Y., and Král, P. (2020). Computational Design of ACE2-Based Peptide Inhibitors of SARS-CoV-2. *ACS Nano* 14, 5143–5147. doi:10.1021/acsnano.0c02857

Huang, J., and Mackerell, A. D., Jr. (2013). CHARMM36 All-Atom Additive Protein Force Field: Validation Based on Comparison to NMR Data. *J. Comput. Chem.* 34, 2135–2145. doi:10.1002/jcc.23354

Huang, X., Pearce, R., and Zhang, Y. (2020). *De Novo* design of Protein Peptides to Block Association of the SARS-CoV-2 Spike Protein with Human ACE2. *Aging (Albany NY)* 12, 11263–11276. doi:10.18632/aging.103416

Ibraheem, D., Elaissari, A., and Fessi, H. (2014). Administration Strategies for Proteins and Peptides. *Int. J. Pharm.* 477, 578–589. doi:10.1016/j.ijpharm.2014.10.059

Johnson, R. J., Mccoy, J. G., Bingman, C. A., Phillips, G. N., Jr., and Raines, R. T. (2007). Inhibition of Human Pancreatic Ribonuclease by the Human Ribonuclease Inhibitor Protein. *J. Mol. Biol.* 368, 434–449. doi:10.1016/j.jmb.2007.02.005

Karoyan, P., Vieillard, V., Gómez-Morales, L., Odile, E., Guihot, A., Luyt, C. E., et al. (2021). Human ACE2 Peptide-Mimics Block SARS-CoV-2 Pulmonary Cells Infection. *Commun. Biol.* 4, 197. doi:10.1038/s42003-021-01736-8

Kim, J. M., Kim, H. M., Lee, E. J., Jo, H. J., Yoon, Y., Lee, N. J., et al. (2020). Detection and Isolation of SARS-CoV-2 in Serum, Urine, and Stool Specimens of COVID-19 Patients from the Republic of Korea. *Osong. Public Health Res. Perspect.* 11, 112–117. doi:10.24171/j.phrp.2020.11.3.02

Lan, J., Ge, J., Yu, J., Shan, S., Zhou, H., Fan, S., et al. (2020). Structure of the SARS-CoV-2 Spike Receptor-Binding Domain Bound to the ACE2 Receptor. *Nature* 581, 215–220. doi:10.1038/s41586-020-2180-5

Li, Y., Wang, H., Tang, X., Fang, S., Ma, D., Du, C., et al. (2020). SARS-CoV-2 and Three Related Coronaviruses Utilize Multiple ACE2 Orthologs and Are Potently Blocked by an Improved ACE2-Ig. *J. Virol.* 94, e01283–20. doi:10.1128/JVI.01283-20

Lizbeth, R.-S. G., Jazmín, G.-M., José, C.-B., and Marlet, M.-A. (2020). Immunoinformatics Study to Search Epitopes of Spike Glycoprotein from SARS-CoV-2 as Potential Vaccine. *J. Biomol. Struct. Dyn.* 39, 4878–4892. doi:10.1080/07391102.2020.1780944

Maqsood, B., Basit, A., Khurshid, M., and Bashir, Q. (2020). Characterization of a Thermostable, Allosteric L-Asparaginase from *Anoxybacillus Flavithermus*. *Int. J. Biol. Macromol.* 152, 584–592. doi:10.1016/j.ijbiomac.2020.02.246

Mercurio, I., Tragni, V., Busto, F., De Grassi, A., and Pierri, C. L. (2021). Protein Structure Analysis of the Interactions between SARS-CoV-2 Spike Protein and the Human ACE2 Receptor: from Conformational Changes to Novel Neutralizing Antibodies. *Cell. Mol. Life Sci.* 78, 1501–1522. doi:10.1007/s00018-020-03580-1

Muralidharan, N., Sakthivel, R., Velmurugan, D., and Gromiha, M. M. (2021). Computational Studies of Drug Repurposing and Synergism of Lopinavir, Oseltamivir and Ritonavir Binding with SARS-CoV-2 Protease against COVID-19. *J. Biomol. Struct. Dyn.* 39, 2673–2678. doi:10.1080/07391102.2020.1752802

Pearce, R., Huang, X., Setiawan, D., and Zhang, Y. (2019). EvoDesign: Designing Protein-Protein Binding Interactions Using Evolutionary Interface Profiles in Conjunction with an Optimized Physical Energy Function. *J. Mol. Biol.* 431, 2467–2476. doi:10.1016/j.jmb.2019.02.028

Pierce, B. G., Wiehe, K., Hwang, H., Kim, B. H., Vreven, T., and Weng, Z. (2014). ZDOCK Server: Interactive Docking Prediction of Protein-Protein Complexes and Symmetric Multimers. *Bioinformatics* 30, 1771–1773. doi:10.1093/bioinformatics/btu097

Rani, N., Vijayakumar, S., Lakshmi, P, T. V, and Arunachalam, A. (2016). Allosteric Site-Mediated Active Site Inhibition of PBP2a Using Quercetin 3-O-Rutinoside and its Combination. *J. Biomol. Struct. Dyn.* 34, 1778–1796. doi:10.1080/07391102.2015.1092096

Rao, S. N., Head, M. S., Kulkarni, A., and Lalonde, J. M. (2007). Validation Studies of the Site-Directed Docking Program LibDock. *J. Chem. Inf. Model.* 47, 2159–2171. doi:10.1021/ci6004299

Ross, G. A., Rustenburg, A. S., Grinaway, P. B., Fass, J., and Chodera, J. D. (2018). Biomolecular Simulations under Realistic Macroscopic Salt Conditions. *J. Phys. Chem. B.* 122, 5466–5486. doi:10.1021/acs.jpcb.7b11734

Schrodinger, L. (2010). *The PyMOL Molecular Graphics System*. Version 1.3r1.

Schymkowitz, J., Borg, J., Stricher, F., Nys, R., Rousseau, F., and Serrano, L. (2005). The FoldX Web Server: an Online Force Field. *Nucleic Acids Res.* 33, W382–W388. doi:10.1093/nar/gki387

Singh, M., Bansal, V., and Feschotte, C. (2020). A Single-Cell RNA Expression Map of Human Coronavirus Entry Factors. *bioRxiv* 32, 108175. doi:10.1016/j.celrep.2020.10817510.1101/2020.05.08.084806

Van Der Spoel, D., Lindahl, E., Hess, B., Groenhof, G., Mark, A. E., and Berendsen, H. J. (2005). GROMACS: Fast, Flexible, and Free. *J. Comput. Chem.* 26, 1701–1718. doi:10.1002/jcc.20291

van Zundert, G. C. P., Rodrigues, J. P. G. L. M., Trellet, M., Schmitz, C., Kastritis, P. L., Karaca, E., et al. (2016). The HADDOCK2.2 Web Server: User-Friendly Integrative Modeling of Biomolecular Complexes. *J. Mol. Biol.* 428, 720–725. doi:10.1016/j.jmb.2015.09.014

Vangone, A., Rodrigues, J. P., Xue, L. C., Van Zundert, G. C., Geng, C., Kurkcuoglu, Z., et al. (2017). Sense and Simplicity in HADDOCK Scoring: Lessons from CASP-CAPRI Round 1. *Proteins* 85, 417–423. doi:10.1002/prot.25198

Wan, Y., Shang, J., Graham, R., Baric, R. S., and Li, F. (2020). Receptor Recognition by the Novel Coronavirus from Wuhan: an Analysis Based on Decade-Long Structural Studies of SARS Coronavirus. *J. Virol.* 94, e00127–20. doi:10.1128/JVI.00127-20

Wang, W., Xu, Y., Gao, R., Lu, R., Han, K., Wu, G., et al. (2020). Detection of SARS-CoV-2 in Different Types of Clinical Specimens. *JAMA* 323, 1843–1844. doi:10.1001/jama.2020.3786

Xia, S., Yan, L., Xu, W., Agrawal, A. S., Algaissi, A., Tseng, C. K., et al. (2019). A Pan-Coronavirus Fusion Inhibitor Targeting the HR1 Domain of Human Coronavirus Spike. *Sci. Adv.* 5, eaav4580. doi:10.1126/sciadv.aav4580

Xue, L. C., Rodrigues, J. P., Kastritis, P. L., Bonvin, A. M., and Vangone, A. (2016). PRODIGY: a Web Server for Predicting the Binding Affinity of Protein-Protein Complexes. *Bioinformatics* 32, 3676–3678. doi:10.1093/bioinformatics/btw514

Yan, R., Zhang, Y., Li, Y., Xia, L., Guo, Y., and Zhou, Q. (2020). Structural Basis for the Recognition of SARS-CoV-2 by Full-Length Human ACE2. *Science* 367, 1444–1448. doi:10.1126/science.abb2762

Yang, J., Yan, R., Roy, A., Xu, D., Poisson, J., and Zhang, Y. (2015). The I-TASSER Suite: Protein Structure and Function Prediction. *Nat. Methods* 12, 7–8. doi:10.1038/nmeth.3213

Zhang, Y., and Skolnick, J. (2005). TM-align: a Protein Structure Alignment Algorithm Based on the TM-Score. *Nucleic Acids Res.* 33, 2302–2309. doi:10.1093/nar/gki524

Conflict of Interest: The authors declare that the research was conducted in the absence of any commercial or financial relationships that could be construed as a potential conflict of interest.

Publisher's Note: All claims expressed in this article are solely those of the authors and do not necessarily represent those of their affiliated organizations, or those of the publisher, the editors and the reviewers. Any product that may be evaluated in this article, or claim that may be made by its manufacturer, is not guaranteed or endorsed by the publisher.

frontiers in Pharmacology

REVIEW
published: 15 September 2021
doi: 10.3389/fphar.2021.708636

Add-On Effect of Honeysuckle in the Treatment of Coronavirus Disease 2019: A Systematic Review and Meta-Analysis

Xu-Qin Du[1,2], *Li-Peng Shi*[1,2]*, *Wen-Fu Cao*[1,2,3]*, *Zhi-Wei Chen*[1,2], *Biao Zuo*[1,2] and *Jin-Yuan Hu*[1,2]

[1]College of Traditional Chinese Medicine, Chongqing Medical University, Chongqing, China, [2]Chongqing Key Laboratory of Traditional Chinese Medicine for Prevention and Cure of Metabolic Diseases, Chongqing, China, [3]Department of Chinese Traditional Medicine, The First Affiliated Hospital of Chongqing Medical University, Chongqing, China

OPEN ACCESS

Edited by:
Brijesh Kumar Singh,
Duke-NUS Medical School, Singapore

Reviewed by:
Patricia Silveyra,
Indiana University Bloomington, United States
Prem Prakash Tripathi,
Indian Institute of Chemical Biology (CSIR), India

***Correspondence:**
Li-Peng Shi
shilipeng0206@163.com
Wen-Fu Cao
caowenfu9316@163.com

Specialty section:
This article was submitted to Respiratory Pharmacology, a section of the journal Frontiers in Pharmacology

Received: *12 May 2021*
Accepted: *18 August 2021*
Published: *15 September 2021*

Citation:
Du X-Q, Shi L-P, Cao W-F, Chen Z-W, Zuo B and Hu J-Y (2021) Add-On Effect of Honeysuckle in the Treatment of Coronavirus Disease 2019: A Systematic Review and Meta-Analysis. Front. Pharmacol. 12:708636. doi: 10.3389/fphar.2021.708636

Background: The outbreak of coronavirus disease 2019 (COVID-19) has rapidly spread to become a global emergency since December 2019. Chinese herbal medicine plays an important role in the treatment of COVID-19. Chinese herbal medicine honeysuckle is an extremely used traditional edible and medicinal herb. Many trials suggest that honeysuckle has obtained a good curative effect for COVID-19; however, no systematic evaluation on the clinical efficacy of honeysuckle in the treatment of COVID-19 is reported. This study aimed to evaluate the efficacy and safety of Chinese herbal medicine honeysuckle in the treatment of COVID-19.

Methods: Seven electronic databases (PubMed, EMBASE, Cochrane Library, China National Knowledge Infrastructure, China Science and Technology Journal Database, Wanfang Database, and China Biology Medicine) were searched to identify randomized controlled trials (RCTs) of honeysuckle for adult patients (aged ≥ 18 years) with COVID-19. The Cochrane Risk of Bias Tool was applied to assess the methodological quality of trials. Review Manager 5.3 software was used for data analysis.

Results: Overall, nine RCTs involving 1,286 patients were enrolled. Our meta-analyses found that combination therapy of honeysuckle and conventional therapy was more effective than conventional therapy alone in lung computed tomography (CT) [relative risk (RR) = 1.24, 95% confidence interval (95%CI) (1.12, 1.37), $P < 0.0001$], clinical cure rate [RR = 1.21, 95%CI (1.12, 1.31), $P < 0.00001$], and rate of conversion to severe cases [RR = 0.50, 95%CI (0.33, 0.76), $P = 0.001$]. Besides, combination therapy can improve the symptom score of fever, cough reduction rate, symptom score of cough, and inflammatory biomarkers (white blood cell (WBC) count; C-reactive protein (CRP)) ($P < 0.05$).

Conclusion: Honeysuckle combined with conventional therapy may be beneficial for the treatment of COVID-19 in improving lung CT, clinical cure rate, clinical symptoms, and laboratory indicators and reducing the rate of conversion to severe cases. Besides, combination therapy did not increase adverse drug events. More high-quality RCTs are needed in the future.

Keywords: coronavirus disease 2019, honeysuckle, systematic review, meta-analysis, randomized controlled trials

INTRODUCTION

Since December 2019, coronavirus disease 2019 (COVID-19) caused by severe acute respiratory syndrome coronavirus 2 (SARS-CoV-2) has become a public health emergency of global concern (Sattler et al., 2020). As of May 6, 2021, more than 154.815 million confirmed cases and more than 3.236 million deaths had been reported globally (World Health Organization (WHO), 2021). Thus, there is an urgent need to prevent and treat COVID-19.

Through a series of prevention and medical treatment measures, the COVID-19 epidemic in China has been effectively controlled by May 6, 2021, with 103,731 confirmed cases and 98,392 cured cases (World Health Organization (WHO), 2021; National Health Commission of the people's Republic of China, 2021). Chinese herbal medicine plays an important role in the treatment of COVID-19 in view of no specific drugs approved for COVID-19. Chinese herbal medicine honeysuckle is an extremely used traditional edible-medicinal herb (Li et al., 2021). Pharmacological studies have already proved honeysuckle's ideal clinical therapeutic effects on inflammation and infectious diseases (Li et al., 2021). Also, it is reported that honeysuckle can effectively alleviate clinical symptoms of COVID-19 (Hu et al., 2020; Zhang et al., 2020) and inhibit SARS-CoV-2 replication (Zhou et al., 2020).

At present, there are only few trials on the treatment of COVID-19 with honeysuckle (Hu et al., 2020; Zhang et al., 2020), but many trials on the treatment of COVID-19 used Chinese herbal medicine including honeysuckle as the main components (Ai et al., 2020; Ding et al., 2020; Duan et al., 2020). These trials suggest that honeysuckle has obtained a good curative effect for COVID-19 (Hu et al., 2020; Zhang et al., 2020). Presently, there is no systematic evaluation report on the clinical efficacy of honeysuckle in the treatment of COVID-19. This review aimed to critically evaluate the effectiveness and safety of honeysuckle for COVID-19.

METHODS

The preferred reporting item for systematic review and meta-analysis (PRISMA) Evaluation Scale was used for reporting the results of this review (Moher et al., 2009). The protocol for this review is available in PROSPERO (https://www.crd.york.ac.uk/prospero/, registration number is CRD42020224312).

Database and Search Strategies

The following seven databases were retrieved, including PubMed, EMBASE, Cochrane Library, China National Knowledge Infrastructure (CNKI), China Science and Technology Journal Database (VIP), Wanfang Database, and China Biology Medicine (CBM), from December 2019 to May 2021. There was no language restriction. The grouped keywords used as search strategy were as follows: ("traditional Chinese medicine" OR "Chinese herbal medicine" OR "honeysuckle" OR "lonicera" OR "jinyinhua") AND ("coronavirus disease 2019" OR "COVID-19" OR "novel coronavirus pneumonia" OR "SARS-CoV-2") AND ("clinical trial" OR "randomized controlled trial" OR "randomised controlled trial" OR "lin chuang yan jiu"). The grouped keywords could be modified according to different databases.

Potentially eligible trials were obtained by manually searching the reference lists of published reviews and meta-analyses. We also retrieved the unpublished papers on honeysuckle for COVID-19.

Inclusion and Exclusion Criteria

We considered the following inclusion criteria: 1) study design: randomized controlled trials (RCTs); 2) participants: adult patients (aged ≥ 18 years) diagnosed with COVID-19; the diagnostic criteria of COVID-19 refer to " Diagnosis and Treatment Guideline for COVID-19 (Trial 8th Edition) " (National Health Commission of the people's Republic of China, 2020); 3) interventions: patients in the treatment group were treated with honeysuckle alone or a combination treatment of honeysuckle and controls; the dose of honeysuckle was 5–30 g, along with a duration range of 5–15 days; the form and dosage of honeysuckle were included in the study description; 4) control: patients in the control group were treated by any conventional therapy or placebo; 5) outcomes: lung computed tomography (CT) was the primary outcome. High-resolution CT was used to observe changes in the lung field before and after treatment. The secondary outcomes included clinical cure rate, viral nucleic acid testing, rate of conversion to severe cases, clinical symptoms (e.g., fever, cough, and fatigue), inflammatory biomarkers [e.g., white blood cell (WBC) count, lymphocyte (LYM) count, and C-reactive protein (CRP)], and adverse drug events (e.g., adverse events rate, diarrhea, and liver damage).

We considered the following exclusion criteria: 1) study design: non-RCTs, such as retrospective studies, observational studies, case reports, and cross-over studies; non-RCTs were excluded due to potential high risk of bias and confounding; 2) participants: patients with a suspected diagnosis of COVID-19; 3) repeated data studies; 4) reviews.

Two reviewers independently screened the trials from seven databases according to the eligibility criteria. Duplicate publications were removed. Through reading the title, abstract, and full text, reviewers excluded the non-RCTs and irrelevant trials. Two reviewers independently extracted data according to the eligibility criteria. Any disagreements were consulted by a third reviewer.

Data Collection

The following information was documented in the data extraction tables: basic characteristics (e.g., the title, first authors' name, publication date, intervention schedule of treatment and control groups, and treatment duration), participant characteristics (e.g., age, gender, and sample size), outcome measures, and adverse drug events.

Quality Assessment

The methodological quality was independently evaluated by two reviewers according to the Cochrane Collaboration's tool (Higgins and Green, 2014). There were seven items of risk of bias (ROB): random sequence generation, allocation

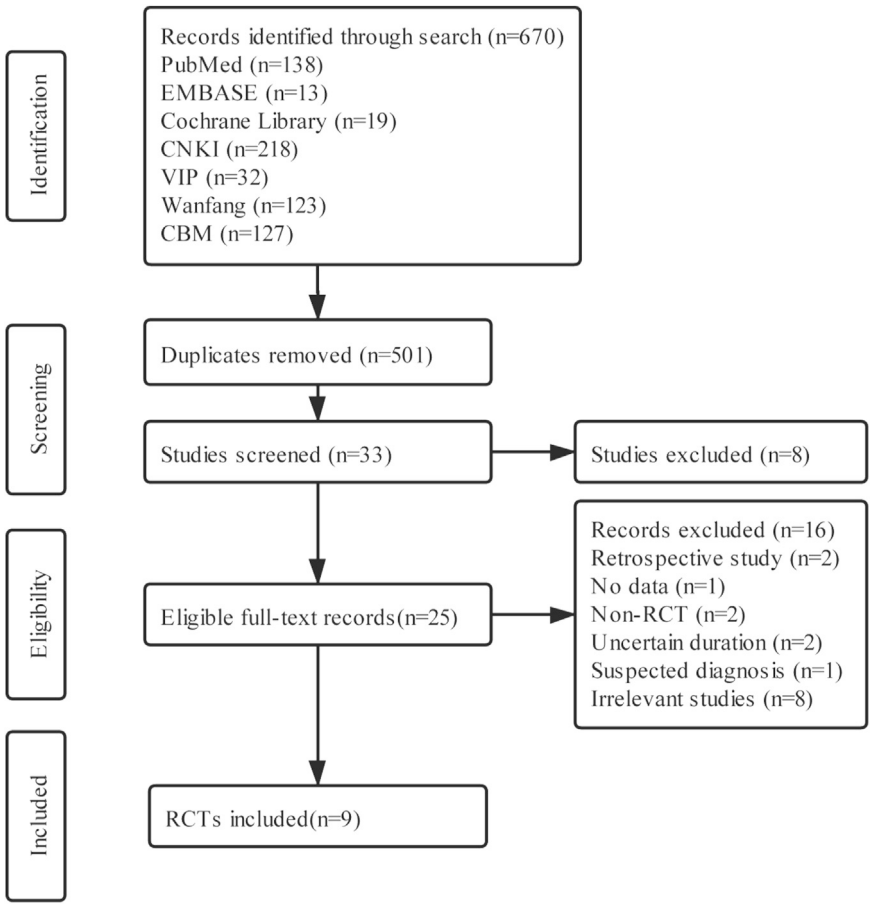

FIGURE 1 | The flowchart of study selection.

concealment, blinding of participants and personnel, blinding of outcome assessment, incomplete outcome data, selective reporting, and other biases. Each item was assessed at low ROB, high ROB, or unclear ROB. Any disagreements between reviewers were resolved by consultation with a third reviewer.

Statistical Analysis

Review Manager 5.3 software (the Cochrane Collaboration, 2014) was used to perform the quantitative synthesis. Relative risk (RR) was used for the dichotomous variables. Mean difference (MD) or standard mean difference (SMD) was used for the continuous variables. Confidence intervals (CIs) were set as 95%. Heterogeneity was tested with the $\chi 2$ test and the I^2 statistical value. Assuming that the p-value from the $\chi 2$ test was more than 0.10 or $I^2 \leq 50\%$, a fixed-effect model was used to assess the differences between two groups; otherwise, a random-effects model was applied. A subgroup analysis of the primary outcome was performed according to the clinical classification of COVID-19. Subgroup analyses of viral nucleic acid testing and rate of conversion to severe cases were performed according to the Chinese herbal medicine component. Sensitivity analysis was conducted by the leave-one-out method (Panahi et al., 2015). When the number of trials on an outcome measure was larger than ten, a funnel plot analysis was performed to evaluate the reporting bias (Liu et al., 2020). Statistically significant results were defined by $p < 0.05$.

RESULTS

Study Selection

The flowchart of study selection is shown in (**Figure 1**). A total of nine eligible trials were included (Fu et al., 2020a; Ai et al., 2020; Ding et al., 2020; Duan et al., 2020; Fu et al., 2020b; Hu et al., 2020; Yu et al., 2020; Zhang et al., 2020; Hu et al., 2021). One article was published online in English (Hu et al., 2021), and the rest were reported online in Chinese.

Study Characteristics

The characteristics of included trials are listed in **Table 1**. All the trials were conducted in China in 2020, among them, two studies were multicentered trials (Hu et al., 2020; Hu et al., 2021) and seven were single-centered trials (Ai et al., 2020; Ding et al., 2020; Duan et al., 2020; Hu et al., 2020; Yu et al., 2020; Zhang et al., 2020; Hu et al., 2021). The sample size of the included trials ranged from 65 to 295 (total 1,286). The treatment duration ranged from 5 to 15 days. Patients in the treatment group were treated with combination

TABLE 1 | The characteristics of included trials.

First author	Type of COVID-19	Sample size (M/F)	Age (yrs)	Intervention	Control	Duration	Outcome measures
Ai et al. (2020)	Nonsevere	T:55 (24/31) C:43 (17/26)	T:57.4 ± 21.3 C:50.8 ± 23.5	Pneumonia No.1 formula (1 dose/d) + conventional therapy	Conventional therapy including arbidol, lopinavir/tonavir, chloroquine, and symptomatic treatment	12 days	Clinical cure rate, inflammatory biomarkers, and adverse events
Ding et al. (2020)	Mild/moderate/severe	T:51 (39/12) C:49 (39/10)	T:57.4 ± 21.3 C:50.8 ± 23.5	Qingfei Touxie Fuzheng recipe (1 dose/d) + conventional therapy	Conventional therapy including interferon-α, ribavirin, quinolones and/or third-generation cephalosporins, and symptomatic treatment	10 days	Lung CT, clinical symptoms, inflammatory biomarkers, and adverse events
Duan et al. (2020)	Mild	T:82 (39/43) C:41 (23/18)	T:51.99 ± 13.88 C:50.29 ± 13.17	Jinhua Qinggan granule (1 dose/time, tid) + conventional therapy	Conventional therapy including antiviral, anti-infection, and other symptomatic treatments	5 days	Clinical symptoms and adverse events
Fu et al. (2020a)	Mild/moderate	T:32 (17/15) C:33 (19/14)	T:43.26 ± 7.15 C:43.68 ± 6.45	Toujie Quwen granule (1 dose/time, bid) + conventional therapy	Conventional therapy including abidor tablets, moxifloxacin tablets, and ambroxol tablets	10 days	Lung CT, clinical cure rate, rate of conversion to severe cases, clinical symptoms, inflammatory biomarkers, and adverse events
Fu et al. (2020b)	Moderate	T:37 (19/18) C:36 (19/17)	T:45.26 ± 7.25 C:44.68 ± 7.45	Toujie Quwen granule (1 dose/time, bid) + conventional therapy	Conventional therapy including abidor tablets and ambroxol tablets	15 days	Clinical cure rate, rate of conversion to severe cases, clinical symptoms, inflammatory biomarkers, and adverse events
Hu et al. (2020)	Moderate	T:100 (49/51) C:100 (55/45)	T:47.00 ± 14.06 C:49.28 ± 11.14	Jinyinhua oral liquid (120 ml/time, tid) + conventional therapy	Conventional therapy including interferon-α, lopinavir/tonavir tablets, and symptomatic treatment	10 days	Lung CT, virus nucleic acid testing, rate of conversion to severe cases, and adverse events
Hu et al. (2020)	Mild/moderate	T:142 (79/63) C:142 (71/71)	T:50.4 ± 15.2 C:51.8 ± 14.8	Lianhua Qingwen capsule (6 g, tid) + conventional therapy	Conventional therapy including oxygen therapy, antiviral medications, and symptomatic therapies	14 days	Lung CT, clinical cure rate, virus nucleic acid testing, rate of conversion to severe cases, clinical symptoms, and adverse events
Yu et al. (2020)	Mild/moderate	T:147 (82/65) C:148 (89/59)	T:48.27 ± 9.56 C:47.25 ± 8.67	Lianhua Qingwen granule (6 g, tid) + conventional therapy	Conventional therapy including abidor tablets, moxifloxacin tablets, and ambroxol tablets	7 days	Lung CT, clinical cure rate, rate of conversion to severe cases, clinical symptoms inflammatory biomarkers, and adverse events
Zhang et al. (2020)	Moderate	T:80 (50/30) C:40 (23/17)	T:53.4 ± 13.70 C:52.0 ± 14.10	Jinyinhua oral liquid (60 ml/time, tid) + conventional therapy	Conventional therapy including interferon-α, lopinavir, tonavir tablets, and symptomatic treatment	10 days	Rate of conversion to severe cases, clinical symptoms, and adverse events

therapy of honeysuckle and controls. Control groups used conventional therapy. In each trial, conventional therapy in the treatment group was identical to the control group. Two trial intervention groups were Chinese medicine compound drugs (Pneumonia No. 1 formula and Qingfei Touxie Fuzheng recipe) (Ai et al., 2020; Ding et al., 2020). And the other trials were Chinese patent medicine (Duan et al., 2020; Fu et al., 2020a; Fu et al., 2020b; Hu et al., 2020; Yu et al., 2020; Zhang et al., 2020; Hu et al., 2021). Conventional therapy included oxygen therapy, drugs, and symptomatic therapies. The drugs used in the control group were arbidol, lopinavir, interferon-α, and ribavirin. Two trial control groups did not provide specific therapy medicine (Duan et al., 2020; Hu et al., 2021).

Description of Honeysuckle

The description of honeysuckle in each trial is shown in **Table 2**. Honeysuckle was used in the dosage formulations of granules (55.55%) (Ai et al., 2020; Duan et al., 2020; Fu et al., 2020a; Fu et al., 2020b; Yu et al., 2020), decoction (11.11%) (Ding et al., 2020), oral liquid (22.22%) (Hu et al., 2020; Zhang et al., 2020), and capsule (11.11%) (Hu et al., 2021). The component of oral liquid (Hu et al., 2020; Zhang et al., 2020) is only honeysuckle.

TABLE 2 | The description of honeysuckle in each trial.

References	Honeysuckle and Chinese herbal medicine	Components
Ai et al. (2020)	Pneumonia No.1 formula (granule)	Honeysuckle 15 g, Lianqiao 30 g, Qingdao 10 g, Huangqi 45 g, Shancigu 20 g, Huangqin 10 g, Daqingye 10 g, Chaihu 5 g, Chantui 10 g, Qianhu 5 g, Chuanbeimu 10 g, Zhebeimu 10 g, Wumei 30 g, Xuanshen 10 g, Fuling 30 g, and Taizishen 15 g
Ding et al. (2020)	Qingfei Touxie Fuzheng recipe (decoction)	Honeysuckle 30 g, Lianqiao 15 g, Mahuang 6 g, Shigao 20 g, Kuxingren 10 g, Lugen 30 g, Yiyiren 30 g, Jiangcan 10 g, Chantui 10 g, Huzhang 15 g, Jianghuang 10 g, Baishaoyao 10 g, Taizishen 20 g, and Gancao 15 g
Duan et al. (2020)	Jinhua Qinggan granule	Honeysuckle 10 g, Shigao 10 g, Mahuang 10 g, Kuxingren 10 g, Huangqin 10 g, Lianqiao 10 g, Zhebeimu 10 g, Zhimu 10 g, Niubangzi 10 g, Qinghao 10 g, Bohe 10 g, and Gancao10 g
Fu et al. (2020a)	Toujie Quwen granule	Honeysuckle 15 g, Lianqiao 30 g, Shancigu 20 g, Huangqin 10 g, Daqingye 10 g, Chaihu 5 g, Qinghao 10 g, Chantui 10 g, Qianhu 5 g, Chuanbeimu 10 g, Zhebeimu 10 g, Wumei 30 g, Xuanshen 10 g, Huangqi 45 g, Fuling 30 g, and Taizishen 15 g
Fu et al. (2020b)	Toujie Quwen granule	Honeysuckle 15 g, Lianqiao 30 g, Shancigu 20 g, Huangqin 10 g, Daqingye 10 g, Chaihu 5 g, Qinghao 10 g, Chantui 10 g, Qianhu 5 g, Chuanbeimu 10 g, Zhebeimu 10 g, Wumei 30 g, Xuanshen 10 g, Huangqi 45 g, Fuling 30 g, and Taizishen 15 g
Hu et al. (2020)	Jinyinhua oral liquid	Honeysuckle 10.8 g
Hu et al. (2020)	Lianhua Qingwen capsule	Honeysuckle, Lianqiao, Mahuang, Kuxingren, Shigao, Banlangen, Mianma, Guanzhong, Yuxingcao, Huoxiang, Dahuang, Hongjingtian, menthol, and Gancao
Yu et al. (2020)	Lianhua Qingwen granule	Honeysuckle, Lianqiao, Mahuang, Kuxingren, Shigao, Banlangen, Mianma, Guanzhong, Yuxingcao, Huoxiang, Dahuang, Hongjingtian, menthol, and Gancao
Zhang et al. (2020)	Jinyinhua oral liquid	Honeysuckle 5.4 g

TABLE 3 | Risk of bias.

References	A	B	C	D	E	F	G
Ai et al. (2020)	L	U	U	U	L	U	U
Ding et al. (2020)	L	U	U	U	L	U	U
Duan et al. (2020)	L	U	U	U	L	U	U
Fu et al. (2020a)	L	U	U	U	L	U	U
Fu et al. (2020b)	L	U	U	U	L	U	U
Hu et al. (2020)	L	U	U	U	L	U	U
Hu et al. (2020)	L	U	U	L	L	U	U
Yu et al. (2020)	L	U	U	U	L	U	U
Zhang et al. (2020)	U	U	U	U	L	U	U

A, random sequence generation (selection bias); B, allocation concealment (selection bias); C, blinding of participants and personnel (performance bias); D, blinding of outcome assessment (detection bias); E, incomplete outcome data (attrition bias); F, selective reporting (reporting bias); G, other biases; L, low risk; H, high risk; U, unclear.

Honeysuckle is one component of Chinese herbal medicine in other dosage formulations.

METHODOLOGICAL QUALITY

The results of the ROB assessment are shown in **Table 3**. In general, there was insufficient information available in all trials included in this study. The risks of bias of included trials were mostly "unclear risk."

Results of the Meta-Analysis

Four trials (Ding et al., 2020; Duan et al., 2020; Hu et al., 2020; Yu et al., 2020) reported lung CT. Compared with conventional therapy alone, combination therapy of honeysuckle and conventional therapy exhibited a significant improvement on lung CT [4 trials, $n = 744$, RR = 1.24, 95%CI (1.12, 1.37), $I^2 = 11\%$, $p < 0.0001$] (**Figure 2A**). Subgroup analysis revealed that combination therapy could better improve the lung CT of nonsevere COVID-19 [3 trials, $n = 644$, RR = 1.22, 95%CI (1.10, 1.35), $I^2 = 25\%$, $p = 0.0002$] (**Figure 2A**).

Five trials (Ai et al., 2020; Fu et al., 2020a; Fu et al., 2020b; Yu et al., 2020; Hu et al., 2021) demonstrated the clinical cure rate. The results showed that clinical cure rate in the combination treatment groups was higher than the control groups [5 trials, $n = 815$, RR = 1.21, 95%CI (1.12, 1.31), $I^2 = 19\%$, $p < 0.00001$] (**Figure 2B**).

Three trials (Hu et al., 2020; Zhang et al., 2020; Hu et al., 2021) described viral nucleic acid testing. Compared with the control groups, no statistical difference on viral nucleic acid testing was identified [3 trials, $n = 532$, RR = 1.06, 95%CI (0.98, 1.15), $I^2 = 0\%$, $p = 0.15$] (**Figure 3A**). Subgroup analysis suggested no statistical difference between honeysuckle alone ($p = 0.32$) and Chinese herbal medicine formula ($p = 0.28$) (**Figure 3A**).

Six trials (Fu et al., 2020a; Fu et al., 2020b; Hu et al., 2020; Yu et al., 2020; Zhang et al., 2020; Hu et al., 2021) reported rate of conversion to severe cases. We found that combination therapy could significantly reduce the rate of conversion to severe cases [6 trials, $n = 965$, RR = 0.50, 95%CI (0.33, 0.76), $I^2 = 0\%$, $p = 0.001$] (**Figure 3B**). Subgroup analysis showed that there was a significant difference between honeysuckle alone ($p = 0.04$) and Chinese herbal medicine formula ($p = 0.01$) (**Figure 3B**).

Six trials (Ding et al., 2020; Duan et al., 2020; Fu et al., 2020a; Fu et al., 2020b; Yu et al., 2020; Zhang et al., 2020) described clinical symptoms of fever, cough, and fatigue. Meta-analyses revealed that combination therapy could better improve the symptoms reduction rate and symptom score than conventional therapy (**Table 4**). As shown in **Table 4**, combination therapy could significantly improve the symptom score of fever, cough reduction rate, symptom score of cough, and symptom score of fatigue ($p < 0.05$). However, there was no significant difference in

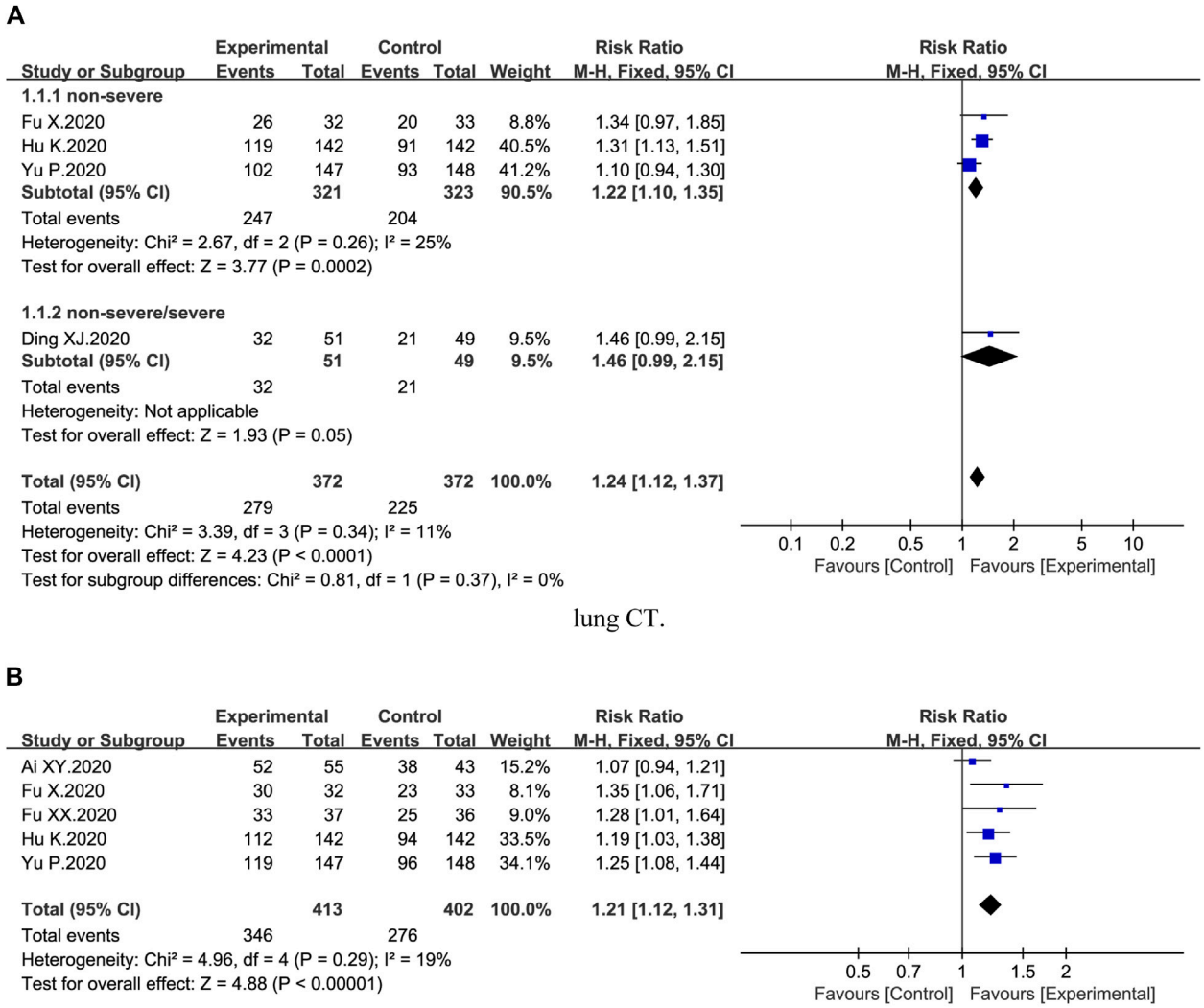

FIGURE 2 | Forest plot of the effects of combination therapy for outcomes of **(A)** lung CT and **(B)** clinical cure rate.

fever reduction rate and fatigue reduction rate between the combination treatment and control groups ($p > 0.05$).

Five trials (Ai et al., 2020; Ding et al., 2020; Fu et al., 2020a; Fu et al., 2020b; Yu et al., 2020) reported inflammatory biomarkers. We found that combination therapy was beneficial for WBC count [3 trials, $n = 433$, MD = 0.38, 95%CI (0.31, 0.44), $I^2 = 22\%$, $p < 0.00001$], LYM count [4 trials, $n = 531$, MD = 0.23, 95%CI (0.05, 0.41), $I^2 = 97\%$, $p = 0.01$], and CRP level [4 trials, $n = 533$, MD = −12.95, 95%CI (−21.18, −4.01), $I^2 = 98\%$, $p = 0.004$] to return to normal. And these differences were statistically significant ($p < 0.05$) (**Table 5**).

All included trials reported adverse drug events. The common adverse drug events of combination therapy were nausea and vomiting, inappetence, diarrhea, headache, renal dysfunction, and abnormal liver function. As shown in **Table 6**, there was no significant difference in adverse events rate, diarrhea, and abnormal liver function between the combination treatment and control groups ($p > 0.05$). Additionally, inappetence, nausea and vomiting, headache, and renal dysfunction were reported in one trial (Hu et al., 2021), and no statistical difference was identified in both combination treatment and control groups.

Sensitivity Analysis

Sensitivity analysis revealed a small change in the effect amount, and a significant difference in lung CT, clinical cure rate, rate of conversion to severe cases, symptom score of fever, cough reduction rate, symptom score of cough, WBC count, and CRP. Sensitivity analysis indicated that the above results were robust.

Publication Bias

As the number of trials in any comparative outcome measure was less than ten, we did not assess the publication bias.

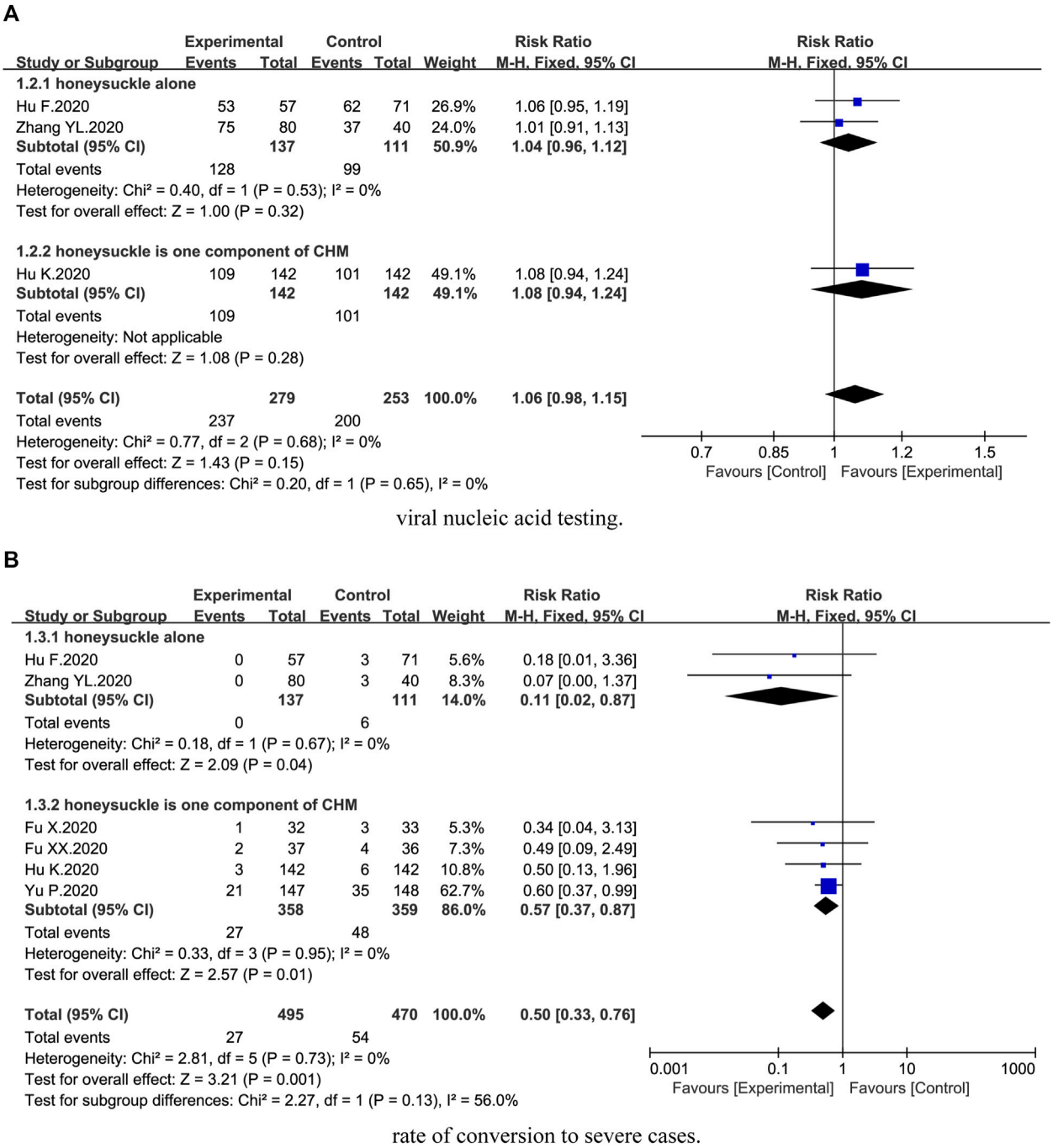

FIGURE 3 | Forest plot of the effects of combination therapy for outcomes of **(A)** viral nucleic acid testing and **(B)** rate of conversion to severe cases.

DISCUSSION

Summary of Findings

In our study, it was found that Chinese herbal medicine honeysuckle could provide additional benefit for the clinical outcomes of COVID-19. This finding was consistent with similar studies (Ang et al., 2020; Xiong et al., 2020). Similar studies have shown that, compared with conventional therapy, Chinese herbal medicine had better effects and fewer adverse drug events (Ang et al., 2020; Xiong et al., 2020). Facing such a severe COVID-19 epidemic, Western countries should pay high attention to the curative effect of Chinese herbal medicine.

Honeysuckle is one of the most widely used traditional Chinese herbal medicines. It is used as an antiviral,

TABLE 4 | Comparison of clinical symptoms between the treatment group and control group.

Outcome measure	No. of trials	Samples			Statistical method	Effect estimate	*p*-value
		Total	Events/intervention	Events/control			
Fever cases	3	296	171/185	90/111	RR (random) 95%CI	0.11 (–0.10, 0.33)	0.31
Cough cases	3	260	135/167	56/93	RR (fixed) 95%CI	1.37 (1.15, 1.65)	0.0006
Fatigue cases	2	163	98/116	32/47	RR (random) 95%CI	1.20 (0.85, 1.69)	0.3
Symptom score of fever	3	433	—	—	RR (random) 95%CI	–0.62 (–0.79, –0.45)	< 0.00001
symptom score of cough	3	433	—	—	RR (random) 95%CI	–1.18 (–1.34, –1.03)	< 0.00001
Symptom score of fatigue	3	433	—	—	RR (random) 95%CI	–0.60 (–1.04, –0.17)	0.007

TABLE 5 | Comparison of inflammatory biomarkers between the treatment group and control group.

Outcome measure	No. of trials	Samples	Statistical method	Effect estimate	*p*-value
WBC count	3	433	MD (fixed) 95%CI	0.38(0.31, 0.44)	< 0.00001
LYM count	4	531	MD (random) 95%CI	0.23(0.05, 0.41)	0.01
CRP	4	533	MD (random) 95%CI	–12.95(–21.18, –4.01)	0.004

TABLE 6 | Comparison of adverse drug events between the treatment group and control group.

Outcome measure	No. of trials	Samples			Statistical method	Effect estimate	*p*-value
		Total	Events/intervention	Events/control			
Adverse events rate	5	755	96/412	80/343	RR (random) 95%CI	1.72(0.44, 6.74)	0.44
Diarrhea	4	655	37/361	19/294	RR (random) 95%CI	2.43(0.20, 29.33)	0.49
Abnormal liver function	2	384	34/193	35/191	RR (fixed) 95%CI	0.97(0.64, 1.47)	0.88

immunomodulator, anti-inflammatory, hepatoprotectant, and nephroprotectant (Miao et al., 2019; Bai et al., 2020; Fang et al., 2020; Alekhya Sita et al., 2019). Honeysuckle is predicted to suppress SARS-CoV-2 replication (Lee et al., 2021). Honeysuckle extracts can inhibit the replication of influenza viruses H1N1, H3N2, and the oseltamivir-resistant mutant strain H1N1-H275Y (Li et al., 2020). Honeysuckle polysaccharides can regulate nonspecific immunity (Zhou et al., 2018) and inhibit the expression of inflammatory factors TNF-α and IL-1β (Bai et al., 2020). Neochlorogenic acid from Lonicera can prevent excessive macrophage-mediated responses associated with acute and chronic inflammatory disorders (Park et al., 2018). *Lonicera caerulea* L. polyphenols (LCPs) can alleviate LPS-induced liver injury by suppressing the nuclear translocation of NF-κB p65 and activation of the MAPK signaling pathway (Li et al., 2020). Luteolin is a pharmacologically active component normally found in honeysuckle, which exhibits antioxidant activity and nephroprotective activity (Alekhya Sita et al., 2019).

In our study, honeysuckle combined with conventional therapy was superior to conventional therapy alone in improving clinical symptoms, imaging, and laboratory indexes. Compared with conventional therapy alone, combination therapy of honeysuckle and conventional therapy could improve symptom score of fever, cough reduction rate, and symptom score of cough. We found that combination therapy could improve lung CT, increase WBC count, and reduce CRP level. This is related to the fact that honeysuckle can affect the immune response and production of inflammatory cytokines (Zhou et al., 2018; Bai et al., 2020). Immunopathological changes, including diminished lymphocytes and elevated cytokines, are important drivers of disease progression and death in coronavirus infections (Tang et al., 2020). Cytokine storm is uncontrolled overproduction of inflammation markers with elevated levels of IL-6, IL-1β, and TNF-α (Coperchini et al., 2020; Kempuraj et al., 2020). This leads to acute lung injury, acute respiratory distress syndrome (ARDS), and widespread tissue damage resulting in multiorgan failure and death (Ragab et al., 2020; Caricchio et al., 2021). In our study, we also found that combination therapy had improvements in clinical parameters including clinical cure rate and rate of conversion to severe cases.

Safety issues should be another concern when honeysuckle combined with conventional therapy is used for COVID-19 patients. In our study, all included trials reported adverse drug events. Compared with conventional therapy alone, combination therapy of honeysuckle and conventional therapy did not increase adverse drug events. This is related to the fact that honeysuckle exhibits hepatoprotective and nephroprotective activity (Alekhya Sita et al., 2019; Li et al., 2020).

Strengths and Limitations

This study is to our knowledge the first systematic review and meta-analysis for the effectiveness and safety of honeysuckle combined with conventional therapy in adult patients with COVID-19. It could help to respond to the current public health emergency. Another advantage could be that only randomized studies are included. Our study was also performed in accordance with Cochrane Handbook and PRISMA checklist to draw quantitative conclusions with scientific and rigorous methods. In addition, we conducted a subgroup analysis and sensitivity analysis. It meant that our meta-analysis results were more robust.

However, our review had several limitations. Merger statistical analysis of some outcomes had unexplained heterogeneity. Most of the included trials had deficiencies in methodology design, including hidden allocation, blinding, and selective reporting. Publication bias was unclear. The drugs used in the control group were different. However, we did not perform subgroup analyses. The treatment duration ranged from 5 to 15 days. We also did not perform subgroup analyses according to treatment duration.

CONCLUSION

In conclusion, honeysuckle combined with conventional therapy may be beneficial for the treatment of COVID-19 in improving clinical symptoms, lung CT, laboratory indicators, and clinical cure rate and reducing the rate of conversion to severe cases. Besides, combination therapy did not increase adverse drug events. However, considering the poor methodology of included trials, more high-quality trials are needed to evaluate the efficacy of honeysuckle in the treatment of COVID-19 in the future.

AUTHOR CONTRIBUTIONS

L-PS and W-FC designed the study. L-PS and X-QD searched databases, collected the data, assessed the quality of study, and performed data analysis. L-PS, X-QD, W-FC, Z-WC, BZ, and J-YH contributed to the rationalization of the results. L-PS, X-QD, and W-FC wrote the manuscript.

FUNDING

This study was funded by the National Natural Science Foundation of China (No. 81573860), Chongqing Medical University Postdoctoral Foundation (No. R11004), and Chongqing Postdoctoral Special Foundation (Yuren Social Office (2020) No. 379). The funding source had no role in the study.

SUPPLEMENTARY MATERIAL

The Supplementary Material for this article can be found online at: https://www.frontiersin.org/articles/10.3389/fphar.2021.708636/full#supplementary-material

REFERENCES

Ai, X., Luo, C., Lin, L., Xie, M., Fan, H., and Tan, X. (2020). Therapeutic effect of integrated traditional Chinese and western medicine on COVID-19 in Guangzhou. *Chin Trop. Med* 20, 746–750. doi:10.13604/j.cnki.46-1064/r.2020.08.12

Alekhya Sita, G. J., Gowthami, M., Srikanth, G., Krishna, M. M., Rama Sireesha, K., Sajjarao, M., et al. (2019). Protective role of luteolin against bisphenol A-induced renal toxicity through suppressing oxidative stress, inflammation, and upregulating Nrf2/ARE/HO-1 pathway. *IUBMB Life* 71, 1041–1047. doi:10.1002/iub.2066

Ang, L., Song, E., Lee, H. W., and Lee, M. S. (2020). Herbal medicine for the treatment of coronavirus disease 2019 (COVID-19): A Systematic Review and Meta-Analysis of Randomized Controlled Trials. *J. Clin. Med.* 9, 1583. doi:10.3390/jcm9051583

Bai, X., Chai, Y., Shi, W., Li, Y., Zhang, T., and Liu, P. (2020). Lonicera japonica polysaccharides attenuate ovalbumin-induced allergic rhinitis by regulation of Th17 cells in BALB/c mice. *J. Funct. Foods* 65, 103758. doi:10.1016/j.jff.2019.103758

Caricchio, R., Gallucci, M., Dass, C., Zhang, X., Gallucci, S., Fleece, D., et al. (2021). Preliminary predictive criteria for COVID-19 cytokine storm. *Ann. Rheum. Dis.* 80, 88–95. doi:10.1136/annrheumdis-2020-218323

Coperchini, F., Chiovato, L., Croce, L., Magri, F., and Rotondi, M. (2020). The cytokine storm in COVID-19: An overview of the involvement of the chemokine/chemokine-receptor system. *Cytokine Growth Factor. Rev.* 53, 25–32. doi:10.1016/j.cytogfr.2020.05.003

Ding, X., Zhang, Y., He, D., Zhang, M., Tan, Y., Yu, A., et al. (2020). Clinical effect and mechanism of Qingfei Touxie Fuzheng recipe in the treatment of COVID-19. *Herald Med.* 39, 640–644. doi:10.3870/j.issn.1004-0781.2020.05.012

Duan, C., Xia, G., Zheng, C., Sun, G., Li, Z., Li, Q., et al. (2020). Clinical observation on Jinhua Qinggan granule combined with conventional western medicine therapy in treating mild cases of coronavirus disease 2019. *J. Tradit Chin. Med.* 61, 1473–1477. doi:10.13288/j.11-2166/r.2020.17.001

Fang, Z., Li, J., Yang, R., Fang, L., and Zhang, Y. (2020). A Review: The triterpenoid saponins and biological activities of lonicera linn. *Molecules* 25, 3773. doi:10.3390/molecules25173773

Fu, X., Lin, L., and Tan, X. (2020a). Clinical observation on effect of Toujie Quwen granules in treatment of COVID-19. *Chin. J. Exp. Tradit Med. Formul* 26, 44–48. doi:10.13422/j.cnki.syfjx.20201314

Fu, X., Lin, L., and Tan, X. (2020b). Clinical study on 37 case of COVID- 19 treated with integrated traditional Chinese and western medicine. *Tradit Chin. Drug Res. Clin. Pharmacol.* 31, 600–604. doi:10.19378/j.issn.1003-9783.2020.05.016

Higgins, J. P. T., and Green, S. (2014). *Cochrane Reviewers' Handbook 5.3.0.* (updated March 2014). Cochrane Collaboration website. Available: www.cochrane-handbook.org (Accessed May 10, 2021).

Hu, F., Guo, A., Huang, L., Yu, W., Liu, G., Gao, X., et al. (2020). Multi-center clinical observation of Jinyinhua oral liquid combined with western medicine in treatment of moderate COVID-19. *J. Tradit Chin. Med.*. Available online at: https://kns.cnki.net/kcms/detail/11.2166.R.20200819.0837.002.html (Accessed May 2, 2021).

Hu, K., Guan, W.-j., Bi, Y., Zhang, W., Li, L., Zhang, B., et al. (2021). Efficacy and safety of Lianhuaqingwen capsules, a repurposed Chinese herb, in patients with coronavirus disease 2019: A multicenter, prospective, randomized controlled trial. *Phytomedicine* 85, 153242. doi:10.1016/j.phymed.2020.153242

Kempuraj, D., Selvakumar, G. P., Ahmed, M. E., Raikwar, S. P., Thangavel, R., Khan, A., et al. (2020). COVID-19, mast cells, cytokine storm, psychological stress, and neuroinflammation. *Neuroscientist* 26, 402–414. doi:10.1177/1073858420941476

Lee, Y.-R., Chang, C.-M., Yeh, Y.-C., Huang, C.-Y., Lin, F.-M., Huang, J.-T., et al. (2021). Honeysuckle aqueous extracts induced let-7a suppress EV71 replication and pathogenesis *in vitro* and *in vivo* and is predicted to inhibit SARS-CoV-2. *Viruses* 13, 308. doi:10.3390/v13020308

Li, B., Cheng, Z., Sun, X., Si, X., Gong, E., Wang, Y., et al. (2020). Lonicera caerulea L. Polyphenols alleviate oxidative stress-induced intestinal environment imbalance and lipopolysaccharide-induced liver injury in HFD-fed rats by regulating the Nrf2/HO-1/NQO1 and MAPK pathways. *Mol. Nutr. Food Res.* 64, e1901315. doi:10.1002/mnfr.201901315

Li, M., Wang, Y., Jin, J., Dou, J., Guo, Q., Ke, X., et al. (2020). Inhibitory activity of honeysuckle extracts against influenza A virus *in vitro* and *in vivo*. *Virol. Sin.* 36, 490–500. doi:10.1007/s12250-020-00302-6

Li, Y., Li, W., Fu, C., Song, Y., and Fu, Q. (2020). Lonicerae japonicae flos and Lonicerae flos: a systematic review of ethnopharmacology, phytochemistry and pharmacology. *Phytochem. Rev.* 19, 1–61. doi:10.1007/s11101-019-09655-7

Liu, M., Gao, Y., Yuan, Y., Yang, K., Shi, S., Zhang, J., et al. (2020). Efficacy and safety of integrated traditional Chinese and western medicine for corona virus disease 2019 (COVID-19): a systematic review and meta-analysis. *Pharmacol. Res.* 158, 104896. doi:10.1016/j.phrs.2020.104896

Miao, H., Zhang, Y., Huang, Z., Lu, B., and Ji, L. (2019). Lonicera japonica attenuates carbon tetrachloride-induced liver fibrosis in mice: molecular mechanisms of action. *Am. J. Chin. Med.* 47, 351–367. doi:10.1142/S0192415X19500174

Moher, D., Liberati, A., Tetzlaff, J., and Altman, D. G.PRISMA Group (2009). Preferred reporting items for systematic reviews and meta-analyses: the PRISMA statement. *BMJ* 339, b2535–W64. doi:10.7326/0003-4819-151-4-200908180-0013510.1136/bmj.b2535

National Health Commission of the people's Republic of China (2021). Epidemic notification. Available: http://www.nhc.gov.cn/xcs/xxgzbd/gzbd_index.shtml2021 (Accessed May 7, 2021).

National Health Commission of the people's Republic of ChinaNational Administration of Traditional Chinese Medicine (2020). Diagnosis and Treatment Guideline for COVID-19 (Trial 8th Edition)]. *Chin. J. Viral Dis.* 10, 321–328. doi:10.16505/j.2095-0136.2020.0071

Panahi, Y., Hosseini, M. S., Khalili, N., Naimi, E., Majeed, M., and Sahebkar, A. (2015). Antioxidant and anti-inflammatory effects of curcuminoid-piperine combination in subjects with metabolic syndrome: A randomized controlled trial and an updated meta-analysis. *Clin. Nutr.* 34, 1101–1108. doi:10.1016/j.clnu.2014.12.019

Park, S. Y., Jin, M. L., Yi, E. H., Kim, Y., and Park, G. (2018). Neochlorogenic acid inhibits against LPS-activated inflammatory responses through up-regulation of Nrf2/HO-1 and involving AMPK pathway. *Environ. Toxicol. Pharmacol.* 62, 1–10. doi:10.1016/j.etap.2018.06.001

Ragab, D., Salah Eldin, H., Taeimah, M., Khattab, R., and Salem, R. (2020). The COVID-19 cytokine storm; what we know so far. *Front. Immunol.* 11, 1446. doi:10.3389/fimmu.2020.01446

Sattler, A., Angermair, S., Stockmann, H., Heim, K. M., Khadzhynov, D., Treskatsch, S., et al. (2020). SARS-CoV-2-specific T cell responses and correlations with COVID-19 patient predisposition. *J. Clin. Invest.* 130, 6477–6489. doi:10.1172/JCI140965

Tang, L., Yin, Z., Hu, Y., and Mei, H. (2020). Controlling cytokine storm is vital in COVID-19. *Front. Immunol.* 11, 570993. doi:10.3389/fimmu.2020.570993

World Health Organization (WHO) (2021). WHO Coronavirus (COVID-19) Dashboard. Available: https://covid19.who.int/2021 (Accessed May 7, 2021).

Xiong, X., Wang, P., Su, K., Cho, W. C., and Xing, Y. (2020). Chinese herbal medicine for coronavirus disease 2019: A systematic review and meta-analysis. *Pharmacol. Res.* 160, 105056. doi:10.1016/j.phrs.2020.105056

Yu, P., Li, Y., Wan, S., and Wang, Y. (2020). Clinical efficacy of Lianhua Qingwen granule combined with abidol in treating coronavirus disease 2019. *Chin. Pharm. J.* 55, 1042–1045. Available online at: http://kns.cnki.net/kcms/detail/11.2162.R.20200422.1429.002.html (Accessed May 2, 2021).

Zhang, Y., Lei, L., Xu, Y., Wei, D., and Hu, F. (2020). Clinical efficacy of Jinyinhua oral liquid in the treatment of 80 patients with coronavirus disease 2019. *Chin. Pharm.* 29, 23–26. doi:10.3969/j.issn.1006-4931.2020.09.006

Zhou, L. K., Zhou, Z., Jiang, X. M., Zheng, Y., Chen, X., Fu, Z., et al. (2020). Absorbed plant MIR2911 in honeysuckle decoction inhibits SARS-CoV-2 replication and accelerates the negative conversion of infected patients. *Cell Discov* 6, 54. doi:10.1038/s41421-020-00197-3

Zhou, X., Dong, Q., Kan, X., Peng, L., Xu, X., Fang, Y., et al. (2018). Immunomodulatory activity of a novel polysaccharide from Lonicera japonica in immunosuppressed mice induced by cyclophosphamide. *PLoS One* 13, e0204152–15. doi:10.1371/journal.pone.0204152

Conflict of Interest: The authors declare that the research was conducted in the absence of any commercial or financial relationships that could be construed as a potential conflict of interest.

Publisher's Note: All claims expressed in this article are solely those of the authors and do not necessarily represent those of their affiliated organizations or those of the publisher, the editors, and the reviewers. Any product that may be evaluated in this article or claim that may be made by its manufacturer is not guaranteed or endorsed by the publisher.

frontiers in Chemistry

ORIGINAL RESEARCH
published: 27 September 2021
doi: 10.3389/fchem.2021.735768

Characterization of Phytochemicals in *Ulva intestinalis* L. and Their Action Against *SARS-CoV-2* Spike Glycoprotein Receptor-Binding Domain

Seema A. Kulkarni[1], Sabari B.B. Krishnan[2†], Bavya Chandrasekhar[2], Kaushani Banerjee[2], Honglae Sohn[3] and Thirumurthy Madhavan[2]**

[1]Department of Biotechnology, School of Bioengineering, SRM Institute of Science and Technology, Chengalpattu, India, [2]Computational Biology Laboratory, Department of Genetic Engineering, School of Bioengineering, SRM Institute of Science and Technology, Chengalpattu, India, [3]Department of Chemistry and Department of Carbon Materials, Chosun University, Gwangju, South Korea

OPEN ACCESS

Edited by:
Sugunadevi Sakkiah,
National Center for Toxicological Research (FDA), United States

Reviewed by:
Albert Poater,
University of Girona, Spain
Utpal Sarkar,
Assam University, India

***Correspondence:**
Honglae Sohn
hsohn@chosun.ac.kr
Thirumurthy Madhavan
thiru.murthyunom@gmail.com

†This author have contributed equally to this work

Specialty section:
This article was submitted to Theoretical and Computational Chemistry, a section of the journal Frontiers in Chemistry

Received: 03 July 2021
Accepted: 10 September 2021
Published: 27 September 2021

Citation:
Kulkarni SA, Krishnan SBB, Chandrasekhar B, Banerjee K, Sohn H and Madhavan T (2021) Characterization of Phytochemicals in Ulva intestinalis *L. and Their Action Against* SARS-CoV-2 *Spike Glycoprotein Receptor-Binding Domain. Front. Chem. 9:735768. doi: 10.3389/fchem.2021.735768*

Coronavirus disease-2019 (COVID-19) has caused a severe impact on almost all aspects of human life and economic development. Numerous studies are being conducted to find novel therapeutic strategies to overcome COVID-19 pandemic in a much effective way. *Ulva intestinalis* L. (*Ui*), a marine microalga, known for its antiviral property, was considered for this study to determine the antiviral efficacy against severe acute respiratory syndrome-associated *Coronavirus-2* (*SARS-CoV-2*). The algal sample was dried and subjected to ethanolic extraction, followed by purification and analysis using gas chromatography-coupled mass spectrometry (GC-MS). Forty-three known compounds were identified and docked against the S_1 receptor binding domain (RBD) of the spike (S) glycoprotein. The compounds that exhibited high binding affinity to the RBD of S_1 protein were further analyzed for their chemical behaviour using conceptual density-functional theory (C-DFT). Finally, pharmacokinetic properties and drug-likeliness studies were carried out to test if the compounds qualified as potential leads. The results indicated that mainly phenols, polyenes, phytosteroids, and aliphatic compounds from the extract, such as 2,4-di-tert-butylphenol (2,4-DtBP), doconexent, 4,8,13-duvatriene-1,3-diol (DTD), retinoyl-β-glucuronide 6′,3′-lactone (RBGUL), and retinal, showed better binding affinity to the target. Pharmacokinetic validation narrowed the list to 2,4-DtBP, retinal and RBGUL as the possible antiviral candidates that could inhibit the viral spike protein effectively.

Keywords: SARS-CoV-2 spike S1 subunit, Ulva intestinalis L., phytochemicals, GC-MS, COVID-19, molecular docking, ADMET studies, conceptual DFT

INTRODUCTION

COVID-19, a contagious viral disease caused by *SARS-CoV-2*, was declared as a public health emergency of international concern by the World Health Organization (WHO) on 30 January 2020, and as a pandemic on March 11, 2020 (Ge et al., 2020). According to the recent pandemic situation report released by the WHO, *SARS-CoV-2* has infected nearly 180 million individuals, causing about four million deaths. Being a positive, single-stranded RNA virus of size 50–200 nm and genome size

of 29.9 k ribonucleotides, it is the most recent member included in the *Betacoronavirus* genus of the *Orthocoranavirinae* subfamily of coronaviruses (Lu et al., 2020). The viral genome was found to encode twelve main proteins, of which two, the spike glycoprotein and the main protease (M^{pro}) have gained attention as potential COVID-19 drug targets (Pavlova et al., 2021). The availability of structural details of these two proteins has accelerated computational studies. The thermodynamically favoured irreversible inhibition of M^{pro} by Michael acceptors has been studied by computational methods such as molecular dynamics and density functional theory (Poater 2020; Ramos-Guzmán et al., 2021; Zanetti-Polzi et al., 2021). The covalent and non-covalent binding free energies of M^{pro}inhibitors have been studied to aid in rational drug discovery and design for targeted antiviral therapy (Awoonor-Williams and Abu-Saleh, 2021). Several experimentations suggest that *SARS-CoV* and *SARS-CoV–2* have a sequence identity of approximately 79 percent, and both variants use angiotensin converting enzyme 2 (ACE2) as their cellular receptor. Similarly, some studies suggest that the infectivity rate varies with amino acid change in the spike protein, and the adsorption of S protein on gold nanoparticles was completely dependant on the size of the core nano-gold (Bette et al., 2021; Yokoyama and Ichiki, 2021). The spike glycoprotein is comprised of two subunits, the S_1, which has the receptor binding domain, and the S_2, which facilitates membrane fusion and endocytosis of the virus (Walls et al., 2020). Several studies have shown that *SARS-CoV-2* utilizes the S_1 protein to bind to the functional receptor human ACE2 (hACE2) at the RBD. The same mechanism was used for viral entry by *SARS-CoV* too. Eventually S_2 protein aids in fusion of viral particles in the host. The receptor-binding motif (RBM) in RBD is the main functional motif and is composed of two regions (region 1 and region 2) that form the interface between the S protein and hACE2. The region outside the RBM in RBD also plays an important role in maintaining the structural stability of the RBD (Li et al., 2003; Yi et al., 2020; Zhou et al., 2020).

The current challenge faced by the health sector is the resistance and insensitivity of the virus to existing drugs, and those drugs that have an edge over the virus were found to have some detrimental side effects. Drugs such as hydroxychloroquine and chloroquine (FDA-approved drugs that are effective against malaria, lupus, and rheumatoid arthritis) were found to hamper this viral infection, but the risks of developing cardiovascular and renal disorders were found in many of its consumers (FDA, 2020). Also, the recovery rate fluctuated from region to region, in fact, from person to person, with varying degrees of side-effects, forcing the WHO to halt the solidarity trial of hydroxychloroquine a few months after the COVID-19 outbreak.

In silico techniques play an important role in accelerating research to identify potential leads against *SARS-CoV*-2. Molecular docking, molecular dynamic simulation and drug repurposing are the strategies currently practiced for drug development against COVID-19 (Acharya et al., 2020). Molecular dynamic simulation studies futher help to substantiate the reciprocity between the protein and the ligand. Such tools can be exploited for drug developmental studies which further aid in lead optimization with increased specificity and selectivity (Raudah et al., 2020). Various herbs and plant-based compounds are being tested for possible antiviral activity against *SARS-CoV-2* (Anand et al., 2021). *Ui*, also called gutweed or grass kelp, a common but often unnoticed macro alga, was mainly studied for its anti-microbial and anti-cancer properties *in vitro*, however, few studies were published on its anti-viral activity (Morán-Santibañez et al., 2016; Klongklaew et al., 2020). It is a member of the *Ulvaceae* family, which belongs to the Chlorophyta (green seaweed) division (Class: Ulvophyceae, Order: Ulvales). It is found to be a euryhaline and thus can grow even in freshwaters, exclusively in nutrient-rich niches such as in water bodies that receive industrial and farm discharges, and low tidal zones. These tubular algae can reach up to 0.3 m in length, with a thickness of about 0.02 m, and exhibit a perennial isomorphic biphasic reproductive cycle. Considering its abundance in the Coromandel coastline of South India, and its possible action against viruses such as the measles *Morbillivirus*in Vero cell lines (Morán-Santibañez et al., 2016), *Ui* was considered as the source of phytochemicals that can serve as possible lead compounds against the S protein RBD of *SARS-CoV-2*.

MATERIALS AND METHODS

Sample Collection and Preparation

The alga *Ui* were collected from the Olaikuda area (Gulf of Mannar) situated near North Mandapam, Rameswaram, Tamil Nadu, India, with the help of the Central Marine Fisheries Research Institute, Mandapam, and Rajendra Kumar Algae Project Center, Mandapam. The algal sample was washed thoroughly with water to remove dirt and debris and packed safely in polythene zip-lock bags. Upon reaching the laboratory it was dried using a tray drier (**Figures 1A,C**), mainly to concentrate the extract, preserve the hydrolabile compounds, and prevent the growth of bacteria and mold.

Isolation and Identification of Phytochemicals

Phytochemical extraction was performed by Soxhlet extraction. The dried sample (~60 g) was pulverized using a mortar and pestle (**Figures 1B,D**), and transferred into a thimble in the extraction tube. The extraction solvent used was 95% ethanol (100 ml). The all-glass Soxhlet apparatus was set up according to the standard protocol and was run for 6 h at 78°C using an isomantle. The extract was analyzed for the phytochemicals using a 7890B GC coupled with a 5977A mass selective detector (MSD). The chromatographic column used for GC was HP-5MS of dimensions 30 m × 250 μm × 0.25 μm (length, inner diameter, and film thickness, respectively). It is a bonded, cross-linked, and solvent-rinsable non-polar column made of (5%-phenyl)-methylpolysiloxane, with a capillary tubing made of fused silica (Agilent Technologies, Santa Clara, CA). The volume of the sample injected was 1 μl and the flow rate of the carrier gas (helium) was 1.0 $ml.min^{-1}$ with a split ratio of 1:1. The injection port temperature was 250°C. The system started with a 2 min-hold at 50°C, then ramped 3°C per minute until the temperature

FIGURE 1 | Samples of *U. intestinalis* used for Soxhlet extraction using ethanol. **(A)** Tray-dried sample **(B)** powdered form of tray-dried sample. **(C)** Freeze-dried sample **(D)** powdered form of freeze-dried sample.

reached 270°C. The system was on hold at this temperature for 20 min. Simultaneously, the separated samples were fed automatically to the MSD at an interface temperature of 280°C. The electron ionization was performed at 70 eV, and the scan range of the system was 40–700 m/*z*. The total run time of the process was 95 min. The retention indices of the compounds were determined relative to trichloromethane, the standard compound selected for data analysis. Further, the compounds were identified by comparing their mass spectra with the data in NIST-14 Mass Spectral Data Library.

Preparation of Ligands and Target

The three-dimensional chemical structures of the identified phytochemicals were obtained from PubChem (https://pubchem.ncbi.nlm.nih.gov/). These were then saved as SDF files. The energy minimization and format conversion of these structures were performed in PyRx software (Dallakyan and Olson 2015). The default energy minimization parameters were the universal force field and the conjugate gradient algorithm. Once energy minimization was completed, the structures were rewritten as PDBQT files. The target protein used in this study was S_1 receptor binding domain of the spike (S) glycoprotein. The three-dimensional structure of RBD was retrieved from a complex of ACE2 and RBD (PDB ID: 6M0J) from the Protein Data Bank (RCSB-PDB; https://www.rcsb.org/). As the first step, the optimization of protein structures was performed using AutoDock Tools by deleting chain A, water molecules, and co-crystal ligands. The missing atoms were then repaired, and polar hydrogens were added. Charges were

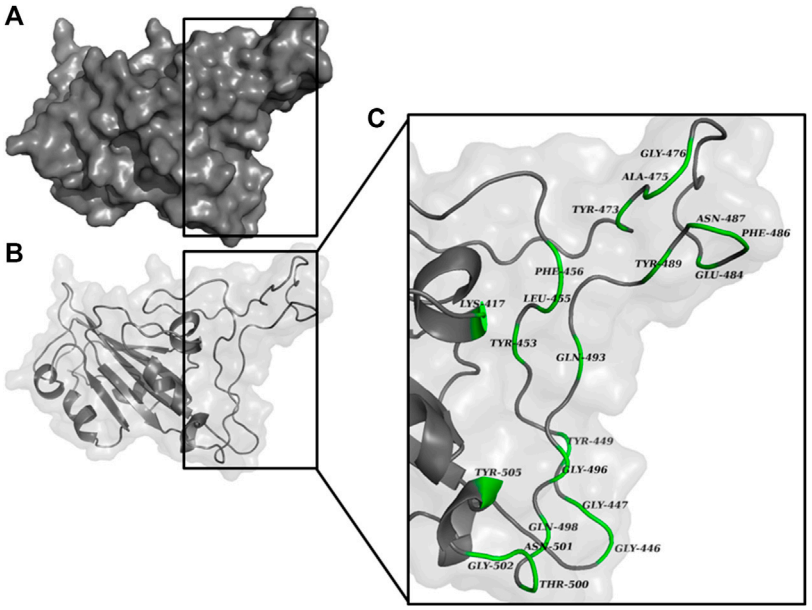

FIGURE 2 | RBD of S_1 protein represented as **(A)** surface, and **(B)** chain. The magnified view of the RBD **(C)** shows the possible interacting residues (green) in <5.0 Å vicinity with ACE2.

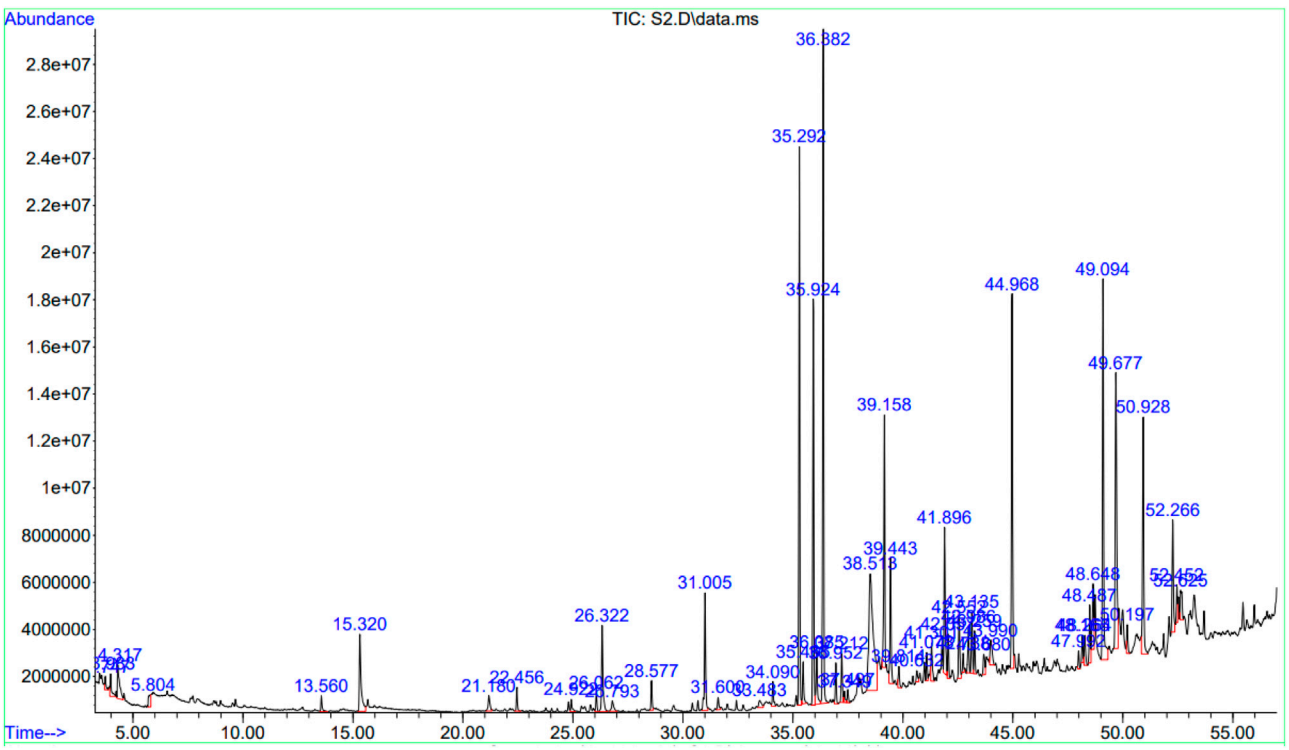

FIGURE 3 | Chromatogram showing the results of GC-MS. The chromatogram was plotted against retention time in minutes (X-axis), and signal abundance (Y-axis). The collected fractions were fed automatically into an MS.

TABLE 1 | GC-MS data of the phytochemicals present in *Ui* extract.

Peak No(s)	Retention time(s) (min)	Compound	$a_{Peak\ Area}$ (%)
1	3.747	Methylglyoxal	0.237
3	4.317	Furfural	1.110
4	5.804	DMSO	0.445
5	13.560	TAA	0.327
6	15.320	Azulene	2.135
7	21.180	Damascone	0.422
8, 13	22.456, 28.577	Cetene	0.877
9	24.922	Myristyl chloride	0.253
10	26.062	Cyclosativene	0.342
11	26.322	2,4-DtBP	1.902
12	26.793	Dihydroactinolide	0.355
14	31.005	8-Heptadecene	2.164
15	31.600	3-DOCH	0.265
16, 27	33.483, 38.513	Palmitic acid	8.207
17, 18	34.090, 35.292	9-Octadecene	9.082
19	35.465	TMHA	0.761
20, 22, 23, 33, 34	35.924, 36.382, 36.952, 41.301, 41.896	Phytol	21.404
21	36.085	HIP	1.134
24	37.212	CMBA	0.904
25, 41	37.349, 43.680	1-Heptatriacotanol	0.740
26	37.497	Methylpalmitate	0.237
28	39.158	Ethylpalmitate	4.206
29	39.443	Butanoic acid	2.250
30	39.814	Paullinic acid	0.428
31, 37	40.632, 42.738	Doconexent	0.524
32	41.078	Allyl stearate	0.445
35	42.057	DTD	0.734
36	42.552	Retinal	1.201
38	42.986	Ethyllinolelaidate	0.866
39	43.135	Ethyllinolenate	1.095
40	43.259	Ethylelaidate	0.658
42	43.990	Icosapent	0.782
43, 50	44.968, 49.677	2-Monopalmitin	13.139
44	47.992	EEBOD	0.293
45	48.165	MHDTE	0.447
46	48.264	BOD4E	0.606
47	48.487	1-Monolinolein	1.059
48, 55	48.648, 52.625	BOD3E	2.347
49	49.094	BTES	7.174
51	50.197	RBGUL	0.487
52	50.928	DPPP	4.517
53	52.266	Oxymesterone	2.362
54	52.452	Propyllinoleate	0.619

a_{Values} indicate the mean relative peak area. For compounds identified with more than one retention time, this value was presented to be a summation of the individual mean relative peak areas.

DMSO: Dimethyl sulfoxide; TAA: Tert-amyl alcohol; 2,4-DtBP: 2,4-Di-tert-butylphenol; 3-DOCH: 3-(6,6-Dimethyl-5-oxohept-2-enyl)cycloheptanone; TMHA: 3,7,11,15-Tetramethylhexadecylacetate; HIP: Hept-3-yl isobutyl ester of phthalic acid; CMBA: Cholestan-3-ol, 2-methylene- (3β,5α)-; DTD: 4,8,13-Duvatriene-1,3-diol; EEBOD: 3-Ethyl-5-(2-ethylbutyl)octadecane; MHDTE: Methyl 4,7,10,13-hexadecatetraenoate; BOD4E: Butyl 6,9,12,15-octadecatetraenoate; BOD3E: Butyl 9,12,15-octadecatrienoate; BTES: But-3-enyl tridecyl ester of sebacic acid; RBGUL: Retinoyl-β-glucuronide 6′,3′-lactone; DPPP: Di-n-2-propylpentylphthalate.

distributed and minimized over the protein structure. The structure was then saved in PDBQT format.

Active Site Prediction and Grid Box Parameters

An active site is defined as a groove or pocket of an enzymatic or non-enzymatic protein which facilitates ligand binding or biochemical reactions (Pravda et al., 2014). The characteristics of the active site are mainly determined by the active site residues (Srinivasan, 2020), and various studies have characterized the possible active site residues of RBD of S_1 subunit of spike protein (**Figure 2**). Tyr449, Tyr453, Arg454, Lys458, Ser459, Ser469, Glu471, Phe486, Asn487, Tyr489, Leu492, Gln493, Gly496, Gln498, Thr500, Asn501, Gly502, and Tyr505 were the reported active site residues (Lan et al., 2020; Kulkarni et al., 2020; Prajapat et al., 2020). These residues were further validated using the 'Zone' function in UCSF Chimera software (https://www.cgl.ucsf.edu/chimera/). The zone parameter was set to "<5.0 Å from currently selected atoms" (Ashraf et al., 2014), where the currently selected atoms were the atoms of chain A. The mean of the X, Y, and Z coordinates of the final atom of each interacting

TABLE 2 | List of selected compounds identified from *Ui* extract with their two-dimensional chemical structures.

Compound	Structure	Compound	Structure
2,4-DtBP	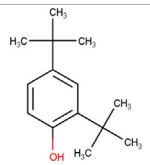	DPPP	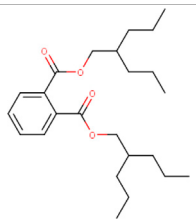
3-DOCH	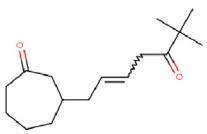	DTD	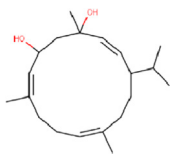
Azulene	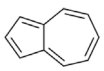	Furfural	
CMBA	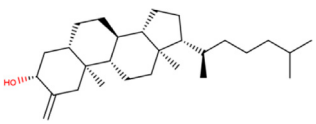	HIP	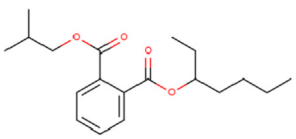
Cyclosativene	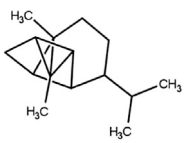	Icosapent	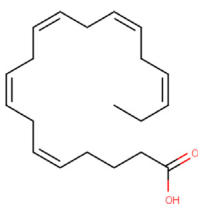
Damascone	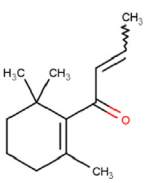	Oxymesterone	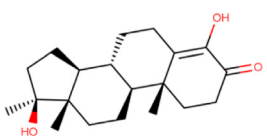

(Continued on following page)

TABLE 2 | (*Continued*) List of selected compounds identified from *Ui* extract with their two-dimensional chemical structures.

Compound	Structure	Compound	Structure
Dihydroactinolide	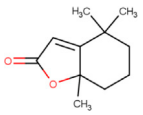	RBGUL	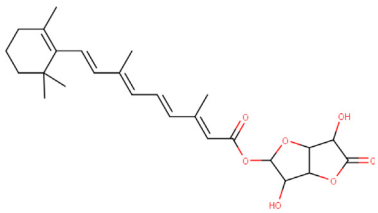
Doconexent	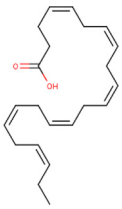	Retinal	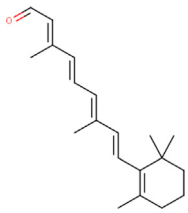

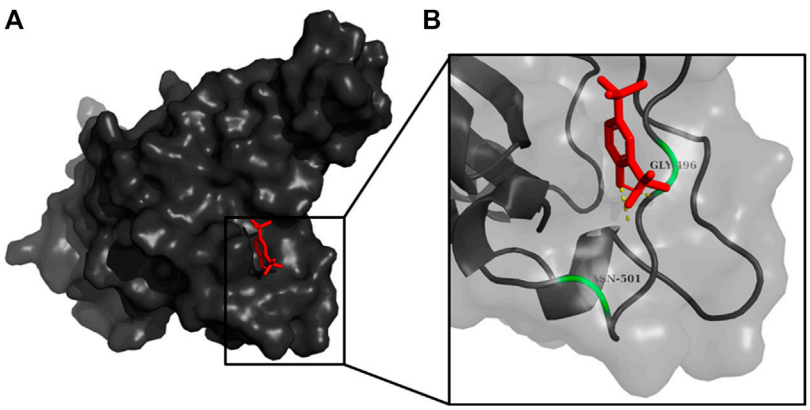

FIGURE 4 | (A) The binding pose of 2,4-DtBP (red) in RBD of S1 protein. **(B)** The hydrogen bonds (yellow) formed between 2,4-DtBP and the interacting residues, Gly496 and Asn501 are also shown.

residue highlighted by UCSF Chimera was calculated and applied as the dimension of the grid-box center. The grid size was manually adjusted to cover the interacting residues. Further, the values of these coordinates were saved as a configuration text file which was later used for docking.

Molecular Docking and Target-Ligand Visualization

Molecular docking is an *in silico* approach which is used to predict the conformational binding energy of ligands to a preferred target using matching and scoring algorithms (Leach et al., 2006). In this experiment, we have used AutoDockVina (Trott and Olson, 2010) in PyRx software as the docking tool, The optimal binding energy of the ligands was obtained based on least root mean square deviation (RMSD) for each conformers of a particular ligand, and arranged in ascending order to select the best ligand(s) for further calculating the chemical behaviour using C-DFT and pharmacokinetic analyses. PyMOL (https://pymol.org/), an open-source molecular visualization software was used to identify the polar contacts (H-bonds) between the ligand and the interacting active site residue, and develop printable figures of this interaction. To analyze hydrophobic interactions between the ligand and residues, another visualization software, BIOVIA Discovery Studio Client 2020 (https://discover.3ds.com/discovery-studio-visualizer-download) was used.

Conceptual DFT Analysis

Conceptual Density-functional theory (C-DFT) is a computational method to predict chemical behaviour of

TABLE 3 | | The binding affinities of selected phytochemicals from *Ui* extract on *SARS-CoV-2* spike RBD with the interacting amino acid residues contributing towards hydrogen bonds and hydrophobic interactions. The top five high scoring compounds have been highlighted (bold).

Compound	Binding affinity (kcal.mol^{-1})	Hydrogen bond interactions	Hydrophobic (pi) interactions
2,4-DtBP	**−5.3**	**Gly496, Asn501**	**Arg403, Tyr505**
3-DOCH	−5.3	–	Tyr505
Azulene	−5.1	–	Arg403, Tyr505
CMBA	−6.4	–	Tyr505
Cyclosativene	−5.3	–	–
Damascone	−5.2	–	Tyr505
Dihydroactinolide	-5.3	–	–
Doconexent	**−5.0**	**Gly496, Asn501**	**Arg403, Tyr495, Phe497, Tyr505**
DPPP	−4.8	Asn501	Tyr449, Tyr505
DTD	**−6.0**	**Gly496**	–
Furfural	−3.8	Arg454, Ser469, Glu471	Arg457, Lys458, Glu471
HIP	−5.2	–	Tyr505
Icosapent	−4.8	Gln498	Arg403, Tyr453, Tyr495, Phe497, Tyr505
Oxymesterone	−6.7	–	Tyr505
RBGUL	**−7.0**	**Gln493**	**Phe490**
Retinal	**−5.9**	**Thr500**	–

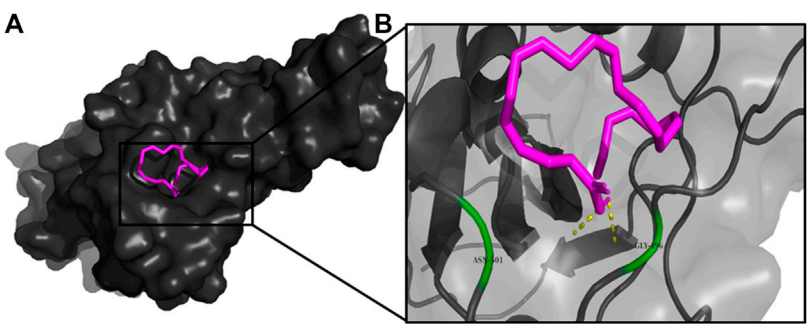

FIGURE 5 | (A) The binding pose of doconexent (magenta) in RBD of S1 protein. **(B)** The hydrogen bonds (yellow) formed between doconexent and the interacting residues, Gly496 and Asn501 are also shown.

the compounds (Poater et al., 2010; Domingo et al., 2016). Density-functional theory(DFT) has been developed from Hohenberg-Kohn theorem, which is an *in-silico* quantum mechanical modeling strategy used to determine the properties of a many-electron systems, using spatially-dependent electron density functionals (Hohenberg and Kohn, 1964; Kohn and Sham, 1965). C-DFT, a sub-field of DFT, helps to analyze the molecular orbital energies of conformers and can give rise to cues for understanding the structure-activity relationship of the molecule (Parr and Yang, 1989; Geerlings et al., 2003; Sarkar and Chattaraj, 2021a; Sarkar and Chattaraj, 2021b). To describe the orbital properties of a molecule, ten different molecular descriptors, known as the global reactivity descriptors and its derivatives, were considered *viz.* total energy (E_y; in eV), molecular dipole moment (D_p; in Debye units), the energy of the lowest unoccupied molecular orbit (LUMO) (E_{LUMO}; in eV), the energy of the highest occupied molecular orbit (HOMO) (E_{HOMO}; in eV), energy gap (ΔE; in eV), absolute hardness (η; in eV), global softness (σ; in eV^{-1}), electronegativity (χ), chemical potential (μ; in eV), and global electrophilicity index (ψ; in eV^{-1}) (Chattaraj et al., 2003; Chattaraj et al., 2006). These molecular descriptors are calculated based on the electron density of molecules using Fukui's molecular orbital theory (Fukui 1982; Ayers and Parr, 2000). E_{LUMO} and E_{HOMO} are the primary and the most important descriptors which determine the ability of a molecule to accept or donate electrons. D_p is the measure of the total polarity of a system. It is also a positive indicator of the reactivity of the molecule. It was found that the higher the

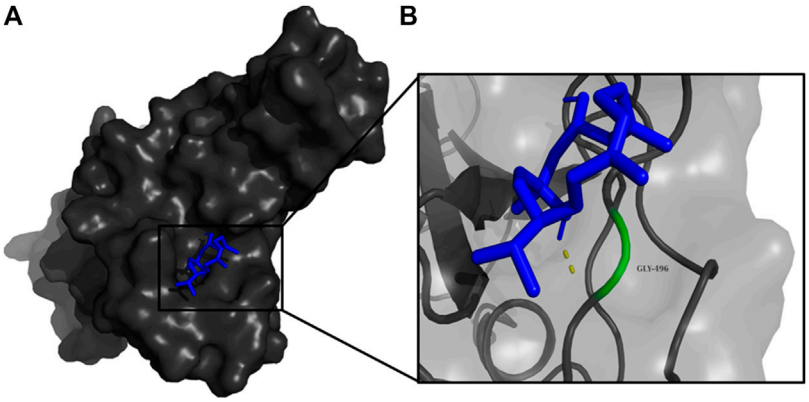

FIGURE 6 | (A) The binding pose of DTD (blue) in RBD of S1 protein. **(B)** The hydrogen bond (yellow) formed between DTD and the interacting residue, Gly496, is also shown.

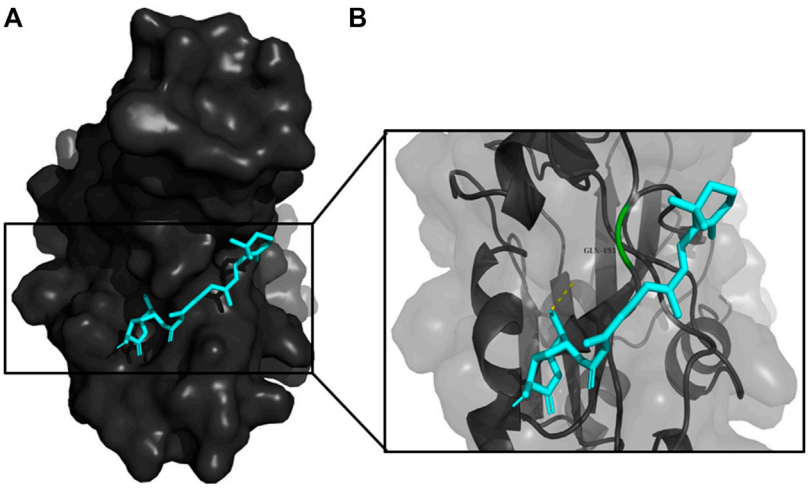

FIGURE 7 | (A) The binding pose of RBGUL (cyan) in RBD of S1 protein. **(B)** The hydrogen bond (yellow) formed between RBGUL and the interacting residue, Gly493, is also shown.

D_p, the greater the reactivity of the molecule (Roy et al., 2006; Mert et al., 2011). The derived descriptors of E_{LUMO} and E_{HOMO} are ΔE, η, σ, χ, μ, and ψ, which also account for the ability of the molecule to interact and contribute to electron sharing or transfer with the target by transiting from HOMO to LUMO. For example, if ΔE is found to be less, the molecule can easily transit from HOMO to LUMO (Chattaraj and Roy, 2007; Bostan et al., 2012). It represents the chemical reactivity and kinetic stability of the molecule; if χ is found to be less, the inhibitory effect of the ligand is higher (Zhan et al., 2003). As the first step in determining these descriptors, the selected ligands were optimized using the Becke-3-parameter, Lee-Yang-Parr (B3LYP) function (Becke 1988; Lee et al., 1988) with 6-311G(2d, p) basis set in Gaussian-16 software (http://gaussian.com/gaussian16/) (Frisch et al., 2016). B3LYP is the most popular functional used in molecular quantum mechanical modeling and is derived from a defined set of atomic/molecular energies and potentials.

Pharmacokinetic and Drug-Likeliness Analyses

The drug-likeliness and pharmacokinetic properties such as Absorption, Distribution, Metabolism, Excretion, and Toxicity (ADMET) of the selected ligands were predicted. The Drug Likeliness Tool (DruLiTo; http://www.niper.gov.in/pi_dev_tools/DruLiToWeb/DruLiTo_index.html), an open-source drug-likeness software developed by the Department of Pharmacoinformatics, National Institute of Pharmaceutical Education and Research (NIPER), Punjab, India was used to analyze drug likeliness by checking whether the ligands violate any of Lipinski's Rule of Five (RO5), or

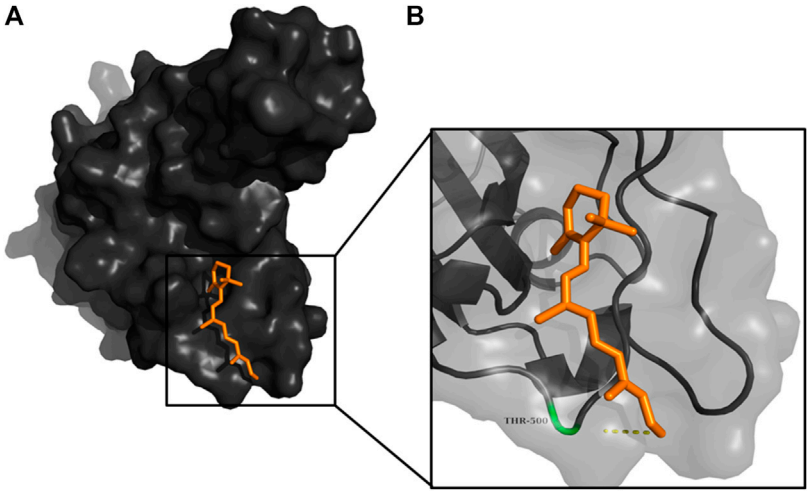

FIGURE 8 | (A) The binding pose of retinal (orange) in RBD of S1 protein. **(B)** The hydrogen bond (yellow) formed between retinal and the interacting residue, Thr500, is also shown.

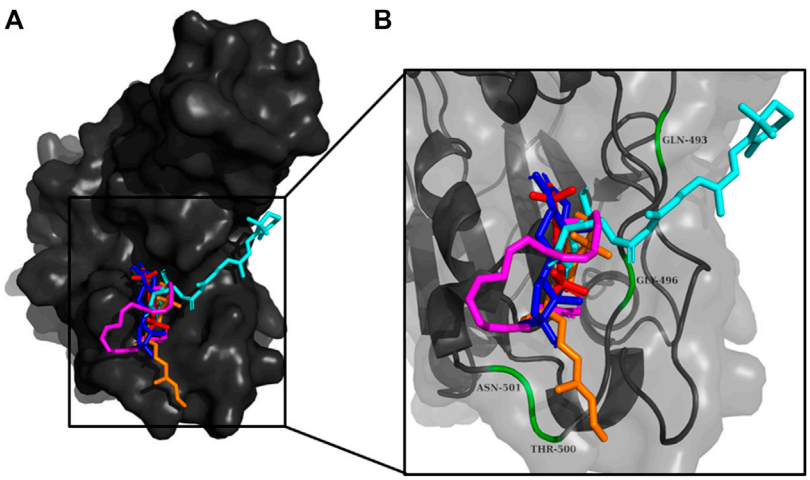

FIGURE 9 | (A) The binding poses of the selected compounds from U. intestinalisextract in one of the active binding pockets of RBD of S1 protein. **(B)** The pocket residues interacting with the compounds are highlighted in green.

would pass the Ghose and Veber filters. A reliable online tool for pharmacokinetic predictions of small molecules, pkCSM (http://biosig.unimelb.edu.au/pkcsm/), was used to predict the ADMET properties of the ligands (Pires et al., 2015), in which the canonical or isomeric SMILES of the ligands from Pub Chem were given as input.

RESULTS

Chemical Composition of Extract

The GC-MS data of the *Ui* ethanolic extract showed 55 peaks (**Figure 3**), and on comparison with NIST-14 library, 43 known phytochemicals were identified (**Table 1**). The phytochemical class analysis revealed that 18 phytochemicals were simple carboxylic acids, fatty acids, or their derivatives (palmitic acid, HIP, methylpalmitate, ethylpalmitate, butanoic acid, paullinic acid, doconexent, allyl stearate, ethyllinolelaidate, ethyllinolenate, ethylelaidate, icosapent, MHDTE, BOD4E, BOD3E, BTES, DPPP, and propyllinoleate), seven belonged to terpenoid class (damascene, cyclosativene, dihydroactinolide, 3-DOCH, phytol, CMBA, and oxymesterone), three (6.98%) each were aldehydes and its derivatives (methylglyoxal, furfural, and retinal), alcohols and its derivatives (TAA, 1-heptatriacotanol, and DTD), alkene hydrocarbons and its derivatives (cetene, 8-heptadecene, and 9-octadecene), and alkane hydrocarbons and its derivatives (myristyl chloride, TMHA, and EEBOD), two were monoglycerides (2-monopalmitin and 1-monolinolein), and one each were an organosulfur compound (DMSO), an aromatic hydrocarbon

TABLE 4 | | Statistics of the conceptual DFT-global reactivity descriptors and their derivatives of the best phytochemicals.

Compound	Total energy, $E_\gamma \times 10^3$(eV)	Dipole moment(Debye)	E_{LUMO}(eV)	E_{HOMO}(eV)	Energy gap (ΔE)	Absolute hardness(η)	Global softness(σ)	Electro negativity (χ)	Chemical potential (μ)	Electro philicity index (ψ)
2,4-DtBP	−16.92	1.32	0.16	−5.68	5.85	2.92	0.17	2.76	-2.76	1.30
Doconexent	−27.43	1.04	0.17	−6.32	6.49	3.24	0.15	3.08	-3.08	1.46
DTD	−25.39	2.64	−0.03	−6.11	6.09	3.04	0.16	3.07	-3.07	1.55
RBGUL	−41.84	3.61	−2.07	−5.27	3.20	1.60	0.31	3.67	-3.67	4.21
Retinal	−23.24	6.33	−2.30	−5.34	3.04	1.52	0.33	3.82	-3.82	4.80

(azulene), a phenol (2,4-DtBP), and a glycoside (RBGUL). The peak corresponding to HIP showed the highest signal abundance of $>2.8\times10^7$, however, the mean relative peak area of phytol (21.404%) was found to be the widest, followed by 2-monopalmitin, 9-octadecene, palmitic acid, and other compounds. The details of the GC-MS analysis such as peak number(s), retention time(s), and mean relative peak area are presented in **Table 1**.

Molecular Docking

Hydroxychloroquine, the control ligand, showed a binding affinity of $-5.7\ kcal.mol^{-1}$ with the optimized structure of RBD. Twenty-one (48.84%) compounds had binding energies ranging from $-4.0\ kcal.mol^{-1}$ to $-4.8\ kcal.mol^{-1}$. Out of the 43 compounds, only 16 were considered for studying their molecular interaction (**Tables 2, 3**). Interaction analysis revealed that furfural had three hydrogen bonds interacting with Arg454, Ser469, and Glu471, but its binding energy was $-3.8\ kcal\ mol^{-1}$. Considering hydrophobic interactions, icosapent interacted with Arg403, Tyr453, Tyr495, Phe497, and Tyr505. The binding energy of this molecule was $-4.8\ kcal.mol^{-1}$. Out of these 16 compounds, only the best five compounds (2,4-DtBP, doconexent, DTD, RBGUL, and retinal) were considered for C-DFT, drug-likeliness studies using DruLiTo, and ADMET properties using pkCSM. The criteria used for this selection was mainly their relative lower binding energy. The conformations were visualized using PyMOL software and depicted in **Figures 4–9**.

Estimated Descriptors of Conceptual DFT

The molecular descriptors were calculated after optimization, based on the FMO theory (**Table 4**). The total energy of the compounds is the total electron energy of the ground state. Lower the total energy, higher is their stability. RBGUL displayed the lowest total energy with value -41.84×10^3 eV. Molecular orbital energies such as HOMO energy (E_{HOMO}) and LUMO energy (E_{LUMO}) were calculated and analyzed (**Table 5**). Retinal showed the least energy gap with an energy difference of 3.04 eV. The energy gap of RBGUL (ΔE = 3.20 eV) was also found to be close enough to that of retinal. The maximum D_p was also shown by retinal (D_p = 6.33 Debye units). Considering derived descriptors, the most electronegative compound in the selected list was retinal (χ = 3.82). The electronegativity of RBGUL (χ = 3.67) was found to be highly similar to that of retinal. Absolute hardness and Global softness are criterions of overall stability of the system and also they are supporting parameters of electronegativity. In our study Retinal and RBGUL showed acceptable values of absolute hardness, 1.52 and 1.60 and softness, 0.33 and 0.31, respectively. Chemical potential of compounds is the negative value of electronegativity values, which is also an indication of high chemical activity. Therefore in this case too, retinal and RGBUL exhibited high chemical potential. High electrophilicity of retinal (4.80) and RBGUL (4.21) suggests their elevated likeliness to accept electrons. According to the above findings, RBGUL, and retinal were considered good inhibitors of S_1 RBD of *SARS-CoV-2*.

Prediction of Pharmacokinetic Properties and Drug-Likeliness

The drug-likeliness prediction from DruLiTo and ADMET results from pkCSM are presented in **Table 6**. Evaluation of drug-likeliness showed that 2,4-DtBP satisfied and passed through the Lipinski's RO5, Ghose, and Veber filters, whereas other ligands violated atleast one of the three parameters. Absorption properties revealed that all ligands were readily absorbed intestinally. 2,4-DtBP, doconexent, DTD, and retinal showed no interference with the P-glycoprotein system, however, RBGUL was found to be both a substrate and an inhibitor in the system. Skin permeability prediction showed that 2,4-DtBP was slightly permeable. Distribution properties showed that these compounds have tendencies to cross the blood-brain barrier (BBB) and central nervous system (CNS). Metabolic properties revealed that no ligand escaped the cytochrome P450 (CYP) system of the liver completely. Amongst the five selected ligands, DTD and RBGUL showed minimum interference with the system (acted as CYP2C19 inhibitor and CYP3A4 substrate, respectively). Considering excretion and toxicity properties, no ligand acted as renal OCT2 substrate, and human *ether-à-go-go*-related gene (*hERG*)-I protein inhibitors. The compounds passed the Ames toxicity test, indicating their inability to be a mutagen and thus a carcinogen. However, hepatotoxicity was predicted with doconexent, RBGUL, and retinal. Except for RBGUL, all other selected ligands showed skin sensitization too.

DISCUSSION

Medicine has started to change from completely "synthetic" to "semi-herbal" in the last couple of decades. Due to the lack of

TABLE 5 | Electron density maps of LUMO and HOMO of the top phytochemicals.

Compound	Optimized structure	LUMO	HOMO
2,4-DtBP	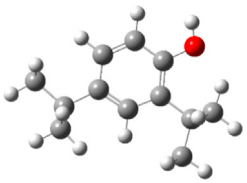	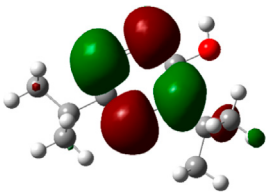	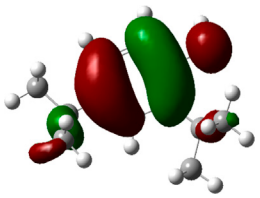
Doconexent	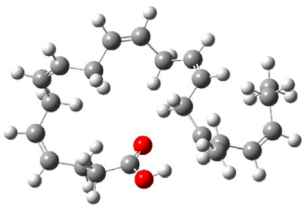	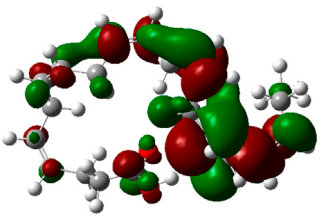	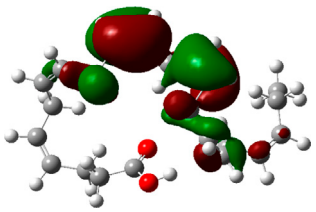
DTD	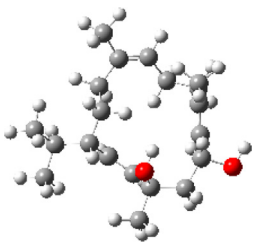	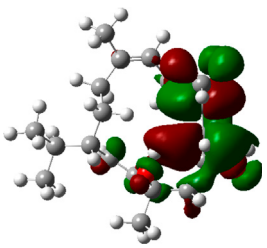	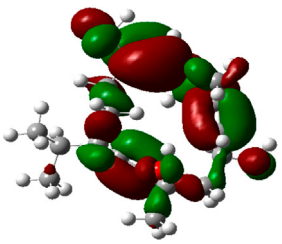
RBGUL	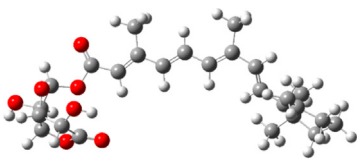	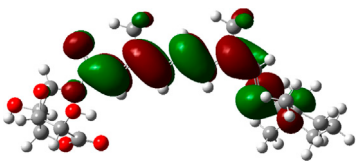	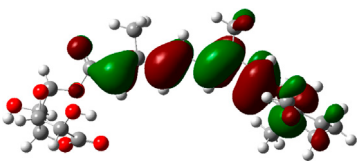
Retinal	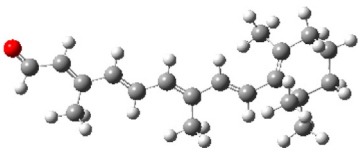	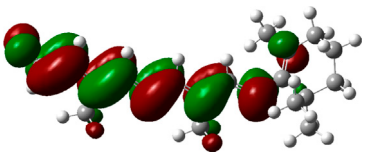	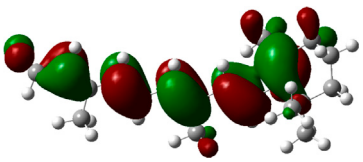

The red blobs represent the negative charge-dense regions and the green blobs represent the positive charge-dense regions of the molecule.

effective treatment and management strategies to treat COVID-19, alternative therapies are being explored. Conventional drug development process involves elaborate and time-consuming protocols, and they seldom produce drugs on demand. To increase the complexity, the causative agent, *SARS-CoV-2*, is a virus with high mutability and variable reproduction number (Rahman et al., 2020) that is slightly greater than its pathological cousins, *SARS-CoV* and *MERS-CoV* (Liu et al., 2020). Due to these facts, it is challenging to develop drugs against this virus presently. However, drugs could be developed against conserved regions of its genome or proteins encoded from these regions, such as spike glycoprotein or main protease, and intense research is being conducted world-wide, for the same. Drug repurposing is the most accepted strategy considered in this approach. Using *in silico* techniques, commercially available drugs are docked with a target protein, and the screened drug could be made available for

TABLE 6 | Molecular and ADMET properties of the selected ligands by DruLiTo and pkCSM online tool.

Property	2,4-DtBP	Doconexent	DTD	RBGUL	Retinal
Drug-likeliness					
Molecular mass (Da)	206.17	328.24	306.26	458.23	284.21
Log*P*	4.279	8.833	5.228	5.067	6.335
No. of H-bond acceptors	1	2	2	7	1
No. of H-bond donors	1	1	2	2	0
Atom molar refractivity	69.37	111.27	96.24	125.44	95.7
No. of atoms	37	56	56	67	49
TPSA (Å^2)	20.23	37.3	40.46	102.29	17.07
No. of rotatable bonds	2	14	1	7	5
Violation of Lipinski's Rule	No	Yes	Yes	Yes	Yes
Pass through Ghose Filter	Yes	No	Yes	Yes	No
Pass through Veber Filter	Yes	No	Yes	Yes	Yes
Absorption					
log*S* (log mol/L)	−3.924	−6.098	−4.709	−4.62	−6.888
Caco2 permeability (logP app in 10^{-6} cm/s)	1.666	1.145	1.636	0.759	1.53
Human intestinal absorption (% absorbed)	92.034	92.98	92.426	72.172	94.747
Log*Kp*	−2.301	−2.731	−2.779	−2.897	−2.491
P-glycoprotein substrate	No	No	No	Yes	No
P-glycoprotein-I inhibitor	No	No	No	Yes	No
P-glycoprotein-II inhibitor	No	No	No	Yes	No
Distribution					
Human VDss (log L/kg)	0.611	−0.709	0.11	0.017	0.506
Human fraction-unbound (Fu)	0.044	0.001	0.256	0.211	0.04
Log*BB*	0.478	−0.203	0.4	−0.088	0.664
Log*PS*	−0.848	−1.169	−2.865	−3.051	−1.863
Metabolism					
CYP2D6 substrate	No	No	No	No	No
CYP3A4 substrate	Yes	Yes	No	Yes	Yes
CYP1A2 inhibitor	Yes	Yes	No	No	Yes
CYP2C19 inhibitor	No	No	Yes	No	No
CYP2C9 inhibitor	No	No	No	No	No
CYP2D6 inhibitor	No	No	No	No	No
CYP3A4 inhibitor	No	No	No	No	No
Excretion					
Total clearance (log mL/min/kg)	0.759	2.264	1.376	0.861	1.563
Renal OCT2 substrate	No	No	No	No	No
Toxicity					
Ames toxicity	No	No	No	No	No
Human MRTD (log mg/kg/day)	0.42	−0.98	0.483	−0.142	−0.341
hERG-I protein inhibitor	No	No	No	No	No
hERG-II protein inhibitor	No	No	No	No	Yes
ORAT-LD50 (mol/kg)	2.351	1.459	1.673	1.913	1.564
ORCT-LOAEL (log mg/kg_bw/day)	1.696	3.208	2.002	2.579	1.065
Hepatotoxicity	No	Yes	No	Yes	Yes
Skin sensitization	Yes	Yes	Yes	No	Yes
*T. pyriformis*toxicity (log μg/L)	1.572	0.451	1.348	0.285	1.515
Minnow toxicity (log mM)	0.006	−1.765	0.528	0.373	−0.56

*log*P: Octanol-water partition coefficient; TPSA: Total polar surface area; log*S*: measure of water solubility; log*K*p: measure of skin permeability; VDss: volume of distribution; log*BB*: measure of BBB permeability; log*PS*: measure of CNS permeability; OCT2: organic cation transporter 2; ORAT-LD50: oral rat acute toxicity-lethal dose 50; ORCT-LOAEL: oral rat chronic toxicity-lowest dose causing observed adverse effects.

patients within a much shorter period because the clinical profile of the drug has been already established. Some drugs repurposed against *SARS-CoV-2* were Remdesivir, Favipiravir, Ribavirin, Lopinavir, Ritonavir, Darunavir, Tocilizumab, type I and type II interferons, chloroquine, hydroxychloroquine, arbidiol and statins (Singh et al., 2020). Though it is a fast-paced approach,

in vitro and *in vivo* studies are required to fully understand its mechanism in the human body, especially when the stakes of comorbid symptoms are high with this disease.

The undesirable side-effects of synthetic drugs has attracted researchers, and scientists towards developing plant-based medicines. Various compounds obtained fromt extracts of plants that belong to families such as *Lamiaceae*, *Fabaceae*, *Geraniaceae*, *Rosaceae*, *Asteraceae*, *Rutaceae* and *Malvaceae*have been reported to exhibit antiviral activity against *SARS-CoV-2* and certain other viruses too (Drevinskas et al., 2018; Denaro et al., 2020; Siddiqui et al., 2020). The top compounds identified as potent antivirals in our study have been previously reported to have exhibited a wide array of functions. 2,4-DtBP is a lipophilic phenol found mostly in higher plants. The phenol and its analogs were reported to have anti-oxidant, anti-inflammatory, anti-cancer, and anti-microbial properties. Considering their anti-viral activities, they reduced the growth of Coxsackievirus B-3 and Herpes Virus type-2 (Zhao et al., 2020). Our study revealed that 2,4-DtBP binds to S_1 RBD of *SARS-CoV-2* with a binding energy of -5.3 kcal.mol^{-1}, and interacted with Gly496 and Asn501 by hydrogen bonds and Arg403 and Tyr505, hydrophobically. Doconexent is a fatty acid which is rich in docosahexaenoic acid (DHA), is a compound with high anti inflammatory properties which is commercially produced from certain microalgae (Milledge, 2011). It has been repurposed to treat cancer and COVID-19 (Li et al., 2020; Singhal et al., 2020; Stanly et al., 2020). Retinal is a vitamin A aldehyde in the most absorbable form. Many studies have pointed the role of vitamins which include retinal, in managing COVID-19 (Michele et al., 2020; Morais et al., 2020; Gröber and Holick, 2021). DTD is a macrocyclicditerpene, primarily isolated from the Tobacco plant (*Nicotianatabacum*). It was found to be a major constituent in the oil extract from the aerial parts of Hercules' all-heal (*Opopanaxchironium*) (Maggio et al., 2013) and has a structural similarity with cembrene (Roberts and Rowland, 1962). Though DTD was not studied for its clinical properties, it was found that cembrenoid derivatives showed anti-cancer properties *in vitro* (Jassbi et al., 2017). With a binding affinity of -6.0 kcal.mol^{-1} against *SARS-CoV-2*, it proved to be a good inhibitor of the virus. RBGUL has similar properties to retinoic acid, and retinol. It was proposed to be a valuable therapeutic compound for the treatment of dermatological conditions and certain cancers, and also a dose-dependent teratogen (Barua, 1997). In our study, RBGUL was found to be the best inhibitor of *SARS-CoV-2*, compared to the other compounds with good binding affinity to the virus (-7.0 kcal.mol^{-1}).

In silico techniques occupy a prominent role in early drug discovery process. A quantitative computational study of the interaction between a particular protein target and a set of ligands, provides a fair idea as to which of the ligands may have an effect on the protein *in vitro*. Screening a large number of compounds against a particular target to narrow down the number of compounds to be tested *in vitro* is easily achievable by bioinformatics techniques. Molecular docking aids in assessing and visualizing the interactions between the ligands and protein. Similarly, the C-DFT study performed by calculating global molecular descriptors based on DFT provides a quantum level understanding of the ligands and helps to construct the relationship between their electronic properties and biological activity. It can also be used to understand the quantitative structure-activity relationship and perform pharmacophore modeling to design effective drugs out of the existing, according to the target. RBGUL and retinal show similar electron density in the orbitals except that the structures look inverted, suggesting that the inhibitory action of both compounds may be similar. They were also considered as highly active compounds as they showed low ΔE, which helps in an easy transition from HOMO to LUMO. Comparing the results of docking and C-DFT, the compounds with higher electronegativity showed better activity. Thus it can be comprehended that smaller ΔE, high D_p, and low electronegativity are essential for the inhibitory effect of a molecule. However, compared to RBGUL, retinal had more disadvantages based on the pharmacokinetic predictions. Besides RBGUL, 2,4-DtBP is also a potential candidate against RBD of *SARS-CoV-2*, considering its less adverse effects. That being said, the most recommended inhibitors against RBD would be 2,4-DtBP and RBGUL. More studies on these phytochemicals can reveal their efficacy, thus validating the results of this experiment.

CONCLUSION

Phytochemicals obtained from *Ui* extract were docked with the *SARS-CoV-2* RBD to ascertain if it exhibited antiviral activity, and also to screen for the compounds that are responsible for the activity. Through this study, we conclude that RBGUL, 2,4-DtBP and Retinal could be used as potent inhibitors against the RBD of coronavirus based on the molecular docking, C-DFT and ADMET studies. However, further studies involving *in vitro* and *in vivo* testing is essential to confirm the antiviral efficiency of the compounds against *SARS-CoV-2*.

DATA AVAILABILITY STATEMENT

The raw data supporting the conclusions of this article will be made available by the authors, without undue reservation.

AUTHOR CONTRIBUTIONS

TM and HS contributed to the conception, design, and data acquisition. SK and SB drafted the manuscript. SK, BC, and KB contributed to data analysis and have critically revised the manuscript. All authors have given final approval and have agreed to be accountable for all aspects of the work.

FUNDING

This study was supported by the Computational Biology Lab, funded by SERB Young Scientist grant (SB/YS/LS-128/2013). This work was supported by the National Research Foundation of Korea (NRF) grant funded by the Korean government (MSIT) (No. 2021R1F1A1062300). This study was also supported by a research fund from Chosun University, 2021. Authors also express gratitude to

StemOnc R and D Private Ltd. and Mr. M. Mahesh Kumar (Assistant Professor, Food and Process Engineering Department, SRMIST, Chennai) for helping through the compound extraction.

REFERENCES

Acharya, A., Agarwal, R., Baker, M. B., Baudry, J., Bhowmik, D., Boehm, S., et al. (2020). Supercomputer-Based Ensemble Docking Drug Discovery Pipeline with Application to COVID-19. *J. Chem. Inf. Model.* 60 (12), 5832–5852. doi:10.1021/acs.jcim.0c01010

Anand, A. V., Balamuralikrishnan, B., Kaviya, M., Bharathi, K., Parithathvi, A., Arun, M., et al. (2021). Medicinal Plants, Phytochemicals, and Herbs to Combat Viral Pathogens Including SARS-CoV-2. *Molecules* 26 (6), 1775. doi:10.3390/molecules26061775

Ashraf, Z., Saeed, A., and Nadeem, H. (2014). Design, Synthesis and Docking Studies of Some Novel Isocoumarin Analogues as Antimicrobial Agents. *RSC Adv.* 4 (96), 53842–53853. doi:10.1039/C4RA07223E

Awoonor-Williams, E., and Abu-Saleh, A. (2021). Covalent and Non-Covalent Binding Free Energy Calculations for Peptidomimetic Inhibitors of SARS-CoV-2 Main Protease. *Phys. Chem. Chem. Phys.* 23 (11), 6746–6757. doi:10.1039/d1cp00266j

Ayers, P. W., and Parr, R. G. (2000). Variational Principles for Describing Chemical Reactions: The Fukui Function and Chemical Hardness Revisited. *J. Am. Chem. Soc.* 122 (9), 2010–2018. doi:10.1021/ja9924039

Barua, A. B. (1997). Retinoyl β-glucuronide: A Biologically Active Form of Vitamin A. *Nutr. Rev.* 55 (7), 259–267. doi:10.1111/j.1753-4887.1997.tb01615.x

Becke, A. D. (1988). Density-Functional Exchange-Energy Approximation with Correct Asymptotic Behavior. *Phys. Rev. A. Gen. Phys.* 38 (6), 3098. doi:10.1103/PhysRevA.38.3098

Bette, K., Will, M. F., Sandrasegaram, G., Hyejin, Y., and James, T. (2021). Tracking Changes in SARS-CoV-2 Spike : Evidence that D614G Increase Infectivity of the COVID-19 Virus. *Cell* 182 (4), 812–827. doi:10.1016/j.cell.2020.06.043

Bostan, R., Varvara, S., Găină, L., and Mureşan, L. M. (2012). Evaluation of Some Phenothiazine Derivatives as Corrosion Inhibitors for Bronze in Weakly Acidic Solution. *Corrosion Sci.* 63, 275–286. doi:10.1016/j.corsci.2012.06.010

Chattaraj, P. K., Maiti, B., and Sarkar, U. (2003). Philicity: a Unified Treatment of Chemical Reactivity and Selectivity. *The J. Phys. Chem. A* 107 (25), 4973–4975. doi:10.1021/jp034707u

Chattaraj, P. K., and Roy, D. R. (2007). Update 1 of: Electrophilicity Index. *Chem. Rev.* 107 (9), PR46–PR74. doi:10.1021/cr078014b

Chattaraj, P. K., Sarkar, U., Roy, D. R., Elango, M., Parthasarathi, R., and Subramanian, V. (2006). Is Electrophilicity a Kinetic or a Thermodynamic Concept? *Indian J. Chem.* 45, 1099–1112.

Dallakyan, S., and Olson, A. J. (2015). "Small-Molecule Library Screening by Docking with PyRx," in *Chemical Biology* (New York, NY: Humana Press), 243–250. doi:10.1007/978-1-4939-2269-7_19

Denaro, M., Smeriglio, A., Barreca, D., De Francesco, C., Occhiuto, C., Milano, G., et al. (2020). Antiviral Activity of Plants and Their Isolated Bioactive Compounds: An Update. *Phytotherapy Res.* 34 (4), 742–768. doi:10.1002/ptr.6575

Domingo, L. R., Ríos-Gutiérrez, M., and Pérez, P. (2016). Applications of the Conceptual Density Functional Theory Indices to Organic Chemistry Reactivity. *Molecules* 21 (6), 748. doi:10.3390/molecules21060748

Drevinskas, T., Mickienė, R., Maruška, A., Stankevičius, M., Tiso, N., Šalomskas, A., et al. (2018). Confirmation of the Antiviral Properties of Medicinal Plants via Chemical Analysis, Machine Learning Methods and Antiviral Tests: A Methodological Approach. *Anal. Methods* 10 (16), 1875–1885. doi:10.1039/C8AY00318A

FDA (2020). FDA Cautions against Use of Hydroxychloroquine or Chloroquine for COVID-19 outside of the Hospital Setting or a Clinical Trial Due to Risk of Heart Rhythm Problems. Available at: https://www.fda.gov/drugs/drug-safety-and-availability/fda-cautions-against-use-hydroxychloroquine-or-chloroquine-covid-19-outside-hospital-setting-or (Accessed November 23, 2020).

Frisch, M., Trucks, G., Schlegel, H., Scuseria, G., Robb, M., Cheeseman, J., et al. (2016). *Gaussian 16*. (Version Revision B. 01)[Linux]. Wallingford CT: Gaussian.

Fukui, K. (1982). The Role of Frontier Orbitals in Chemical Reactions (Nobel Lecture). *Angew. Chem. Int. Edition English* 21 (11), 801–809. doi:10.1002/anie.198208013

Ge, H., Wang, X., Yuan, X., Xiao, G., Wang, C., Deng, T., et al. (2020). The Epidemiology and Clinical Information about COVID-19. *Eur. J. Clin. Microbiol. Infect. Dis.* 39 (6), 1011–1019. doi:10.1007/s10096-020-03874-z

Geerlings, P., DeProft, F., and Langenaeker, W. (2003). Conceptual Density Functional Theory. *Chem. Rev.* 103 (5), 1793–1874. doi:10.1021/cr990029p

Gröber, U., and Holick, M. F. (2021). The Coronavirus Disease (COVID-19)A Supportive Approach with Selected Micronutrients. *Int. J. Vitamin Nutr. Res.*, 1–12. doi:10.1024/0300-9831/a000693

Hohenberg, P., and Kohn, W. (1964). Density Functional Theory (DFT). *W.J.P.R. Phys. Rev.* 136, B864. doi:10.1103/physrev.136.b864

Jassbi, A. R., Vafapour, M., Shokrollahi, A., Firuzi, O., Zare, M., Chandran, J. N., et al. (2017). Cytotoxic Activity of Two Cembranoidditerpenes from Nicotianasylvestris against Three Human Cancer Cell Lines. *Open Bioactive Compd. J.* 5 (1), 1–8. doi:10.2174/1874847301705010001

Klongklaew, N., Praiboon, J., Tamtin, M., and Srisapoome, P. (2020). Antibacterial and Antiviral Activities of Local Thai green Macroalgae Crude Extracts in pacific white Shrimp (Litopenaeusvannamei). *Mar. Drugs* 18 (3), 140. doi:10.3390/md18030140

Kohn, W., and Sham, L. J. (1965). Self-consistent Equations Including Exchange and Correlation Effects. *Phys. Rev.* 140 (4A), A1133. doi:10.110310.1103/physrev.140.a1133

Kulkarni, S. A., Nagarajan, S. K., Ramesh, V., Palaniyandi, V., Selvam, S. P., and Madhavan, T. (2020). Computational Evaluation of Major Components from Plant Essential Oils as Potent Inhibitors of SARS-CoV-2 Spike Protein. *J. Mol. Struct.* 1221, 128823. doi:10.1016/j.molstruc.2020.128823

Lan, J., Ge, J., Yu, J., Shan, S., Zhou, H., Fan, S., et al. (2020). Structure of the SARS-CoV-2 Spike Receptor-Binding Domain Bound to the ACE2 Receptor. *Nature* 581 (7807), 215–220. doi:10.1038/s41586-020-2180-5

Leach, A. R., Shoichet, B. K., and Peishoff, C. E. (2006). Prediction of Protein–Ligand Interactions. Docking and Scoring: Successes and Gaps. *J. Med. Chem.* 49 (20), 5851–5855. doi:10.1021/jm060999m

Lee, C., Yang, W., and Parr, R. G. (1988). Development of the Colle-Salvetti Correlation-Energy Formula into a Functional of the Electron Density. *Phys. Rev. B Condens Matter* 37 (2), 785. doi:10.1103/PhysRevB.37.785

Li, W., Moore, M. J., Vasilieva, N., Sui, J., Wong, S. K., Berne, M. A., et al. (2003). Angiotensin-Converting Enzyme 2 Is a Functional Receptor for the SARS Coronavirus. *Nature* 426, 450–454. doi:10.1038/nature02145

Liu, Y., Gayle, A. A., Wilder-Smith, A., and Rocklöv, J. (2020). The Reproductive Number of COVID-19 Is Higher Compared to SARS Coronavirus. *J. Trav. Med.* 27 (2), taaa021. doi:10.1093/jtm/taaa021

Lu, R., Zhao, X., Li, J., Niu, P., Yang, B., Wu, H., et al. (2020). Genomic Characterisation and Epidemiology of 2019 Novel Coronavirus: Implications for Virus Origins and Receptor Binding. *The lancet* 395 (10224), 565–574. doi:10.1016/S0140-6736(20)30251-8

Maggio, A., Bruno, M., Formisano, C., Rigano, D., and Senatore, F. (2013). Chemical Composition of the Essential Oils of Three Species of Apiaceae Growing Wild in Sicily: Bonanniagraeca, Eryngiummaritimum and Opopanaxchironium. *Nat. Product. Commun.* 8 (6), 1934578X1300800640. doi:10.1177/1934578X1300800640

Mert, B. D., Mert, M. E., Kardaş, G., and Yazıcı, B. (2011). Experimental and Theoretical Investigation of 3-amino-1, 2, 4-Triazole-5-Thiol as a Corrosion Inhibitor for Carbon Steel in HCl Medium. *Corrosion Sci.* 53 (12), 4265–4272. doi:10.1016/j.corsci.2011.08.038

Michele, C. A., Angel, B., Valeria, L., Teresa, M., Giuseppe, C., Giovanni, M., et al. (2020). Vitamin Supplements in the Era of SARS-Cov2 Pandemic. *GSC Biol. Pharm. Sci.* 11 (2), 007–019. doi:10.30574/gscbps.2020.11.2.0114

Milledge, J. J. (2011). Commercial Application of Microalgae Other Than as Biofuels: A Brief Review. *Rev. Environ. Sci. Bio/Technology* 10 (1), 31–41. doi:10.1007/s11157-010-9214-7

Morais, A. H., Passos, T. S., Maciel, B. L., and da Silva-Maia, J. K. (2020). Can Probiotics and Diet Promote Beneficial Immune Modulation and Purine Control in Coronavirus Infection? *Nutrients* 12 (6), 1737. doi:10.3390/nu12061737

Morán-Santibañez, K., Cruz-Suárez, L. E., Ricque-Marie, D., Robledo, D., Freile-Pelegrín, Y., Peña-Hernández, M. A., et al. (2016). Synergistic Effects of Sulfated Polysaccharides from Mexican Seaweeds against Measles Virus. *Biomed. Research International* 2016. doi:10.1155/2016/8502123

Parr, R. G., and Yang, W. (1989). *Density-functional Theory of Atoms and Molecules*. New York: Oxford University Press. doi:10.1007/978-94-009-9027-2_2

Pavlova, A., Lynch, D. L., Daidone, I., Zanetti-Polzi, L., Smith, M. D., Chipot, C., et al. (2021). Inhibitor Binding Influences the Protonation States of Histidines in SARS-CoV-2 Main Protease. *Chem. Sci.* 12 (4), 1513–1527. doi:10.1039/D0SC04942E

Pires, D. E., Blundell, T. L., and Ascher, D. B. (2015). pkCSM: Predicting Small-Molecule Pharmacokinetic and Toxicity Properties Using Graph-Based Signatures. *J. Med. Chem.* 58 (9), 4066–4072. doi:10.1021/acs.jmedchem.5b00104

Poater, A. (2020). Michael Acceptors Tuned by the Pivotal Aromaticity of Histidine to Block COVID-19 Activity. *J. Phys. Chem. Lett.* 11 (15), 6262–6265. doi:10.1021/acs.jpclett.0c01828

Poater, A., Saliner, A. G., Solà, M., Cavallo, L., and Worth, A. P. (2010). Computational Methods to Predict the Reactivity of Nanoparticles through Structure–Property Relationships. *Expert Opin. Drug Deliv.* 7 (3), 295–305. doi:10.1517/17425240903508756

Prajapat, M., Shekhar, N., Sarma, P., Avti, P., Singh, S., Kaur, H., et al. (2020). Virtual Screening and Molecular Dynamics Study of Approved Drugs as Inhibitors of Spike Protein S1 Domain and ACE2 Interaction in SARS-CoV-2. *J. Mol. Graphics Model.* 101, 107716. doi:10.1016/j.jmgm.2020.107716

Pravda, L., Berka, K., Vařeková, R. S., Sehnal, D., Banáš, P., Laskowski, R. A., et al. (2014). Anatomy of Enzyme Channels. *BMC bioinformatics* 15 (1), 1–8. doi:10.1186/s12859-014-0379-x

Rahman, B., Sadraddin, E., and Porreca, A. (2020). The Basic Reproduction Number of SARS CoV2 in Wuhan is About to die out, How About the Rest of the World?. *Rev. Med. Virol.* 30 (4), e2111. doi:10.1002/rmv.2111

Ramos-Guzmán, C. A., Ruiz-Pernía, J. J., and Tuñón, I. (2021). A Microscopic Description of SARS-CoV-2 Main Protease Inhibition with Michael Acceptors. Strategies for Improving Inhibitor Design. *Chem. Sci.* 12 (10), 3489–3496. doi:10.1039/D0SC04978F

Raudah, L., Donghyuk, S., and Sun, C. (2020). Advances in Molecular Dynamics Simulations and Enhanced Sampling Methods for the Study of Protein Systems. *Int. J. Mol. Sci.* 21 (17), 6339. doi:10.3390/ijms21176339

Roberts, D. L., and Rowland, R. L. (1962). MacrocyclicDiterpenes. α-and β-4, 8, 13-Duvatriene-1, 3-diols from Tobacco. *J. Org. Chem.* 27 (11), 3989–3995. doi:10.1021/jo01058a056

Roy, D. R., Parthasarathi, R., Padmanabhan, J., Sarkar, U., Subramanian, V., and Chattaraj, P. K. (2006). Careful Scrutiny of the Philicity Concept. *J. Phys. Chem. A* 110 (3), 1084–1093. doi:10.1021/jp053641v

Sarkar, U., and Chattaraj, P. K. (2021a). Conceptual DFT Based Electronic Structure Principles in a Dynamical Context. *J. Indian Chem. Soc.* 98 (7), 100098. doi:10.1039/D0SC07017C10.1016/j.jics.2021.100098

Sarkar, U., and Chattaraj, P. K. (2021b). Reactivity Dynamics. *J. Phys. Chem. A* 125 (10), 2051–2060. doi:10.1021/acs.jpca.0c10788

Siddiqui, A. J., Danciu, C., Ashraf, S. A., Moin, A., Singh, R., Alreshidi, M., et al. (2020). Plants-Derived Biomolecules as Potent Antiviralphytomedicines: New Insights on Ethnobotanical Evidences against Coronaviruses. *Plants* 9 (9), 1244. doi:10.3390/plants9091244

Singh, T. U., Parida, S., Lingaraju, M. C., Kesavan, M., Kumar, D., and Singh, R. K. (2020). Drug Repurposing Approach to Fight COVID-19. *Pharmacol. Rep.* 72 (6), 1479–1508. doi:10.1007/s43440-020-00155-6

Singhal, T., Chansoria, A., and Kothari, S. (2020). Evaluation of Anti-Inflammatory Activity of Docosahexanoic Acid on Carrageenan Induced Paw Oedema in Rats. *Int. J. Basic Clin. Pharmacol.* 9 (5), 718–721. doi:10.18203/2319-2003.ijbcp20201745

Srinivasan, B. (2020). Words of Advice: Teaching Enzyme Kinetics. *FEBS J.* 288, 2068–2083. doi:10.1111/febs.15537

Stanly, C., Alfieri, M., Ambrosone, A., Leone, A., Fiume, I., and Pocsfalvi, G. (2020). Grapefruit-Derived Micro and Nanovesicles Show Distinct Metabolome Profiles and Anticancer Activities in the A375 Human Melanoma Cell Line. *Cells* 9 (12), 2722. doi:10.3390/cells9122722

Trott, O., and Olson, A. J. (2010). AutoDockVina: Improving the Speed and Accuracy of Docking with a New Scoring Function, Efficient Optimization, and Multithreading. *J. Comput. Chem.* 31 (2), 455–461. doi:10.1002/jcc.21334

Walls, A. C., Park, Y. J., Tortorici, M. A., Wall, A., McGuire, A. T., and Veesler, D. (2020). Structure, Function, and Antigenicity of the SARS-CoV-2 Spike Glycoprotein. *Cell* 181 (2), 281–292. doi:10.1016/j.cell.2020.02.058

Yi, C., Sun, X., Ye, J., Ding, L., Liu, M., Yang, Z., et al. (2020). Key Residues of the Receptor Binding Motif in the Spike Protein of SARS-CoV-2 that Interact with ACE2 and Neutralizing Antibodies. *Cell Mol. Immunol.* 17 (6), 621–630. doi:10.1038/s41423-020-0458-z

Yokoyama, K., and Ichiki, A. (2021). Nano-Size Dependence in the Adsorption by the SARS-CoV-2 Spike Protein Over Gold Colloid. *Colloids Surf. A: Physicochemical Eng. Aspects* 615, 126275. doi:10.1016/j.colsurfa.2021.126275

Zanetti-Polzi, L., Smith, M. D., Chipot, C., Gumbart, J. C., Lynch, D. L., Pavlova, A., et al. (2021). Tuning Proton Transfer Thermodynamics in SARS-Cov-2 Main Protease: Implications for Catalysis and Inhibitor Design. *J. Phys. Chem. Lett.* 12 (17), 4195–4202. doi:10.1021/acs.jpclett.1c00425

Zhan, C. G., Nichols, J. A., and Dixon, D. A. (2003). Ionization Potential, Electron Affinity, Electronegativity, Hardness, and Electron Excitation Energy: Molecular Properties from Density Functional Theory Orbital Energies. *J. Phys. Chem. A* 107 (20), 4184–4195. doi:10.1021/jp0225774

Zhao, F., Wang, P., Lucardi, R. D., Su, Z., and Li, S. (2020). Natural Sources and Bioactivities of 2, 4-Di-Tert-Butylphenol and its Analogs. *Toxins* 12 (1), 35. doi:10.3390/toxins12010035

Zhou, P., Xing-Lou, Y., Xian-Guang, W., Hu, B., Zhang, L., Zhang, W., et al. (2020). A Pneumonia Outbreak Associated with a New Coronavirus of Probable Bat Origin. *Nature* 579, 270–273. doi:10.1038/s41586-020-2012-7

Conflict of Interest: The authors declare that the research was conducted in the absence of any commercial or financial relationships that could be construed as a potential conflict of interest.

Publisher's Note: All claims expressed in this article are solely those of the authors and do not necessarily represent those of their affiliated organizations, or those of the publisher, the editors and the reviewers. Any product that may be evaluated in this article, or claim that may be made by its manufacturer, is not guaranteed or endorsed by the publisher.

frontiers in Chemistry

ORIGINAL RESEARCH
published: 08 October 2021
doi: 10.3389/fchem.2021.744376

Inhibition Potencies of Phytochemicals Derived from Sesame Against SARS-CoV-2 Main Protease: A Molecular Docking and Simulation Study

Anuj Kumar[1], *Dwijesh Chandra Mishra*[1], *Ulavappa Basavanneppa Angadi*[1]*, *Rashmi Yadav*[2], *Anil Rai*[1] *and Dinesh Kumar*[1]

[1]*Centre for Agricultural Bioinformatics (CABin), ICAR- Indian Agricultural Statistics Research Institute, New Delhi, India,* [2]*Division of Germplasm Evaluation, ICAR-National Bureau of Plant Genetic Resources, New Delhi, India*

The ongoing COVID-19 pandemic, caused by SARS-CoV-2, has now spread across the nations with high mortality rates and multifaceted impact on human life. The proper treatment methods to overcome this contagious disease are still limited. The main protease enzyme (M^{pro}, also called $3CL^{pro}$) is essential for viral replication and has been considered as one of the potent drug targets for treating COVID-19. In this study, virtual screening was performed to find out the molecular interactions between 36 natural compounds derived from sesame and the M^{pro} of COVID-19. Four natural metabolites, namely, sesamin, sesaminol, sesamolin, and sesamolinol have been ranked as the top interacting molecules to M^{pro} based on the affinity of molecular docking. Moreover, stability of these four sesame-specific natural compounds has also been evaluated using molecular dynamics (MD) simulations for 200 nanoseconds. The molecular dynamics simulations and free energy calculations revealed that these compounds have stable and favorable energies, causing strong binding with M^{pro}. These screened natural metabolites also meet the essential conditions for drug likeness such as absorption, distribution, metabolism, and excretion (ADME) properties as well as Lipinski's rule of five. Our finding suggests that these screened natural compounds may be evolved as promising therapeutics against COVID-19.

Keywords: COVID-19, main protease, sesame, natural compounds, molecular docking, molecular dynamics simulations, therapeutics

OPEN ACCESS

Edited by:
Sugunadevi Sakkiah, National Center for Toxicological Research (FDA), United States

Reviewed by:
Subhash Chandra, Kumaun University, India
Md Tabish Rehman, King Saud University, Saudi Arabia

***Correspondence:**
Ulavappa Basavanneppa Angadi
ub.angadi@icar.gov.in

Specialty section:
This article was submitted to Theoretical and Computational Chemistry, a section of the journal Frontiers in Chemistry

Received: *20 July 2021*
Accepted: *06 September 2021*
Published: *08 October 2021*

Citation:
Kumar A, Mishra DC, Angadi UB, Yadav R, Rai A and Kumar D (2021) Inhibition Potencies of Phytochemicals Derived from Sesame Against SARS-CoV-2 Main Protease: A Molecular Docking and Simulation Study. Front. Chem. 9:744376. doi: 10.3389/fchem.2021.744376

INTRODUCTION

The ongoing pandemic eruption due to the worldwide spread of coronavirus disease (COVID-19) is caused by the novel virus strain severe acute respiratory syndrome coronavirus-2 (SARS-CoV-2; previously named 2019-nCoV) (Wu et al., 2020b). This viral disease is an unprecedented global public health care threat (Jamwal et al., 2020). The first case of COVID-19 disease was originated from Wuhan, Hubei Province, China, and quickly spread across 219 countries and territories around the world with high mortality rates in immunocompromised patients (Enayatkhani et al., 2020; Mackenzie and Smith, 2020; Xu et al., 2020). Based on the recommendations of the Emergency

Committee, the World Health Organization (WHO) has declared this respiratory infectious disease as a Public Health Emergency of International Concern (PHEIC) on 30 January, 2020 and a pandemic on 11 March, 2020 (Shi et al., 2020; Yu et al., 2020). As on 10 July 2021, this contagious disease had led to more than 185,291,530 confirmed cases and 4,010,834 fatalities (https://covid19.who.int/), with the number of cases increasing abruptly across the globe. At present, India is fighting hard against the second wave of COVID-19. The ongoing pandemic has now initiated taking a toll on India's economy. A large population of India is facing disproportionately higher rates of COVID-19 infection, morbidity, and mortality. As of 10 July 2021, the total COVID-19 caseload has now soared to 30,752,950 with 405,939 deaths (https://covid19.who.int/table). India is the most severely affected Asian country. The ongoing pandemic has been considered more dreadful than the previous global outbreaks, namely, SARS-CoV (2002–2003) and Middle East respiratory syndrome (MERS) (2012–present) (de Wit et al., 2016; Gupta et al., 2020; Wang et al., 2020b; Wu and McGoogan, 2020; Yuan et al., 2020). Based on previous investigations, the fatality rate of SARS-CoV and MERS has been calculated as 10 and 35%, respectively (Lee et al., 2004; Cheng et al., 2007). It has been well-reported that COVID-19 affects the lower respiratory tract of the body, which causes pneumonia and affects the gastrointestinal system, kidney, heart, and central nervous system. Fever, cough, diarrhea, and tiredness have been considered the most common symptoms (Chen et al., 2020a; Tang et al., 2020), while aches and pains, sore throat, conjunctivitis, headache, loss of taste or smell, a rash on skin, or discoloration of fingers or toes are the less common symptoms of this infectious disease (Backer et al., 2020; Rothe et al., 2020; Russell et al., 2020; Verdoni et al., 2020; Yu and Yu, 2020).

The coronaviruses have been recognized as a large enveloped positive-sense single-strand RNA viruses from Nidovirales (order) of the Coronaviridae family and subfamily Coronavirinae (Raj et al., 2021; Shamsi et al., 2021). This subfamily is classified into four genera including *alpha-*, *beta-*, *gamma-*, and *deltacoronavirus* (*α-*, *β-*, *γ-*, and *δ-CoV*) based on evolutionary methods (Hulswit et al., 2016). In view of previous reports, coronaviruses have been considered as highly evolving viruses, with a high rate of mutation and genomic recombination (Chen et al., 2020b). In the past, six species of human coronavirus associated with different respiratory tract diseases have been reported, which include HCoV-NL63, HCoV-229E, HCoV-OC34, HCoV-HKU1, SARS-CoV, and MERS-CoV (Arden et al., 2005; Woo et al., 2005; Su et al., 2016). The novel strain SARS-CoV-2 has been characterized as the seventh strain of the human coronavirus. Based on the significant nucleotide sequence similarity with SARS and MERS coronaviruses, the International Committee on Taxonomy of Viruses (ICTV) coined the nomenclature of SARS-COV-2 (Hasan et al., 2020). The ICTV taxonomically placed the SARS-COV-2 in the genus *Betacoronavirus* (Helmy et al., 2020; Wang et al., 2020b).

The genome size of SARS-CoV-2 is ~29.9 kb (29,903 nucleotides) (Wu et al., 2020a). The first whole-genome sequencing data for SARS-CoV-2 (~30 kb) were submitted to the Genbank with the accession number MN908947 and isolated from Wuhan (Wu et al., 2020a). The genome of SARS-CoV-2 encodes approximately 13–15 open reading frames (ORFs) which are flanked by 5′ and 3′ UTRs (Chen et al., 2020b; Elfiky and Azzam, 2020; Gordon et al., 2020). These ORFs constitute a replicase assembly during the replication process of the central dogma of molecular biology and encode 27 distinct structural and non-structural proteins (NSPs) (Liu et al., 2021; Shamsi et al., 2021). The 5′ end of the SARS-CoV-2 genome encodes 16 NSPs (Nsp1-16) and constitutes the replicase/transcriptase complex (RTC). These 16 proteins are conserved in all SARS viruses and play a critical role in a set of biological processes such as viral replication, assembly, and immune response modulation (Shamsi et al., 2021). The 3′ end of the viral genome encodes four conical structural proteins including E (envelope protein), M (membrane protein), N (nucleocapsid protein), and S (spike protein), and nine putative accessory factors. The main protease enzyme (M^{pro} also called $3CL^{pro}$) is essential for viral replication and has been considered as one of the potent drug targets for treating COVID-19 (Joshi et al., 2020; Khan et al., 2020; Kumar et al., 2020; Pant et al., 2020; Wu et al., 2020a; Zhang et al., 2020). In cooperation with other components, this important enzyme also helps in the transcription of the viral RNA. M^{pro} is a key enzyme that exclusively cleaves the polyproteins (pp1a and pp1ab) which is essential for the assembly of virus drugs (Jin et al., 2020). The molecular mass of M^{pro} is 33,797 Da with length of 306 amino acid residues and structurally possesses the three functional domains, namely, domain I (8–101 residues), domain II (102–184 residues), and domain III (201–306 residues) (Jin et al., 2020; Khan et al., 2020). Among them, domains I and II have an antiparallel β-barrel structure, while domain III represents a group of five α-helices organized as a large antiparallel cluster. Domain III is connected to domain II by a 15-residue-long loop region (185–200 residues). The active site is composed of a catalytic dyad having Cys145 and His41 residues (Khan et al., 2020). The functional role of M^{pro} in the viral replication highlights its importance that can be used to identify the potential drug therapeutics against COVID-19 (Ullrich and Nitsche, 2020). Solved crystal structures of M^{pro} provide a platform to develop and design the antiviral drugs to combat COVID-19 (Jin et al., 2020; Zhang et al., 2020). In response to the COVID-19 outbreak, several studies have been performed using integrated bioinformatics and molecular modeling approaches for the screening of novel natural metabolites as potential drug targets against M^{pro} (Chikhale et al., 2020a; Kumar et al., 2020; Maurya and Sharma, 2020; Rout et al., 2020; Tripathi et al., 2020; Mishra et al., 2021; Romeo et al., 2021; Tock et al., 2021). But no effective method has been developed yet to prevent and treat the COVID-19 disease in a significant manner. In addition to the aforementioned approaches, several other viral protease inhibitors like remdesivir, hydroxychloroquine, chloroquine, lopinavir, ritonavir, oseltamivir, and fapilavir have been explored as repurposed drugs for COVID-19 treatment (Chang et al., 2016; Chang et al., 2020; Contini, 2020; Das et al., 2020; Elfiky, 2020; Gonzalez–Paz et al., 2020; Islam et al., 2020; Khan et al., 2020; Sinha et al., 2020; Wahedi et al., 2020; Abdelli et al., 2021). The antimalarial drug named as

chloroquine has been proposed as the potential inhibitor of M^{pro} activity (Ou et al., 2021). In a recent follow-up study, Pathak et al. (2021) explored the potential of rifampicin and letermovir as repurposed drug candidates against COVID-19. On the contrary, several studies reported the severe adverse effects of these repurposed drugs in different countries (Sultana et al., 2020; Wang et al., 2020a). Therefore, it is imperative to discover natural compound–based drug targets that could serve as potential inhibitors of different SARS-CoV-2 proteins and aid in controlling viral replication to enhance efficacy in COVID-19 treatment.

Sesame (*Sesamum indicum* L.) is an herbaceous annual plant cultivated for its edible seed, oil, and flavorsome value, belonging to the order Tubiflorae, family Pedaliaceae with many common names including gingelly, til, and benne seed (Bhat et al., 2014; Pathak et al., 2019). This oil crop is regarded as "queen of oilseeds" because of its property of resistance to oxidation and rancidity (Dalibalta et al., 2020). Sesame is widely cultivated in the tropical parts of Africa and Asia, India being one of the major producers with Myanmar, China, and Sudan (Majdalawieh et al., 2017). A plethora of nutrients including proteins, carbohydrates, antioxidants, lignans, tocopherols, phytates, phytosterols, and polyunsaturated fatty acids are exclusively found in sesame (Nagendra Prasad et al., 2012; Kumar et al., 2018; Pathak et al., 2019). These bioactive compounds possess certain medicinal properties like hepatoprotective, hypoglycemic, antihypertensive, anti-estrogenic, and anticancer (Kumar and Singh, 2014; Majdalawieh et al., 2017). Active ingredients of sesame have also been investigated as potential inhibitors of Parkinson's disease (PD) (Kappo et al., 2016). There are very few reports available for the screening of sesame-derived compounds against main protease of COVID-19. So far, only one compound of sesame, namely, sesamin has been well-explored against COVID-19 using *in silico* approach. Kodchakorn et al. (2020) investigated the potential of sesamin along with other herbal medicines (andrographolide, anthocyanin-b-D-glucoside, capsaicin, curcumin, cyanidin, cyanidin-3-O-glucoside, and hesperidin) against the M^{pro} of SARS-CoV-2 using molecular docking. Docking complexes of these nutraceuticals with M^{pro} were further validated for their atomic stability using molecular dynamics (MD) simulations on 50 ns, and suggested that the screened compounds may be considered for coprotection and treatment against COVID-19. In a recent study, Pandey and Verma (2020) also studied the potential of sesamin and four other dietary components (galangin, ellagic acid, capsaicin, and epicatechin) as structural inhibitors of SARS-CoV-2 M^{pro} using the molecular docking approach. In a very recent study, Allam et al. (2021) reported seven sesame-derived natural compounds (sesamin, sesamolin, pinoresinol, hydroxymatairesinol, spicatolignan, ferulic acid, and vanillic acid) as potential inhibitors against three proteins of SARS-CoV-2 including M^{pro}, papain-like protease (PL^{pro}), and the RNA-dependent RNA polymerase (RdRp) using the molecular docking analysis followed by MD simulations on 50 ns for representative complexes. However, there is no significant evidence of docking results evaluation available for MD simulations on high nanosecond scale (up to 200 ns) to understand the inhibitory mechanism of all sesame-derived compounds against the SARS-CoV-2 proteins. Despite the medicinal importance of sesame, all bioactive molecules derived from this important medicinal plant have not been well-explored in a significant manner yet for the treatment of COVID-19. With the fruitful utilization of molecular modeling methods including molecular docking and MD simulations, sesame-derived bioactive compounds may be utilized to design the alternative natural compound–based effective therapeutics against COVID-19.

Keeping this in view, in the present study, we have undertaken a thorough attempt to investigate the inhibition potencies of 36 phytochemicals from sesame against M^{pro} of SARS-CoV-2 using the molecular docking approach. Four natural metabolites, namely, sesamin, sesaminol, sesamolin, and sesamolinol, were further subjected to conformational stability using MD simulations followed by free energy calculations. The knowledge generated in the current study encourages and suggests that the sesame-derived phytochemicals have enough potential of being effective in treatment of COVID-19.

MATERIALS AND METHODS

A flowchart depicting the pipeline involved in the identification of interaction between sesame-derived bioactive molecules and M^{pro} is presented in **Figure 1**.

Ligand Selection

An extensive literature survey was conducted to prepare a library of sesame-derived natural compounds reported with therapeutic potential. Chemical structures of 36 phytochemicals (**Supplementary Table S1**) were obtained from the PubChem database (Kim et al., 2020) in a Spatial Data File (SDF) format. All these molecules were optimized prior to molecular docking using a set of AutoDock tools (Morris et al., 2009). Each and every molecule embedded in thse library was prepared with the addition of polar hydrogens and Gasteiger charges calculation. For the docking purpose, the molecules were saved in a pdbqt format using PyRx Open Babble tools (O'Boyle et al., 2011).

Preparation of Receptor

The crystal structure of the M^{pro} of SARS-CoV-2 in a complex with Z45617795 (PDB ID: 5R7Y) was attained from the RCSB-Protein Data Bank (Berman, 2000; Burley et al., 2018) for docking purposes. This protein crystal structure was solved by the PanDDA analysis group (https://www.rcsb.org/structure/5R7Y). Preprocessing of the M^{pro} of SARS-CoV-2 was carried out by removing water atoms and heteroatoms, and adding polar hydrogen atoms and Kollman charges on it using AutoDockTools version 1.5.6. Swiss-pdb Viewer (Guex and Peitsch, 1997) was employed to structure optimization and energy minimization. The clean geometry module available in the Discovery Studio platform was utilized for the side chain correction.

Virtual Screening Based on Molecular Docking

In a search for a drug against COVID-19, we performed a site-specific docking screen for the M^{pro} of SARS-CoV-2 against the prepared library of sesame-derived natural compounds

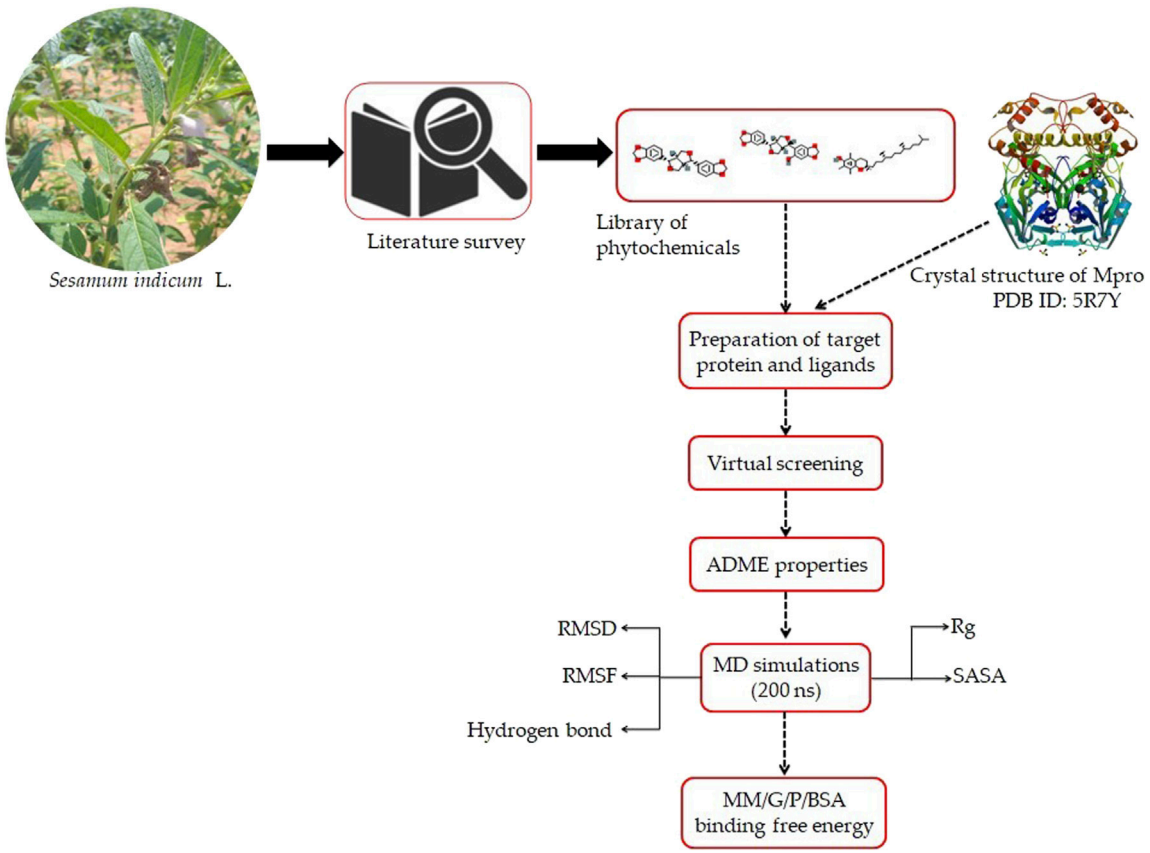

FIGURE 1 | Representation of pipeline utilized in the present study to identify the inhibitors of M^{pro} of SARS-CoV-2 using an extensive molecular modeling approach.

containing 36 compounds. AutoDock Vina program was employed for virtual screening. The grid box was created with the size of 70 Å × 70 Å × 70 Å, with a total of 50 genetic run. For the purpose of docking, amino acid residues such as Thr24, Thr26, Asn119, Phe140, Gly143, Cys145, His163, His164, Glu166, Gln189, and Thr190 were considered as active sites, as earlier reported by Khan et al. (2020) and Kumar et al. (2020). Other parameters were set as default while docking process. The carmofur (CID_2577) compound was selected as the positive control (Jin et al., 2020) for docking process. After docking, the top ranked compounds (based on docking score, number of hydrogen bonds, and specificity) (**Table1**) were chosen and visually inspected using PyMol and Discovery Studio (DeLano, 2002).

Drug-Likeness and Absorption, Distribution, Metabolism, and Excretion Profiling

The automated Swiss ADME server (Daina et al., 2017) was employed to calculate the drug-likeness attributes of screened molecules. Different molecular properties such as molecular weight, number of hydrogen bond accepters, number of hydrogen bond donors, number of rotatable bonds, molar refractivity, bioavailability score, synthetic accessibility, TPSA, and solubility were calculated with utilizing Lipinski's rule of five (Lipinski, 2004) and Veber's rule (Veber et al., 2002).

Molecular Dynamics Simulations

In order to assess the stabilities of docking conformation complexes of the four bioactive compounds sesamin, sesaminol, sesamolin, and sesamolinol with SARS-CoV-2 M^{pro}, MD simulations were performed using GROMOS9643a1 force field embedded in GROMACS 5.1.1 package installed on Linux-based workstation (Abraham et al., 2015; Kutzner et al., 2019). For the MD simulations, we followed the protocol previously described by Gajula et al. (2016) and Jee et al. (2017). The automatic PRODRG server was employed to prepare the topology files of ligand molecules (Schüttelkopf and van Aalten, 2004). The docking complexes were solvated in a dodecahedron box. In order to make the whole system neutral, the appropriate Na+ ions were added to the system. The steepest descent algorithm was applied to perform the energy minimization of the prepared system with 50,000 iteration steps and cutoff up to 1,000 $kjmol^{-1}$ with a primary goal of reducing the steric clashes during simulations. The long-range electrostatic interactions were calculated by using particle mesh Ewald (PME) truncation method (Abraham and Gready, 2011). Prior to a

TABLE 1 | List of top four natural compounds shortlisted based on binding energy score as a result of virtual screening.

S. No.	Compound	2D structure	Binding energy (kcal/mol)	Molecular interactions
1	M^{pro} (active site residues)	Thr24, Thr26, Asn119, Phe140, Gly143, Cys145, His163, His164, Glu166, Gln189, and Thr190		
2	Sesamin (CID_72307)	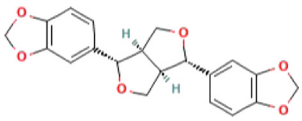	−6.7	Hydrogen bond: ASN151 (5.46 Å), SER158 (4.38 Å), and ARG298 (6.05 Å) Carbon–hydrogen bond: ASP295 (5.38 Å) Alkyl: VAL104 (5.27 Å) Pi–sigma: VAL104 (4.29 Å)
3	Sesaminol (CID_94672)	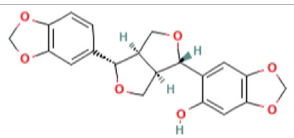	−6.6	Hydrogen bond: ARG105 (6.59 Å), ASN151 (5.39 Å), and ARG298 (6.05 Å) Carbon–hydrogen bond: ASP295 (5.27 Å) Pi-Sigma: VAL104 (4.30 Å)
4	Sesamolin (CID_131801617)	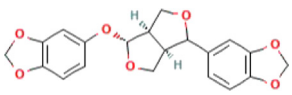	−6.4	Hydrogen bond: ARG105 (6.03 Å), GLN110 (4.52 Å), and SER158 (4.08 Å) Pi–sigma: VAL104 (4.89 Å)
5	Sesamolinol (CID_443019)	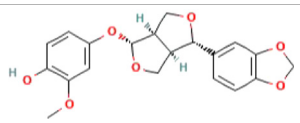	−6.1	Hydrogen bond: SER158 (4.10 Å) Carbon–hydrogen bond: ILE106 (4.45 Å), and GLN110 (5.21 Å) Pi–sigma: VAL104 (5.04 Å) Alkyl: VAL202 (5.45 Å), and ILE249 (5.21 Å) Pi-Alkyl: HIS246 (5.26 Å)

production run, the process of equilibrium was completed in two phases. In the first phase, equilibration was established with a constant number of particles, volume, and temperature (NVT), with each step 2 femtosecond (fs). The second phase was performed with a constant number of particles, pressure, and temperature NPT, with the ensemble at 300 K. After determining the coordinates, LINCS algorithm was considered to constrain the covalent bonds involving hydrogen atoms (Hess et al., 1997; Hess, 2007). Temperature was regulated inside the box using V-rescale, a popular Berendsen temperature coupling method. Finally, a production run of 200 ns was run with each step of 2 fs.

Trajectory Analysis

After the successful completion of MD simulations, trajectories were analyzed using a set of tools implemented in GROMACS package. The gRMS tool of GROMACS was utilized to calculate the root-mean-square deviation (RMSD) variation in protein backbone, while the overall root-mean-square fluctuation (RMSF) in the atomic positions of protein C backbone was generated by using the grmsf module. The gyrate, gmxsasa, and g h bond tools were employed to estimate the radius of gyration (Rg), solvent accessible surface area (SASA), and hydrogen bonds, respectively.

Molecular Mechanic/Poisson–Boltzmann Surface Area Binding Free Energy Calculations

The Molecular Mechanic/Poisson–Boltzmann Surface Area (MM/PBSA) was performed on g mmpbsa script program to calculate the binding free energy of interactions between the docking complexes (Kumari et al., 2014; Aldeghi et al., 2017). After the simulation of docking complexes, all the trajectories of 200 ns were used for MM/PBSA-based binding free energy analysis. The major energy components such as binding energy (kJ/mol), van der Waals energy (DEvdW), electrostatic energy, polar solvation energy, and SASA energy all together contributed to calculate the MM/PBSA relative binding affinity. The MM/PBSA method–based binding free energy of the protein–ligand systems were calculated using the following equation:

$$\Delta G_{MMPBSA} = \langle G_{complex} - G_{protein} - G_{ligand} \rangle_{complex},$$

where $G_{complex}$ represents the total free energy of the docking complex, and $G_{protein}$ and G_{ligand} depict the total free energies of the isolated protein and ligand in the solvent, respectively.

RESULTS AND DISCUSSION

Molecular Docking

Molecular docking is one of the most applied methods in the process of computer-aided drug design (CADD) to identify potential inhibitors against various pathogens. With this revolutionary method, an immense amount of energy, time, and costs of the drug discovery process can be saved to screen the large drug libraries for the discovery of potential drug compounds (Wadood et al., 2013; Yu and MacKerell, 2016). There is no effective cure for COVID-19 so far; therefore, identification of potential drug compounds is required on an urgent basis. In the present study, we screened an in-house library of sesame-derived bioactive molecules against M^{pro} of SARS-CoV-2 using a molecular docking approach. In total, 36 natural compounds

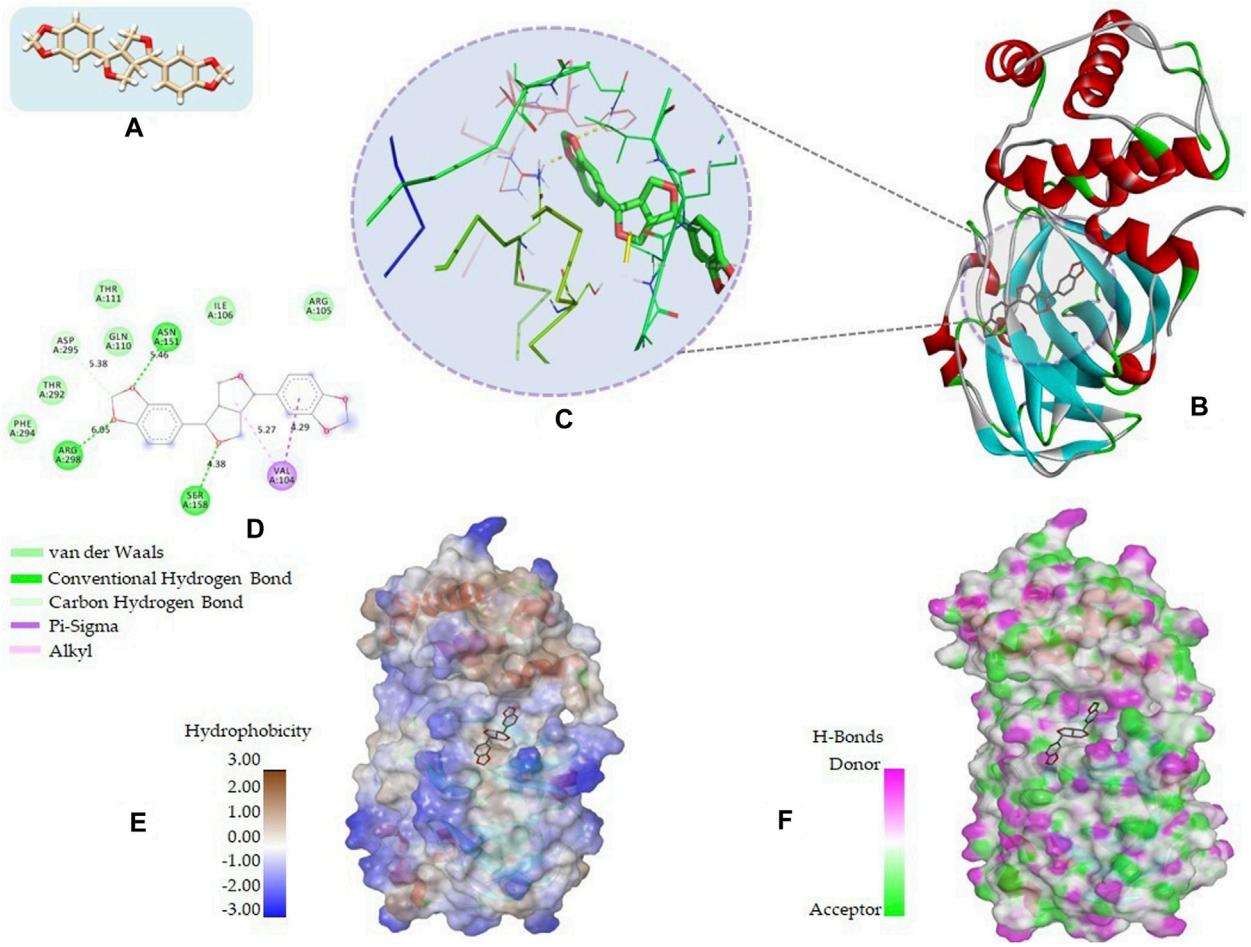

FIGURE 2 | 2D and 3D representation of molecular interaction between the M^{pro} of COVID-19 (PDB ID: 5R7Y) and sesamin compound (CID_72307): **(A)** 3D structure presentation of sesamin; **(B)** Molecular docking complex of a crystal structure of M^{pro} with sesamin molecule, docked using AutoDock implemented in PyRx package; **(C)** close view of pocket with sesamin structure in the stick model colored by atom types, yellow dashed lines represent the hydrogen bond networks; **(D)** 2D representation of different types of interactions with sesamin including van der Waals, conventional hydrogen bond, carbon hydrogen bond, Pi–sigma, and alkyl; **(E)** hydrophobicity surface representation of the overall structure of Mpro in complex with Sesamin; and **(F)** pocket view of sesamin binding with M^{pro} and the representation of residues involved in hydrogen bond donor acceptor. The docking complex of M^{pro} with sesamin was rendered in different CPK using UCSF Chimera, Discovery Studio, and PyMol.

(**Supplementary Table S1**) were docked into the binding pocket of M^{pro}. The docking results demonstrated that out of 36 selected natural compounds used in the present study, four bioactive molecules, namely, sesamin, sesaminol, sesamolin, and sesamolinol were found to have a higher binding energy of −6.7, −6.6, −6.4, and −6.1 kcal/mol^{-1}, respectively, than the positive control compound carmofur whose binding energy was determined to be −5.2 kcal/mol^{-1}. These four natural compounds (sesamin, sesaminol, sesamolin, and sesamolinol) ranked as top interacting with M^{pro} based on the affinity of molecular docking, number of hydrogen bonds and compound specificity.

The 2D structures, binding score, and details of interactions of the top four screened compounds are displayed in **Table 1**. Docking complexes of these natural metabolites with M^{pro} have been considered for further evaluation using MD simulations and MM/PBSA energy calculations. Discovery studio and PyMOL programs were employed to prepare the two- and three-dimensional plots of molecular interaction networks, respectively. After visualizing the 2D and 3D interaction plots, it was observed that the sesamin compound formed hydrogen bonds with three residues, namely, Asn151 (5.46 Å), Ser158 (4.38 Å), and Arg298 (6.05 Å). This compound was found to have one carbon–hydrogen (C–H) bond with Asp295 (5.38 Å), alkyl bond with Val104 (5.27 Å), and Pi–sigma bond with Val104 (4.29 Å) residue. It also manifests van der Waals (VdW) interaction with six residues including Arg105, Ile106, Gln110, Thr111, Thr292, and Phe294 (**Figure 2**).

In the case of sesaminol, three residues, namely, Arg105 (6.59 Å), Asn151 (5.39 Å), and Arg298 (6.05 Å), formed the hydrogen bonds. Residues Asp295 (5.27 Å) and Val104 (4.30 Å) interacted via C–H bond and Pi–sigma, respectively. Five residues including Ile106, Gln110, Thr111, Thr292, and

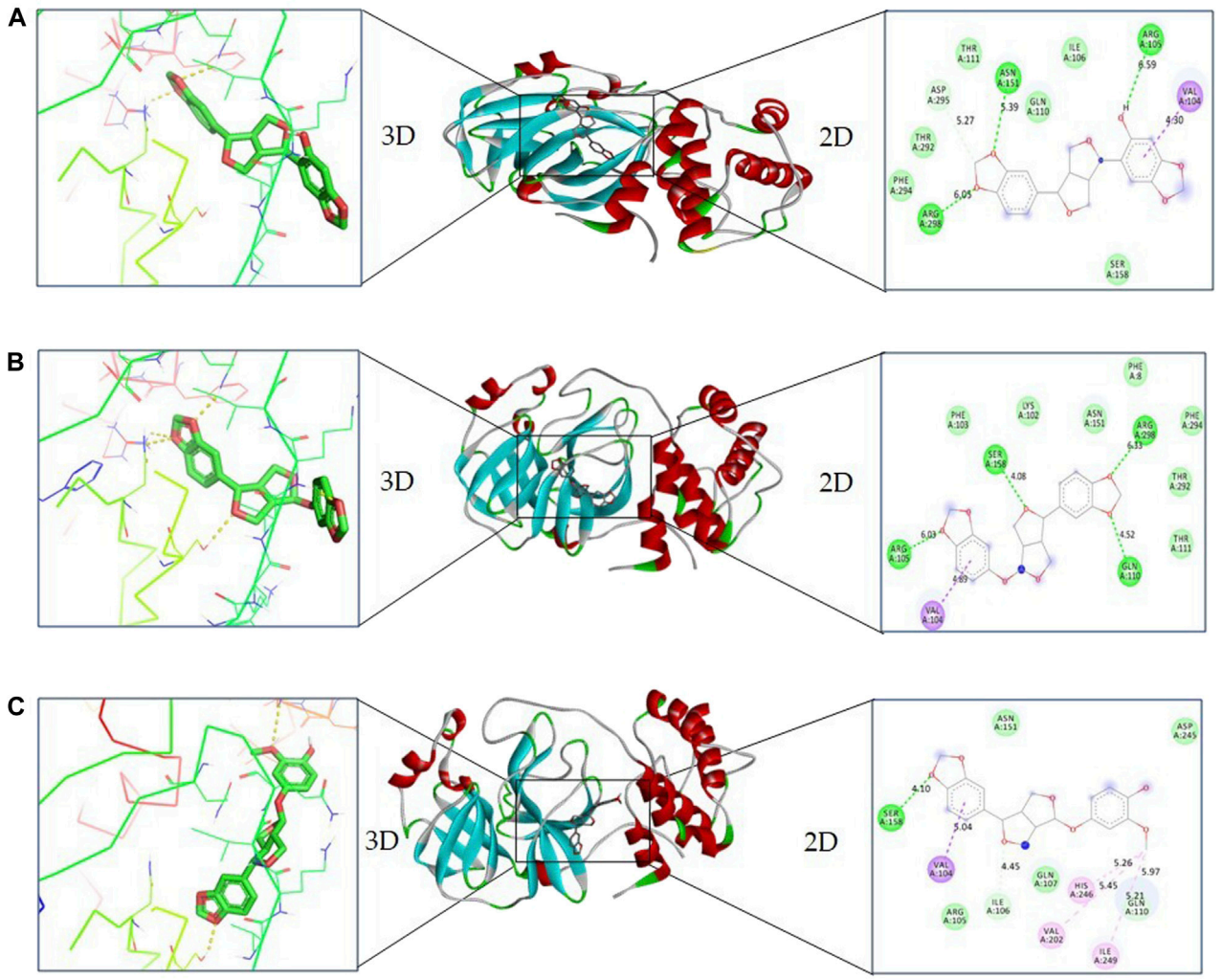

FIGURE 3 | 2D and 3D representation of docking complexes: **(A)** M^{pro} and sesaminol complex; **(B)** M^{pro} and sesamolin complex; **(C)** M^{pro} and sesamolinol complex visualized using UCSF Chimera and Discovery Studio.

Phe294 manifest VdW interaction (**Figure 3A**). As shown in **Figure 3B**, sesamolin molecule exhibits the hydrogen bond with three residues, namely, Arg105 (6.03 Å), Gln110 (4.52 Å), and Ser158 (4.08 Å), and one Pi–sigma with Val104 (4.89 Å). VdW interaction with residues Phe8, Lys102, Phe103, Thr111, Asn151, Thr292, and Phe294 was also formed. In the sesamolinol molecule, one residue Ser158 (4.10 Å) formed hydrogen bond (**Figure 3C**). Several other residues formed other types of molecular interactions such as Ile106 (4.45 Å), Gln110 (5.21 Å) (C–H bond), Val104 (5.04 Å) (Pi–sigma), Val202 (5.45 Å), Ile249 (5.21 Å) (alkyl), His246 (5.26 Å) (Pi–alkyl), and residues Arg105, Gln107, Asn151, Asp245 demonstrated VdW interactions.

Consistent with previous studies which reported the potential inhibitors of M^{pro} (Park et al., 2015; Aanouz et al., 2020; Bello et al., 2020; Chikhale et al., 2020b; Krupanidhi et al., 2020; Matveeva et al., 2020; Muhammad et al., 2020; Tripathi et al., 2020; Mitra et al., 2021; Prasanth et al., 2021; Varadharajan et al., 2021), in our study, screened four compounds (sesamin, sesaminol, sesamolin, and sesamolinol) were found to be tightly fit into the binding pocket of the M^{pro} of COVID-19. In previous studies, the potential of herb-derived natural compounds have been explored to inhibit the M^{pro} of COVID-19 using integrated bioinformatics and molecular modeling approaches (Kumar et al., 2020; Suravajhala et al., 2020; Gunda et al., 2021; Mishra et al., 2021). Three natural metabolites, namely, ursolic acid, carvacrol, and oleanolic acid have been reported as the potential inhibitors of M^{pro} of COVID-19. The molecular docking study of ursolic acid, carvacrol, and oleanolic acid with the M^{pro} protein demonstrated the binding energy of −5.9, −4.0, and −6.0 kcal/mol, respectively (Kumar et al., 2020). The ursolic acid formed a strong hydrogen bond with Ser46 residues, while the docking study of carvacrol and oleanolic acid with the M^{pro} protein exhibits hydrogen bonding with Gly143 and Gln189 residues of the active site, respectively. In a recent study, Gunda et al. (2021) proposed the natural xanthone compounds as promising drug inhibitors against the M^{pro} of

COVID-19 based on their significant antiviral power, which is well-documented in literatures. In a recent follow-up study, Mishra et al. (2021) explored a set of natural compounds to investigate their binding potential to the M^{pro} of COVID-19. Based on the docking and MD simulations, the four natural compounds, namely, amentoflavone, guggulsterone, puerarin, and piperine have been reported as antiviral compounds against the M^{pro} of COVID-19. The binding affinity of these natural metabolites with M^{pro} protein confirms the results of the present study.

Several compounds of sesame possess the natural antibacterial, antifungal, antiviral, and anti-inflammatory properties, and lignans such as sesamin, sesaminol, sesamolin, and sesamolinol are good examples (Uncu et al., 2015; Dravie et al., 2020). Sesamin is exclusively found in the sesame plant, and its antioxidant, antibacterial, antiviral, and antifungal activities are well-reported. Kodchakorn et al. (2020) identified that sesamin interacts with the M^{pro} of SARS-CoV-2 and affects the thermal stability of M^{pro} using in silico methods, providing evidence for sesamin as a structural inhibitor against the M^{pro} of SARS-CoV-2. Other studies also indicated that the sesamin compound might interact with amino acid residues Ser144, Cys145, Gln189, and Gln192 and showed significant interactions with effective residues His41, Met49, and Met165 of the M^{pro} of COVID-19 (Pandey and Verma, 2020). In a follow-up study, Allam et al. (2021) explored the sesamin and sesamolin compounds along with other natural compounds against M^{pro}, PL^{pro}, and RdRp proteins. Sesamin was found to be interacted with M^{pro} with three residues including Gln189, Thr190, and His41, while the sesamolin molecule was reported to interact with two amino acid residues, namely, Gln189 and Thr190. Our results may support the previous findings on the inhibitory effect of sesamin and sesamolin against the M^{pro} of COVID-19. Previous reports demonstrated the docking results only for few compounds including sesamin and sesamolin but did not consider all compounds of sesame reported in the literature, which have significant medicinal properties as well. In the present study, we explored the potential of 36 sesame-derived natural compounds against the M^{pro} of COVID-19, and based on the docking results, the four natural compounds were selected, namely, sesamin, sesaminol, sesamolin, and sesamolinol for further evaluation using MD simulations on 200 ns. The previous studies lack the evidence of docking results evaluated using MD simulations on high ns scale. The screened natural compounds based on the present study were also well-studied for their central role in different biological activities. Several *in vitro* and *in vivo* studies illustrate the neuroprotective role of sesamin against cerebral ischemia (Chung et al., 2010; Dar and Arumugam, 2013). Also, this major lignin compound has demonstrated other biological activities such as antihypertensive, atherosclerosis, thrombosis, antidiabetic, anticancer, cardiovascular, and anti-inflammatory (Kumar et al., 2018; Dalibalta et al., 2020). Of note, sesamin has been previously shown to be effective against swine flu (influenza type A H1N1) through in silico and *in vitro* studies (Fanhchaksai et al., 2015). This compound was established as a novel inhibitor of pro-inflammatory cytokines, IL-1β and TNF-α. Sesaminol is one type of sesame lignan compound commonly found in sesame seeds and well known for its strong antioxidant and anticancer properties (Miyahara et al., 2001; Watanabe et al., 2017).

TABLE 2 | ADME properties of screened top four compounds from sesame (*S. indicum* L.).

Drug-likeliness properties	MW (g/mol)	Consensus log Po/w	No. of H bond acceptors	No. of H bond donors	Molar refractivity	Lipinski	Veber	Bioavailability score (range 0.4–0.6)	Synthetic accessibility (range >6)	TPSA (Å2)	No. of rotatable bonds	Solubility (mg/ml)
Phytochemical	(range ≤500 g)	(range ≤5)	(range ≤10)	(range ≤5)	(range 40–130)					(range >100)	(range 1–10)	
Sesamin (CID_72307)	354.35	2.79	6	0	90.00	Yes	Yes	0.55	4.12	55.38	2	8.98e-03
Sesaminol (CID_94672)	370.35	2.37	7	1	92.02	Yes	Yes	0.55	4.31	75.61	2	3.62e-02
Sesamolin (CID_131801617)	370.35	2.74	7	3	91.52	Yes	Yes	0.55	4.43	64.61	3	1.75e-02
Sesamolinol (CID_443019)	372.37	2.56	7	1	93.98	Yes	Yes	0.55	4.50	75.61	4	2.80e-02

Using *in vitro* and *in vivo* models, Kaji et al. (2020) reported the preventive effect of sesaminol on a neurodegenerative disease named as Parkinson's disease (PD). Sesamolin, the second major lignan, found in sesame oil has been regarded as a natural therapeutic agent because of its various therapeutic properties (Michailidis et al., 2019). Free radical scavenging activity of sesamolin provides protection to neuronal hypoxia (Park et al., 2010). Sesamolinol has also been considered the important lignin compound due to its various biological activities (Grougnet et al., 2011). The present study reported bioactive molecules (sesaminol, sesamolin, and sesamolinol) which are established as potential inhibitors of M^{pro} having enough bibliographical research support.

Evaluation of Drug Likeness

Prior to conducting MD simulation analysis, we evaluated the pharmacokinetic properties of the screened compounds of sesame. The ADME results of the shortlisted molecules calculated using SWISSADME server are shown in **Table 2**. Sesamin, sesaminol, sesamolin, and sesamolinol have the following molecular weights, respectively: 354.35, 370.35, 370.35, and 372.37 g/mol; these four natural compounds have a molecular weight ≤500 g/mol, which indicated that these screened natural compounds may easily be transported, diffused, and absorbed by the body (Lipinski et al., 2001; Lipinski, 2004).The LogP values of sesamin, sesaminol, sesamolin, and sesamolinol molecules were found to have 2.79, 2.37, 2.74, and 2.56, respectively, which are in accordance with Lipinski's rule of five. For these four compounds, the number of hydrogen bond donors was less than five, which meets the criteria of ADME as the number of H bond donors should be ≤5. The ADME analysis revealed that sesamin, sesaminol, sesamolin, and sesamolinol molecules present the following values of the topological polar surface (TPSA): 55.38, 75.61, 64.61, and 75.61 Å2. The range of lower TPSA values represents the acceptable results, as described by Ahuja et al. (2021) and Singh et al. (2021) in previous studies. It has been noted that the natural compounds derived from sesame are better behaved than the co-crystallized molecule. These screened molecules also validate Veber's rule which state the oral bioavailability of drug-like compounds. These four metabolites, namely, sesamin, sesaminol, sesamolin, and sesamolinol have the molar refractivity values 90, 92.02, 91.52, and 93.98, respectively; these compounds also present the scores of the synthetic accessibility (SA): 4.12, 4.31, 4.43, and 4.50, respectively. SA is one of the important parameters of synthesis during the process of drug designing (Ertl and Schuffenhauer, 2009). The predicted SA score of these screened compounds was <10, which suggested that these compounds can be easily synthesized. Taken together, the drug-likeness analysis indicated that these sesame-derived natural metabolites possess favorable pharmacokinetic properties, and thus can be considered drug-like molecules.

Conformation of Stability of Docking Complexes for Natural Compounds and SARS-CoV-2 M^{pro} by Molecular Dynamics Simulations

In order to determine the structural stability of docking complexes, MD simulations were run with the most stable docked models on 200 ns. Based on docking scores, hydrogen bonds, and compound specificity, four docking complexes, namely, sesamin, sesaminol, sesamolin, and sesamolinol were subjected to MD simulations. High binding energy scores of docking complexes allowed for the estimation of the amino acid residue interactions over time. The RMSD, RMSF, SASA, and Rg plots were calculated to evaluate the stability of simulated systems.

Root-Mean-Square Deviation

The RMSD is a most commonly used quantitative method to evaluate the stability of the docking complexes and measures the conformational stability perturbations within the protein backbone during MD simulations on different nanosecond scales (Sargsyan et al., 2017). In order to investigate the stability of the ligand molecules to the protein, all the ligand and backbone RMSDs were graphically measured. As evident from **Figure 4A**, the protein backbone of M^{pro} showed constant stability throughout the simulation with a range between 0.37 and 0.47 nm. The average RMSD values for complexes with sesamin, sesaminol, sesamolin, and sesamolinol were ~0.37, ~ 0.38, ~ 0.31, and ~0.38 nm, respectively. Likewise, the control (blue) element also showed the average value of RMSD to be around 0.47 nm. The complex with sesaminol (yellow) and sesamolinol (cyan) displayed higher simulation trajectory after ~50 ns than the complex with sesamin (red) and sesamolin (green). The compound sesamolin has shown two fluctuations throughout the simulations on 200 ns time scale. The first stable conformation was noted between 25 and 100 ns, and the second stable conformation was found between 110 and 200 ns. The RMSD constant was at ~0.25, and a large fluctuation was observed between 10 and 25 ns. However, there was no significant effect of this fluctuation was found on the protein structure. Sesamolinol showed slight changes in the starting period of simulation between 2 and 25 ns. After 25 ns, sesamolinol was found to be constant at ~0.35 throughout the simulations. It may be because of the binding region size and loop presence at the pocket site. All the four ligand molecules shared the almost similar trend of stability and RMSD values with small conformational changes. As depicted in **Figure 4B**, the calculated ligand RMSD plot is the conformation of the measured protein backbone; RMSD plot shows the stability of target compounds throughout the simulation with fluctuation in sesamolinol at starting point between 5 and 15 ns on ~0.50 nm. In the same plot, the sesamolin compound also showed the fluctuation between 160 and 170 ns on ~0.25 nm. Based on the minimal fluctuations and low difference in values depicted in the protein backbone and ligand RMSD plots, it can be predicted that protein–ligand complexes were stable and comparable to solved structures. The docked pose of our ligands is fixed in the active region, same as the crystal structure ligand Z45617795, which is quite acceptable in protein–ligand interaction (**Table 1**). The RMSDs of our ligands with heavy atoms are similar to crystal structure resolution which is higher than 1.65 Å and is accurately ordered and exactly fitted in the electron density map. Therefore, RMSDs obtained from MD simulation also showed the structure stability during simulation (each ligand has remained constant

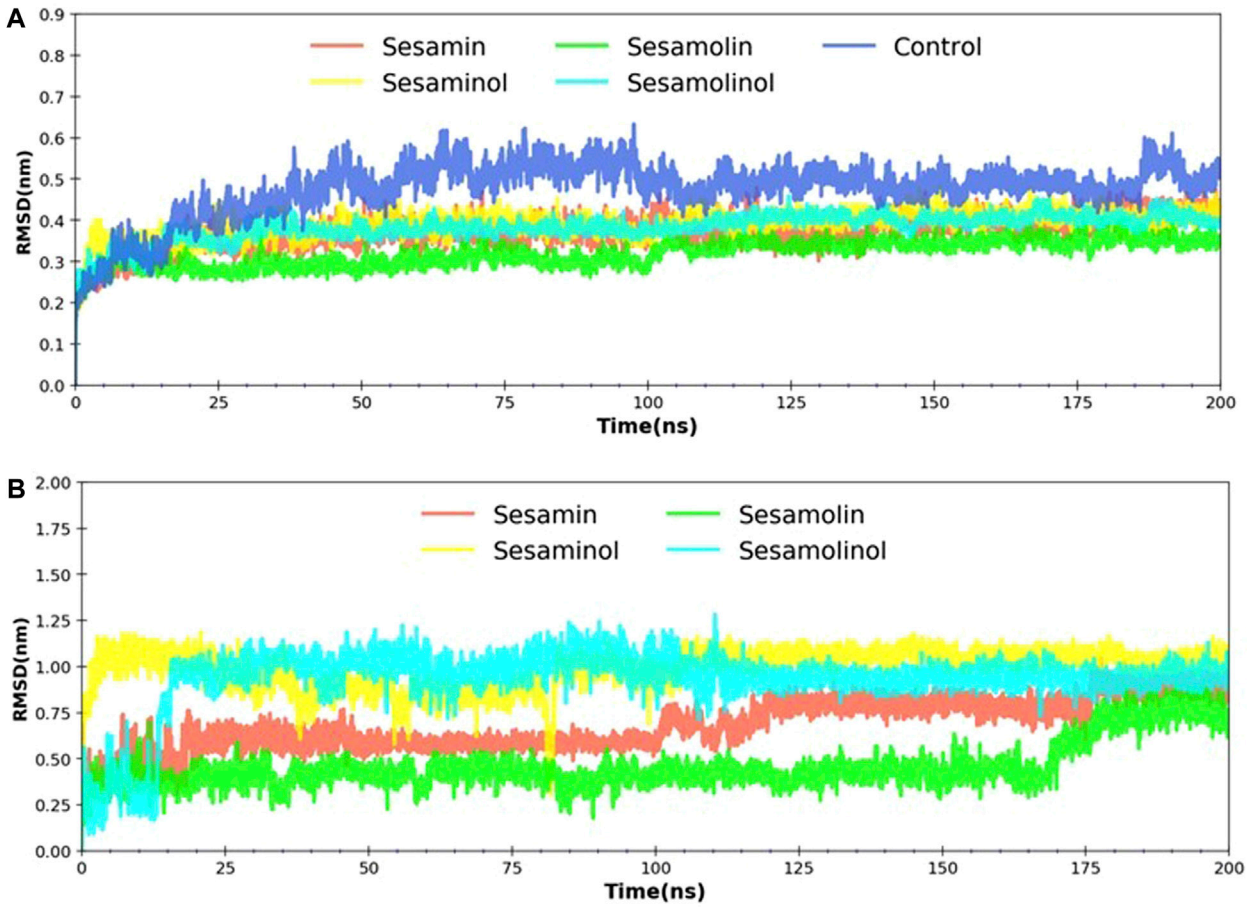

FIGURE 4 | RMSD analysis. **(A)** Backbone RMSD plot of docking complexes; and **(B)** ligand RMSD plot of complexes [M^{pro} – sesamin complex (red), M^{pro} – sesamolin complex (green), M^{pro} – sesaminol complex (yellow), M^{pro} – sesamolinol complex (cyan), and control (blue)].

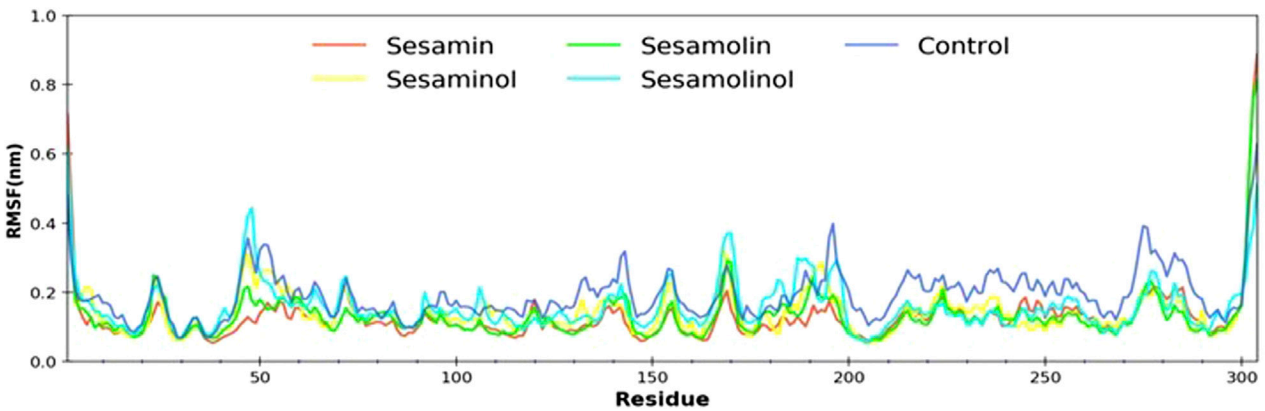

FIGURE 5 | Calculated RMSF plot of docking complexes[M^{pro} – sesamin complex (red), M^{pro} – sesamolin complex (green), M^{pro} – sesaminol complex (yellow), M^{pro} – sesamolinol complex (cyan), and control (blue)].

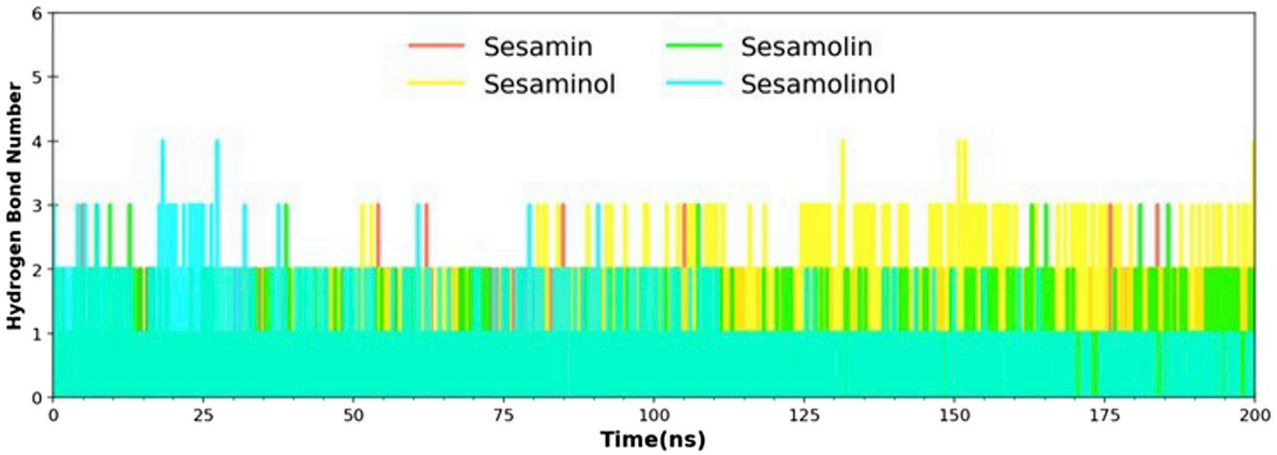

FIGURE 6 | Hydrogen bond analysis of docking complexes [M^{pro} – sesamin complex (red), M^{pro} – sesamolin complex (green), M^{pro} – sesaminol complex (yellow), and M^{pro} – sesamolinol complex (cyan)].

and has a constant range of RMSDs). From these observations, we assume that our ligand RMSDs (0.25–1 nm) showed similar stability as crystal ligand pose has in resolutions.

Root-Mean-Square Fluctuation

In order to determine the individual residue flexibility of the system with the time, RMSF was calculated, in which high fluctuation score indicates more flexibility and unstable bonds, while a low score reflects well-structured regions in the protein–ligand complexes (Gajula et al., 2016). The RMSF of alpha-carbon atoms of all system was investigated and is given in **Figure 5**. All the five systems (control, M^{pro}–sesamin, M^{pro}–sesaminol, M^{pro}–sesamolin, and M^{pro}–sesamolinol complexes) demonstrated almost a similar pattern of fluctuation across the whole structure during simulation. The average RMSF values of control, M^{pro}– sesamin, M^{pro}– sesaminol, M^{pro}– sesamolin, and M^{pro}– sesamolinol complexes were ~0.25, ~0.20, ~0.23, ~0.21, and ~0.35 nm, respectively. These values revealed that all the subjected docking complexes exhibit relatively less conformation fluctuation than the control system. These less fluctuations of the docking complexes suggested that the residues distributed across the active site of M^{pro} interact with sesamin, sesaminol, sesamolin, and sesamolinol in a significant manner.

Hydrogen Bond Analysis

Hydrogen bonds play an essential role in establishing molecular interactions of biological systems. The molecular interaction between M^{pro} and sesame-derived bioactive molecules was explored by the secondary structure changes, which is, in turn, regulated by a number of hydrogen bonds. For selected complexes (M^{pro}– sesamin, M^{pro}– sesaminol, M^{pro}– sesamolin, and M^{pro}– sesamolinol), a number of formed hydrogen bonds were calculated throughout the MD simulation on the scale of 200 ns. The number of hydrogen bonds and hydrogen bond distribution is represented in **Figure 6**. In complex with sesaminol (yellow) and sesamolinol (cyan), the numbers of hydrogen bonds were three, with few conformations showing up to 4 hydrogen bonds throughout the simulations. Sesamin (red) and sesamolin (green) have a constant range of hydrogen bonds between two and three in whole simulation. These results showed that the screened natural metabolites were able to maintain a strong interaction with a pocket site and suggested that all four docking complexes were stable throughout the simulation.

Radius of Gyration, and Solvent Accessible Surface Area Analysis

MD trajectories corresponding to four complexes (M^{pro}–sesamin, M^{pro}– sesaminol, M^{pro}– sesamolin, and M^{pro}–sesamolinol) were further investigated with the aid of Rg and SASA analysis. Rg was calculated with a primary goal to determine the compactness of the system with the time. As depicted in **Figure 7A**, the Rg values of all four systems with control were reported as 2.08–2.15 nm throughout the simulation. Rg value analysis affirms the stability of each system and suggested that the binding of screened natural phytochemicals does not induce structural changes during whole simulation. During simulation, SASA values were calculated to measure the receptor exposed to the solvents. It is well-documented that a higher SASA value reflects the expansion of protein volume during MD simulation (Kumar et al., 2020). Always, a low fluctuation is expected during whole simulation. Interaction with ligand compounds may influence SASA and sometimes affect the protein structure in a significant manner. The calculated SASA values showed between 130 and 148 nm^2, reflecting that the binding of sesamin, sesaminol, sesamolin, and sesamolinol does not affect the folding of protein (**Figure 7B**). The calculated SASA values for these ligand compounds are the consent of previous reports (Kumar et al., 2020; Mishra et al., 2021) and suggested that all of the four complexes were stable after the binding of sesamin, sesaminol, sesamolin, and sesamolinol to the M^{pro} active site.

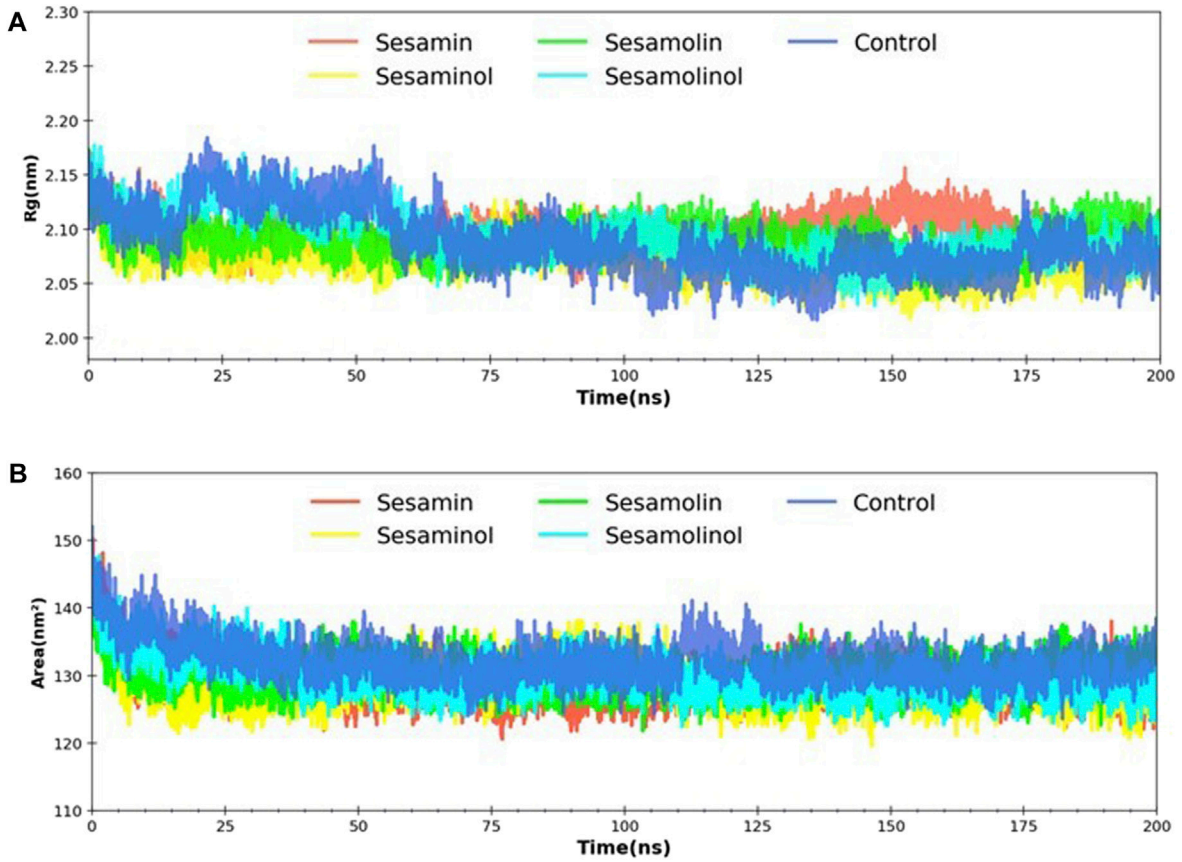

FIGURE 7 | Rg and SASA analysis. **(A)** Predicted Rg plot of docking complexes; and **(B)** SASA plot of selected complexes [M^{pro} – sesamin complex (red), M^{pro} – sesamolin complex (green), M^{pro} – sesaminol complex (yellow), M^{pro} – sesamolinol complex (cyan), and control (blue)].

TABLE 3 | Calculated total binding energy, van der Waals energy, electrostatic energy, polar solvation energy, and SASA energy of the docking complexes.

Complex	Binding energy (kJ/mol)	van der Waals energy (ΔEvdW) (kJ/mol)	Electrostatic energy (ΔElec), (kJ/mol)	Polar solvation energy (ΔG polar) (kJ/mol)	SASA energy (kJ/mol)
Sesamin	−145.511 ± 17.054	−185.239 ± 12.497	−1.331 ± 2.720	56.328 ± 10.084	−15.269 ± 0.859
Sesamolin	−211.240 ± 14.034	−244.688 ± 13.232	−2.394 ± 2.452	53.429 ± 6.865	−17.587 ± 0.839
Sesaminol	−149.078 ± 9.043	−158.179 ± 8.593	−1.087 ± 1.785	24.598 ± 4.487	−14.410 ± 0.870
Sesamolinol	−199.110 ± 15.881	−233.811 ± 13.828	2.162 ± 2.619	51.381 ± 7.632	−18.842 ± 0.954

Estimation of Binding Free Energy

The average free binding energy of selected complexes (M^{pro}–sesamin, M^{pro}– sesaminol, M^{pro}– sesamolin, and M^{pro}–sesamolinol) was calculated by using a python script MmPbSaStat.py embedded in g_mmpbsa package. The molecular mechanic/Poisson–Boltzmann surface area (MM/PBSA) is one of the popular and accurate methods to estimate the ligand binding affinities in the protein system. To calculate the binding free energy, we have utilized the steps previously described (Gajula et al., 2016; Jee et al., 2017). The MM/PBSA-based binding energy score extracted after the systematical calculation is provided in **Table 3**. The cumulative sum of different energies such as van der Walls, electrostatic, polar solvation, and SASA is presented as the final binding energy. All types of the energy significantly contributed to the molecular interaction between the ligand compounds and M^{pro}. The evaluated binding free energy of screened molecules exhibited as sesamin (−145.511 ± 17.054 kJ/mol), sesamolin (−211.240 ± 14.034 kJ/mol), sesaminol (−149.078 ± 9.043 kJ/mol) and sesamolinol (−199.110 ± 15.881 kJ/mol). The negative values of the binding energy reflect that the targeted compound favorably interact with the receptor protein. As compared with other screened compounds, the sesamolin (−211.240 ± 14.034 kJ/mol) showed the maximum negative

binding energy. The MM/PBSA results clearly suggest that sesamolinol (−199.110 ± 15.881 kJ/mol) possessed the second least binding energy. These natural compounds with the maximum negative binding energy and better binding affinity could be utilized as potential inhibitors against the M^{pro} of COVID-19.

CONCLUSION

The inhibition of M^{pro} protein represents a promising strategy for controlling viral replication leading to discovery of potential drug candidates. The current extensive study concludes four phytochemicals, namely, sesamin, sesaminol, sesamolin, and sesamolinol as potential inhibitors against the M^{pro} of SARS-CoV-2. The integrated molecular docking and MD simulation study revealed that these bioactive molecules form a very stable complex with M^{pro} that shows excellent binding affinities higher than other sesame-derived molecules. Docking complexes of these natural metabolites with M^{pro} showed a stable conformation on 200 ns, which is further supported by the results of binding free energy. Moreover, the proposed potential inhibitors also meet the criteria of drug likeness based on Lipinski's rule of five and ADME properties. The inhibitory effect of these sesame-derived natural compounds against the M^{pro} of SARS-CoV-2 may also be further validated using a plethora of *in vitro* and *in vivo* experiments. The current study suggested that the screened phytochemicals (sesamin, sesaminol, sesamolin, and sesamolinol) have shown enough potential to inhibit the M^{pro} and may be utilized as effective drug candidates for the development of new treatment against COVID-19 infection.

DATA AVAILABILITY STATEMENT

The datasets presented in this study can be found in online repositories. The names of the repository/repositories and accession number(s) can be found in the article/ **Supplementary Material**.

AUTHOR CONTRIBUTIONS

AK and UA contributed to conception, design, and data acquisition. AK drafted the manuscript. DM contributed to data analysis. UA, RY, AR, and DK proofread the final manuscript. All authors gave final approval and agreed to be accountable for all aspects of the work.

FUNDING

This research was funded by the Department of Biotechnology, Ministry of Science and Technology, government of India (grant number BT/Ag/Network/Sesame/2019-20).

ACKNOWLEDGMENTS

The authors are thankful to Gourav Choudhir, Indian Institute of Technology, Delhi, for his technical support in molecular dynamics simulations. The authors are also thankful to Indian Council of Agricultural Research, Ministry of Agriculture and Farmers' Welfare, government of India, for use of Advanced Super Computing Hub for Omics Knowledge in Agriculture (ASHOKA) facility.

SUPPLEMENTARY MATERIAL

The Supplementary Material for this article can be found online at: https://www.frontiersin.org/articles/10.3389/fchem.2021.744376/full#supplementary-material

REFERENCES

Aanouz, I., Belhassan, A., El-Khatabi, K., Lakhlifi, T., El-ldrissi, M., and Bouachrine, M. (2020). Moroccan Medicinal Plants as Inhibitors against SARS-CoV-2 Main Protease: Computational Investigations. *J. Biomol. Struct. Dyn.* 39, 2971–2979. doi:10.1080/07391102.2020.1758790

Abdelli, I., Hassani, F., Bekkel Brikci, S., and Ghalem, S. (2021). In Silico study the Inhibition of Angiotensin Converting Enzyme 2 Receptor of COVID-19 by Ammoides Verticillata Components Harvested from Western Algeria. *J. Biomol. Struct. Dyn.* 39, 1–14. doi:10.1080/07391102.2020.1763199

Abraham, M. J., and Gready, J. E. (2011). Optimization of Parameters for Molecular Dynamics Simulation Using Smooth Particle-Mesh Ewald in GROMACS 4.5. *J. Comput. Chem.* 32, 2031–2040. doi:10.1002/jcc.21773

Abraham, M. J., Murtola, T., Schulz, R., Páll, S., Smith, J. C., Hess, B., et al. (2015). GROMACS: High Performance Molecular Simulations through Multi-Level Parallelism from Laptops to Supercomputers. *SoftwareX* 1–2, 19–25. doi:10.1016/j.softx.2015.06.001

Ahuja, A., Tyagi, P. K., Tyagi, S., Kumar, A., Kumar, M., and Sharifi-Rad, J. (2021). Potential of Pueraria Tuberosa (Willd.) DC. To rescue Cognitive Decline Associated with BACE1 Protein of Alzheimer's Disease on Drosophila Model: An Integrated Molecular Modeling and *In Vivo* Approach. *Int. J. Biol. Macromolecules* 179, 586–600. doi:10.1016/j.ijbiomac.2021.03.032

Aldeghi, M., Bodkin, M. J., Knapp, S., and Biggin, P. C. (2017). Statistical Analysis on the Performance of Molecular Mechanics Poisson-Boltzmann Surface Area versus Absolute Binding Free Energy Calculations: Bromodomains as a Case Study. *J. Chem. Inf. Model.* 57, 2203–2221. doi:10.1021/acs.jcim.7b00347

Allam, A. E., Amen, Y., Ashour, A., Assaf, H. K., Hassan, H. A., Abdel-Rahman, I. M., et al. (2021). In Silico study of Natural Compounds from Sesame against COVID-19 by Targeting Mpro, PLpro and RdRp. *RSC Adv.* 11, 22398–22408. doi:10.1039/D1RA03937G

Arden, K. E., Nissen, M. D., Sloots, T. P., and Mackay, I. M. (2005). New Human Coronavirus, HCoV-NL63, Associated with Severe Lower Respiratory Tract Disease in Australia. *J. Med. Virol.* 75, 455–462. doi:10.1002/jmv.20288

Backer, J. A., Klinkenberg, D., and Wallinga, J. (2020). Incubation Period of 2019 Novel Coronavirus (2019-nCoV) Infections Among Travellers from Wuhan, China, 20-28 January 2020. *Eurosurveillance* 25, 2000062. doi:10.2807/1560-7917.ES.2020.25.5.2000062

Bello, M., Martínez-Muñoz, A., and Balbuena-Rebolledo, I. (2020). Identification of Saquinavir as a Potent Inhibitor of Dimeric SARS-CoV2 Main Protease through MM/GBSA. *J. Mol. Model.* 26, 340. doi:10.1007/s00894-020-04600-4

Berman, H. M. (2000). The Protein Data Bank. *Nucleic Acids Res.* 28, 235–242. doi:10.1093/nar/28.1.235

Bhat, K. V., Kumari, R., Pathak, N., and Rai, A. K. (2014). Value Addition in Sesame: A Perspective on Bioactive Components for Enhancing Utility and Profitability. *Phcog Rev.* 8, 147. doi:10.4103/0973-7847.134249

Burley, S. K., Berman, H. M., Bhikadiya, C., Bi, C., Chen, L., Di Costanzo, L., et al. (2018). RCSB Protein Data Bank: Biological Macromolecular Structures Enabling Research and Education in Fundamental Biology, Biomedicine, Biotechnology and Energy. *Nucleic Acids Res.* 47, D464–D474. doi:10.1093/nar/gky1004

Chang, C.-k., Lo, S.-C., Wang, Y.-S., and Hou, M.-H. (2016). Recent Insights into the Development of Therapeutics against Coronavirus Diseases by Targeting N Protein. *Drug Discov. Today* 21, 562–572. doi:10.1016/j.drudis.2015.11.015

Chang, Y.-C., Tung, Y.-A., Lee, K.-H., Chen, T.-F., Hsiao, Y.-C., Chang, H.-C., et al. (2020). Potential Therapeutic Agents for COVID-19 Based on the Analysis of Protease and RNA Polymerase Docking. *Preprints*, 2020020242. doi:10.20944/preprints202002.0242.v1

Chen, T., Wu, D., Chen, H., Yan, W., Yang, D., Chen, G., et al. (2020a). Clinical Characteristics of 113 Deceased Patients with Coronavirus Disease 2019: Retrospective Study. *BMJ* 368, m1091. doi:10.1136/bmj.m1091

Chen, Y., Liu, Q., and Guo, D. (2020b). Emerging Coronaviruses: Genome Structure, Replication, and Pathogenesis. *J. Med. Virol.* 92, 418–423. doi:10.1002/jmv.25681

Cheng, V. C. C., Lau, S. K. P., Woo, P. C. Y., and Yuen, K. Y. (2007). Severe Acute Respiratory Syndrome Coronavirus as an Agent of Emerging and Reemerging Infection. *Clin. Microbiol. Rev.* 20, 660–694. doi:10.1128/cmr.00023-07

Chikhale, R. V., Gurav, S. S., Patil, R. B., Sinha, S. K., Prasad, S. K., Shakya, A., et al. (2020a). Sars-cov-2 Host Entry and Replication Inhibitors from Indian Ginseng: an In-Silico Approach. *J. Biomol. Struct. Dyn.* 39, 4510–4521. doi:10.1080/07391102.2020.1778539

Chikhale, R. V., Sinha, S. K., Patil, R. B., Prasad, S. K., Shakya, A., Gurav, N., et al. (2020b). In-silico Investigation of Phytochemicals from *Asparagus racemosus* as Plausible Antiviral Agent in COVID-19. *J. Biomol. Struct. Dyn.* 39, 5033–5047. doi:10.1080/07391102.2020.1784289

Chung, B.-H., Lee, J. J., Kim, J.-D., Jeoung, D., Lee, H., Choe, J., et al. (2010). Angiogenic Activity of Sesamin through the Activation of Multiple Signal Pathways. *Biochem. Biophysical Res. Commun.* 391, 254–260. doi:10.1016/j.bbrc.2009.11.045

Contini, A. (2020). Virtual Screening of an FDA Approved Drugs Database on Two COVID-19 Coronavirus Proteins. *Life Sci.* 251, 117627. doi:10.26434/chemrxiv.11847381.v1

Daina, A., Michielin, O., and Zoete, V. (2017). SwissADME: A Free Web Tool to Evaluate Pharmacokinetics, Drug-Likeness and Medicinal Chemistry Friendliness of Small Molecules. *Sci. Rep.* 7, 42717. doi:10.1038/srep42717

Dalibalta, S., Majdalawieh, A. F., and Manjikian, H. (2020). Health Benefits of Sesamin on Cardiovascular Disease and its Associated Risk Factors. *Saudi Pharm. J.* 28, 1276–1289. doi:10.1016/j.jsps.2020.08.018

Dar, A. A., and Arumugam, N. (2013). Lignans of Sesame: Purification Methods, Biological Activities and Biosynthesis - A Review. *Bioorg. Chem.* 50, 1–10. doi:10.1016/j.bioorg.2013.06.009

Das, S., Sarmah, S., Lyndem, S., and Singha Roy, A. (2020). An Investigation into the Identification of Potential Inhibitors of SARS-CoV-2 Main Protease Using Molecular Docking Study. *J. Biomol. Struct. Dyn.* 39, 3347–3357. doi:10.1080/07391102.2020.1763201

de Wit, E., van Doremalen, N., Falzarano, D., and Munster, V. J. (2016). SARS and MERS: Recent Insights into Emerging Coronaviruses. *Nat. Rev. Microbiol.* 14, 523–534. doi:10.1038/nrmicro.2016.81

DeLano, W. L. (2002). *The PyMOL Molecular Graphics System*. San Carlos, CA: DeLano Scientific.

Dravie, E. E., Kortei, N. K., Essuman, E. K., Tettey, C. O., Boakye, A. A., and Hunkpe, G. (2020). Antioxidant, Phytochemical and Physicochemical Properties of Sesame Seed (Sesamum indicum L). *Scientific Afr.* 8, e00349. doi:10.1016/j.sciaf.2020.e00349

Elfiky, A. A., and Azzam, E. B. (2020). Novel Guanosine Derivatives against MERS CoV Polymerase: An In Silico Perspective. *J. Biomol. Struct. Dyn.* 39, 2923–2931. doi:10.1080/07391102.2020.1758789

Elfiky, A. A. (2020). SARS-CoV-2 RNA Dependent RNA Polymerase (RdRp) Targeting: An *In Silico* Perspective. *J. Biomol. Struct. Dyn.* 39, 3204–3212. doi:10.1080/07391102.2020.1761882

Enayatkhani, M., Hasaniazad, M., Faezi, S., Gouklani, H., Davoodian, P., Ahmadi, N., et al. (2020). Reverse Vaccinology Approach to Design a Novel Multi-Epitope Vaccine Candidate against COVID-19: an In Silico Study. *J. Biomol. Struct. Dyn.* 39, 2857–2872. doi:10.1080/07391102.2020.1756411

Ertl, P., and Schuffenhauer, A. (2009). Estimation of Synthetic Accessibility Score of Drug-like Molecules Based on Molecular Complexity and Fragment Contributions. *J. Cheminform* 1, 8. doi:10.1186/1758-2946-1-8

Fanhchaksai, K., Kodchakorn, K., Pothacharoen, P., and Kongtawelert, P. (2015). Effect of Sesamin against Cytokine Production from Influenza Type A H1N1-Induced Peripheral Blood Mononuclear Cells: Computational and Experimental Studies *In Vitro*. *Cell. Dev. Biol.* 52, 107–119. doi:10.1007/s11626-015-9950-7

Gajula, M., Kumar, A., and Ijaq, J. (2016). Protocol for Molecular Dynamics Simulations of Proteins. *Bio-protocol* 85, 159–166. doi:10.21769/bioprotoc.2051

Gonzalez-Paz, L. A., Lossada, C. A., Moncayo, L. S., Romero, F., Paz, J. L., Vera-Villalobos, J., et al. (2020). *Theoretical Molecular Docking Study of the Structural Disruption of the Viral 3CL-Protease of COVID19 Induced by Binding of Capsaicin, Piperine and Curcumin Part 1: A Comparative Study with Chloroquine and Hydrochloroquine Two Antimalaric Drugs*. Research Square. doi:10.21203/rs.3.rs-21206/v1

Gordon, D. E., Jang, G. M., Bouhaddou, M., Xu, J., Obernier, K., O'Meara, M. J., et al. (2020). A SARS-CoV-2-Human Protein-Protein Interaction Map Reveals Drug Targets and Potential Drug-Repurposing. *Nature* 583, 459–468. doi:10.1101/2020.03.22.002386

Grougnet, R., Magiatis, P., Laborie, H., Lazarou, D., Papadopoulos, A., and Skaltsounis, A.-L. (2011). Sesamolinol Glucoside, Disaminyl Ether, and Other Lignans from Sesame Seeds. *J. Agric. Food Chem.* 60, 108–111. doi:10.1021/jf2040687

Guex, N., and Peitsch, M. C. (1997). SWISS-MODEL and the Swiss-Pdb Viewer: An Environment for Comparative Protein Modeling. *Electrophoresis* 18, 2714–2723. doi:10.1002/elps.1150181505

Gunda, S. K., P, H. K., Kumar, A., Kishor, P. B. K., and S, A. K. (2021). *Natural Xanthone Compounds as Promising Drug Candidates against COVID-19 - an Integrated Molecular Docking and Dynamics Simulation Study*. Research Square. doi:10.21203/rs.3.rs-102884/v2

Gupta, A., Madhavan, M. V., Sehgal, K., Nair, N., Mahajan, S., Sehrawat, T. S., et al. (2020). Extrapulmonary Manifestations of COVID-19. *Nat. Med.* 26, 1017–1032. doi:10.1038/s41591-020-0968-3

Hasan, A., Paray, B. A., Hussain, A., Qadir, F. A., Attar, F., Aziz, F. M., et al. (2020). A Review on the Cleavage Priming of the Spike Protein on Coronavirus by Angiotensin-Converting Enzyme-2 and Furin. *J. Biomol. Struct. Dyn.* 39, 3025–3033. doi:10.1080/07391102.2020.1754293

Helmy, Y. A., Fawzy, M., Elaswad, A., Sobieh, A., Kenney, S. P., and Shehata, A. A. (2020). The COVID-19 Pandemic: A Comprehensive Review of Taxonomy, Genetics, Epidemiology, Diagnosis, Treatment, and Control. *Jcm* 9, 1225. doi:10.3390/jcm9041225

Hess, B., Bekker, H., Berendsen, H. J. C., and Fraaije, J. G. E. M. (1997). LINCS: A Linear Constraint Solver for Molecular Simulations. *J. Comput. Chem.* 18, 1463–1472. doi:10.1002/(sici)1096-987x(199709)18:12<1463:aid-jcc4>3.0.co;2-h

Hess, B. (2007). P-LINCS: A Parallel Linear Constraint Solver for Molecular Simulation. *J. Chem. Theor. Comput.* 4, 116–122. doi:10.1021/ct700200b

Hulswit, R. J. G., de Haan, C. A. M., and Bosch, B.-J. (2016). Coronavirus Spike Protein and Tropism Changes. *Adv. Virus. Res.* 96, 29–57. doi:10.1016/bs.aivir.2016.08.004

Islam, R., Parves, M. R., Paul, A. S., Uddin, N., Rahman, M. S., Mamun, A. A., et al. (2020). A Molecular Modeling Approach to Identify Effective Antiviral Phytochemicals against the Main Protease of SARS-CoV-2. *J. Biomol. Struct. Dyn.* 39, 3213–3224. doi:10.1080/07391102.2020.1761883

Jamwal, S., Gautam, A., Elsworth, J., Kumar, M., Chawla, R., and Kumar, P. (2020). An Updated Insight into the Molecular Pathogenesis, Secondary Complications and Potential Therapeutics of COVID-19 Pandemic. *Life Sci.* 257, 118105. doi:10.1016/j.lfs.2020.118105

Jee, B., Kumar, S., Yadav, R., Singh, Y., Kumar, A., and Sharma, N. (2017). Ursolic Acid and Carvacrol May Be Potential Inhibitors of Dormancy Protein Small Heat Shock protein16.3 of *Mycobacterium tuberculosis*. *J. Biomol. Struct. Dyn.* 36, 3434–3443. doi:10.1080/07391102.2017.1389305

Jin, Z., Zhao, Y., Sun, Y., Zhang, B., Wang, H., Wu, Y., et al. (2020). Structural Basis for the Inhibition of SARS-CoV-2 Main Protease by Antineoplastic Drug Carmofur. *Nat. Struct. Mol. Biol.* 27, 529–532. doi:10.1038/s41594-020-0440-6

Joshi, R. S., Jagdale, S. S., Bansode, S. B., Shankar, S. S., Tellis, M. B., Pandya, V. K., et al. (2020). Discovery of Potential Multi-Target-Directed Ligands by

Targeting Host-specific SARS-CoV-2 Structurally Conserved Main Protease. *J. Biomol. Struct. Dyn.* 39, 3099–3114. doi:10.1080/07391102.2020.1760137

Kaji, H., Matsui-Yuasa, I., Matsumoto, K., Omura, A., Kiyomoto, K., and Kojima-Yuasa, A. (2020). Sesaminol Prevents Parkinson's Disease by Activating the Nrf2-ARE Signaling Pathway. *Heliyon* 6, e05342. doi:10.1016/j.heliyon.2020.e05342

Kappo, A., Oyinloye, B., Ajiboye, B., Ojo, O., and Nwozo, S. (2016). Cardioprotective and Antioxidant Influence of Aqueous Extracts from Sesamum indicum Seeds on Oxidative Stress Induced by Cadmium in Wistar Rats. *Phcog Mag.* 12, 170. doi:10.4103/0973-1296.182155

Khan, S. A., Zia, K., Ashraf, S., Uddin, R., and Ul-Haq, Z. (2020). Identification of Chymotrypsin-like Protease Inhibitors of SARS-CoV-2 via Integrated Computational Approach. *J. Biomol. Struct. Dyn.* 39, 2607–2616. doi:10.1080/07391102.2020.1751298

Kim, S., Chen, J., Cheng, T., Gindulyte, A., He, J., He, S., et al. (2020). PubChem in 2021: New Data Content and Improved Web Interfaces. *Nucleic Acids Res.* 49, D1388–D1395. doi:10.1093/nar/gkaa971

Kodchakorn, K., Poovorawan, Y., Suwannakarn, K., and Kongtawelert, P. (2020). Molecular Modelling Investigation for Drugs and Nutraceuticals Against Protease of SARS-CoV-2. *J. Mol. Graphics Model.* 101, 107717. doi:10.1016/j.jmgm.2020.107717

Krupanidhi, S., Abraham Peele, K., Venkateswarulu, T. C., Ayyagari, V. S., Nazneen Bobby, M., John Babu, D., et al. (2020). Screening of Phytochemical Compounds of Tinospora Cordifolia for Their Inhibitory Activity on SARS-CoV-2: an In Silico Study. *J. Biomol. Struct. Dyn.* 39, 5799–5803. doi:10.1080/07391102.2020.1787226

Kumar, A., Choudhir, G., Shukla, S. K., Sharma, M., Tyagi, P., Bhushan, A., et al. (2020). Identification of Phytochemical Inhibitors against Main Protease of COVID-19 Using Molecular Modeling Approaches. *J. Biomol. Struct. Dyn.* 39, 3760–3770. doi:10.1080/07391102.2020.1772112

Kumar, A., Kumar, R., Sharma, M., Kumar, U., Gajula, M., and Singh, K. (2018). Uttarakhand Medicinal Plants Database (UMPDB): A Platform for Exploring Genomic, Chemical, and Traditional Knowledge. *Data* 3, 7. doi:10.3390/data3010007

Kumari, R., Kumar, R., and Lynn, A. (2014). g_mmpbsa-A GROMACS Tool for High-Throughput MM-PBSA Calculations. *J. Chem. Inf. Model.* 54, 1951–1962. doi:10.1021/ci500020m

Kutzner, C., Páll, S., Fechner, M., Esztermann, A., Groot, B. L., and Grubmüller, H. (2019). More Bang for Your Buck: Improved Use of GPU Nodes for GROMACS 2018. *J. Comput. Chem.* 40, 2418–2431. doi:10.1002/jcc.26011

Lee, N., Allen Chan, K. C., Hui, D. S., Ng, E. K. O., Wu, A., Chiu, R. W. K., et al. (2004). Effects of Early Corticosteroid Treatment on Plasma SARS-Associated Coronavirus RNA Concentrations in Adult Patients. *J. Clin. Virol.* 31, 304–309. doi:10.1016/j.jcv.2004.07.006

Lipinski, C. A., Lombardo, F., Dominy, B. M., and Feeney, P. J. (2001). Experimental and computational approaches to estimate solubility and permeability in drug discovery and development settings. *Adv. Drug Deliv. Rev.* 46, 3–26. doi:10.1016/s0169-409x(00)00129-0

Lipinski, C. A. (2004). Lead- and Drug-like Compounds: the Rule-Of-Five Revolution. *Drug Discov. Today Tech.* 1, 337–341. doi:10.1016/j.ddtec.2004.11.007

Liu, X.-h., Zhang, X., Lu, Z.-h., Zhu, Y.-s., and Wang, T. (2021). Potential Molecular Targets of Nonstructural Proteins for the Development of Antiviral Drugs against SARS-CoV-2 Infection. *Biomed. Pharmacother.* 133, 111035. doi:10.1016/j.biopha.2020.111035

Mackenzie, J. S., and Smith, D. W. (2020). COVID-19: A Novel Zoonotic Disease Caused by a Coronavirus from China: what We Know and what We Don't. *Microbiol. Aust.* 41, 45. doi:10.1071/ma20013

Mahendra Kumar, C., and Singh, S. A. (2014). Bioactive Lignans from Sesame (*Sesamum indicum* L.): Evaluation of Their Antioxidant and Antibacterial Effects for Food Applications. *J. Food Sci. Technol.* 52, 2934–2941. doi:10.1007/s13197-014-1334-6

Majdalawieh, A. F., Massri, M., and Nasrallah, G. K. (2017). A Comprehensive Review on the AnticancerProperties and Mechanisms of Action of Sesamin, a Lignan in Sesame Seeds (*Sesamum indicum*). *Eur. J. Pharmacol.* 815, 512–521. doi:10.1016/j.ejphar.2017.10.020

Matveeva, T., Khafizova, G., and Sokornova, S. (2020). In Search of Herbal Anti-SARS-cov2 Compounds. *Front. Plant Sci.* 11, 589998. doi:10.3389/fpls.2020.589998

Maurya, D. K., and Sharma, D. (2020). Evaluation of Traditional Ayurvedic Kadha for Prevention and Management of the Novel Coronavirus (SARS-CoV-2) Using *In Silico* Approach. *J. Biomol. Struct. Dyn.* 30, 1–16. doi:10.1080/07391102.2020.1852119

Michailidis, D., Angelis, A., Aligiannis, N., Mitakou, S., and Skaltsounis, L. (2019). Recovery of Sesamin, Sesamolin, and Minor Lignans from Sesame Oil Using Solid Support-free Liquid-Liquid Extraction and Chromatography Techniques and Evaluation of Their Enzymatic Inhibition Properties. *Front. Pharmacol.* 10, 723. doi:10.3389/fphar.2019.00723

Mishra, A., Pathak, Y., Kumar, A., Mishra, S. K., and Tripathi, V. (2021). Natural Compounds as Potential Inhibitors of SARS-CoV-2 Main Protease: An In-Silico Study. *Asian Pac. J. Trop. Biomed.* 11, 155–163. doi:10.4103/2221-1691.310202

Mitra, D., Verma, D., Mahakur, B., Kamboj, A., Srivastava, R., Gupta, S., et al. (2021). Molecular Docking and Simulation Studies of Natural Compounds of *Vitex negundo* L. Against Papain-Like Protease (PLpro) of SARS CoV-2 (Coronavirus) to Conquer the Pandemic Situation in the World. *J. Biomol. Struct. Dyn.* 18, 1–22. doi:10.1080/07391102.2021.1873185

Miyahara, Y., Hibasami, H., Katsuzaki, H., Imai, K., Osawa, T., Ina, K., et al. (2001). Sesaminol from Sesame Seed Induces Apoptosis in Human Lymphoid Leukemia Molt 4B Cells. *Int. J. Mol. Med.* 7, 485–488. doi:10.3892/ijmm.7.5.485

Morris, G. M., Huey, R., Lindstrom, W., Sanner, M. F., Belew, R. K., Goodsell, D. S., et al. (2009). AutoDock4 and AutoDockTools4: Automated Docking with Selective Receptor Flexibility. *J. Comput. Chem.* 30, 2785–2791. doi:10.1002/jcc.21256

Muhammad, I. A., Muangchoo, K., Muhammad, A., Ajingi, Y. S., Muhammad, I. Y., Umar, I. D., et al. (2020). A Computational Study to Identify Potential Inhibitors of SARS-CoV-2 Main Protease (Mpro) from Eucalyptus Active Compounds. *Computation* 8, 79. doi:10.3390/computation8030079

Nagendra Prasad, M. N., Sanjay, K. R., and Prasad, D. (2012). A Review on Nutritional and Nutraceutical Properties of Sesame. *J. Nutr. Food Sci.* 02, 2. doi:10.4172/2155-9600.1000127

O'Boyle, N. M., Banck, M., James, C. A., Morley, C., Vandermeersch, T., and Hutchison, G. R. (2011). Open Babel: An Open Chemical Toolbox. *J. Cheminform* 3, 33. doi:10.1186/1758-2946-3-33

Ou, T., Mou, H., Zhang, L., Ojha, A., Choe, H., and Farzan, M. (2021). Hydroxychloroquine-mediated Inhibition of SARS-CoV-2 Entry is Attenuated by TMPRSS2. *PLOS Pathog.* 17, e1009212. doi:10.1371/journal.ppat.1009212

Pandey, A. K., and Verma, S. (2020). An In-Silico Evaluation of Dietary Components for Structural Inhibition of SARS-Cov-2 Main Protease. *J. Biomol. Struct. Dyn.* 0, 1–7. doi:10.1080/07391102.2020.1809522

Pant, S., Singh, M., Ravichandiran, V., Murty, U. S. N., and Srivastava, H. K. (2020). Peptide-like and Small-Molecule Inhibitors against Covid-19. *J. Biomol. Struct. Dyn.* 39, 2904–2913. doi:10.1080/07391102.2020.1757510

Park, J.-Y., Ko, J.-A., Kim, D. W., Kim, Y. M., Kwon, H.-J., Jeong, H. J., et al. (2015). Chalcones Isolated fromAngelica Keiskeiinhibit Cysteine Proteases of SARS-CoV. *J. Enzyme Inhib. Med. Chem.* 31, 23–30. doi:10.3109/14756366.2014.1003215

Park, S.-H., Ryu, S.-N., Bu, Y., Kim, H., Simon, J. E., and Kim, K.-S. (2010). Antioxidant Components as Potential Neuroprotective Agents in Sesame (Sesamum indicumL.). *Food Rev. Int.* 26, 103–121. doi:10.1080/87559120903564464

Pathak, N., Bhaduri, A., and Rai, A. K. (2019). "Sesame: Bioactive Compounds and Health Benefits," in *Bioactive Molecules in Food* (Switzerland: Springer International Publishing), 181–200. doi:10.1007/978-3-319-78030-6_59

Pathak, Y., Mishra, A., Choudhir, G., Kumar, A., and Tripathi, V. (2021). Rifampicin and Letermovir as Potential Repurposed Drug Candidate for COVID-19 Treatment: Insights from an In-Silico Study. *Pharmacol. Rep.* 73, 926–938. doi:10.1007/s43440-021-00228-0

Prasanth, D. S. N. B. K., Murahari, M., Chandramohan, V., Bhavya, G., Lakshmana Rao, A., Panda, S. P., et al. (2021). In-silico Strategies of Some Selected Phytoconstituents from Melissa Officinalis as SARS CoV-2 Main Protease and Spike Protein (COVID-19) Inhibitors. *Mol. Simulation* 47, 457–470. doi:10.1080/08927022.2021.1880576

Raj, V., Park, J. G., Cho, K.-H., Choi, P., Kim, T., Ham, J., et al. (2021). Assessment of Antiviral Potencies of Cannabinoids against SARS-CoV-2 Using Computational and *In Vitro* Approaches. *Int. J. Biol. Macromolecules* 168, 474–485. doi:10.1016/j.ijbiomac.2020.12.020

Romeo, I., Mesiti, F., Lupia, A., and Alcaro, S. (2021). Current Updates on Naturally Occurring Compounds Recognizing SARS-CoV-2 Druggable Targets. *Molecules* 26, 632. doi:10.3390/molecules26030632

Rothe, C., Schunk, M., Sothmann, P., Bretzel, G., Froeschl, G., Wallrauch, C., et al. (2020). Transmission of 2019-nCoV Infection from an Asymptomatic Contact in Germany. *N. Engl. J. Med.* 382, 970–971. doi:10.1056/nejmc2001468

Rout, J., Swain, B. C., and Tripathy, U. (2020). In Silico investigation of Spice Molecules as Potent Inhibitor of SARS-CoV-2. *J. Biomol. Struct. Dyn.* 17, 1–15. doi:10.1080/07391102.2020.1819879

Russell, T. W., Golding, N., Golding, N., Hellewell, J., Abbott, S., Wright, L., et al. (2020). Reconstructing the Early Global Dynamics of Under-ascertained COVID-19 Cases and Infections. *BMC Med.* 18, 332. doi:10.1186/s12916-020-01790-9

Sargsyan, K., Grauffel, C., and Lim, C. (2017). How Molecular Size Impacts RMSD Applications in Molecular Dynamics Simulations. *J. Chem. Theor. Comput.* 13, 1518–1524. doi:10.1021/acs.jctc.7b00028

Schüttelkopf, A. W., and van Aalten, D. M. F. (2004). PRODRG: a Tool for High-Throughput Crystallography of Protein-Ligand Complexes. *Acta Crystallogr. D Biol. Cryst.* 60, 1355–1363. doi:10.1107/s0907444904011679

Shamsi, A., Mohammad, T., Anwar, S., Amani, S., Khan, M. S., Husain, F. M., et al. (2021). Potential Drug Targets of SARS-CoV-2: From Genomics to Therapeutics. *Int. J. Biol. Macromolecules* 177, 1–9. doi:10.1016/j.ijbiomac.2021.02.071

Shi, Y., Yu, X., Zhao, H., Wang, H., Zhao, R., and Sheng, J. (2020). Host Susceptibility to Severe COVID-19 and Establishment of a Host Risk Score: Findings of 487 Cases Outside Wuhan. *Crit. Care* 24, 108. doi:10.1186/s13054-020-2833-7

Singh, G., Tiwari, A., Choudhir, G., P, H., Kumar, A., and Sharma, S. (2021). Unraveling the Potential Role of Bioactive Molecules Produced by *Trichoderma* spp. As Inhibitors of Tomatinase Enzyme Having an Important Role in Wilting Disease: An *In-Silico* Approach. *J. Biomol. Struct. Dyn.* 15, 1–10. doi:10.1080/07391102.2021.1898476

Sinha, S. K., Shakya, A., Prasad, S. K., Singh, S., Gurav, N. S., Prasad, R. S., et al. (2020). An In-Silico Evaluation of Different Saikosaponins for Their Potency Against SARS-CoV-2 Using NSP15 and Fusion Spike Glycoprotein as Targets. *J. Biomol. Struct. Dyn.* 39, 3244–3255. doi:10.1080/07391102.2020.1762741

Su, S., Wong, G., Shi, W., Liu, J., Lai, A. C. K., Zhou, J., et al. (2016). Epidemiology, Genetic Recombination, and Pathogenesis of Coronaviruses. *Trends Microbiol.* 24, 490–502. doi:10.1016/j.tim.2016.03.003

Sultana, J., Crisafulli, S., Gabbay, F., Lynn, E., Shakir, S., and Trifirò, G. (2020). Challenges for Drug Repurposing in the COVID-19 Pandemic Era. *Front. Pharmacol.* 11, 588654. doi:10.3389/fphar.2020.588654

Suravajhala, R., Parashar, A., Malik, B., Nagaraj, A. V., Padmanaban, G., Kavi Kishor, P., et al. (2020). Comparative Docking Studies on Curcumin with COVID-19 Proteins. *Netw. Model. Anal. Health Inform. Bioinform* 10, 44. doi:10.20944/preprints202005.0439.v1

Tang, W., Hu, T., Hu, B., Jin, C., Wang, G., Xie, C., et al. (2020). Prevalence and Correlates of PTSD and Depressive Symptoms One Month after the Outbreak of the COVID-19 Epidemic in a Sample of home-quarantined Chinese university Students. *J. Affective Disord.* 274, 1–7. doi:10.1016/j.jad.2020.05.009

Tock, M. J., Chen, W., Combrinck, S., Sandasi, M., Kamatou, G. P. P., and Viljoen, A. M. (2021). Exploring the Phytochemical Variation of Non-volatile Metabolites within Three South African Salvia Species Using UPLC-MS Fingerprinting and Chemometric Analysis. *Fitoterapia* 152, 104940. doi:10.1016/j.fitote.2021.104940

Tripathi, M. K., Singh, P., Sharma, S., Singh, T. P., Ethayathulla, A. S., and Kaur, P. (2020). Identification of Bioactive Molecule from Withania Somnifera (Ashwagandha) as SARS-CoV-2 Main Protease Inhibitor. *J. Biomol. Struct. Dyn.* 39, 5668–5681. doi:10.1080/07391102.2020.1790425

Ullrich, S., and Nitsche, C. (2020). The SARS-CoV-2 Main Protease as Drug Target. *Bioorg. Med. Chem. Lett.* 30, 127377. doi:10.1016/j.bmcl.2020.127377

Uncu, A. Ö., Gultekin, V., Allmer, J., Frary, A., and Doganlar, S. (2015). Genomic Simple Sequence Repeat Markers Reveal Patterns of Genetic Relatedness and Diversity in Sesame. *Plant Genome* 8, 0087. doi:10.3835/plantgenome2014.11.0087

Varadharajan, V., Arumugam, G. S., and Shanmugam, S. (2021). Isatin-based Virtual High Throughput Screening, Molecular Docking, DFT, QM/MM, MD and MM-PBSA Study of Novel Inhibitors of SARS-CoV-2 Main Protease. *J. Biomol. Struct. Dyn.* 25, 1–16. doi:10.1080/07391102.2021.1904003

Veber, D. F., Johnson, S. R., Cheng, H.-Y., Smith, B. R., Ward, K. W., and Kopple, K. D. (2002). Molecular Properties that Influence the Oral Bioavailability of Drug Candidates. *J. Med. Chem.* 45, 2615–2623. doi:10.1021/jm020017n

Verdoni, L., Mazza, A., Gervasoni, A., Martelli, L., Ruggeri, M., Ciuffreda, M., et al. (2020). An Outbreak of Severe Kawasaki-like Disease at the Italian Epicentre of the SARS-CoV-2 Epidemic: An Observational Cohort Study. *The Lancet* 395, 1771–1778. doi:10.1016/s0140-6736(20)31103-x

Wadood, A., Ahmed, N., Shah, L., Ahmad, A., Hassan, H., and Shams, S. (2013). In-silico Drug Design: An Approach Which Revolutionarised the Drug Discovery Process. *OA Drug Des. Deliv.* 1, 3. doi:10.13172/2054-4057-1-1-1119

Wahedi, H. M., Ahmad, S., and Abbasi, S. W. (2020). Stilbene-based Natural Compounds as Promising Drug Candidates against COVID-19. *J. Biomol. Struct. Dyn.* 39, 3225–3234. doi:10.1080/07391102.2020.1762743

Wang, L., Wang, Y., Ye, D., and Liu, Q. (2020a). Review of the 2019 Novel Coronavirus (SARS-CoV-2) Based on Current Evidence. *Int. J. Antimicrob. Agents* 55, 105948. doi:10.1016/j.ijantimicag.2020.105948

Wang, W., Xu, Y., Gao, R., Lu, R., Han, K., Wu, G., et al. (2020b). Detection of SARS-CoV-2 in Different Types of Clinical Specimens. *JAMA* 323, 1843–1844. doi:10.1001/jama.2020.3786

Watanabe, M., Iizumi, Y., Sukeno, M., Iizuka-Ohashi, M., Sowa, Y., and Sakai, T. (2017). The Pleiotropic Regulation of Cyclin D1 by Newly Identified Sesaminol-Binding Protein ANT2. *Oncogenesis* 6, e311. doi:10.1038/oncsis.2017.10

Woo, P. C. Y., Lau, S. K. P., Chu, C.-m., Chan, K.-h., Tsoi, H.-w., Huang, Y., et al. (2005). Characterization and Complete Genome Sequence of a Novel Coronavirus, Coronavirus HKU1, from Patients with Pneumonia. *J. Virol.* 79, 884–895. doi:10.1128/jvi.79.2.884-895.2005

Wu, A., Peng, Y., Huang, B., Ding, X., Wang, X., Niu, P., et al. (2020a). Genome Composition and Divergence of the Novel Coronavirus (2019-nCoV) Originating in China. *Cell Host Microbe* 27, 325–328. doi:10.1016/j.chom.2020.02.001

Wu, Y.-C., Chen, C.-S., and Chan, Y.-J. (2020b). The Outbreak of COVID-19: An Overview. *J. Chin. Med. Assoc.* 83, 217–220. doi:10.1097/jcma.0000000000000270

Wu, Z., and McGoogan, J. M. (2020). Characteristics of and Important Lessons from the Coronavirus Disease 2019 (COVID-19) Outbreak in China. *JAMA* 323, 1239. doi:10.1001/jama.2020.2648

Xu, X.-W., Wu, X.-X., Jiang, X.-G., Xu, K.-J., Ying, L.-J., Ma, C.-L., et al. (2020). Clinical Findings in a Group of Patients Infected with the 2019 Novel Coronavirus (SARS-Cov-2) outside of Wuhan, China: Retrospective Case Series. *BMJ* 368, m606. doi:10.1136/bmj.m606

Yu, S., and Yu, M. (2020). Severe Acute Respiratory Syndrome Coronavirus 2-induced Neurological Complications. *Front. Cell Dev. Biol.* 8, 8. doi:10.3389/fcell.2020.605972

Yu, W., and MacKerell, A. D. (2016). "Computer-Aided Drug Design Methods," in *Methods in Molecular Biology*. (New York: Springer), 85–106. doi:10.1007/978-1-4939-6634-9_5

Yu, Y., Xu, D., Fu, S., Zhang, J., Yang, X., Xu, L., et al. (2020). Patients with COVID-19 in 19 ICUs in Wuhan, China: a Cross-Sectional Study. *Crit. Care* 24, 219. doi:10.1186/s13054-020-02939-x

Yuan, M., Wu, N. C., Zhu, X., Lee, C.-C. D. D., So, R. T. Y., Lv, H., et al. (2020). A Highly Conserved Cryptic Epitope in the Receptor Binding Domains of SARS-CoV-2 and SARS-CoV. *Science* 368, 630–633. doi:10.1126/science.abb7269

Zhang, L., Lin, D., Sun, X., Curth, U., Drosten, C., Sauerhering, L., et al. (2020). Crystal Structure of SARS-CoV-2 Main Protease Provides a Basis for Design of Improved α-ketoamide Inhibitors. *Science* 368, 409–412. doi:10.1126/science.abb3405

Conflict of Interest: The authors declare that the research was conducted in the absence of any commercial or financial relationships that could be construed as a potential conflict of interest.

Publisher's Note: All claims expressed in this article are solely those of the authors and do not necessarily represent those of their affiliated organizations, or those of the publisher, the editors, and the reviewers. Any product that may be evaluated in this article, or claim that may be made by its manufacturer, is not guaranteed or endorsed by the publisher.

frontiers in Pharmacology

ORIGINAL RESEARCH
published: 14 October 2021
doi: 10.3389/fphar.2021.746729

Effect of Prophylactic Use of Intranasal Oil Formulations in the Hamster Model of COVID-19

Zaigham Abbas Rizvi[1], Manas Ranjan Tripathy[1], Nishant Sharma[2], Sandeep Goswami[1], N Srikanth[3], J. L. N. Sastry[4], Shailendra Mani[2], Milan Surjit[2], Amit Awasthi[1] and Madhu Dikshit[5]**

[1]Immuno-biology Laboratory, Infection and Immunology Centre, Translational Health Science and Technology Institute, NCR-Biotech Science Cluster, Faridabad, India, [2]Infection and Immunology Centre, Translational Health Science and Technology Institute, NCR-Biotech Science Cluster, Faridabad, India, [3]DG(I/C), Central Council for Ayurvedic Sciences, New Delhi, India, [4]CEO-National Medicinal Plants Board, Ministry of AYUSH, New Delhi, India, [5]Non-communicable Disease Centre, Translational Health Science and Technology Institute, NCR-Biotech Science Cluster, Faridabad, India

Severe acute respiratory syndrome coronavirus 2 (SARS-CoV2) infection initiates with viral entry in the upper respiratory tract, leading to coronavirus disease 2019 (COVID-19). Severe COVID-19 is characterized by pulmonary pathologies associated with respiratory failure. Thus, therapeutics aimed at inhibiting the entry of the virus or its internalization in the upper respiratory tract are of interest. Herein, we report the prophylactic application of two intranasal formulations provided by the National Medicinal Plant Board (NMPB), Anu oil and til tailya, in the hamster model of SARS-CoV-2 infection. Prophylactic intra-nasal instillation of these oil formulations exhibited reduced viral load in lungs and resulted in reduced body weight loss and lung-pneumonitis. In line with reduced viral load, histopathological analysis revealed a reduction in lung pathology in the Anu oil group as compared to the control infected group. However, the til tailya group did not show a significant reduction in lung pathology. Furthermore, molecular analysis using mRNA expression profiling indicated reduced expression of pro-inflammatory cytokine genes, including Th1 and Th17 cytokines for both the intranasal formulations as a result of decreased viral load. Together, the prophylactic intranasal application of Anu oil seems to be useful in limiting both viral load and severity in SARS-CoV2 infection in the hamster model.

Keywords: COVID-19, intranasal, herbal, AYUSH, prophylactic

OPEN ACCESS

Edited by:
Brijesh Kumar Singh,
Duke-NUS Medical School, Singapore

Reviewed by:
Pradeep Bist,
Duke-NUS Medical School, Singapore
Francesco Sessa,
University of Foggia, Italy

****Correspondence:***
Madhu Dikshit
drmadhudikshit@gmail.com
Amit Awasthi
aawasthi@thsti.res.in

Specialty section:
This article was submitted to Experimental Pharmacology and Drug Discovery, a section of the journal Frontiers in Pharmacology

Received: *24 July 2021*
Accepted: *10 September 2021*
Published: *14 October 2021*

Citation:
Rizvi ZA, Tripathy MR, Sharma N, Goswami S, Srikanth N, Sastry JN, Mani S, Surjit M, Awasthi A and Dikshit M (2021) Effect of Prophylactic Use of Intranasal Oil Formulations in the Hamster Model of COVID-19. Front. Pharmacol. 12:746729. doi: 10.3389/fphar.2021.746729

INTRODUCTION

Since the first report of Coronavirus Disease (COVID-19) in Wuhan in December 2019, a number of COVID-19 incidences have exploded around the globe leading it to be declared a pandemic by the WHO (Chen and Li, 2020; Wang et al., 2020) (https://www.ecdc.europa.eu/en/geographical-distribution-2019-ncov-cases). As of September 6, 2021, the total number of coronavirus infection incidences was 221,846,104 with around 4,586,516 deaths globally, with 441,075 mortalities in India alone. The majority of the coronavirus cases are asymptomatic and do not require aggressive treatment. However, an estimated 13.8% of the infected individuals are at risk of developing a severe form of COVID-19, which could be characterized by either one or all of the following COVID-19 symptoms: respiratory distress, high fever, loss of taste and smell, and diarrhea (Chen and Li, 2020; Wang et al., 2020). In addition, up to around 6% of COVID-19 cases end up with respiratory failure due to cytokine storm, cardiovascular complications, and

multiple organ failure (https://www.who.int/emergencies/diseases/novel-coronavirus-2019) (Guan et al., 2020; Wang et al., 2020). As is known for other respiratory viruses, SARS-CoV2 initially infects the upper respiratory tract and then rapidly spreads to the lower respiratory tract (Chen and Li, 2020). During an active infection, the virus can be transmitted and spread from both symptomatic and asymptomatic individuals via respiratory droplets generated through coughing, sneezing, or hyperventilation via the airborne route (Gandhi et al., 2020; Guan et al., 2020).

Global health research has primarily focused on vaccine development against COVID-19, with active vaccination being the current strategy to protect COVID-19–related mortalities (Poland et al., 2020a; Dong et al., 2020). Given the emergence of new SARS-CoV2 variants, the protective efficacy of vaccines could be reduced; hence, therapeutics that may prevent viral entry, replication, and transmission are highly desirable. In line with this, pharmacological agents such as intranasal delivery of TLR2/6 agonist or lipopeptide agents, intranasal administration of neutralizing antibodies, and intranasal gene therapy are currently being explored as potential strategies to inhibit the host–pathogen interaction and limit the infection (Hassan et al., 2020; Boiardi and Stebbing, 2021; Ku et al., 2021; Kunzelmann, 2021; Proud et al., 2021; Vries et al., 2021). For example, intranasal corticosteroid spray for the recovery of the sense of smell is under clinical trials for COVID-19 patients (Abdelalim et al., 2021). Since pharmaceutical drugs may have many off-target effects, therapeutics based on herbal extracts have recently gained much attention (Matveeva et al., 2020; De Pellegrin et al., 2021; Jan et al., 2021; Li et al., 2021). Here, we evaluated the efficacy of two ayurvedic intranasal (herbal) oil formulations, Anu oil and til tailya (Duraipandi and Selvakumar, 2020), in hamster SARS-CoV2 challenge model.

Sesame oil (til tailya, TT) is the oil derived from a plant (*Sesamum indicum*) which is a classical ayurvedic medicine mentioned in Charak Samhita (https://niimh.nic.in/ebooks/ecaraka/). On the other hand, a classical ayurvedic medicine, Anu tailya was used by Maharishi Charak more than 5,000 years ago for therapeutic purposes. Anu oil consists of extracted oils from several important medicinal plants like nāgarmothā (*Cyperus scariosus*), jīvantī (*Leptadenia reticulata*), sweta candana (*Santalum album*), jala (*Pavonia odorata*), Pṛśniparṇī (*Uraria picta*), bela (*Aegle marmelos*), devdāru (*Cedrus deodara*), dāruharidrā (*Berberis aristata*), tejpatra (*Cinnamomum tamala*), dālacīnī (*Cinnamomum verum*), kamala keṣara (*Nelumbo nucifera*), sevya (*Chrysopogon zizanioides*), viḍañga (*Embelia ribes*), utpala (*Nymphaeanouchali*), anantmūla (*Hemidesmus indicus*), tila tailya (*Sesamum indicum*), muleṭhī (*Glycyrrhiza glabra*), plawa (*Cyperus platyphyllus*), agarū (*Aquilaria agallocha*), satāvarī (*Asparagus racemosus*), bṛhatī (*Solanum indicum*), kaṇṭakārī (*Solanum surattense*), surbhi (*Pluchea lanceolata*), sālaparṇī (*Desmodium gangeticum*), truṭi (*Elettaria* cardamomum), reṇukā (*Vitex agnus-castus*), and ajadugdha (Duraipandi and Selvakumar, 2020; see the enclosed supplement information). Here, we report that intranasal instillation of both til tailya and Anu oil limited the viral entry and replication in the lungs associated with SARS-CoV2 infection in hamsters. However, Anu oil but not til tailya was able to rescue the lung pneumonitis and injury partly due to suppression of inflammatory cytokine response.

MATERIALS AND METHODS

Sesame oil and Anu oil (a polyherbal medicine) used in the study were prepared as per pharmacopoeial standards and were provided by the National Medicinal Plant Board (NMPB) for the study.

Animal Ethics and Biosafety Statement

6- to 9-week-old golden Syrian hamsters were acclimatized in biosafety level-2 (BSL-2) for 1 week and then infected in the animal BSL3 (ABSL-3) institutional facility. The animals were maintained under the 12-h light and dark cycle and fed a standard pellet diet and water ad libitum. All the experimental protocols involving the handling of virus culture, and animal infection were approved by RCGM, institutional biosafety, and IAEC Animal Ethics Committee (IAEC/THSTI/105).

Virus Culture and Titration

SARS-related coronavirus 2, isolate USA-WA1/2020 virus was grown and titrated in vero E6 cell line cultured in Dulbecco's modified Eagle medium (DMEM) complete media containing 4.5 g/L D-glucose, 100,000 U/L penicillin–streptomycin, 100 mg/L sodium pyruvate, 25 mM HEPES, and 2% FBS. The stocks of the virus were plaque purified at the THSTI IDRF facility inside ABSL3 following institutional biosafety guidelines.

SARS-CoV2 Infection in Golden Syrian Hamster and Ayush Herbal Extracts Dosing Regime

6- to 9-week-old golden Syrian hamsters were procured from CDRI and quarantined for 1 week at the small animal facility (SAF), THST before starting the experiment. The animals were then randomly divided into five groups containing five animals/group, namely, uninfected (UI), infected (I), and two infected groups receiving til tailya (TT) or Anu oil (AO) as therapeutic interventions, respectively. One group received intranasal installation of Anu oil, while the other group received intranasal installation of til tailya (50 ul/nostril/day) starting 5 days before infection and continued till 4 days postinfection (DPI). On the day of the challenge, intranasal administration of Anu oil and til tailya was carried out 30 min before infection. On the day of the challenge, the animals were shifted to ABSL3. Intranasal infection with live SARS-CoV2 10^5PFU/100 µl or with the DMEM mock control (for uninfected control group) was established with the help of a catheter under mild anesthetized by using ketamine (150 mg/kg) and xylazine (10 mg/kg) intraperitoneal injection inside the ABSL3 facility. All the experimental protocols involving the handling of virus culture and animal infection were approved by the RCGM, Institutional Biosafety and IAEC Animal Ethics Committee.

Gross Clinical Parameters of SARS-CoV2 Infection

All infected animals were euthanized after 4 days post-infection at ABSL3. Changes in body weight were observed each day post-challenge and plotted as percent change in the body weight. Post-sacrifice, the lungs and spleen of the animals were excised and imaged

for gross morphological changes. The left lower lobe of the lung was fixed in 10% formalin and used for histological analysis. The remaining part of the lung's left lobe was homogenized in 2 ml TRIzol solution for viral load estimation. The spleen was homogenized in 2 ml of TRIzol solution. The TRIzol samples were stored immediately at −80°C until further use. Blood of the animals was drawn through direct heart puncture, and serum was isolated and stored at -80°C until further use.

Viral Load

For viral load, estimated lungs were homogenized in TRIzol reagent (Invitrogen), and their supernatant was collected after centrifugation at 4,000 rpm for 15 min at 4°C. Thereafter, RNA was isolated by TRIzol–choloform method, and RNA yield was quantitated by nano-drop; 1 µg of total RNA was then reverse-transcribed to cDNA using the iScript cDNA synthesis kit (Biorad; #1708891) (Roche). Diluted cDNAs (1:5) were used for qPCR by using the KAPA SYBR® FAST qPCR Master Mix (5X) Universal Kit (KK4600) on the Fast 7,500 Dx real-time PCR system (Applied Biosystems), and the results were analyzed with SDS2.1 software. In brief, 200 ng of RNA was used as a template for reverse transcription polymerase chain reaction (RT-PCR). The CDC-approved commercial kit was used for the SARS-CoV-2 N gene: 5′-GACCCCAAAATCAGCGAAAT-3′ (forward), 5′-TCTGGTTAC TGCCAGTTGAATCTG-3′ (reverse). The hypoxanthine–guanine phosphoribosyltransferase (HGPRT) gene was used as an endogenous control for normalization through quantitative RT-PCR. The relative expression of each gene was expressed as fold change and was calculated by subtracting the cycling threshold (Ct) value of hypoxanthine–guanine phosphoribosyltransferase (HGPRT-endogenous control gene) from the Ct value of the target gene (ΔCT). The fold change was then calculated according to the formula POWER(2,-ΔCT)*10,000 (Malik et al., 2017).

qPCR

RNA from spleen samples was isolated as described earlier for the lung samples, and cDNA was prepared. Thereafter, the relative expression of each gene was expressed as fold change and was calculated by subtracting the cycling threshold (Ct) value of hypoxantine–guanine phosphoribosyltransferase (HGPRT-endogenous control gene) from the Ct value of target gene (ΔCT). Fold change was calculated according to the formula POWER(2,-ΔCT)*10,000 (Malik et al., 2017; Rizvi et al., 2021a). The list of the primers is provided as follows in **Table 1**

Histology

The lung of the euthanized animals was fixed in 10% formalin solution and then embedded in paraffin. Sample embedded paraffin blocks were then cut into 3-µm fine sections and mounted on silicone-coated glass slides. The slides were then stained with hematoxylin and eosin dye, as previously described (Rizvi et al., 2018). Each stained sample was then analyzed and captured at ×40 magnification. Assessment for the histological score was carried out through blind scoring for each sample by a professional histologist.

Statistical Analysis

Results from the experiments were analyzed and plotted by using GraphPad Prism 7.0 software. The graph for percent change in body weight, gene expression, and lung histology scores were compared and analyzed by using the Student t-test or one-way ANOVA, with $n = 5$ samples per group. The p-value of less than 0.05 and was considered as statistically significant.

RESULTS

Prophylactic Use of Intranasal Instillation of Ayush Oil Formulations Prevents SARS-CoV2 Infection and Associated Gross Clinical Parameters

SARS-CoV2 infection in hamsters peaks in 4–5 days and is characterized by a reduction in body weight and appearance of pneumonitis in the lungs and splenomegaly (Imai et al., 2020; Sia et al., 2020; Rizvi et al., 2021b; Chan et al., 2020). These defined gross clinical parameters were recorded for all the groups,

TABLE 1 | Primer sequences.

Gene	Forward	Reverse
HGPRT	GATAGATCCACTCCCATAACTG	TACCTTCAACAATCAAGACATTC
Tryptase β2	TCGCCACTGTATCCCCTGAA	CTAGGCACCCTTGACTTTGC
Chymase	ATGAACCACCCTCGGACACT	AGAAGGGGGCTTTGCATTCC
muc1	CGGAAGAACTATGGGCAGCT	GCCACTACTGGGTTGGTGTAAG
Sftpd	TGAGCATGACAGACGTGGAC	GGCTTAGAACTCGCAGACGA
Eotaxin	ATGTGCTCTCAGGTCATCGC	TCCTCAGTTGTCCCCATCCT
PAI-1	CCGTGGAACCAGAACGAGAT	ACCAGAATGAGGCGTGTCAG
IFNy	TGTTGCTCTGCCTCACTCAGG	AAGACGAGGTCCCCTCCATTC
TNFa	AGAATCCGGGCAGGTCTACT	TATCCCGGCAGCTTGTGTTT
IL13	AAATGGCGGGTTCTGTGC	AATATCCTCTGGGTCTTGTAGATGG
IL17 A	ATGTCCAAACACTGAGGCCAA	GCGAAGTGGATCTGTTGAGGT
IL10	GGTTGCCAAACCTTATCAGAA ATG	TTCACCTGTTCCACAGCCTTG
IL6	GGACAATGACTATGTGTTGTTAGAA	AGGCAAATTTCCCAATTGTATCCAG
CXCL10	TGGAAATTATTCCTGCAAGTCA	GTG ATC GGC TTC TCT CTG GT

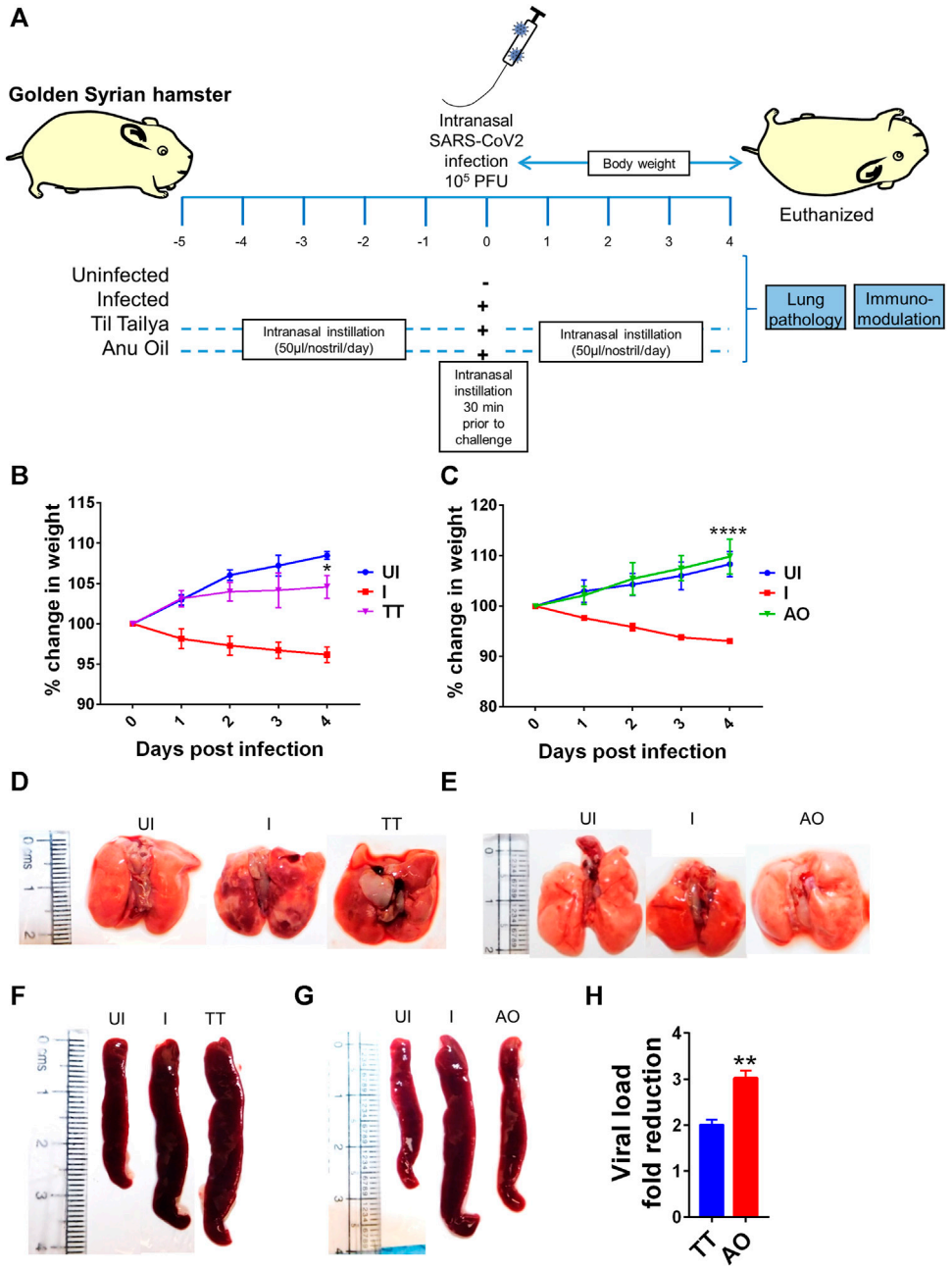

FIGURE 1 | Effect of intranasal instillation of Anu oil and til tailya on gross clinical parameters and lung viral load in SARS-CoV2 infected hamsters. **(A)** Schematic outlines the study design. Prophylactic treatment regime was adopted for Anu oil (AO) and til tailya (TT) with each animal receiving (50 µl/nostril/day) intranasal instillation of Anu oil, til tailya, or mock control 5 days before challenge and then continued till after infection till end point (i.e., 4 days postinfection). One group was challenge and received live infection (I); the other group of animals was unchallenged healthy control (UI). On the day of challenge, the animals were given intranasal oil-instillation 30 min prior to challenge with SARS-CoV2. **(B and C)** Line graph showing mean % change in body weight post-infection ±standard error mean (SEM). **(D and E)** Images of the excised lungs showing gross morphology with pneumonitis region (dark red patches). **(F and G)** Images of excised spleen indicating changes in the spleen length. **(H)** Bar graph showing mean fold reduction in lung viral load ±SEM as compared to the infected **(I)** control. *$p < 0.05$, **$p < 0.01$, ****$p < 0.0001$ (t-test).

that is, uninfected control (UI), infected control (I), and infected hamsters receiving either Til tailya (TT) or Anu oil (AO) intranasal formulations (50 µl/nostril/day). Treatment of TT and AO was started 5 days before SARS-CoV2 live virus challenge and was continued till the end of the experiment, that is, 4 days postinfection (dpi), as presented schematically

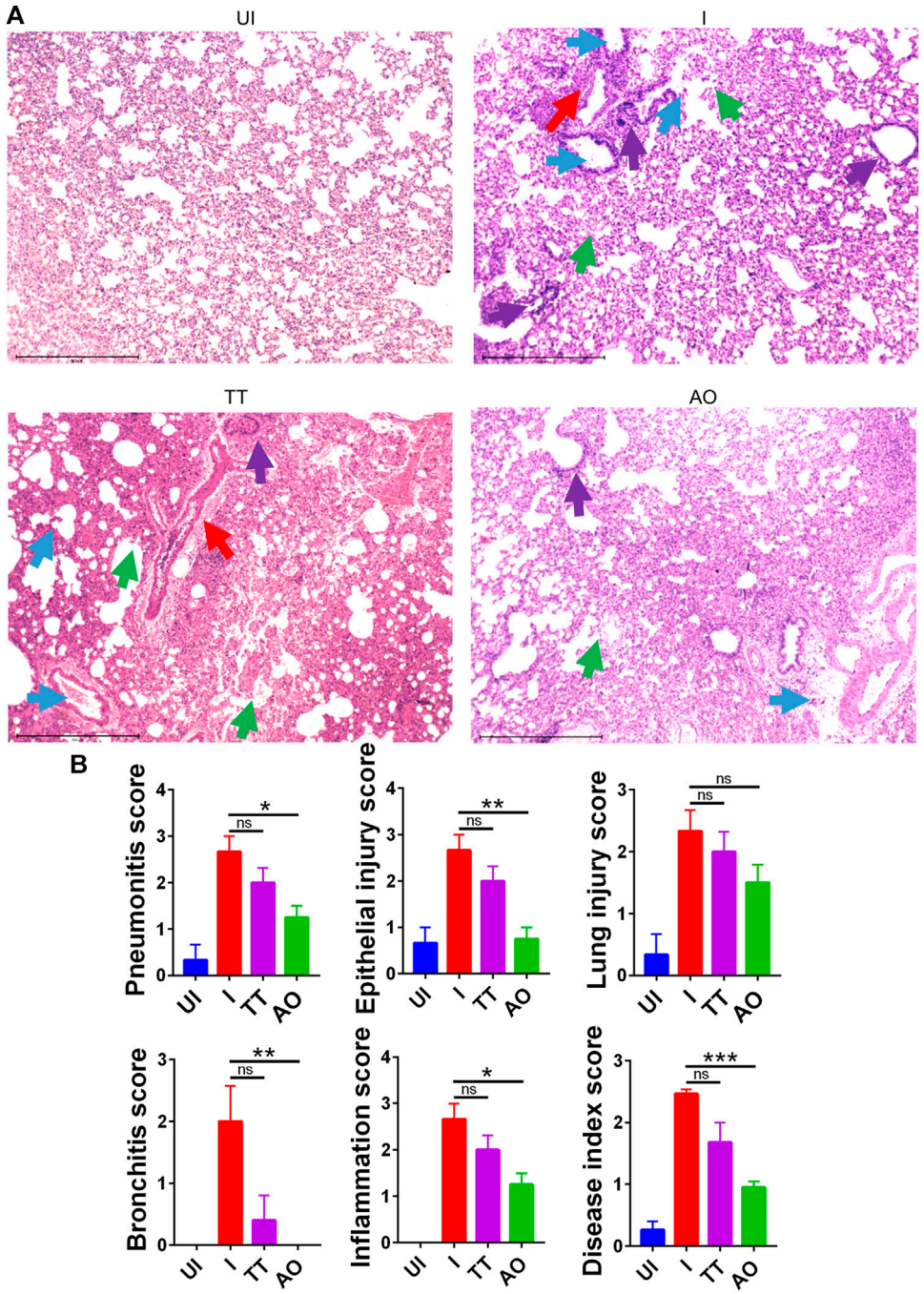

FIGURE 2 | H&E–stained lung sections showing histopathology and its assessment. **(A)** images of H&E-stained lungs at ×40 magnification showing regions of pneumonitis (blue arrow), bronchitis (red arrow), epithelial injury (green arrow), and inflammation (purple arrow) along with their **(B)** histological score for pneumonitis, inflammation, lung injury, alveolar epithelial cells, bronchitis, and overall disease score for different groups UI, I, TT, and AO on day 4 postinfection. *$p < 0.05$, **$p < 0.01$, ***$p < 0.001$ (one-way ANOVA).

in the study design (**Figure 1A**). In line with the earlier published reports, a decrease in the body weight of SARS-CoV2–infected hamsters was observed with 5–8% body weight reduction on 4 days dpi. Hamsters receiving TT or AO, before SARS-CoV2 infection, did not lose body weight as observed in the SARS-CoV2–infected group (**Figures 1B,C**). SARS-CoV2 infection in the hamster model is characterized by lung inflammation, pneumonitis, and cytokines release (Afrin et al., 2020; Chen and Li, 2020; Moore and June 2020). To further understand the lung-associated pathologies, gross morphological changes of the excised lungs were compared between healthy, SARS-CoV2–infected, and SARS-CoV2–infected plus oil formulated

groups. There was a reduction in the regions of pneumonitis in the excised lungs of the AO group, but not the TT group, as compared to infection control (**Figures 1D,E**). As reported earlier, splenomegaly is one of the critical parameters indicating active infection (Rizvi et al., 2021b). Thus, we tested the splenomegaly between different groups and found that AO, but not TT, showed inhibition in splenomegaly as compared to the SARS-CoV2–infected hamsters (**Figures 1F,G**). We also evaluated the lung viral load at four dpi and calculated the fold reduction in viral load in AO- and TT-treated groups as compared to the SARS-CoV2–infected groups. Our data indicate that compared to the SARS-CoV2–infected group, viral loads in AO- and TT-treated groups were ~3- and ~2-fold less, respectively (**Figure 1H**). Together, these data indicated that prophylactic use of intranasal instillation of TT and AO resulted in decreased lung viral load with the AO group, showing better protection in gross clinical parameters.

Prophylactic Use of Anu Oil Reduces SARS-CoV2–Induced Lung Pathology in Hamsters

Since gross clinical parameters and lung viral load data suggested protection from SARS-CoV2 infection in AO and TT groups, we set out to study the mitigation of pulmonary pathologies such as lung injury, alveolar epithelial injury, bronchitis, pneumonitis, and inflammation using histological analysis (Bao et al., 2020; Lee et al., 2020; Leng et al., 2020; Rizvi et al., 2021b). Hematoxylin and eosin (H and E)–stained lung data showed a reduction in alveolar epithelial injury, inflammation, and pneumonitis in SARS-CoV2–infected AO-treated hamsters as compared to SARS-CoV2–infected hamsters. There was no sign of bronchitis in SARS-CoV2–infected AO-treated hamsters with overall significant mitigation in the disease score as compared to SARS-CoV2–infected hamsters (**Figures 2A,B**). Hamsters treated with TT however showed little or no improvement in lung injury and overall disease score as compared to the infected control (**Figures 2A,B**). Together, lung pathology associated with SARS-CoV2 was found to be resolved in the AO group but not in the TT group, with around 1.5-fold rescue in disease index in the AO group as compared to the infected control group.

Prophylactic Use of Anu Oil Prevent Lung Injury in Hamsters Associated With SARS-CoV2 Infection

Lung histology data indicated overall improvment in histological changes of SARS-CoV2–infected AO-treated groups as compared to SARS-CoV2–infected group. These data compelled us to explore the mechanism involved in the rescue of lung pathologies. Injury to the pulmonary region is characterized by elevated expression of surfactant D (sftp-D), increased mucus (muc-1) secretion, and increased expression of eotaxin, which promotes infiltration of granulocytes and mast cells and an increased risk of pulmonary thrombosis as seen in COVID-19 patients (Crouch, 2000; Guo et al., 2001; Prabhakaran et al., 2003; Xie et al., 2017; Chatterjee et al., 2020). We observed elevated levels of sftp-D, muc-1, eotaxin, muc-1, chymase, tryptase, and plasmonigen activator inhibitor-I (PAI-1: a key factor for lung fibrosis) in the lungs of infected hamsters (**Figures 3A–C**). However, prophylactic intranasal use of AO in SARS-CoV2–infected hamster significantly reduced the mRNA expression of these lung injury genes and genes that are required for chemotaxis of granulocytes and function of mast cells (**Figures 3A,B**). Prophylactic use of AO in SARS-CoV2–infected hamsters did not reduce PAI-1 expression (**Figure 3C**). In contrast to AO, TT data showed no reduction in lung injury as compared to infected control (**Figure 3A**). Surprisingly, there was a marked increase in mast cell markers in the TT group as compared to the infected control (**Figure 3B**). Overall, consistent with our lung histology data, a profound reduction in the expression of lung injury genes and mast cell markers as compared to the infected control was observed in AO-treated groups.

AO and TT Treatment Inhibits the Expression of SARS-CoV2–Induced Pro-Inflammatory Cytokines

COVID-19–related respiratory distress is associated with inflammation in the lungs. The increase in lung inflammation is characterized by the secretion of pro-inflammatory cytokines in COVID-19 patients (Iwasaki and Yang, 2020; Mathew et al., 2020; Moore and June 2020; Verity et al., 2020). Cytokine expression data from splenocytes indicate elevated expression of Th1 cytokines (IFNγ and TNFα), Th2 cytokine (IL-4, IL-13), Th17 cytokine (IL-17 A), and various other pro-inflammatory cytokine-like IL-6 and IL-13 in SARS-CoV2–infected group as compared to uninfected hamsters (**Figures 4A–D**). However, there was not much change observed in anti-inflammatory cytokine IL-10 expression as compared to the challenge control group. Prophylactic intranasal installation of AO and TT in SARS-CoV2–infected hamsters resulted in the reduction in Th1 and Th17 cell cytokines, together with pro-inflammatory cytokine expression (**Figures 4A,B,D**). However, surprisingly, only TT but not AO was able to reduce the Th2 cytokine gene expression (**Figures 4A,C**). Furthermore, we found an elevated IFN-gamma secretion in both AO- and TT-treated animals (**Figures 4A,C**). Since C-X-C motif chemokine ligand 10 (CXCL10), a chemoattractant, is an important mediator of IFN-gamma response and is secreted by various immune cells, we evaluated the mRNA expression of CXCL10 from treated (AO/TT) vs challenge (I) samples (Zhang et al., 2020). As compared to the challenge control group, neither the AO nor TT group did not show significant changes (**Figures 4B,D**). Together, we show that AO and TT reduced the pro-inflammatory cytokines.

Anu Oil Intranasal Formulation Shows More Protective Efficacy Against SARS-CoV2 Infection in Hamsters as Compared to Til Tailya Intranasal Formulation

We summarize the finding of our study and provide the first evidence that intranasal formulation such as Anu oil and til tailya

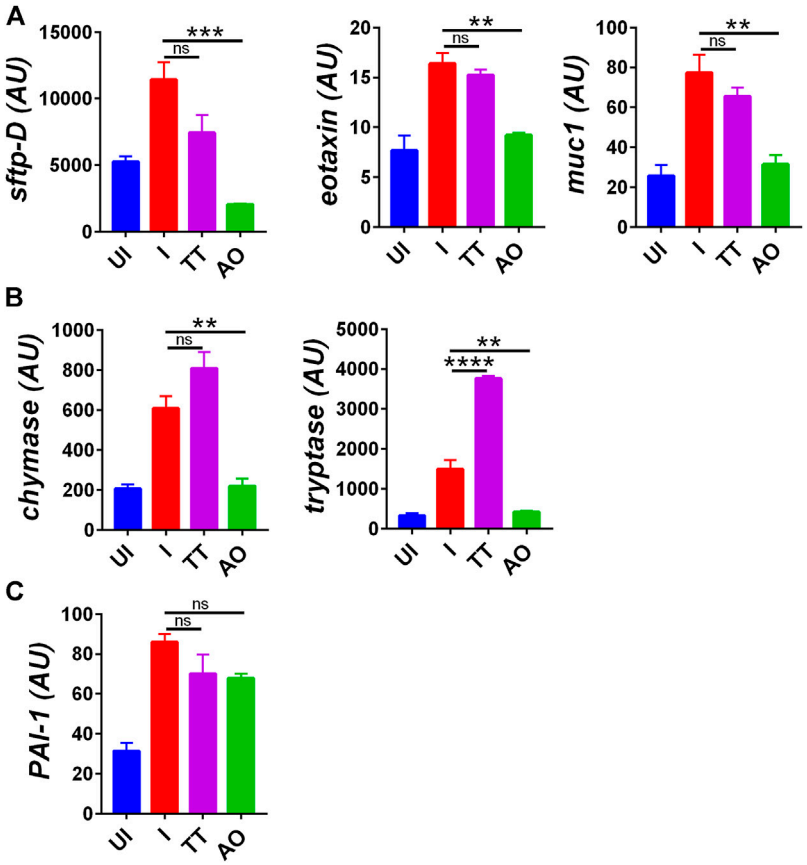

FIGURE 3 | Changes in mRNA expression of genes involved in lung injury upon AO or TT intranasal administration in hamsters infected with SARS-CoV2. Relative mRNA expression profiling was carried out in UI, I, TT, and AO lung samples for **(A)** lung injury genes **(B)** mast cell activation markers **(C)** thrombosis factor. Mean ± SEM. $^{**}p < 0.01$, $^{***}p < 0.001$, $^{****}p < 0.0001$ (one-way ANOVA).

limits viral entry and replication. However, only Anu oil but not til tailya was effective in reducing the SARS-CoV2–associated pulmonary pathologies and lung injuries, even though both AO and TT were effective in reducing the pro-inflammatory cytokine response in hamsters (**Figure 5**).

DISCUSSION

Advances in vaccine development against SARS-CoV2 Wuhan strain and aggressive vaccination strategy have significantly reduced the SARS-CoV2 infection and COVID-19 deaths worldwide (Dong et al., 2020; Poland et al., 2020a, 2020b). However, the recent rise in variant strains that show high transmission and disease severity is of concern, primarily, due to the reduced efficacy of virus neutralization in vaccinated individuals for some variant strains (Garcia-Beltran et al., 2021; Planas et al., 2021; Supasa et al., 2021). Therefore, therapeutic options are paramount in combating COVID-19.

Although several repurposed drugs are currently being used for the treatment of COVID-19 patients, they have limited efficacy. Herbal medicines or medicines derived from herbal extracts offer a safer alternative therapy due to their prolonged human use, acceptability with lesser side effects (Matveeva et al., 2020; Jan et al., 2021; Li et al., 2021). Recently, Chinese traditional medicine has gained popularity due to its antiviral efficacy in *in vitro* and animal models of SARS-CoV2 (Ling, 2020; Xiong et al., 2020; Yang et al., 2020; Jan et al., 2021; Lee et al., 2021). In India, going back to more than 3,000 years, ayurvedic medicines are considered useful for both lifestyle disorders and infectious conditions. The word ayurveda is derived from two Sanskrit words ayur (life) and veda (knowledge) (Subrahmanya et al., 2013; Banerjee et al., 2020; Girija and Sivan, 2020; Golechha, 2020; Joshi and Puthiyedath, 2020; Rastogi et al., 2020). In the present study, we investigated antiviral activity of two oil formulations, namely, til tailya and Anu oil against SARS-CoV2. Due to immiscibility of these oil formulations with culture medium, it was not possible to test them *in vitro* for their antiviral activity using VeroE6 cell line.

Therefore, in the current study, we describe the efficacy of prophylactic use of two intranasal ayurvedic oil formulations using the hamster model for SARS-CoV2 challenge. Hamsters are one of the best small animal models for SARS-CoV2 infection which mimics the viral entry and replication of the upper and the lower respiratory tract of humans (Sia et al., 2020; Rizvi et al., 2021b). Hamsters receiving Anu oil or til tailya intranasally before

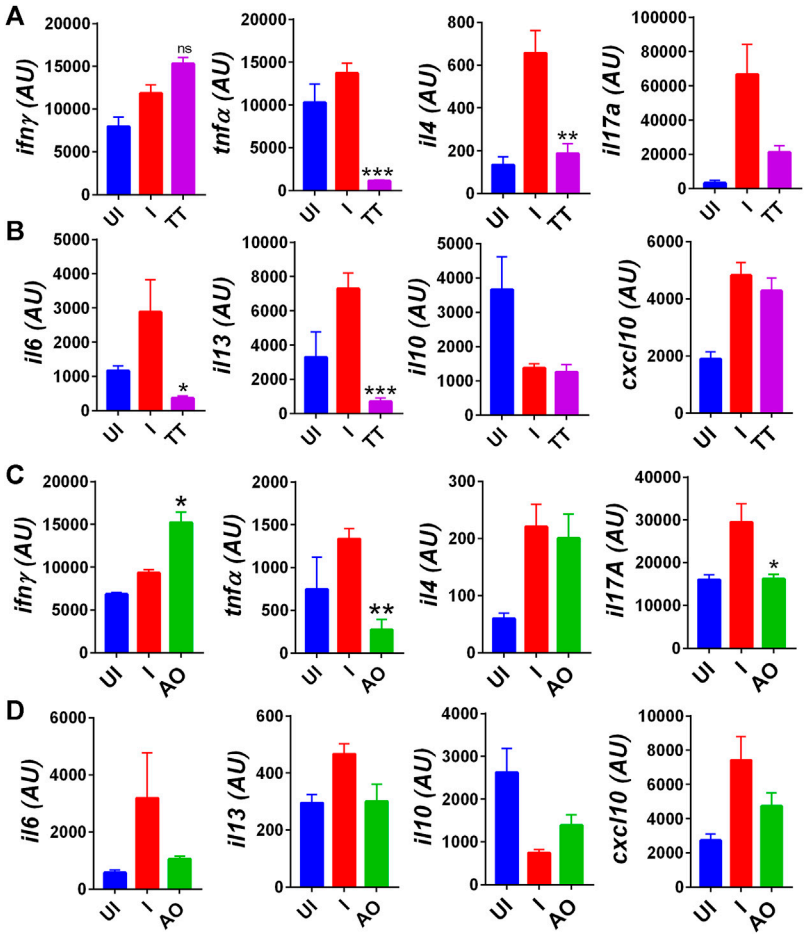

FIGURE 4 | Immuno-modulatory effect of TT and AO on cytokine expression in splenocytes. Relative mRNA expression profiling was carried out in UI, I, TT, and AO splenocytes samples for **(A)** T helper cell cytokines for TT samples. **(B)** pro-inflammatory and anti-inflammatory cytokines for TT samples. **(C)** T helper cell cytokines for AO samples. **(D)** pro-inflammatory and anti-inflammatory cytokines for AO samples. Bar graph showing mean ± SEM. ns = non-significant $^{**}p < 0.05$ $^{**}p < 0.01$, $^{***}p < 0.001$, $^{****}p < 0.0001$ (one-way ANOVA).

SARS-CoV2 infection showed reduced weight loss. Lung histology data corroborated with the gross parameter findings showed lesser SARS-CoV2–related histopathology in Anu oil–treated hamsters, while there was little or no protection in the til tailya group. It has been shown earlier that even low dose of intranasal SARS-CoV2 infection in hamsters could result in pneumonitis and lung pathologies (Rizvi et al., 2021b). It might be possible that even though both til tailya and Anu oil could limit the entry of SARS-CoV2 and replication, only Anu oil–treated group exhibited a greater reduction in the lung viral load (around three folds). Expectedly, the Anu oil group also showed lesser lung injury than the til tailya group. Pulmonary damage and pneumonitis have been reported as the major causes of respiratory failure in patients suffering from a severe form of SARS-CoV2 infection (Moore and June 2020). Prophylactic use of Anu oil showed significant reduction in the overall disease index as compared to the infected control, suggesting some degree of protection against SARS-CoV2–induced lung injury and pathology. The reagents and antibodies specific to hamster CD molecules and signaling proteins were commercially not available, thus limiting the scope of finding the molecular mechanisms and cellular characterization of the protective response. We therefore carried out mRNA expression profiling to assess the role of cytokines and chemokines involved in the inflammatory response and lung injury parameters. mRNA expression data suggest that Anu oil intervention also reduced the expression of lung injury markers and lung inflammation, indicating that Anu oil was able to protect against the pulmonary damage caused by SARS-CoV2 infection. Finally, we studied the expression of cytokines to understand if intranasal formulation could help prevent the inflammatory cytokine response within the lung. Interestingly, both Anu oil and til tailya were able to limit the expression of pro-inflammatory cytokines as compared to the infected hamsters.

Taken together, in the current study, using the hamster SARS-CoV2 model, we report that prophylactic intranasal treatment with Anu oil and til tailya reduced the lung viral load. However, SARS-CoV2–related pulmonary pathologies were prevented only

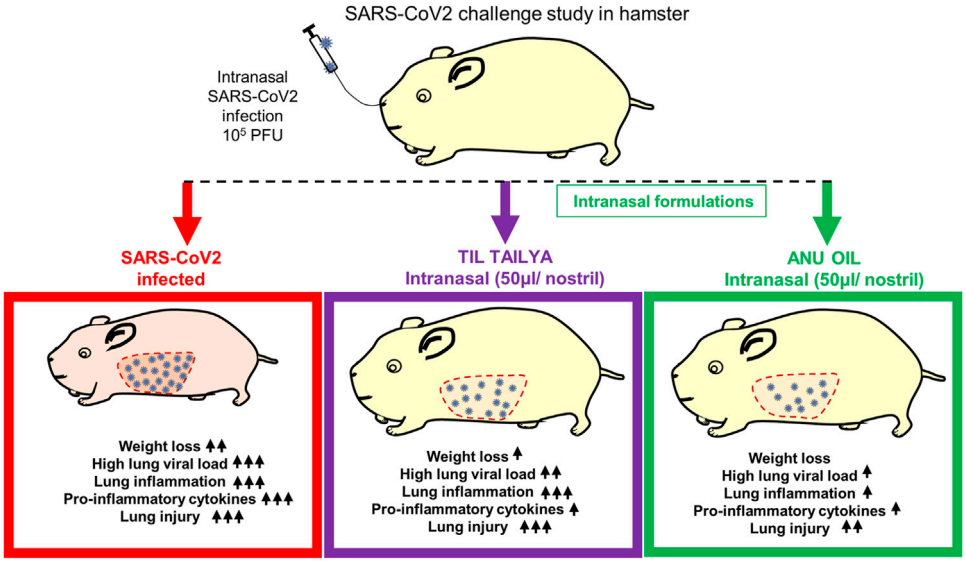

FIGURE 5 | Summary representing the important findings of the study. Diagrammatic representation of the effect of pretreatment of intranasal til tailya and Anu oil against SARS-CoV2–associated pathologies in golden Syrian hamster. ns = non-significant.

in Anu oil–treated hamsters as demonstrated by histopathological lung injury scores and expression of injury markers and inflammatory cytokines. Although the chemical constituents of Anu oil and til tailya remain to be investigated. The protection against SARS-CoV2 infection and related pathologies seem to be in part due to the significant reduction in the viral entry and replication in the upper respiratory tract. This preclinical study in the hamster model points to the prophylactic potential of intranasal Anu oil in COVID and necessitates further studies to understand its observed effect.

DATA AVAILABILITY STATEMENT

The original contributions presented in the study are included in the article/**Supplementary Files;** further inquiries can be directed to the corresponding authors.

ETHICS STATEMENT

The animal study was reviewed and approved by the Institutional Animal Ethics Committee, Translational Health Science and Technology Institute.

AUTHOR CONTRIBUTIONS

Conceived, designed, and supervised the study: MD and AA; performed the experiments: ZR and NS; ABSL3 procedures: ZR, MT, and NS; qPCR primer designing and analysis: ZR; histology and analysis: ZR and MT; viral load: ZR, MT, and SG; qPCR: ZR, MT, and SG; virus stock: SM; contributed reagents/materials/analysis tools: AA, NShastri, JS, and MS; wrote the manuscript: ZR; and revised the manuscript: MD and AA.

ACKNOWLEDGMENTS

MD and AA received financial support for this study from Ayush-DBT (BT/PR40378/TRM/120/486/2020 and NMPB/IFD/GIA/NR/PL/2020–21/53). We acknowledge the financial support from THSTI Core to establish the hamster model for SARS-CoV2 infection. We greatly acknowledge the support and critical inputs of Pramod Kumar Garg in the manuscript. We acknowledge the IDRF (THSTI) for the support at the ABSL3 facility. Pankaj Lawania and Prabhanjan Diwedi for their support in conducting ABSL3 animal experiments and Jitender Chandel for providing technical help. A small animal facility and immunology core for providing support in experimentation. Hamsters were procured from CDRI, Lucknow. The ILBS for support in histological analysis and assessment. The following reagent was deposited by the Centers for Disease Control and Prevention and obtained through BEI Resources, NIAID, NIH: SARS Related Coronavirus 2, Isolate United States-WA1/2020, NR-52281.

SUPPLEMENTARY MATERIAL

The Supplementary Material for this article can be found online at: https://www.frontiersin.org/articles/10.3389/fphar.2021.746729/full#supplementary-material

REFERENCES

Abdelalim, A. A., Mohamady, A. A., Elsayed, R. A., Elawady, M. A., and Ghallab, A. F. (2021). Corticosteroid Nasal spray for Recovery of Smell Sensation in COVID-19 Patients: A Randomized Controlled Trial. *Am. J. Otolaryngol.* 42, 102884. doi:10.1016/j.amjoto.2020.102884

Afrin, L. B., Weinstock, L. B., and Molderings, G. J. (2020). Covid-19 Hyperinflammation and post-Covid-19 Illness May Be Rooted in Mast Cell Activation Syndrome. *Int. J. Infect. Dis.* 100, 327–332. doi:10.1016/j.ijid.2020.09.016

Banerjee, S., Kar, A., Mukherjee, P. K., Haldar, P. K., Sharma, N., and Katiyar, C. K. (2020). Immunoprotective Potential of Ayurvedic Herb Kalmegh (Andrographis Paniculata) against Respiratory Viral Infections - LC-MS/MS and Network Pharmacology Analysis. *Phytochem. Anal.* 32, 629–639. doi:10.1002/pca.3011

Bao, L., Deng, W., Huang, B., Gao, H., Liu, J., Ren, L., et al. (2020). The Pathogenicity of SARS-CoV-2 in hACE2 Transgenic Mice. *Nature* 583, 830–833. doi:10.1038/s41586-020-2312-y

Boiardi, F., and Stebbing, J. (2021). Reducing Transmission of SARS-CoV-2 with Intranasal Prophylaxis. *EBioMedicine* 63, 103170. doi:10.1016/j.ebiom.2020.103170

Chan, J. F.-W., Zhang, A. J., Yuan, S., Poon, V. K.-M., Chan, C. C.-S., Lee, A. C.-Y., et al. (2020). Simulation of the Clinical and Pathological Manifestations of Coronavirus Disease 2019 (COVID-19) in a Golden Syrian Hamster Model: Implications for Disease Pathogenesis and Transmissibility. *Clin. Infect. Dis.* doi:10.1093/cid/ciaa325

Chatterjee, M., van Putten, J. P. M., and Strijbis, K. (2020). Defensive Properties of Mucin Glycoproteins during Respiratory Infections-Relevance for SARS-CoV-2. *mBio* 11, e02374–20. doi:10.1128/mBio.02374-20

Chen, Y., and Li, L. (2020). SARS-CoV-2: Virus Dynamics and Host Response. *Lancet Infect. Dis.* 20, 515–516. doi:10.1016/S1473-3099(20)30235-8

Crouch, E. C. (2000). Surfactant Protein-D and Pulmonary Host Defense. *Respir. Res.* 1, 93–108. doi:10.1186/rr19

De Pellegrin, M. L., Rohrhofer, A., Schuster, P., Schmidt, B., Peterburs, P., and Gessner, A. (2021). The Potential of Herbal Extracts to Inhibit SARS-CoV-2: a Pilot Study. *Clin. Phytosci* 7, 29. doi:10.1186/s40816-021-00264-6

Dong, Y., Dai, T., Wei, Y., Zhang, L., Zheng, M., and Zhou, F. (2020). A Systematic Review of SARS-CoV-2 Vaccine Candidates. *Signal. Transduct Target. Ther.* 5, 237–314. doi:10.1038/s41392-020-00352-y

Duraipandi, S., and Selvakumar, V. (2020). Reinventing Nano Drug Delivery Systems for Hydrophilic Active Ingredients in Ayurvedic Lipid Based Formulations Containing Poly Herbal Decoction. *J. Ayurveda Integr. Med.* 11, 224–227. doi:10.1016/j.jaim.2018.01.008

Gandhi, R. T., Lynch, J. B., and del Rio, C. (2020). Mild or Moderate Covid-19. *N. Engl. J. Med.* 383, 1757–1766. null. doi:10.1056/NEJMcp2009249

Garcia-Beltran, W. F., Lam, E. C., Denis, K. S., Nitido, A. D., Garcia, Z. H., Hauser, B. M., et al. (2021). Multiple SARS-CoV-2 Variants Escape Neutralization by Vaccine-Induced Humoral Immunity. *medRxiv*. doi:10.1101/2021.02.14.21251704

Girija, P. L. T., and Sivan, N. (2020). Ayurvedic Treatment of COVID-19/SARS-CoV-2: A Case Report. *J. Ayurveda Integr. Med.* doi:10.1016/j.jaim.2020.06.001

Golechha, M. (2020). Time to Realise the True Potential of Ayurveda against COVID-19. *Brain Behav. Immun.* 87, 130–131. doi:10.1016/j.bbi.2020.05.003

Guan, W. J., Ni, Z. Y., Hu, Y., Liang, W. H., Ou, C. Q., He, J. X., et al. (2020). Clinical Characteristics of Coronavirus Disease 2019 in China. *N. Engl. J. Med.* 382, 1708–1720. doi:10.1056/NEJMoa2002032

Guo, R. F., Lentsch, A. B., Warner, R. L., Huber-Lang, M., Sarma, J. V., Hlaing, T., et al. (2001). Regulatory Effects of Eotaxin on Acute Lung Inflammatory Injury. *J. Immunol.* 166, 5208–5218. doi:10.4049/jimmunol.166.8.5208

Hassan, A. O., Kafai, N. M., Dmitriev, I. P., Fox, J. M., Smith, B. K., Harvey, I. B., et al. (2020). A Single-Dose Intranasal ChAd Vaccine Protects Upper and Lower Respiratory Tracts against SARS-CoV-2. *Cell* 183, 169–184.e13. doi:10.1016/j.cell.2020.08.026

Imai, M., Iwatsuki-Horimoto, K., Hatta, M., Loeber, S., Halfmann, P. J., Nakajima, N., et al. (2020). Syrian Hamsters as a Small Animal Model for SARS-CoV-2 Infection and Countermeasure Development. *Proc. Natl. Acad. Sci. U S A.* 117, 16587–16595. doi:10.1073/pnas.2009799117

Iwasaki, A., and Yang, Y. (2020). The Potential Danger of Suboptimal Antibody Responses in COVID-19. *Nat. Rev. Immunol.* 20, 339–341. doi:10.1038/s41577-020-0321-6

Jan, J. T., Cheng, T. R., Juang, Y. P., Ma, H. H., Wu, Y. T., Yang, W. B., et al. (2021). Identification of Existing Pharmaceuticals and Herbal Medicines as Inhibitors of SARS-CoV-2 Infection. *Proc. Natl. Acad. Sci. U S A.* 118, e2021579118. doi:10.1073/pnas.2021579118

Joshi, J. A., and Puthiyedath, R. (2020). Outcomes of Ayurvedic Care in a COVID-19 Patient with Hypoxia - A Case Report. *J. Ayurveda Integr. Med.* doi:10.1016/j.jaim.2020.10.006

Ku, M.-W., Bourgine, M., Authié, P., Lopez, J., Nemirov, K., Moncoq, F., et al. (2021). Intranasal Vaccination with a Lentiviral Vector Protects against SARS-CoV-2 in Preclinical Animal Models. *Cell Host Microbe* 29, 236–249.e6. doi:10.1016/j.chom.2020.12.010

Kunzelmann, K. (2021). Getting Hands on a Drug for Covid-19: Inhaled and Intranasal Niclosamide. *Lancet Reg. Health Eur.* 4, 100094. doi:10.1016/j.lanepe.2021.100094

Lee, A. C., Zhang, A. J., Chan, J. F., Li, C., Fan, Z., Liu, F., et al. (2020). Oral SARS-CoV-2 Inoculation Establishes Subclinical Respiratory Infection with Virus Shedding in Golden Syrian Hamsters. *Cell Rep Med* 1, 100121. doi:10.1016/j.xcrm.2020.100121

Lee, D. Y. W., Li, Q. Y., Liu, J., and Efferth, T. (2021). Traditional Chinese Herbal Medicine at the Forefront Battle against COVID-19: Clinical Experience and Scientific Basis. *Phytomedicine* 80, 153337. doi:10.1016/j.phymed.2020.153337

Leng, L., Cao, R., Ma, J., Mou, D., Zhu, Y., Li, W., et al. (2020). Pathological Features of COVID-19-Associated Lung Injury: a Preliminary Proteomics Report Based on Clinical Samples. *Signal. Transduct Target. Ther.* 5, 240. doi:10.1038/s41392-020-00355-9

Li, S., Cheng, C.-S., Zhang, C., Tang, G.-Y., Tan, H.-Y., Chen, H.-Y., et al. (2021). Edible and Herbal Plants for the Prevention and Management of COVID-19. *Front. Pharmacol.* 12. doi:10.3389/fphar.2021.656103

Ling, C. Q. (2020). Traditional Chinese Medicine Is a Resource for Drug Discovery against 2019 Novel Coronavirus (SARS-CoV-2). *J. Integr. Med.* 18, 87–88. doi:10.1016/j.joim.2020.02.004

Malik, S., Sadhu, S., Elesela, S., Pandey, R. P., Chawla, A. S., Sharma, D., et al. (2017). Transcription Factor Foxo1 Is Essential for IL-9 Induction in T Helper Cells. *Nat. Commun.* 8, 815. doi:10.1038/s41467-017-00674-6

Mathew, D., Giles, J. R., Baxter, A. E., Oldridge, D. A., Greenplate, A. R., Wu, J. E., et al. (2020). Deep Immune Profiling of COVID-19 Patients Reveals Distinct Immunotypes with Therapeutic Implications. *Science* 369, eabc8511. doi:10.1126/science.abc8511

Matveeva, T., Khafizova, G., and Sokornova, S. (2020). In Search of Herbal Anti-SARS-Cov2 Compounds. *Front. Plant Sci.* 11, 589998. doi:10.3389/fpls.2020.589998

Moore, J. B., and June, C. H. (2020). Cytokine Release Syndrome in Severe COVID-19. *Science* 368, 473–474. doi:10.1126/science.abb8925

Planas, D., Bruel, T., Grzelak, L., Guivel-Benhassine, F., Staropoli, I., Porrot, F., et al. (2021). Sensitivity of Infectious SARS-CoV-2 B.1.1.7 and B.1.351 Variants to Neutralizing Antibodies. *Nat. Med.* 27, 917–924. doi:10.1038/s41591-021-01318-5

Poland, G. A., Ovsyannikova, I. G., Crooke, S. N., and Kennedy, R. B. (2020a). SARS-CoV-2 Vaccine Development: Current Status. *Mayo Clin. Proc.* 95, 2172–2188. doi:10.1016/j.mayocp.2020.07.021

Poland, G. A., Ovsyannikova, I. G., and Kennedy, R. B. (2020b). SARS-CoV-2 Immunity: Review and Applications to Phase 3 Vaccine Candidates. *Lancet* 396, 1595–1606. doi:10.1016/S0140-6736(20)32137-1

Prabhakaran, P., Ware, L. B., White, K. E., Cross, M. T., Matthay, M. A., and Olman, M. A. (2003). Elevated Levels of Plasminogen Activator Inhibitor-1 in Pulmonary Edema Fluid Are Associated with Mortality in Acute Lung Injury. *Am. J. Physiol. Lung Cel Mol Physiol.* 285, L20–L28. doi:10.1152/ajplung.00312.2002

Proud, P. C., Tsitoura, D., Watson, R. J., Chua, B. Y., Aram, M. J., Bewley, K. R., et al. (2021). Prophylactic Intranasal Administration of a TLR2/6 Agonist Reduces Upper Respiratory Tract Viral Shedding in a SARS-CoV-2 challenge Ferret Model. *EBioMedicine* 63, 103153. doi:10.1016/j.ebiom.2020.103153

Rastogi, S., Pandey, D. N., and Singh, R. H. (2020). COVID-19 Pandemic: A Pragmatic Plan for Ayurveda Intervention. *J. Ayurveda Integr. Med.* S0975-9476, 30019–X. doi:10.1016/j.jaim.2020.04.002

Rizvi, Z. A., Dalal, R., Sadhu, S., Kumar, Y., Kumar, S., Gupta, S. K., et al. (2021a). High-Salt Diet Mediates Interplay Between NK Cells and Gut Microbiota to Induce Potent Tumor Immunity. *Sci. Adv.* 7, eabg5016. doi:10.1126/sciadv.abg5016

Rizvi, Z. A., Dalal, R., Sadhu, S., Kumar, Y., Srivastava, T., Gupta, S. K., et al. (2021b). Immunological and Cardio-Vascular Pathologies Associated with SARS-CoV-2 Infection in Golden Syrian Hamster. *bioRxiv*. doi:10.1101/2021.01.11.426080

Rizvi, Z. A., Puri, N., and Saxena, R. K. (2018). Evidence of CD1d Pathway of Lipid Antigen Presentation in Mouse Primary Lung Epithelial Cells and its Up-Regulation upon Mycobacterium Bovis BCG Infection. *PLOS ONE* 13, e0210116. doi:10.1371/journal.pone.0210116

Sia, S. F., Yan, L. M., Chin, A. W. H., Fung, K., Choy, K. T., Wong, A. Y. L., et al. (2020). Pathogenesis and Transmission of SARS-CoV-2 in golden Hamsters. *Nature* 583, 834–838. doi:10.1038/s41586-020-2342-5

Subrahmanya, N. K., Patel, K. S., Kori, V. K., and Shrikrishna, R. (2013). Role of Kasahara Dashemani Vati in Kasa and Vyadhikshamatva in Children with Special Reference to Recurrent Respiratory Tract Infections. *Ayu* 34, 281–287. doi:10.4103/0974-8520.123124

Supasa, P., Zhou, D., Dejnirattisai, W., Liu, C., Mentzer, A. J., Ginn, H. M., et al. (2021). Reduced Neutralization of SARS-CoV-2 B.1.1.7 Variant by Convalescent and Vaccine Sera. *Cell* 184, 2201–e7. doi:10.1016/j.cell.2021.02.033

Verity, R., Okell, L. C., Dorigatti, I., Winskill, P., Whittaker, C., Imai, N., et al. (2020). Estimates of the Severity of Coronavirus Disease 2019: a Model-Based Analysis. *Lancet Infect. Dis.* 20, 669–677. doi:10.1016/S1473-3099(20)30243-7

de Vries, R. D., Schmitz, K. S., Bovier, F. T., Predella, C., Khao, J., Noack, D., et al. (2021). Intranasal Fusion Inhibitory Lipopeptide Prevents Direct-Contact SARS-CoV-2 Transmission in Ferrets. *Science* 371, 1379–1382. doi:10.1126/science.abf4896

Wang, T., Du, Z., Zhu, F., Cao, Z., An, Y., Gao, Y., et al. (2020). Comorbidities and Multi-Organ Injuries in the Treatment of COVID-19. *Lancet* 395, e52. doi:10.1016/S0140-6736(20)30558-4

Xie, G., Liu, Y., Yao, Q., Zheng, R., Zhang, L., Lin, J., et al. (2017). Hypoxia-induced Angiotensin II by the Lactate-chymase-dependent Mechanism Mediates Radioresistance of Hypoxic Tumor Cells. *Sci. Rep.* 7, 42396. doi:10.1038/srep42396

Xiong, X., Wang, P., Su, K., Cho, W. C., and Xing, Y. (2020). Chinese Herbal Medicine for Coronavirus Disease 2019: A Systematic Review and Meta-Analysis. *Pharmacol. Res.* 160, 105056. doi:10.1016/j.phrs.2020.105056

Yang, Y., Islam, M. S., Wang, J., Li, Y., and Chen, X. (2020). Traditional Chinese Medicine in the Treatment of Patients Infected with 2019-New Coronavirus (SARS-CoV-2): A Review and Perspective. *Int. J. Biol. Sci.* 16, 1708–1717. doi:10.7150/ijbs.45538

Zhang, N., Zhao, Y. D., and Wang, X. M. (2020). CXCL10 an Important Chemokine Associated with Cytokine Storm in COVID-19 Infected Patients. *Eur. Rev. Med. Pharmacol. Sci.* 24, 7497–7505. doi:10.26355/eurrev_202007_21922

Conflict of Interest: The authors declare that the research was conducted in the absence of any commercial or financial relationships that could be construed as a potential conflict of interest.

Publisher's Note: All claims expressed in this article are solely those of the authors and do not necessarily represent those of their affiliated organizations, or those of the publisher, the editors, and the reviewers. Any product that may be evaluated in this article, or claim that may be made by its manufacturer, is not guaranteed or endorsed by the publisher.

frontiers in Pharmacology

ORIGINAL RESEARCH
published: 19 January 2022
doi: 10.3389/fphar.2021.755600

Antidepressant and Antipsychotic Drugs Reduce Viral Infection by SARS-CoV-2 and Fluoxetine Shows Antiviral Activity Against the Novel Variants *in vitro*

Senem Merve Fred[1], *Suvi Kuivanen*[2], *Hasan Ugurlu*[2], *Plinio Cabrera Casarotto*[1], *Lev Levanov*[2], *Kalle Saksela*[2], *Olli Vapalahti*[2,3,4] *and Eero Castrén*[1]*

[1]Neuroscience Center–HiLIFE, University of Helsinki, Helsinki, Finland, [2]Department of Virology, University of Helsinki, Helsinki, Finland, [3]Department of Veterinary Biosciences, University of Helsinki, Helsinki, Finland, [4]HUS Diagnostic Center, HUSLAB, Clinical Microbiology, University of Helsinki and Helsinki University Hospital, Helsinki, Finland

OPEN ACCESS

Edited by:
Salvatore Salomone,
University of Catania, Italy

Reviewed by:
Sebastian Schloer,
University of Münster, Germany
Jing Xing,
Michigan State University,
United States
Silke Walter,
Saarland University Hospital, Germany

***Correspondence:**
Eero Castrén
eero.castren@helsinki.fi

Specialty section:
This article was submitted to Experimental Pharmacology and Drug Discovery, a section of the journal Frontiers in Pharmacology

Received: 09 August 2021
Accepted: 09 December 2021
Published: 19 January 2022

Citation:
Fred SM, Kuivanen S, Ugurlu H, Casarotto PC, Levanov L, Saksela K, Vapalahti O and Castrén E (2022) Antidepressant and Antipsychotic Drugs Reduce Viral Infection by SARS-CoV-2 and Fluoxetine Shows Antiviral Activity Against the Novel Variants in vitro. Front. Pharmacol. 12:755600. doi: 10.3389/fphar.2021.755600

Repurposing of currently available drugs is a valuable strategy to tackle the consequences of COVID-19. Recently, several studies have investigated the effect of psychoactive drugs on SARS-CoV-2 in cell culture models as well as in clinical practice. Our aim was to expand these studies and test some of these compounds against newly emerged variants. Several antidepressants and antipsychotic drugs with different primary mechanisms of action were tested in ACE2/TMPRSS2-expressing human embryonic kidney cells against the infection by SARS-CoV-2 spike protein-dependent pseudoviruses. Some of these compounds were also tested in human lung epithelial cell line, Calu-1, against the first wave (B.1) lineage of SARS-CoV-2 and the variants of concern, B.1.1.7, B.1.351, and B.1.617.2. Several clinically used antidepressants, including fluoxetine, citalopram, reboxetine, imipramine, as well as antipsychotic compounds chlorpromazine, flupenthixol, and pimozide inhibited the infection by pseudotyped viruses with minimal effects on cell viability. The antiviral action of several of these drugs was verified in Calu-1 cells against the B.1 lineage of SARS-CoV-2. By contrast, the anticonvulsant carbamazepine, and novel antidepressants ketamine, known as anesthetic at high doses, and its derivatives as well as MAO and phosphodiesterase inhibitors phenelzine and rolipram, respectively, showed no activity in the pseudovirus model. Furthermore, fluoxetine remained effective against pseudoviruses with common receptor binding domain mutations, N501Y, K417N, and E484K, as well as B.1.1.7 (alpha), B.1.351 (beta), and B.1.617.2 (delta) variants of SARS-CoV-2. Our study confirms previous data and extends information on the repurposing of these drugs to counteract SARS-CoV-2 infection including different variants of concern, however, extensive clinical studies must be performed to confirm our *in vitro* findings.

Keywords: antidepressants (AD), fluoxetine, SARS-CoV-2, alpha variant, beta variant, delta variant

INTRODUCTION

Coronaviruses, members of the enveloped RNA virus family *Coronaviridae* (Lai & Cavanagh, 1997), are known to infect multiple species ranging from birds to mammals (To et al., 2013). In humans, in addition to four coronaviruses causing common colds, high level of pathogenicity of viruses from this family, such as severe acute respiratory syndrome coronavirus (SARS-CoV) and Middle East respiratory syndrome coronavirus (MERS-CoV), were observed in epidemics that emerged in 2003 and 2012, respectively (Tang et al., 2015). The pandemic that started in December 2019 in Wuhan, China, caused by SARS-CoV-2 infection, and the dramatic increase in the number of infected people and death due to COVID-19, has shifted the efforts of scientists towards investigating this virus more closely (F. Wu et al., 2020; Zhou et al., 2020). Autopsies of patients who died from COVID-19 have reported the spread of virus to lungs, kidneys, liver, heart, brain, and blood (Puelles et al., 2020). Taken together, severity of cases and high infectivity of the virus requires more attention and effort towards controlling the global epidemic and developing treatment options.

The spike protein (S protein) localized to the viral envelope has been annotated as one of the critical parts of this group of viruses because of its role in attachment and fusion to host target cells (Li et al., 2005). Angiotensin-converting enzyme 2 (ACE2) located on the surface of the target cells is recognized by S protein of SARS-CoV and SARS-CoV-2 (Li et al., 2003; Walls et al., 2020; Wang et al., 2020; Hoffmann, et al., 2020b). A distinct location, the receptor-binding domain (RBD), in S protein is important for binding to ACE2 (Li et al., 2005; Wan et al., 2020). ACE2-binding alone may allow the viral entry to target cells, however, proteolytic processing of S protein by transmembrane protease/serine subfamily member 2 (TMPRSS2) has been shown to enhance viral entry (Shulla et al., 2011; Hoffmann, et al., 2020b). Recent data on SARS-CoV-2 also suggest that the S protein cleavage by furin proprotein convertase (Hoffmann, et a., 2020a; Johnson et al., 2021) and binding of the C-end of the S1 to the cellular receptor neuropilin-1 can also increase infectivity (Cantuti-Castelvetri et al., 2020; Daly et al., 2020). Lysosomal enzyme Cathepsin L has been shown to regulate priming of SARS-CoV-2 S protein for the entry of viral RNA genome into the host cytoplasm (Ou et al., 2020). Although many key players facilitating viral entry and the routes of infection have been identified since the emergence of COVID-19, effective drugs that can alleviate or eliminate the viral infection remain to be found.

A number of SARS-CoV-2 variants of concern have been identified, including B.1.1.7 lineage (alpha) (Rambaut, 2020), B.1.351 lineage (beta) (Tegally et al., 2020), B.1.1.28 lineage and the descendent P1 lineage (gamma) (Voloch et al., 2020; Faria et al., 2021; PAOLA, 2021), and one of the recent ones, B.1.617 and its sub-linage B.1.617.2 (delta) (Cherian et al., 2021; Mlcochova et al., 2021). Several common and critical mutations in the RBD of S protein have been detected in these variants which can affect the ACE2 affinity (Khateeb et al., 2021). A common RBD mutation, N501Y, is shared by alpha, beta, and gamma, while K417N and E484K are found in beta and gamma (Khateeb et al., 2021). The delta variant contains a non-RBD mutation, D614G, shared by alpha and gamma variants, as well as an RBD mutation, E484Q, which is similar to E484K in other variants (Khateeb et al., 2021). These mutations detected in the RBD domain of spike have been associated with antibody neutralization (Gu et al., 2020; Starr et al., 2020; Alenquer et al., 2021; Nelson et al., 2021; Wibmer et al., 2021; Greaney, et al., 2021a; Greaney, et al., 2021b). Moreover, they have also put the currently available vaccines and vaccine candidates under dispute (Fontanet et al., 2021).

The strategy of drug repurposing has been used as a method of searching novel treatments for virus-related diseases (Dyall et al., 2014; Mercorelli et al., 2018; Serra et al., 2021). A pre-clinical study has shown that the antidepressant drugs, such as sertraline, paroxetine, and clomipramine, can reduce the *Zaire* Ebola virus (EBOV) entry to target cells (Johansen et al., 2015). Recently, a number of studies presented evidence supporting the effects of antidepressant drugs and related psychoactive drugs as antiviral compounds against SARS-CoV-2 (Carpinteiro et al., 2020; Drayman et al., 2020; Schloer et al., 2020; Yang et al., 2020; Zimniak et al., 2021). In line with preclinical studies, the treatment of COVID-19 patients with fluoxetine, escitalopram, and venlafaxine for 20 days has been found to reduce the risk of intubation or death by COVID-19 (Hoertel, et al., 2021b). Treatment of COVID-19 patients with fluvoxamine for 2 weeks was also effective to decrease the development of clinical deterioration (Lenze et al., 2020). A follow up randomized controlled trial which was performed with higher number of patients has reached to the same conclusion about fluvoxamine that this compound helps with the reduction of hospitalization risk due to COVID-19 (Reis et al., 2021). Another study reported that the prevalence of COVID-19 was higher in health care professionals compared to patients in psychiatric ward of a hospital in Paris, which prompted the authors to suggest that the consumption of chlorpromazine protects against COVID-19 (Plaze et al., 2020a; Plaze et al., 2020b).

In the present study, we addressed if the psychoactive drugs can be used to reduce SARS-CoV-2 infection of host cells *in vitro*. We show that pharmacologically diverse antidepressant drugs, as well as several antipsychotics were able to reduce the infection by pseudotyped viruses harboring SARS-CoV-2 S protein. Treatment of human lung epithelial cell line Calu-1 infected with the B.1 lineage of SARS-CoV-2 with these drugs was also successful in reducing the amount of infectious virus. Moreover, infection by pseudotyped viruses carrying N501Y, K417N, or E484K single point mutations or triple mutation (N501Y/K417N/E484K) in the spike protein was shown to be reduced by fluoxetine. Fluoxetine was also effective against the variants of SARS-CoV-2, B.1.1.7 (alpha), B.1.351 (beta), and B.1.617.2 (delta) in Calu-1 cells.

MATERIALS AND METHODS

Ethical Statement

Not applicable, all the experiments were performed using cells.

Drugs

Fluoxetine (#H6995, Bosche Scientific), citalopram (#C505000, Toronto Research Chemicals), paroxetine (#2141, Tocris),

TABLE 1 | Psychoactive drugs implicated in our study and the doses used for the treatment of HEK 293T-ACE2-TMPRSS2 and Calu-1 cells.

Category of drugs tested	Name of drugs	Dose (μM)
Selective serotonin reuptake inhibitors (SSRIs)	Fluoxetine	0.01–20
	Citalopram	0.01–50
	Paroxetine	0.01–20
	Fluvoxamine	0.01–50
Selective norepinephrine reuptake inhibitor (NRI)	Reboxetine	0.1–50
Serotonin - norepinephrine reuptake inhibitor (SNRI)	Venlafaxine	0.01–50
Tricyclic antidepressants	Clomipramine	0.01–10
	Imipramine	0.01–50
	Desipramine	0.01–20
Rapid-acting antidepressants	Ketamine	0.01–50
	2R, 6R-Hydroxynorketamine (2R, 6R-HNK)	
	2S, 6S-Hydroxynorketamine (2S, 6S-HNK)	
Phosphodiesterase-4 inhibitor	Rolipram	0.01–50
Monoamine oxidase inhibitor	Phenelzine	0.01–50
Antipsychotic	Chlorpromazine	0.01–5
	Flupenthixol	0.01–10
	Pimozide	1–10
Anticonvulsant	Carbamazepine	0.1–50

fluvoxamine (#1033), venlafaxine (#2917, Tocris), reboxetine (#1982, Tocris), imipramine (#I7379-5G, Sigma–Aldrich), clomipramine (#C7291**,** Sigma–Aldrich), desipramine (#3067, Tocris), phenelzine (#P6777, Sigma–Aldrich), rolipram (#R6520, Sigma–Aldrich), ketamine (#3131, Tocris), 2R, 6R-Hydroxynorketamine and 2S, 6S-Hydroxynorketamine (#6094 and #6095, respectively, Tocris), carbamazepine (#4098, Tocris), chlorpromazine (#C8138, Sigma–Aldrich), flupenthixol (#4057, Tocris), and pimozide (#0937, Tocris) were investigated in this study. The compounds were dissolved in dimethyl sulfoxide (DMSO) that was also used as a vehicle in all the experiments. Concentrations tested (**Table 1**) were selected based on earlier *in vitro* studies from our research group (Fred et al., 2019; Casarotto et al., 2021) and other laboratories (Johansen et al., 2015).

Cell Lines

TMPRSS2 (NM_001135099.1) and ACE2 (AB046569.1) cDNAs were sequentially transfected into HEK293T cells using lentiviral vectors. The positive colonies were selected by blasticidin or puromycin resistance for TMPRSS2 and ACE2, respectively. The viral vectors were generated by transfecting HEK293T cells using polyethylenimine with the packaging vector pCMV-dR8.91 and the vesicular stomatitis virus (VSV-G) envelope expression vector pMD2.G (#12259, Addgene) with either pLenti6.3/V5-DEST-TMPRSS2 (from UH Biomedicum Functional Genomic Unit) or pWPI-puro [modified from, #12254, Addgene, (Zhao et al., 2019)] expressing ACE2 (cDNA from Dr. Markku Varjosalo). Six hours after transfection, media was replaced with fresh Dulbecco's Modified Eagle Medium (DMEM) containing high glucose (Sigma–Aldrich) supplemented with 10% fetal calf serum (FCS). Culture supernatant was collected 2 days after transfection and passed through a 0.22-micron filter. The supernatant containing TMPRSS2 lentivector was added to human embryonic kidney cells, HEK293T, seeded on 6-well plates. Following 2 days of selection with 15 μg/ ml of blasticidin (Invitrogen), the cells were incubated with the medium containing the ACE2 lentivector, and supplemented with 3 μg/ ml puromycin (Sigma–Aldrich). After selection with puromycin, single cell lines were established by serial dilution. Both the double-transduced pool and the cloned cell lines were analyzed with SDS-PAGE using an anti-V5 antibody (#MA5-15253, Invitrogen) for TMPRSS2 and an anti-ACE2-antibody (#15983, Cell Signaling Technology).

HEK293T and HEK293T-ACE2-TMPRSS2 cells were maintained in DMEM supplemented with 10% FCS, 2% L-Glutamine, and 1% penicillin/streptomycin. Human lung epithelial cell line Calu-1 was kept in Roswell Park Memorial Institute (RPMI) 1640 medium supplemented with 10% FCS, 1% L-Glutamine, and 1% penicillin/streptomycin. Another human lung epithelial cell line Calu-3 and human colorectal adenocarcinoma cell line Caco-2 were kept in Minimum Essential Medium Eagle (MEM) supplemented with 20% FCS, 1% L-Glutamine, 1% penicillin/streptomycin, and 1% MEM Non-essential Amino acid Solution (100X). VeroE6 cells (ATCC® CRL-1586) were maintained in MEM supplemented with 10% FCS, 1% L-Glutamine and 1% penicillin/streptomycin. All the cell lines were incubated at 5% CO2 and 37°C.

We compared the expression level of *ACE2, TMPRSS2, FURIN* and *GAPDH* with qPCR in all the cell lines (**Supplementary Figure S1**) by using human specific primers (**Supplementary Table S1**).

Production of Luciferase-Encoding Lentiviral Vector Pseudotyped with WT and Mutant SARS-CoV-2 S-Glycoprotein, and VSV-Glycoprotein

HEK293T cells grown in T175 flask were transfected by using TransIT-2020 reagent (Mirus Bio) with p8.9NDSB (Berthoux et al., 2004), pWPI-puro expressing *Renilla* luciferase, pEBB-

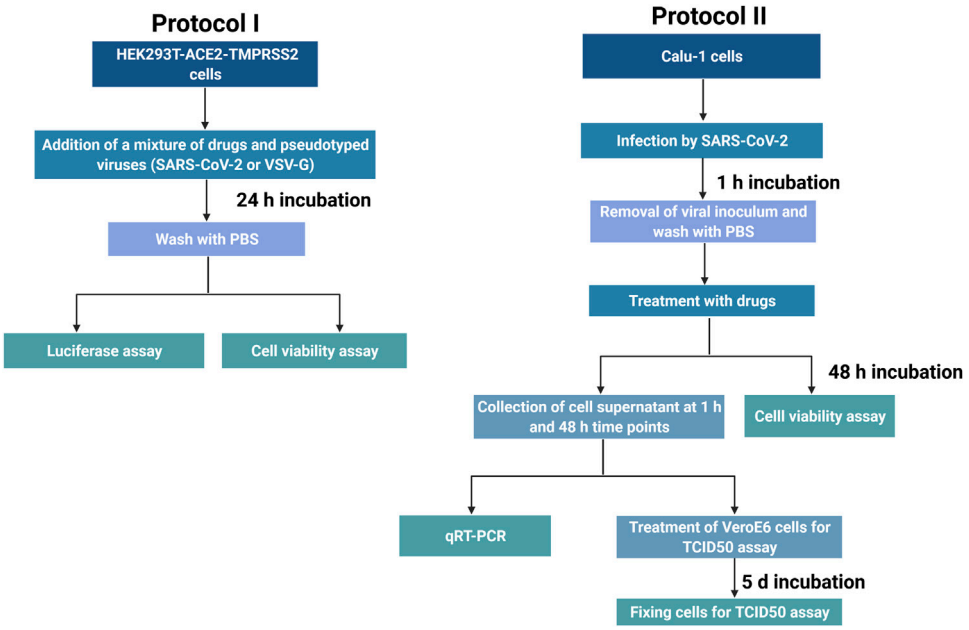

FIGURE 1 | Protocols used in the study. Protocol I represents the experiments in HEK293T-ACE-TMPRSS2 cell line, while Protocol II corresponds to the experiments conducted in Calu-1 cell line. created with BioRender.com.

GFP, and pCAGGS, an expression vector containing the SARS-CoV-2 spike glycoprotein cDNA of the Wuhan-Hu-1 reference strain (NC_045512.2). The last 18 codons of spike glycoprotein were deleted to enhance the plasma membrane transport. Pseudotyped viruses harbouring the glycoprotein of vesicular stomatitis virus (VSV-G) were produced following the same protocol by using VSV-G envelope expression vector pMD2.G (#12259, Addgene). The culture media was replaced 12–16 h after transfection with fresh DMEM High Glucose (Sigma–Aldrich) supplemented with 10% FBS. The supernatant containing the SARS-CoV-2 spike glycoprotein- or VSV-G-harboring pseudoviruses was collected 48 h after transfection, and passed through a 0.22-micron filter.

Mutations in RBD regions were generated by synthetic DNA (Integrated DNA Technologies) using PvuII and HpaI restriction sites. Lentiviral vectors pseudotyped with mutant spikes were produced by following a similar protocol as the wild type particles with minor changes. Instead of pWPI-puro expressing *Renilla* luciferase, pWPI plasmid carrying both GFP and *Renilla* luciferase were used to eliminate the use of pEBB-GFP plasmid.

Detection of Viral Infection by Pseudotyped SARS-CoV-2 or VSV-G Viruses and Native SARS-CoV-2

In the Protocol I (**Figure 1**), infection and treatment of HEK293T-ACE2-TMPRSS2 cells was used. Because of the replication-deficient nature of pseudo-viruses, we aimed at understanding the effect of drugs on the initial viral entry to cells. Therefore, we exposed cells to the compounds and the pseudoviruses simultaneously.

HEK293T-ACE2-TMPRSS2 cells were cultured in poly-L-lysine coated 96-well plates (ViewPlate 96, PerkinElmer Life Sciences). Next day, the cells received varying concentrations of listed drugs (**Table 1**) and pseudotyped lentiviruses harboring S-protein of SARS-CoV-2 or glycoprotein of VSV. Following 24 h incubation with drugs and viral particles, cells were washed once with PBS. After cells were lysed for 15 min at RT, *Renilla* luciferase reporter was used to measure viral entry. For this purpose, luciferase activity was measured with a plate reader employing dispenser feature (Varioskan Flash, ThermoFisher Scientific) after substrate addition to each well (*Renilla* luciferase Assay System, E2820, Promega or Coelenterazine native, cat#303, Nanolight Technology). In order to measure background signal, uninfected cells and empty wells were included into the assay plate.

Calu-1 cells were used in the Protocol II (**Figure 1**) to address the drug effect on the replication and secondary wave of infection by SARS-CoV-2 virus. Protocol II, while complementing protocol I, addresses the efficiency of drug treatment on infection by the native virus. After identifying selective serotonin reuptake inhibitors (SSRIs), selective norepinephrine reuptake inhibitor (NRI), serotonin - norepinephrine reuptake inhibitor (SNRI), tricyclics, and antipsychotics that reduced the pseudoviral infection in HEK cells, we shortlisted candidates to be tested in Calu-1 cells with the native virus. Therefore, we ensured that there is, at least, one representative from one of these groups (**Table 1**). All work with infectious SARS-CoV-2 virus was conducted in a Biosafety Level 3 (BSL-3) laboratory of UH at Haartman Institute. SARS-CoV-2 virus isolates (wild type, B.1.1.7, B.1.351, and B.1.617.2), obtained from nasopharyngeal swabs of patients (Cantuti-Castelvetri et al., 2020) (MOI 0.05),

were incubated with Calu-1 cells in 48-well plates (40.000 cells/well) for 1 h at 37°C and 5% CO_2, after which virus inoculum was removed and cells were washed twice with PBS. The compounds were added to the cells in six replicates, diluted in virus growth medium (VGM) (RPMI-1640 supplemented with 2% FCS, L-glutamine, penicillin and streptomycin), and 0.1% DMSO in VGM was used as control. Samples of the supernatant were collected at 1 and 48 h post infection for qRT-PCR and at 48 h for the TCID50 assay. Viral RNA was extracted using RNeasy Mini Kit (Qiagen, Germany), and SARS-CoV-2 qRT-PCR was performed using primers, probe and an *in vitro* synthesized control for RNA-dependent RNA polymerase (RdRp) as described earlier (Corman et al., 2020; Lin et al., 2021). Infectious virus titers were determined by TCID50 measurement of VeroE6 cells. Shortly, 10-fold dilutions of the samples were inoculated to VeroE6 cells, incubated for 5 days, fixed with 10% formaldehyde for 30 min RT and stained with crystal violet.

A flow chart was prepared to summarize the timeline of experiments regarding the pseudotyped viruses and the native virus (**Figure 1**).

Cell Viability Assay

Cell culturing, treatment, and infection protocols were followed as described for HEK293T-ACE2-TMPRSS2 and Calu-1 cells (**Figure 1**). At the end of 24 h or 48 h period, cells were washed once with PBS and their viability was measured with a kit designed to quantify ATP level according to instructions of the manufacturer (CellTiterGlo 2.0 Luminescent Cell Viability Assay, Promega).

Data and Statistical Analysis

Pseudotyped Viruses

The number of samples per treatment group was determined based on our earlier studies (Fred et al., 2019; Casarotto et al., 2021). Each "n" represents the number of wells used for the indicated treatment. Some drugs were tested in the same plate, therefore, the same control group values were used for the analysis. Data were normalized to control groups to avoid unwanted sources of variation, pooled together, and analyzed in GraphPad Prism 6.0 software. Pseudotyped virus experiments were analyzed by unpaired *t*-test or one-way analysis of variance (or their nonparametric equivalents) followed by Dunnett or Dunn's post hoc tests if a significant overall effect was observed. Cell viability of non-infected and infected cells treated with indicated compounds were analyzed by two-way analysis of variance followed by Sidak's post hoc test, again only if we observed a treatment or interaction effect between the factors. The luciferase activity readings from pseudotyped viruses (SARS-CoV-2 and VSV-G) were replotted together to run a comparative analysis. We compared the drug effect on the infection by SARS-CoV-2 spike and VSV-G pseudotyped viruses by two-way analysis of variance followed by Sidak's multiple comparison test. The mutant pseudotyped virus experiments (infection) were also analyzed by two-way analysis of variance followed by Sidak's multiple comparison. IC50 values were calculated in GraphPad Prism software by using the non-linear curve fitting of the data with log (inhibitor) *vs.* response-Variable slope function after conversion of drug concentrations to logarithmic scale.

Protein bands detected in Western Blotting were subtracted from background and normalized to total protein of beta actin. Data were analyzed by the two-way analysis of variance followed by Sidak's post hoc test. Same analysis was applied to the qPCR assessment of *ACE2* and *TMPRSS2* expression in infected and non-infected HEK cells.

Native SARS-CoV-2 Viruses

Each "n" represents the number of wells used for the indicated treatment. The control group of some samples were the same, as they were tested in the same plate. Therefore, the same control group was represented in different plots. The plots representing changes in the genome copy number were plotted in linear scale, whereas TCID50 values were represented in log10 scale in GraphPad Prism.

For all the experiments, values of $p < 0.05$ were considered significant. Presence of any outliers was calculated by using Grubb's test on GraphPad Prism website (https://www.graphpad.com/quickcalcs/grubbs1), and excluded from the analysis. We performed one-way ANOVA, two-way ANOVA or unpaired *t*-test, followed by Dunnet's, Dunn's or Sidak post hoc analysis for the experiments with the native virus. Statistical analysis were provided in **Supplementary Table S2** for the corresponding figures.

RESULTS

HEK293T-ACE2-TMPRSS2 Cell Line Is Responsive to Camostat Mesylate

Camostat mesylate, a clinically tested serine protease inhibitor, has been shown to inhibit the activity of TMPRSS2 and reduce the SARS-CoV-2 infection in cell lines expressing TMPRSS2 (Kawase et al., 2012; Hoffmann, et al., 2020b; Hoffmann, et al., 2020c). In order to confirm the activity of TMPRSS2 in the HEK293T-ACE2-TMPRSS2 cell line, we treated the cells with different doses of camostat mesylate for 24 h and measured the level of viral infection. The infection of HEK293T-ACE2-TMPRSS2 cell line by the pseudotyped lentiviruses was significantly reduced suggesting that these cells express TMPRSS2 and the activity of this protease is blocked by camostat mesylate (**Supplementary Figure S2**).

Antidepressant Drugs Show Antiviral Activity Against Pseudotyped Viruses and the First wave (B.1) Lineage of SARS-CoV-2

In the Protocol I, HEK293T-ACE2-TMPRSS2 cells were treated with a mixture of pseudotyped viral particles and one of the following antidepressants: fluoxetine, citalopram, paroxetine, fluvoxamine, venlafaxine, reboxetine, clomipramine, imipramine, or desipramine (**Table 1**) for 24 h. We found that all the drugs significantly reduced the viral infection, as measured by luciferase reporter activity (**Figure 2**). According to the cell viability assay where ATP level was measured in infected

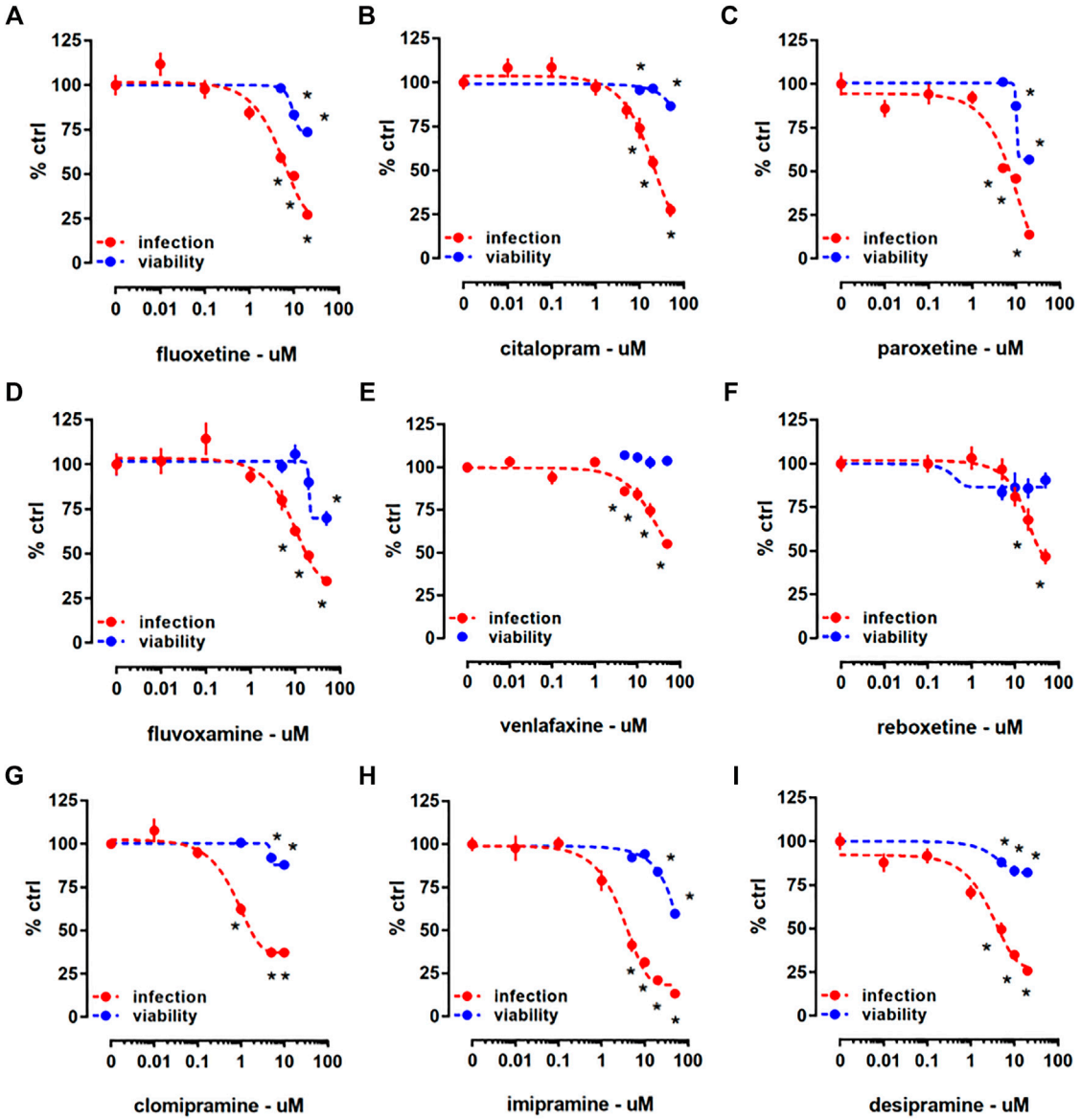

FIGURE 2 | The effect of antidepressant drugs on HEK293T-ACE2-TMPRSS2 cells challenged with SARS-CoV-2 pseudotyped viruses. Treatment with **(A)** fluoxetine (luciferase assay: n = 18–26; cell viability: n = 6; IC50 = 5.992 μM), **(B)** citalopram (luciferase assay: n = 16–22; cell viability: n = 6; IC50 = 27.51 μM), **(C)** paroxetine (luciferase assay: n = 12; cell viability: n = 5; IC50 = 12.55 μM), **(D)** fluvoxamine (luciferase assay: n = 14–24; cell viability: n = 6; IC50 = 10.54 μM), **(E)** venlafaxine (luciferase assay: n = 11–12; cell viability: n = 5; IC50 = 36.35 μM), **(F)** reboxetine (luciferase assay: n = 12; cell viability: n = 6; IC50 = 17.69 μM), **(G)** clomipramine (luciferase assay: n = 12–24; cell viability: n = 6; IC50 = 0.75 μM), **(H)** imipramine (luciferase assay: n = 6–18; cell viability: n = 6; IC50 = 3 μM), and **(I)** desipramine (luciferase assay: n = 12; cell viability: n = 5; IC50 = 8.097 μM) significantly reduced luciferase reporter activity. At higher concentrations, all the compounds, except **(E)** venlafaxine and **(F)** reboxetine reduced ATP levels in the luminescent cell viability assay after 24 h incubation. *p < 0.05 from control group (0). Data represented as mean ± SEM.

HEK293T-ACE2-TMPRSS2 cells, all the tested compounds, except venlafaxine (**Figure 2E**) and reboxetine (**Figure 2F**), were slightly toxic at higher concentrations (**Figure 2**). Combination of infection with drug treatment did not induce any further toxicity (**Supplementary Figure S3**). We also examined the changes in mRNA level of *ACE2* and *TMPRSS2* by the viral infection combined with 24 h of fluoxetine (10 μM), clomipramine (10 μM), and chlorpromazine (5 μM) treatment (**Supplementary Figure S4**). The *ACE2* expression remained unaltered upon fluoxetine treatment, while clomipramine in infected cells, and chlorpromazine in non-infected cells induced a reduction of this target (**Supplementary Figure S4A**). *TMPRSS2* level was increased by fluoxetine in non-infected and infected cells, while the other compounds remained ineffective (**Supplementary Figure S4B**). Furthermore, by addressing the protein levels (**Supplementary**

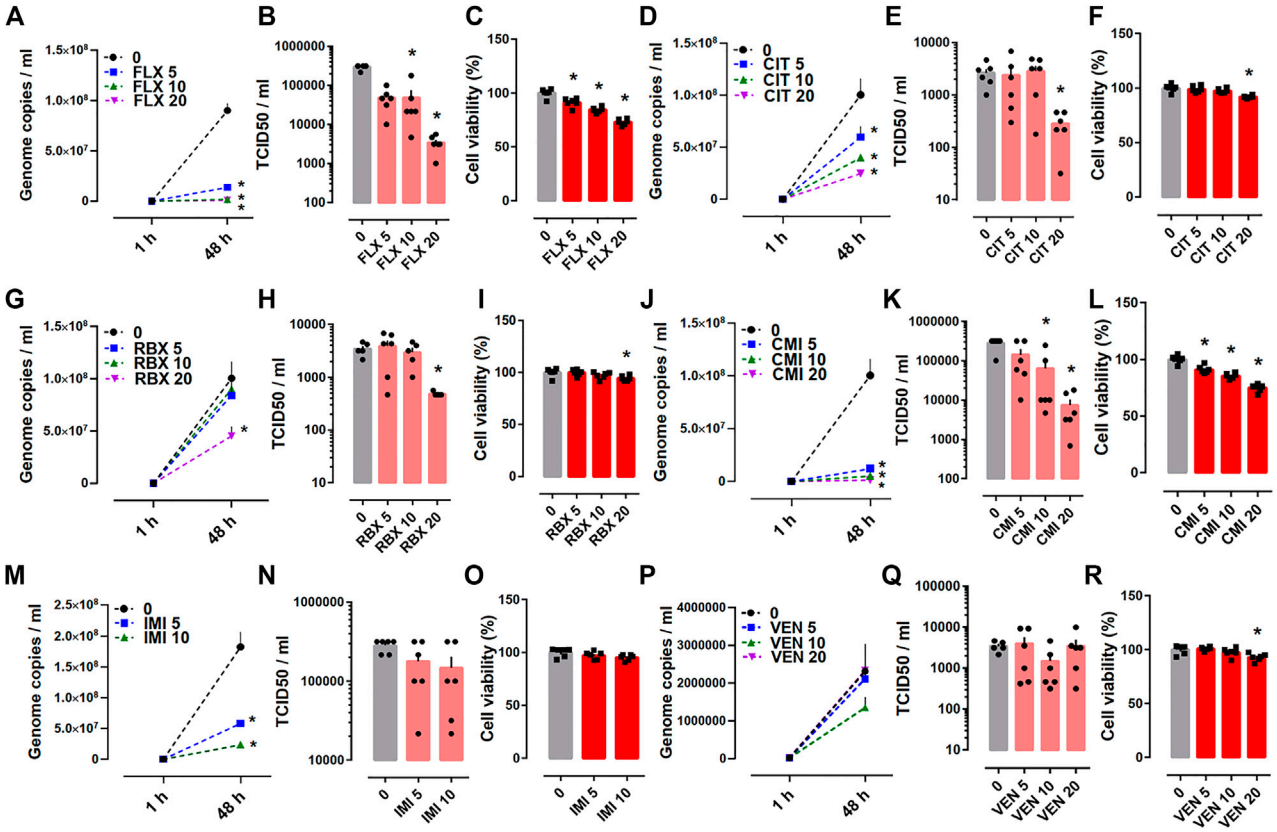

FIGURE 3 | The effect of antidepressant drugs on SARS-CoV-2 (B.1) infection in Calu-1 cells. **(A,B)** Fluoxetine (n = 6), **(D,E)** citalopram (n = 4–6), **(G,H)** reboxetine (n = 5–6), and **(J,K)** clomipramine (n = 6) reduced the genome copy number of SARS-CoV-2 measured by qRT-PCR and also the amount of infectious viral particles detected by TCID50 assay after 48 h of treatment. **(M)** Imipramine (n = 6) reduced the genome copy number, while **(N)** failed to reduce TCID50 (n = 6). **(P,Q)** Venlafaxine (n = 5–6) was ineffective for changing the genome copy number of SARS-CoV-2 and TCID50. **(C,F,I,L,R)** All the compounds, **(O)** except imipramine, reduced the viability of Calu-1 cells infected with the native SARS-CoV-2 (n = 6). Genome copies were plotted in linear scale, while TCID50 values in log scale. Fluoxetine: FLX, Citalopram: CIT, Reboxetine: RBX, Clomipramine: CMI, Imipramine: IMI, Venlafaxine: VEN. *p < 0.05 from control group (0) at corresponding time point. Data represented as mean ± SEM.

Figure S4C), we found that fluoxetine does not exert any effect on the ACE2 expression (**Supplementary Figure S4D**), while TMPRSS2 is significantly increased in non-infected cells after 24 h (**Supplementary Figure S4E**). Despite not being statistically significant, fluoxetine also increased TMPRSS2 in the infected cells (**Supplementary Figure S4E**).

In the Protocol II experiments, SARS-CoV-2 infected Calu-1 cells were treated with fluoxetine, reboxetine, clomipramine, imipramine, citalopram or venlafaxine up to 48 h at concentrations of 5, 10, and 20 μM. The base level of viral RNA that was measured 1 h after drug treatment revealed no significant changes between control and treatment groups (**Figure 3**). However, at 48 h after infection, fluoxetine (**Figures 3A,B**), citalopram (**Figures 3D,E**), reboxetine (**Figures 3G,H**), and clomipramine (**Figures 3J,K**) clearly reduced the genome copies of SARS-CoV-2 and infectious virus particles measured by TCID50 assay. Despite reducing the genome copies (**Figure 3M**), imipramine failed to effect the TCID50 (**Figure 3N**).Venlafaxine was ineffective on reducing the viral replication and infectious particles of native SARS-CoV-2 (**Figures 3P,Q**). Viability of Calu-1 cells was measured in infected cells after 48 h treatment with the compounds. All compounds, except for imipramine, decreased the cell viability (**Figures 3C,F,I,L,O,R**).

Antipsychotics can Decrease the Viral Infection

The antiviral activity of antipsychotics chlorpromazine, flupenthixol, and pimozide were tested through the Protocol I in HEK293T-ACE2-TMPRSS2 cells against the pseudotyped viruses harboring SARS-CoV-2 spike protein (**Table 1**). Following 24 h incubation, all of these compounds were able to prevent viral infection, although we also observed slight reduction of cell viability (**Figures 4A–C**).

Chlorpromazine (1, 2.5, and 5 μM) was also tested through the Protocol II in SARS-CoV-2 (B.1 lineage) infected Calu-1 cells. Treatment for 48 h with all the tested concentrations of chlorpromazine were able to reduce the total amount of virus (**Figure 4D**), but we failed to observe diminished amount of

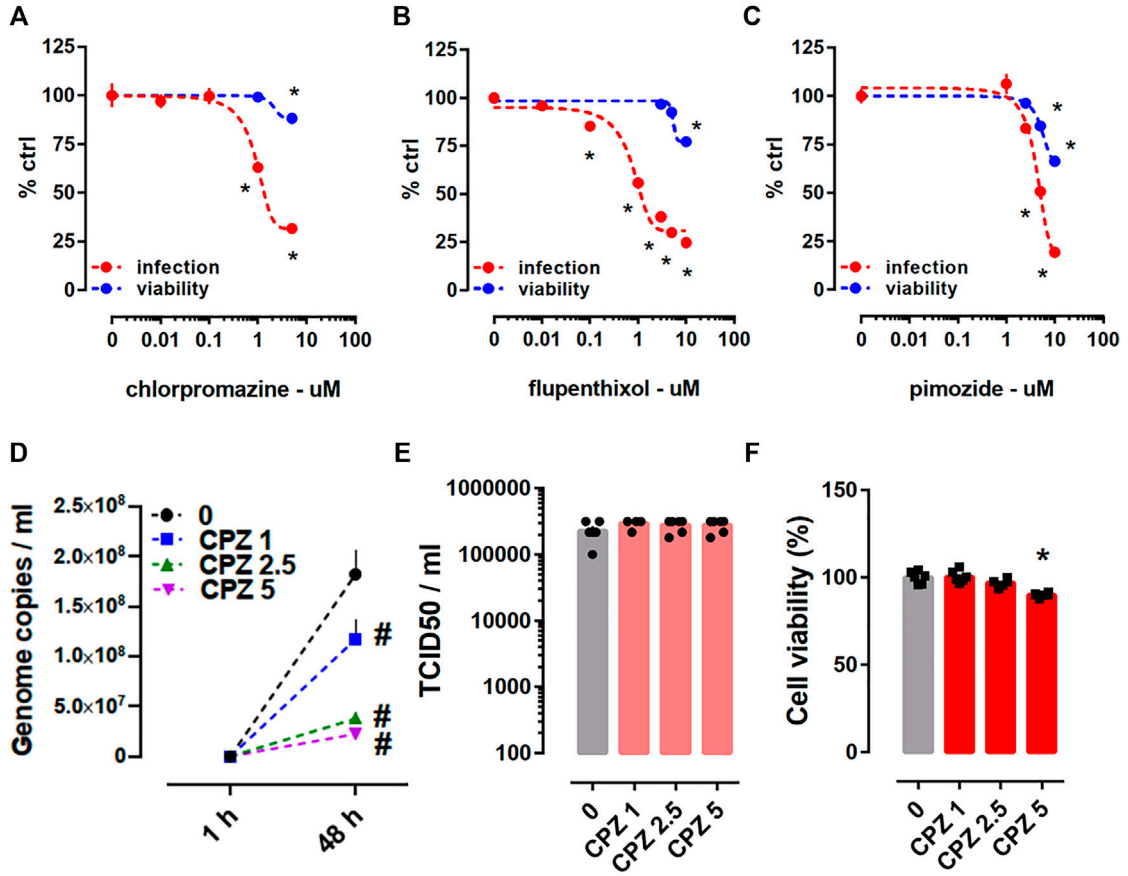

FIGURE 4 | Antiviral activity of antipsychotics in HEK293T-ACE2-TMPRSS2 cells challenged with pseudotyped viruses and in Calu-1 cells infected with SARS-CoV-2 (B.1). Decline of luciferase reporter activity was observed at multiple doses of **(A)** chlorpromazine (luciferase assay: $n = 8–20$; cell viability: $n = 8$; IC50 = 0.972 μM), **(B)** flupenthixol (luciferase assay: $n = 12$; cell viability: $n = 5$; IC50 = 1.072 μM), and **(C)** pimozide (luciferase assay: $n = 12$; cell viability: n = 5; IC50 = 4.539 μM) following 24 h incubation suggesting reduced infection. Treatment of cells with **(A)** chlorpromazine, **(B)** flupenthixol, and **(C)** pimozide combined with viral infection decreased cell viability indicated by the ATP level. **(D)** Treatment with chlorpromazine for 48 h decreased the genome copy number of SARS-CoV-2 ($n = 5–6$) in qRT-PCR, but **(E)** failed to reduce the amount of infectious virus in TCID50 assay ($n = 6$). **(F)** The highest dose of chlorpromazine treatment increased the toxicity in infected Calu-1 cells indicated by the ATP level. Genome copies were plotted in linear scale, while TCID50 values in log scale. Chlorpromazine: CPZ. *$p < 0.05$ from control group (0). #$p < 0.05$ from control group (0) at corresponding time point. Data represented as mean ± SEM.

infectious virus after 48 h treatment (**Figure 4E**). There was a slight but significant reduction in the viability of infected Calu-1 cells after 48 h treatment with chlorpromazine (5 μM) (**Figure 4F**).

Some Psychoactive Drugs Fail to Prevent the Infection by the Pseudotyped Viruses

Ketamine, used for many decades as anesthetic drug in clinics, has been shown to induce antidepressant-like effects when administered in sub-anesthetic doses (Berman et al., 2000; Zarate et al., 2006; Abdallah et al., 2015). Therefore, we next tested whether ketamine and ketamine metabolites (2S,6S-HNK and 2R,6R-HNK), which have also received attention as rapid-acting antidepressants during recent years (Abdallah et al., 2015; Zanos et al., 2018), might also inhibit infection by the pseudotyped virus. We found that neither ketamine nor the metabolites were effective in reducing the viral infection within 24 h of incubation period (**Supplementary Figures S5A–C**). Furthermore, other classical antidepressant drugs, phosphodiesterase-4 inhibitor rolipram and monoamine oxidase inhibitor phenelzine (**Table 1**) also failed to prevent the viral entry (**Supplementary Figures S5D,E**). We also tested carbamazepine, an anticonvulsant, which is also used as mood stabilizer for the treatment of bipolar disorder (Mitchell & Malhi, 2002). This compound also failed to change the viral infection in ACE2/TMPRSS2-expressing HEK cells after 24 h of treatment (**Supplementary Figure S5F**).

Some of the Tested Drugs Show SARS-CoV-2 Spike Specificity

We used pseudotyped viruses harboring glycoprotein of vesicular stomatitis virus (VSV) to address the specificity and potential viral-entry independent effects of tested compounds. HEK293T-ACE2-TMPRSS2 cells were treated with a mixture of VSV-G

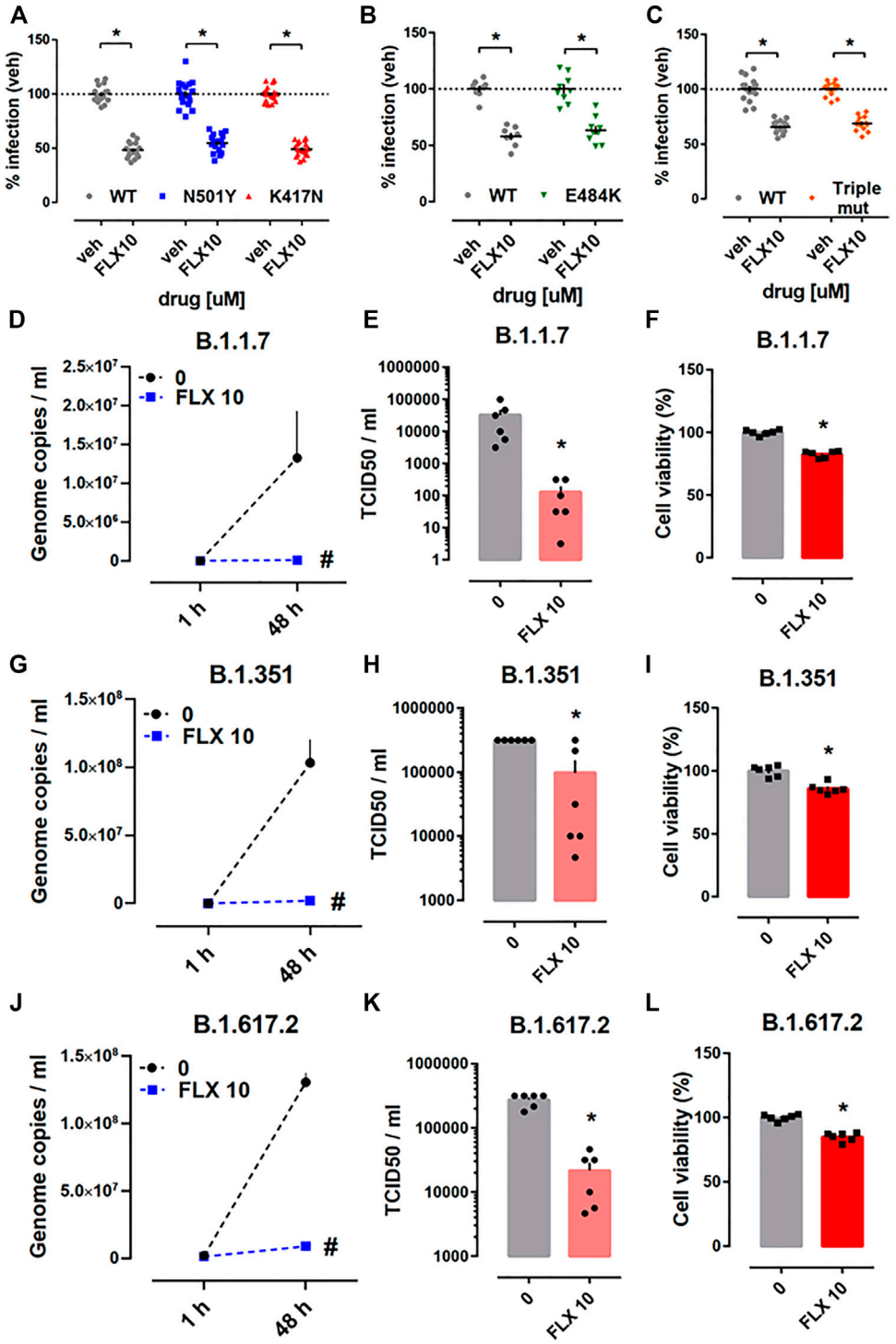

FIGURE 5 | Antiviral activity of fluoxetine against the mutant pseudo-viruses and the native variants of SARS-CoV-2. Treatment with fluoxetine (10 μM, 24 h) significantly reduced the luciferase reporter activity in HEK293T-ACE2-TMPRSS2 cells infected with **(A)** WT (grey, $n = 16$), N501Y (blue, $n = 18$), K417N (red, $n = 18$), **(B)** E484K (green, $n = 8$–9) and **(C)** triple mutant (N501Y/K417N/E484K, orange, $n = 13$–16), viral particles. Fluoxetine (10 μM) reduced genome copy number and TCID50 in Calu-1 cells infected with **(D,E)** B.1.1.7 (alpha), **(G,H)** B.1.351 (beta), and **(J,K)** B.1.617.2 (delta) variants, measured by qRT-PCR and TCID50 assay, respectively ($n = 6$). **(F,I,L)** Fluoxetine also slightly reduced the Calu-1 viability in cells infected with the variants ($n = 6$) measured by the ATP levels. Fluoxetine: FLX and wild type: WT. *$p < 0.05$ from control group (veh). #$p < 0.05$ from control group (0). Data represented as mean ± SEM.

pseudotyped viruses and drugs including fluoxetine, citalopram, paroxetine, fluvoxamine, reboxetine, clomipramine, desipramine, chlorpromazine, flupenthixol, or pimozide for 24 h. Viral infection was quantified by measuring the luciferase activity (**Supplementary Figure S6**; **Supplementary Figure S7**). While fluoxetine (**Supplementary Figure S6A**), clomipramine (**Supplementary Figure S6C**), chlorpromazine (**Supplementary Figure S6E**), flupenthixol (**Supplementary Figure S6G**), pimozide (**Supplementary Figure S6I**), and reboxetine (**Supplementary Figure S6K**) reduced the infection by the VSV-G pseudotyped viruses; citalopram (**Supplementary Figure S7A**), desipramine (**Supplementary Figure S7C**), paroxetine (**Supplementary Figure S7E**), and fluvoxamine (**Supplementary Figure S7G**) remained ineffective. Slight reduction of cell viability was observed in infected HEK293T-ACE2-TMPRSS2 cells after fluoxetine, clomipramine, chlorpromazine, pimozide, and reboxetine treatment (**Supplementary Figure S6**), while flupenthixol, citalopram, desipramine, paroxetine, or fluvoxamine did not exert a toxic effect (**Supplementary Figure S6**; **Supplementary Figure S7**).

We compared the effectiveness of the tested antidepressants and antipsychotics against SARS-CoV-2 spike- and VSV-G-pseudotyped viruses. We compiled the data from these viruses, and found higher effectiveness of drugs in reducing the luciferase activity in SARS-CoV-2 pseudoviruses compared to VSV-G (**Supplementary Figures S6B,D,F,H,J,L**; **Supplementary Figures S7B,D,F,H**).

Fluoxetine Remains Effective Against Pseudotyped Viruses Harboring the S Protein RBD Mutations and Native Variants B.1.1.7 (Alpha), B.1.351 (Beta), and B.1.617.2 (Delta)

Next, we addressed the effectiveness of fluoxetine against the pseudotyped viruses carrying mutations in the S protein that have been observed in some of the emerging SARS-CoV-2 variants. We found that fluoxetine (10 μM) treatment for 24 h was effective against pseudotyped viruses carrying single point mutations in their S protein (N501Y, K417N, or E484K) (**Figures 5A,B**), and also a triple mutant harboring combination of these three point mutations (N501Y/K417N/E484K) (**Figure 5C**). Calu-1 cells which were infected with B.1.1.7 (alpha), B.1.351 (beta), or B.1.617.2 (delta) variants, and challenged with fluoxetine (10 μM) showed reduced amount of genome copies (**Figures 5D,G,J**) and infectious virus (**Figures 5E,H,K**). The viability of Calu-1 cells infected with these variants and treated with fluoxetine for 48 h was slightly reduced (**Figures 5F,I,L**).

DISCUSSION

In the present study, we identified the potential of some widely consumed antidepressant and antipsychotic drugs against the infection by SARS-CoV-2 (B.1) and the variants B.1.1.7 (alpha), B.1.351 (beta), and B.1.617.2 (delta). The experiments using pseudotyped viruses to infect HEK293T cells overexpressing ACE2 and TMPRSS2 were aimed at identifying the direct effect of drugs on the entry phase of the viral infection, as we added the virus and drugs around the same time. The outcome measure by luciferase assay was a direct indication of the number of infected cells, due to replication-deficient nature of pseudotyped viruses. In experiments with human respiratory/lung epithelial cells and native virus, Calu-1 cells were first exposed to the SARS-CoV-2 virus, which was followed by the removal of this inoculum and addition of drugs to be tested. In this scenario, drugs do not necessarily interfere with the initial infection of cells by the virus, which was at low multiplicity of infection (MOI 0.05), but with viral particle production and infection of the neighboring cells. The decrease in viral replication that we observed after treating the cells for 48 h with the tested drugs and the reduction of TCID50 as a secondary outcome could be caused by 1) the blockade of virus entry during the subsequent waves of Calu-1 cell infection; 2) a direct effect on the mechanisms of viral replication, packaging and release of new viral particles; 3) an indirect effect through the regulation of innate immunity; or 4) a combination of the above effects. The first alternative, that the drugs interfere with viral infection of Calu-1 cells later on when the cells release newly packed viruses to medium thereby explaining the decline of viral genome copies and TCID50, would also be compatible with our findings with the pseudotyped virus.

By testing pseudotyped viruses harboring the VSV-G, we found that some compounds, including fluoxetine, clomipramine, chlorpromazine, flupenthixol, pimozide, and reboxetine, counteract the infection in HEK-ACE2-TMPRSS2 cells suggesting that these drugs are not specific for SARS-CoV-2 spike protein. On the other hand, the effect was significantly smaller against the VSV-G pseudoviruses compared to the SARS-CoV-2 pseudoviruses. Although the reduction of viability may have contributed to the diminished VSV-G infection, it should be noted that these compounds are effective against the entry of other viruses, as this has been reported in studies testing clomipramine and flupenthixol against Ebola virus (Johansen et al., 2015). Moreover, as these drugs also counteract VSV-G pseudoviruses, it is unlikely that mechanism of action is on the luciferase transcription. Interestingly, fluvoxamine, paroxetine, desipramine, nor citalopram exerted any effect on VSV-G infection suggesting the SARS-CoV-2 spike specificity of these compounds.

Accumulating data suggest that the psychoactive drugs that have been categorized as functional inhibitors of acid sphingomyelinase activity (FIASMA) (Kornhuber et al., 2010; Kornhuber et al., 2011) can significantly reduce the SARS-CoV-2 infection through cellular events associated with cholesterol-trapping, luminal pH changes in endolysosomal compartments, and ceramide manipulation (Carpinteiro et al., 2020; Schloer et al., 2020). FIASMA compounds, other than psychoactive drugs, have been reported to reduce SARS-CoV-2

infection *in vitro* (i.e., ambroxol, a mucolytic drug) (Carpinteiro et al., 2021), and also diminished the risk of intubation or death from COVID-19 in patients (i.e., cardiovascular system medications) (Hoertel, et al., 2021a). Most of the compounds we tested in the present study that showed antiviral activity are considered FIASMAs. On the other hand, we found that non-FIASMA compounds reboxetine, in both HEK and Calu-1 cells, and venlafaxine (Kornhuber et al., 2011; Zeitler et al., 2019), in HEK cells, demonstrate antiviral activity. However, the failure of venlafaxine against the native SARS-CoV-2 was unexpected. The data prompted us to assume that HEKs and Calu-1 cells might show differential expression and/or recruitment of distinct molecular targets for the infection by pseudoviruses and the native SARS-CoV-2, respectively. Therefore, availability or absence of specific targets might affect the drug response. Altogether, inhibition of ASM by these drugs can only partially explain the role of psychoactive drugs for the reduction of SARS-CoV-2 infection. Recently, some of these FIASMA compounds, including cationic amphiphilic drugs (CADs), have been suggested to induce phospholipidosis, which can explain the antiviral action of these drugs (Tummino et al., 2021).

Another mechanism of action proposed for these compounds, is the Sigma-1 receptor (S1R) agonism, as the activation of this receptor is known to regulate cytokine production (Lenze et al., 2020). Many psychoactive drugs bind to S1R, including fluvoxamine, sertraline, fluoxetine, citalopram, imipramine, paroxetine, and desipramine (Narita et al., 1996; Sukhatme et al., 2021). However, venlafaxine, one of the compounds that showed antiviral activity in our study in HEK cells, has a very weak affinity to this chaperone (Ishima et al., 2014). Moreover, ketamine can bind to both S1R and S2R (Robson et al., 2012), but this drug was ineffective as an antiviral agent in the present study. Therefore, S1R agonism and the regulation of cytokine levels through this chaperon does not appear to fully explain how these drugs act as antiviral agents.

Our data on chlorpromazine are in agreement with the earlier studies that have demonstrated antiviral activity against other coronaviruses (Cong et al., 2018; Dyall et al., 2014; Wilde et al., 2014). Other antipsychotics, flupenthixol and pimozide, identified as inhibitors of pseudotyped viral infection of HEK cells in our study, have also been confirmed by others as antiviral agents (Drayman et al., 2020; Yang et al., 2020). Pimozide, tested by computational docking analysis and *in vitro* assays, has been suggested to inhibit main protease of SARS-CoV-2 (M^{Pro}) (Vatansever et al., 2020).

Emergence of the novel variants raises concern on the effectiveness of currently available SARS-CoV-2 vaccines for the neutralization of these variants (Callaway, 2021; Callaway and Ledford, 2021; Fontanet et al., 2021). Recent *in vitro* studies reported that some of these vaccines remain effective against the variants carrying a set of mutations (Muik et al., 2021; Wu et al., 2021; Xie et al., 2021); however, others have shown decreased effectiveness, particularly to those carrying the E484K mutation (Wadman, 2020; Callaway and Mallapaty, 2021; Collier et al., 2021; Wang et al., 2021). Our data suggest that fluoxetine remains effective against the pseudotyped viruses harboring single mutations (N501Y, K417N, E484K), or a triple mutation (N501Y/K417N/E484K) present in beta and gamma variants. In line with this, inhibitory effect of fluoxetine persists against the SARS-CoV-2 variants alpha, beta, and delta. Therefore, it is plausible to argue that antidepressants, as well as related-psychoactive compounds can be considered as an alternative treatment method for people infected with SARS-CoV-2.

One of the limitations of our study is that inferring the drug concentrations required for the inhibition of SARS-CoV-2 infection at the clinical level from *in vitro* data is difficult, as these drugs accumulate in different organs, including brain and lungs, and show variance among individuals (Karson et al., 1993; Bolo, 2000; Johnson et al., 2007). Samples collected from pilot fatalities show 19.6 μg/ g mean concentration of fluoxetine in lungs (~7.6 μM) which is in the concentration range that is effective against SARS-CoV-2. Although further experiments are needed to address the tissue concentrations for the other molecules tested, these data suggest that due to accumulation into lung tissue (R. D. Johnson et al., 2007) (60-fold higher concentrations were found in lungs than in plasma), the concentrations tested here have been estimated to be clinically relevant against the SARS-CoV-2 infection (Eugene, 2021). We have also listed the IC50, CC50, and selectivity index (SI) parameters in **Supplementary Table S3**, which were calculated from the HEK cell response. We almost never reached to 50% drop in the cell viability test with the concentrations tested, which might have affected the CC50 values calculated by curve fitting. Therefore, interpretation of CC50 and SI values to suggest a safe antiviral window might be misleading.

Another interesting result we observed was the increase of TMPRSS2 in HEK cells after 24 h fluoxetine treatment. The TMPRSS2 increase by fluoxetine was detected in both non-infected and infected cells suggesting that the infection alone has no impact on this event. In fact, we expected to observe a reduction of TMPRSS2 by fluoxetine. However, the increase of TMPRSS2 after 24 h fluoxetine treatment might not be related with the antiviral action of fluoxetine. To gain an insight into this issue, testing fluoxetine with different treatment regimens is needed.

Dissecting the viral entry routes provides the opportunity for alternative strategies for prevention and management of the viral infection. Since the emergence of COVID-19, substantial progress has been made towards understanding the life cycle of SARS-CoV-2 and particularly how the virus can enter target cells (T. Tang et al., 2020). Earlier studies on viruses including SARS-CoV, Ebola, and influenza shed a light on the mechanism of viral entry and accentuated the importance of endolysosomal compartments and cholesterol (Mingo et al., 2015; Kühnl et al., 2018), which led to the recent discoveries of repurposed drugs against SARS-CoV-2 (Carpinteiro et al., 2020; Schloer et al., 2020). Alternative strategies, including the combination of compounds that can target machineries in host cells and the virus itself have also been developed to increase the effectiveness of the treatment (Schloer et al., 2021). For instance,

combination of fluoxetine with remdesivir, a nucleotide analog interfering RNA-dependent RNA polymerase, was shown to be more effective than either of these compounds alone (Schloer et al., 2021).

Together with other recent studies, our data suggest that antidepressant drugs might become an additional tool against the COVID-19 pandemic, therefore, further clinical studies implicating bigger sample size and longer follow-up periods should be conducted.

DATA AVAILABILITY STATEMENT

The original contributions presented in the study are included in the article/**Supplementary Material**, further inquiries can be directed to the corresponding author. Data produced in the present study is openly available in FigShare (DOI: 10.6084/m9.figshare.14248856).

AUTHOR CONTRIBUTIONS

SF, PC, and EC conceptualization; SF, SK, HU, LL investigation; SF, SK, KS, HU writing first draft, reviewed by SF, SK, KS, OV, PC, and EC.

FUNDING

This study was supported by the Academy of Finland Grant # 335527 to EC and OV, # 1336490 to OV, and Turkish Ministry of Education to HU.

ACKNOWLEDGMENTS

We thank Seija Lagas, Sulo Kolehmainen, Elsa Meshi and Mira Utriainen for technical assistance. We extend our gratitude to Leonora Szirovicza for maintaining Calu-3 and Caco-2 cell lines. Dr. Emmy Verschuren is thanked for providing the Calu-1 cell line, Dr. Mirja Puolakkainen for Calu-3 cell line, Prof. Carl-Henrik von Bonsdorf for Caco-2 cell line, and Dr. Didier Trono for plasmids that were acquired through Addgene. We also thank Dr. Jussi Hepojoki for the ACE2 antibody.

SUPPLEMENTARY MATERIAL

The Supplementary Material for this article can be found online at: https://www.frontiersin.org/articles/10.3389/fphar.2021.755600/full#supplementary-material

REFERENCES

Abdallah, C. G., Sanacora, G., Duman, R. S., and Krystal, J. H. (2015). Ketamine and Rapid-Acting Antidepressants: A Window into a New Neurobiology for Mood Disorder Therapeutics. *Annu. Rev. Med.* 66 (1), 509–523. doi:10.1146/annurev-med-053013-062946

Alenquer, M., Ferreira, F., Lousa, D., Valério, M., Medina-Lopes, M., Bergman, M. L., et al. (2021). Signatures in SARS-CoV-2 Spike Protein Conferring Escape to Neutralizing Antibodies. *Plos Pathog.* 17 (8), e1009772. doi:10.1371/journal.ppat.1009772

Berman, R. M., Cappiello, A., Anand, A., Oren, D. A., Heninger, G. R., Charney, D. S., et al. (2000). Antidepressant Effects of Ketamine in Depressed Patients. *Biol. Psychiatry* 47 (4), 351–354. doi:10.1016/S0006-3223(99)00230-9

Berthoux, L., Sebastian, S., Sokolskaja, E., and Luban, J. (2004). Lv1 Inhibition of Human Immunodeficiency Virus Type 1 Is Counteracted by Factors that Stimulate Synthesis or Nuclear Translocation of Viral cDNA. *J. Virol.* 78 (21), 11739–11750. doi:10.1128/JVI.78.21.11739-11750.2004

Bolo, N. R., Hodé, Y., Nédélec, J. F., Lainé, E., Wagner, G., and Macher, J. P. (2000). Brain Pharmacokinetics and Tissue Distribution *In Vivo* of Fluvoxamine and Fluoxetine by Fluorine Magnetic Resonance Spectroscopy. *Neuropsychopharmacology* 23 (4), 428–438. doi:10.1016/S0893-133X(00)00116-0

Callaway, E., and Ledford, H. (2021). How to Redesign COVID Vaccines So They Protect against Variants. *Nature* 590 (7844), 15–16. doi:10.1038/d41586-021-00241-6

Callaway, E., and Mallapaty, S. (2021). Novavax Offers First Evidence that COVID Vaccines Protect People against Variants. *Nature* 590 (7844), 17. doi:10.1038/d41586-021-00268-9

Callaway, E. (2021). Could New COVID Variants Undermine Vaccines? Labs Scramble to Find Out. *Nature* 589 (7841), 177–178. doi:10.1038/d41586-021-00031-0

Cantuti-Castelvetri, L., Ojha, R., Pedro, L. D., Djannatian, M., Franz, J., Kuivanen, S., et al. (2020). Neuropilin-1 Facilitates SARS-CoV-2 Cell Entry and Infectivity. *Science* 370 (6518), 856–860. doi:10.1126/science.abd2985

Carpinteiro, A., Edwards, M. J., Hoffmann, M., Kochs, G., Gripp, B., Weigang, S., et al. (2020). Pharmacological Inhibition of Acid Sphingomyelinase Prevents Uptake of SARS-CoV-2 by Epithelial Cells. *Cel Rep. Med.* 1, 100142. doi:10.1016/j.xcrm.2020.100142

Carpinteiro, A., Gripp, B., Hoffmann, M., Pöhlmann, S., Hoertel, N., Edwards, M. J., et al. (2021). Inhibition of Acid Sphingomyelinase by Ambroxol Prevents SARS-CoV-2 Entry into Epithelial Cells. *J. Biol. Chem.* 296, 100701. doi:10.1016/j.jbc.2021.100701

Casarotto, P. C., Girych, M., Fred, S. M., Kovaleva, V., Moliner, R., Enkavi, G., et al. (2021). Antidepressant Drugs Act by Directly Binding to TRKB Neurotrophin Receptors. *Cell* 184 (0), 1299–1313. doi:10.1016/j.cell.2021.01.034

Cherian, S., Potdar, V., Jadhav, S., Yadav, P., Gupta, N., Das, M., et al. (2021). Convergent Evolution of SARS-CoV-2 Spike Mutations, L452R, E484Q and P681R, in the Second Wave of COVID-19 in Maharashtra, India. *Microorganisms* 9 (7), 1542. doi:10.1101/2021.04.22.440932

Collier, D. A., De Marco, A., Ferreira, I. A. T. M., Meng, B., Datir, R., Walls, A. C., et al. (2021). SARS-CoV-2 B.1.1.7 Sensitivity to mRNA Vaccine-Elicited, Convalescent and Monoclonal Antibodies. *Infect. Dis. (except HIV/AIDS)*. 1. 1. doi:10.1101/2021.01.19.21249840

Cong, Y., Hart, B. J., Gross, R., Zhou, H., Frieman, M., Bollinger, L., et al. (2018). MERS-CoV Pathogenesis and Antiviral Efficacy of Licensed Drugs in Human Monocyte-Derived Antigen-Presenting Cells. *PLoS ONE* 13 (3). doi:10.1371/journal.pone.0194868

Corman, V. M., Landt, O., Kaiser, M., Molenkamp, R., Meijer, A., Chu, D. K., et al. (2020). Detection of 2019 Novel Coronavirus (2019-nCoV) by Real-Time RT-PCR. *Euro Surveill.* 25 (3), 2000045. doi:10.2807/1560-7917.ES.2020.25.3.2000045

Daly, J. L., Simonetti, B., Klein, K., Chen, K. E., Williamson, M. K., Antón-Plágaro, C., et al. (2020). Neuropilin-1 Is a Host Factor for SARS-CoV-2 Infection. *Science* 370 (6518), 861–865. doi:10.1126/science.abd3072

Drayman, N., Jones, K. A., Azizi, S.-A., Froggatt, H. M., Tan, K., Maltseva, N. I., et al. (2020). Drug Repurposing Screen Identifies Masitinib as a 3CLpro Inhibitor that Blocks Replication of SARS-CoV-2 *In Vitro*. *Microbiology*. 1. 1. doi:10.1101/2020.08.31.274639

Dyall, J., Coleman, C. M., Hart, B. J., Venkataraman, T., Holbrook, M. R., Kindrachuk, J., et al. (2014). Repurposing of Clinically Developed Drugs for Treatment of Middle East Respiratory Syndrome Coronavirus Infection. *Antimicrob. Agents Chemother.* 58 (8), 4885–4893. doi:10.1128/AAC.03036-14

Eugene, A. R. (2021). Fluoxetine Pharmacokinetics and Tissue Distribution Suggest a Possible Role in Reducing SARS-CoV-2 Titers. *F1000Res* 10, 477. doi:10.12688/f1000research.53275.1

Faria, N. R., Mellan, T. A., Whittaker, C., Claro, I. M., Candido, D. da. S., Mishra, S., et al. (2021). Genomics and Epidemiology of the P.1 SARS-CoV-2 Lineage in Manaus, Brazil. *Science*, 372 (6544), 815–821. doi:10.1126/science.abh2644

Fontanet, A., Autran, B., Lina, B., Kieny, M. P., Karim, S. S. A., and Sridhar, D. (2021). SARS-CoV-2 Variants and Ending the COVID-19 Pandemic. *The Lancet*, 397 (10278), 952–954. doi:10.1016/S0140-6736(21)00370-6

Fred, S. M., Laukkanen, L., Brunello, C. A., Vesa, L., Göös, H., Cardon, I., et al. (2019). Pharmacologically Diverse Antidepressants Facilitate TRKB Receptor Activation by Disrupting its Interaction with the Endocytic Adaptor Complex AP-2. *J. Biol. Chem.* 294, 18150–18161. doi:10.1074/jbc.RA119.008837

Greaney, A. J., Loes, A. N., Crawford, K. H. D., Starr, T. N., Malone, K. D., Chu, H. Y., et al. (2021a). Comprehensive Mapping of Mutations in the SARS-CoV-2 Receptor-Binding Domain that Affect Recognition by Polyclonal Human Plasma Antibodies. *Cell Host & Microbe* 29, 463–476. doi:10.1016/j.chom.2021.02.003

Greaney, A. J., Starr, T. N., Gilchuk, P., Zost, S. J., Binshtein, E., Loes, A. N., et al. (2021b). Complete Mapping of Mutations to the SARS-CoV-2 Spike Receptor-Binding Domain that Escape Antibody Recognition. *Cell Host & Microbe* 29 (1), 44–57. e9. doi:10.1016/j.chom.2020.11.007

Gu, H., Chen, Q., Yang, G., He, L., Fan, H., Deng, Y. Q., et al. (2020). Adaptation of SARS-CoV-2 in BALB/c Mice for Testing Vaccine Efficacy. *Science* 369 (6511), 1603–1607. doi:10.1126/science.abc4730

Hoertel, N., Sánchez-Rico, M., Gulbins, E., Kornhuber, J., Carpinteiro, A., Lenze, E. J., et al. (2021a). Association between FIASMAs and Reduced Risk of Intubation or Death in Individuals Hospitalized for Severe COVID-19: An Observational Multicenter Study. *Clin. Pharmacol. Ther.* 110 (6), 1498–1511. doi:10.1002/cpt.2317

Hoertel, N., Sánchez-Rico, M., Vernet, R., Beeker, N., Jannot, A.-S., Neuraz, A., et al. (2021b). Association between Antidepressant Use and Reduced Risk of Intubation or Death in Hospitalized Patients with COVID-19: Results from an Observational Study. *Mol. Psychiatry* 26, 5199–5212. doi:10.1038/s41380-021-01021-4

Hoffmann, M., Kleine-Weber, H., and Pöhlmann, S. (2020a). A Multibasic Cleavage Site in the Spike Protein of SARS-CoV-2 Is Essential for Infection of Human Lung Cells. *Mol. Cell* 78 (4), 779–e5. doi:10.1016/j.molcel.2020.04.022

Hoffmann, M., Kleine-Weber, H., Schroeder, S., Krüger, N., Herrler, T., Erichsen, S., et al. (2020b). SARS-CoV-2 Cell Entry Depends on ACE2 and TMPRSS2 and Is Blocked by a Clinically Proven Protease Inhibitor. *Cell* 181 (2), 271–e8. doi:10.1016/j.cell.2020.02.052

Hoffmann, M., Hofmann-Winkler, H., Smith, J. C., Krüger, N., Sørensen, L. K., Søgaard, O. S., et al. (2020c). Camostat Mesylate Inhibits SARS-CoV-2 Activation by TMPRSS2-Related Proteases and its Metabolite GBPA Exerts Antiviral Activity. *BioRxiv*. 1. 1. doi:10.1101/2020.08.05.237651

Ishima, T., Fujita, Y., and Hashimoto, K. (2014). Interaction of New Antidepressants with Sigma-1 Receptor Chaperones and Their Potentiation of Neurite Outgrowth in PC12 Cells. *Eur. J. Pharmacol.* 727, 167–173. doi:10.1016/j.ejphar.2014.01.064

Johansen, L. M., DeWald, L. E., Shoemaker, C. J., Hoffstrom, B. G., Lear-Rooney, C. M., Stossel, A., et al. (2015). A Screen of Approved Drugs and Molecular Probes Identifies Therapeutics with Anti-ebola Virus Activity. *Sci. Transl Med.* 7 (290), 290ra89. doi:10.1126/scitranslmed.aaa5597

Johnson, R. D., Lewis, R. J., and Angier, M. K. (2007). The Distribution of Fluoxetine in Human Fluids and Tissues. *J. Anal. Toxicol.* 31 (7), 409–414. doi:10.1093/jat/31.7.409

Johnson, B. A., Xie, X., Bailey, A. L., Kalveram, B., Lokugamage, K. G., Muruato, A., et al. (2021). Loss of Furin Cleavage Site Attenuates SARS-CoV-2 Pathogenesis. *Nature* 591, 293–299. doi:10.1038/s41586-021-03237-4

Karson, C. N., Newton, J. E., Livingston, R., Jolly, J. B., Cooper, T. B., Sprigg, J., et al. (1993). Human Brain Fluoxetine Concentrations. *J. Neuropsychiatry Clin. Neurosci.* 5 (3), 322–329. doi:10.1176/jnp.5.3.322

Kawase, M., Shirato, K., van der Hoek, L., Taguchi, F., and Matsuyama, S. (2012). Simultaneous Treatment of Human Bronchial Epithelial Cells with Serine and Cysteine Protease Inhibitors Prevents Severe Acute Respiratory Syndrome Coronavirus Entry. *J. Virol.* 86 (12), 6537–6545. doi:10.1128/JVI.00094-12

Khateeb, J., Li, Y., and Zhang, H. (2021). Emerging SARS-CoV-2 Variants of Concern and Potential Intervention Approaches. *Crit. Care* 25 (1), 244. doi:10.1186/s13054-021-03662-x

Kornhuber, J., Tripal, P., Reichel, M., Mühle, C., Rhein, C., Muehlbacher, M., et al. (2010). Functional Inhibitors of Acid Sphingomyelinase (FIASMAs): A Novel Pharmacological Group of Drugs with Broad Clinical Applications. *Cell Physiol Biochem* 26 (1), 9–20. doi:10.1159/000315101

Kornhuber, J., Muehlbacher, M., Trapp, S., Pechmann, S., Friedl, A., Reichel, M., et al. (2011). Identification of Novel Functional Inhibitors of Acid Sphingomyelinase. *PLoS ONE* 6 (8), e23852. doi:10.1371/journal.pone.0023852

Kühnl, A., Musiol, A., Heitzig, N., Johnson, D. E., Ehrhardt, C., Grewal, T., et al. (2018). Late Endosomal/Lysosomal Cholesterol Accumulation Is a Host Cell-Protective Mechanism Inhibiting Endosomal Escape of Influenza A Virus. *MBio* 9 (4), e01345–18. doi:10.1128/mBio.01345-18

Lai, M. M., and Cavanagh, D. (1997). The Molecular Biology of Coronaviruses. *Adv. Virus. Res.* 48, 1–100. doi:10.1016/S0065-3527(08)60286-9

Lenze, E. J., Mattar, C., Zorumski, C. F., Stevens, A., Schweiger, J., Nicol, G. E., et al. (2020). Fluvoxamine vs Placebo and Clinical Deterioration in Outpatients with Symptomatic COVID-19: A Randomized Clinical Trial. *JAMA* 324, 2292. doi:10.1001/jama.2020.22760

Li, W., Moore, M. J., Vasilieva, N., Sui, J., Wong, S. K., Berne, M. A., et al. (2003). Angiotensin-converting Enzyme 2 Is a Functional Receptor for the SARS Coronavirus. *Nature* 426 (6965), 450–454. doi:10.1038/nature02145

Li, F., Li, W., Farzan, M., and Harrison, S. C. (2005). Structure of SARS Coronavirus Spike Receptor-Binding Domain Complexed with Receptor. *Science* 309 (5742), 1864–1868. doi:10.1126/science.1116480

Lin, J.-W., Tang, C., Wei, H.-C., Du, B., Chen, C., Wang, M., et al. (2021). Genomic Monitoring of SARS-CoV-2 Uncovers an Nsp1 Deletion Variant that Modulates Type I Interferon Response. *Cell Host & Microbe* 29, 489–502. doi:10.1016/j.chom.2021.01.015

Mercorelli, B., Palù, G., and Loregian, A. (2018). Drug Repurposing for Viral Infectious Diseases: How Far Are We? *Trends Microbiol.* 26 (10), 865–876. doi:10.1016/j.tim.2018.04.004

Mingo, R. M., Simmons, J. A., Shoemaker, C. J., Nelson, E. A., Schornberg, K. L., D'Souza, R. S., et al. (2015). Ebola Virus and Severe Acute Respiratory Syndrome Coronavirus Display Late Cell Entry Kinetics: Evidence that Transport to NPC1+ Endolysosomes Is a Rate-Defining Step. *J. Virol.* 89 (5), 2931–2943. doi:10.1128/JVI.03398-14

Mitchell, P. B., and Malhi, G. S. (2002). The Expanding Pharmacopoeia for Bipolar Disorder. *Annu. Rev. Med.* 53, 173–188. doi:10.1146/annurev.med.53.082901.103933

Mlcochova, P., Kemp, S., Dhar, M. S., Papa, G., Meng, B., Mishra, S., et al. (2021). SARS-CoV-2 B.1.617.2 Delta Variant Replication, Sensitivity to Neutralising Antibodies and Vaccine Breakthrough. *BioRxiv*. 1. 1. doi:10.1101/2021.05.08.443253

Muik, A., Wallisch, A.-K., Sänger, B., Swanson, K. A., Mühl, J., Chen, W., et al. (2021). Neutralization of SARS-CoV-2 Lineage B.1.1.7 Pseudovirus by BNT162b2 Vaccine-Elicited Human Sera. *BioRxiv*. 1. 1. doi:10.1101/2021.01.18.42698410.1126/science.abg6105

Narita, N., Hashimoto, K., Tomitaka, S., and Minabe, Y. (1996). Interactions of Selective Serotonin Reuptake Inhibitors with Subtypes of Sigma Receptors in Rat Brain. *Eur. J. Pharmacol.* 307 (1), 117–119. doi:10.1016/0014-2999(96)00254-3

Nelson, G., Buzko, O., Spilman, P., Niazi, K., Rabizadeh, S., and Soon-Shiong, P. (2021). Molecular Dynamic Simulation Reveals E484K Mutation Enhances Spike RBD-ACE2 Affinity and the Combination of E484K, K417N and N501Y Mutations (501Y.V2 Variant) Induces Conformational Change Greater Than N501Y Mutant Alone, Potentially Resulting in an Escape Mutant. *BioRxiv*. 1. 1. doi:10.1101/2021.01.13.426558

Ou, X., Liu, Y., Lei, X., Li, P., Mi, D., Ren, L., et al. (2020). Characterization of Spike Glycoprotein of SARS-CoV-2 on Virus Entry and its Immune Cross-Reactivity with SARS-CoV. *Nat. Commun.* 11 (1), 1620. doi:10.1038/s41467-020-15562-9

PAOLA. *Phylogenetic relationship of SARS-CoV-2 sequences from Amazonas with emerging Brazilian variants harboring mutations E484K and N501Y in the Spike*

protein—SARS-CoV-2 coronavirus / nCoV-2019 Genomic Epidemiology. (2021), January 11. Virological. Available at: https://virological.org/t/phylogenetic-relationship-of-sars-cov-2-sequences-from-amazonas-with-emerging-brazilian-variants-harboring-mutations-e484k-and-n501y-in-the-spike-protein/585

Plaze, M., Attali, D., Petit, A. C., Blatzer, M., Simon-Loriere, E., Vinckier, F., et al. (2020a). Repurposing Chlorpromazine to Treat COVID-19: The reCoVery Study. *Encephale* 46 (3), 169–172. doi:10.1016/j.encep.2020.05.006

Plaze, M., Attali, D., Prot, M., Petit, A. C., Blatzer, M., Vinckier, F., et al. (2021b). Inhibition of the Replication of SARS-CoV-2 in Human Cells by the FDA-Approved Drug Chlorpromazine. *Int. J. Antimicrob. Agents* 57, 106274. doi:10.1016/j.ijantimicag.2020.106274

Puelles, V. G., Lütgehetmann, M., Lindenmeyer, M. T., Sperhake, J. P., Wong, M. N., Allweiss, L., et al. (2020). Multiorgan and Renal Tropism of SARS-CoV-2. *N. Engl. J. Med.* 383 (6), 590–592. doi:10.1056/NEJMc2011400

Rambaut, A. (2020). Preliminary genomic characterisation of an emergent SARSCoV-2 lineage in the UK defined by a novel set of spike mutations—SARSCoV-2 coronavirus / nCoV-2019 Genomic Epidemiology. Virological. Available at: https://virological.org/t/preliminary-genomic-characterisationof-an-emergent-sars-cov-2-lineage-in-the-uk-defined-by-a-novel-set-of-spikemutations/563 (Accessed December 18, 2020).

Reis, G., Moreira-Silva, E. A. D. S., Silva, D. C. M., Thabane, L., Milagres, A. C., Ferreira, T. S., et al. (2021). Effect of Early Treatment with Fluvoxamine on Risk of Emergency Care and Hospitalisation Among Patients with COVID-19: The TOGETHER Randomised, Platform Clinical Trial. *Lancet Glob. Health*. S2214-109X(21)00448-4. doi:10.1016/S2214-109X(21)00448-4

Robson, M. J., Elliott, M., Seminerio, M. J., and Matsumoto, R. R. (2012). Evaluation of Sigma (σ) Receptors in the Antidepressant-like Effects of Ketamine *In Vitro* and *In Vivo*. *Eur. Neuropsychopharmacol.* 22 (4), 308–317. doi:10.1016/j.euroneuro.2011.08.002

Schloer, S., Brunotte, L., Goretzko, J., Mecate-Zambrano, A., Korthals, N., Gerke, V., et al. (2020). Targeting the Endolysosomal Host-SARS-CoV-2 Interface by Clinically Licensed Functional Inhibitors of Acid Sphingomyelinase (FIASMA) Including the Antidepressant Fluoxetine. *Emerg. Microbes Infect.* 9 (1), 2245–2255. doi:10.1080/22221751.2020.1829082

Schloer, S., Brunotte, L., Mecate-Zambrano, A., Zheng, S., Tang, J., Ludwig, S., et al. (2021). Drug Synergy of Combinatory Treatment with Remdesivir and the Repurposed Drugs Fluoxetine and Itraconazole Effectively Impairs SARS-CoV-2 Infection *In Vitro*. *Br. J. Pharmacol.* 178 (11), 2339–2350. doi:10.1111/bph.15418

Serra, A., Fratello, M., Federico, A., Ojha, R., Provenzani, R., Tasnadi, E., et al. (2021). Computationally Prioritized Drugs Inhibit SARS-CoV-2 Infection and Syncytia Formation. *BioRxiv*. 1. 1. doi:10.1101/2021.04.15.440004

Shulla, A., Heald-Sargent, T., Subramanya, G., Zhao, J., Perlman, S., and Gallagher, T. (2011). A Transmembrane Serine Protease Is Linked to the Severe Acute Respiratory Syndrome Coronavirus Receptor and Activates Virus Entry. *J. Virol.* 85 (2), 873–882. doi:10.1128/JVI.02062-10

Starr, T. N., Greaney, A. J., Hilton, S. K., Ellis, D., Crawford, K. H. D., Dingens, A. S., et al. (2020). Deep Mutational Scanning of SARS-CoV-2 Receptor Binding Domain Reveals Constraints on Folding and ACE2 Binding. *Cell* 182 (5), 1295–1310. doi:10.1016/j.cell.2020.08.012

Sukhatme, V. P., Reiersen, A. M., Vayttaden, S. J., and Sukhatme, V. V. (2021). Fluvoxamine: A Review of its Mechanism of Action and its Role in COVID-19. *Front. Pharmacol.* 12, 763. doi:10.3389/fphar.2021.652688

Tang, Q., Song, Y., Shi, M., Cheng, Y., Zhang, W., and Xia, X. Q. (2015). Inferring the Hosts of Coronavirus Using Dual Statistical Models Based on Nucleotide Composition. *Sci. Rep.* 5 (1), 17155. doi:10.1038/srep17155

Tang, T., Bidon, M., Jaimes, J. A., Whittaker, G. R., and Daniel, S. (2020). Coronavirus Membrane Fusion Mechanism Offers a Potential Target for Antiviral Development. *Antivir. Res* 178, 104792. doi:10.1016/j.antiviral.2020.104792

Tegally, H., Wilkinson, E., Giovanetti, M., Iranzadeh, A., Fonseca, V., Giandhari, J., et al. (20202020). Emergence and Rapid Spread of a New Severe Acute Respiratory Syndrome-Related Coronavirus 2 (SARS-CoV-2) Lineage with Multiple Spike Mutations in South Africa. *MedRxiv* 1221, 20248640. doi:10.1101/2020.12.21.20248640

To, K. K., Hung, I. F., Chan, J. F., and Yuen, K. Y. (2013). From SARS Coronavirus to Novel Animal and Human Coronaviruses. *J. Thorac. Dis.* 5(Suppl. 2), S103–S108. doi:10.3978/j.issn.2072-1439.2013.06.02

Tummino, T. A., Rezelj, V. V., Fischer, B., Fischer, A., O'Meara, M. J., Monel, B., et al. (2021). Drug-induced Phospholipidosis Confounds Drug Repurposing for SARS-CoV-2. *Science* 373 (6554), 541–547. doi:10.1126/science.abi4708

Vatansever, E. C., Yang, K., Kratch, K. C., Drelich, A., Cho, C.-C., Mellott, D. M., et al. (2020). Bepridil Is Potent against SARS-CoV-2 *In Vitro*. *BioRxiv*. 1. 1. doi:10.1101/2020.05.23.112235

Voloch, C. M., da Silva, F. R., de Almeida, L. G. P., Cardoso, C. C., Brustolini, O. J., Gerber, A. L., et al. (2020). Genomic characterization of a novel SARS-CoV-2 lineage from Rio de Janeiro, Brazil. *MedRxiv* 95, 10. doi:10.1101/2020.12.23.20248598

Wadman, M. (2020). The Long Shot. *Science* 370 (6517), 649–653. doi:10.1126/science.370.6517.649

Walls, A. C., Park, Y. J., Tortorici, M. A., Wall, A., McGuire, A. T., and Veesler, D. (2020). Structure, Function, and Antigenicity of the SARS-CoV-2 Spike Glycoprotein. *Cell* 181 (2), 281–e6. doi:10.1016/j.cell.2020.02.058

Wan, Y., Shang, J., Graham, R., Baric, R. S., and Li, F. (2020). Receptor Recognition by the Novel Coronavirus from Wuhan: An Analysis Based on Decade-Long Structural Studies of SARS Coronavirus. *J. Virol.* 94 (7). 1. doi:10.1128/JVI.00127-20

Wang, Q., Zhang, Y., Wu, L., Niu, S., Song, C., Zhang, Z., et al. (2020). Structural and Functional Basis of SARS-CoV-2 Entry by Using Human ACE2. *Cell* 181 (4), 894–e9. doi:10.1016/j.cell.2020.03.045

Wang, P., Nair, M. S., Liu, L., Iketani, S., Luo, Y., Guo, Y., et al. (2021). Antibody Resistance of SARS-CoV-2 Variants B.1.351 and B.1.1.7. *BioRxiv*. 1. 1. doi:10.1101/2021.01.25.428137

Wibmer, C. K., Ayres, F., Hermanus, T., Madzivhandila, M., Kgagudi, P., Oosthuysen, B., et al. (2021). SARS-CoV-2 501Y.V2 Escapes Neutralization by South African COVID-19 Donor Plasma. *Nat. Med.* 27 (4), 622–625. doi:10.1038/s41591-021-01285-x

Wilde, A. H., de Jochmans, D., Posthuma, C. C., Zevenhoven-Dobbe, J. C., Nieuwkoop, S., van Bestebroer, T. M., et al. (2014). Screening of an FDA-Approved Compound Library Identifies Four Small-Molecule Inhibitors of Middle East Respiratory Syndrome Coronavirus Replication in Cell Culture. *Antimicrob. Agents Chemother.* 58 (8), 4875–4884. doi:10.1128/AAC.03011-14

Wu, F., Zhao, S., Yu, B., Chen, Y. M., Wang, W., Song, Z. G., et al. (2020). A New Coronavirus Associated with Human Respiratory Disease in China. *Nature* 579 (7798), 265–269. doi:10.1038/s41586-020-2008-3

Wu, K., Werner, A. P., Moliva, J. I., Koch, M., Choi, A., Stewart-Jones, G. B. E., et al. (2021). mRNA-1273 Vaccine Induces Neutralizing Antibodies against Spike Mutants from Global SARS-CoV-2 Variants. *Immunology*. 1. 1. doi:10.1101/2021.01.25.427948

Xie, X., Liu, Y., Liu, J., Zhang, X., Zou, J., Fontes-Garfias, C. R., et al. (2021). Neutralization of SARS-CoV-2 Spike 69/70 Deletion, E484K and N501Y Variants by BNT162b2 Vaccine-Elicited Sera. *Nat. Med.* 27, 620–621. doi:10.1038/s41591-021-01270-4

Yang, L., Pei, R. J., Li, H., Ma, X. N., Zhou, Y., Zhu, F. H., et al. (2020). Identification of SARS-CoV-2 Entry Inhibitors Among Already Approved Drugs. *Acta Pharmacol. Sin* 1–7. doi:10.1038/s41401-020-00556-6

Zanos, P., Moaddel, R., Morris, P. J., Riggs, L. M., Highland, J. N., Georgiou, P., et al. (2018). Ketamine and Ketamine Metabolite Pharmacology: Insights into Therapeutic Mechanisms. *Pharmacol. Rev.* 70 (3), 621–660. doi:10.1124/pr.117.015198

Zarate, C. A., Singh, J. B., Carlson, P. J., Brutsche, N. E., Ameli, R., Luckenbaugh, D. A., et al. (2006). A Randomized Trial of an N-Methyl-D-Aspartate Antagonist in Treatment-Resistant Major Depression. *Arch. Gen. Psychiatry* 63 (8), 856–864. doi:10.1001/archpsyc.63.8.856

Zeitler, S., Ye, L., Andreyeva, A., Schumacher, F., Monti, J., Nürnberg, B., et al. (2019). Acid Sphingomyelinase - a Regulator of Canonical Transient Receptor Potential Channel 6 (TRPC6) Activity. *J. Neurochem.* 150 (6), 678–690. doi:10.1111/jnc.14823

Zhao, Z., Kesti, T., Uğurlu, H., Baur, A. S., Fagerlund, R., and Saksela, K. (2019). Tyrosine Phosphorylation Directs TACE into Extracellular Vesicles

via Unconventional Secretion. *Traffic* 20 (3), 202–212. doi:10.1111/tra.12630

Zhou, P., Yang, X. L., Wang, X. G., Hu, B., Zhang, L., Zhang, W., et al. (2020). A Pneumonia Outbreak Associated with a New Coronavirus of Probable Bat Origin. *Nature* 579 (7798), 270–273. doi:10.1038/s41586-020-2012-7

Zimniak, M., Kirschner, L., Hilpert, H., Geiger, N., Danov, O., Oberwinkler, H., et al. (2021). The Serotonin Reuptake Inhibitor Fluoxetine Inhibits SARS-CoV-2 in Human Lung Tissue. *Sci. Rep.* 11 (1), 5890. doi:10.1038/s41598-021-85049-0

Conflict of Interest: The authors declare that the research was conducted in the absence of any commercial or financial relationships that could be construed as a potential conflict of interest.

Publisher's Note: All claims expressed in this article are solely those of the authors and do not necessarily represent those of their affiliated organizations, or those of the publisher, the editors and the reviewers. Any product that may be evaluated in this article, or claim that may be made by its manufacturer, is not guaranteed or endorsed by the publisher.

Advantages of publishing in Frontiers

OPEN ACCESS
Articles are free to read for greatest visibility and readership

FAST PUBLICATION
Around 90 days from submission to decision

HIGH QUALITY PEER-REVIEW
Rigorous, collaborative, and constructive peer-review

TRANSPARENT PEER-REVIEW
Editors and reviewers acknowledged by name on published articles

Frontiers
Avenue du Tribunal-Fédéral 34
1005 Lausanne | Switzerland

Visit us: www.frontiersin.org
Contact us: frontiersin.org/about/contact

REPRODUCIBILITY OF RESEARCH
Support open data and methods to enhance research reproducibility

DIGITAL PUBLISHING
Articles designed for optimal readership across devices

FOLLOW US
@frontiersin

IMPACT METRICS
Advanced article metrics track visibility across digital media

EXTENSIVE PROMOTION
Marketing and promotion of impactful research

LOOP RESEARCH NETWORK
Our network increases your article's readership